Fisheries and Oceans Canada | Pêches et Océans Canada
Ecosystems and Oceans Science | Sciences des écosystèmes et des océans

Canadian Science Advisory Secretariat (CSAS)

Research Document 2022/010

Pacific Region

Yellowmouth Rockfish (*Sebastes reedi*) stock assessment for British Columbia in 2021

Paul J. Starr[1] and Rowan Haigh[2]

[1]Canadian Groundfish Research and Conservation Society
1406 Rose Ann Drive
Nanaimo, BC V9T 4K8

[2]Pacific Biological Station, Science Branch
Fisheries and Oceans Canada
3190 Hammond Bay Road
Nanaimo, BC V9T 6N7

December 2022

Canada

Foreword

This series documents the scientific basis for the evaluation of aquatic resources and ecosystems in Canada. As such, it addresses the issues of the day in the time frames required and the documents it contains are not intended as definitive statements on the subjects addressed but rather as progress reports on ongoing investigations.

Published by:

Fisheries and Oceans Canada
Canadian Science Advisory Secretariat
200 Kent Street
Ottawa ON K1A 0E6

http://www.dfo-mpo.gc.ca/csas-sccs/
csas-sccs@dfo-mpo.gc.ca

ISSN 1919-5044
ISBN 978-0-660-42109-4 Cat. No. Fs70-5/2022-010E-PDF

Correct citation for this publication:

Starr, P.J. and Haigh, R. 2022. Yellowmouth Rockfish (*Sebastes reedi*) stock assessment for British Columbia in 2021. DFO Can. Sci. Advis. Sec. Res. Doc. 2022/010. viii + 288 p.

Aussi disponible en français :

*Starr, P.J. and Haigh, R. 2022. Évaluation du stock de sébaste à bouche jaune (*Sebastes reedi*) de la Colombie-Britannique en 2021. DFO Can. Sci. Advis. Sec. Res. Doc. 2022/010. viii + 319 p.*

TABLE OF CONTENTS

LIST OF MAIN TABLES

LIST OF MAIN FIGURES

ABSTRACT

Yellowmouth Rockfish (*Sebastes reedi*, YMR) ranges from the Gulf of Alaska southward to northern California near San Francisco. In British Columbia (BC), the apparent area of highest concentration occurs in Queen Charlotte Sound with isolated hotspots west of Haida Gwaii and at the northern end of Vancouver Island. This species occurs along the west coast of Vancouver Island, but its density appears to be low south of Brooks Peninsula.

In 2010, the Committee on the Status of Endangered Wildlife in Canada (COSEWIC) assessed the coastal population of YMR in British Columbia as 'Threatened', based on an analysis of survey indices and the threat from commercial fishing. As a result, the species was considered for legal listing under the *Species at Risk Act* (SARA). In a 2011 stock assessment (also acting as a recovery potential assessment), Edwards et al. (2012a) put forward two base case runs ('Estimate *M*' and *M*=0.047), which both estimated that the B_{2011} stock status was well above the upper stock reference level for a healthy stock in the Fisheries and Oceans Canada (DFO) Sustainable Fisheries Framework (DFO 2009). In 2017, a decision was made not to list Yellowmouth Rockfish under Schedule 1 of the SARA. In 2019, Bill-C-68 was enacted to amend the Fisheries Act with the Fish Stocks provisions, prompting a national review of the approximately 180 stocks using Sustainability Surveys with the aim to include the majority of those stocks in regulation over the next five years. Yellowmouth Rockfish is one of 18 groundfish stocks in the Pacific Region being considered for inclusion. The purpose of this YMR stock assessment is to evaluate the current stock status and provide advice suitable for input to a sustainable fisheries management plan.

This stock assessment evaluates a BC coastwide population harvested by a single fishery dominated by bottom trawl. Midwater trawl catches of YMR were combined with bottom trawl for the purposes of this stock assessment. YMR catches by capture methods other than trawl were negligible, averaging less than 1% over the period 1996 to 2020. Analyses of biology and distribution did not support separate regional stocks for YMR. A single coastwide stock was also assumed by Edwards et al. (2012a).

We use an annual catch-at-age model tuned to four fishery-independent trawl survey series, a bottom trawl Commercial catch per unit effort (CPUE) series, annual estimates of commercial catch since 1935, and age composition data from survey series (25 years of data from four surveys) and the commercial fishery (28 years of data). The model starts from an assumed equilibrium state in 1935, the survey data cover the period 1967 to 2020 (although not all years are represented) and the CPUE series provides an annual index from 1996 to 2020.

A two-sex model was implemented in a Bayesian framework, using the Markov Chain Monte Carlo (MCMC) 'No U-Turn Sampling' procedure, to estimate models which fixed natural mortality to one of five levels (0.04, 0.045, 0.05, 0.055, 0.06), spanning a range that was considered plausible and which returned acceptable MCMC diagnostics. The parameters estimated by these models included average recruitment over the period 1950–2012, and selectivity for the four surveys and the commercial trawl fleet. The survey and CPUE scaling coefficients (q) were determined analytically. These five model runs were combined into a composite base case which explored the major axis of parameter uncertainty in this stock assessment. Fourteen sensitivity analyses were performed relative to the central run (M=0.05) of the composite base case to test the effect of alternative model assumptions.

The composite base case estimated the YMR female spawning population biomass at the end of 2021 to be 0.69 (0.44, 1.08) relative to B_0 and to be 2.4 (1.5, 3.7) relative to B_{MSY}. This latter result suggests that the YMR spawning population currently lies well in the Healthy zone (with a probability >0.99). Projections predicted that the stock will remain in the Healthy zone up to the

end of 2031 at all evaluated catch levels up to 3000 t/y. However, these projections also predicted that the stock would decline at catch levels greater than 500 t/y, under the assumption that recruitment will be average over that time period. None of the fourteen sensitivity analyses changed this conclusion. These analyses included, estimating M, higher and lower pre-1996 catch histories, higher and lower recruitment standard deviation (σ_R) assumptions, dropping the CPUE series and substituting an alternative CPUE series, omitting ageing error, restricting the period over which recruitments were estimated to 1970–2012, and upweighting the age frequency data for the Queen Charlotte Sound synoptic survey. The most pessimistic sensitivity run was the one which omitted the ageing error, an option that we consider unrealistic.

1. INTRODUCTION

In 2010, the Committee on the Status of Endangered Wildlife in Canada (COSEWIC) assessed the coastal population of Yellowmouth Rockfish (YMR, *Sebastes reedi*) in British Columbia (BC) as 'Threatened', based on an analysis of survey indices and the threat from commercial fishing. As a result, the species was considered for legal listing under the *Species at Risk Act* (SARA). In a 2011 stock assessment (also acting as a recovery potential assessment), Edwards et al. (2012a) put forward two base case models, one which estimated natural mortality (M) for males at 0.060 (0.054, 0.065)[1] and for females at 0.056 (0.051, 0.061) while the other model fixed M for both sexes at 0.047. The 'estimate M' base case modelled the 2011 beginning year stock status of YMR as 0.61 (0.43, 0.83) of the unfished equilibrium spawning biomass (B_0), and 2.69 (1.61, 4.57) of the spawning biomass at maximum sustainable yield (B_{MSY}), while B_0 was estimated to be 46,300 tonnes (35,700, 70,300). The equivalent estimates for the 'fix M' base case were B_{2011}/B_0 = 0.41 (0.29, 0.55), B_{2011}/B_{MSY} = 1.92 (1.09, 3.20) and B_0 = 37,300 (33,500, 42,400). Both base case model estimates for the B_{2011} stock status were well above the upper stock reference level for a healthy stock in the DFO Sustainable Fisheries Framework (DFO 2009).

In 2017, a decision was made not to list Yellowmouth Rockfish under Schedule 1 of the SARA. While DFO will continue to manage this species under the *Fisheries Act*, actions to address conservation concerns were outlined in the order not to list (SI/2017-24 May 3, 2017). In 2019, Bill-C-68 was enacted to amend the Fisheries Act with the Fish Stocks provisions, prompting a national review of the approximately 180 stocks using Sustainability Surveys with the aim to include the majority of those stocks in regulation over the next five years. Yellowmouth Rockfish are one of 18 groundfish stocks in the Pacific Region being considered for inclusion.

Based on the distribution of catches and CPUE over the period 1996–2020, the bulk of the BC population of YMR is centred in Queen Charlotte Sound (central BC coast), specifically in association with the three main gullies – Goose Island, Mitchell's, and Moresby. There are also density 'hotspots' off the southwest coast of Haida Gwaii (near Cape St. James), off Rennell Sound, off the northwest coast of Haida Gwaii, and off the northwest coast of Vancouver Island. Densities of YMR appear to be low off the west coast of Vancouver Island south of Brooks Peninsula. Preliminary analyses showed no strong evidence for stock separation along the BC coast based on growth and size frequency; therefore, the coastwide population was assessed, as it was in 2011.

In 2011, data for YMR were deemed sufficient (given available index series and age structures) to conduct a statistical catch-at-age analysis which allowed Edwards et al. (2012a) to use a model variant of Coleraine (Hilborn et al. 2003) called 'Awatea'. For this stock assessment, we have used the National Oceanic and Atmospheric Administration's (NOAA's) Stock Synthesis (SS, version 3.30.17, Methot and Wetzel 2013, Methot et al. 2021) model, which has been adopted by many United States assessment scientists in the Pacific region. This stock assessment software has more flexibility in fitting data and provides some useful diagnostics (e.g., retrospective analysis) that are not available in Awatea.

The SS statistical catch-at-age software (see APPENDIX E for equations) was used to model the YMR population. The assessment model included:

- sex-specific parameters;
- abundance indices by year (y):

[1] denoting median and 0.05 and 0.95 quantiles of the Bayesian posterior distribution

- one bottom trawl CPUE series (25y, 1996-2020);
- three synoptic bottom trawl surveys:
  QCS = Queen Charlotte Sound (10y, spanning 2003 to 2019),
  WCVI = west coast Vancouver Island (8y, spanning 2004 to 2018),
  WCHG = west coast Haida Gwaii (8y, spanning 2006 to 2020);
- one historical bottom trawl survey:
  GIG = Goose Island Gully (8y, spanning 1967 to 1994);

- proportions-at-age data (also called age frequencies or 'AF') by year (y), five sets:
  - commercial trawl catch (28y, spanning 1979 to 2019),
  - QCS Synoptic (9y, spanning 2003 to 2019),
  - WCVI Synoptic (4y, spanning 1996 to 2012),
  - WCHG Synoptic (9y, spanning 1997 to 2018),
  - GIG Historical (3y spanning 1979 to 1995);
- maximum modelled age of 60 y, with older ages accumulated into the final age class;
- estimated selectivities for the commercial fishery and for the four sets of survey indices.

The input data were reweighted once based on the recommendations of Francis (2011) for abundance and McAllister and Ianelli (1997) for composition data (APPENDIX E). The age frequency weightings used in the component runs of the base case appear in Table F.2 and in Table F.18 for the sensitivity runs.

This stock assessment is being conducted at the request of Fisheries and Oceans Canada (DFO) Fisheries Management Branch made to the DFO Science Branch for advice regarding the status of YMR relative to reference points that are consistent with the DFO's *Fishery Decision-Making Framework Incorporating the Precautionary Approach* (DFO 2009), including the implications of various harvest strategies on expected stock status. In the absence of updated science advice, there is uncertainty about the risks posed to the BC YMR stock at current levels of catch. This advice is reviewed at a Canadian Science Advisory Secretariat (CSAS) Regional Peer Review (RPR) that considers the scientific capability of the assessment to inform fisheries management decisions when establishing catch levels for the species. This work also informs and supplements decisions external to DFO, specifically COSEWIC.

1.1. ASSESSMENT BOUNDARIES

This assessment includes Pacific Marine Fisheries Commission (PMFC[2]) major areas (3CD and 5ABCDE) along the BC coast (Figure 1). The available biological data were examined for evidence of stock separation (see Section D.3) between the most northerly component of the YMR stock (west coast Haida Gwaii) and the remaining southerly sections of the population. This potential split was chosen as the scenario with the greatest potential to show population differences. This was because a separation of the west coast Haida Gwaii finfish populations from the remainder of the coast has been observed in other BC finfish populations (e.g., Pacific Ocean Perch, Walleye Pollock, Rougheye/Blackspotted Rockfish complex). While some differences (growth, size, and composition taken by gear type) among areas were found, the differences were generally small and not always consistent across years or sexes. Furthermore, YMR data from the west coast Haida Gwaii were sparse and this part of the coast only accounted for a relatively small proportion of the catch (mean 1996–2020 percentage=12%). Consequently, we elected to make the same single stock assumption that had been made by Edwards et al. (2012a).

[2] See APPENDIX A for historical background on the PMFC.

The PMFC areas are similar but not identical to the management areas used by the Groundfish Management Unit (GMU), which uses combinations of DFO Pacific Fishery Management Areas. A further complication for YMR and Pacific Ocean Perch is that the GMU areas were modified in 1997 for these two species so that GMU area 5C was expanded around Cape St. James, incorporating parts of PMFC areas 5B and 5E. We have not used GMU management areas for catch reconstruction because catch reporting from these areas has only been available since 1996; however, we have adjusted the 5C boundary for biological analyses. Although traditional PMFC areas are somewhat different than the GMU areas for YMR, managers can prorate any catch policy using historical catch ratios as outlined in 0, Section A.3.

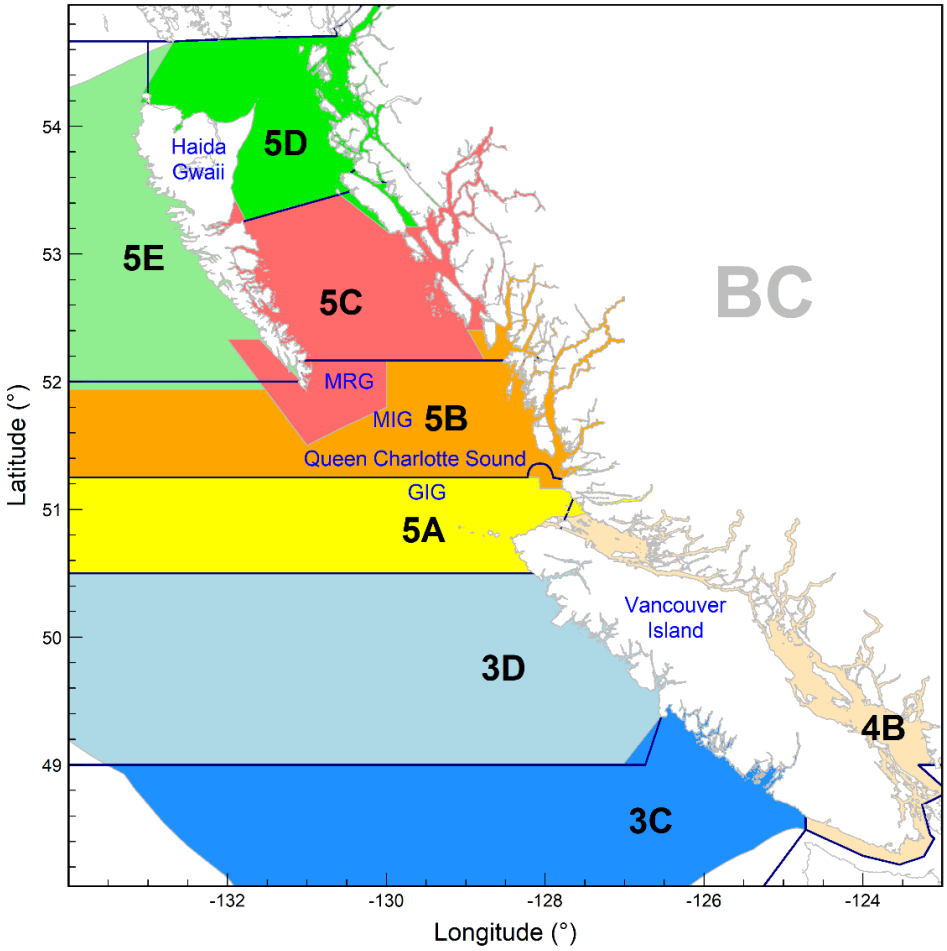

Figure 1. Pacific Marine Fisheries Commission (PMFC) major areas (outlined in dark blue) compared with Groundfish Management Unit areas for YMR (shaded). For reference, the map indicates Moresby Gully (MRG), Mitchell's Gully (MIG), and Goose Island Gully (GIG). This assessment covers one coastwide stock: PMFC 3CD + 5ABCDE.

1.2. RANGE AND DISTRIBUTION

Yellowmouth Rockfish range from the Gulf of Alaska southward to northern California near San Francisco, typically at depths between 180 and 275 m (Love et al. 2002). In BC, the apparent area of highest concentration occurs in Queen Charlotte Sound (PMFC areas 5A and 5B in Figure 2) with isolated hotspots west of Haida Gwaii (PMFC area 5E in Figure 2) and at the northern end of Vancouver Island (PMFC area 5A in Figure 2). This species occurs along the west coast of Vancouver Island (3C/3D in Figure 2), but its density appears to be low south of

Brooks Peninsula. Adults occur on the bottom and in midwater above high-relief rocks, and have been aged up to 99 years in BC. This species has been encountered by the BC bottom trawl fleet over an estimated 30,192 km^2 (Figure 2 top left, based on a roughly 32-km^2 grid size and tow start positions in the commercial fishery), and the bulk of the BC population has been captured by the trawl fleet between depths of 130 m and 402 m (see Appendix G). Maps of catch hotspots by fishing locality indicate the top three localities to be 'Triangle', 'South Triangle', and 'SE Cape St. James' (Figure G.8).

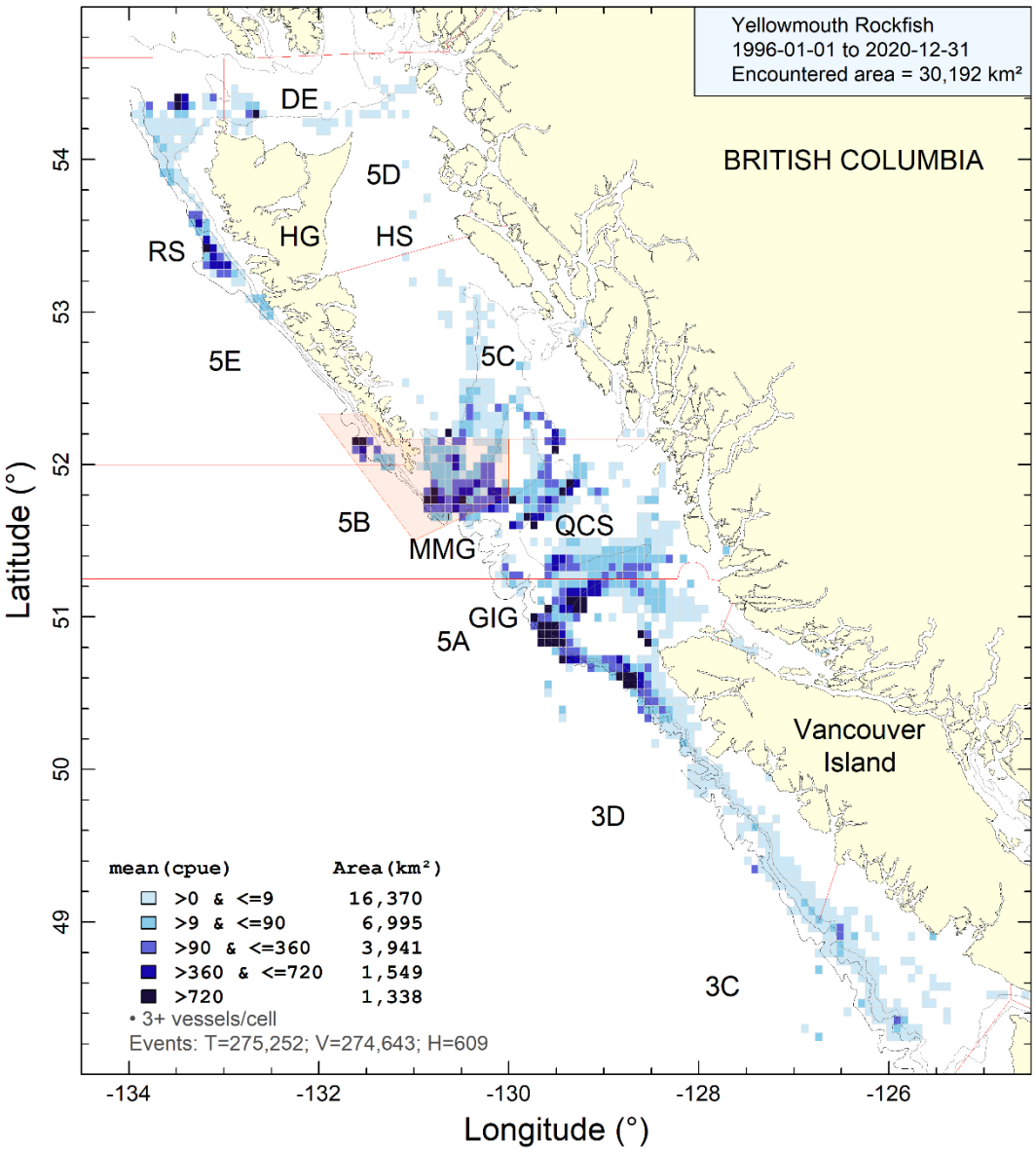

Figure 2. Areal distribution of YMR mean trawl (bottom + midwater) catch per unit effort (kg/hour) from 1996 to 2020 in grid cells 0.075° longitude by 0.055° latitude (roughly 32 km² each). Isobaths show the 100, 200, 500, and 1000 m depth contours. Cells with <3 fishing vessels are not displayed. DE=Dixon Entrance, GIG=Goose Island Gully, HG=Haida Gwaii, HS=Hecate Strait, MMG=Mitchell's and Moresby Gullies, QCS=Queen Charlottes Sound, RS=Rennell Sound. Shaded polygon shows the extension of area 5C for managing Pacific Ocean Perch and Yellowmouth Rockfish, primarily to capture Moresby Gully as a single management unit.

2. CATCH DATA

This stock assessment recognises one commercial fishery dominated by trawl (bottom + midwater), with minor removals by halibut longline, sablefish trap, lingcod longline, inshore longline, and salmon troll. Recreational YMR catches were assumed to be non-existent or negligible. Commercial discards, as reported by full-time observer coverage since 1996, are small, averaging less than 2% over the 25-year period.

The methods used to prepare a catch history for this YMR assessment, along with the full catch history, are presented in detail in APPENDIX A. Information about species caught concurrently with YMR commercial catches is presented in APPENDIX G. The average annual YMR catch for all capture methods over the most recent five years (2016–20) was 1,272 metric tonnes (t) coastwide.

The catch for 2021 was incomplete and so we used the catch from 2020 (1057 t) for 2021. The 2020 catch was lower than the five-year average (1,272 t), which likely reflected the impact from the Covid19 disruptions (e.g., lockdowns) as well as changes in market demand. We consulted with Industry and were told that this estimate for the YMR catch in 2021 (of around 1000 t) was reasonable given the ongoing circumstances. The current year catch was added to the model to provide managers with advice that starts at the end of 2021.

We compared length and age distributions for bottom and midwater trawl data across years and sexes and found some differences in the respective distributions (see Appendix D, Section D.3.2), mainly that the bottom trawl fishery tended to sample older fish than were seen in the midwater trawl fishery. There was also a suggestion that midwater trawl captures were smaller and younger than bottom trawl fish, but this difference was not consistent across years. While these differences may be sufficient to treat midwater trawl as a separate fishery, there were inadequate age data to fully characterise the midwater fishery across years as well as the observation that this fishery only accounts for 16% of the total annual catch of YMR from 1996 to 2020. Consequently, we chose to combine the AF data from midwater trawl gear with the bottom trawl data.

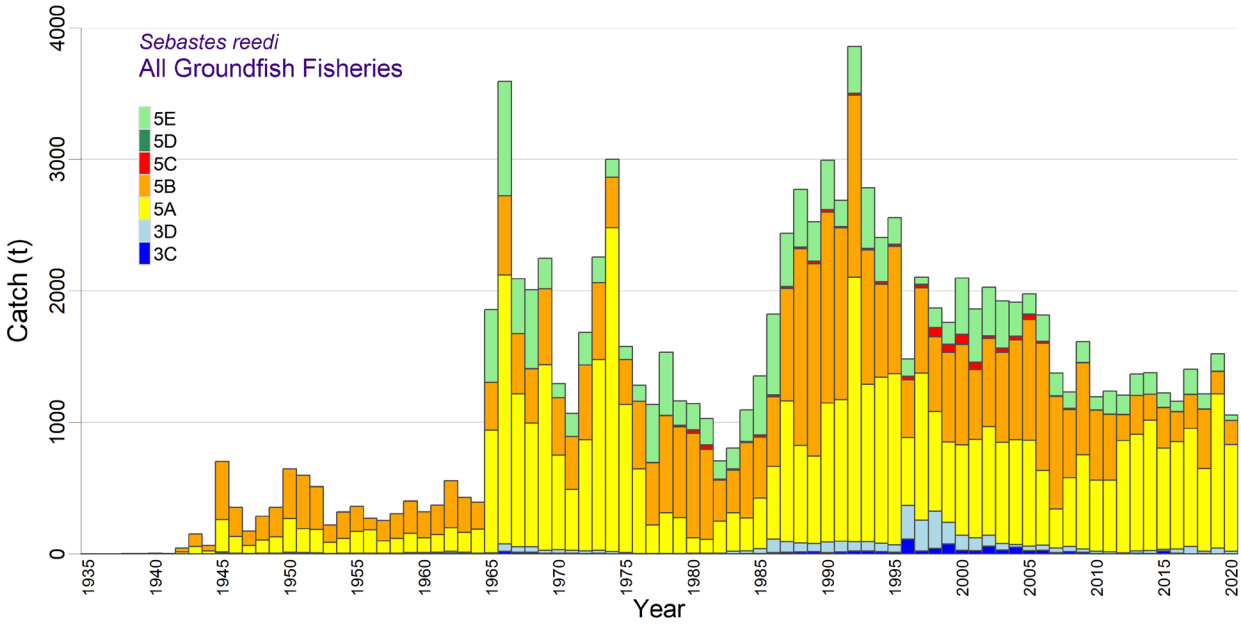

Figure 3. Catch reconstruction of Yellowmouth Rockfish from 1935 to 2020 used in the stock assessment model. The 2021 catch was assigned the same value (1057 t) as the 2020 catch.

3. FISHERIES MANAGEMENT

Before 1977, no quotas were in effect for any slope rockfish species. Since then, the DFO groundfish management unit (GMU) imposed a combination of species/area quotas, area/time closures, and trip limits on major finfish species. Quotas in the form of total allowable catches (TACs) were first introduced specifically for YMR in 1979 for the BC coast (Table A.1, and see Table A.2 for additional management actions taken).

A coastwide YMR stock assessment (and recovery potential assessment) was conducted in 2011 (Edwards et al. 2012a) to address concerns by COSEWIC which listed the species as 'Threatened', with the commercial fishery being the primary threat (COSEWIC 2010). Estimates for the ratio of spawning biomass (mature females only) at the beginning of 2011 to the unfished equilibrium spawning biomass were 0.61 (0.43-0.83) and 0.41 (0.29-0.55) for runs 'Estimate M' and 'Fix M' respectively. Exploitation rates for 2010 were estimated to be 0.020 (0.010-0.036) for run 'Estimate M' and 0.038 (0.026-0.059) for run 'Fix M', compared to respective historic highs of 0.090 (0.059-0.123) and 0.130 (0.110-0.154) estimated for 1966 during intense fishing by foreign fleets. The low estimated exploitation rates in 2010 (0.02-0.04 y^{-1}) led to the conclusion that coastwide BC YMR did not appear to have any sustainability issues, especially as they were lower than *M*, either fixed at 0.047 or estimated to be 0.060 (0.054, 0.065) for females. Typically, rockfish experience slow declines in stock size in between episodic large recruitment events. Consequently, even though a persistent *F*+*M* mortality occurs, it can be considered 'sustainable' over long periods as long as these episodic recruitment events replenish the population and fishing mortality is kept to low levels.

Yellowmouth Rockfish has the third highest total allowable catch (TAC) for rockfish in BC (after Pacific Ocean Perch and Yellowtail Rockfish), with an annual coastwide TAC of 2,444 t. The combined midwater and bottom trawl fishery accounts for 97% of the coastwide TAC of YMR, with the rest allocated to the hook and line fishery. Appendix 8 of the 2021 DFO Integrated Fisheries Management Plan (IFMP) reports the coastwide trawl TAC for YMR at 2,361 t. This has not changed since 2001.

4. SURVEY DESCRIPTIONS

Four sets of fishery independent survey indices were used to track changes in the biomass of this population coastwide (APPENDIX B):

1. *QCS Synoptic* – a random-stratified synoptic (species comprehensive) trawl survey covering all of Queen Charlotte Sound (QCS) and targeting a wide range of finfish species. This survey has been repeated 10 times between 2003 to 2019, using three different commercial vessels but with a consistent design, including the same net. An 11th QCS survey was conducted in July/August 2021 but these data were not available for inclusion in this stock assessment.
2. *WCVI Synoptic* – a random-stratified synoptic trawl survey covering the west coast of Vancouver Island (WCVI). This survey was repeated eight times between 2004 to 2018 using the research vessel FV *Ricker* and was conducted in 2018 using a commercial vessel after the retirement of the *Ricker*. The scheduled 2020 WCVI synoptic survey was delayed until 2021 due to concerns caused by the COVID-19 pandemic. This survey employs a consistent design, including the same net, and targets a wide range of finfish species.
3. *WCHG Synoptic* – a random-stratified synoptic trawl survey covering the west coast (WC) of Graham Island in Haida Gwaii (HG) and the western part of Dixon Entrance. This survey has

been repeated eight[3] times between 2006 to 2020 using three commercial vessels and a consistent design, including the same net and targeting a wide range of finfish species. In 2020, during the COVID pandemic, this survey was conducted without any DFO personnel on board, but the data from this survey have been included in this stock assessment. The 2014 survey was omitted from the series because less than ½ of the tows were completed. A random stratified WCHG trawl survey that operated in 1997 under a slightly different design was not included in this series, although it was included in a sensitivity run.

4. *GIG Historical* – a composite series of seven indices extending from 1967 to 1984 in Goose Island Gully (GIG). Most of these surveys were performed by the research vessel *G.B. Reed*, but two commercial vessels (*Eastward Ho* and *Ocean Selector*) were used in 1984 and 1994 respectively. Only tows located in Goose Island Gully (GIG) have been used to ensure continuity across all surveys.

The Hecate Strait (HS) multi-species assemblage bottom trawl survey, HS synoptic survey, and the two shrimp trawl surveys (WCVI and QCS) have been omitted from this stock assessment (even though the QCS shrimp survey was included in the 2011 stock assessment) because either the presence of YMR in these surveys has been sporadic or the coverage, spatial or by depth, has been incomplete, rendering these surveys poor candidates to provide reliable abundance series for this species. Rockfish stock assessments, beginning with Yellowtail Rockfish (DFO 2015), have explicitly omitted using the WCVI and QCS shrimp surveys because of the truncated depth coverage, which ends at 160 m for the WCVI shrimp survey and at 231 m for the QCS survey. Both surveys have constrained spatial coverage with the WCVI survey confined to the centre of WCVI and the QCS survey only covering the inshore (head) end of Goose Island Gully.

The relative biomass survey indices were used as data in the models along with the associated relative error for each index value. No process error was added to the survey relative errors because the observation errors were already high (Appendix B).

5. COMMERCIAL CPUE

Commercial catch per unit effort (CPUE) data were used to generate indices of abundance as input to the model fitting procedure (see Appendix C). This series of annual indices, extending from 1996 to 2020, provided a more informative abundance signal to the model than did the four survey series, probably due to the higher relative error among the survey series, the shorter period covered by the surveys and the greater number and frequency of index values in the CPUE series. There was concern that using CPUE from a targeted fishery might not reflect abundance but be contaminated by fisher behaviour responses to economic considerations. This concern was addressed in a number of ways. First, the CPUE series was compared with each survey series (see Section C.6 in Appendix C). This comparison is equivocal for all surveys because of the large relative errors associated with the survey estimates for this species. The best comparison was for the QCS synoptic survey, which showed an acceptable match (see Figure C.18) in spite of the large relative errors. Second, the CPUE analysis was repeated two more times, with each iteration successively removing the DFO localities that returned the highest catch rates (once for the top five localities in the lognormal analysis and then removing an additional four localities which had the highest binomial catch rates). The logic underlying this procedure was that, if targeting of YMR were affecting the estimated relative series, the localities with the highest catch rates would be the areas that fishers use preferentially for targeting YMR. However, these sensitivity analyses returned CPUE series that

[3] The 2014 West Coast Haida Gwaii survey did not complete and is not usable.

differed little from the original series (see Figure C.22), a result which suggests that the CPUE abundance indices estimated from these commercial data show good consistency between the low- and high-catch rate localities.

The CPUE abundance index series was standardised for changes to vessel configuration, catch timing (seasonality), and location of catch (e.g., latitude, DFO locality, and depth) to remove potential biases in CPUE that may result from changes in fishing practices and other non-abundance effects. This procedure was followed in two steps, with the model fitted to the positive catches assuming a lognormal distribution and to the presence/absence of YMR assuming a binomial distribution. These two models were then combined using a multiplicative "delta-lognormal" model (Eq. C.4). In these models, abundance was represented as a 'year effect' and the explanatory variables were selected sequentially by a General Linear Model, which accounted for variation in the available data. Other factors that might affect the behaviour of fishers, particularly economic factors, do not enter these models due to a lack of applicable data, thus resulting in indices that may not entirely reflect changes in the underlying stock abundance. APPENDIX C provides details on the CPUE analyses and APPENDIX F provides one sensitivity to the removing of the CPUE index series and another that uses a CPUE series derived from using a Tweedie distribution (Jorgensen 1987). Process error of 0.3296 was added to the CPUE observation errors (see APPENDIX E, Section E.6.1 for its derivation).

6. BIOLOGICAL INFORMATION

6.1. BIOLOGICAL SAMPLES

Age proportion samples from 1979 to 2019 were available from commercial trawl (combined bottom and midwater) catches of YMR, with a total of 28 years covered by at least two samples per year. Age frequency (AF) samples were also available from the four surveys: QCS (2003-2019 with 9y AF), WCVI (1996-2012 with 4y AF), WCHG (1997-2018 with 9y AF), and GIG (1979-1995 with 3y AF). Only otoliths aged using the 'break and burn' (B&B) method were included in age samples used in this assessment because an earlier surface ageing method was shown to be biased, especially with increasing age (Stanley 1987). However, surface ageing is currently the preferred method for ageing very young rockfish (≤ 3y) by the ageing lab (DFO, 2022.). Commercial fishery age frequency data were summarised for each quarter, weighted by the YMR catch weight for the sampled trip. The total quarterly samples were scaled up to the entire year using the quarterly landed commercial catch weights of YMR. See APPENDIX D (Section D.2.1) for details.

Sampled AFs from bottom and midwater trawl were combined after comparing cumulative AFs for each gear type by sex and capture year and concluding that the AF series from the two capture methods were reasonably consistent and that there were insufficient data to construct independent midwater trawl AFs (see Section D.3.2). Consequently, the model was run assuming a joint selectivity for these two trawl methods by combining the AFs and the catch data into a single trawl fishery. There were no ageing data for the other fisheries.

Moderate amounts of age frequency data were available from the four survey series used in the model. While sample sizes were reasonable, the number of fish aged was marginal (<200 fish by sex per year). The survey AFs were scaled to represent the total survey in a manner similar to that used for the commercial samples: within an area stratum, samples were weighted by the YMR catch density in the sampled tows; stratum samples were then weighted by the stratum areas (section D.2.2). Survey selectivity priors were based on posterior medians from various Pacific Ocean Perch (POP) stock assessments in 2017 for Trawl, QCS, and GIG (Haigh et al.

2018), and in 2012 for WCVI (Edwards et al. 2014a) and WCHG (Edwards et al. 2014b). Standard deviations for the normal priors were calculated as 20% of the mean.

Examination of the resulting scaled survey AFs indicated poor consistency across years and between sexes within a survey year. That is, strong and weak year classes did not track properly, with a strong year class not showing up in the following survey or a strong year class for males being weak for females within the same year. Early model runs which gave these data appropriate weights led to what appeared to be spurious year class strengths that were in conflict with the year class estimates coming from the commercial age data. Consequently, we decided to only use the commercial age frequency data to estimate year class deviations and to severely downweight the survey age data. This approach allowed the model to estimate appropriate selectivity functions for each survey while not allowing the survey age data to contribute to the estimation of year class strength. We ran a single sensitivity run which upweighted the QC Sound survey age data to illustrate the effect of giving too much weight to these data.

6.2. AGEING ERROR

Ageing error is a common issue in most age-structured stock assessments. Figure D.17 (see Section D.2.3 in Appendix D) suggests that YMR ages estimated by the primary readers were reproduced reasonably consistently by secondary readers when performing spot-check analyses, but there were some large discrepancies. The base population model for YMR used an ageing error vector based on the CVs of observed lengths-at-age (Figure D.18). This ageing error vector resolved recruitment events in the data such that four large recruitment spikes were identified (in 1952, 1961, 1982, and 2006). A sensitivity run using no ageing error was performed for comparison.

6.3. GROWTH PARAMETERS

Growth and allometric length-weight parameters were estimated from YMR length and age data using biological samples collected from the synoptic surveys conducted between 2003 and 2019 (Section D.1.1 in APPENDIX D). Allometric parameters were similar for females and males: (log α, β) = F (-11.76, 3.18), M (-11.95, 3.24).

Previous attempts to incorporate ageing error when fitting growth parameters (for Bocaccio, Starr and Haigh, in press[a]) did not show much difference compared to fitting without ageing error, and the same was found for YMR (results not presented); therefore, we use the standard maximum likelihood estimation [MLE] fits for YMR using both research and surveys. Females are only marginally bigger than males (L_∞: F=48.2 cm, M=46.7 cm). Growth models were also estimated using a Bayesian procedure that included random effects that incorporate ageing error (see Appendix D, section D.3). A comparison of the coast-wide Bayesian models from this procedure with the equivalent MLE models used in the stock assessment shows no functional difference for either sex (Figure D.24 right panel).

Research survey data are preferred over commercial data when estimating allometric and growth parameters because surveys generally capture a wider variety of sizes and ages. Commercial data lack information on smaller fish because the cod ends deliberately exclude small, less marketable fish, while a survey attempts to capture a wide range of sizes. Consequently the growth functions derived from commercial data will be poorly determined at the lower end. There are usually sufficient aged otoliths just from the research data that there is no need to include commercial data. The stock assessment assumes that YMR has a time invariant set of biological parameters which exist regardless of the gear used to collect the data.

6.4. MATURITY AND FECUNDITY

The proportions of females that mature at ages 1 through 40 were computed from biological samples collected from the commercial fishery and research surveys. Although it is preferable to use research data to estimate biological functions, this is not always possible for species which mature in the late autumn, winter or early spring months. This is because the research surveys generally only cover the period May to September, when the weather tends to be better.

Maturity stage was determined macroscopically by either the research technicians on the survey vessels or the commercial fishery observers, partitioning the samples into one of seven maturity stages (Stanley and Kronlund 2000; described in APPENDIX D, Section D.1.3). Fish assigned to stages 1 or 2 were considered immature while those assigned to stages 3-7 were considered mature. Data representing staged and aged females (using the B&B method) were pooled from research and commercial trips and the observed proportion mature at each age was calculated. All months were used in creating the maturity curve because these data provided cleaner fits than using a subset of months. Yellowmouth Rockfish spawn in winter, so winter data are needed to estimate a credible function. A monotonic increasing maturity-at-age vector was constructed by fitting a half-Gaussian function (Equation D.3) to the observed maturity values (APPENDIX D, Section D.1.3). The ogive used in the model assigned proportions mature to zero for ages 1 to 4, then switched to the fitted monotonic function for ages 5 to 40, all forced to 1.0 (fully mature) from age 17 to age 60. This strategy follows previous BC rockfish stock assessments where it was recognised that younger ages are not well sampled, and those that are, tend to be larger and more likely to be mature (e.g., Stanley et al. 2009). Females older than age 10 were assumed to be at least 50% mature and maturity was assumed to be constant over time (an examination of maturity ogives in 5-year periods from 1996 to 2020 showed no substantial changes over time).

Fecundity was assumed to be proportional to the female body weight (approximately length cubed); however, researchers have demonstrated that this assumption may have consequences for sustainability. Specifically, if larger and older females produce more eggs of higher quality, the removal of these productive females by fishing will have a disproportionate effect on recruitment (He et al. 2015). Dick et al. (2017) concluded that relative fecundity (eggs per gram body weight) increased with size in *Sebastes*, and estimated the length-fecundity relationship median exponent for POP to be 4.97, which is considerably larger than the cubic length-weight exponents typically used for BC rockfish stock assessments (e.g., Table D.2). Another issue affecting reproductive output is ‘skip spawning’ where some species do not spawn in every year (Rideout and Tomkiewicz 2011). Conrath (2017) found varying rates of skipped spawning in three deepwater rockfish species. It is not known if YMR exhibit skipped spawning.

6.5. NATURAL MORTALITY

Using the natural mortality estimators of Hoenig (1983) and Gertseva (Starr and Haigh, 2021), Table D.8 explored various ages associated with the upper tail of the YMR age distribution (Figure D.7). For ages 50 and above (at 10-y increments), estimates of M span 0.047 to 0.108. We were able to estimate YMR natural mortality (M) within the model – female: mode of the posterior distribution [MPD] M = 0.066, MCMC M = 0.070 (0.060, 0.078); male: MPD M = 0.064, MCMC M = 0.068 (0.058, 0.076). However, the MCMC estimate moved well above the normal prior N(0.05,0.01) and sample diagnostics were poor, indicating that the model could not converge when M was estimated, even with a tight prior. This is likely due to the lack of a strong abundance signal in the survey data. Given the poor MCMC performance of the model which

estimated M, we opted to fix M at values that spanned a credible range for this parameter guided by the analyses summarised in Table D 8: M Î {0.04, 0.045, 0.05, 0.055, 0.06}.

6.6. STEEPNESS

The 'steepness' parameter, h, specifies the proportion of the maximum recruitment that is available at $0.2B_0$, where B_0 is the unfished equilibrium spawning biomass (mature females). This stock assessment fixed steepness to 0.7, partly to reduce the number of parameters estimated by the model and partly because there was no indication that the coastwide stock was depleted (approaching $0.2B_0$) so that this parameter will have very little impact in the stock reconstruction.

7. AGE-STRUCTURED MODEL

A two-sex, age-structured, stochastic model was used to reconstruct the population trajectory of YMR from 1935 to the end of 2021 using the National Oceanic and Atmospheric Administration's (NOAA's) Stock Synthesis 3 (SS) model platform. Ages were tracked from 1 to 60, where 60 acted as an accumulator age category. The population was assumed to be in equilibrium with average recruitment and with no fishing at the beginning of the reconstruction. Female selectivities for the four surveys and the predominantly trawl commercial fishery were determined by a flexible selectivity function parameterised in SS with six β parameters (described in Appendix E). For this assessment, only two β parameters were estimated: β_1, equivalent to the μ parameter (age at which selectivity first reaches maximum selectivity) in Awatea, and β_3, equivalent to the log v_L parameter (variance that determines the width of the ascending limb of a double normal curve) in Awatea. The right-hand (descending limb) was assumed to be fixed at the maximum selectivity to avoid the creation of a cryptic population. Dome-shaped selectivity was explored, but the resulting estimated parameters did not include values for descending curves. Additionally, when forcing the right-hand limb to descend, there was no apparent improvement in the fits to the AF data. The male offset parameters ($\Delta_{1,2,3,4}$) were also fixed at 0 as exploratory runs indicated that male selectivity did not vary greatly from that for females. The remaining four β parameters ($\beta_{2,4,5,6}$) available in SS were not used in this assessment. The model and its equations are described more fully in Appendix E.

Sample sizes are used to calculate the variance for a data source and are useful to indicate the relative differences in uncertainty across years within each data source. However, sample size may not represent the relative difference in the variance between different data sources (usually abundance vs. composition). Therefore, the relative weights for each data source in an integrated stock assessment should be adjusted to reflect the information content of each, while retaining the relative differences across years. This can be accomplished by applying adjustment factors to abundance and composition data to weight either data source up or down relative to the other. In this stock assessment, we used the Francis (2011) method for reweighting the abundance data: adding spline smoother-derived process error to the CPUE relative errors and no process error to the survey index relative errors, which were already high. For the composition data, we used a ratio method available in support code for SS that calculated the harmonic mean of effective sample sizes (McAllister and Ianelli 1997) over the arithmetic mean of observed sample sizes to scale observed sample sizes up closer to effective sample sizes. This adjustment factor was only applied to the commercial AF data whereas survey AF data were downweighted to 0.25. The result of this reweighting emphasized the composition data over the abundance data, counter to what the Francis mean-age method did for previous stock assessments using Awatea. However, we found the YMR abundance data relatively uninformative in this stock because of the large associated relative errors.

Generally, the modelling procedure first determined the best fit, or mode of the posterior distribution (MPD), to the data by minimising the negative log likelihood. Each MPD run was used as the respective starting point for the Markov Chain Monte Carlo (MCMC) simulations. Unlike previous BC rockfish assessments, which used a random walk Metropolis procedure, each run was evaluated using a "No U-Turn Sampling" (NUTS) algorithm (Monnahan and Kristensen 2018, Monnahan et al. 2019) which reduced the evaluation time from days to hours and which employed more efficient search algorithms. In this assessment, 4000 NUTS iterations were evaluated by parsing the workload into eight parallel chains (using the R package '`snowfall`', Knaus 2015) of 500 iterations each, discarding the first 250 iterations and saving the last 250 samples per chain. The parallel chains were then merged for a total of 2000 samples for use in the MCMC analysis.

A composite base case for YMR comprised five model runs (10,000 pooled MCMC posterior samples) to estimate stock status and to make projections and to provide scientific advice to managers. Decisions made during the stock assessment of YMR included:

- fixed natural mortality M to five levels, for a total of five reference models:
    - B1 (Run77): M = 0.04,
    - B2 (Run71): M = 0.045,
    - B3 (Run75): M = 0.05,
    - B4 (Run72): M = 0.055,
    - B5 (Run76): M = 0.06;
- set accumulator age A = 60 (pooled age for ages $a \geq 60$);
- used four survey abundance index series (QCS Synoptic, WCVI Synoptic, WCHG Synoptic, GIG Historical), all four with age frequency (AF) data;
- used one commercial fishery abundance index series (bottom trawl CPUE index);
- used a model-derived analytical solution for the abundance series scaling parameters (q_g), where q values are not estimated as active parameters (Methot et al. 2021);
- assumed one fishery, predominantly trawl with minor catches by non-trawl gear, with pooled catches and AF data;
- assumed two sexes (females, males);
- used informed selectivity priors based on median values from MCMC posteriors from the 2012 and 2017 POP stock assessments; assumed no age shift for males relative to females;
- estimated recruitment deviations from 1950 to 2012 and allowed post-2012 recruitments to vary given a data signal;
- applied abundance reweighting: added CV process error to the CPUE index CVs, c_p=0.3296 (see Appendix E) and added no process to the survey indices (relative error was high);
- applied composition reweighting: adjusted AF effective sample sizes, using the harmonic mean ratio method based on McAllister and Ianelli (1997) for the commercial fishery AFs, and fixed the four sets of survey AFs with an arbitrary low weight of 0.25;
- fixed the standard deviation of recruitment residuals (σ_R) to 0.9;
- excluded the 1995 survey index from the GIG Historical series (design incompatible);

- excluded the 1997 WCHG survey index (an oversight but checked its influence in a sensitivity run);
- used an ageing error vector based on CVs of observed lengths-at-age.

All base component model runs were reweighted one time for (i) abundance, by adding process error c_p = 0.3296 to the standard errors of the commercial trawl CPUE indices and no process error to the relative errors of the survey indices, and (ii) composition using either a harmonic mean ratio procedure outlined in Section E.6.2.2 of Appendix E for commercial trawl AFs or a fixed value of 0.25 for survey AFs.

Fourteen sensitivity analyses were run (with full MCMC simulations) relative to the central run of the composite base case (Run75: M=0.05, A=60, incorporating ageing error [AE] based on CVs of length-at-age) to test the sensitivity of the outputs to alternate model assumptions:

- S01 (Run78) – add 1997 index to WCHG survey series: (label: 'add 1997 WCHG index');
- S02 (Run79) – estimate M using a normal prior: N(0.05, 0.01) (label: 'estimate M');
- S03 (Run80) – drop commercial CPUE series (label: 'drop CPUE');
- S04 (Run81) – use CPUE series fitted by Tweedie distribution (label: 'Tweedie CPUE');
- S05 (Run82) – reduce std. dev. of recr. residuals σ_R from 0.9 to 0.6 (label: 'sigmaR=0.6');
- S06 (Run83) – increase std. dev. of recr. residuals σ_R from 0.9 to 1.2 (label: 'sigmaR=1.2');
- S07 (Run84) – reduce commercial catch for 1965-1995 by 33% (label: 'reduce catch 33%');
- S08 (Run85) – increase comm. catch for 1965-1995 by 50% (label: 'increase catch 50%');
- S09 (Run86) – upweight QCS AF samples by 3.5 (label: 'upweight QCS AF');
- S10 (Run87) – delay recruitment deviations from 1950 to 1970 (label: 'start Rdevs in 1970');
- S11 (Run88) – remove ageing error (label: 'no ageing error');
- S12 (Run91) – reduce steepness from h=0.7 to h=0.5 (label: 'steepness h=0.5');
- S13 (Run92) – double 2021 catch from 1,057 t to 2,114 t (label: 'double 2021 catch');
- S14 (Run93) – use AE based on ageing precision (label: 'AE from age readers').

All sensitivity runs were reweighted once in a manner similar to that described above for the base component runs. The process error added to the commercial CPUE for all sensitivities (except S04 because Tweedie CPUE standard error was already high) was the same as that adopted in the central run B3 (R75) (c_p=0.3296), based on a spline analysis (Appendix E).

As for the component base runs, each sensitivity run was evaluated using the NUTS procedure (described above) to generate 2000 MCMC samples each.

8. MODEL RESULTS

8.1. BASE CASE

8.1.1. Central Run (B3, M=0.05, Run75)

The model fits to the survey abundance indices were generally satisfactory (Figure F.2), although some index values were missed entirely (2013 QCS, 2010 WCVI, 2012 WCHG, 1994 GIG). The fit to the commercial CPUE indices showed a downward trend from 1996 to 2010 and

remained fairly flat thereafter. The model was unable to fit the initial peak in the CPUE series, passing well below the 1998 and 1999 index values. None of the CPUE index values were missed, largely due to adding process error of 33%. Nevertheless, the series pattern appeared to be matched by the model. Likelihood profile analysis indicated that the CPUE index series was the only abundance series that provided information on stock size, with the four survey series showing little contrast and all index values having high relative errors.

Only the commercial AF were used to estimate recruitments. This was done by upweighting the commercial AF data using the ratio of the harmonic mean of the effective sample size relative to the arithmetic mean of the observed sample size. These ratios tended to be large (6–10), giving a high weight to these data. The AF data for the surveys were deliberately given very low weights (0.25). This was done to eliminate any impact on the year class strength estimates from these data, while still estimating an appropriate selectivity function. The reason for this approach was that the quality of the survey AF data seemed low, given the inconsistencies in the apparent year class strength between survey years and between sexes within the same survey year. These inconsistencies led to conflicting estimates of recruitment deviations which were undesirable.

The ratios of the harmonic mean of effective sample size vs. the arithmetic mean of observed sample size (Figure F.13) shows ratios of 6.4, 3.6, 3.0, 4.7, and 6.7 for the five AF data sets calculated for the central run. However, only the value for the commercial AF was used (6.4, see Table F.2 for all weights used) and the remaining values were discarded by downweighting the survey AFs by assigning a low weight of 0.25, for reasons discussed above. The resulting model estimates of mean age matched the adjusted mean ages very well for all five AF data sets (Figure F.14).

Fits to the commercial trawl fishery age frequency data were excellent, with the model tracking year classes consistently across the 41 year time span represented by the commercial AF data (Figure F.3). There are some large departures at various ages classes (standardised residuals >2; Figure F.4), but that is not surprising given the large number of age-year categories to fit (there are 1680 categories=28 y times 60 ages). Residuals by year show that there are about 9-10 age-year categories in the 1990s that are greater than 2 and four greater than 3. The 1952 and 1982 cohorts show some residuals greater than 2 as well; however, most of the age-year residuals are below 2. Fits to AFs from the four surveys were mixed as expected, given the low weight used to fit these data (Figures F.5 to F.12).

The survey selectivity parameter estimates did not move very far from the priors, which differed by survey (Figure F.1). However, the parameter estimates for the commercial trawl fishery moved well away from the prior, indicating the presence of a strong signal from the data. The maturity ogive, generated from an externally fitted model (see Appendix D, Section D.1.3), was situated to the right of the commercial fishery selectivity function, indicating that sub-mature fish were harvested by this fishery (Figure F.15). The survey selectivity functions were also situated to the left of the maturity function, indicating that the surveys were sampling sub-mature year classes.

The spawning biomass (female) trajectory for the central run lies between 12,000 and 40,000 tonnes (Figure F.16, top) and reached the lowest point in the trajectory in 2013 or 2014 and has since increased, with the lowest point just below $0.5B_0$ (Figure F.16, bottom).

The recruitment estimates show four large events in 1952, 1961, 1982, and 2006 (Figure F.17). These events appear to be well defined in the data, with the definition greatly improved after the implementation of ageing error based on the coefficient of variation (CV) of length-at-age (see Section 8.2). The model estimates two periods of prolonged below average recruitment deviations, the first between 1970 and 1980 and the second between 1990 and 2000. The four

recruitment ‘spikes’ correspond to recruitments around three times the long-term average recruitment (Figure F.17, middle).

8.1.2. Composite Base Case

The composite base case comprised five runs which explored the effect of a range of fixed *M* values (for both sexes) for this stock assessment: (B1) *M* = 0.04, (B2) *M* = 0.045, (B3) *M* = 0.05, (B4) *M* = 0.055, and (B5) *M* = 0.06. While estimating *M* was possible (see Section 8.2), the MCMC diagnostics were unstable and the resulting posterior sample did not converge.

Unlike the 2011 YMR stock assessment (Edwards et al. 2012a), we were not able to estimate *M* reliably in this assessment, given the change in modelling software as well as the lack of contrast in the survey data accompanied by very large relative errors. Model runs which estimated *M* gave an MPD estimate of female *M* of 0.066 and an MCMC estimate of 0.070 (0.060, 0.078). While these estimates were at the lower end of the range for externally estimated *M* (see Appendix D, Section D.1.4), model behaviour when *M*>0.06 appeared to be unstable and the MCMC diagnostics were unacceptable. Natural mortality appears to be the most important component of uncertainty in this stock assessment. Consequently, a composite base case was constructed by assembling model runs which spanned a plausible range of *M* values for this stock as well as providing acceptable fits and MCMC diagnostics. Various other sources of uncertainty were explored in sensitivity runs based on central Run 75.

The composite base case was used to calculate a set of parameter estimates (Table 1) and derived quantities at equilibrium and those associated with MSY (Table 2). The distribution of all the estimated parameters among the five component runs (Figure F.25) show overlapping distributions of parameter estimates. The parameter which differed the most among the five runs was R_0, which increased as *M* increased, while the selectivity parameters differed little among the component runs. This latter result shows why the model cannot estimate *M* because the AF data fits are equivalent across this range of *M* values, indicating that there is no information in the available data to estimate this parameter.

Given the sensitivity of the stock size estimate to the assumed value of *M*, the derived quantities that reflect stock size (Figure F.26) also varied by *M*. Not surprisingly, B_0, MSY, B_{MSY}, and current stock status relative to B_0 all increased with increasing *M*. The exploitation rate at MSY, u_{MSY}, also increased with increasing *M*. The ratio of B_{MSY}/B_0 remained constant but uncertainty around the median estimate expanded. Given a catch of 1,057 t in 2021, the mid-year harvest rates become lower with increasing *M* because estimated spawning biomass (and consequently vulnerable biomass) increased.

Estimated recruitments show four main recruitment pulses (1952, 1961/62, 1982, and 2006), typical of deepwater rockfish species (Figure 4). The composite base case population trajectory from 1935 to 2022 and projected biomass to 2032 (Figure 5), assuming three constant catch policies of 0, 1,250, and 2,500 t/y, show that catches greater than MSY (1,039 t, Table 2) result in biomass declines. Figure 5 also indicates that the median stock biomass will remain above the upper stock reference (USR) for the next ten years for catches on the order of the five-year mean (1,250 t/y). Exploitation rates have largely stayed below u_{MSY} for most of the fishery’s history (Figure F.29).

Table 1. Quantiles of the posterior distribution based on 10,000 MCMC samples for the main estimated model parameters for the composite base case YMR stock assessment. Selectivity parameters are expressed in terms compatible with Awatea; SS counterparts: $\mu_g = \beta_{1g}$ and log $v_{Lg} = \beta_{3g}$ (see Appendix E).

Parameter	5%	25%	50%	75%	95%
log R_0	7.525	7.774	8.070	8.411	8.820
μ_1 (TRAWL+)	10.98	11.34	11.60	11.88	12.28
μ_2 (QCS)	10.07	12.09	13.65	15.38	17.99
μ_3 (WCVI)	8.951	11.64	13.67	15.68	18.61
μ_4 (WCHG)	8.474	9.900	10.72	11.52	12.75
μ_5 (GIG)	10.67	13.61	15.85	18.21	21.68
log v_{L1} (TRAWL+)	1.703	1.917	2.063	2.203	2.394
log v_{L2} (QCS)	3.056	3.622	3.982	4.342	4.829
log v_{L3} (WCVI)	2.812	3.427	3.837	4.225	4.784
log v_{L4} (WCHG)	1.376	1.772	2.046	2.314	2.707
log v_{L5} (GIG)	3.463	4.358	4.934	5.518	6.352

Table 2. Parameter and derived parameter quantiles from the 10,000 samples of the MCMC posterior of the composite base case. Definitions: B_0 – unfished equilibrium spawning biomass (mature females), B_{2022} – spawning biomass at the start of 2022, u_{2021} – exploitation rate (ratio of total catch to vulnerable biomass) in the middle of 2021, u_{max} – maximum exploitation rate (calculated for each sample as the maximum exploitation rate from 1935-2021), B_{MSY} – equilibrium spawning biomass at MSY (maximum sustainable yield), u_{MSY} – equilibrium exploitation rate at MSY. All biomass values (including MSY) are in tonnes. The average catch over the last 5 years (2016-20) was 1,272 t.

Quantity	5%	25%	50%	75%	95%
B_0	20,898	23,707	26,386	30,528	41,314
B_{2022}	10,070	13,848	18,001	24,978	42,533
B_{2022} / B_0	0.4446	0.5708	0.6922	0.8417	1.080
u_{2021}	0.01012	0.01697	0.02357	0.03048	0.04154
u_{max}	0.02686	0.03845	0.04837	0.0573	0.06531
MSY	696	845	1,039	1,327	1,919
B_{MSY}	6,063	6,894	7,656	8,810	11,938
0.4B_{MSY}	2,425	2,758	3,063	3,524	4,775
0.8BMSY	4,850	5,515	6,125	7,048	9,550
B_{2022} / B_{MSY}	1.535	1.969	2.394	2.905	3.727
B_{MSY} / B_0	0.2702	0.2847	0.2917	0.2971	0.3036
u_{MSY}	0.04063	0.04356	0.04636	0.04893	0.05117
u_{2021} / u_{MSY}	0.2019	0.3471	0.5082	0.7066	1.001

A phase plot of the time-evolution of spawning biomass and exploitation rate by the modelled fishery in MSY space (Figure 6) suggests that the stock is firmly in the Healthy zone, with a current position at B_{2022}/B_{MSY} = 2.39 (1.54, 3.73) and u_{2021}/u_{MSY} =0.51 (0.20,1.00). The current-year stock status figure (Figure F.32) shows the position of the composite base case in DFO's Healthy zone, and demonstrates how the individual component runs contribute to the composite base case. Values of M higher than 0.06 will push the stock status further into the Healthy zone.

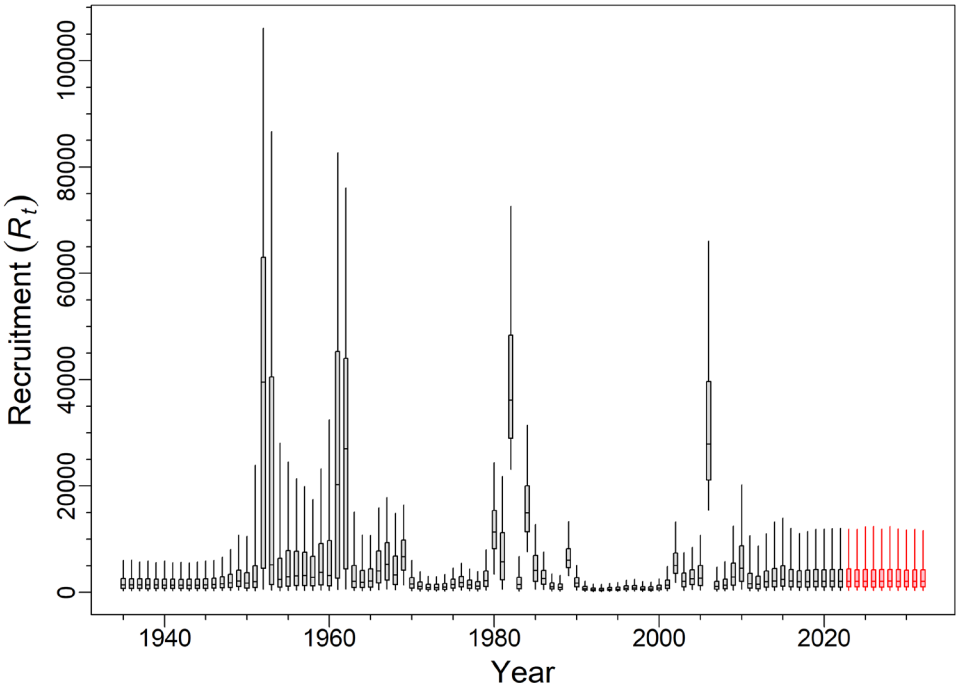

Figure 4. Recruitment trajectory and projection (1000s age-0 fish) for the composite base case. Boxplots delimit the 0.05, 0.25, 0.5, 0.75, and 0.95 quantiles.

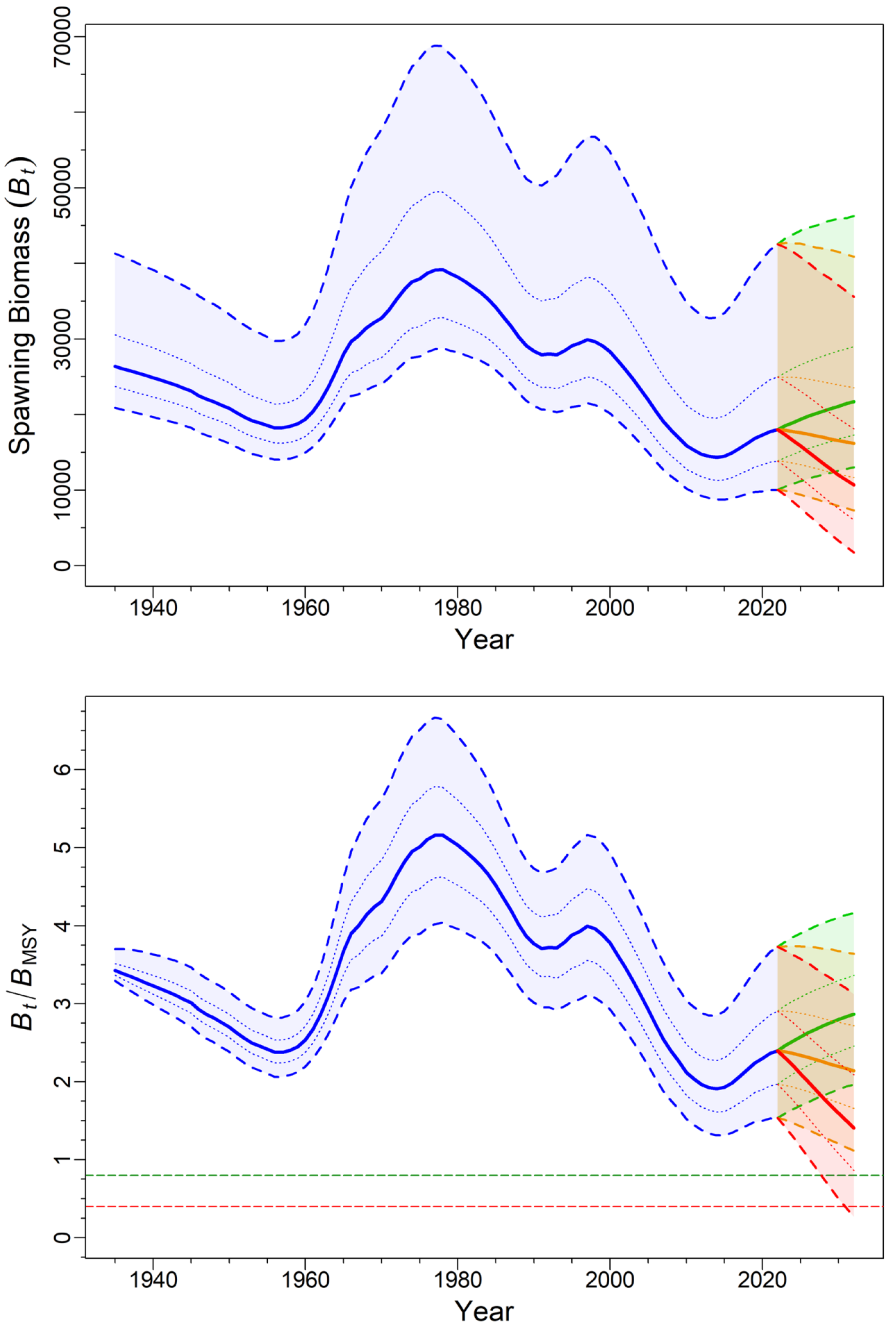

Figure 5. Estimates of spawning biomass B_t (tonnes, top) and B_t relative to B_{MSY} (bottom) for the composite base case. The median biomass trajectory appears as a solid curve surrounded by a 90% credibility envelope (quantiles: 0.05-0.95) in light blue and delimited by dashed lines for years t=1935-2022; projected biomass (2023-2032) appears for three catch policies: green for no catch (0 t/y), orange for average catch (1,250 t/y), and red for high catch (2,500 t/y). Also delimited is the 50% credibility interval (quantiles: 0.25-0.75) delimited by dotted lines. The horizontal dashed lines show the median LRP = $0.4B_{MSY}$ and USR = $0.8B_{MSY}$.

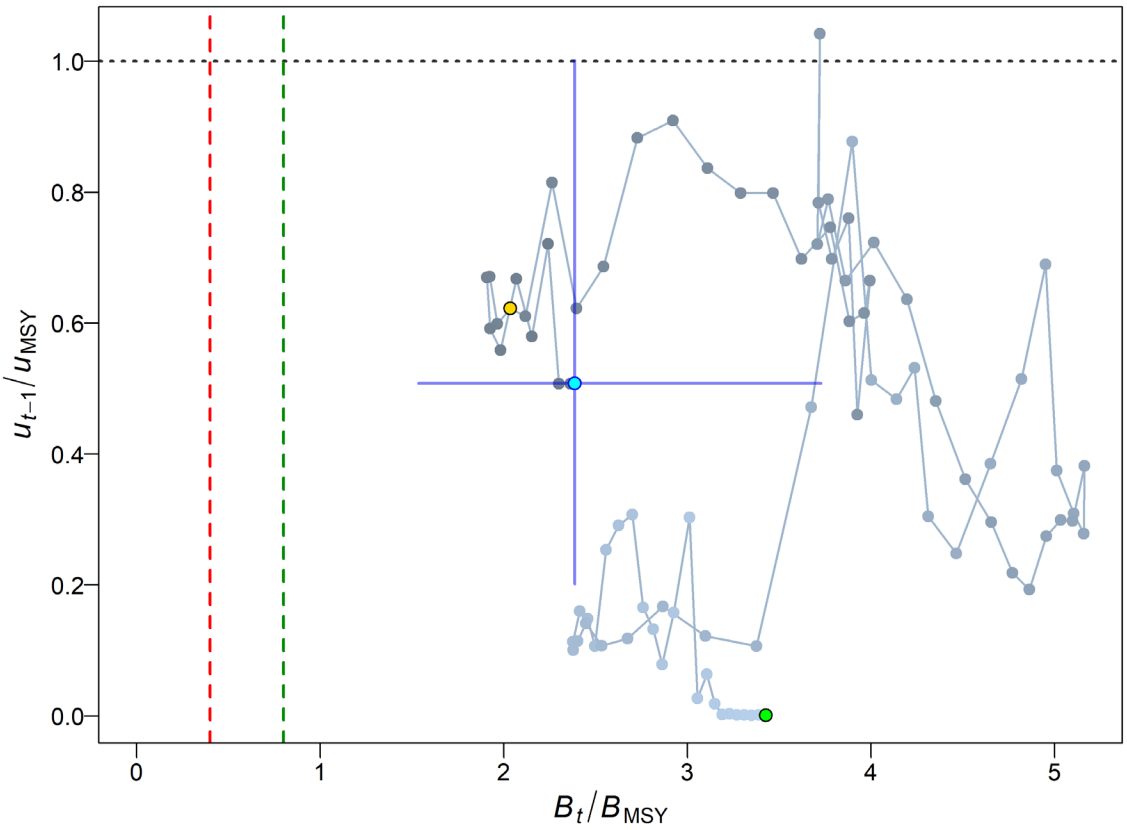

Figure 6. Phase plot through time of the medians of the ratios B_t/B_{MSY} (the spawning biomass at the start of year t relative to B_{MSY}) and fishing pressure relative to u_{MSY} (u_{t-1}/u_{MSY}, where the exploitation rate occurs in the middle of year t-1) for the composite base case. The filled green circle is the equilibrium starting year (1935). Years then proceed from lighter shades through to darker with the final year (t=2022) as a filled cyan circle, and the blue cross lines represent the 0.05 and 0.95 quantiles of the posterior distributions for the final year. Previous assessment year (2011) is indicated by gold circle. Red and green vertical dashed lines indicate the PA provisional LRP = $0.4B_{MSY}$ and USR = $0.8B_{MSY}$, and the horizontal grey dotted line indicates u_{MSY}.

8.2. SENSITIVITY ANALYSES

Fourteen sensitivity analyses were run (with full MCMC simulations) relative to the central run (Run75: M=0.05, CPUE c_p=0.3296) to test the sensitivity of the outputs to alternative model assumptions (see Section 7 for sensitivity run details). The differences among the sensitivity runs (including the central run) are summarised in tables of median parameter estimates (Table F.19) and median MSY-based quantities (Table F.20).

Three additional runs were requested by the RPR participants to be added to the original eleven sensitivity analyses (Figure 7) to explore the effects of lower steepness (h=0.5, S12), doubling the 2021 catch (S13), and using an alternative ageing error structure based on precision inferred by secondary readers' age assignments for primary reader's age determination (S14).

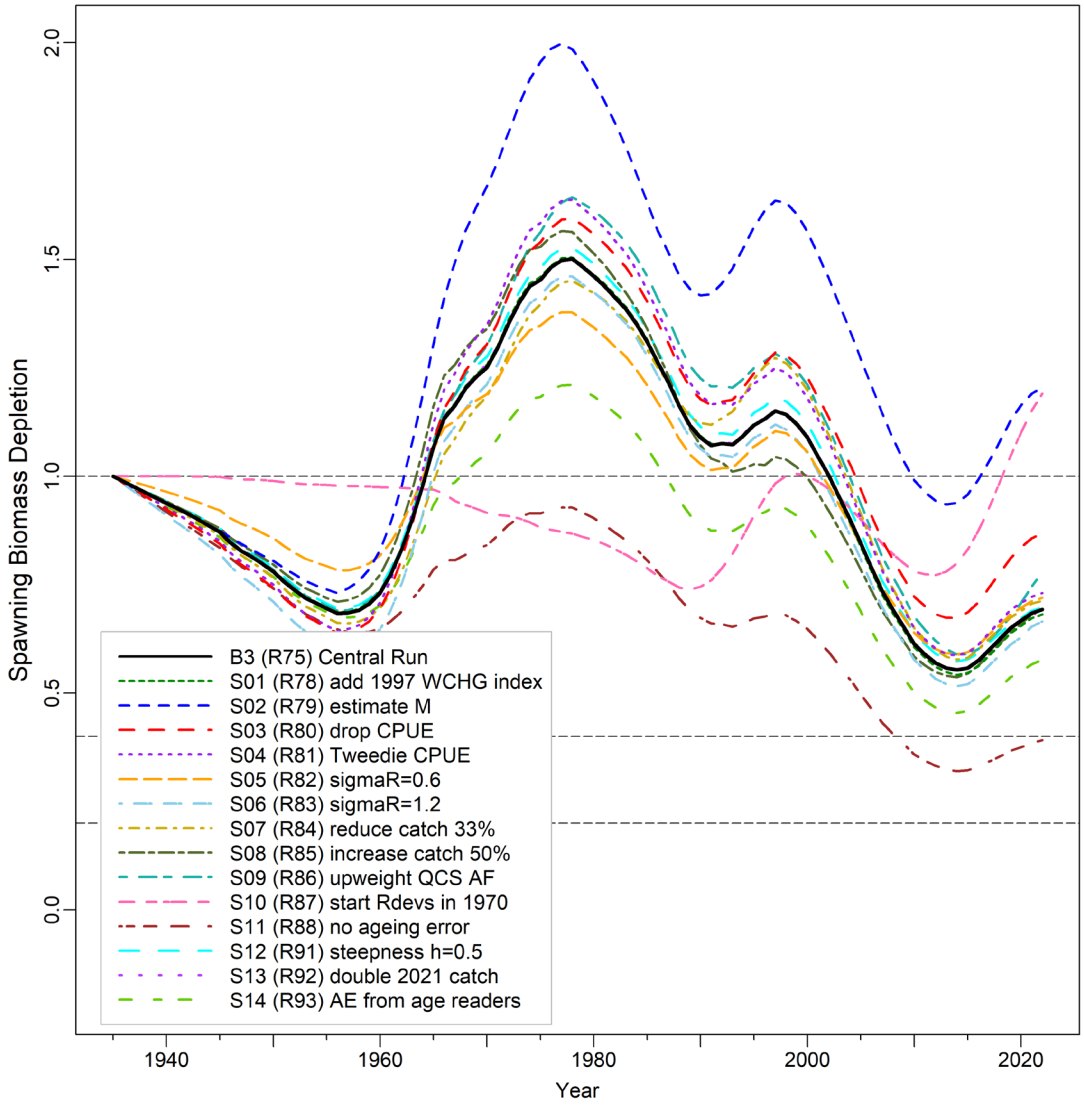

Figure 7. Model median trajectories of spawning biomass as a proportion of unfished equilibrium biomass (B_t/B_0) for the central run and fourteen sensitivity runs (see legend lower left). Horizontal dashed lines show alternative reference points used by other jurisdictions: $0.2B_0$ (~DFO's USR), $0.4B_0$ (often a target level above B_{MSY}), and B_0 (equilibrium spawning biomass).

The diagnostic plots (Figures F.33 to F.35) suggest that eight sensitivity runs exhibited good MCMC behaviour, four were fair, one was poor, and one was unacceptable with little credibility:

- Good – no trend in traces, split-chains align, no autocorrelation
    - S01 (add 1997 WCHG index)
    - S04 (Tweedie CPUE)
    - S06 (sigmaR=1.2)
    - S07 (reduce catch 33%)
    - S08 (increase catch 50%)
    - S12 (steepness h=0.5)
    - S13 (double 2021 catch)
    - S14 (AE from age readers)

- Fair – trace trend temporarily interrupted, split-chains somewhat frayed, some autocorrelation
    - S03 (drop CPUE)
    - S05 (sigmaR=0.6)
    - S09 (upweight QCS AF)
    - S11 (no ageing error)
- Poor – trace trend fluctuates substantially or shows a persistent increase/decrease, split-chains differ from each other, substantial autocorrelation
    - S10 (start Rdevs in 1970)
- Unacceptable – trace trend shows a persistent increase/decrease that has not levelled, split-chains differ markedly from each other, persistent autocorrelation
    - S02 (estimate M)

The run that estimated *M* (S02) may not have converged and the unacceptable diagnostics suggested instability in the model. Additionally, the posterior for M_1 (females), 0.070 (0.060, 0.078), moved well above the prior N (0.05, 0.01). While a higher *M* may be suitable for this species, it was not supported by the available data while using the SS modelling platform.

The trajectories of the B_t medians relative to B_0 (Figure 7) showed that most sensitivities followed the trajectory of the central run with some variation, while three scenarios departed markedly (S02, S10, S11). Although estimating *M* (S02) followed the trajectory of the central run, it remained consistently above the latter and resulted in the most optimistic scenario. However, it is likely that this run did not converge and these results should be interpreted with caution. The run that estimated recruitment deviations starting in 1970 rather than 1950 (S10) followed a path well below the central run before trending up to an estimate for current (2022) stock status that was similar to that of the run that estimated *M* (S02). The reason for this result can be seen in Figure F.38, where run S10 estimated the highest recruitment deviations of all the runs during the low period in the late 1990s. Run S10 then estimated higher recruitment deviations in the following years compared to most of the other runs. This compensatory behaviour is responsible for the very optimistic stock status estimated by this run. S10 also estimated an unrealistically high level of female spawning biomass compared to all other runs, save S02 (Figure F.36).

The most pessimistic run was the one without ageing error (AE) corrections (S11), followed by the run using an alternative AE based on CVs of age calculated from otolith readers' estimates of precision (S14), suggesting that accounting for ageing error is important to remove bias, in both cases negative. While S11 and S14 estimated higher B_0 values compared to the central run, the median estimates of current stock status relative to B_0 were lower (S11=0.39, S14=0.55, B3=0.69). The higher B_0 suggests that the runs using absent/weaker AE adjustments were estimating a more productive stock (the median MSY is 62% and 24% greater than the central run estimate; Table F.20). However, what is more likely, is that these models traded off initial equilibrium biomass and early recruitments to get the best fit to the data. Figure F.36 shows this, with the two runs with alternative AE assumptions (S11 and S14) starting off at levels higher than B3 (median B_0: S11=41,767; S14=32,151, B3=26,065; Table F.20), but between 1970 and 1980 all three models converged to similar levels of absolute biomass after the constraint of data took effect. The S11 and S14 runs adjusted the initial biomass and early recruitments to get a better fit to the data, given the different AE assumptions. By the time the three model trajectories reached 2022, they estimated similar levels of median female spawning biomass: S11=16,389; S14=18,482, B3=18,027 (Table F.20). The lower estimate for B_{2022} by

S11 (compared to B3 and S14) is explained by the low recruitment deviations estimated by this model in the late 1990s (Figure F.38).

The use (or lack) of ageing error (AE), showed that this process had an important impact on model results. The model with no ageing error (S11) estimated recruitment peaks spread broadly across adjacent years, while a strong AE assumption (B3, central run) concentrated recruitment into single years. The intermediate AE assumption (S14) lay between the two extremes of S11 and B3, with the first two recruitment peaks spread less broadly across years than in S11. This issue emerged as a potential axis of uncertainty during the RPR meeting and should be explored in future assessments. The authors chose the strong AE assumption because the single-year recruitment events were consistent with expected rockfish life history patterns.

Dropping the CPUE series (S03) resulted in higher estimates for current status. This run increased the fishery AF weight, possibly because, without the presence of the CPUE series, the dominant uncertainty in S03 was the high relative error associated with the surveys. If this is correct, the harmonic mean ratio procedure increased the weight associated with the fishery AF data (Table F.18) because these data were relatively more informative than the other data in the model.

Run S09, which upweighted the QC Sound survey AFs, illustrates why we chose to downweight the available survey age frequency data. This run estimated an age at maximum selectivity that was shifted downward by three years compared to the central run (S09 median μ_2=10.8; B3 median μ_2=13.7; Table F.19). By adjusting the selectivity function to the left, this model estimated two large recent year classes (in 2010 and 2015) that were absent in all the other model runs (Figure F.38). These strong year classes resulted in a very optimistic estimate of current stock status (median=0.75B_0) and would likely propagate into optimistic projections. While these year classes may in fact exist, it seemed unwise to allow these few uncertain observations in a single survey to drive such a high degree of optimism.

Parameter estimates varied little among sensitivity runs (Figure 8), with the exception of S02 (estimating M) and S09 (upweighting the QCS survey AFs). Derived quantities based on MSY (Figure 9) exhibited high values of MSY and B_0 for S02 and S10 (delayed estimation of recruitment deviations).

The stock status (B_{2022}/B_{MSY}) for the sensitivities (Section 9.2) are all in the DFO Healthy zone, including the most pessimistic S11 run that does not correct for ageing error.

9. ADVICE FOR MANAGERS

9.1. REFERENCE POINTS

The Sustainable Fisheries Framework (SFF, DFO 2009) established provisional reference points, which incorporate the ‘precautionary approach’ (PA), to guide management and assess harvest in relation to sustainability. These reference points are the limit reference point (LRP) of 0.4B_{MSY} and the upper stock reference point (USR) of 0.8B_{MSY}, which have been adopted by previous rockfish assessments (Edwards et al. 2012 a,b, 2014 a,b; DFO 2015, Starr et al. 2016; Haigh et al. 2018; Starr and Haigh 2021 a,b) and are used here. Note that to determine the suitability of these reference points for this stock (or any *Sebastes* stock) would require a separate investigation involving simulation testing using a range of operating models.

The zone below 0.4B_{MSY} is termed the ‘Critical zone’ by the SFF, the zone lying between 0.4B_{MSY} and 0.8B_{MSY} is termed the ‘Cautious zone’, and the region above the upper stock reference point (0.8B_{MSY}) is termed the ‘Healthy zone’. Generally, stock status is evaluated as

the probability of the spawning female biomass in year t being above the reference points, i.e., $P(B_t > 0.4B_{MSY})$ and $P(B_t > 0.8B_{MSY})$. The SFF also stipulates that, when in the Healthy zone, the fishing mortality (u_t) must be at or below that associated with MSY under equilibrium conditions (u_{MSY}), i.e., $P(u_t < u_{MSY})$. Furthermore, fishing mortality is to be proportionately ramped down when the stock is deemed to be in the Cautious zone, and set equal to zero when in the Critical zone.

The term 'stock status' should be interpreted as 'perceived stock status at the time of the assessment for the year ending in 2021 (i.e., beginning of year 2022)' because the value is calculated as the ratio of two estimated biomass values (B_{2022}/B_{MSY}) by a specific model using the data available up to 2021. Further, the estimate of B_{MSY} depends on the model assessment of stock productivity as well as the catch split among fisheries (if there are more than one). Therefore, comparisons of stock status among various model scenarios can be misleading because the B_{MSY} space is not the same from one model to the next. For example, the estimated median B_{2022}/B_{MSY} for the central YMR run was 0.69, but for the comparable Awatea run, it was 0.44; however, estimated median B_{2022} values were 18,027 t and 17,222 t, respectively. Current spawning stock size estimates were similar but the B_{MSY} estimates were very different (7,593 t vs. 11.046 t), largely due to assumptions about AF error distributions.

MSY-based reference points estimated within a stock assessment model can be sensitive to model assumptions about natural mortality and stock recruitment dynamics (Forrest et al. 2018). As a result, other jurisdictions use reference points that are expressed in terms of B_0 rather than B_{MSY} (Edwards et al. 2012, N.Z. Ministry of Fisheries 2011). These reference points, for example, are default values used in New Zealand, with $0.2B_0$ as the 'soft limit', below which management action needs to be taken, and $0.4B_0$ considered a 'target' biomass for low productivity stocks, a mean around which the biomass is expected to vary. The 'soft limit' is equivalent to the upper stock reference (USR, $0.8B_{MSY}$) in the DFO Sustainable Fisheries Framework (SFF) while a 'target' biomass is not specified by the DFO SFF. Results are provided comparing projected spawning biomass to B_{MSY} and to current spawning biomass B_{2022}, and comparing projected harvest rate to current harvest rate u_{2021} (APPENDIX F).

9.2. STOCK STATUS AND DECISION TABLES

In this stock assessment, projections extend to the end of 2031 (beginning 2032). Projections out to 3 generations (90 years), where one generation was determined to be 30 years (see Appendix D), were not completed due to technical reasons associated with the new model framework (SS) and time constraints; however, the stock status of YMR in the Healthy zone does not warrant such projections at this time.

Stock status for DFO managers is usually defined as the current spawning biomass relative to the estimated spawning biomass required for maximum sustainable yield (MSY). Plots that depict distributions of B_{2022}/B_{MSY} in three zones (Critical, Cautious, Healthy) delimited by $0.4B_{MSY}$ (LRP) and $0.8B_{MSY}$ (USR), show that the YMR composite base case lies in the Healthy zone with a probability >0.999 in 2022, as do the five component runs (Figure 8). Projections of the composite base case stock remain above $0.8B_{MSY}$ with at least a 50% probability up to 2032 at all catch policies up to 3000 t/y (Table F.9). However, these projections also predict that the stock will decline at catch levels above 500 t/y, under the assumption that recruitment will be average over that time period (Table F.12).

Stock status plots for sensitivity runs based on the central run of the YMR composite base case (Figure 9) show that all of the sensitivity runs also lie with a high probability in the Healthy zone. The only run that approaches the USR is S11 (no ageing error); however, the probability that this run is in the Healthy zone remains high at 0.998.

Decision tables for the YMR composite base case provide advice to managers as probabilities that projected biomass B_t (t = 2023, ..., 2032) will exceed biomass-based reference points (or that projected exploitation rate u_t (t = 2022, ..., 2031) will fall below harvest-based reference points) under constant-catch policies (Table 3). That is, the table presents probabilities that projected B_t using the composite base case will exceed the LRP and the USR or will be less than the harvest rate at MSY. All decision tables (including those for alternate reference points) for the composite base case can be found in APPENDIX F (Tables F8 to F17).

Assuming that a catch of 1,250 t (close to the recent 5-y mean) will be taken each year for the next 10 years, Table 3 indicates that a manager would be >99% certain that both B_{2027} and B_{2032} lie above the LRP of $0.4B_{MSY}$, >99% certain that B_{2027} and 99% certain that B_{2032} lie above the USR of $0.8B_{MSY}$, and 83% certain that u_{2027} lies below u_{MSY} and 78% certain that u_{2032} lies below u_{MSY} for the composite base case. Generally, it is up to managers to choose the preferred catch levels or harvest levels (if available) using their preferred risk levels. For example, it may be desirable to be 95% certain that B_{2032} exceeds an LRP whereas exceeding a USR might only require a 50% probability. Assuming this risk profile, a catch policy of <=2,000 t/y satisfies the LRP constraint in Table 3. Assuming that u_{MSY} is a target exploitation rate, only catch policies <= 750 t/y have a probability greater than 95% of the harvest rate remaining below u_{MSY} in 10 years, whereas catch policies <=1,500 t/y would have a probability greater than 50%.

We caution that, although uncertainty is built into the assessment and its projections by taking a Bayesian approach for parameter estimation and by constructing a composite base case that spans ranges of inestimable parameter values, these results depend heavily on the assumed model structure, the informative priors, and data assumptions (particularly the average recruitment assumptions) used for the projections.

Table 3. Decision tables for the reference points $0.4B_{MSY}$, $0.8B_{MSY}$, and u_{MSY} for 1-10 year projections for a range of constant catch policies (in tonnes) using the composite base case. Values are the probability (proportion of 10,000 MCMC samples) of the female spawning biomass at the start of year t being greater than the B_{MSY} reference points, or the exploitation rate of vulnerable biomass in the middle of year t-1 being less than the u_{MSY} reference point. For reference, the average catch over the last 5 years (2016-2020) was 1,272 t.

$P(B_t > 0.4B_{MSY})$

Catch policy	Projection year (start)										
	2022	2023	2024	2025	2026	2027	2028	2029	2030	2031	2032
0	1	1	1	1	1	1	1	1	1	1	1
500	1	1	1	1	1	1	1	1	1	1	1
750	1	1	1	1	1	1	1	1	1	1	1
1000	1	1	1	1	1	1	1	1	1	1	1
1250	1	1	1	1	1	1	1	1	1	1	1
1500	1	1	1	1	1	1	1	1	>0.99	>0.99	>0.99
2000	1	1	1	1	1	>0.99	>0.99	>0.99	>0.99	0.99	0.98
2500	1	1	1	1	>0.99	>0.99	>0.99	0.99	0.97	0.95	0.92
3000	1	1	1	1	>0.99	0.99	0.98	0.95	0.91	0.87	0.81

$P(B_t > 0.8B_{MSY})$

Catch policy	Projection year (start)										
	2022	2023	2024	2025	2026	2027	2028	2029	2030	2031	2032
0	1	1	1	1	1	1	1	1	1	1	1
500	1	1	1	1	1	1	1	1	1	1	1
750	1	1	1	1	1	1	1	>0.99	>0.99	>0.99	>0.99
1000	1	1	1	1	1	>0.99	>0.99	>0.99	>0.99	>0.99	>0.99
1250	1	1	1	1	>0.99	>0.99	>0.99	>0.99	>0.99	>0.99	0.99
1500	1	1	1	>0.99	>0.99	>0.99	>0.99	0.99	0.99	0.98	0.98
2000	1	1	>0.99	>0.99	>0.99	0.99	0.98	0.97	0.95	0.92	0.90
2500	1	1	>0.99	>0.99	0.99	0.97	0.94	0.91	0.87	0.82	0.78
3000	1	1	>0.99	0.99	0.97	0.93	0.88	0.82	0.76	0.70	0.64

$P(u_t < u_{MSY})$

Catch policy	Projection year (start)										
	2022	2023	2024	2025	2026	2027	2028	2029	2030	2031	2032
0	0.95	1	1	1	1	1	1	1	1	1	1
500	0.95	1	1	1	1	1	1	1	1	1	1
750	0.95	>0.99	>0.99	>0.99	>0.99	>0.99	>0.99	>0.99	>0.99	0.99	0.99
1000	0.95	0.96	0.96	0.96	0.95	0.95	0.94	0.94	0.94	0.93	0.93
1250	0.95	0.87	0.86	0.85	0.84	0.83	0.82	0.81	0.80	0.79	0.78
1500	0.95	0.74	0.73	0.71	0.70	0.69	0.67	0.66	0.65	0.64	0.62
2000	0.95	0.52	0.50	0.48	0.47	0.45	0.43	0.42	0.41	0.39	0.38
2500	0.95	0.36	0.35	0.33	0.31	0.29	0.28	0.27	0.25	0.24	0.23
3000	0.95	0.25	0.23	0.22	0.20	0.19	0.18	0.16	0.15	0.14	0.13

Table 4. Decision tables for the reference points $0.2B_0$ and $0.4B_0$ for 1-10 year projections for a range of constant catch policies (in tonnes) using the composite base case. Values are the probability (proportion of 10,000 MCMC samples) of the female spawning biomass at the start of year t being greater than the B_0 reference points. For reference, the average catch over the last 5 years (2016-2020) was 1,272 t. .

$P(B_t > 0.2B_0)$

Catch											
										Projection year (start)	
Policy	2022	2023	2024	2025	2026	2027	2028	2029	2030	2031	2032
0	1	1	1	1	1	1	1	1	1	1	1
500	1	1	1	1	1	1	1	1	1	1	1
750	1	1	1	1	1	1	1	1	1	1	1
1000	1	1	1	1	1	1	1	>0.99	>0.99	>0.99	>0.99
1250	1	1	1	1	1	>0.99	>0.99	>0.99	>0.99	>0.99	>0.99
1500	1	1	1	1	>0.99	>0.99	>0.99	>0.99	>0.99	0.99	0.99
2000	1	1	1	>0.99	>0.99	>0.99	0.99	0.98	0.97	0.95	0.93
2500	1	1	1	>0.99	>0.99	0.98	0.96	0.94	0.9	0.87	0.82
3000	1	1	>0.99	>0.99	0.98	0.96	0.92	0.86	0.81	0.75	0.69

$P(B_t > 0.4B_0)$

Catch											
										Projection year (start)	
policy	2022	2023	2024	2025	2026	2027	2028	2029	2030	2031	2032
0	0.98	0.99	0.99	>0.99	>0.99	>0.99	>0.99	>0.99	>0.99	>0.99	>0.99
500	0.98	0.98	0.98	0.99	0.99	0.99	0.99	0.99	0.99	0.99	0.99
750	0.98	0.98	0.98	0.98	0.98	0.98	0.97	0.97	0.97	0.97	0.97
1000	0.98	0.98	0.97	0.97	0.97	0.96	0.96	0.95	0.94	0.93	0.93
1250	0.98	0.98	0.97	0.96	0.95	0.94	0.93	0.91	0.90	0.89	0.87
1500	0.98	0.97	0.96	0.95	0.93	0.92	0.89	0.87	0.85	0.83	0.81
2000	0.98	0.97	0.95	0.92	0.88	0.85	0.81	0.77	0.73	0.69	0.66
2500	0.98	0.96	0.92	0.88	0.82	0.77	0.71	0.66	0.60	0.55	0.51
3000	0.98	0.95	0.9	0.83	0.76	0.69	0.61	0.54	0.49	0.44	0.40

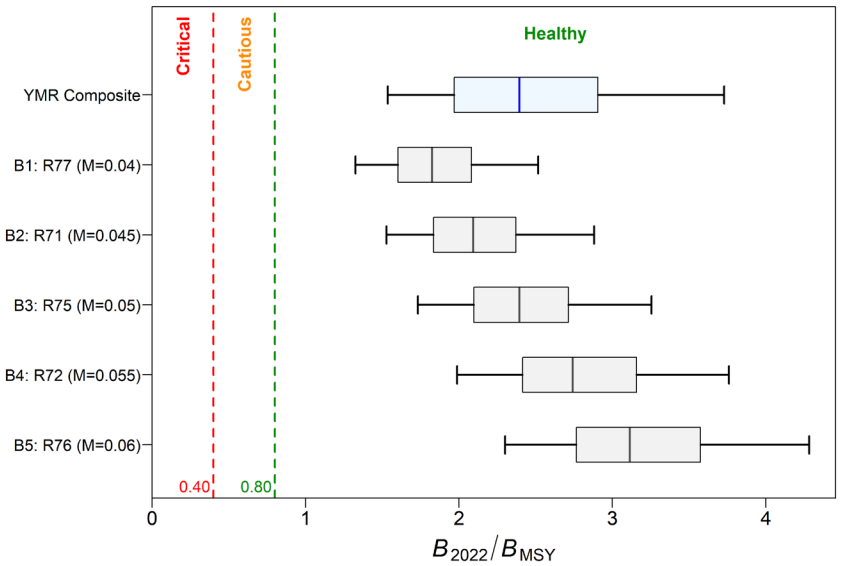

Figure 8. Status of the coastal YMR stock relative to the DFO PA provisional reference points of $0.4B_{MSY}$ and $0.8B_{MSY}$ for the t=2022 composite base case and the component base runs that are pooled to form the composite base case. Boxplots show the 0.05, 0.25, 0.5, 0.75 and 0.95 quantiles from the MCMC posterior.

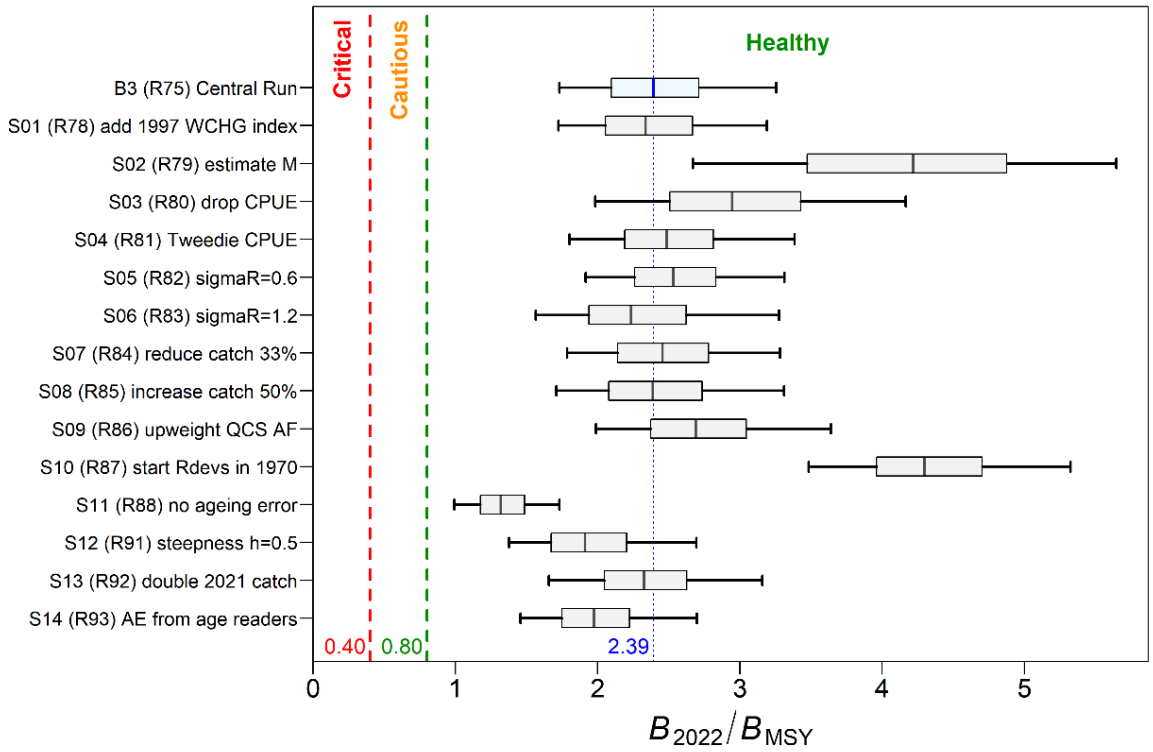

Figure 9. Stock status at beginning of 2022 of the YMR stock relative to the DFO PA provisional reference points of $0.4B_{MSY}$ and $0.8B_{MSY}$ for the central run (B3, M=0.05) of the composite base case and fourteen sensitivity runs (see y-axis notation and sensitivity descriptions in the main text). Boxplots show the 0.05, 0.25, 0.5, 0.75 and 0.95 quantiles from the MCMC posterior. APPENDIX F contains the details of these sensitivity runs.

9.3. STOCK REBUILDING

There is no rebuilding plan for YMR mentioned in the most recent IFMP, and considering its assessed status as 'Healthy', there is no need for a rebuilding plan at present.

The COSEWIC assessment criteria are based on a decline in the total number of mature individuals over the most recent 10 years or 3 generations, whichever is longer. The generation time for YMR is estimated to be 30 years; however, due to the working paper deadline and the learning curve for SS, we have not projected out to three generations (90 years). This long-term projection was not requested by the Regional Peer Review participants. Such projections would be exceedingly unrealistic for YMR, given that it is very unlikely that a constant catch policy could be maintained for such a long period of time without modification, particularly if the stock were reaching low levels. Furthermore, such projections assume randomised recruitment centred around the long-term mean recruitment, assuming the fixed σ_R standard deviation. However, the recruitment trajectories shown in Figure F.30 clearly show that such a recruitment assumption is unrealistic, with YMR showing a typical *Sebastes* recruitment strategy: long periods of poor recruitment punctuated by occasional strong recruitment events. This type of recruitment series is difficult to simulate, particularly when the frequency of strong recruitment events will be poorly determined due to their infrequency. The short term projections (presented in Table 3 and Tables F.8 to F.17 in Appendix F) are less affected by this problem, particularly in the early years. This is because many of the projected year classes were estimated during the stock reconstruction and the median value of μ_1 (trawl) at 11.6 years introduces a long lag period before new recruits are contributing to the vulnerable biomass.

COSEWIC indicator A1 is reserved for those species where the causes of the reduction are clearly reversible, understood, and ceased. Indicator A2 is used when the population reduction may not be reversible, may not be understood, or may not have ceased. The 2011 Yellowmouth Rockfish recovery potential analysis (Edwards et al 2012a) placed YMR into category A2b (where the 'b' indicates that the original COSEWIC designation was based on 'an index of abundance appropriate to the taxon'). Under A2, a species is considered Endangered or Threatened if the decline has been ≥50% or ≥30%, respectively. Using these guidelines, the recovery reference criteria become $0.5B_{t\text{-}3G}$ (a 50% decline) and $0.7B_{t\text{-}3G}$ (a 30% decline), where $B_{t\text{-}3G}$ is the biomass three generations (90 years) previous to the biomass in year t, e.g., $P(B_{2023,\ldots,2112} > 0.5|0.7\ B_{1933,\ldots B2022})$. We did not evaluate this criterion for reasons mentioned above; however, we did include the probabilities $P(B_{2023,\ldots,2032} > 0.5|0.7B_0)$.

9.4. ASSESSMENT SCHEDULE

Advice was also requested concerning the appropriate time interval between future stock assessments and, for the interim years between stock updates, potential values of indicators that could trigger a full assessment earlier than usual (as per DFO 2016). While the existing synoptic trawl surveys, particularly the QCS, WCVI, and WCHG surveys, are uninformative with respect to YMR stock size, they should be adequate to signal a major reduction in stock abundance. The next full stock assessment should be scheduled no earlier than 2031, given the currently assessed Healthy state and low exploitation rates. Large recruitment events appear to happen every 10-25 years, the last one occurring in 2006. While the episodic nature of these events cannot be accurately predicted, we might see another high-recruitment event in the next decade. Regardless of when a new stock assessment is to be initiated, at least 6-12 months lead time is required before the new stock assessment is initiated to allow for the reading of new ageing structures that will be needed for the interpretation of the population trajectory. Advice for interim years is explicitly included in the decision tables and managers can select another line on the table if stock abundance appears to have changed or if greater certainty of staying above the reference point is desired. During intervening years the trend in abundance can be

tracked by commercial fishery CPUE and, less reliably (because of the high relative error), by the fishery independent surveys used in this stock assessment. The groundfish synopsis report (Anderson et al. 2019), which will be periodically updated as a Science Response, summarises these trends and can be used as a tracking tool.

10. GENERAL COMMENTS

10.1. SOFTWARE IMPLEMENTATION ISSUES

This rockfish stock assessment marks a departure from those conducted since 2007 by adopting the Stock Synthesis 3 (SS) generic stock assessment platform maintained by NOAA (Methot and Wetzel 2013). Previously, rockfish were assessed using a simpler age-structured model called 'Awatea'[4], a version of Coleraine (Hilborn et al. 2003) that was developed and maintained by Allan Hicks (then at Univ. Washington, now at IPHC). Both Awatea and SS are platforms for implementing the Automatic Differentiation Model Builder software (ADMB Project 2009), which provides (a) maximum posterior density estimates using a function minimiser and automatic differentiation, and (b) an approximation of the posterior distribution of the parameters using the Markov Chain Monte Carlo (MCMC) method, specifically using the Hastings-Metropolis algorithm (Gelman et al. 2004). For SS, MCMCs were generated using a 'no U-turn sampler' (NUTS, Monnahan and Kristensen 2018, Monnahan et al. 2019) which shortened run time considerably from days to hours compared to using the traditional random-walk Metropolis method. The implementation of NUTS in R uses the package '`adnuts`' (Monnahan 2018); a useful synopsis of the procedure can be found in Appendix H of the 2020 Pacific Hake assessment (Grandin et al. 2020).

The SS model framework is maintained by a dedicated group of scientists at NOAA's SS Virtual Lab headed by Richard Methot. A very useful R package for processing SS output data, called '`r4ss`', is maintained by Ian Taylor. While `r4ss` (Taylor et al. 2021) facilitates the exploration of SS model results, we adapted some of their code and that of PBSawatea to provide a more familiar stock assessment output. However, the transition in stock assessment environments was challenging and not all of SS'/r4ss' capabilities (e.g., retrospective analysis, fecundity choices, parameter options) have been implemented in this stock assessment. These will be explored in future BC stock assessments.

One of the biggest challenges that we faced with the YMR stock assessment was the lack of information provided by the survey abundance indices. This was explored through likelihood profile analysis and fits of expected index relative to the observed index. The likelihood profile plot (Figure 10, left panel) shows no minimum negative log likelihood associated with a value for LN(R_0) for any of the four surveys used in the model, allowing the model to accept very large biomass estimates, while there is a clear LN(R_0) minimum for the CPUE series (blue line). The two panels on the right are observed and expected plots generated by `r4ss`, showing the CPUE indices (top right, Figure 10) and the QCS survey indices (lower right, Figure 10). The CPUE index values (apart from 1998 and 1999) lie on the 1:1 line, showing good contrast, while the QCS survey index values show no contrast in the expected indices across a wide range of observed indices. We explored many runs using Francis (2011) reweighting before we realised that the last thing we wanted to do was downweight the composition data in favour of the abundance data. The strongest (apart from the CPUE) signal we had for successfully fitting the YMR data was contained in the commercial trawl AF data. Once we determined that we could

[4] Some stock assessments lacked reliable age frequency data and so a delay-difference model under the name 'iSCAM' was used.

obtain credible results by increasing the weight on the commercial trawl AFs, we switched to a reweighting method based on r4ss' comparing the harmonic mean of annual effective sample sizes, using McAllister and Ianelli (1997) equation (2.5), to the arithmetic mean of observed sample sizes to derive new weights w_g for AF data. In the end, we applied w_1 to the trawl AF sample sizes and downweighted those of the surveys using $w_{2,3,4,5}$=0.25.

The second challenge we had with SS was the limited choice of error distributions for fitting AF data. The SS platform offered the Multinomial and a self-weighting Dirichlet-Multinomial (Thorson et al. 2017). The latter provided no benefit to this assessment over the former, and the Multinomial was insensitive to outliers in the AF data, which, along with the very large relative errors associated with the fishery-independent surveys, allowed the model to find good fits to the data at unrealistically high estimates of R_0. Awatea, on the other hand, uses a robust normal method that reduces the influence of observations with standardised residuals > 3 standard deviations (Fournier 1990). This feature constrained the excursions into very large biomass estimates and allowed Awatea to estimate both *M* and *h* using the same data offered to the SS platform, and produced MCMCs with good diagnostics.

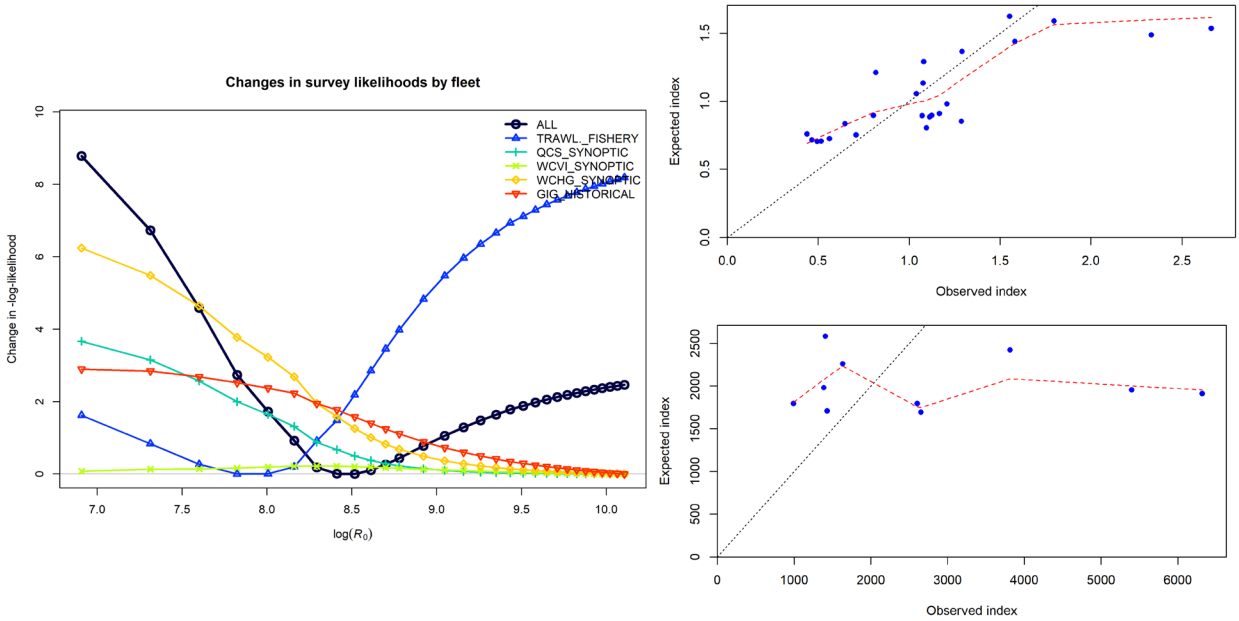

Figure 10. Left: Likelihood profile of survey indices at various fixed values of log R_0 (R53, M=0.055); upper right: expected CPUE index vs. observed CPUE index (R75); lower right: expected QCS survey index vs. observed QCS survey index (R75).

10.2. YMR MODELLING ISSUES

In common with stock assessments for other BC rockfish, this stock assessment depicts a slow-growing, low productivity stock. Similar to several of the more recent BC *Sebastes* stock assessments, we were unable to obtain a credible estimate for *M*. This was largely due to the lack of contrast and the high relative errors in the survey biomass indices. In effect, this stock assessment is a complex catch curve analysis which includes recruitment deviations. Nevertheless, *M* remains confounded with exploitation rate, as it is in all such analyses. If the surveys were more informative, the model would be able to estimate stock size, thus narrowing the range of possible *M* estimates. Instead, we were forced to come up with a range of plausible *M* values to use as fixed estimates in the model and then construct a composite base case from

which to provide management advice. The sensitivity run that estimated *M* (S02) demonstrates the futility of estimating natural mortality in this stock assessment using the multinomial distribution.

None of the *M* values used in the composite base case indicated that there was a sustainability issue with this stock. Even the lowest investigated value of *M* (0.04, model B1, Table F.7) returned a median estimate for B_{2022}/B_0 of 0.53 (0.38, 0.73) and for B_{2022}/B_{MSY} of 1.8 (1.3, 2.5). Consequently, we can be reasonably confident that the YMR stock is in the Healthy zone and is likely to stay there for 5-10 years at current levels of catch (around 1,000 to 1,200 t/y). Unfortunately, there is less confidence in the estimate of stock size and hence of long-term yield. The median B_0 estimate from the composite base case (26,386 t; Table 2), along with the corresponding estimate of MSY (1,039 t) is simply an average across five plausible values of *M* that were based on the observed distribution of maximum age in the GFBio database. This problem will not be easily resolved, given the low precision associated with the fishery independent surveys for this species.

The 2011 (Awatea) YMR stock assessment estimated a larger stock size than that in this assessment. Even the fixed *M* base case (M=0.047) had a median estimate for B_0 of 37,290 t which is 41% higher than the median composite base case estimate of B_0. Similarly, the previous YMR assessment estimated the median MSY to be 1,693 t, which is 63% greater than the MSY estimate for the composite base case. Appendix H demonstrates that the most likely cause of the difference in the estimated size of the initial biomass by the two models lies in the different distributional assumptions used to fit the AF data made by the two modelling platforms. SS uses the multinomial to fit these data while Awatea uses the robust normal. Figure H.11 shows that the two models converge in the mid-1960s and continue with similar estimates of biomass to the end of the reconstruction at the beginning of 2022. However, the initial estimates of equilibrium biomass differ, with the SS model estimating a large recruitment in 1952 which is omitted by the Awatea model. This behaviour demonstrates the trade-off in these models between initial stock size and recruitment, with the models obtaining similar fits to the data with either strategy. This trade-off occurs before there are data to constrain the model. Once there are available data, the models converge in their biomass estimates, resulting in uncertainty for the reference levels but less so in the estimates of recent biomass.

Foreign fleet effort in 1965-76 along the BC coast targeted POP, and YMR catch for these years was estimated as an assumed bycatch; therefore, the magnitude of the foreign fleet removals of YMR is uncertain. Another source of uncertainty in the catch series comes from domestic landings from the mid-1980s to 1995 (pre-observer coverage) which may have misreported lesser rockfish species to bypass quota restrictions on more desirable species like POP (Starr and Haigh 2021). However, the sensitivity runs on catch (S07: -33%; S08: +50%) showed that catch uncertainty did not have a major effect on the model's biomass trajectory or on the estimates of the relative stock size at the end of 2021 (Figure 7, Figure 9).

In the past, the use of commercial CPUE as an index of abundance has been generally avoided in BC rockfish stock assessments (primarily due to uncertainty in vessel behaviour in response to regulations). However, we have successfully used CPUE based on the bycatch of the evaluated species in the BC bottom trawl fishery in five recent stock assessments (Rougheye/Blackspotted Rockfish complex: Starr and Haigh in press[b]; Bocaccio: Starr and Haigh, in 2022b; Widow Rockfish: Starr and Haigh 2021b; Redstripe Rockfish: Starr and Haigh 2021a; Shortspine Thornyhead: Starr and Haigh 2017). Unlike the above five analyses, which were presumed to be based on catch/effort data collected from a passive bycatch fishery, YMR is frequently a target species as well as a bycatch species. However, because of the lack of real abundance information in the trawl survey data (see Figure 10), we were constrained to add this series to provide a usable abundance series. The CPUE likelihood profile in Figure 10 (left)

demonstrates the additional information this series adds to the model. In the case of the bycatch models, we reasoned that as long as the CPUE estimation model included the incidence of zero tows as well as the tows which captured the species, the resulting series would potentially track abundance. There was confidence that zero tows were being recorded reasonably well as a result of the high level of observer coverage in the BC bottom trawl fishery. Because the YMR fishery is both a target and bycatch fishery, we tested the robustness of the CPUE series by dropping the DFO localities with the highest catch rates, under the hypothesis that target fishing for YMR was most likely to be occurring in these "hot spots". This analysis, reported in Section C.8 (Appendix C), demonstrated that the CPUE trajectory was effectively unchanged.

Two runs relating to CPUE were included in the suite of YMR sensitivity runs:

- Sensitivity run S03 dropped the CPUE series but the B_0 median estimate was nearly the same as for model B3 (S03=26,252 t; B3=26,065 t), although the upper 95% quantile was greater (S03=34,660 t; B3=32,811 t). However, this model estimated a larger B_{2022} than did B3 (median=22,521 t compared to 18,027 t for run B3), resulting in a higher estimate of stock status for run S03.
- Sensitivity run S04 substituted an alternative CPUE model based on the Tweedie distribution which can accommodate zero and positive tows in the same model, thus removing the need to estimate separate models and combining them using the multiplicative delta-lognormal procedure (Equation C.4 in Appendix C). However, the two CPUE series did not differ much (see Figure C.21) and model S04 estimated similar, but slightly more optimistic, derived parameter estimates (Figure 9) compared to the central run.

We investigated a range of other sensitivity runs, most of which had little effect on the estimated stock status or overall model performance:

- There was little effect from raising (S06) or lowering (S05) the standard deviation of recruitment residuals (σ_R).
- Adding in the additional 1997 WCHG survey index (S01) had no impact on the assessment, a result consistent with uninformative nature of the survey data.
- Upweighting the QCS survey AF data (S09) was discussed in Section 8.2. Although this sensitivity run did not materially alter the advice, it would have affected the projections through the estimation of possibly spurious recent strong year classes.
- It is surprising that beginning recruitment deviation estimates in 1970 rather than 1950 (S10) had such a strong impact on the stock assessment because it is rare to have such informative age information that can be used to estimate early year class strengths. However, this effect may be caused by an interaction with the uninformative survey information and may not be a result that can be generalised.
- Finally, it is apparent that this stock assessment did not fully explore the uncertainty associated with ageing error. Sensitivity run S11, which did not use any ageing error, indicated that model results were sensitive to the presence or absence of this procedure. We were asked in the RPR to do a run which used an alternative implementation of ageing error based on the error of secondary readers relative to the first reader (run S14). This run resulted in an intermediate effect (relative to the central run and run S11) on the estimate of stock status (Figure 9). We are satisfied with the performance of the implementation of ageing error in the composite base case, which gave punctuated estimates of recruitment that conform with our understanding of *Sebastes* recruitment strategy (see Figure 4 and Figure H.10). We also feel that the ageing error implemented in run S14 likely underestimated this error, particularly at older ages where data were sparse. However,

ageing error is more typically estimated using statistical models that use multiple age readings from individual fish to derive a classification matrix that defines the probability of assigning an observed age to a fish based on its true age, which is statistically inferred (Richards et al. 1992). Future *Sebastes* stock assessments should more fully explore this axis of uncertainty.

The decision tables provide guidance to the selection of short-term catch recommendations and describe the range of possible future outcomes over the projection period at fixed levels of annual catch. The accuracy of the projections is predicated on the model being correct. Uncertainty in the parameters is explicitly addressed using a Bayesian approach but reflects only the specified model and weights assigned to the various data components.

11. FUTURE RESEARCH AND DATA REQUIREMENTS

The following issues should be considered when planning future stock assessments and management evaluations for Yellowmouth Rockfish:

1. Continue the suite of fishery-independent trawl surveys that have been established across the BC coast. This includes obtaining age and length composition samples, which will allow the estimation of survey-specific selectivity ogives.
2. Explore how single populations, such as YMR, are part of a complex system consisting of biological and economic components (Walker and Salt 2006). Such systems can have multiple stable states, which may have implications in our understanding of YMR population dynamics and resilience.
3. Explore the effects of climate change on YMR populations and identify how shifts in the ecosystem affect our perception of equilibrium conditions under different climate regimes. This could include exploring the use of environmental covariates as predictors of recruitment, as well as investigating the role of episodic recruitment in the evolutionary strategy used by YMR.
4. If sufficient midwater trawl fishery biological data become available, consider using a two-fishery model.
5. Estimate both M and h in Stock Synthesis.
6. Explore using a single sex model, with the growth functions differing little by sex.
7. Explore how hyperallometry in the length relationship influences fecundity (e.g., exponent greater than 3).
8. Investigate using a smoothing function or possibly binning ages to explore how best to incorporate ageing error into this stock assessment.
9. Try using constant harvest rates to project farther than 10 years. As well, investigate if more realistic recruitment procedures for rockfish species have been implemented in SS3. Such improvements may increase the reliability of the projections.
10. Explore retrospective patterns, fecundity, and parameter options in this stock assessment.
11. Explore the addition of climate-based variables, which might be especially important for sporadically recruiting species. The authors could address this as a sensitivity analysis for next time. The authors also indicated that SS has the option to include environmental indices as abundance indices.
12. Overlay Pacific Decadal Oscillation bands on recruitment trajectories (see Figure F.30.) to see if there are any patterns.

12. ACKNOWLEDGEMENTS

The switch in model platforms from Awatea to Stock Synthesis was greatly facilitated by the help from the following people: Richard Methot (NOAA[5]), Ian Taylor (NWFSC[6], NOAA), Chantel Wetzel (NWFSC, NOAA), Kathryn Doering (NWFSC, NOAA), Adam Langley (FIS[7], NZ), Allan Hicks (IPHC[8]), and Chris Grandin (PBS[9], DFO[10]). Additional guidance on data inputs was provided by Sean Anderson (PBS, DFO), Bruce Turris (CGRCS[11]) and Brian Mose (CIC[12] Trawl). The staff in the Sclerochronology Laboratory at the PBS were, as always, quick to process YMR otolith requests. Written peer reviews by Andrew Edwards (PBS, DFO) and Bob Rogers (NAFC[13], DFO) provided helpful guidance and discussion during the regional peer review (RPR) meeting. Greg Workman facilitated the RPR meeting as Chair and Jill Campbell acted as rapporteur. Additional feedback by other RPR participants contributed greatly to the process. Jon T. Schnute provided guidance on the mathematical notation for ageing error in Appendix E.

13. REFERENCES CITED

Anderson, S.C., Keppel, E.A., and Edwards, A.M. 2019. A reproducible data synopsis for over 100 species of British Columbia groundfish. DFO Can. Sci. Advis. Sec. Res. Doc. 2019/041. vii + 321 p.

Conrath, C.L. 2017. Maturity, spawning omission, and reproductive complexity of deepwater rockfish. Trans. Am. Fish. Soc. 145. 495-507.

COSEWIC. 2010. COSEWIC assessment and status report on the Yellowmouth Rockfish *Sebastes reedi* in Canada. Committee on the Status of Endangered Wildlife in Canada, Ottawa ON, vii + 57 p.

DFO. 2009. A fishery decision-making framework incorporating the Precautionary Approach. Accessed Aug 17, 2021.

DFO. 2015. Yellowtail Rockfish (Sebastes Flavidus) Stock Assessment for the Coast of British Columbia, Canada. DFO Can. Sci. Advis. Sec. Sci. Advis. Rep. 2015/010.

DFO. 2016. Guidelines for providing interim-year updates and science advice for multi-year assessments. DFO Can. Sci. Advis. Sec. Sci. Advis. Rep. 2016/020.

DFO. 2022. Proceedings of the Pacific regional peer review on Redstripe Rockfish (*Sebastes proriger*) stock assessment for British Columbia in 2018; June 13-14, 2018. DFO Can. Sci. Advis. Sec. Proceed. Ser. 2022/014.

Dick, E.J., Beyer, S., Mangel, M., and Ralston, S. 2017. A meta-analysis of fecundity in rockfishes (genus *Sebastes*). Fish. Res. 187. 73-85.

[5] National Oceanic and Atmospheric Administration, Dept. Commerce, USA

[6] Northwest Fisheries Science Center, Seattle WA

[7] Fisheries Information Systems, Ltd., Nelson NZ

[8] International Pacific Halibut Commission, Seattle WA

[9] Pacific Biological Station, Nanaimo BC

[10] Fisheries and Oceans Canada (aka Dept. Fisheries and Oceans)

[11] Canadian Groundfish Research and Conservation Society, New Westminster BC

[12] Commercial Industry Caucus, BC

[13] Northwest Atlantic Fisheries Centre, St. John's NL

Edwards, A.M., Haigh, R., and Starr, P.J. 2012a. Stock assessment and recovery potential assessment for Yellowmouth Rockfish (*Sebastes reedi*) along the Pacific coast of Canada. DFO Can. Sci. Advis. Sec. Res. Doc. 2012/095: iv + 188 p.

Edwards, A.M., Haigh, R., and Starr, P.J. 2014a. Pacific Ocean Perch (*Sebastes alutus*) stock assessment for the north and west coasts of Haida Gwaii, British Columbia. DFO Can. Sci. Advis. Sec. Res. Doc. 2013/092: vi + 126 p.

Edwards, A.M., Haigh, R., and Starr, P.J. 2014b. Pacific Ocean Perch (*Sebastes alutus*) stock assessment for the west coast of Vancouver Island, British Columbia. DFO Can. Sci. Advis. Sec. Res. Doc. 2013/093: vi + 135 p.

Edwards, A.M., Starr, P.J., and Haigh, R. 2012b. Stock assessment for Pacific ocean perch (*Sebastes alutus*) in Queen Charlotte Sound, British Columbia. DFO Can. Sci. Advis. Sec. Res. Doc. 2011/111: viii + 172 p.

Fournier, D.A., Sibert, J.R., Majkowski, J., and Hampton, J. 1990. MULTIFAN a likelihood-based method for estimating growth parameters and age composition from multiple length frequency data sets illustrated using data for southern bluefin tuna (*Thunnus maccoyii*). Can. J. Fish. Aquat. Sci. 47(2). 301-317.

Francis, R.I.C.C. 2011. Data weighting in statistical fisheries stock assessment models. Can. J. Fish. Aquat. Sci. 68(6): 1124–1138.

Gelman, A., Carlin, J.B., Stern, H.S., and Rubin, D.B. 2004. Bayesian Data Analysis, 2nd edition. Chapman and Hall/CRC, New York.

Grandin, C.J., Johnson, K.F., Edwards, A.M., and Berger, A.M. 2020. Status of the Pacific Hake (whiting) stock in U.S. and Canadian waters in 2020. Prepared by the Joint Technical Committee of the U.S. and Canada Pacific Hake/Whiting Agreement, National Marine Fisheries Service and Fisheries and Oceans Canada. 273 p.

Haigh, R., Starr, P.J., Edwards, A.M., King, J.R., and Lecomte, J.B. 2018. Stock assessment for Pacific Ocean Perch (*Sebastes alutus*) in Queen Charlotte Sound, British Columbia in 2017. DFO Can. Sci. Advis. Sec. Res. Doc. 2018/038: v + 227 p.

He, X., Field, J.C., Beyer, S.G., and Sogard, S.M. 2015. Effects of size-dependent relative fecundity specifications in fishery stock assessments. Fish. Res. 165. 54-62.

Hilborn, R., Maunder, M., Parma, A., Ernst, B., Payne, J., and Starr, P. 2003. Coleraine: A generalized age-structured stock assessment model. User's manual version 2.0. University of Washington Report SAFS-UW-0116. Tech. rep., University of Washington.

Hoenig, J.M. 1983. Empirical use of longevity data to estimate mortality rates. Fish. Bull. 82(1): 898-903.

Jorgensen, B. 1987. Exponential dispersion models. J. Royal Stat. Soc. Series B (Methodological) 49(2). 127-162.

Knaus, J. 2015. snowfall: Easier cluster computing (based on snow). R package ver. 1.84-6.1.

Love, M.S., Yoklavich, M., and Thorsteinson, L. 2002. The Rockfishes of the Northeast Pacific. University of California Press, Berkeley and Los Angeles, California.

McAllister, M.K., and Ianelli, J.N. 1997. Bayesian stock assessment using catch-age data and the sampling – importance resampling algorithm. Can. J. Fish. Aquat. Sci. 54(2). 284-300.

Methot Jr, R.D., and Wetzel, C.R. 2013. Stock Synthesis: A biological and statistical framework for fish stock assessment and fishery management. Fish. Res. 142. 86-99.

Methot Jr, R.D., Wetzel, C.R., Taylor, I.G., Doering, K.L., and Johnson, K.F. 2021. Stock Synthesis User Manual, version 3.30.17. NOAA Fisheries, Seattle WA. iv + 233 p.

Monnahan, C.C. 2018. adnuts: No-U-Turn MCMC Sampling for ADMB Models. R package ver. 1.1.2.

Monnahan, C.C., Branch, T.A., Thorson, J.T., Stewart, I.J., and Szuwalski, C.S. 2019. Overcoming long Bayesian run times in integrated fisheries stock assessments. ICES J. Mar. Sci. 76(6). 1477-1488.

Monnahan, C.C., and Kristensen, K. 2018. No-U-turn sampling for fast Bayesian inference in ADMB and TMB: Introducing the adnuts and tmbstan R packages. PLoS ONE 13(5). e0197,954.

New Zealand Ministry of Fisheries. 2011. Operational Guidelines for New Zealand's Harvest Strategy Standard. Ministry of Fisheries, New Zealand.

Rideout, R.M., and Tomkiewicz, J. 2011. Skipped spawning in fishes: More common than you might think. Mar. Coast. Fish. 3. 176-189.

Richards, L.J., Schnute, J.T., Kronlund, A.R. and Beamish, R.J. 1992. Statistical models for the analysis of ageing error. Can. J. Fish. Aquat. Sci. 49(9). 1801-1815.

Stanley, R.D. 1987. A comparison of age estimates derived from the surface and cross-section methods of otolith reading for Pacific ocean perch (*Sebastes alutus*). In Proceedings of the International Rockfish Symposium, Anchorage, Alaska USA, October 20-22, 1986, Lowell Wakefield Fisheries Symposium, Alaska Sea Grant Rep. No. 87-2, p. 187-196

Stanley, R.D., and Kronlund, A.R. 2000. Silvergray rockfish (*Sebastes brevispinis*) assessment for 2000 and recommended yield options for 2001/2002. DFO Can. Sci. Advis. Sec. Res. Doc. 2000/173. 116 p.

Stanley, R.D., Starr, P., and Olsen, N. 2009. Stock assessment for Canary rockfish (*Sebastes pinniger*) in British Columbia waters. DFO Can. Sci. Advis. Sec. Res. Doc. 2009/013. xxii + 198 p.

Starr, P.J., and Haigh, R. 2017. Stock assessment of the coastwide population of Shortspine Thornyhead (*Sebastolobus alascanus*) in 2015 off the British Columbia coast. DFO Can. Sci. Advis. Sec. Res. Doc. 2017/015. ix + 174 p.

Starr, P.J. and Haigh, R. 2022. Bocaccio (*Sebastes paucispinis*) stock assessment for British Columbia in 2019, including guidance for rebuilding plans. DFO Can. Sci. Advis. Sec. Res. Doc. 2022/001. vii + 292 p.

Starr, P.J., and Haigh, R. 2022b. Rougheye/Blackspotted Rockfish (*Sebastes aleutianus/ melanostictus*) stock assessment for British Columbia in 2020. DFO Can. Sci. Advis. Sec. Res. Doc. 2020/022. In press

Starr, P.J. and Haigh, R. 2021a. Redstripe Rockfish (*Sebastes proriger*) stock assessment for British Columbia in 2018. DFO Can. Sci. Advis. Sec. Res. Doc. 2021/014. vii + 340 p.

Starr, P.J., and Haigh, R. 2021b. Widow Rockfish (*Sebastes entomelas*) stock assessment for British Columbia in 2019. DFO Can. Sci. Advis. Sec. Res. Doc. 2021/039.

Starr, P.J., Haigh, R., and Grandin, C. 2016. Stock assessment for Silvergray Rockfish (*Sebastes brevispinis*) along the Pacific coast of Canada. DFO Can. Sci. Advis. Sec. Res. Doc. 2016/042: vi + 170 p.

Taylor, I.G., Doering, K.L., Johnson, K.F., Wetzel, C.R., and Stewart, I.J. 2021. Beyond visualizing catch-at-age models: Lessons learned from the r4ss package about software to support stock assessments. Fisheries Research 239. e105924.

Thorson, J.T., Johnson, K.F., Methot, R.D., and Taylor, I.G. 2017. Model-based estimates of effective sample size in stock assessment models using the Dirichlet-multinomial distribution. Fish. Res. 192. 84-93.

Walker, B., and Salt, D. 2006. Resilience Thinking: Sustaining Ecosystems and People in a Changing World. Island Press. Washington DC. 192 p.

APPENDIX A. CATCH DATA

A.1. BRIEF HISTORY OF THE FISHERY

Forrester (1969) provides a brief history of the Pacific Marine Fisheries Commission (PMFC), which is reproduced (with some modification) below. Currently, the PMFC is called the Pacific States Marine Fisheries Commission; however, this document retains the acronym 'PMFC' for historical context.

> *The Pacific Marine Fisheries Commission (PMFC) was created in 1947 when the states of Washington, Oregon, and California jointly formed an interstate agreement (called a 'compact') with the consent of the 80th Congress of the USA. In 1956, informal agreement was reached among various research agencies along the Pacific coast to establish a uniform description of fishing areas as a means of coordinating the collection and compilation of otter trawl catch statistics. This work was undertaken by the PMFC with the informal cooperation of the Fisheries Research Board of Canada. Areas 1A, 1B, and 1C encompass waters off the California coast, while Areas 2A-2D involve waters adjacent to Oregon and a small part of southern Washington. The remainder of the Washington coast and the waters off the west coast of Vancouver Island comprise Areas 3A-3D, while United States and Canadian inshore waters (Juan de Fuca Strait, Strait of Georgia, and Puget Sound) are represented by Areas 4A and 4B, respectively. Fishing grounds between the northern end of Vancouver Island and the British Columbia-Alaska boundary are represented by Areas 5A-5E. The entire Alaskan coast is designated as Area 6, but except for a small amount of fishing in inshore channels, this area has not been trawled intensively by North American nationals.*

The early history of the British Columbia (BC) trawl fleet was covered by Forrester and Smith (1972). A trawl fishery for slope rockfish has existed in BC since the 1940s. Aside from Canadian trawlers, foreign fleets targeted Pacific Ocean Perch (POP, *Sebastes alutus*) in BC waters for approximately two decades. These fleets were primarily from the USA (1959–1976), the USSR (1965–1968), and Japan (1966–1976). Consequently, the foreign vessels removed large amounts of rockfish biomass, including species other than POP, in Queen Charlotte Sound (QCS, Ketchen 1976, 1980b), off the west coast of Haida Gwaii (WCHG, Ketchen 1980a,b), and off the west coast of Vancouver Island (WCVI, Ketchen 1976, 1980a,b). All foreign fleets were excluded from Canadian waters inside of 200 nm with the declaration of the Exclusive Economic Zone in 1977. Canadian effort escalated in 1985, and for the next decade, landings by species were often misreported to avoid species-specific trip limits.

Yellowmouth Rockfish (YMR) ranges from the Gulf of Alaska southward to northern California near San Francisco, typically at depths between 180 and 275 m (Love et al. 2002). In BC, the apparent area of highest concentration occurs in Queen Charlotte Sound (PMFC areas 5A and 5B in Figure A.1) with isolated hotspots west of Haida Gwaii (PMFC area 5E in Figure A.1). This species occurs along the west coast of Vancouver Island (3C in Figure A.1), but its density appears to be low there. Adults occur on the bottom and in midwater above high-relief rocks, and have been aged up to 99 years. This species has been encountered by the BC bottom trawl fleet over an estimated 26,315 km^2 (Figure A.1 top left, based on a roughly 32-km^2 grid size and tow start positions in the commercial fishery), and the bulk of the population lies between depths of 130 m and 402 m (see Appendix G).

In 2012, measures were introduced to reduce and manage the bycatch of corals and sponges by the BC groundfish bottom trawl fishery. These measures were developed jointly by industry

and environmental non-governmental organisations (Wallace et al. 2015), and included: limiting the footprint of groundfish bottom trawl activities, establishing a combined bycatch conservation limit for corals and sponges, and establishing an encounter protocol for individual trawl tows when the combined coral and sponge catch exceeded 20 kg. These measures have been incorporated into DFO's Pacific Region Groundfish Integrated Fisheries Management Plan (Feb 21, 2021, version 1.1) and apply to all vessels using trawl gear in BC.

Table A.1. Annual Total Allowable Catch (TAC tonnes/year) for YMR caught in BC waters: year can either be calendar year (1993-1996) or fishing year (1997 on). Sector allocations remained constant from 2001 on: Trawl 96.77%, ZN Outside 2.49%, Halibut 0.74%. Annual TACs (t/y) also remained unchanged from 2001 on – Trawl: 3C=219, 3D5AB=1135, 5CD=685, 5E=325; ZN Outside: 3C=4, 3D5AB=20, 5CD=13, 5E=24; Halibut: 3C=1, 3D5AB=6, 5CD=4, 5E=7. Research allocations were generally 3 t/y for the longline surveys and ranged from 3-7 t/y for the trawl surveys.

Year	Start	End	3C	3D+5AB	5CD	5E [5ES,5EN]	Coast
1979	1/1/1979	12/31/1979	---	50	---	[750,---]	800
1980	1/1/1980	12/31/1980	---	250	---	[800,---]	1050
1981	1/1/1981	12/31/1981	---	---	---	[800,---]	800
1982	1/1/1982	12/31/1982	---	250	---	[100,600]	950
1983	1/1/1983	12/31/1983	---	250	---	[agg,open]	---
1984	1/1/1984	12/31/1984	---	250	300	[agg,open]	---
1985	1/1/1985	12/31/1985	---	350	250	[agg,open]	---
1986	1/1/1986	12/31/1986	---	---	250	[agg,open]	---
1987	1/1/1987	12/31/1987	---	350	250	[agg,open]	---
1988	1/1/1988	12/31/1988	---	375	250	[agg,open]	---
1989	1/1/1989	12/31/1989	---	500	350	[agg,open]	1450
1990	1/1/1990	12/31/1990	---	500	330	[agg,open]	1380
1991	1/1/1991	12/31/1991	---	500	330	[550,0]	1380
1992	1/1/1992	12/31/1992	---	500	330	[550,0]	1380
1993	1/1/1993	12/31/1993	---	500	330	[550,0]	1380
1994	1/15/1994	12/31/1994	---	---	---	[---,0]	---
1995	1/1/1995	12/31/1995	---	---	---	---	---
1996	2/6/1996	3/31/1997	---	---	---	---	---
1997	4/1/1997	3/31/1998	100	1866	360	104	2430
1998	4/1/1998	3/31/1999	221	1145	691	328	2385
1999	4/1/1999	3/31/2000	223	1156	697	331	2407
2000	4/1/2000	3/31/2001	223	1156	697	331	2408
2001	4/1/2001	3/31/2002	224	1162	702	357	2444
2002	4/1/2002	3/31/2003	224	1162	702	357	2444
2003	4/1/2003	3/31/2004	224	1162	702	357	2444
2004	4/1/2004	3/31/2005	224	1162	702	357	2444
2005	4/1/2005	3/31/2006	224	1162	702	357	2444
2006	4/1/2006	3/31/2007	224	1162	702	357	2444
2007	3/10/2007	3/31/2008	224	1162	702	357	2444
2008	3/8/2008	2/20/2009	224	1162	702	357	2444
2009	2/21/2009	2/20/2010	224	1162	702	357	2444
2010	2/21/2010	2/20/2011	224	1162	702	357	2444
2011	2/21/2011	2/20/2013	224	1162	702	357	2444
2012	2/21/2011	2/20/2013	224	1162	702	357	2444
2013	2/21/2013	2/20/2014	224	1162	702	357	2444
2014	2/21/2014	2/20/2015	224	1162	702	357	2444
2015	2/21/2015	2/20/2016	224	1162	702	357	2444
2016	2/21/2016	2/20/2017	224	1162	702	357	2444
2017	2/21/2017	2/20/2018	224	1162	702	357	2444
2018	2/21/2018	2/20/2019	224	1162	702	357	2444
2019	2/21/2019	2/20/2020	224	1162	702	357	2444
2020	2/21/2020	2/20/2021	224	1162	702	357	2444
2021	2/21/2021	2/20/2022	224	1162	702	357	2444

Table A.2. Codes to notes on management actions and quota adjustments that appear in Table A.1. Abbreviations that appear under 'Management Actions': Agg = Aggregate, DFO = Department of Fisheries & Oceans, DMP = dockside monitoring program, GTAC =Groundfish Trawl Advisory Committee, H&L = hook and line, IFMP = Integrated Fisheries Management Plan, IVQ = individual vessel quota, MC =Mortality Cap, TAC =Total Allowable Catch, TWL = Trawl. See Archived Integrated Fisheries Management Plans - Pacific Region for further details. Rockfish species codes: BKR=Black, CAR=Canary, CHR=China, CPR=Copper, LST=Longspine Thornyhead, ORF=Other rockfish, POP=Pacific Ocean Perch, QBR=Quillback, RER=Rougheye/Blackspotted, RSR=Redstripe, SCR=Sharpchin, SGR=Silvergray, SKR=Shortraker, SST=Shortspine Thornyhead, TIR=Tiger, WWR=Widow, YMR=Yellowmouth, YTR=Yellowtail.

Year	Management Actions
1986	SRF: Slope rockfish (POP, YMR, RER) coastwide quota = 5000t.
1988	YMR: The quota for Yellowmouth Rockfish only applies to areas 127, 108, 109, 110, 111 and 130-1. Evidence from surveys and from commercial fishery suggests a common stock from the mouth of Queen Charlotte Sound and possibly to Cape Cook.
1989	TWL: In 1989, quota rockfish comprising Pacific Ocean Perch, Yellowmouth Rockfish, Canary Rockfish and Silvergray Rockfish, will be managed on a coastwide basis.
1994	TWL: Started a dockside monitoring program (DMP) for the Trawl fleet.
1994	TWL: As a means of both reducing at-sea discarding and simplifying the harvesting regime, rockfish aggregation was implemented. Through consultation with GTAC, the following aggregates were identified: Agg 1= POP, YMR, RER, CAR, SGR, YTR; Agg 2= RSR, WWR; Agg 3= SKR, SST, LST; Agg 4= ORF.
1995	TWL: Trawl aggregates established in 1994 changed: Agg 1= CAR, SGR, YTR, WWR, RER; Agg 2= POP, YMR, RSR; Agg 3= SKR, SST, LST; Agg 4= ORF.
1996	TWL: Started 100% onboard observer program for offshore Trawl fleet.
1996	H&L: Rockfish aggregation will continue on a limited basis in 1996: Agg 1= YTR, WWR; Agg 2= CAR, SGR; Agg 3= POP, YMR; Agg 4= RER, SKR; Agg 5= RSR, SCR; Agg 6= ORF incl. SST, LST
1997	TWL: Started IVQ system for Trawl \Total Allowable Catch (TAC) species (April 1, 1997)
1997	YMR: Permanent boundary adjustment -- Pacific Ocean Perch and Yellowmouth Rockfish caught within Subarea 102-3 and those portions of Subareas 142-1, 130-3 and 130-2 found southerly and easterly of a straight line commencing at 52°20'00"N 131°36'00"W thence to 52°20'00"N 132°00'00"W thence to 51°30'00"N 131°00'00"W and easterly and northerly of a straight line commencing at 51°30'00"N 131°00'00"W thence to 51°39'20"N 130°30'30"W will be deducted from the vessel's 5CD IVQ for those two species.
1997	H&L: All H&L rockfish, with the exception of YYR, shall be managed under the following rockfish aggregates: Agg 1= QBR, CPR; Agg 2= CHR, TIR; Agg 3= CAR, SGR; Agg 4= RER, SKR, SST, LST; Agg 5= POP, YMR, RSR; Agg 6= YTR, BKR, WWR; Agg 7= ORF excluding YYR.
2000	ALL: Formal discussions between the hook and line rockfish (ZN), halibut and trawl sectors were initiated in 2000 to establish individual rockfish species allocations between the sectors to replace the 92/8 split. Allocation arrangements were agreed to for rockfish species that are not currently under TAC. Splits agreed upon for these rockfish will be implemented in the future when or if TACs are set for those species.
2002	TWL: Closed areas to preserve four hexactinellid (glassy) sponge reefs.
2003	YMR: Species at Risk Act (SARA) came into force in 2003.
2006	ALL: Introduced an \Integrated Fisheries Management Plan (IFMP) for all directed groundfish fisheries.
2006	H&L: Implemented 100% at-sea electronic monitoring and 100% dockside monitoring for all groundfish H&L fisheries.
2012	TWL: Froze the footprint of where groundfish bottom trawl activities can occur (all vessels under the authority of a valid Category T commercial groundfish trawl license selecting Option A as identified in the IFMP).
2013	TWL: To support groundfish research, the groundfish trawl industry agreed to the trawl TAC offsets to account for unavoidable mortality incurred during the joint DFO-Industry groundfish multi-species surveys in 2013.
2015	ALL: Research allocations were specified starting in 2015 to account for the mortalities associated with survey catches to be covered by TACs.

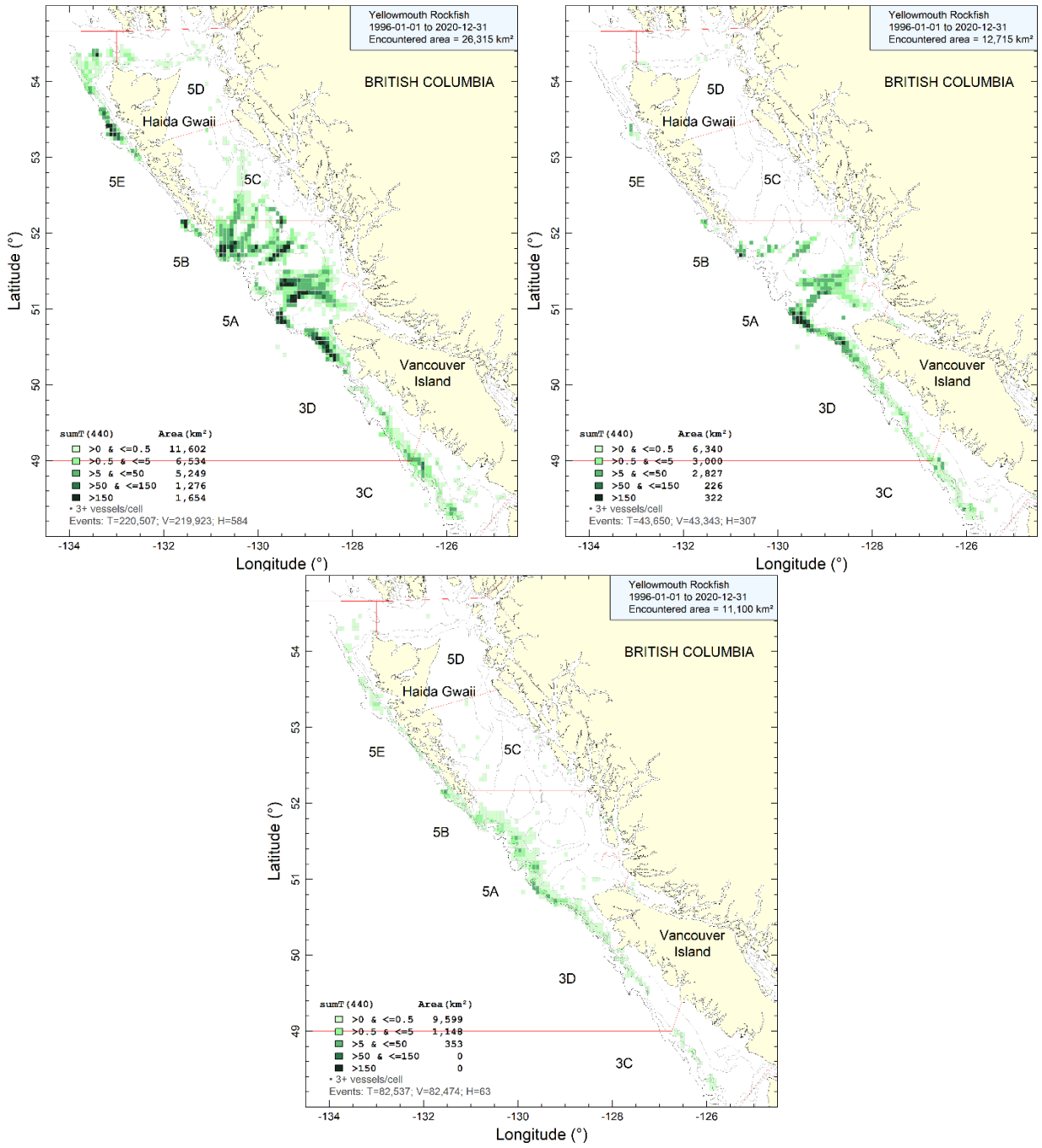

Figure A.1. Aerial distribution of accumulated YMR catch (tonnes) by bottom trawl (upper left), midwater trawl (upper right), hook and line (lower middle, no trap records) from 1996 to 2020 in grid cells 0.075° longitude by 0.055° latitude (roughly 32 km²). Isobaths show the 100, 200, 500, and 1200 m depth contours. Note that cells with <3 fishing vessels are not displayed.

A.2. CATCH RECONSTRUCTION

This assessment reconstructs YMR catch back to 1918 but considers the start of the fishery to be 1935 (Figure A.2) before the fishery started to increase during World War II. Prior to this, trawl catches were negligible and halibut fleet catches were estimated to be <20 tonnes per stock per year. During the period 1950–1975, US vessels routinely caught more rockfish than did Canadian vessels. Additionally, from the mid-1960s to the mid-1970s, foreign fleets (Russian and Japanese) removed large amounts of rockfish, primarily POP. These large catches were first reported by various authors (Westrheim et al. 1972; Gunderson et al. 1977; Leaman and Stanley 1993); however, Ketchen (1980a,b) re-examined the foreign fleet catch, primarily because statistics from the USSR called all rockfish 'perches' while the Japanese used the term 'Pacific ocean perch' indiscriminately. In the catch reconstruction, all historical foreign catches (annual rockfish landings) were tracked separately from Canadian YMR landings, converted to YMR (Section A.2.2), and added to the latter during the reconstruction process.

A.2.1. Data sources

Starting in 2015, all official Canadian catch tables from the databases below (except PacHarv3) have been merged into one table called 'GF_MERGED_CATCH', which is available in DFO's GFFOS database. All groundfish DFO databases are now housed on the DFBCV9TWVASP001 server. YMR catch by fishery sector ultimately comes from the following seven DFO databases:

- PacHarv3 sales slips (1982-1995) – hook and line only;
- GFCatch (1954-1995) – trawl and trap;
- PacHarvHL merged data table (1986-2006) – halibut, Dogfish+Lingcod, H&L rockfish;
- PacHarvSable fisherlogs (1995-2005) – Sablefish;
- PacHarvest observer trawl (1996-2007) – trawl;
- GFFOS groundfish subset from Fishery Operation System (2006-pressent) – all fisheries and modern surveys; and
- GFBioSQL joint-venture hake and research survey catches (1947-presen) – multiple gear types. GFBioSQL is an SQL Server database that mirrors the GFBio Oracle database.

All data sources other than PacHarv3 were superseded by GFFOS from 2007 on because this latter repository was designed to record all Canadian west coast landings and discards from commercial fisheries and research activities.

Prior to the modern catch databases, historical landings of aggregate rockfish – either total rockfish (TRF) or rockfish other than POP (ORF) – are reported by eight different sources (see Haigh and Yamanaka 2011). The earliest historical source of rockfish landings comes from Canada Dominion Bureau of Statistics (1918-1950).

The purpose of this procedure is to estimate the reconstructed catch of any rockfish species (generically designated as RRF) from ratios of RRF/ORF or RRF/TRF, add the estimated discards from the ratio RRF/TAR (where TAR is the target species landed by fishery), to reconstruct the total catch of species RRF.

A.2.2. Reconstruction details

A.2.2.1. Definition of terms

A brief synopsis of the catch reconstruction (CR) follows, with a reminder of the definition of terms:

Fisheries: there are five fisheries in the reconstruction (even though trawl dominates the YMR fishery):

- T = groundfish trawl (bottom + midwater),
- H = Halibut longline,
- S = Sablefish trap/longline,
- DL = Dogfish and Lingcod troll/longline (originally called 'Schedule II'),
- ZN = hook and line rockfish (sector called 'ZN' from 1986 to 2006 and 'Rockfish Outside' and 'Rockfish Inside' from 2007 on).

TRF: acronym for 'total rockfish' (all species of *Sebastes* + *Sebastolobus*)

ORF*:* acronym for 'other rockfish' (= TRF minus POP), landed catch aggregated by year, fishery, and PMFC (Pacific Marine Fisheries Commission) major area

POP: Pacific Ocean Perch

RRF: Reconstructed rockfish species – in this case, YMR

TAR*:* Target species landed catch

L & D: L =landed catch, D =releases (formerly called 'discards')

gamma: mean of annual ratios, $\sum_i \mathrm{RRF}_i^L / \mathrm{ORF}_i^L$, grouped by major PMFC area and fishery. For YMR, the reference years were set to 1996-2019 for the trawl fishery and 1996-2019 for the non-trawl fisheries.

delta: mean of annual ratios, $\sum_i \mathrm{RRF}_i^D / \mathrm{TAR}_i$, grouped by major PMFC area and fishery using reference years i = 1997-2006 for the trawl fishery and 2000-2004 for all other fisheries. Observer records were used to gather data on releases.

The stock assessment population model uses calendar year, requiring calendar year catch estimates. The reconstruction defaults to using 'official' (reported) catch numbers by fishery starting in years 1996 (T), 2000 (H), 2007 (S,DL), and 1986 (ZN), which are the years when these fisheries implemented reliable observer coverage. These defaults were not used for YMR. Instead, landings were reconstructed before 1996 for the trawl fishery and before 2006 for the non-trawl fisheries. Although reported data existed in earlier time periods, previous TWGs considered that reported catches of less desirable rockfish species from 1985 (start of restrictive trip limits) to 1994 (start of the DMP) were likely inflated, given the incentives for operators to misreport their catch of desirable species during this period.

The reconstruction of Canadian YMR catch estimated landings for years before those with credible records using gamma ratios (Table A.3). These ratios were also used to convert foreign landings of ORF to YMR. The ratios were calculated from a relatively modern period (1996-2019 for all fisheries); therefore, an obvious caveat to this procedure is that ratios derived from a modern fishery may not reflect catch ratios during the historical foreign fleet activity or regulatory regimes not using IVQs (individual vessel quotas). Consequently, we use sets of years where gamma does not fluctuate wildly in an attempt to minimise this potential issue.

After YMR landings were estimated, non-retained catch (releases or discards) were estimated and added during years identified by fishery: T = 1954-1995, H = 1918-2005, S/DL = 1950-2005, and ZN = 1986-2005. The non-retained catch was estimated using the `delta` ratios of YMR discarded by a fishery to fishery-specific landed targets (TAR): T = YMR, H = Pacific Halibut, S = Sablefish, DL = Spiny Dogfish + Lingcod, ZN = YMR (Table A.3).

The current annual YMR catches by trawl fishery and those from the non-trawl fisheries appear in Table A.4 and Figure A.2. The combined fleet catches were used in the population models as plotted in Figure A.8. The catch reconstruction used for YMR was built on Jan 26, 2021, with an updated 2020 catch obtained on Jul 7, 2021. The 2021 catch was set equal to the 2020 catch.

A.2.2.2. Reconstruction results

Table A.3. Estimated 'gamma' (YMR/ORF) and 'delta' (discard) ratios for each fishery and PMFC area used in the catch reconstruction of YMR.

gamma (proportion YMR/ORF)

PMFC	Trawl	Halibut	Sablefish	Dogfish/ Lingcod	H&L Rockfish
3C	0.00600	0.00115	0.00014	0.00048	0.00007
3D	0.01104	0.00109	0.00005	0.00211	0.00019
5A	0.24891	0.03481	0.00471	0.00152	0.01532
5B	0.23423	0.01586	0.00124	0.00023	0.00510
5C	0.01268	0.00080	0	0.00026	0.00003
5D	0.00020	0.00033	0	0	0.00006
5E	0.12055	0.00092	0.00002	0.00347	0.00154

delta (discard rate)

PMFC	Trawl	Halibut	Sablefish	Dogfish/ Lingcod	H&L Rockfish
3C	0.00644	0	0	0	0
3D	0.00509	0.00002	0.00011	0.00002	0
5A	0.00244	0.00089	0.00023	0	0.00115
5B	0.00524	0.00013	0.00069	0	0
5C	0.00265	0.00002	0	0	0
5D	0.01707	0	0	0	0
5E	0.00066	0.00003	0	0	0.00047

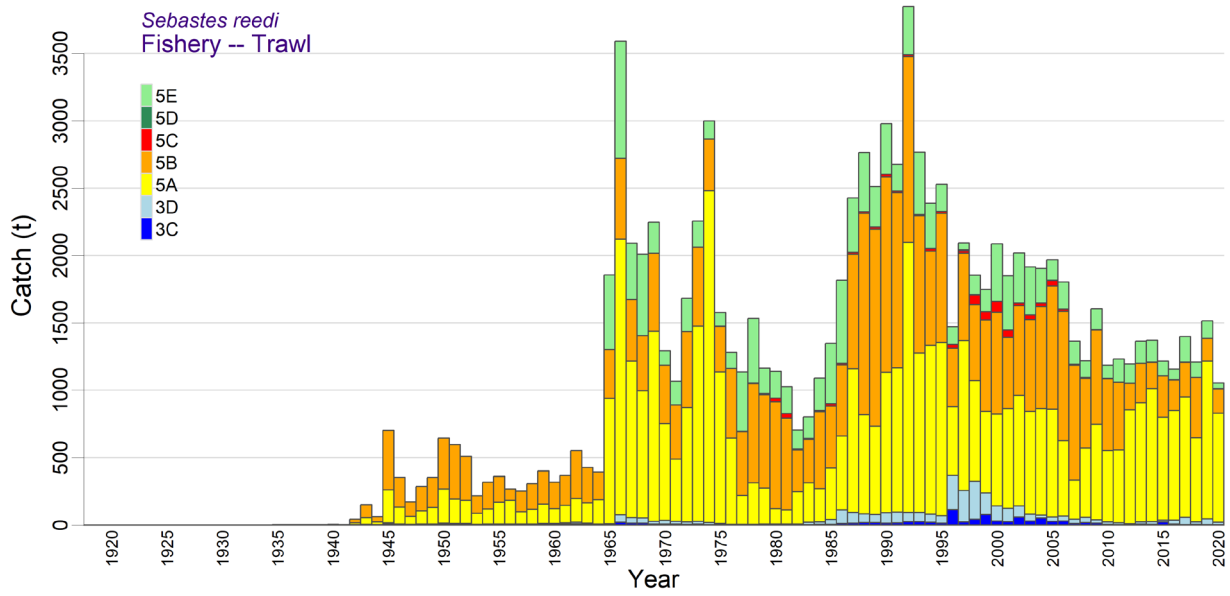

*Figure A.2. Reconstructed total (landed + released) catch (t) for YMR from the **trawl** fishery in PMFC major areas 3C to 5E.*

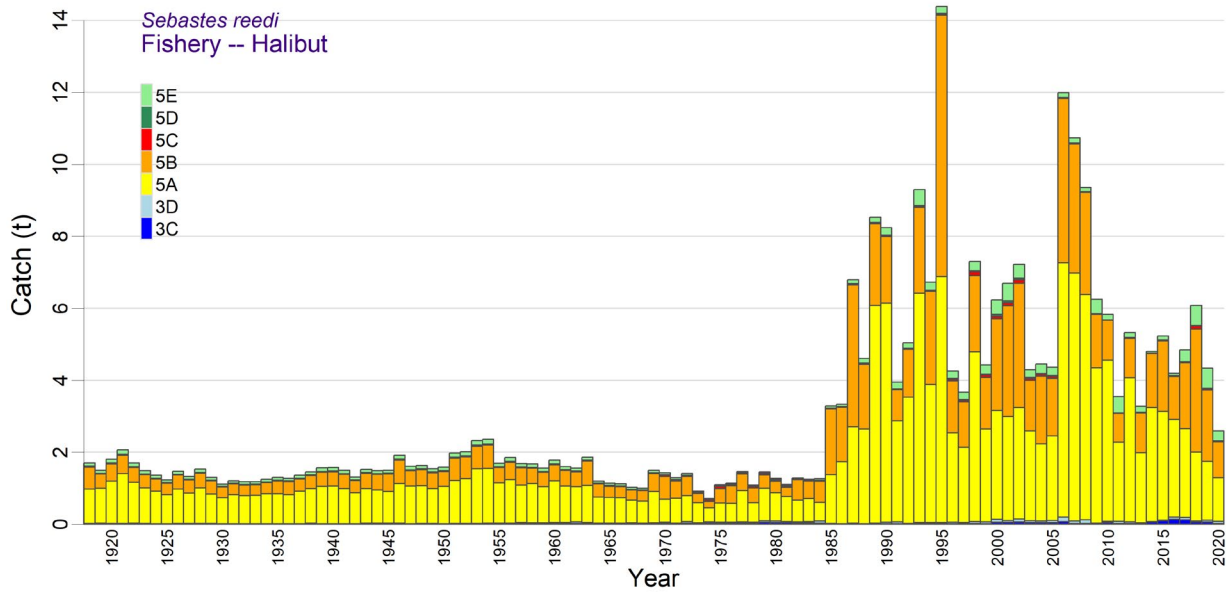

*Figure A.3. Reconstructed total (landed + released) catch (t) for YMR from the **halibut** fishery in PMFC major areas 3C to 5E.*

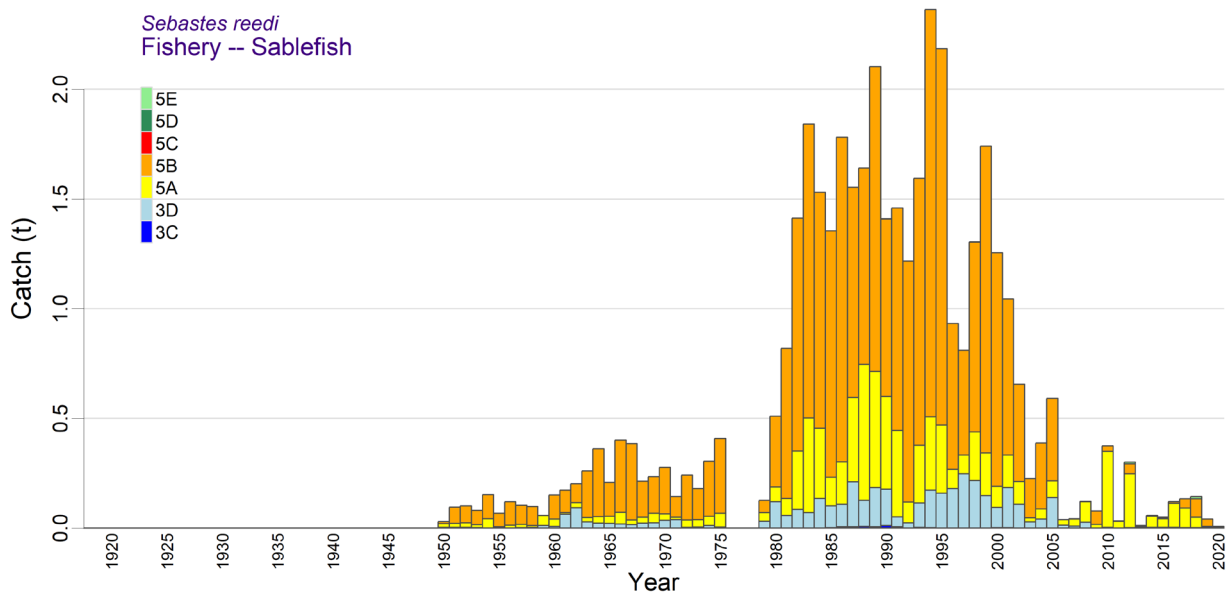

*Figure A.4. Reconstructed total (landed + released) catch (t) for YMR from the **sablefish** fishery in PMFC major areas 3C to 5E.*

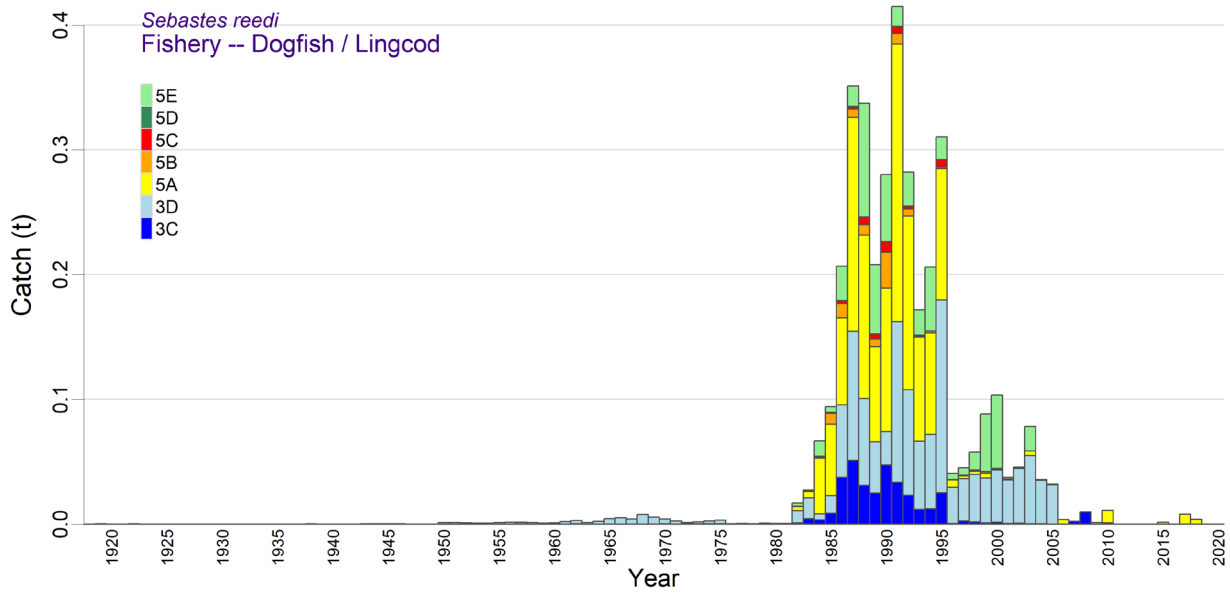

*Figure A.5. Reconstructed total (landed + released) catch (t) for YMR from the **dogfish/lingcod** fishery in PMFC major areas 3C to 5E.*

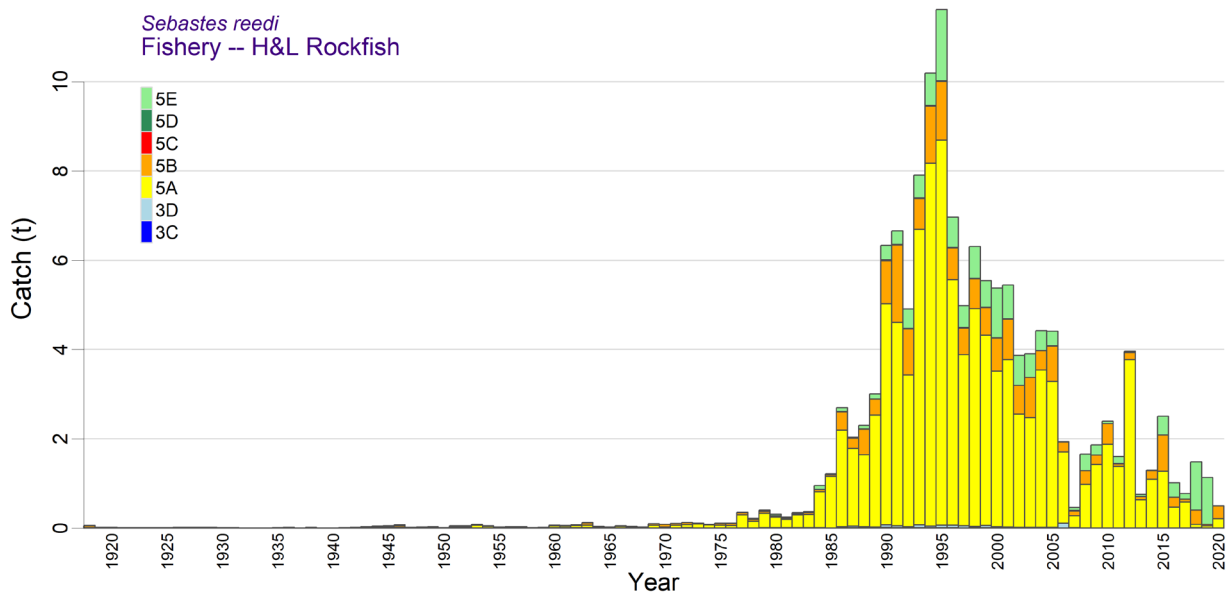

*Figure A.6. Reconstructed total (landed + released) catch (t) for YMR from the **hook and line rockfish** fishery in PMFC major areas 3C to 5E.*

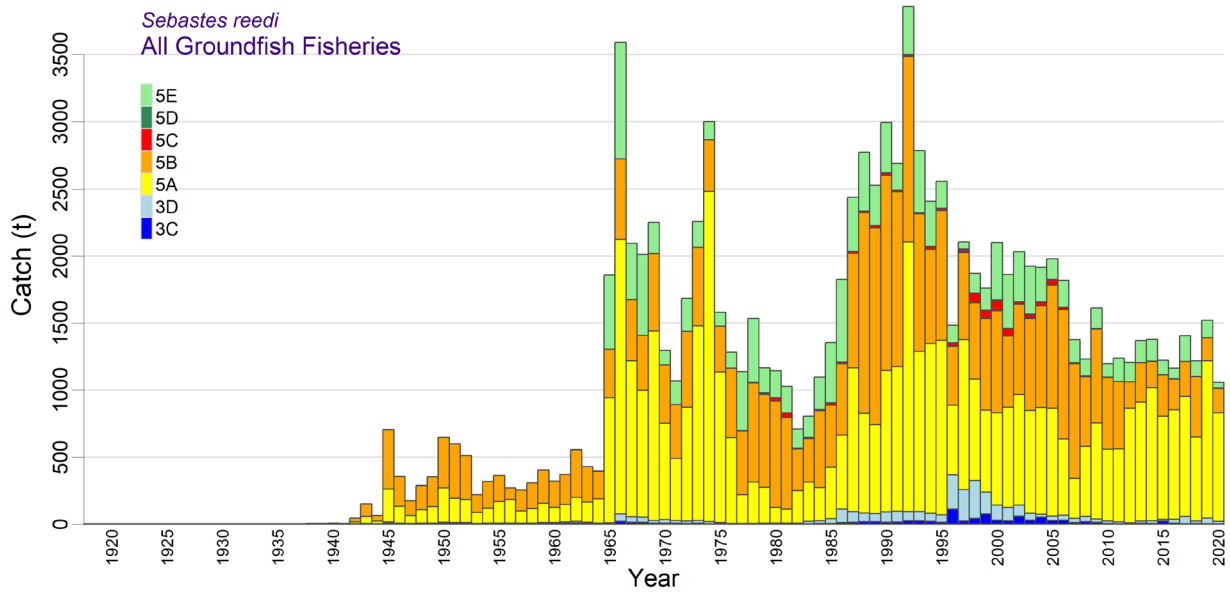

*Figure A.7. Reconstructed total (landed + released) catch (t) for YMR from the **combined** commercial groundfish fisheries in PMFC major areas 3C to 5E.*

Table A.4. Reconstructed catches (in tonnes, landings + releases) of YMR coastwide from trawl and non-trawl fisheries (Halibut, Sablefish, Dogfish/Lingcod, and H&L Rockfish). Shaded columns (with an asterisk) indicate catches used in the population model. Catch for 2021 is that reported for the end of June 2021; used same catch as 2020 (1057 t) for 2021 in model.

Year	Trawl	Other	*Coast	Year	Trawl	Other	*Coast	Year	Trawl	Other	*Coast
1918	0.759	1.76	2.52	1952	510	2.16	512	1987	2427	10.7	2438
1919	0.138	1.51	1.65	1953	217	2.48	220	1988	2764	8.88	2773
1920	0.154	1.82	1.97	1954	317	2.56	319	1989	2513	13.8	2527
1921	0.022	2.07	2.10	1955	360	1.78	362	1990	2979	16.2	2995
1922	0.039	1.71	1.75	1956	268	2.00	270	1991	2677	12.4	2689
1923	0.029	1.49	1.52	1957	252	1.82	254	1992	3848	11.4	3859
1924	0.047	1.36	1.41	1958	306	1.78	307	1993	2766	19.0	2785
1925	0.058	1.23	1.29	1959	401	1.62	403	1994	2388	19.5	2408
1926	0.128	1.48	1.61	1960	319	1.99	321	1995	2528	28.5	2556
1927	0.197	1.34	1.54	1961	369	1.83	371	1996	1471	12.2	1484
1928	0.147	1.54	1.69	1962	554	1.83	556	1997	2095	9.49	2104
1929	0.205	1.31	1.52	1963	427	2.25	429	1998	1855	14.9	1870
1930	0.110	1.12	1.23	1964	394	1.59	395	1999	1748	11.8	1760
1931	0.030	1.21	1.24	1965	1856	1.37	1858	2000	2086	13.0	2099
1932	0.033	1.18	1.21	1966	3591	1.57	3592	2001	1849	13.2	1862
1933	0.007	1.18	1.19	1967	2092	1.45	2093	2002	2018	11.8	2030
1934	0.164	1.25	1.42	1968	2010	1.24	2011	2003	1916	8.49	1924
1935	1.37	1.30	2.68	1969	2246	1.83	2248	2004	1905	9.30	1914
1936	1.82	1.29	3.11	1970	1293	1.79	1295	2005	1968	9.38	1978
1937	1.49	1.36	2.85	1971	1068	1.54	1069	2006	1804	14.0	1818
1938	2.26	1.46	3.73	1972	1682	1.78	1683	2007	1364	11.2	1375
1939	2.41	1.56	3.97	1973	2255	1.21	2256	2008	1219	11.1	1230
1940	5.45	1.57	7.02	1974	2999	1.10	3000	2009	1604	8.18	1612
1941	2.70	1.50	4.20	1975	1577	1.62	1578	2010	1187	8.60	1196
1942	43.8	1.32	45.1	1976	1281	1.25	1282	2011	1233	5.18	1238
1943	150	1.55	151	1977	1135	1.81	1137	2012	1196	9.59	1206
1944	61.7	1.52	63.2	1978	1534	1.30	1535	2013	1364	4.03	1368
1945	702	1.55	704	1979	1163	1.98	1165	2014	1373	6.16	1379
1946	353	1.98	355	1980	1141	2.10	1143	2015	1215	7.78	1223
1947	172	1.61	173	1981	1026	2.16	1028	2016	1157	5.33	1162
1948	286	1.65	288	1982	704	3.06	707	2017	1398	5.75	1404
1949	352	1.56	353	1983	802	3.49	805	2018	1209	7.71	1216
1950	645	1.62	646	1984	1091	3.82	1095	2019	1515	5.50	1521
1951	596	2.11	598	1985	1350	5.94	1356	2020	1054	3.09	1057
1952	510	2.16	512	1986	1817	8.02	1825	2021	293	4.93	298

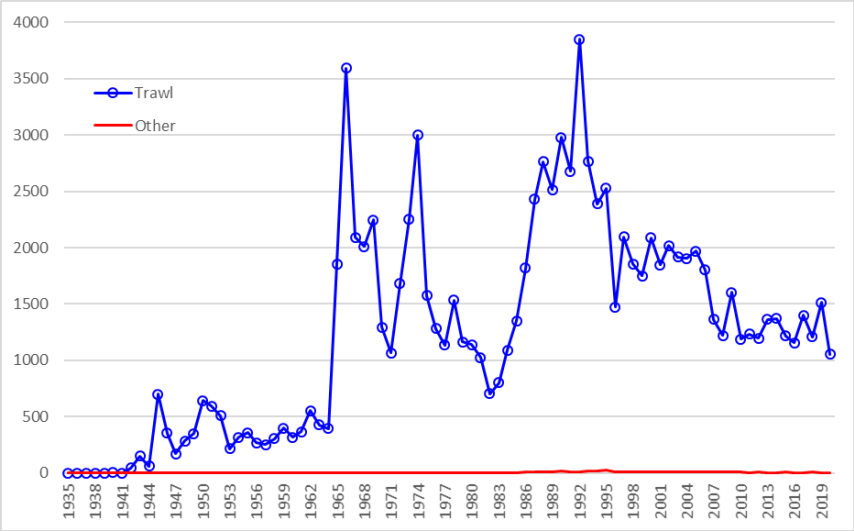

Figure A.8. Plots of catch by fishery for YMR from 1935 to 2020 used in the population model. Data values provided in Table A.4.

A.2.3. Changes to the reconstruction algorithm since 2011

A.2.3.1. Pacific Ocean Perch (2012)

In two previous stock assessments for POP in areas 3CD and 5DE (Edwards et al. 2014a,b), the authors documented two departures from the catch reconstruction algorithm introduced by Haigh and Yamanaka (2011). The first dropped the use of trawl and trap data from the sales slip database `PacHarv3` because catches were sometimes reported by large statistical areas that could not be clearly mapped to PMFC areas. In theory, `PacHarv3` should report the same catch as that in the `GFCatch` database (Rutherford 1999), but area inconsistencies cause catch inflation when certain large statistical areas cover multiple PMFC areas. Therefore, only the `GFCatch` database for the trawl and trap records from 1954 to 1995 were used, rather than trying to mesh `GFCatch` and `PacHarv3`. The point is somewhat moot as assessments since 2015 by the Offshore Rockfish Program use the merged-catch data table (Section A.2.1). Data for the H&L fisheries from `PacHarv3` are still used as these do not appear in other databases.

The second departure was the inclusion of an additional data source for BC rockfish catch by the Japanese fleet reported in Ketchen (1980a).

A.2.3.2. Yellowtail Rockfish (2014)

The Yellowtail Rockfish assessment (DFO 2015) selected offshore areas that reflected the activity of the foreign fleets' impact on this species to calculate `gamma` (RRF/ORF) and `delta` ratios (RRF/TAR). This option was not used in the YMR reconstruction.

A.2.3.3. Shortspine Thornyhead (2015)

The Shortspine Thornyhead assessment (Starr and Haigh 2017) was the first to use the merged catch table (`GF_MERGED_CATCH` in `GFFOS`). Previous assessments required the meshing together of caches from six separate databases: `GFBioSQL` (research, midwater joint-venture Hake, midwater foreign), `GFCatch` (trawl and trap), `GFFOS` (all fisheries), `PacHarvest` (trawl),

PacHarvHL (hook and line), and PacHarvSable (trap and longline). See Section A.2.1 for further details.

A.2.3.4. Yelloweye Rockfish Outside (2015)

The Yelloweye Rockfish (YYR) assessment (Yamanaka et al. 2018) introduced the concept of depth-stratified gamma and delta ratios; however, this functionality has not been used for offshore rockfish to date.

Also in the YYR assessment, rockfish catch from seamounts was removed (implemented in all subsequent reconstructions, including the YMR one), as well as an option to exclude rockfish catch from the foreign fleet and the experimental Langara Spit POP fishery (neither were excluded from the YMR reconstruction). The latter option is more likely appropriate for inshore rockfish species because they did not experience historical offshore foreign fleet activity or offshore experiments.

A.2.3.5. Redstripe Rockfish (2018)

The Redstripe Rockfish assessment (Starr and Haigh, 2021a), introduced the use of summarising annual gamma and delta ratios from reference years (Section A.2.2) by calculating the geometric mean across years instead of using the arithmetic mean. This choice reduces the influence of single anomalously large annual ratios. The geometric mean was used in the YMR reconstruction.

Also new in 2018 was the ability to estimate RRF (using gamma) for landings later than 1996, should the user have reason to replace observed landings with estimated ones. For YMR, observed landings by fishery were used starting in 1996 for the trawl fishery and 2006 for the non-trawl fisheries; prior to these years, landings were estimated using gamma.

Another feature introduced in 2018 was the ability to specify years by fishery for discard regimes, that is, when discard ratios were to be applied. Previously, these had been fixed to 1954-1995 for the trawl fishery and 1986-2005 for the non-trawl fisheries. For YMR, discard regimes by fishery were set to T = 1954-1995, H = 1918-2005, S/DL = 1950-2005, and ZN = 1986-2005. As previously, years before the discard period assume no discarding, and years after the discard period assume that discards have been reported in the databases.

A.2.3.6. Widow Rockfish (2019)

The Widow Rockfish (WWR) assessment (Starr and Haigh, 2021b) found a substantial amount of WWR reported as foreign catch in the database GFBioSQL that came from midwater gear off WCVI. Subsequently, the catch reconstruction algorithm was changed to assign GFBio foreign catch to four of the five fisheries based on gear type:

- bottom and midwater trawl gear assigned to the T fishery,
- longline gear assigned to the H fishery,
- trap and line-trap mix gear assigned to the S fishery, and
- h&l gear assigned to the ZN fishery.

The assignment only happens if the user chooses to use foreign catch in the reconstruction (see Section A.2.3.3). These foreign catches occurred well after the foreign fleet activity between 1965 and the implementation of an exclusive economic zone in 1977. YMR foreign catches in GFBio occurred primarily in 1987-1989 (43 t).

A.2.3.7. Bocaccio (2019)

The Bocaccio rockfish (BOR) assessment (Starr and Haigh, 2022) used advice from the technical working group, which identified specific reference years for the calculation of `gamma`: 1990-2000 for trawl (to capture the years before decreasing mortality caps for BOR were placed on the trawl fleet) and 2007-2011 for non-trawl (to capture years after some form of observer program like electronic monitoring was applied to the hook and line fleets). The catch reconstruction algorithm was previously coded to only allow one set of reference years to be applied across all fisheries. The algorithm was changed so that a user can now specify separate reference years for each fishery.

Once the merged catch table (`GF_MERGED_CATCH` in `GFFOS`) was introduced (Section A.2.3.3), catch from all databases other than `PacHarv3` have been reconciled so that caches are not double counted. In this assessment, the remaining two catch data sources (GFM and PH3, for brevity) were re-assessed by comparing ORF data, and the CR algorithm was changed in how the data sources were merged for the categories RRF landed, RRF discarded, ORF landed, POP landed, and TRF landed:

- GFM catch is the only source needed for FID 1 (Trawl fishery), as was previously assumed;
- GFM and PH3 catches appear to supplement each other for FIDs 2 (Halibut fishery), 3 (Sablefish fishery), and 4 (Dogfish/Lingcod fishery), and the catches were added in any given year up to 2005 (electronic monitoring started in 2006 and so the GFFOS database was reporting all catch for these fisheries by then);
- GFM and PH3 catches appear to be redundant for FID 5 (H&L Rockfish fishery), and so the maximum catch was used in any given year.

Also new in the BOR assessment was the introduction of historical Sablefish (SBF) and Lingcod (LIN) trawl landings from 1950 to 1975 (Ketchen 1976) for use in calculating historical discards for FIDs 3 and 4 during this period. These landings could not be used directly because they were taken by the trawl fleet; therefore, an estimation of SBF and LIN landed catch by FIDs 3 and 4, respectively, relative to SBF and LIN landed catch by FID 1 (trawl) was calculated from GFM. Annual ratios of SBF_3/SBF_1 and LIN_4/LIN_1 from 1996-2011 were chosen to calculate a geometric mean; the ratios from 2012 on started to diverge from those in the chosen period. The procedure yielded average ratios: $SBF_3/SBF_1 = 10.235$ and $LIN_4/LIN_1 = 0.351$, which were used to scale the 1950-75 trawl landings of SBF and LIN, respectively. From these estimated landings, discards of YMR were calculated by applying `delta` (see Section A.2.2.1).

Another departure was the re-allocation of PH3 records to the various catch reconstruction fisheries based on data from 1952-95. The distribution of effort (events) and catch by species for each gear type (Table A.5) led to the code revision in Table A.6.

Table A.5. PacHarv3 (PH3) number of events reportedly catching each species and catch (t) of species from 1952-95 by gear type and species code, where SCO = Scorpionfishes, POP = Pacific Ocean Perch, YTR = Yellowtail Rockfish, YMR =Yellowmouth Rockfish, YYR = Yelloweye Rockfish, SST = Shortspine Thornyhead, PAH = Pacific Halibut, SBF = Sablefish, DOG = Spiny Dogfish, and LIN = Lingcod.

EVENTS

Code	PH3 Gear Description	SCO	POP	YTR	YMR	YYR	SST	PAH	SBF	DOG	LIN
10	GILL NET, SALMON	55	-	-	-	17	-	-	-	-	164
11	NET, SET	-	-	-	-		-		-	1	-
20	SEINE, PURSE, SALMON	4	-	-	-	2	-	-	-	-	14
30	TROLL, SALMON	4281	49	69	1	2587	11	613	40	77	5201
31	TROLL, FREEZER, SALMON	614	1	14	2	294	2	91	8	31	1752
36	JIG, HAND, NON-SALMON	1126	25	241	13	914	4	1	1	152	845
40	LONGLINE	2893	109	355	100	2738	327	4484	603	1248	2377
50	TRAWL, OTTER, BOTTOM	3910	2419	2335	1521	557	1435	-	2469	748	3098
51	TRAWL, MIDWATER	770	155	770	175	21	26	-	51	210	173
57	SHRIMP TRAWL	173	10	2	-	21	-	-	2	12	82
70	SEINE, BEACH	4	-	-	-	-	-	-	-	-	2
90	TRAP	74		1	1	14	18		753	3	34

CATCH

Code	PH3 Gear Description	SCO	POP	YTR	YMR	YYR	SST	PAH	SBF	DOG	LIN
10	GILL NET, SALMON	3.6	-	-	-	1.0	-	-	-	-	16
11	NET, SET	-	-	-	-		-	-	-	2.5	-
20	SEINE, PURSE, SALMON	0.2	-	-	-	0.7	-	-	-	-	4.3
30	TROLL, SALMON	3060	1.3	5.6	0.0	925	2.0	538	20	70	5757
31	TROLL, FREEZER, SALMON	73	0.0	2.2	0.4	31	4.0	52	0.1	99	695
36	JIG, HAND, NON-SALMON	2133	5.2	40	4.6	745	0.1	0.3	1.1	175	1883
40	LONGLINE	6921	11	29	35	7922	91	48384	10785	21799	6119
50	TRAWL, OTTER, BOTTOM	117534	79327	28758	17609	1818	3468	-	6090	12637	45811
51	TRAWL, MIDWATER	17737	469	14867	735	3.3	7.7	-	7.9	1400	103
57	SHRIMP TRAWL	23	0.6	2.1	-	0.3	-	-	0.0	18	34
70	SEINE, BEACH	0.1	-	-	-	-	-	-	-	-	0.6
90	TRAP	76	-	0.0	0.6	3.6	6.4	-	50886	34	4.4

Table A.6. Code extract from Oracle SQL query 'ph3_fcatORF.sql' that defines catch reconstruction FIDs (1=Trawl, 2=Halibut, 3=Sablefish, 4=Dogfish/Lingcod, 5=H&L Rockfish) from gear types and dominant species caught (by weight) per event in PH3 table 'CATCH_SUMMARY'.

FID definition in SQL query 'ph3_fcatORF.sql'

```
(CASE  -- in order of priority
-- originally TRAWL (otter bottom, midwater, shrimp, herring)
WHEN TAR.GR_GEAR_CDE IN (50,51,57,59) THEN 1
-- Partition LONGLINE
WHEN TAR.GR_GEAR_CDE IN (40) AND TAR.Target IN ('614') THEN 2
WHEN TAR.GR_GEAR_CDE IN (40) AND TAR.Target IN ('455') THEN 3
WHEN TAR.GR_GEAR_CDE IN (40) AND TAR.Target IN ('044','467') THEN 4
WHEN TAR.GR_GEAR_CDE IN (40) AND TAR.Target NOT IN ('614','455','044','467')) THEN 5
-- Partition TROLL (salmon, freezer salmon)
WHEN TAR.GR_GEAR_CDE IN (30,31) AND TAR.Target IN ('614') THEN 2
WHEN TAR.GR_GEAR_CDE IN (30,31) AND TAR.Target IN ('455') THEN 3
WHEN TAR.GR_GEAR_CDE IN (30,31) AND TAR.Target IN ('044','467') THEN 4
WHEN TAR.GR_GEAR_CDE IN (30,31) AND TAR.Target  NOT IN ('614','455','044','467')) THEN 5
-- Partition JIG (hand non-salmon)
WHEN TAR.GR_GEAR_CDE IN (36) AND TAR.Target IN ('614') THEN 2
WHEN TAR.GR_GEAR_CDE IN (36) AND TAR.Target IN ('455') THEN 3
WHEN TAR.GR_GEAR_CDE IN (36) AND TAR.Target IN ('044','467') THEN 4
WHEN TAR.GR_GEAR_CDE IN (36) AND TAR.Target  NOT IN ('614','455','044','467')) THEN 5
-- originally TRAP (experimental, salmon, longline, shrimp & prawn, crab)
WHEN TAR.GR_GEAR_CDE IN (86,90,91,92,97,98) THEN 3
-- Unassigned Trawl, Halibut, Sablefish, Dogfish-Lingcod, H&L Rockfish
WHEN TAR.Target IN ('394','396','405','418','440','451') THEN 1
WHEN TAR.Target IN ('614') THEN 2
WHEN TAR.Target IN ('455') THEN 3
WHEN TAR.Target IN ('044','467') THEN 4
WHEN TAR.Target IN ('388','401','407','424','431','433','442') THEN 5
ELSE 0 END) AS \"fid\",
```

A.2.3.8. Rougheye/Blackspotted Rockfish (2020)

During the Rougheye/Blackspotted Rockfish (REBS) catch reconstruction, a close look at annual gammas revealed large fluctuations from 1991 to 2019 (Starr and Haigh 2022). Based on these findings, the reference years chosen to calculate a geometric mean gamma by fishery were: 1997:2005 for Trawl and 2007:2009 for non-trawl. These intervals were selected to reflect times of credible data: (i) reconciled observer logs with DMP landings in PacHarvest for the trawl fishery, and (ii) least volatility in GFFOS for the non-trawl fisheries.

A.2.3.9. Yellowmouth Rockfish (2021)

During the YMR catch reconstruction, the annual gammas only experienced moderate fluctuations from 1996 to 2019 (Figure A.9, Figure A.10). Based on these figures, the reference years chosen to calculate a geometric mean gamma by fishery were: 1996:2019 for Trawl (Figure A.9) and 1996:2019 for the non-trawl fisheries (Figure A.10). Normally, intervals are selected to reflect times of credible data (see Section A.2.3.8); however, all available years were chosen because no management changes had occurred for YMR since the inception of the Trawl observer program, and the other fisheries were largely irrelevant for this species.

Figure A.9. Annual gamma ratios (YMR/ORF) for the trawl commercial groundfish fishery (solid lines). Dotted lines trace the running geometric mean. Vertical dashed lines delimit 5-yr intervals.

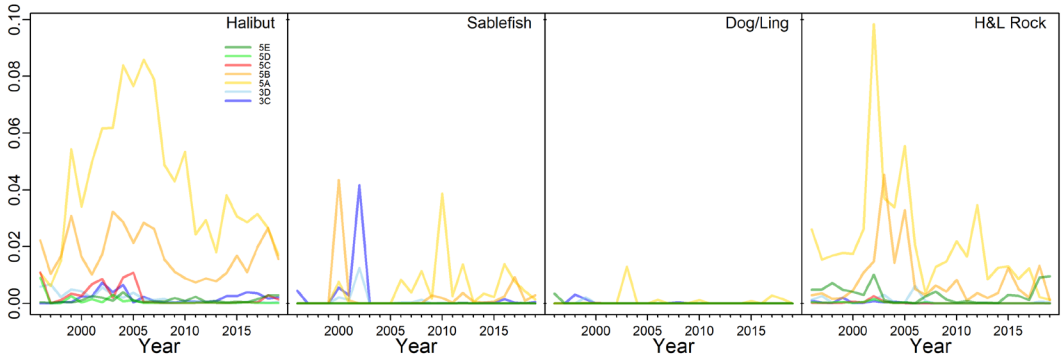

Figure A.10. Annual gamma ratios (YMR/ORF) for the four non-trawl commercial groundfish fisheries.

A.2.4. Caveats

The available catch data before 1996 (first year of onboard observer program) present difficulties for use in a stock assessment model without some form of interpretation, both in terms of misreporting (i.e., reporting catches of one species as another) or misidentifying species. There is also the possible existence of at-sea discarding due to catches exceeding what was permitted for retention. Although there were reports that fishermen misreported the location of catches, this issue is not a large problem for an assessment of a coastwide stock. Additionally, there was a significant foreign fishery for rockfish in BC waters, primarily by the United States, the Soviet Union and Japan from 1965 to 1976. These countries tended to report their catches in aggregate form, usually lumping rockfish into a single category. These fisheries ceased after the declaration of the 200 nm exclusive economic zone by Canada in 1977.

The accuracy and precision of reconstructed catch series inherently reflect the problems associated with the development of a commercial fishery:

- trips offloading catch with no area information,
- unreported discarding,
- recording catch of one species as another to avoid quota violations,
- developing expertise in monitoring systems,
- shifting regulations,
- changing data storage technologies, etc.

Many of these problems have been eliminated through the introduction of observer programs (onboard observers starting in 1996 for the offshore trawl fleet, electronic monitoring starting in 2006 for the H&L fleets), dockside [observer] monitoring, and tradeable individual vessel quotas (starting in 1997) that confer ownership of the resource to the fishing sector.

The catch reconstruction procedure does not rebuild catch by gear type (e.g., bottom trawl vs. midwater trawl, trap vs. longline). While adding this dimension is possible, it would mean splitting catches back in time using ratios observed in the modern fishery, which likely would not accurately represent historical activity by gear type (see Section A.2.2 for similar caveats regarding the use of modern catch ratios to reconstruct the catch of one species from a total rockfish catch). In this assessment, we combined the catches of YMR by bottom and midwater trawl because the biological data (Appendix D) by gear did not support two fleets in the population model and it was inconclusive whether there was a demonstrable difference in selectivity. Table A.7 and Figure A.11 show the reported coastwide catch (landings plus non-retained) by gear type. Note that the catch reconstruction allocates catch of RRF from unknown areas to PMFC areas proportionally by known catch in PMFC areas to reflect all potential removals of biomass from BC waters. Consequently, reported catches by area are often less than the reconstructed catches by area.

The catch for 2021 was incomplete and so we used the catch from 2020 (1057 t) for 2021. The 2020 catch was lower than the five-year average, which likely reflected the impact from the Covid19 disruptions (e.g., lockdowns) as well as changes in market demand. We consulted with Industry and were told that the estimate for the YMR catch in 2021 (of around 1000 t) was reasonable under the ongoing circumstances.

Table A.7. Reported catch (tonnes) by gear type, sector, and fishery for the BC YMR coastwide starting when trawl fleet activity was monitored by onboard observers. BT=bottom trawl, MW=midwater trawl, HL=hook and line, GFT=groundfish trawl, ZN=license for hook and line, RO=HL rockfish outside, H=halibut longline, S=sablefish trap, HS=halibut + sablefish, DL=dogfish/lingcod.

Year	Gear				Sector						Fishery				
	BT	MW	HL	Trap	GFT	ZN	RO	H	HS	S	T	H	S	DL	HL
1996	1342	70.2	11.0	--	1412	9.67	--	1.32	--	--	1412	1.32	--	--	9.67
1997	2000	72.0	4.92	--	2072	4.76	--	0.165	--	--	2072	0.165	--	--	4.76
1998	1813	37.4	9.59	--	1850	7.62	--	1.96	--	0.012	1850	1.96	0.012	--	7.62
1999	1659	87.0	8.35	--	1746	5.84	--	2.52	--	--	1746	2.52	--	--	5.84
2000	1878	201	10.1	--	2079	7.08	--	2.97	--	--	2079	2.97	--	--	7.08
2001	1696	149	11.9	--	1845	7.83	--	4.11	--	--	1845	4.11	--	--	7.83
2002	1812	203	25.0	--	2015	19.4	--	5.60	--	--	2015	5.60	--	--	19.4
2003	1761	150	19.3	--	1911	13.1	--	6.15	--	0.047	1911	6.15	0.047	0.040	13.1
2004	1796	95.7	18.1	--	1891	9.29	--	8.78	--	--	1891	8.78	--	--	9.29
2005	1822	136	23.5	--	1957	16.6	--	6.91	--	--	1957	6.91	--	--	16.6
2006	1618	162	13.4	--	1780	1.91	0.007	10.7	0.752	0.037	1780	11.4	0.037	0.004	1.92
2007	1154	197	10.2	--	1352	--	0.146	8.98	1.02	0.031	1352	10.0	0.031	0.002	0.146
2008	893	306	10.8	0.001	1198	--	1.65	8.01	1.04	0.110	1198	9.05	0.110	0.010	1.65
2009	1479	110	7.82	--	1589	--	1.83	4.31	1.59	0.075	1589	5.91	0.075	0.001	1.83
2010	1119	61.2	8.43	0.001	1180	--	2.38	4.27	1.40	0.374	1180	5.67	0.374	0.011	2.38
2011	1062	160	4.86	--	1222	--	1.56	2.28	1.00	0.022	1222	3.28	0.022	--	1.56
2012	754	432	8.89	0.104	1186	--	3.92	3.51	1.40	0.162	1186	4.91	0.162	--	3.92
2013	790	526	3.53	--	1316	--	0.681	1.40	1.45	0.008	1316	2.85	0.008	--	0.681
2014	652	716	6.00	--	1367	--	1.28	2.60	2.07	0.040	1367	4.68	0.040	--	1.28
2015	640	548	7.31	--	1188	--	2.50	2.17	2.62	0.015	1188	4.79	0.015	0.001	2.50
2016	797	353	4.86	--	1150	--	1.00	2.43	1.34	0.091	1150	3.77	0.091	--	1.00
2017	852	532	5.40	--	1384	--	0.769	1.97	2.54	0.111	1384	4.51	0.111	0.008	0.769
2018	850	349	7.29	--	1199	--	1.49	2.67	2.99	0.130	1199	5.67	0.130	0.004	1.49
2019	1110	395	5.23	--	1505	--	1.09	2.66	1.45	0.036	1505	4.11	0.036	--	1.09
2020	911	127	2.68	0.005	1037	--	0.494	1.28	0.908	--	1037	2.18	0.005	--	0.494

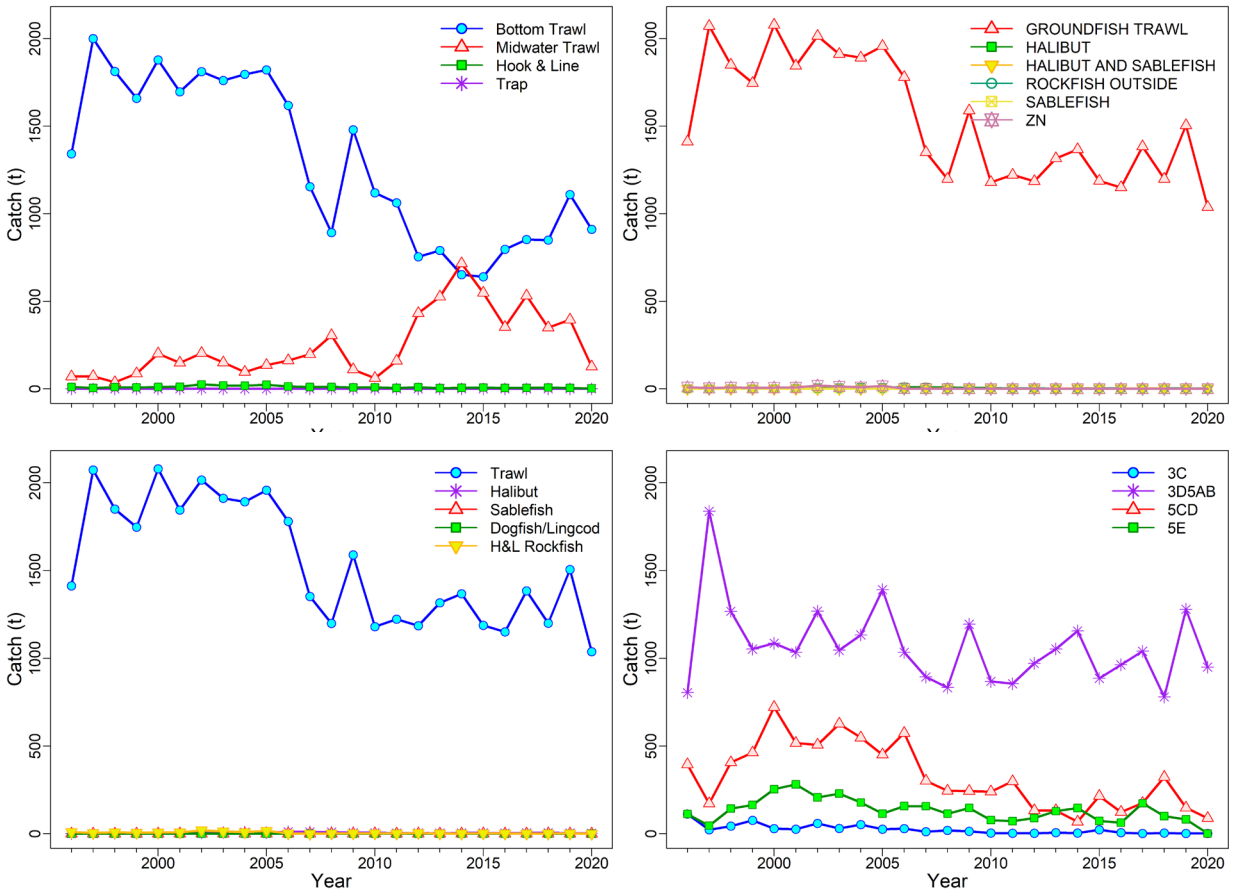

Figure A.11. Reported YMR catch (landings + released) by gear (top left), by sector (top right), by fishery (bottom left), and by groundfish management area (bottom right) since the implementation of the trawl fishery onboard-observer program in 1996.

A.3. SCALING CATCH POLICY TO GMU AREA TACS

The area definitions used by DFO Groundfish Science (PMFC areas) differ somewhat from those used by the DFO Groundfish Management (GMU), which uses Pacific Fishery Management Areas (PFMA). The reasons for these discrepancies vary depending on the species, but they occur to address different requirements by Science and Management. For Science, there is a need to reference historical catch using areas that are consistently reported across all years in the databases and catch records. The PMFC and GMU areas, while similar but not identical (Figure 1), address current management requirements.

As this assessment covers a coastwide stock, and GMU issues four area-specific TACs, a catch policy for the coastwide stock could be allocated to PMFC areas (adjusted for the 5C expansion) using the average 5-year proportional catch ratios in Table A.8. For example, a catch policy of 1000 tonnes/year of YMR would be allocated as follows:

- 3C = 2 t/y 0.0021 * 1000 t/y
- 3D5AB = 832 t/y (0.0252 + 0.7161 + 0.0905) * 1000 t/y
- 5CD = 132 t/y (0.1321 + 0.0001) * 1000 t/y
- 5E = 34 t/y0.0338 * 1000 t/y

Table A.8. Catch of YMR from the combined fishery in PMFC areas (adjusted for the 5C expansion specific to management of POP and YMR) from the last 5 years of complete catch statistics. Annual proportions of catch by area are shown in rows marked by year. Area-specific 5-year geometric means of annual proportions (normalised) are shown in the final row.

Catch(t)

Year	3C	3D	5A	5B	5C	5D	5E	BC
2016	6.277	30.150	813.375	118.968	123.253	0.009	63.142	1155.175
2017	1.777	54.461	891.231	94.344	174.537	0.001	173.328	1389.679
2018	3.264	18.039	623.204	138.420	323.316	0.000	100.202	1206.445
2019	1.817	43.094	1167.250	68.572	148.019	0.000	81.529	1510.281
2020	1.487	17.772	803.334	128.483	87.916	0.061	1.113	1040.166

Proportion

Year	3C	3D	5A	5B	5C	5D	5E	BC
2016	0.0054	0.0261	0.7041	0.1030	0.1067	0.0001	0.0547	1
2017	0.0013	0.0392	0.6413	0.0679	0.1256	0.0001	0.1247	1
2018	0.0027	0.0150	0.5166	0.1147	0.2680	0.0001	0.0831	1
2019	0.0012	0.0285	0.7729	0.0454	0.0980	0.0001	0.0540	1
2020	0.0014	0.0171	0.7723	0.1235	0.0845	0.0001	0.0011	1
GeoMean	0.0020	0.0237	0.6741	0.0852	0.1244	0.0001	0.0318	0.9414
Normalise	0.0021	0.0252	0.7161	0.0905	0.1321	0.0001	0.0338	1

A.4. REFERENCES – CATCH

Canada Dominion Bureau of Statistics. 1918-1950. Fisheries Statistics of Canada (British Columbia). Tech. rep., Canada Dominion Bureau of Statistics, Ottawa, ON.

DFO. 2015. Yellowtail Rockfish (*Sebastes Flavidus*) Stock Assessment for the Coast of British Columbia, Canada. DFO Can. Sci. Advis. Sec. Sci. Advis. Rep. 2015/010.

Edwards, A.M., Haigh, R., and Starr, P.J. 2014a. Pacific Ocean Perch (*Sebastes alutus*) stock assessment for the north and west coasts of Haida Gwaii, British Columbia. DFO Can. Sci. Advis. Sec. Res. Doc. 2013/092: vi + 126 p.

Edwards, A.M., Haigh, R., and Starr, P.J. 2014b. Pacific Ocean Perch (*Sebastes alutus*) stock assessment for the west coast of Vancouver Island, British Columbia. DFO Can. Sci. Advis. Sec. Res. Doc. 2013/093: vi + 135 p.

Forrester, C.R. 1969. Results of English Sole tagging in British Columbia waters. Bull. Pac. Mar. Fish. Comm. 7: 1-10.

Forrester, C.R., and Smith, J.E. 1972. The British Columbia groundfish fishery in 1971, some aspects of its investigation and related fisheries. Fish. Res. Board Can. Tech. Rep. 338: 67 p.

Gunderson, D.R., Westrheim, S.J., Demory, R.L., and Fraidenburg, M.E. 1977. The status of Pacific Ocean Perch (*Sebastes alutus*) stocks off British Columbia, Washington, and Oregon in 1974. Fish. Mar. Serv. Tech. Rep. 690: iv + 63 p.

Haigh, R., and Yamanaka, K.L. 2011. Catch history reconstruction for rockfish (*Sebastes* spp.) caught in British Columbia coastal waters. Can. Tech. Rep. Fish. Aquat. Sci. 2943: viii + 124 p.

Ketchen, K.S. 1976. Catch and effort statistics of the Canadian and United States trawl fisheries in waters adjacent to the British Columbia coast 1950-1975. Fisheries and Marine Service, Nanaimo, BC, Data Record 6.

Ketchen, K.S. 1980a. Assessment of groundfish stocks off the west coast of Canada (1979). Can. Data Rep. Fish. Aquat. Sci. 185: xvii + 213 p.

Ketchen, K.S. 1980b. Reconstruction of Pacific Ocean Perch (*Sebastes alutus*) stock history in Queen Charlotte sound. Part I. Estimation of foreign catches, 1965–1976. Can. Manuscr. Rep. Fish. Aquat. Sci. 1570: iv + 46 p.

Leaman, B.M., and Stanley, R.D. 1993. Experimental management programs for two rockfish stocks off British Columbia, Canada. In S. J. Smith, J. J. Hunt and D. Rivard, eds., Risk evaluation and biological reference points for fisheries management, p. 403-418. Canadian Special Publication of Fisheries and Aquatic Sciences 120.

Rutherford, K.L. 1999. A brief history of GFCatch (1954-1995), the groundfish catch and effort database at the Pacific Biological Station. Can. Tech. Rep. Fish. Aquat. Sci. 2299: v + 66 p.

Starr, P.J., and Haigh, R. 2017. Stock assessment of the coastwide population of Shortspine Thornyhead (*Sebastolobus alascanus*) in 2015 off the British Columbia coast. DFO Can. Sci. Advis. Sec. Res. Doc. 2017/015: ix + 174 p

Starr, P.J., and Haigh, R. 2021a. Redstripe Rockfish (*Sebastes proriger*) stock assessment for British Columbia in 2018. DFO Can. Sci. Advis. Sec. Res. Doc. 2021/014. vii + 340 p.

Starr, P.J. and Haigh, R. 2021b. Widow Rockfish (*Sebastes entomelas*) stock assessment for British Columbia in 2019. DFO Can. Sci. Advis. Sec. Res. Doc. 2021/039. viii + 238 p

Starr, P.J., and Haigh, R. 2022a. Bocaccio (*Sebastes paucispinis*) stock assessment for British Columbia in 2019, including guidance for rebuilding plans. DFO Can. Sci. Advis. Sec. Res. In press[a].

Starr, P.J., and Haigh, R. 2022b. Rougheye/Blackspotted Rockfish (*Sebastes aleutianus/ melanostictus*) stock assessment for British Columbia in 2020. DFO Can. Sci. Advis. Sec. Res. Doc. In press[b].

Wallace, S., Turris, B., Driscoll, J., Bodtker, K., Mose, B., and Munro, G. 2015. Canada's Pacific groundfish trawl habitat agreement: A global first in an ecosystem approach to bottom trawl impacts. Mar. Pol. 60: 240-248.

Westrheim, S.J., Gunderson, D.R., and Meehan, J.M. 1972. On the status of Pacific Ocean Perch (*Sebastes alutus*) stocks off British Columbia, Washington, and Oregon in 1970. Fish. Res. Board Can. Tech. Rep. 326: 48 p.

Yamanaka, K.L., McAllister, M.M., Etienne, M.P., Edwards, A.M., and Haigh, R. 2018. Assessment for the outside population of Yelloweye Rockfish (*Sebastes ruberrimus*) for British Columbia, Canada in 2014. DFO Can. Sci. Advis. Sec. Res. Doc. 2018/001: ix + 150 p.

APPENDIX B. TRAWL SURVEYS

B.1. INTRODUCTION

This appendix summarises the derivation of relative abundance indices for Yellowmouth Rockfish (YMR) from the following bottom trawl surveys:

- a set of historical surveys operated in the Goose Island Gully of Queen Charlotte Sound (Section B.3);
- Queen Charlotte Sound (QCS) synoptic survey (Section B.3);
- West coast Vancouver Island (WCVI) synoptic survey (Section B.5);
- West coast Haida Gwaii (WCHG) synoptic survey (Section B.6);

Only surveys used in the YMR stock assessment are presented in this appendix. The Hecate Strait multi-species survey and the WCVI shrimp and Queen Charlotte Sound shrimp surveys have been omitted because the presence of YMR in these surveys has been either sporadic or the coverage, either spatial or by depth, has been incomplete, rendering these surveys poor candidates to provide abundance series for this species. Rockfish stock assessments, beginning with Yellowtail Rockfish (DFO 2015 a,b), have explicitly omitted using the two shrimp surveys because of the truncated depth coverage, which ends at 160 m for the WCVI shrimp survey, and the constrained spatial coverage of the QC Sound shrimp survey as well as its truncated depth coverage, which ends at 231 m. For similar reasons, the early Goose Island Gully surveys used in other rockfish stock assessments (0.99 quantile of start depth=294 m), the Hecate Strait synoptic survey (0.99 quantile of start depth=287 m), and the first four index years of the NMFS Triennial survey (0.99 quantile of start depth=329 m) have also been dropped. The hook and line surveys were not considered because the mean positive sets per year were very low for this species (Anderson et al. 2019), indicating an expectation that these surveys will not provide reliable abundance indices.

B.2. ANALYTICAL METHODS

Catch and effort data for strata i in year y yield catch per unit effort (CPUE) values U_{yi}. Given a set of data $\{C_{yij}, E_{yij}\}$ for tows $j = 1,\ldots,n_{yi}$,

Eq. B.1 $$U_{yi} = \frac{1}{n_{yi}} \sum_{j=1}^{n_{yi}} \frac{C_{yij}}{E_{yij}},$$

where C_{yij} = catch (kg) in tow j, stratum i, year y;
E_{yij} = effort (h) in tow j, stratum i, year y;
n_{yi} = number of tows in stratum i, year y.

CPUE values U_{yi} convert to CPUE densities δ_{yi} (kg/km^2) using:

Eq. B.2 $$\delta_{yi} = \frac{1}{vw} U_{yi},$$

where v = average vessel speed (km/h);
w = average net width (km).

Alternatively, if vessel information exists for every tow, CPUE density can be expressed

Eq. B.3 $$\delta_{yi} = \frac{1}{n_{yi}} \sum_{j=1}^{n_{yi}} \frac{C_{yij}}{D_{yij} w_{yij}},$$

where C_{yij} = catch weight (kg) for tow j, stratum i, year y;

D_{yij} = distance travelled (km) for tow j, stratum i, year y;

w_{yij} = net opening (km) for tow j, stratum i, year y;

n_{yi} = number of tows in stratum i, year y.

The annual biomass estimate is then the sum of the product of CPUE densities and bottom areas across m strata:

Eq. B.4 $$B_y = \sum_{i=1}^{m} \delta_{yi} A_i = \sum_{i=1}^{m} B_{yi},$$

where δ_{yi} = mean CPUE density (kg/km^2) for stratum i, year y;

A_i = area (km^2) of stratum i;

B_{yi} = biomass (kg) for stratum i, year y;

m = number of strata.

The variance of the survey biomass estimate V_y (kg^2) follows:

Eq. B.5 $$V_y = \sum_{i=1}^{m} \frac{\sigma_{yi}^2 A_i^2}{n_{yi}} = \sum_{i=1}^{m} V_{yi},$$

where σ_{yi}^2 = variance of CPUE density (kg^2/km^4) for stratum i, year y;

V_{yi} = variance of the biomass estimate (kg^2) for stratum i, year y.

The coefficient of variation (CV) of the annual biomass estimate for year y is

Eq. B.6 $$CV_y = \frac{\sqrt{V_y}}{B_y}.$$

B.3. EARLY SURVEYS IN QUEEN CHARLOTTE SOUND GOOSE ISLAND GULLY (GIG)

B.3.1. Data selection

Tow-by-tow data from a series of historical trawl surveys were available for 12 years spanning the period from 1965 to 1995. The first two surveys, in 1965 and 1966, were wide-ranging, with the 1965 survey extending from near San Francisco to halfway up the Alaskan Panhandle (Westrheim 1966a, 1967b). The 1966 survey was only slightly less ambitious, ranging from the southern US-Canada border in Juan de Fuca Strait into the Alaskan Panhandle (Westrheim 1966b, 1967b). It was apparent that the design of these two early surveys was exploratory and that these surveys would not be comparable to the subsequent Queen Charlotte Sound (QCS) surveys which were much narrower in terms of area covered and which had a much higher

density of tows in the Goose Island Gully (GIG). This can be seen in the small number of tows used by the first two surveys in GIG (Table B.1). As a consequence, these surveys are not included in this series.

The 1967 ([left panel]: Figure B.1) and 1969 ([left panel]: Figure B.2) surveys (Westrheim 1967a, 1969; Westrheim et al. 1968) also performed tows on the west coast of Vancouver Island, the west coast of Haida Gwaii and SE Alaska, but both of these surveys had a reasonable number of tows in the GIG grounds (Table B.1). The 1971 survey ([left panel]: Figure B.3) was entirely confined to GIG (Harling et al. 1971) while the 1973 ([left panel]: Figure B.4), 1976 ([left panel]: Figure B.5) and 1977 ([left panel]: Figure B.6) surveys covered both Goose Island and Mitchell Gullies in QCS (Harling et al. 1973; Westrheim et al. 1976; Harling and Davenport 1977).

A 1979 survey (Nagtegaal and Farlinger 1980) was conducted by a commercial fishing vessel (*Southward Ho*, Table B.1), with the distribution of tows being very different from the preceding and succeeding surveys (plot not provided; see Figure C5 in Edwards et al. 2012). As well, the distribution of tows by depth was also different from the other surveys Table B.2.

These observations imply a substantially different survey design and consequently this survey was not included in the time series.

The 1984 survey was conducted by two vessels: the *G.B. Reed* and the *Eastward Ho* (Nagtegaal et al. 1986). Part of the design of this survey was to compare the catch rates of the two vessels (one was a commercial fishing vessel and the other a government research vessel – Greg Workman, DFO, pers. comm.), thus they both followed similar design specifications, including the configuration of the net. Unfortunately, the tows were not distributed similarly in all areas, with the *G.B. Reed* fishing mainly in the shallower portions of the GIG, while the *Eastward Ho* fished more in the deeper and seaward parts of the GIG ([left panel]: Figure B.7) although the two vessels fished more contiguously in Mitchell Gully (immediately to the north). When the depth-stratified catch rates for Pacific Ocean Perch (the main design species of the surveys) of the two vessels were compared within the GIG only (using a simple Analysis of Variance [ANOVA]), the *Eastward Ho* catch rates were significantly higher ($p=0.049$) than those observed for the *G.B. Reed*. However, the difference in catch rates was no longer significant when tows from Mitchell's Gully were added to the analysis ($p=0.12$). Given the lack of significance when the full suite of available tows was compared, along with the uneven spatial distribution of tows among vessels within the GIG (although the ANOVA was depth-stratified, it is possible that the depth categories were too coarse), the most parsimonious conclusion was that there was no detectable difference between the two vessels. Consequently, all the GIG tows from both vessels were pooled for this survey year.

The 1994 survey, also conducted by a commercial vessel (the *Ocean Selector*, Table B.2

was modified by the removal of 19 tows which were part of an acoustic experiment and therefore were not considered appropriate for biomass estimation (they were tows used to estimate species composition for ensonified schools). Although this survey was designed to emulate as closely as possible the previous *G.B. Reed* surveys in terms of tow location selection (same fixed tow locations, G. Workman, DFO, pers. comm.), the timing of this survey was about two to three months earlier than the previous surveys (starting in mid-June rather than August or September, Table B.3).

A 1995 survey, conducted by two commercial fishing vessels: the *Ocean Selector* and the *Frosti*

Table B.2, used a random stratified design with each vessel duplicating every tow (G. Workman, DFO, pers. comm.). This type of design was entirely different from the fixed station (based on Loran coordinates) used in the previous surveys. As well, the focus of this survey was on Pacific

Ocean Perch (POP), with tows optimised to capture this species. Given the difference in design (random stations rather than fixed locations), this survey was not used in the stock assessment.

Given that the only area that was consistently monitored by these surveys was the GIG grounds, tows lying between 50.9°N & 51.6°N latitude from the seven acceptable survey years, covering the period from 1967 to 1994, were used to index the YMR population (Table B.1).

Table B.1. Number of tows in GIG and in other areas (Other) by survey year and vessel conducting the survey for the 12 historical (1965 to 1995) surveys. Survey years in grey were not used in the assessment

Survey	GB Reed		Southward Ho		Eastward Ho		Ocean Selector			Frosti
Year	Other	GIG	Other	GIG	Other	GIG	Other	GIG	Other	GIG
1965	76	8	-	-	-	-	-	-	-	-
1966	49	15	-	-	-	-	-	-	-	-
1967	17	33	-	-	-	-	-	-	-	-
1969	3	32	-	-	-	-	-	-	-	-
1971	3	36	-	-	-	-	-	-	-	-
1973	13	33	-	-	-	-	-	-	-	-
1976	23	33	-	-	-	-	--	-	-	-
1977	15	47	-	-	-	-		-	-	-
1979			20	59						
1984	19	42	-	-	15	27	-	-	-	-
1994	-	-	-	-	-	-	2	69	-	-
1995	-	-	-	-	-	-	2	55	1	57

Table B.2. Total number of tows by 20 fathom depth interval (in metres) in GIG and in other areas (Other) by survey year for the 12 historical (1965 to 1995) surveys. Survey years in grey were not used in the assessment. Some of the tows in the GIG portion of the table have usability codes other than 0,1,2, or 6.

Areas other than GIG

Survey year	20 fathom depth interval (m)									Total Tows
	66-146	147-183	184-219	220-256	257-292	293-329	330-366	367-402	440-549	
1965	3	15	26	17	6	6	1	1	1	76
1966	3	11	18	8	2	1	3	2	1	49
1967	1	-	6	1	2	1	1	4	-	16
1969	-	1	-	1	-	1	-	-	-	3
1971	-	-	-		-	-	-	-	-	
1973	-	-	4	3	2	2	2	-	-	13
1976	-	-	4	4	4	4	4	-	-	20
1977	-	-	3	2	2	3	2	-	-	12
1979	11	2	1	5	1	-		-	-	20
1984	-	-	4	10	7	7	6	-	-	34
1994	-	-	-	-	-	-	-	-	-	-
1995	-	-	-	-	-	-	-	-	-	-

GIG

Survey year	20 fathom depth interval (m)									Total Tows
	66-146	147-183	184-219	220-256	257-292	293-329	330-366	367-402	440-549	
1965	-	2	4	1	1	-	-	-	-	8
1966	3	2	3	5	2	-	-	-	-	15
1967	1	6	11	6	10	-	-	-	-	34
1969	-	9	11	6	6	-	-	-	-	32
1971	-	5	15	9	10	-	-	-	-	39
1973	-	7	11	7	8	-	-	-	-	33
1976	-	7	15	8	6	-	-	-	-	36
1977	1	12	14	14	9	-	-	-	-	50
1979	23	12	18	6	-	-	-	-	-	59
1984	-	13	25	17	13	1	-	-	-	69
1994	-	15	18	20	18	-	-	-	-	71
1995	2	23	47	22	15	6	-	-	-	115

The original depth stratification of these surveys was in 20 fathom (36.1 m) intervals, ranging from 36 fathoms (66 m) to 300 fathoms (549 m). These depth strata were combined for analysis into three ranges which encompassed most rockfish: 120–183 m, 184–218 m and 219–300 m, for a total of 332 tows from the eight accepted survey years (Table B.3).

Table B.3. Number of tows available by survey year and depth stratum for the analysis of the historical GIG trawl survey series. Survey year in grey was not used in the YMR stock assessment.

Survey Year	Depth stratum			Total	Start Date	End Date
	120-183 m (70–100 fm)	184-218 m (100–120 fm)	219-300 m (120–160 fm)			
1967	7	11	15	33	07-Sep-67	03-Oct-67
1969	8	11	12	31	14-Sep-69	24-Sep-69
1971	4	15	17	36	14-Oct-71	28-Oct-71
1973	7	11	15	33	07-Sep-73	24-Sep-73
1976	7	13	13	33	09-Sep-76	26-Sep-76
1977	13	14	20	47	24-Aug-77	07-Sep-77
1984	13	23	33	69	05-Aug-84	08-Sep-84
1994	10	16	24	50	21-Jun-94	06-Jul-94
1995	22	45	45	112	11-Sep-95	22-Sep-95

A doorspread density (Eq. B.3) was calculated for each tow based on the catch of YMR, using a fixed doorspread value of 61.6 m (Yamanaka et al. 1996) for every tow and the recorded distance travelled. Unfortunately, the speed, effort and distance travelled fields were not well

populated for these surveys. Therefore, missing values for these fields were filled in with the mean values for the survey year. This resulted in the majority of the tows having distances towed near 3 km, which was the expected result given the design specification of ½ hour tows at an approximate speed of 6 km/h (about 3.2 knots).

B.3.2. Results

Maps showing the locations where YMR were caught in the Goose Island Gully (GIG) indicate that this species is found throughout the gully, although in small amounts, in every year as well as extending into the south-eastern branch of the gully (see Figure B.1 to Figure B.8). YMR was taken relatively frequently, but in small amounts, with 193 of the 444 (including 1995; 43%) valid tows capturing YMR with a median catch weight of 9.5 kg. The largest valid YMR tow in terms of catch weight was 1,587 kg in 1976. YMR were mainly taken at depths from 154 to 275 m (5% and 95% quantiles of the starting depth empirical distribution), with the minimum and maximum observed YMR catch weights at starting tow depths of 150 and 299 m respectively (Figure B.9).

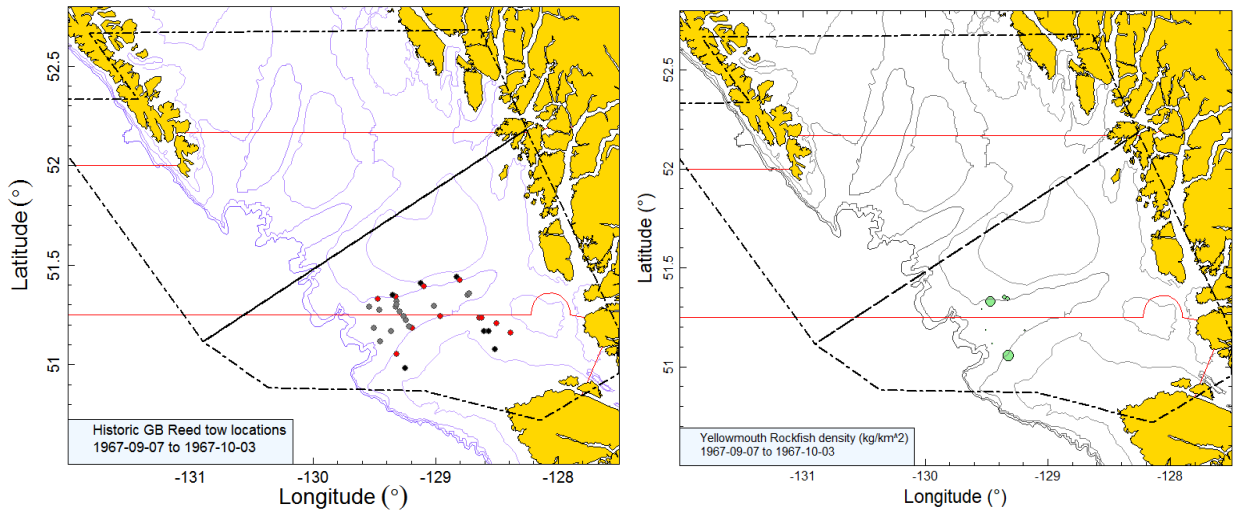

Figure B.1. Valid tow locations and density plots for the historic 1967 Goose Island Gully (GIG) survey. Tow locations are colour-coded by depth range: black=120–183m; red=184-218m; grey=219-300m. Circle sizes in the right-hand density plot scaled across all years (1967, 1969, 1971, 1973, 1976, 1977, 1984, and 1994), with the largest circle = 8,112 kg/km^2 in 1971. Black boundary lines show the extent of the modern Queen Charlotte Sound synoptic survey and the red solid lines indicate the boundaries between PMFC areas 5A, 5B and 5C.

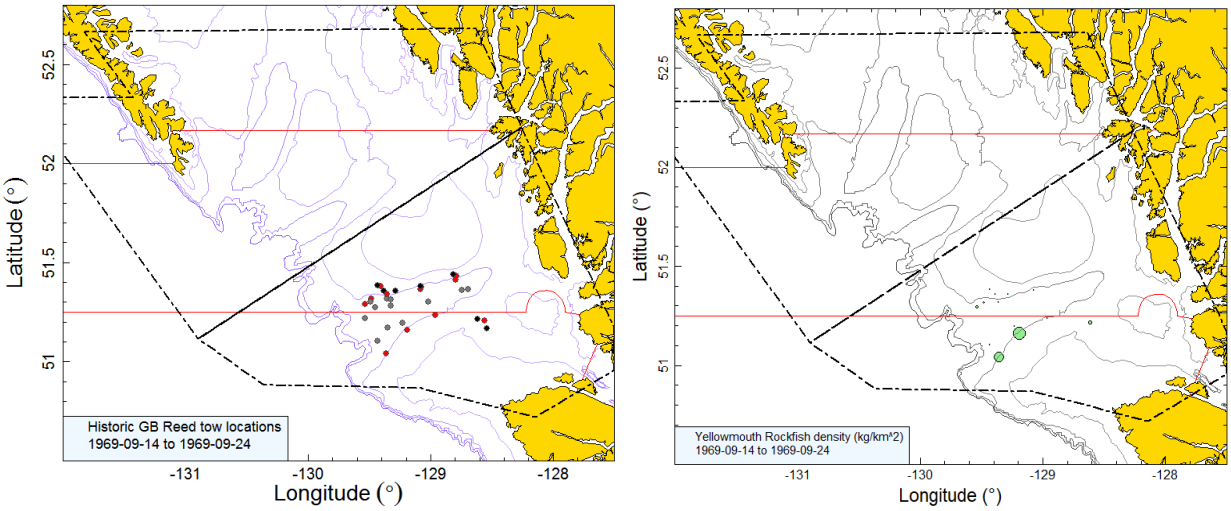

Figure B.2. Tow locations and density plots for the historic 1969 Goose Island Gully (GIG) survey (see Figure B.1 caption).

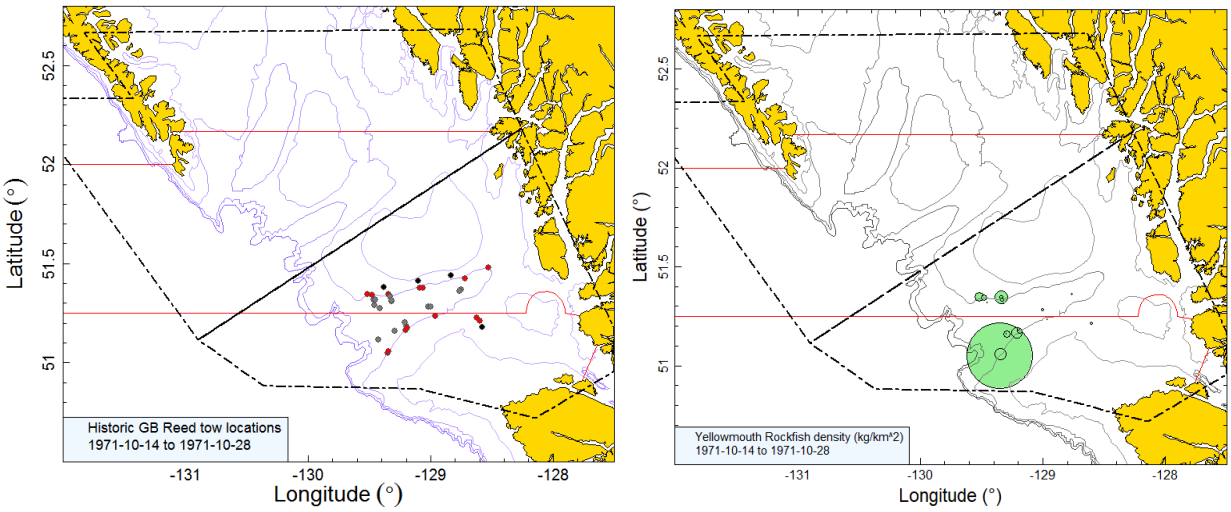

Figure B.3. Tow locations and density plots for the historic 1971 Goose Island Gully (GIG) survey (see Figure B.1 caption).

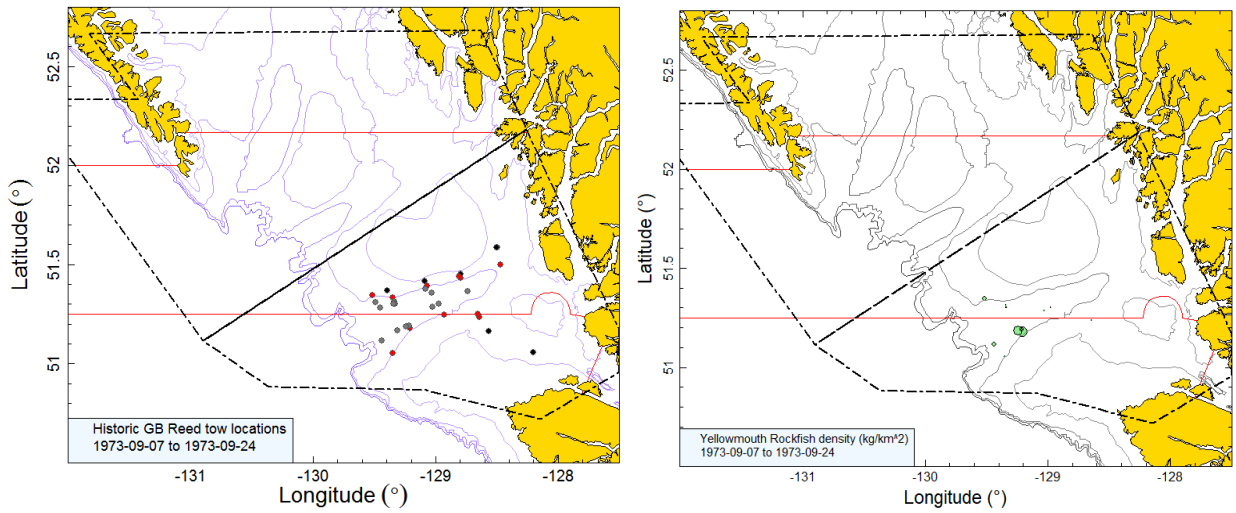

Figure B.4. Tow locations and density plots for the historic 1973 Goose Island Gully (GIG) survey (see Figure B.1 caption).

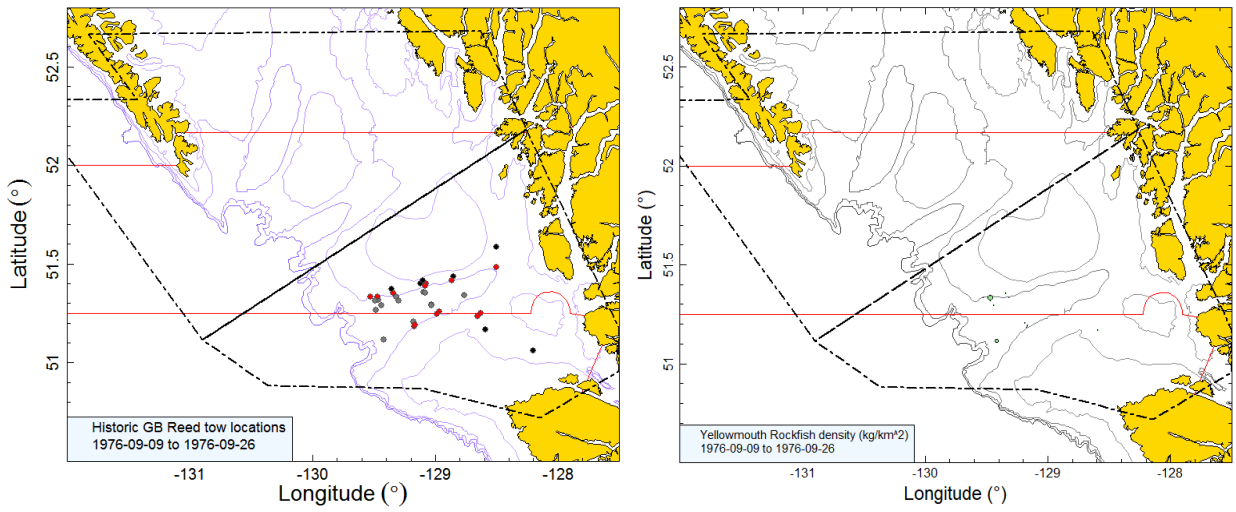

Figure B.5. Tow locations and density plots for the historic 1976 Goose Island Gully (GIG) survey (see Figure B.1 caption).

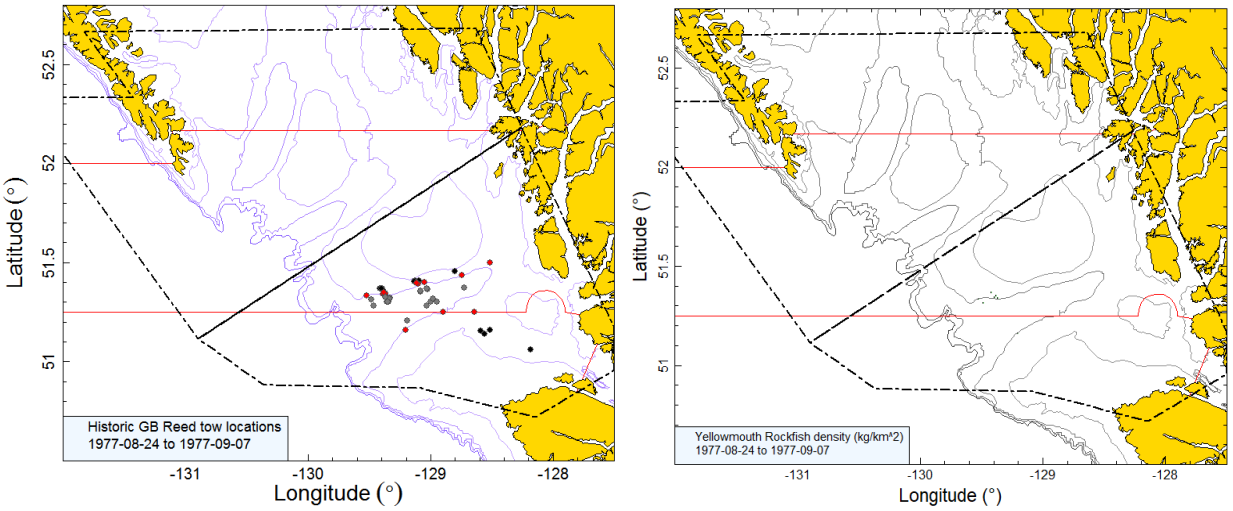

Figure B.6. Tow locations and density plots for the historic 1977 Goose Island Gully (GIG) survey (see Figure B.1 caption).

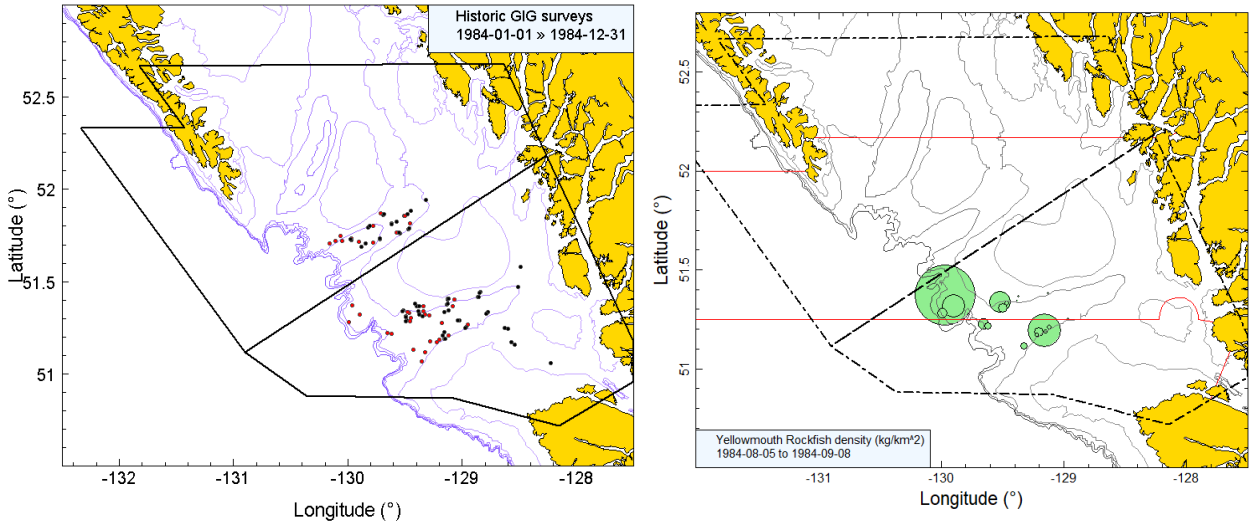

Figure B.7. [left panel]: Tow location colours indicate the vessel fishing rather than depth: black=G.B. Reed; red=Eastward Ho. Additional locations fished by vessel in Mitchell Gully are also shown; [right panel]: density plot for the historic 1984 Goose Island Gully (GIG) survey (see Figure B.1 caption).

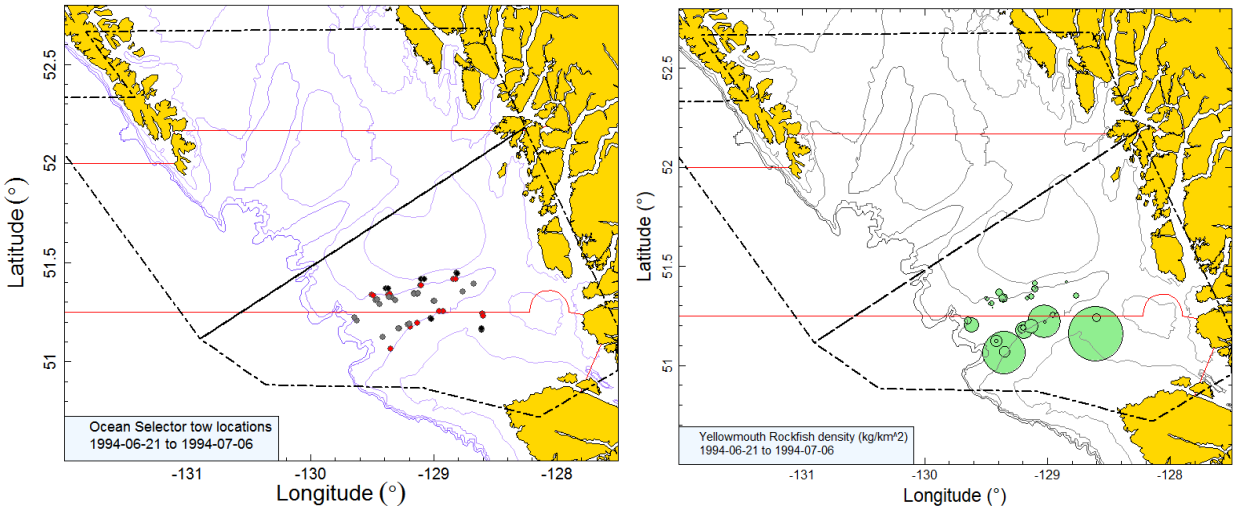

Figure B.8. Tow locations and density plots for the Ocean Selector 1994 Goose Island Gully (GIG) survey (see Figure B.1 caption).

Estimated biomass levels in the GIG for Yellowmouth Rockfish from the historical GIG trawl surveys were variable, with the maximum biomass recorded in 1994 (at 2,624 t) and the minimum biomass in 1977 (at 27 t) (Figure B.10; Table B.4). Survey relative errors were very variable for this species, ranging from a low of 0.16 in 1967 to 0.63 in 1976 (Table B.4). The proportion of tows which caught YMR tended to be higher than the later synoptic surveys and a more variable between years, ranging between 17% in 1977 and 66% in 1994 (Figure B.11). Overall, 123 tows from a total 332 valid tows (37%) contained YMR.

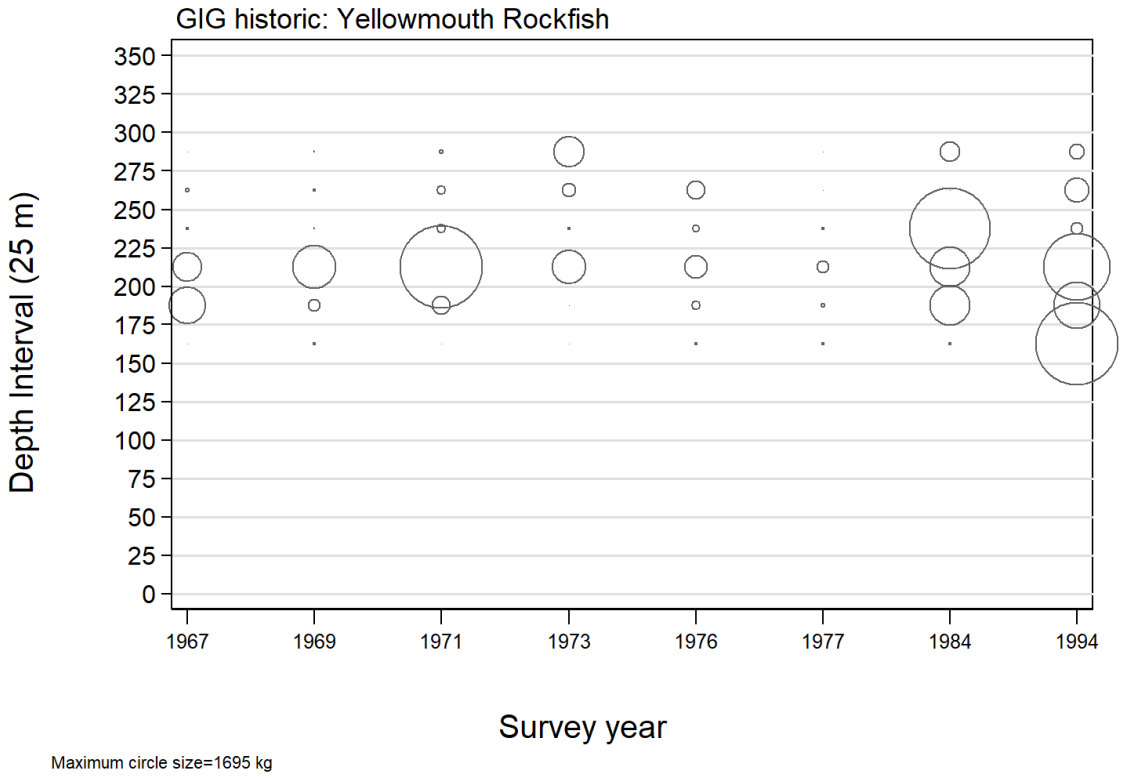

Figure B.9. Distribution of observed catch weights of Yellowmouth Rockfish (YMR) for the historic Goose Island Gully (GIG) surveys (Table B.3) by survey year and 25 m depth zone. Depth zones are indicated by the mid point of the depth interval and circles in the panel are scaled to the maximum value (1695 kg) in the 150–175 m interval in 1994. The 1% and 99% quantiles for the YMR empirical start of tow depth distribution= 154 m and 287 m respectively.

Table B.4. Biomass estimates for Yellowmouth Rockfish from the historical Goose Island Gully trawl surveys for the years 1967 to 1994. Biomass estimates are based on three depth strata (Table B.3), assuming that the survey tows were randomly selected within these areas. Bootstrap bias corrected confidence intervals and CVs are based on 1000 random draws with replacement.

Survey Year	**Biomass (t)** (Eq. B.4)	**Mean bootstrap biomass (t)**	**Lower bound biomass (t)**	**Upper bound biomass (t)**	**Bootstrap CV**	**Analytic CV** (Eq. B.6)
1967	397.8	394.4	64.4	862.4	0.497	0.504
1969	359.9	359.9	50.2	813.1	0.543	0.546
1971	765.8	760.5	78.4	2,249.2	0.805	0.839
1973	371.7	370.8	87.3	833.3	0.510	0.507
1976	157.1	155.5	35.0	362.6	0.516	0.520
1977	27.2	27.2	4.4	68.9	0.615	0.625
1984	686.6	703.7	136.1	1,757.3	0.575	0.606
1994	2,623.7	2,583.0	544.2	6,719.9	0.575	0.574

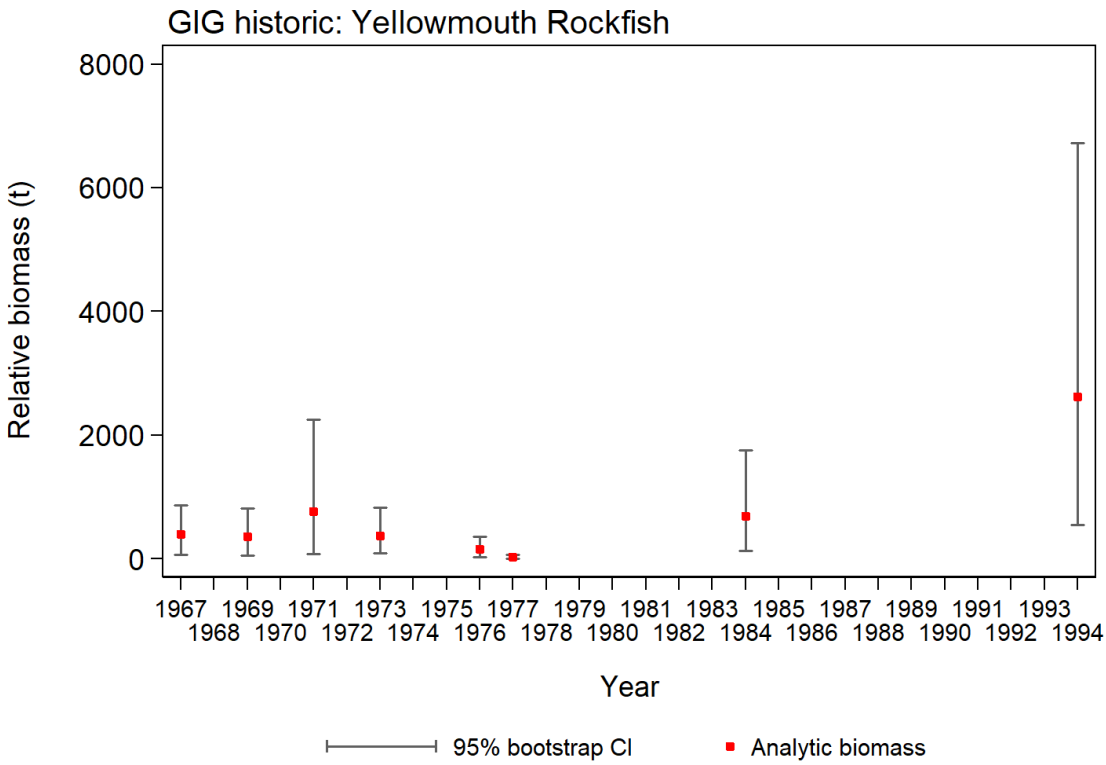

Figure B.10. Plot of biomass estimates for the YMR historic Goose Island Gully (GIG) surveys: 1967 to 1994 (values provided in Table B.4). Bias corrected 95% confidence intervals from 1000 bootstrap replicates are plotted.

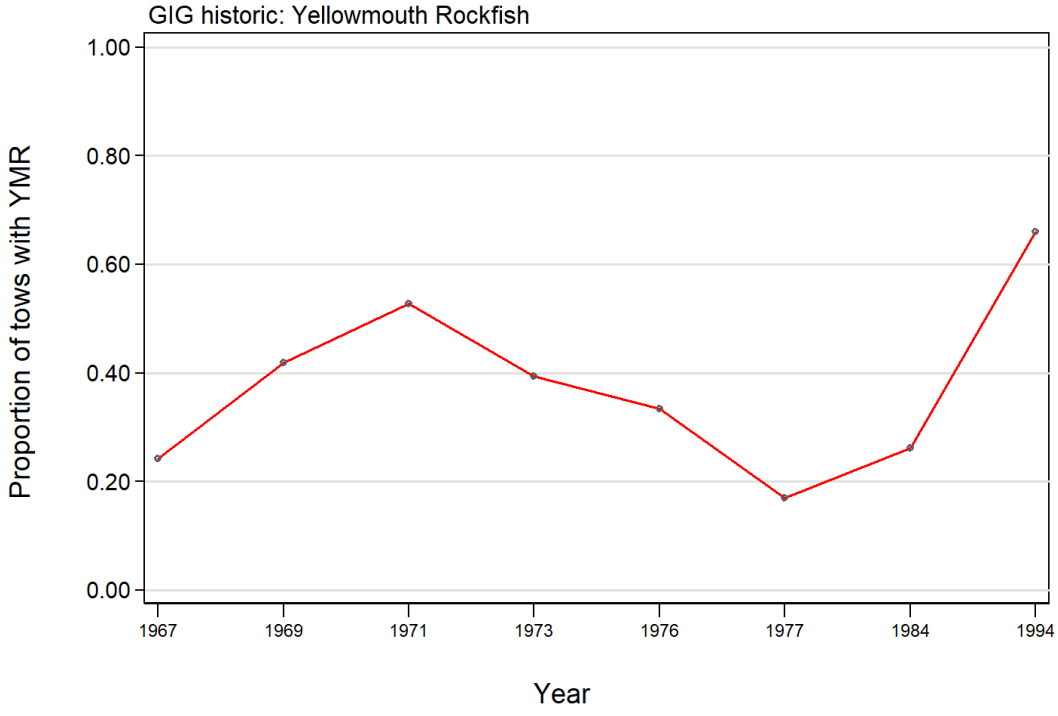

Figure B.11. Proportion of tows by year which contain YMR from the historic Goose Island Gully (GIG) surveys: 1967 to 1994.

B.4. QUEEN CHARLOTTE SOUND SYNOPTIC TRAWL SURVEY

B.4.1. Data selection

This survey has been conducted ten times over the period 2003 to 2019 in the Queen Charlotte Sound (QCS), which lies between the top of Vancouver Island and the southern portion of Moresby Island and extends into the lower part of Hecate Strait between Moresby Island and the mainland. The design divided the survey into two large areal strata which roughly correspond to the PMFC regions 5A and 5B while also incorporating part of 5C (all valid tow starting positions are shown by survey year in Figure B.12 to Figure B.21). Each of these two areal strata was divided into four depth strata: 50–125 m; 125–200 m; 200–330 m; and 330–500 m (Table B.5).

Table B.5. Number of usable tows for biomass estimation by year and depth stratum for the Queen Charlotte Sound synoptic survey over the period 2003 to 2019. Also shown is the area of each stratum for the 2019 survey and the vessel conducting the survey by survey year.

Year	Vessel	South depth strata				North depth strata				Total tows[1]
		50-125	125-200	200-330	330-500	50-125	125-200	200-330	330-500	
2003	*Viking Storm*	29	56	29	6	5	38	46	19	228
2004	*Viking Storm*	42	48	30	8	20	38	37	6	229
2005	*Viking Storm*	29	60	28	8	8	43	37	8	221
2007	*Viking Storm*	33	61	24	7	19	56	48	7	255
2009	*Viking Storm*	34	60	27	8	10	43	42	6	230
2011	*Nordic Pearl*	38	67	23	8	10	51	43	8	248
2013	*Nordic Pearl*	32	65	29	10	9	45	41	5	236
2015	*Frosti*	30	65	26	4	12	49	44	8	238
2017	*Nordic Pearl*	36	57	28	8	12	51	40	7	239
2019	*Nordic Pearl*	35	62	26	9	15	52	35	8	242
Area (km^2)[2]		5,012	5,300	2,640	528	1,740	3,928	3,664	1,236	24,048[2]

[1] GFBio usability codes=0,1,2,6 [2] Total area (km^2) for 2019 synoptic survey

Table B.6. Number of missing doorspread values by year for the Queen Charlotte Sound synoptic survey over the period 2003 to 2019 as well as showing the number of available doorspread observations and the mean doorspread value for each survey year.

Year	Number tows with missing doorspread [1]	Number tows with doorspread observations [2]	Mean doorspread (m) used for tows with missing values [2]
2003	13	236	72.1
2004	8	267	72.8
2005	1	258	74.5
2007	5	262	71.8
2009	2	248	71.3
2011	30	242	67.0
2013	42	226	69.5
2015	0	249	70.5
2017	1	264	64.7
2019	8	264	62.9
Total	110	2,516	69.7

[1] valid biomass estimation tows only [2] includes tows not used for biomass estimation

A doorspread density value (Eq. B.3) was generated for each tow based on the catch of YMR (YMR) from the mean doorspread for the tow and the distance travelled. [`distance travelled`] is a database field which is calculated directly from the tow track. This field is used preferentially for the variable D_{yij} in Eq. B.3. A calculated value ([`vessel speed`] X [`tow duration`]) is used for this variable if [`distance travelled`] is missing, but there were only two instances of this occurring in the ten trawl surveys. Missing values for the [`doorspread`] field were filled in with the mean doorspread for the survey year (110 values over all years, Table B.6).

B.4.2. Results

An examination of the spatial plots provided from Figure B.12 to Figure B.21 shows that most YMR were caught along the western shelf edge along the drop-off to deeper water. In some years, small amounts of YMR were captured to the east of the shelf edge in several of the central gullies (e.g., Figure B.16). YMR were found in moderate to deep tows, with the 1% to 99% quantiles ranging from 97 m to 312 m (Figure B.22). The YMR biomass estimates ranged from 990 to 6,300 t, although the two years with high biomass (2017 and 2019) are also associated with high relative error (0.46 and 0.71 respectively) in the series (Table B.7, Figure B.23). Both of these survey years were associated with the some very large tows, which result in high levels of relative error. All estimates of relative error are very high, ranging from 0.31 in 2007 to 0.71 in 2019 (Table B.7).

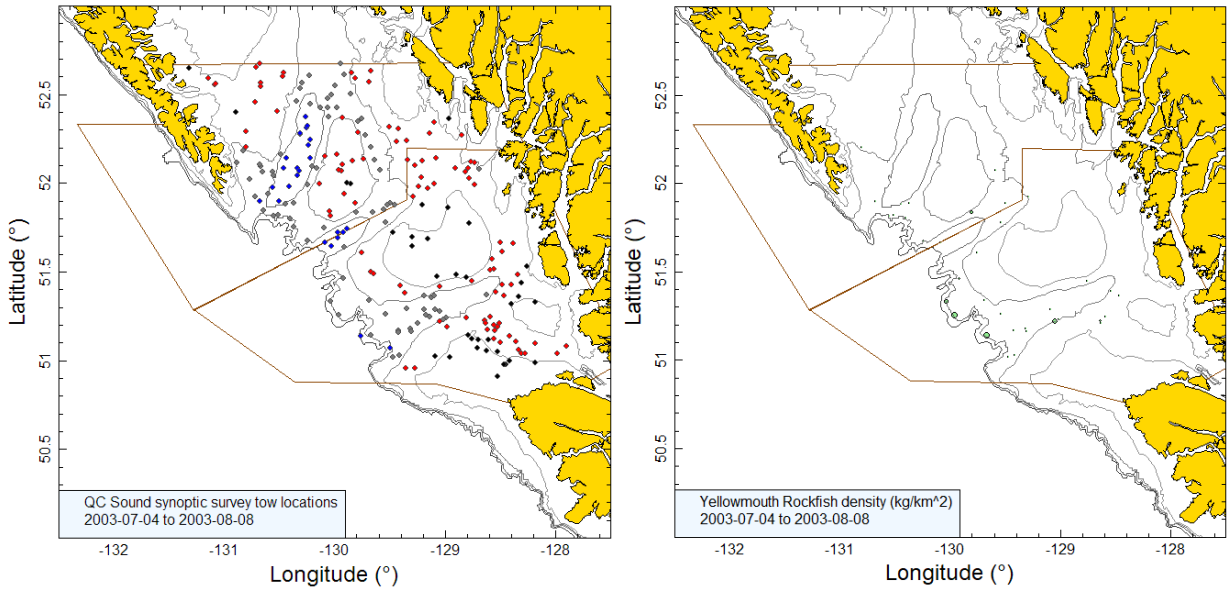

Figure B.12. Valid tow locations (50-125m stratum: black; 126-200m stratum: red; 201-330m stratum: grey; 331-500m stratum: blue) and density plots for the 2003 QC Sound synoptic survey. Circle sizes in the right-hand density plot scaled across all years (2003–2005, 2007, 2009, 2011, 2013, 2015, 2017, 2019), with the largest circle = 37,379 kg/km^2 in 2019. Boundaries delineate the North and South areal strata.

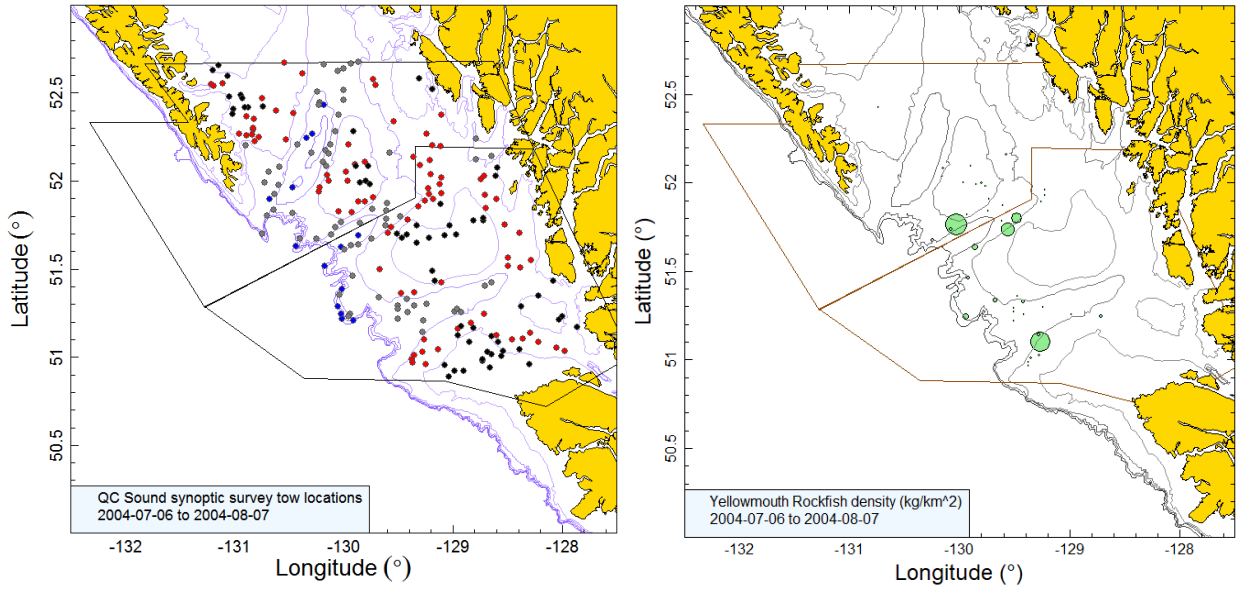

Figure B.13. Tow locations and density plots for the 2004 Queen Charlotte Sound synoptic survey (see Figure B.12 caption).

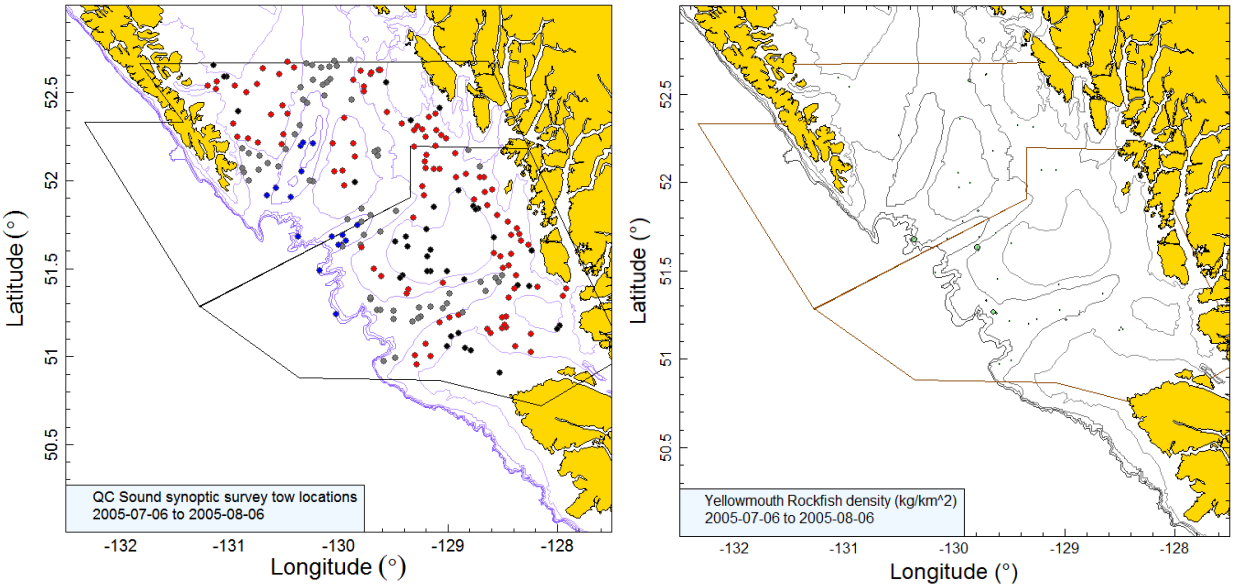

Figure B.14. Tow locations and density plots for the 2005 Queen Charlotte Sound synoptic survey (see Figure B.12 caption).

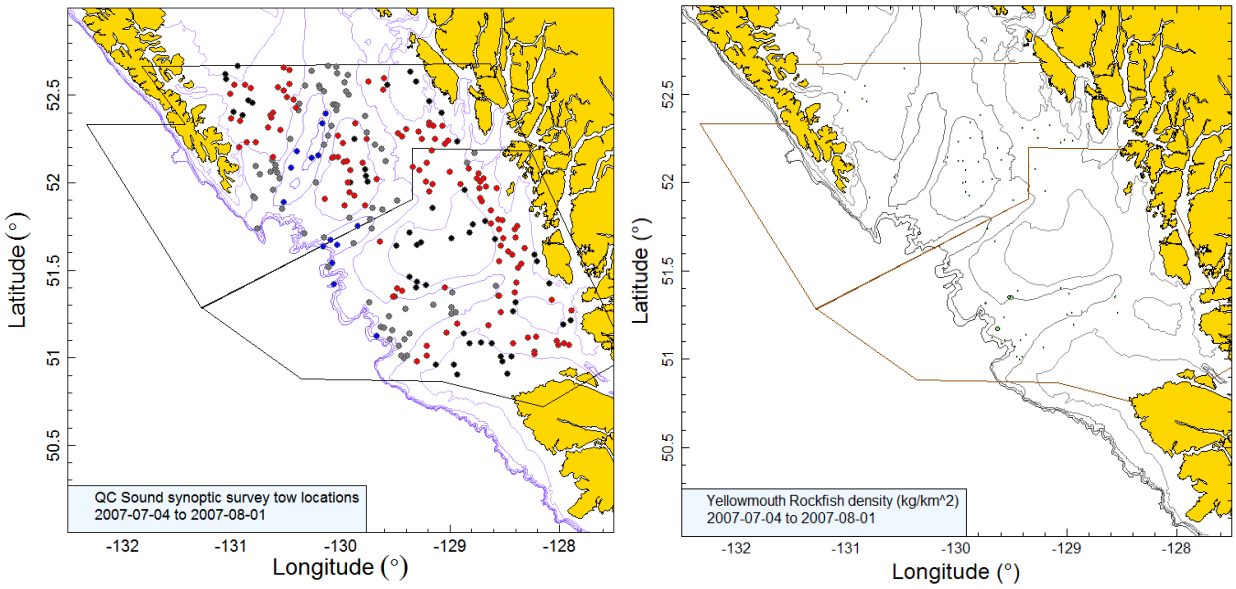

Figure B.15. Tow locations and density plots for the 2007 Queen Charlotte Sound synoptic survey (see Figure B.12 caption).

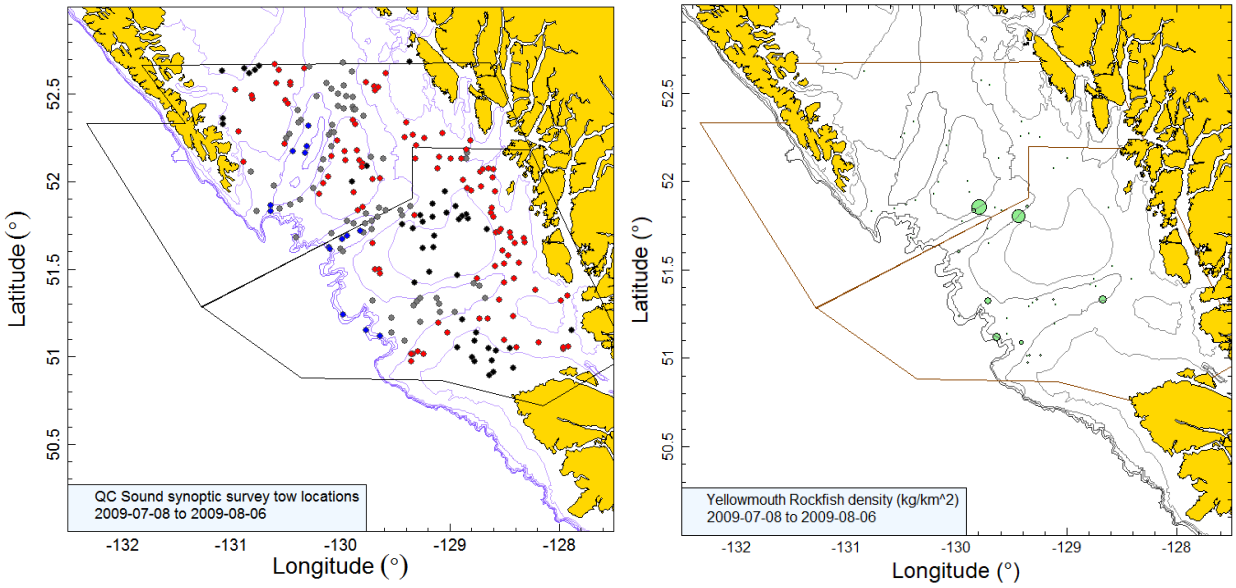

Figure B.16. Tow locations and density plots for the 2009 Queen Charlotte Sound synoptic survey (see Figure B.12 caption).

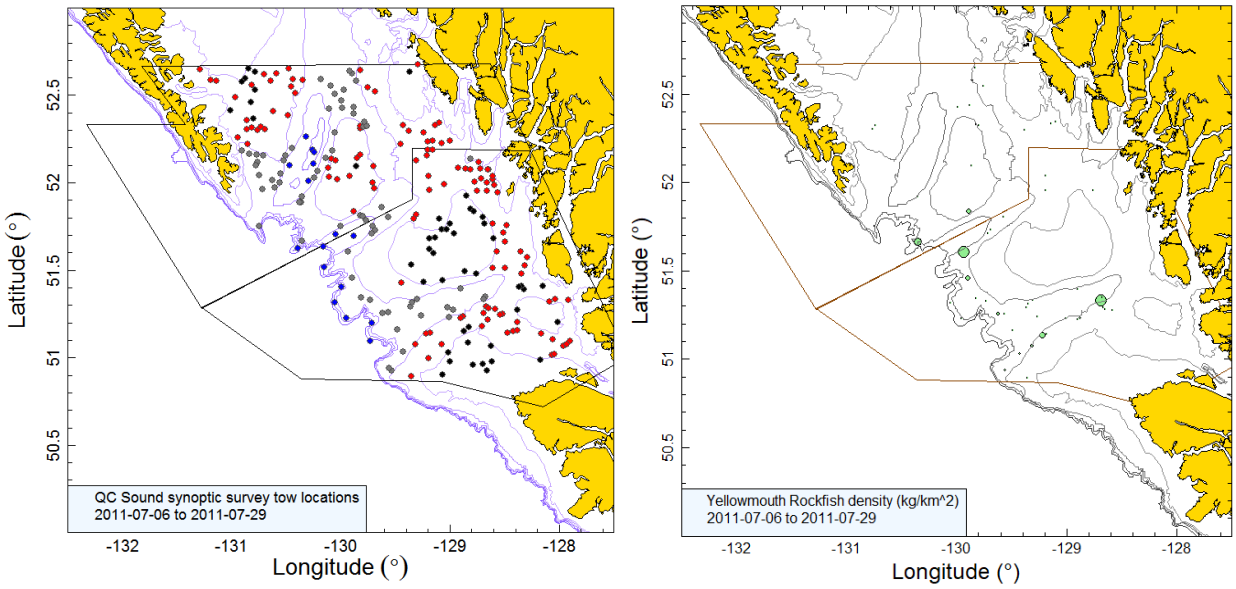

Figure B.17. Tow locations and density plots for the 2011 Queen Charlotte Sound synoptic survey (see Figure B.12 caption).

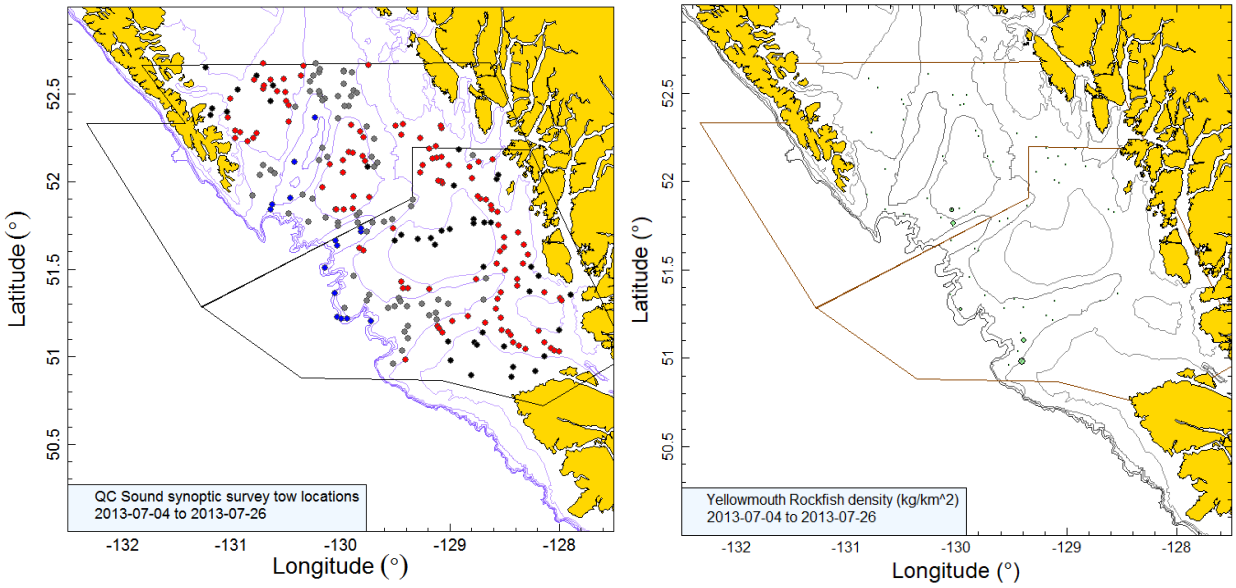

Figure B.18. Tow locations and density plots for the 2013 Queen Charlotte Sound synoptic survey (see Figure B.12 caption).

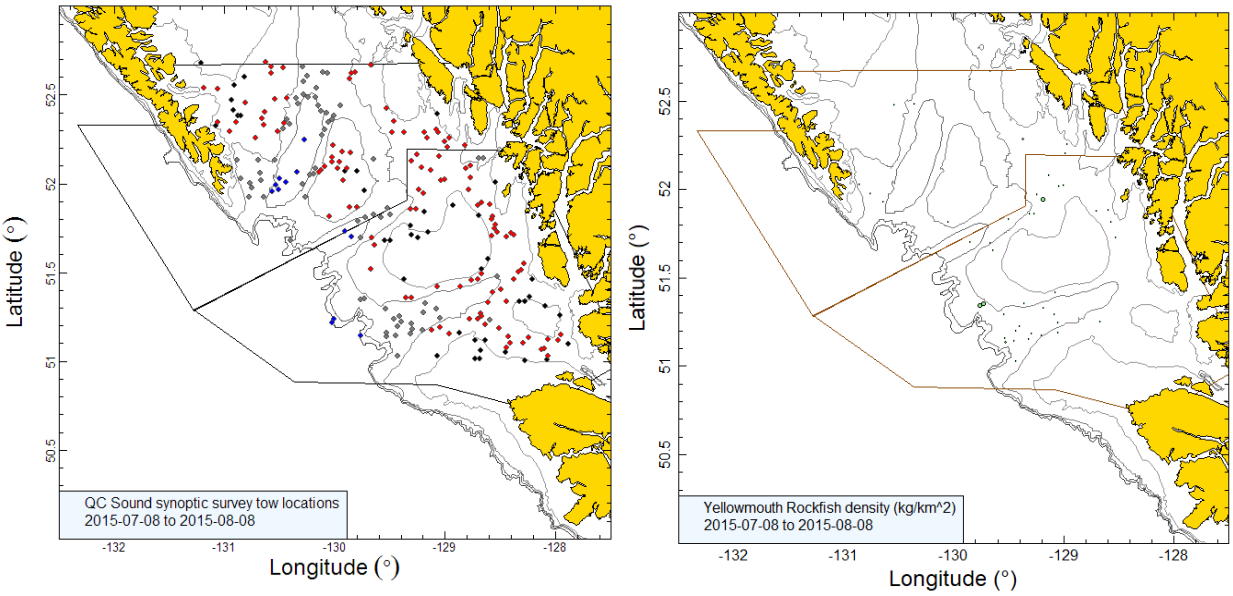

Figure B.19. Tow locations and density plots for the 2015 Queen Charlotte Sound synoptic survey (see Figure B.12 caption).

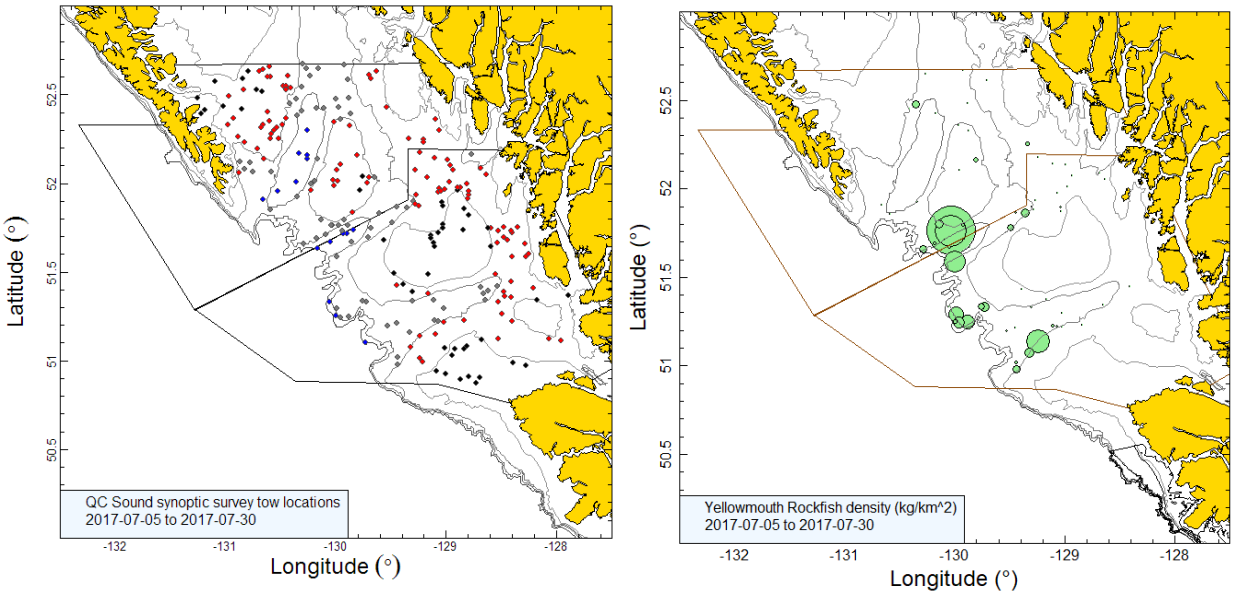

Figure B.20. Tow locations and density plots for the 2017 Queen Charlotte Sound synoptic survey (see Figure B.12 caption).

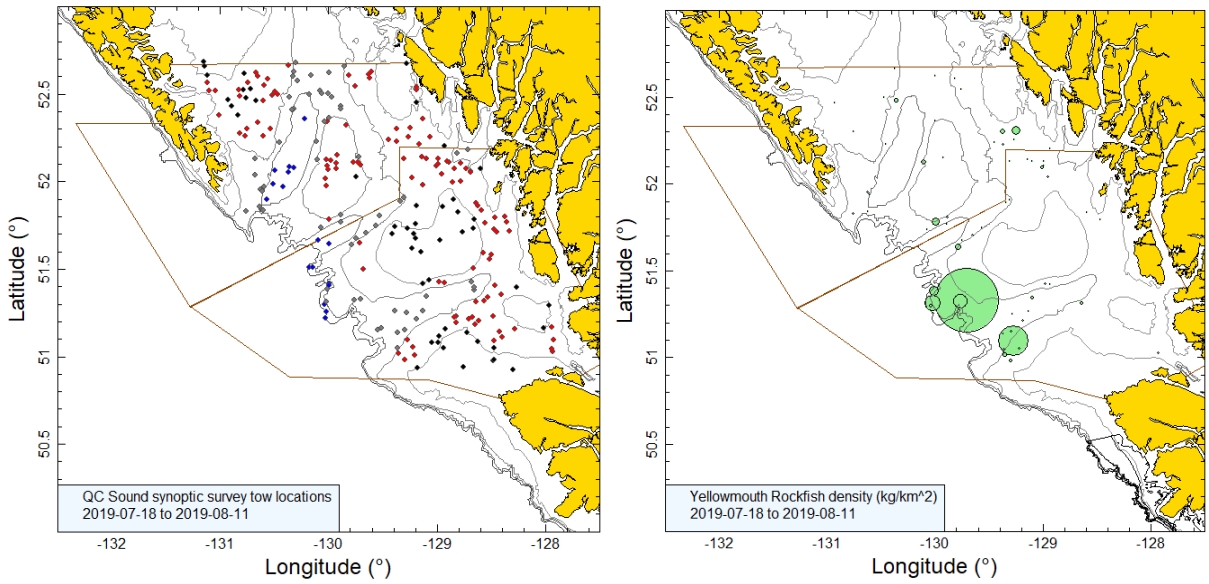

Figure B.21. Tow locations and density plots for the 2019 Queen Charlotte Sound synoptic survey (see Figure B.12 caption).

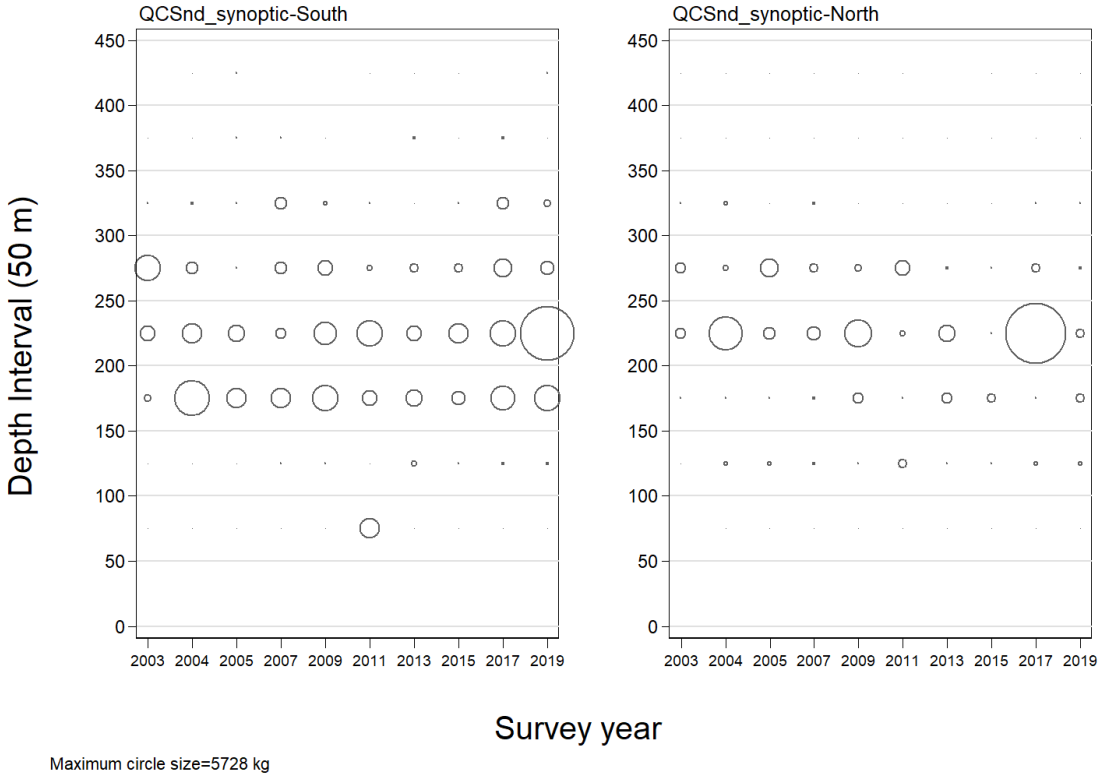

Figure B.22. Distribution of observed catch weights for tows used in biomass estimation for YMR in the two main Queen Charlotte Sound synoptic survey areal strata (Table B.5) by survey year and 50 m depth zone. Catches are plotted at the mid-point of the interval and circles in the panel are scaled to the maximum value (5728 kg) in the 200–250 m interval in the 2017 northern stratum. The 1% and 99% quantiles for the YMR start of tow depth distribution= 97 m and 312 m respectively.

Table B.7. Biomass estimates for YMR from the Queen Charlotte Sound synoptic trawl survey for the survey years 2003 to 2019. Bootstrap bias corrected confidence intervals and CVs are based on 1000 random draws with replacement.

Survey Year	Biomass (t) (Eq. B.4)	Mean bootstrap biomass (t)	Lower bound biomass (t)	Upper bound biomass (t)	Bootstrap CV	Analytic CV (Eq. B.6)
2003	1,407.2	1,391.9	598.0	2,692.6	0.366	0.372
2004	3,812.8	3,759.4	950.1	8,314.0	0.483	0.473
2005	1,632.6	1,638.5	636.6	3,468.2	0.425	0.425
2007	1,388.2	1,407.5	653.6	2,409.1	0.320	0.309
2009	2,604.8	2,640.4	883.4	5,163.7	0.417	0.427
2011	2,651.5	2,607.8	1,015.9	5,032.5	0.389	0.406
2013	1,432.8	1,415.8	673.6	2,506.6	0.321	0.333
2015	989.9	978.2	333.7	1,920.8	0.406	0.401
2017	6,318.2	6,330.6	2,312.7	13,689.6	0.447	0.455
2019	5,400.8	5,411.3	728.2	14,942.6	0.700	0.713

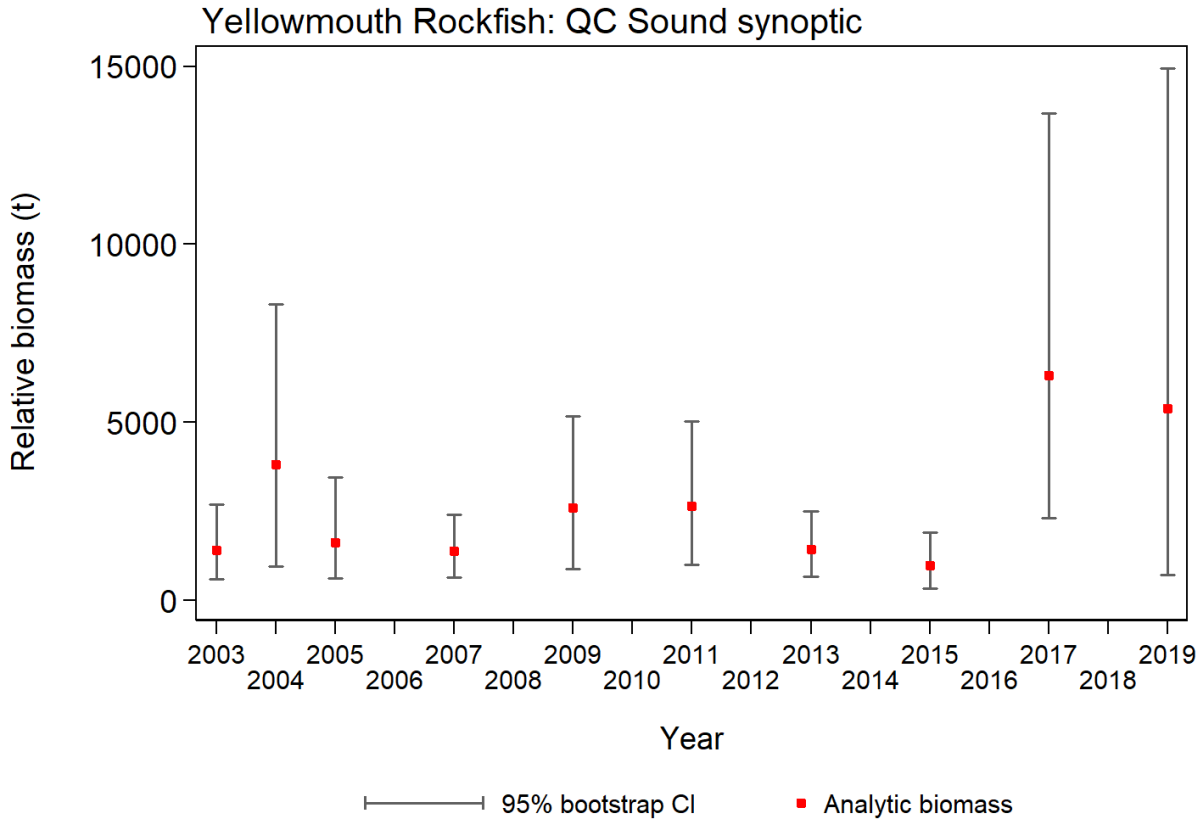

Figure B.23. Plot of biomass estimates for YMR (values provided in Table B.7) from the Queen Charlotte Sound synoptic survey over the period 2003 to 2019. Bias corrected 95% confidence intervals from 1000 bootstrap replicates are plotted.

On average, YMR were captured in around 23% of tows in both areal strata, ranging from 20% to 33% of the tows in the South stratum and 10% to 32% of the tows in the North stratum (Figure B.24). Overall, 547 of the 2,366 valid survey tows (23%) contained YMR. The median catch weight for positive tows used in biomass estimation was 4.0 kg/tow across the ten surveys, and the maximum catch weight in a tow was 4,921 kg in the 2019 survey.

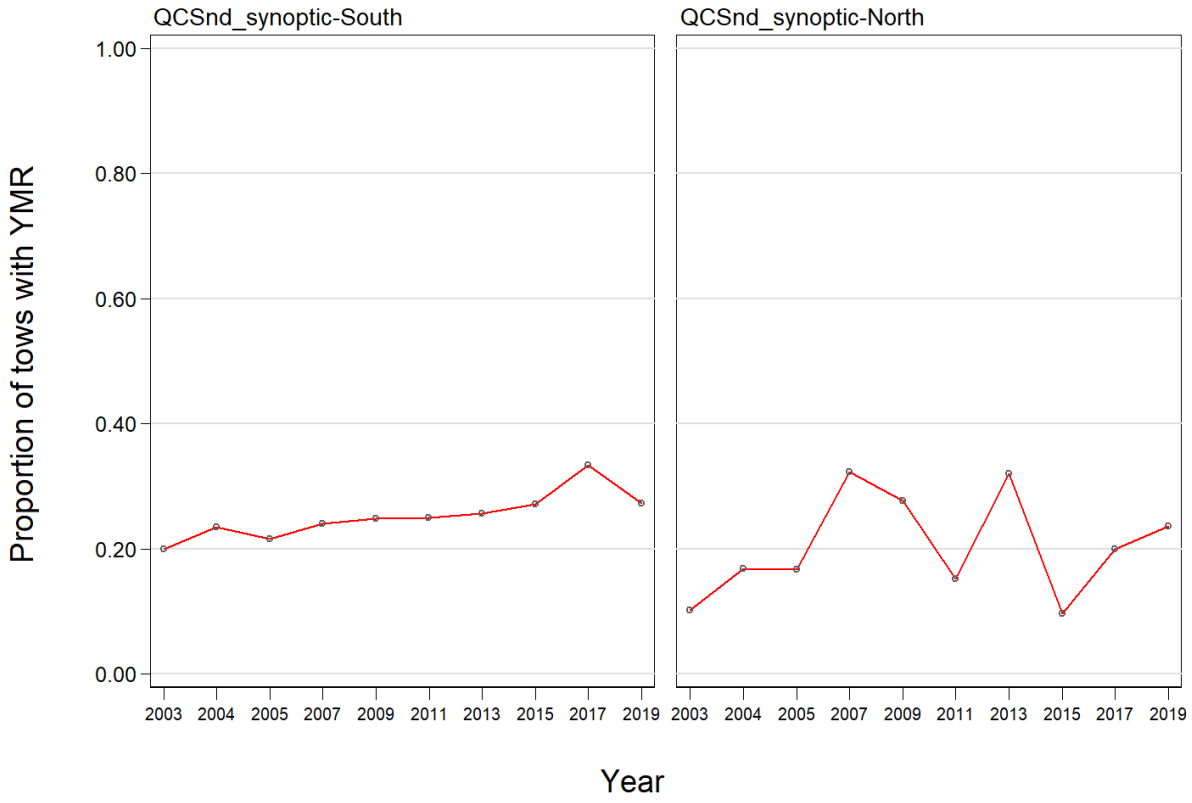

Figure B.24. Proportion of tows by stratum and year which contain YMR from the Queen Charlotte Sound synoptic survey over the period 2003 to 2019.

B.5. WEST COAST VANCOUVER ISLAND SYNOPTIC TRAWL SURVEY

B.5.1. Data selection

This survey has been conducted seven times in the period 2004 to 2016 off the west coast of Vancouver Island by RV *W.E. Ricker*. An eighth survey was conducted in 2018 by the RV *Nordic Pearl* due to the decommissioning of the *W.E. Ricker*. The scheduled 2020 survey was cancelled due to restrictions on the deployment of government vessels imposed by Canadian policy pertaining to the ongoing COVID-19 epidemic. It comprises a single areal stratum, separated into four depth strata: 50-125 m; 125-200 m; 200-330 m; and 330-500 m (Table B.8). Approximately 150 to 200 2-km^2 blocks are selected randomly among the four depth strata when conducting each survey (Olsen et. al. 2008).

A “doorspread density” value was generated for each tow based on the catch of YMR, the mean doorspread for the tow and the distance travelled (Eq. B.3). The distance travelled was provided as a data field, determined directly from vessel track information collected during the tow. There were only two missing values in this field (in 2004 and 2010) which were filled in by multiplying the vessel speed by the time that the net was towed. There were a large number of missing values for the doorspread field, which were filled in using the mean doorspread for the survey year or a default value of 64.6 m for the three years with no doorspread data (Table B.9). The

default value is based on the mean of the observed doorspread from the net mensuration equipment, averaged across the years with doorspread estimates.

Table B.8. Stratum designations, number of usable and unusable tows, for each year of the west coast Vancouver Island synoptic survey. Also shown is the area of each depth stratum in 2018 and the start and end dates for each survey.

Survey year	Stratum depth zone				Total Tows[1]	Unusable tows	Start date	End date
	50-125 m	125-200 m	200-330 m	330-500 m				
2004	34	34	13	8	89	17	26-May-04	09-Jun-04
2006	61	62	28	13	164	12	24-May-06	18-Jun-06
2008	54	50	32	23	159	19	27-May-08	21-Jun-08
2010	58	47	22	9	136	8	08-Jun-10	28-Jun-10
2012	60	46	25	20	151	6	23-May-12	15-Jun-12
2014	55	49	29	13	146	7	29-May-14	20-Jun-14
2016	54	41	26	19	140	7	25-May-16	15-Jun-16
2018	69	64	36	21	190	12	19-May-18	12-Jun-18
Area (km^2)	5,716	3,768	708	572	10,764[2]	–	–	–

[1] GFBio usability codes=0,1,2,6
[2] Total area (km^2) for 2018 synoptic survey

Table B.9. Number of tows with and without doorspread measurements by survey year for the WCVI synoptic survey. Mean doorspread values for those tows with measurements are provided.

Survey Year	Number tows		Mean doorspread (m)
	Without doorspread	With doorspread	
2004	89	0	–
2006	96	69	64.3
2008	58	107	64.5
2010	136	0	–
2012	153	0	–
2014	14	139	64.3
2016	0	147	65.5
2018	0	202	64.3
All surveys	546	664	64.6

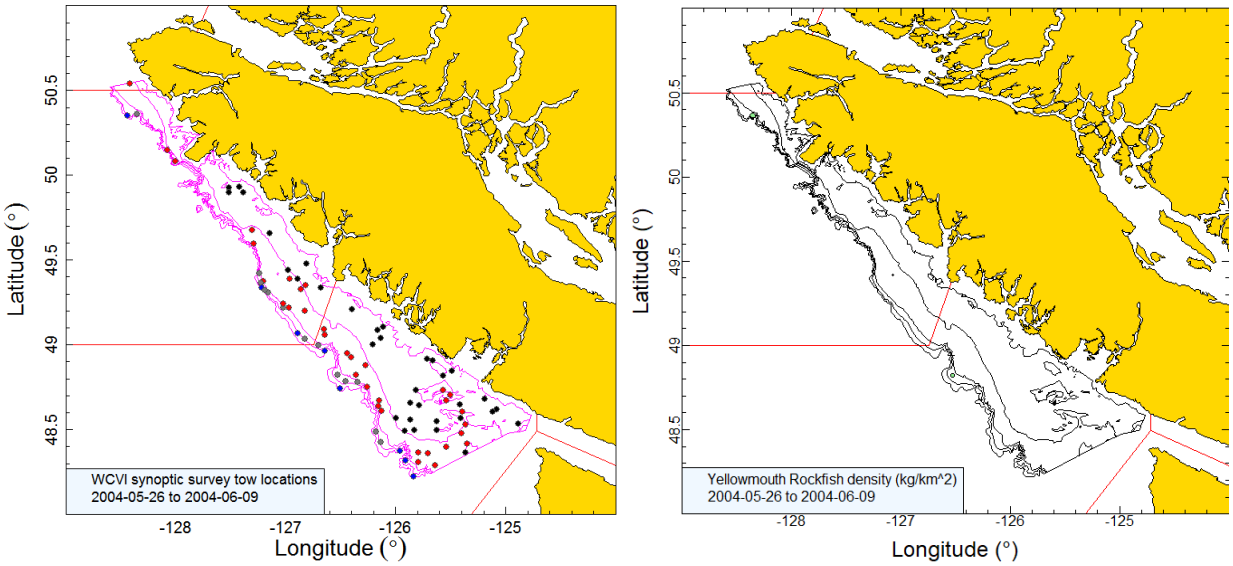

Figure B.25. Valid tow locations (50-125m stratum: black; 126-200m stratum: red; 201-330m stratum: grey; 331-500m stratum: blue) and density plots for the 2004 west coast Vancouver Island synoptic survey. Circle sizes in the right-hand density plot scaled across all years (2004, 2006, 2008, 2010, 2012, 2014, 2016, 2018), with the largest circle = 3,875 kg/km^2 in 2010. The red solid lines indicate the boundaries for PMFC areas 3C, 3D and 5A.

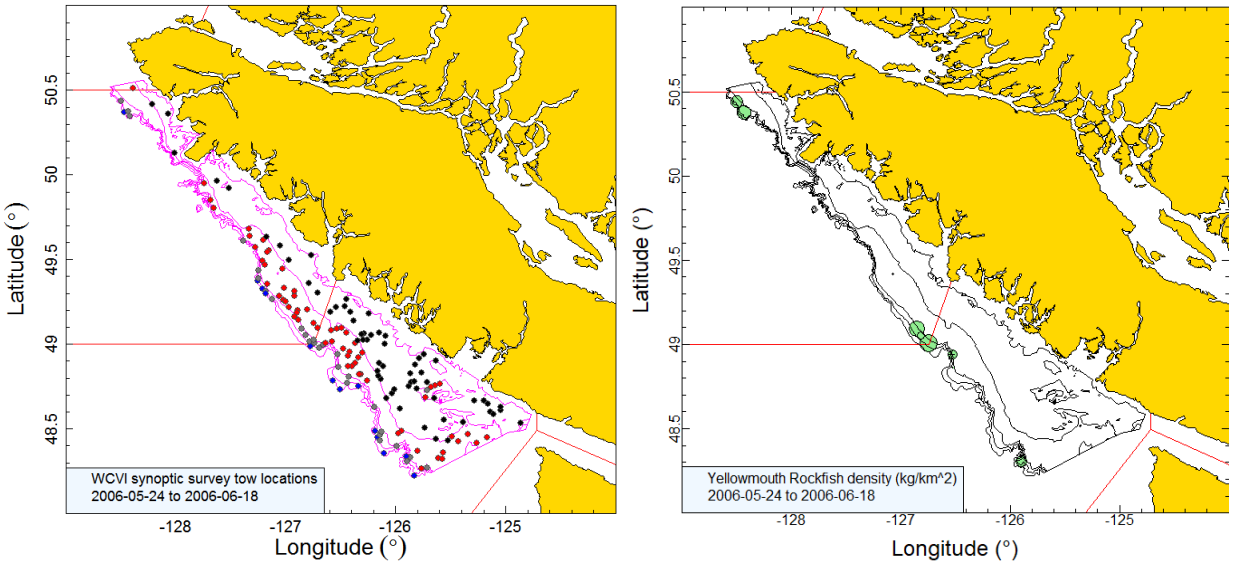

Figure B.26. Tow locations and density plots for the 2006 west coast Vancouver Island synoptic survey (see Figure B.25 caption).

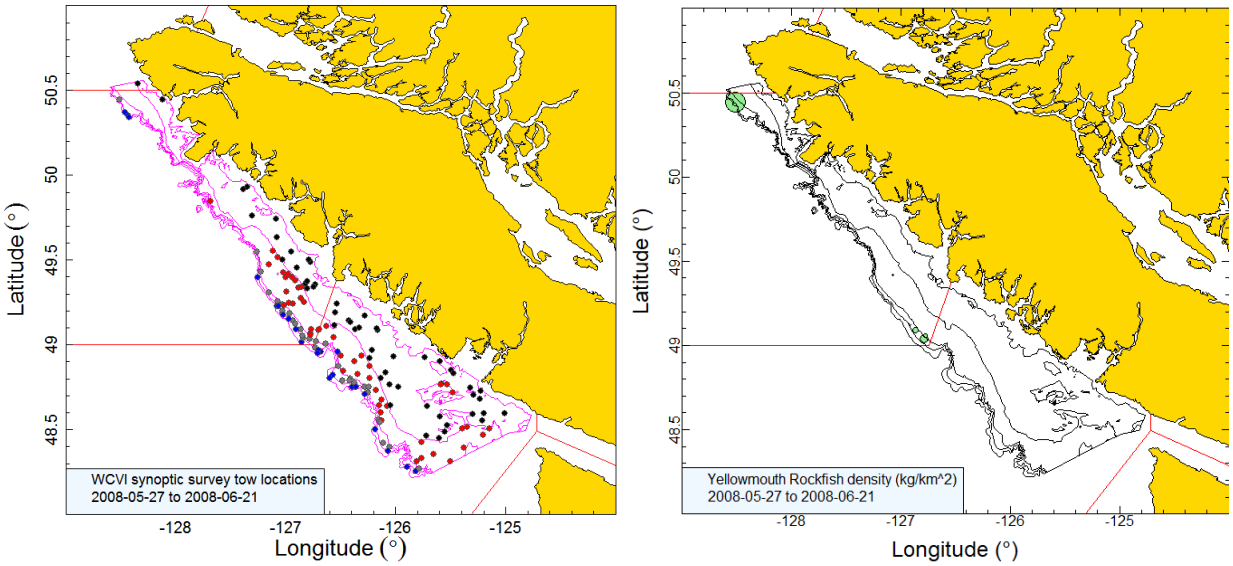

Figure B.27. Tow locations and density plots for the 2008 west coast Vancouver Island synoptic survey (see Figure B.25 caption).

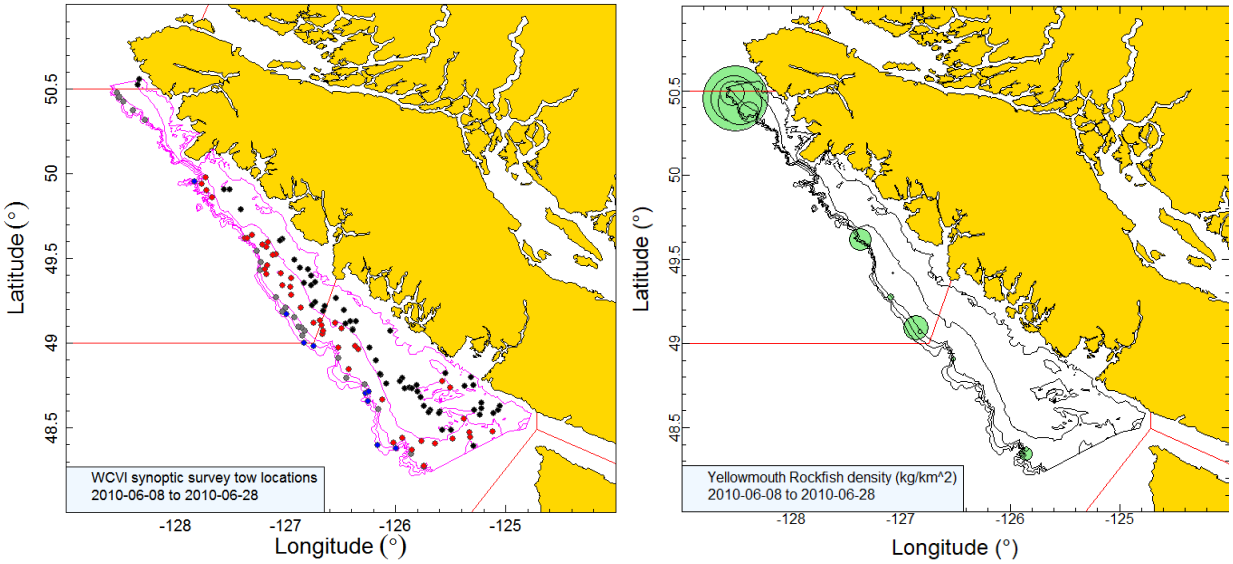

Figure B.28. Tow locations and density plots for the 2010 west coast Vancouver Island synoptic survey (see Figure B.25 caption).

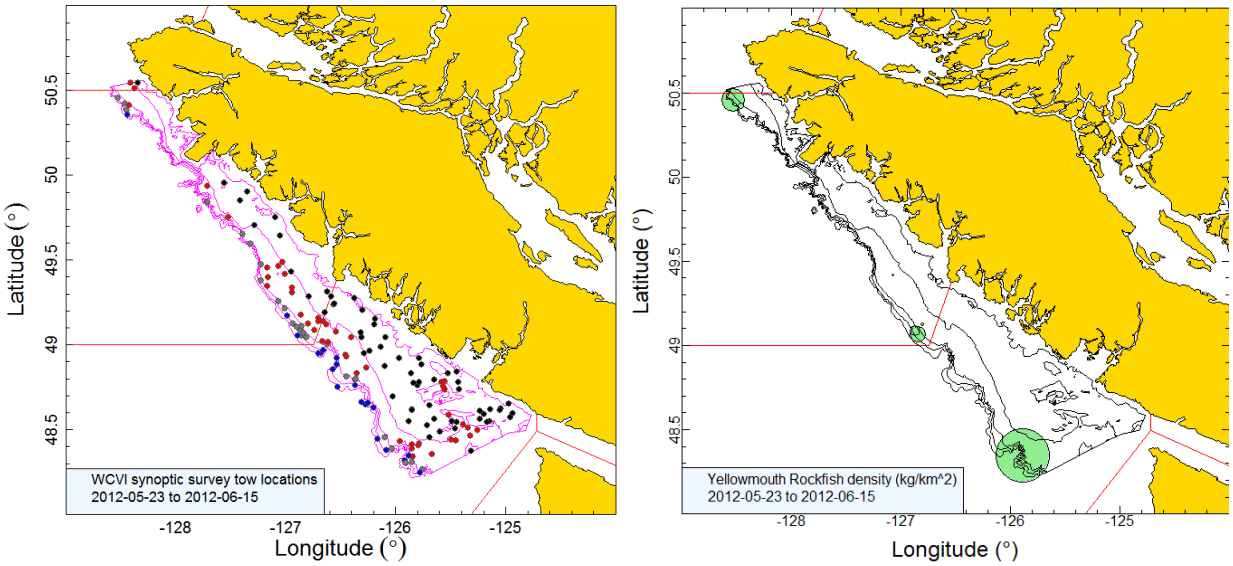

Figure B.29. Tow locations and density plots for the 2012 west coast Vancouver Island synoptic survey (see Figure B.25 caption).

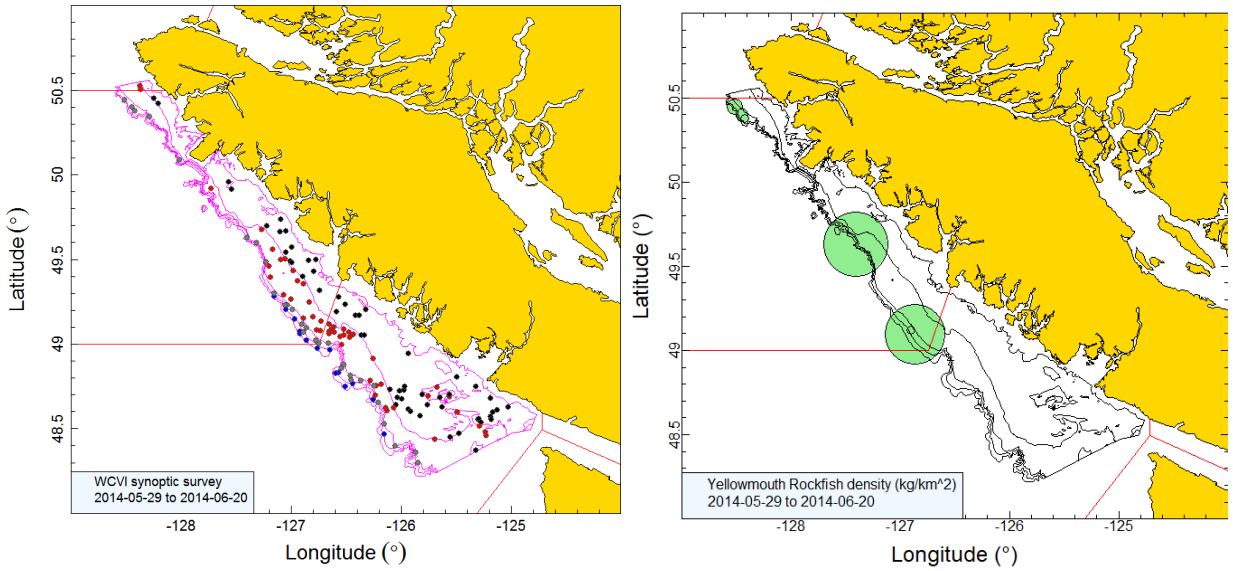

Figure B.30. Tow locations and density plots for the 2014 west coast Vancouver Island synoptic survey (see Figure B.25 caption).

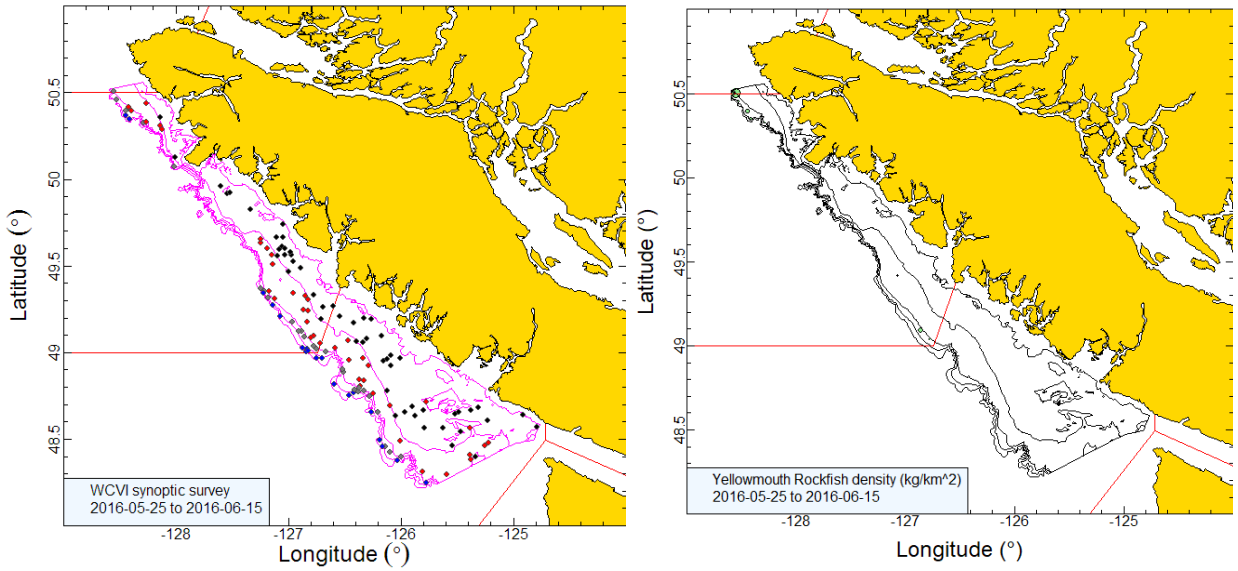

Figure B.31. Tow locations and density plots for the 2016 west coast Vancouver Island synoptic survey (see Figure B.25 caption).

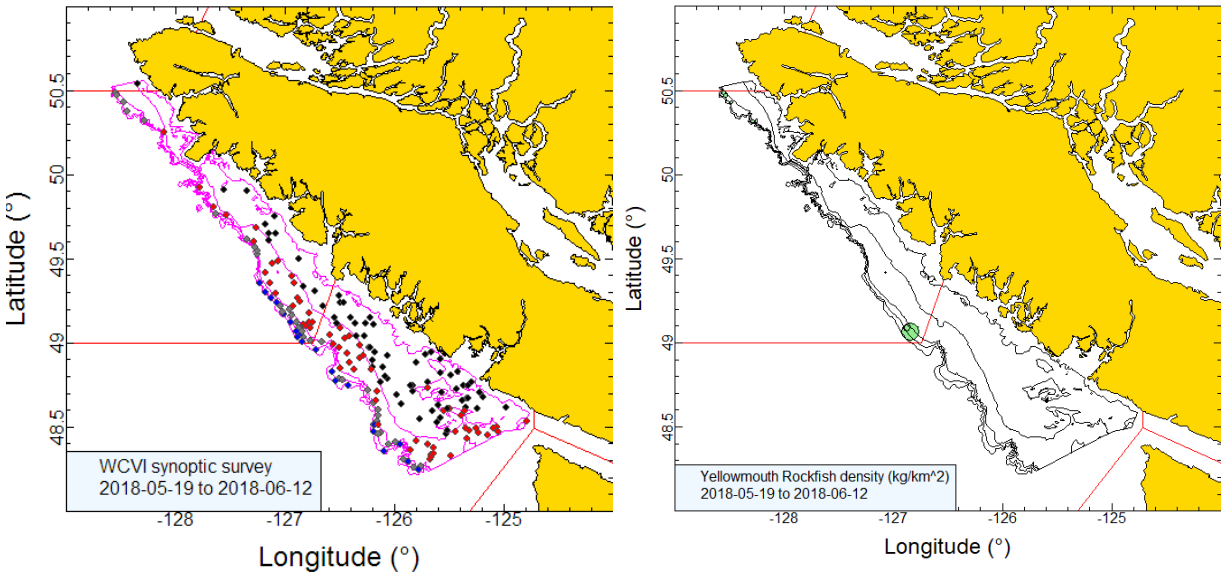

Figure B.32. Tow locations and density plots for the 2018 west coast Vancouver Island synoptic survey (see Figure B.25 caption).

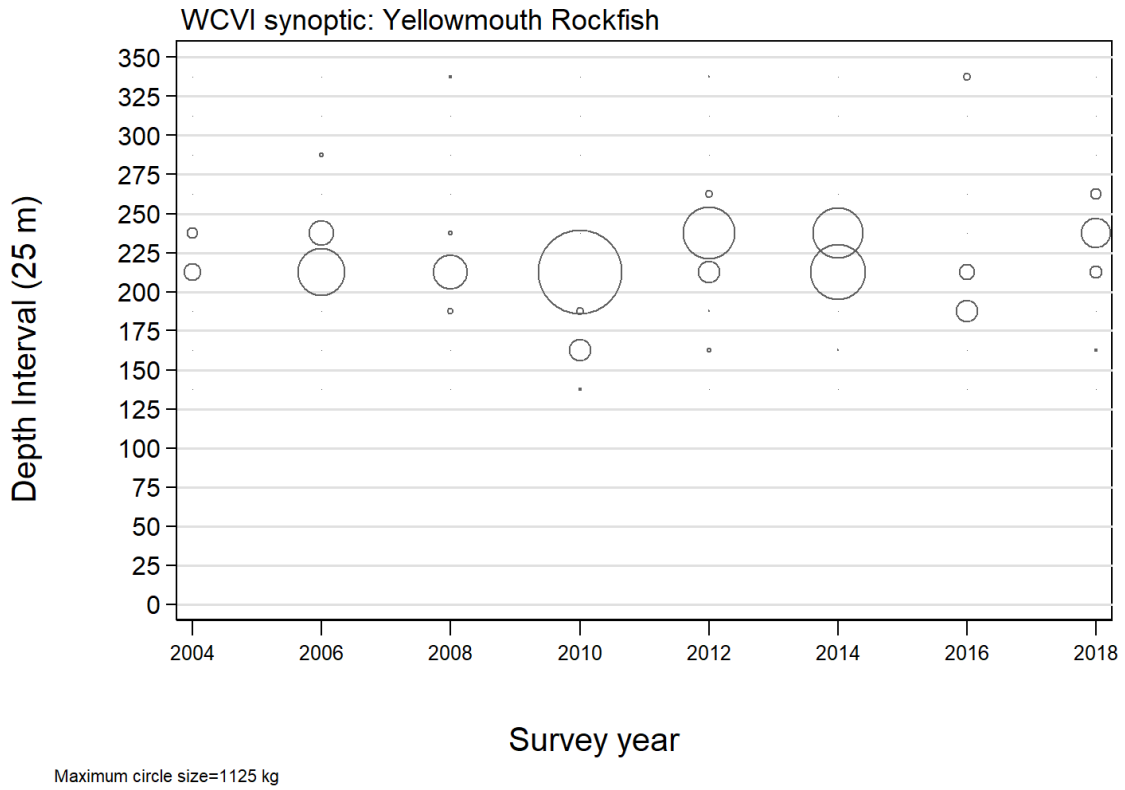

Figure B.33. Distribution of observed weights of YMR by survey year and 25 m depth zone. Catches are plotted at the mid-point of the interval and circles in the panel are scaled to the maximum value (1,125 kg) in the 200-225 m interval in 2010. The 1st and 99th percentiles for the YMR start of tow depth distribution = 169 m and 251 m, respectively.

B.5.2. Results

YMR were taken exclusively along the shelf edge from near the US border to the most northern section of the survey, well above Brooks Peninsula near the top of Vancouver Island (Figure B.25 to Figure B.32). The distribution appeared to predominate in the upper half of Vancouver Island, with the highest density tows taken above Brooks Peninsula. YMR were mainly taken in the very narrow depth range 200 to 250 m (5–95 percentiles=201 to 234 m) (Figure B.33). Relative biomass levels for YMR from this trawl survey were low, ranging from 28 to 343 t, with high relative errors, which ranged from 0.34 to 0.74 (Figure B.34; Table B.10).

The proportion of tows capturing YMR was very low, and showed little year-to-year variation, ranging between 2 and 9% over the eight surveys and with a mean value of 5% (Figure B.35). Only 63 of the 1175 usable tows (19%) from this survey contained YMR, with a median catch weight for positive tows of 14 kg/tow and maximum catch weight across all eight surveys of 485 kg (in 2010).

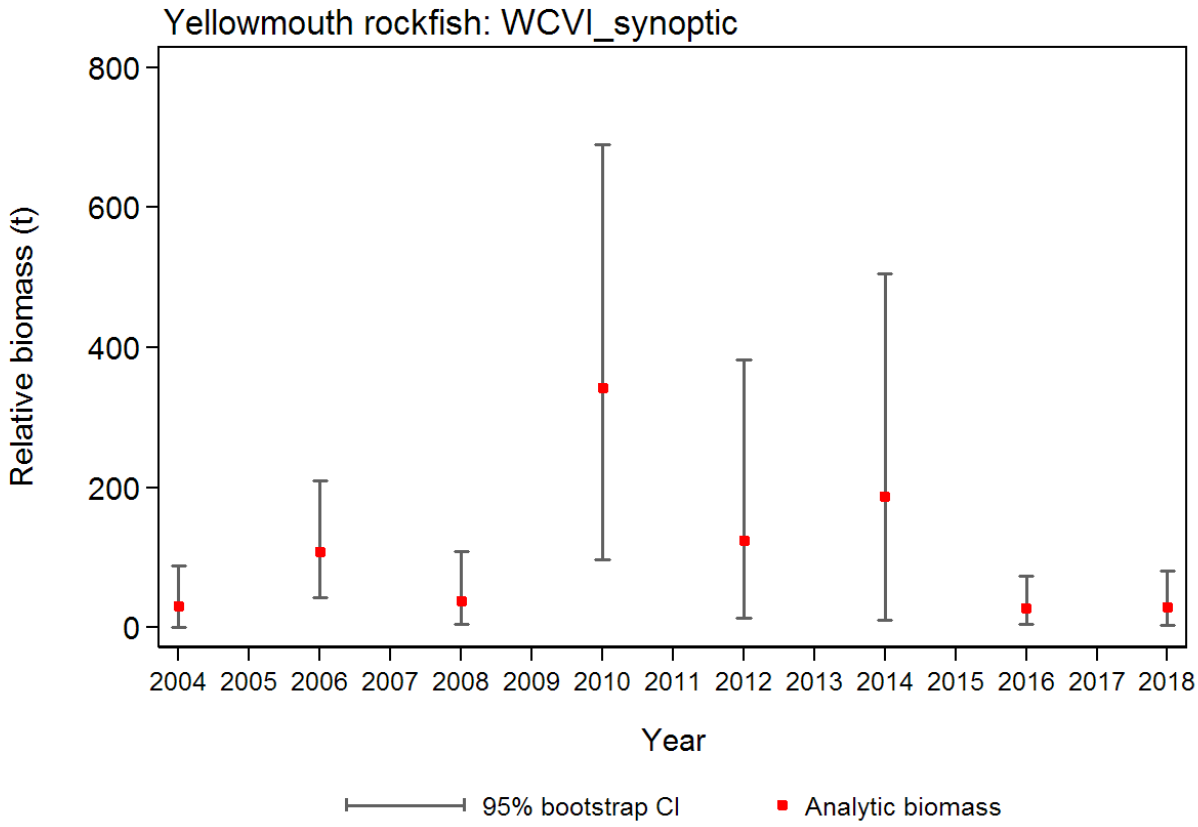

Figure B.34. Plot of biomass estimates for YMR from the 2004 to 2018 west coast Vancouver Island synoptic trawl surveys (Table B.10). Bias-corrected 95% confidence intervals from 1000 bootstrap replicates are plotted.

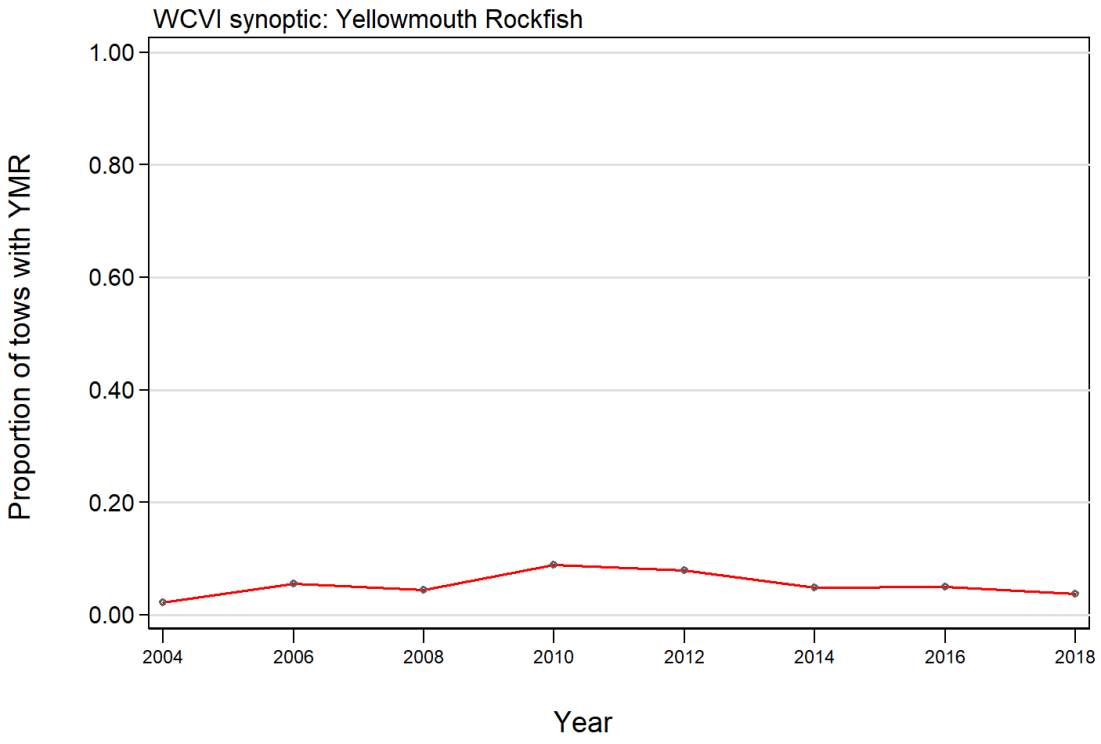

Figure B.35. Proportion of tows by stratum and year capturing YMR in the WCVI synoptic trawl surveys, 2004–2018.

Table B.10. Biomass estimates for YMR from the WCVI synoptic trawl survey for the survey years 2004 to 2018. Bootstrap bias-corrected confidence intervals and CVs are based on 1000 random draws with replacement.

Survey Year	Biomass (t) (Eq. B.4)	Mean bootstrap biomass (t)	Lower bound biomass (t)	Upper bound biomass (t)	Bootstrap CV	Analytic CV (Eq. B.6)
2004	30.5	29.9	0.0	88.0	0.725	0.739
2006	108.5	106.4	42.3	209.2	0.380	0.371
2008	38.8	39.4	4.5	109.3	0.690	0.700
2010	342.9	341.2	97.7	689.7	0.433	0.432
2012	125.2	125.7	13.2	383.1	0.732	0.741
2014	188.3	190.7	10.3	504.9	0.665	0.644
2016	27.7	27.6	5.5	74.5	0.617	0.620
2018	29.0	29.9	3.6	81.3	0.707	0.726

B.6. WEST COAST HAIDA GWAII SYNOPTIC TRAWL SURVEY

B.6.1. Data selection

The west coast Haida Gwaii (WCHG) survey has been conducted eight times in the period 2006 to 2018 off the west coast of Haida Gwaii. This includes a survey conducted in 2014 which did not complete a sufficient number of tows for it to be considered comparable to the remaining surveys and which is consequently omitted from Table B.11. An earlier survey, conducted in 1997, also using a random stratified design similar to the current synoptic survey design along with an Atlantic Western II box trawl net (Workman et al. 1998), has been included in this time series. This survey comprises a single areal stratum extending from 53°N to the BC-Alaska border and east to 133°W (e.g., Olsen et al. 2008). The 1997 survey (depth stratification: 180-275 m, 275-365 m, 365-460 m, 460-625 m) and the 2006 survey (depth stratification: 150–

200 m, 200–330 m, 330–500 m, 500–800 m, and 800–1300 m) have been re-stratified into the four depth strata used from 2007 onwards: 180–330 m; 330–500 m; 500–800 m; and 800–1300 m, based on the mean of the beginning and end depths of each tow (Table B.11). All tows S of 53°N from the two earlier surveys have been dropped from biomass estimation. Plots of the locations of all valid tows by year and stratum are presented in Figure B.36 (1997), Figure B.37 (2006), Figure B.38 (2007), Figure B.39 (2008), Figure B.40 (2010), Figure B.41 (2012), Figure B.42 (2016), Figure B.43 (2018) and Figure B.44 (2020). Note that the depth stratum boundaries for this survey differ from those used for the Queen Charlotte Sound (Edwards et al. 2012) and west coast Vancouver Island (Edwards et al. 2014) synoptic surveys due to the considerable difference in the seabed topography of the area being surveyed. The deepest stratum (800–1300 m) has been omitted from this analysis because of lack of coverage in 2007.

Table B.11. Stratum designations, vessel name, number of usable and unusable tows, for each completed year of the west coast Haida Gwaii synoptic survey. Also shown are the dates of the first and last survey tow in each year.

		Depth stratum							
Survey year	Vessel	180-330m	330-500m	500-800m	800-1300m	Total tows[1]	Unusable tows	Minimum date	Maximum date
1997	*Ocean Selector*	39	57	6	0	102	5	07-Sep-97	21-Sep-97
2006	*Viking Storm*	54	26	14	54	94	14[2]	30-Aug-06	22-Sep-06
2007	*Nemesis*	67	33	8	67	108	8	14-Sep-07	12-Oct-07
2008	*Frosti*	70	31	8	70	109	10	28-Aug-08	18-Sep-08
2010	*Viking Storm*	81	28	11	81	120	5	28-Aug-10	16-Sep-10
2012	*Nordic Pearl*	75	28	9	75	112	13	27-Aug-12	16-Sep-12
2016	*Frosti*	67	28	5	67	100	10	28-Aug-16	24-Sep-16
2018	*Nordic Pearl*	67	30	10	67	107	12	05-Sep-18	20-Sep-18
2020	*Nordic Pearl*	65	26	3	65	94	16	29-Aug-20	18-Sep-20
Area (km^2)		1,076	1,004	952	2,248	5,280[3]	–	–	–

[1] GFBio usability codes=0,1,2,6 and omitting the 800-1300 m stratum; [2] excludes 2 tows S of 53°N; [3] Total area in 2020 (km^2)

Table B.12. Number of valid tows with doorspread measurements, the mean doorspread values (in m) from these tows for each survey year and the number of valid tows without doorspread measurements.

Year	Tows with doorspread	Tows missing doorspread	Mean doorspread (m)
1997	107	0	61.6
2006	93	30	77.7
2007	113	3	68.5
2008	123	4	80.7
2010	129	2	79.1
2012	92	49	73.8
2016	105	15	74.1
2018	130	0	67.0
2020	107	5	67.5
Total/Average	1,000	108	73.0[1]

[1] average 2007–2020: all observations

A doorspread density (Eq. B.3) was generated for each tow based on the catch of YMR from the mean doorspread for the tow and the distance travelled. [`distance travelled`] is a database field which is calculated directly from the tow track. This field is used preferentially for the variable D_{yij} in Eq. B.3. A calculated value ([`vessel speed`] X [`tow duration`]) is used for this variable if [`distance travelled`] is missing, but there were no instances of this occurring in the eight trawl surveys. Missing values for the [`doorspread`] field were filled in with the mean doorspread for the survey year (103 values over all years, Table B.12).

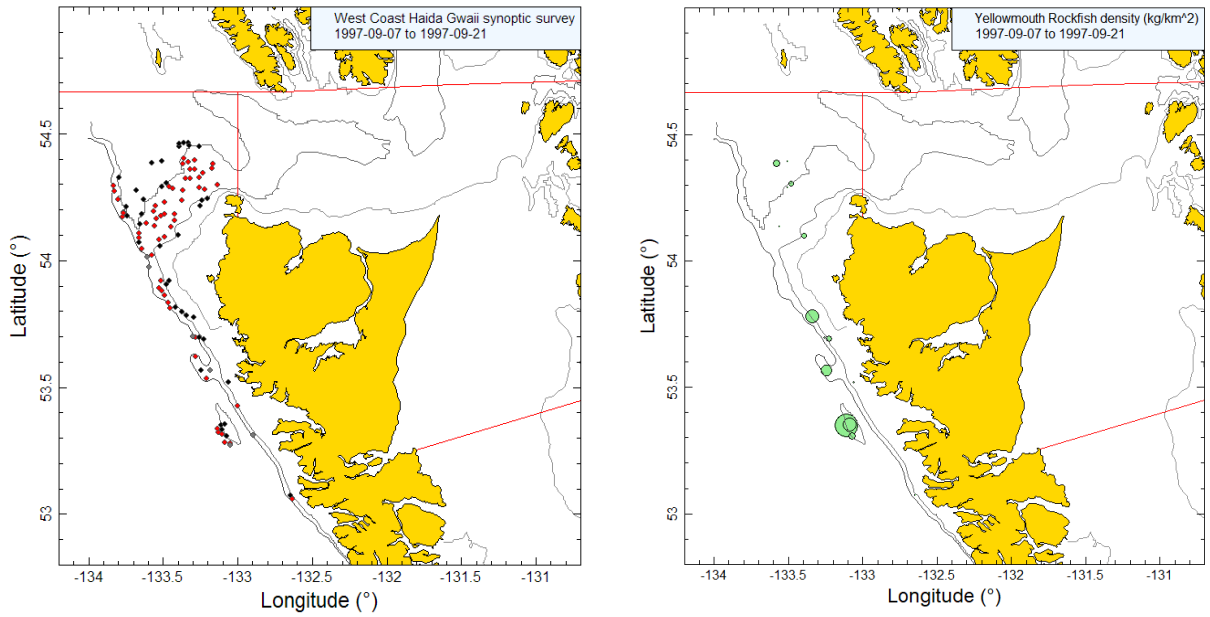

Figure B.36. Valid tow locations by stratum (180-330m: black; 330-500m: red; 500-800m: grey; 800-1300m: blue) and density plots for the 1997 Ocean Selector synoptic survey. Circle sizes in the right-hand density plot scaled across all years (1997–2020), with the largest circle =30,479 kg/km^2 in 2016. The red lines show the Pacific Marine Fisheries Commission 5E and 5D major area boundaries.

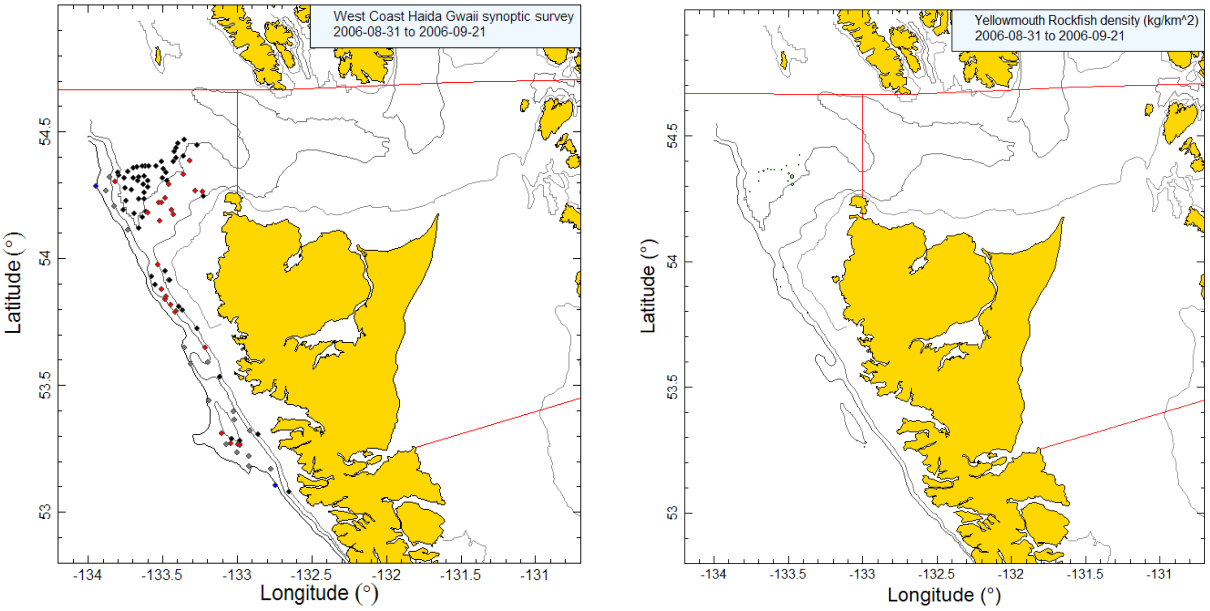

Figure B.37. Tow locations and density plots for the 2006 Viking Storm synoptic survey (see Figure B.36 caption).

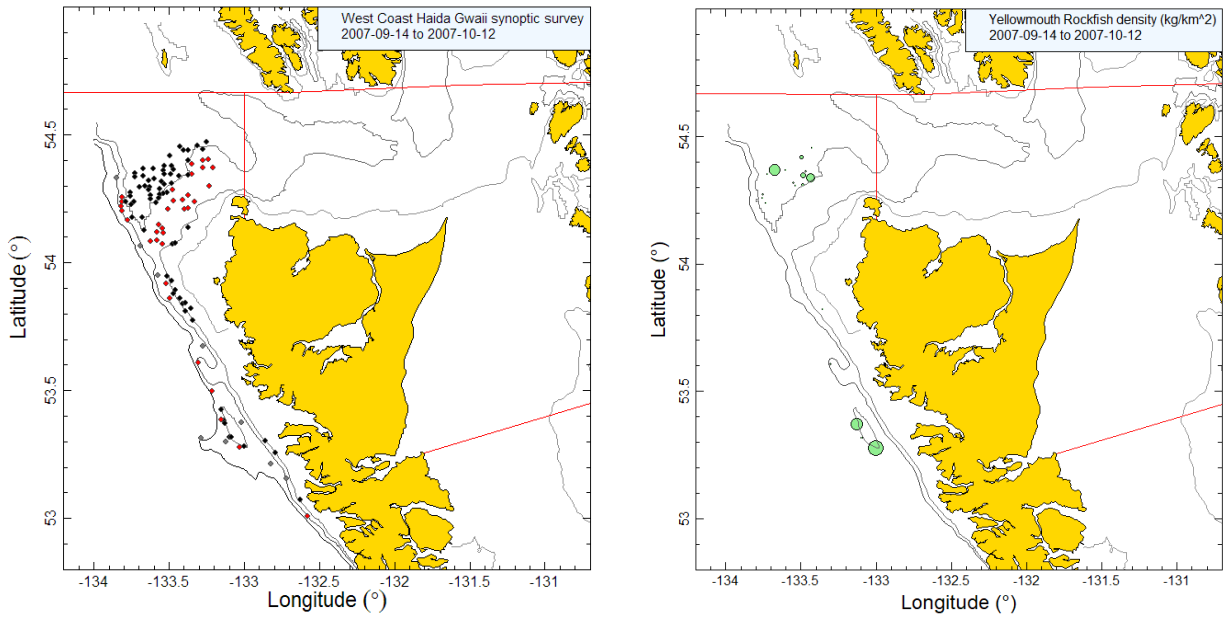

Figure B.38. Tow locations and density plots for the 2007 Nemesis synoptic survey (see Figure B.36 caption).

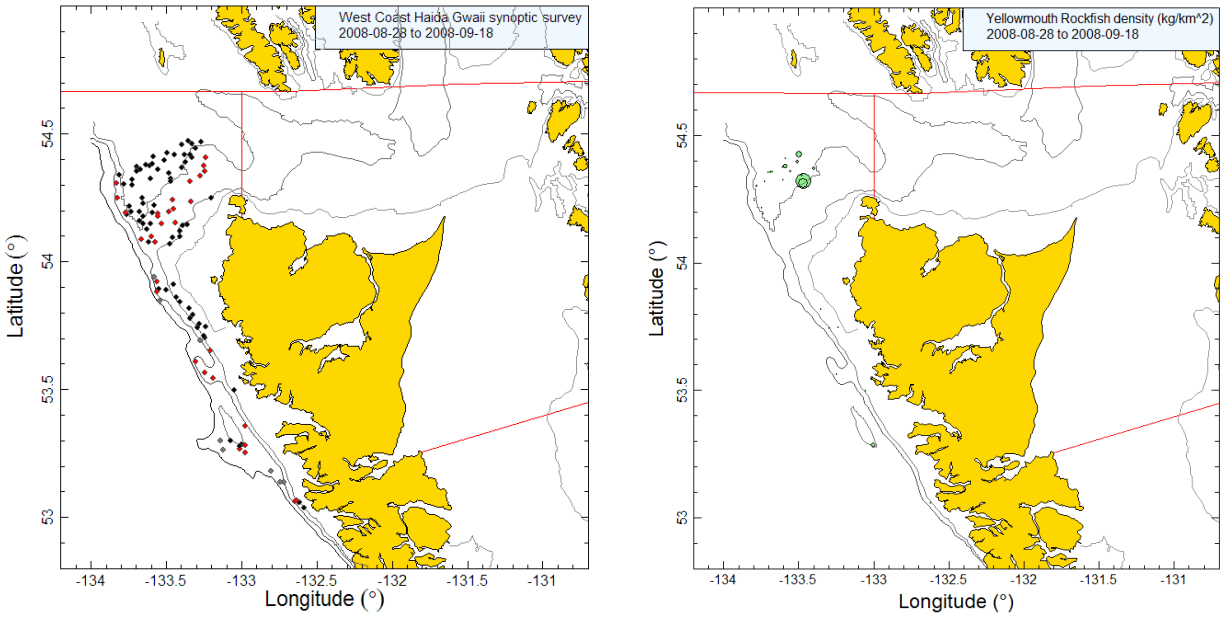

Figure B.39. Tow locations and density plots for the 2008 Frosti synoptic survey (see Figure B.36 caption).

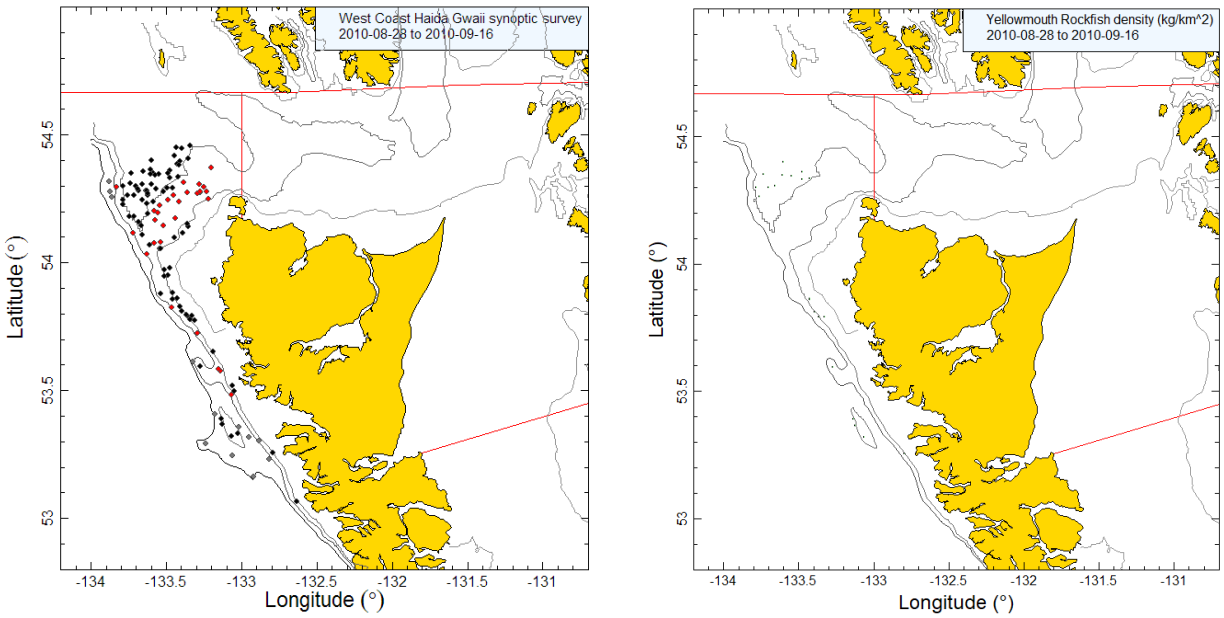

Figure B.40. Tow locations and density plots for the 2010 Viking Storm synoptic survey (see Figure B.36 caption).

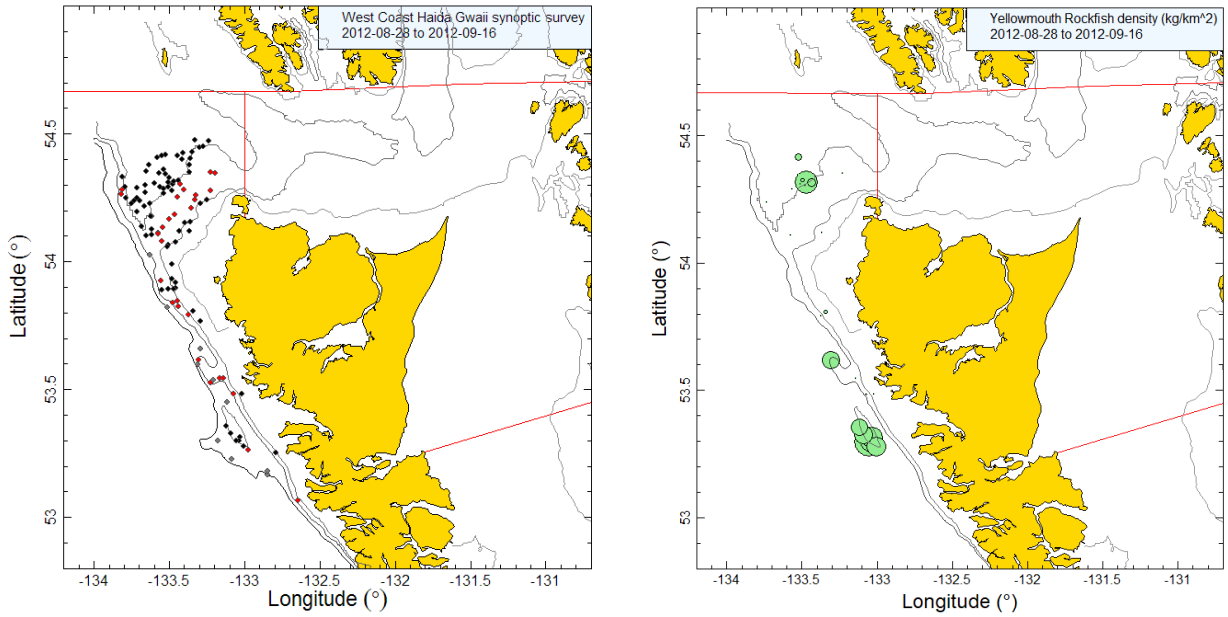

Figure B.41. Tow locations and density plots for the 2012 Nordic Pearl synoptic survey (see Figure B.36 caption).

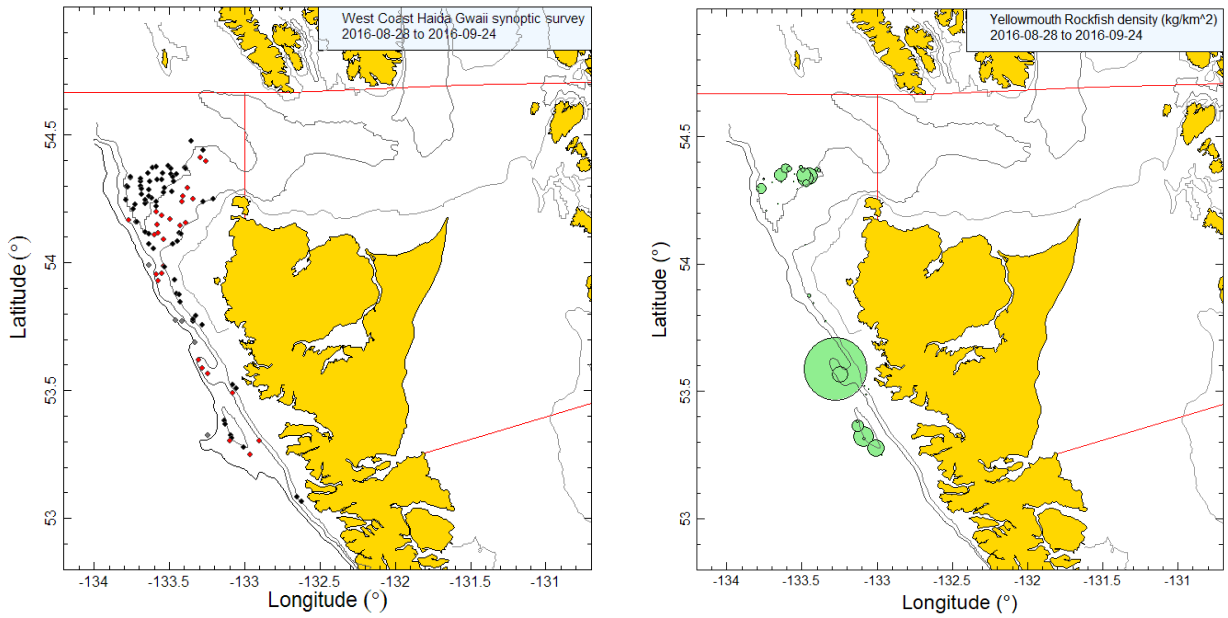

Figure B.42. Tow locations and density plots for the 2016 Frosti synoptic survey (see Figure B.36 caption).

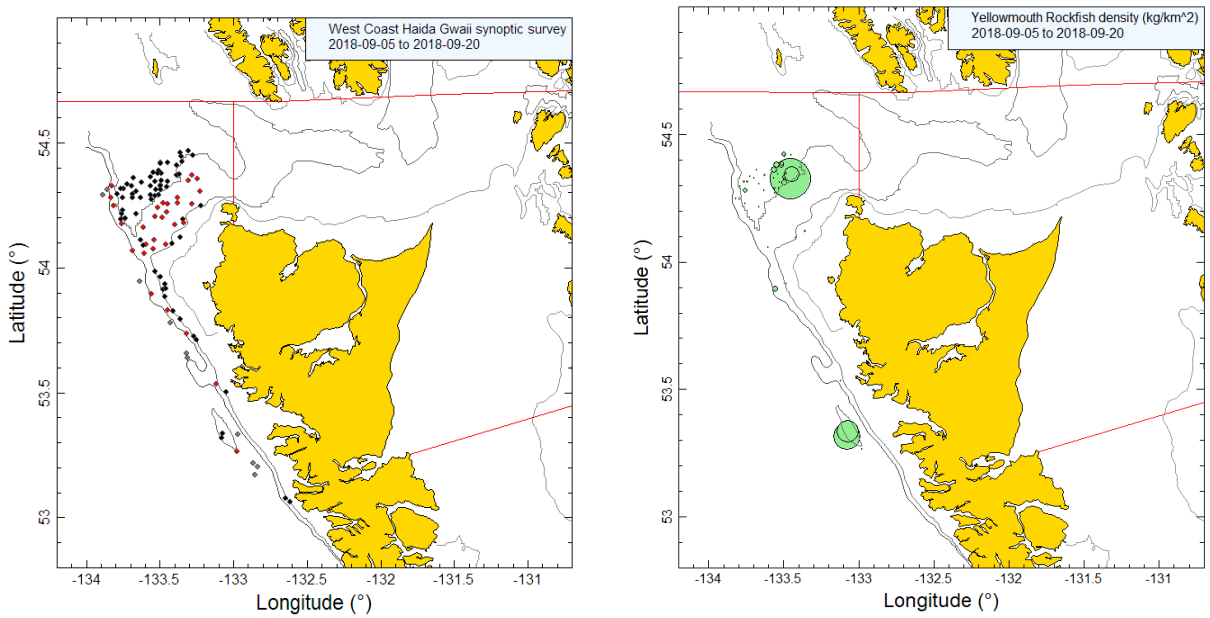

Figure B.43. Tow locations and density plots for the 2018 Nordic Pearl synoptic survey (see Figure B.36 caption).

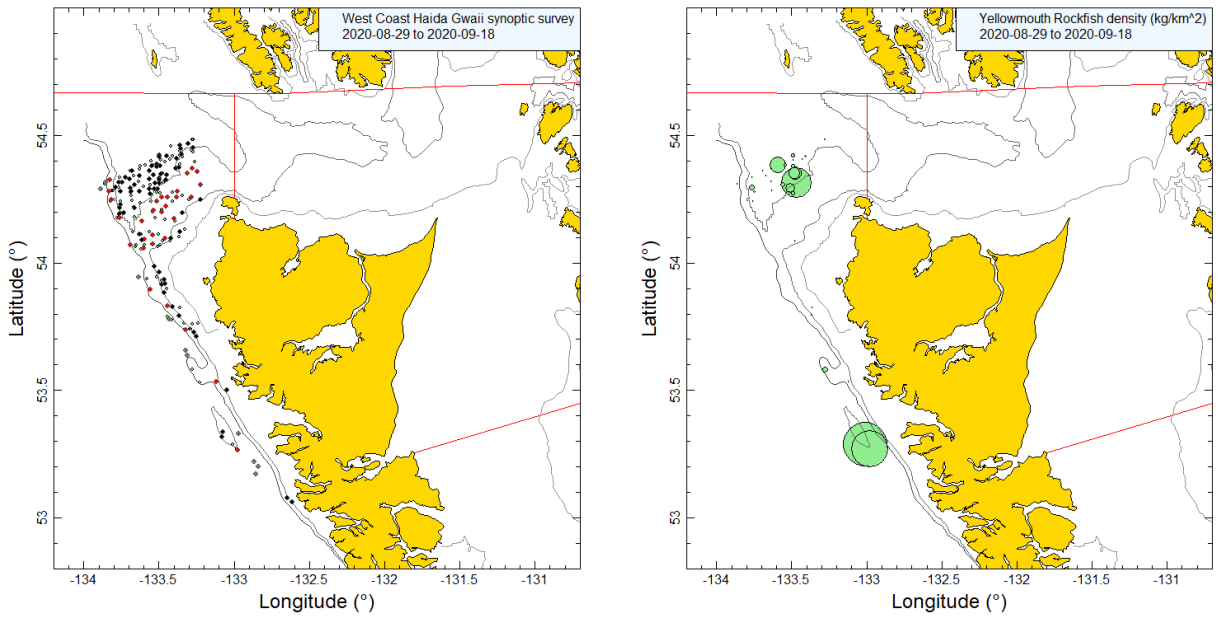

Figure B.44. Tow locations and density plots for the 2020 Nordic Pearl synoptic survey (see Figure B.36 caption).

B.6.2. Results

All nine usable surveys have taken YMR along the shelf edge off the west coast of Graham Island, down to 53°N, the southernmost extent of this survey and into the western reaches of Dixon Entrance (Figure B.36 to Figure B.44). YMR were mainly taken at in a narrow depth range from 200 m to 300 m (5 to 95% quantiles of the starting tow depth=209–299), with 50% of the observations lying in an extremely narrow range between 221 m and 260 m depth (25–75% quantiles, Figure B.45).

The proportion of tows that captured YMR averaged near 20% for the first six surveys and then appeared to rise to near 40% for the final three surveys, ranging from 16 to 41% of tows over the nine survey years and with an overall mean of 26% (243 of 948 tows)(Figure B.47). The median YMR catch weight for positive tows was 7.3 kg/tow and the maximum catch weight across the nine surveys was 3,762 kg in 2020.

Estimated biomass levels for YMR from these trawl surveys vary considerably over the 23 year period, with the first four synoptic surveys (2006–2010) being quite low (all below 400 t and one at only 41 t), followed by four surveys with much larger biomass estimates (Figure B.46; Table B.13). The estimated relative errors (RE) for these surveys are variable and large, ranging from 0.36 in 2012 to 0.73 in 2016 (Table B.13).

Table B.13. Biomass estimates for YMR from the eight west coast Haida Gwaii synoptic surveys used in the stock assessment. Bootstrap bias-corrected confidence intervals and coefficients of variation (CVs) are based on 1000 random draws with replacement.

Survey Year	Biomass (t) (Eq. B.4)	Mean bootstrap biomass (t)	Lower bound biomass (t)	Upper bound biomass (t)	Bootstrap CV	Analytic CV (Eq. B.6)
1997	786.9	811.6	253.3	1,655.0	0.455	0.463
2006	133.9	134.6	48.2	296.8	0.443	0.428
2007	344.9	350.5	101.7	710.6	0.444	0.457
2008	232.4	235.4	58.4	609.0	0.540	0.544
2010	41.1	42.1	11.8	78.4	0.415	0.420
2012	1,039.0	1,036.5	433.2	1,953.5	0.363	0.351
2016	1,454.7	1,446.9	233.5	4,092.1	0.727	0.753
2018	666.0	652.0	165.8	1,565.8	0.549	0.539
2020	932.7	914.3	263.1	2,085.0	0.483	0.487

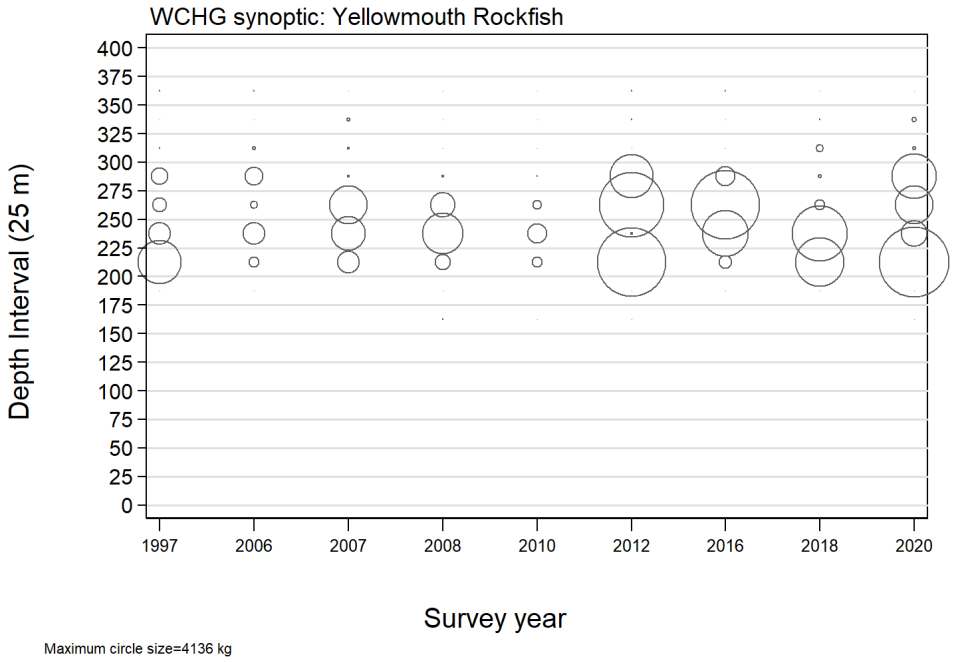

Figure B.45. Distribution of observed weights of YMR by survey year and 25 m depth zone intervals. Catches are plotted at the mid-point of the interval and circles in the each panel are scaled to the maximum value (4,136 kg – 200-225 m interval in 2020). Minimum and maximum depths observed for YMR: 157 m and 558 m, respectively.

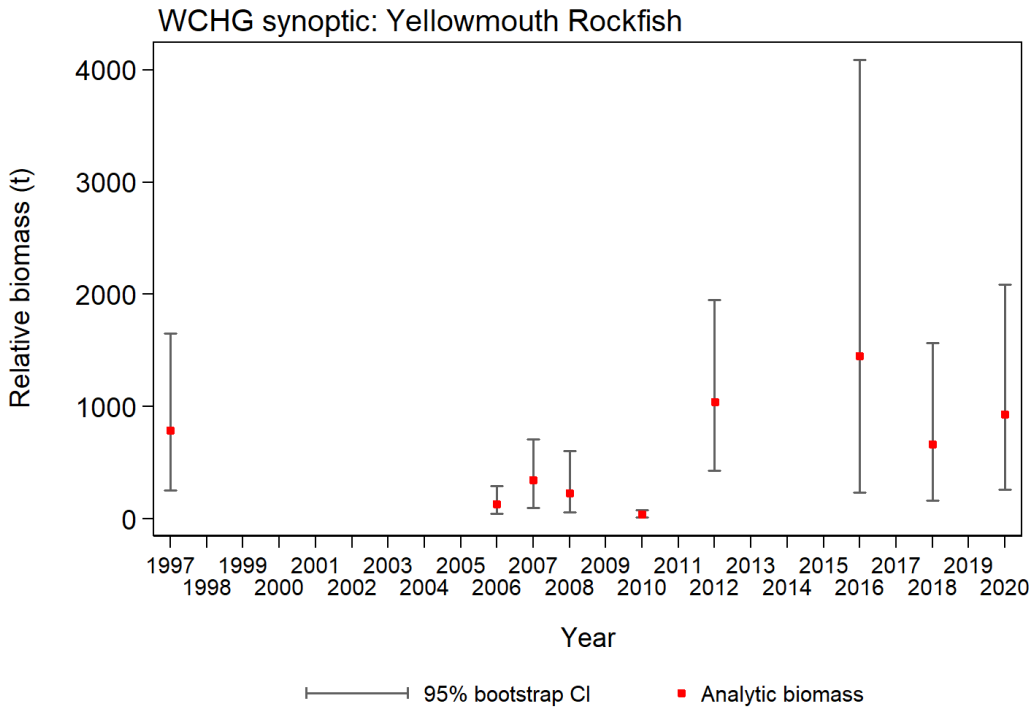

Figure B.46. Biomass estimates for YMR from the 2006 to 2018 west coast Haida Gwaii synoptic surveys (Table B.13). Bias-corrected 95% confidence intervals from 1000 bootstrap replicates are plotted.

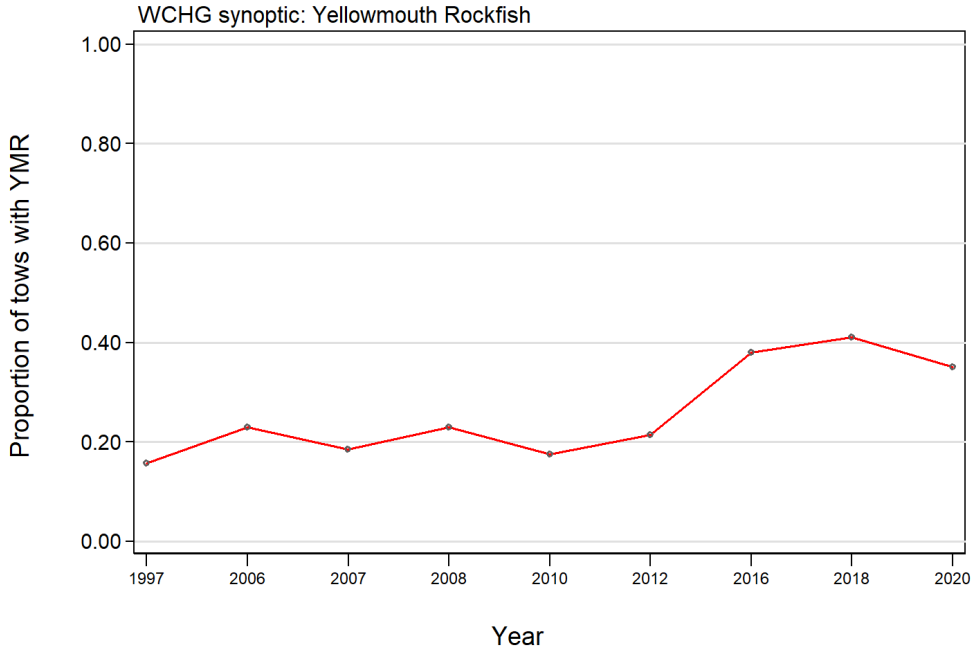

Figure B.47. Proportion of tows by year that contain YMR for the seven west coast Haida Gwaii synoptic surveys.

B.7. REFERENCES – SURVEYS

Anderson, S.C., Keppel, E.A., and Edwards, A.M. 2019. A reproducible data synopsis for over 100 species of British Columbia groundfish. DFO Can. Sci. Advis. Sec. Res. Doc. 2019/041. vii + 321 p.

DFO. 2015a. Yellowtail Rockfish (*Sebastes flavidus*) stock assessment for the coast of British Columbia, Canada. DFO Can. Sci. Advis. Sec. Sci. Advis. Rep. 2015/010. 14 p.

DFO. 2015b. Proceedings of the Pacific regional peer review on Stock assessment for Yellowtail Rockfish (*Sebastes flavidus*) in British Columbia; November 18-19, 2014. DFO Can. Sci. Advis. Sec. Proceed. Ser. 2015/020.

Edwards, A.M., Haigh, R., and Starr, P.J. 2014. Pacific Ocean Perch (*Sebastes alutus*) stock assessment for the west coast of Vancouver Island, British Columbia. DFO Can. Sci. Advis. Sec. Res. Doc. 2013/093: vi + 135 pp.

Edwards, A.M., Starr, P.J., and Haigh, R. 2012. Stock assessment for Pacific ocean perch (*Sebastes alutus*) in Queen Charlotte Sound, British Columbia. DFO Can. Sci. Advis. Sec. Res. Doc. 2011/111: viii + 172 pp.

Harling, W.R., and Davenport, D. 1977. *G.B. Reed* Groundfish Cruise No. 77-3 August 22 to September 8, 1977. Fish. Mar. Serv. Data Rep. 42: iii + 46 pp.

Harling, W.R., Davenport, D., Smith, H.S., Wowchuk, R.H., and Westrheim, S.J. 1971. *G.B. Reed* Groundfish Cruise No. 71-3, October 1-29, 1971. Fish. Res. Board Can. Tech. Rep. 290: 35 pp.

Harling, W.R., Davenport, D., Smith, M.S., Phillips, A.C., and Westrheim, S.J. 1973. *G.B. Reed* Groundfish Cruise No. 73-2, September 5-25, 1973. Fish. Res. Board Can. Tech. Rep. 424: 37 pp.

Nagtegaal, D.A., and Farlinger, S.P. 1980. Catches and trawl locations of the M/V *Southward Ho* during a rockfish exploration and assessment cruise to Queen Charlotte Sound, September 7-27, 1979. Can. Data Rep. Fish. Aquat. Sci. 216: iii + 95 pp.

Nagtegaal, D.A., Leaman, B.M., and Stanley, R.D. 1986. Catches and trawl locations of R/V *G.B. Reed* and M/V *Eastward Ho* during the Pacific Ocean Perch assessment cruise to Queen Charlotte Sound, August-September, 1984. Can. Data Rep. Fish. Aquat. Sci. 611: iii + 109 pp.

Olsen, N., Rutherford, K.L., and Stanley, R.D. 2008. West Coast Queen Charlotte Islands Groundfish Bottom Trawl Survey, August 25th to September 21st , 2008. Can. Manuscr. Rep. Fish. Aquat. Sci. 2858: vii + 50 pp.

Westrheim, S.J. 1966a. Report on the trawling operations of the Canadian Research Vessel *G.B. Reed* from Queen Charlotte Sound, British Columbia to Cape Spencer, Alaska, August 23 to September 7, 1965. Fish. Res. Board Can. Manuscr. Rep. 890: 27 pp.

Westrheim, S.J. 1966b. Report on the trawling operations of the Canadian Research Vessel *G.B. Reed* from Queen Charlotte Sound, British Columbia to Sitka Sound, Alaska, August 24 to September 15, 1966. Fish. Res. Board Can. Manuscr. Rep. 891: 27 pp.

Westrheim, S.J. 1967a. Report on the trawling operations of the Canadian Research Vessel *G.B. Reed* off British Columbia and Southeastern Alaska, September 6 - October 4, 1967. Fish. Res. Board Can. Manuscr. Rep. 934: 8 pp.

Westrheim, S.J. 1967b. *G.B. Reed* groundfish cruise reports, 1963-66. Fish. Res. Board Can. Tech. Rep. 30: ii + 286 pp.

Westrheim, S.J. 1969. Report of the trawling operations of the Canadian Research Vessel *G.B. Reed* off British Columbia, September 1969. Fish. Res. Board Can. Manuscr. Rep. 1063: 6 pp.

Westrheim, S.J., Harling, W.R., and Davenport, D. 1968. *G.B. Reed* Groundfish Cruise No. 67-2, September 6 to October 4, 1967. Fish. Res. Board Can. Tech. Rep. 46: 45 pp.

Westrheim, S.J., Leaman, B.M., Harling, W.R., Davenport, D., Smith, M.S., and Wowchuk, R.M. 1976. *G.B. Reed* Groundfish Cruise No. 76-3, September 8-27, 1976. Fish. Mar. Serv. Data Rec. 21: 47 pp.

Workman, G.D., Olsen, N. and Kronlund, A.R. 1998. Results from a bottom trawl survey of rockfish stocks off the west coast of the Queen Charlotte Islands, September 5 to 23, 1997. Can. Manuscr. Rep. Fish. Aquat. Sci. 2457: viii + 86 p.

Yamanaka, K.L., Richards, L.J., and Workman, G.D. 1996. Bottom trawl survey for rockfish in Queen Charlotte Sound, September 11 to 22, 1995. Can. Manuscr. Rep. Fish. Aquat. Sci. 2362: iv + 116 pp.

APPENDIX C. COMMERCIAL TRAWL CPUE

C.1. INTRODUCTION

Commercial catch and effort data have been used to generate indices of abundance in several ways. The simplest indices are derived from the arithmetic mean or geometric mean of catch divided by an appropriate measure of effort (Catch Per Unit Effort or CPUE) but such indices make no adjustments for changes in fishing practices or other non-abundance factors that may affect catch rates. Consequently, methods to standardise for changes to vessel configuration, the timing or location of catch and other possible effects have been developed to remove potential biases to CPUE that may result from such changes. In these models, abundance is represented as a "year effect" and the dependent variable is either an explicitly calculated CPUE represented as catch divided by effort, or an implicit CPUE represented as catch per tow or catch per record. In the latter case, additional effort terms can be offered as explanatory variables, allowing the model to select the effort term with the greatest explanatory power. It is always preferable to standardise for as many factors as possible when using CPUE as a proxy for abundance. Unfortunately, it is often not possible to adjust for factors that might affect the behaviour of fishers, particularly economic factors, resulting in indices that may not entirely reflect the underlying stock abundance.

C.2. METHODS

C.2.1. Arithmetic and Unstandardised CPUE

Arithmetic and unstandardised CPUE indices provide potential measures of relative abundance, but are generally considered unreliable because they fail to take into account changes in the fishery, including spatial and temporal changes as well as behavioural and gear changes. They are frequently calculated because they provide a measure of the overall effect of the standardisation procedure.

Arithmetic CPUE (Eq. C.1) in year y was calculated as the total catch for the year divided by the total effort in the year using Eq. C.1:

Eq. C.1 $$\hat{A}_y = \sum_{i=1}^{n_y} C_{i,y} \Big/ \sum_{i=1}^{n_y} E_{i,y}$$

where $C_{i,y}$ is the field name `[catch]` and $E_{i,y}$ is the field name `[tows]` or `[hours_fished]` in the data object for record i in year y; n_y is the number of records in year y.

Unstandardised (geometric) CPUE assumes a log-normal error distribution. An unstandardised index of CPUE (Eq. C.2) in year y was calculated as the geometric mean of the ratio of catch to effort for each i in year y, using Eq. C.2:

Eq. C.2 $$\hat{G}_y = \exp\left[\frac{1}{n_y}\sum_{i=1}^{n_y} \ln\left(\frac{C_{i,y}}{E_{i,y}}\right)\right].$$

C.2.2. Standardised CPUE

These models are preferred over the unstandardised models described above because they can account for changes in fishing behaviour and other factors which may affect the estimated abundance trend, as long as the models are provided with adequate data. In the models

described below, catch per record is used as the dependent variable and the associated effort is treated as an explanatory variable.

C.2.2.1. Lognormal Model

Standardised CPUE often assumes a lognormal error distribution, with explanatory variables used to represent changes in the fishery. A standardised CPUE index (Eq. C.3) is calculated from a generalised linear model (GLM) (Quinn and Deriso 1999) using a range of explanatory variables including `[Year]`, `[month]`, `[depth]`, `[vessel]` and other available factors:

Eq. C.3 $$\ln\left(I_i\right) = B + Y_{y_i} + \alpha_{a_i} + \beta_{b_i} + ... + f\left(\chi_i\right) + f\left(\delta_i\right) + ... + \varepsilon_i$$

where I_i = C_i or catch;

B = the intercept;

Y_{y_i} = year coefficient for the year corresponding to record i;

α_{a_i} and β_{b_i} = coefficients for factorial variables a and b corresponding to record i;

$f\left(\chi_i\right)$ and $f\left(\delta_i\right)$ are polynomial functions (to the 3rd order) of the continuous variables χ_i and δ_i corresponding to record i;

ε_i = an error term.

The actual number of factorial and continuous explanatory variables in each model depends on the model selection criteria and the nature of the data. Because each record represents a single tow, $C_{i,y}$ has an implicit associated effort of one tow. Hours fished for the tow is represented on the right-hand side of the equation as a continuous (polynomial) variable.

Note that calculating standardised CPUE with Eq. C.3, while assuming a lognormal distribution and without additional explanatory variables, is equivalent to using Eq. C.2 as long as the same definition for $E_{i,y}$ is used.

Canonical coefficients and standard errors were calculated for each categorical variable (Francis 1999). Standardised analyses typically set one of the coefficients to 1.0 without an error term and estimate the remaining coefficients and the associated error relative to the fixed coefficient. This is required because of parameter confounding. The Francis (1999) procedure rescales all coefficients so that the geometric mean of the coefficients is equal to 1.0 and calculates a standard error for each coefficient, including the fixed coefficient.

Coefficient-distribution-influence (CDI) plots are visual tools to facilitate understanding of patterns which may exist in the combination of coefficient values, distributional changes, and annual influence (Bentley et al. 2012). CDI plots were used to illustrate each explanatory variable added to the model.

C.2.2.2. Binomial Logit Model

The procedure described by Eq. C.3 is necessarily confined to the positive catch observations in the data set because the logarithm of zero is undefined. Observations with zero catch were modelled by fitting a logit regression model based on a binomial distribution and using the presence/absence of the species being modelled as the dependent variable (where 1 is substituted for $\ln(I_i)$ in Eq. C.3 if it is a successful catch record and 0 if it is not successful) and using the same data set. Explanatory factors are estimated in the model in the same manner as described in Eq. C.3. Such a model provides an alternative series of standardised coefficients of

relative annual changes that is analogous to the series estimated from the lognormal regression.

C.2.2.3. Combined Model

A combined model (sometimes termed a “hurdle” model), integrating the two sets of relative annual changes estimated by the lognormal and binomial models, can be estimated using the delta distribution, which allows zero and positive observations (Fletcher et al. 2005). Such a model provides a single index of abundance which integrates the signals from the positive (lognormal) and binomial series.

This approach uses the following equation to calculate an index based on the two contributing indices, after standardising each series to a geometric mean=1.0:

Eq. C.4 $$ {}^{C}Y_{y} = {}^{L}Y_{y}\,{}^{B}Y_{y} $$

where ${}^{C}Y_{y}$ = combined index for year y,

${}^{L}Y_{y}$ = lognormal index for year y,

${}^{B}Y_{y}$ = binomial index for year y

Francis (2001) suggests that a bootstrap procedure is the appropriate way to estimate the variability of the combined index. Therefore, confidence bounds for the combined model were estimated using a bootstrap procedure based on 100 replicates, drawn with replacement, operated by re-estimating each component model and then repeating Eq. C.4 for each bootstrap replicate.

The index series plots below present normalised values, i.e., each series is divided by its geometric mean so that the series is centred on 1. This facilitates comparison among series.

C.3. PRELIMINARY INSPECTION OF THE DATA

The analyses reported in this Appendix are based on tow-by-tow total catch (landings + discards) data collected over the period 1996–2020 for which detailed positional data for every tow are available. Each tow has an estimate of retained and discarded catch because of the presence of an observer on board the vessel. These data are held in the DFO PacHarvTrawl (PacHarvest) and GFFOS databases (Fisheries and Oceans Canada, Pacific Region, Groundfish Data Unit).

Tow-by-tow catch and effort data for Yellowmouth Rockfish (YMR) from the BC trawl fishery operating from Juan de Fuca Strait to the Dixon Entrance from 1996 to 2020 were selected using the following criteria:

- Tow start date between 1 January 1996 and 31 December 2020;
- Bottom trawl type (includes ‘unknown’ trawl gear);
- Fished in PMFC regions: 3C, 3D, 5A, 5B, 5C, 5D or 5E;
- Fishing success code <=1 (code 0= unknown; code 1= useable);
- Catch of at least one fish or invertebrate species (no water hauls or inanimate object tows);
- Valid depth field;
- Valid latitude and longitude co-ordinates;

- Valid estimate of time towed that was > 0 hours and <= 6 hours.

Each record represents a single tow, which results in equivalency between the number of records and number of tows. Catch per record can therefore be used to represent CPUE because each record (tow) has an implicit effort component.

The catch and effort data for YMR were treated as a single area (totBC) representing all catch outside of the Strait of Georgia, upper Johnstone Strait and Juan de Fuca Strait, based on the declared distribution of trawl catches (see Appendix A). Only bottom trawl data were used as this is by far the most prevalent capture method for this species. Figure C.1 plots the distribution of depth for all successful YMR bottom trawl tows in the designated region. A depth range for this analysis was selected from this plot and is summarised in Table C.1.

Table C.1. Depth bins used in CPUE analyses of stock by gear.

Analysis	Trawl Gear	First year	Depth range (m)	Upper bound effort (h)	Minimum bin + records	N depth bins	N latitude bins	N locality bins
totBC (3CD5ABCDE)	Bottom trawl	1996	100–425	6	140	13	31	33

Vessel qualification criteria for the bottom trawl fisheries were based on number of trips per year and number of years fishing to avoid including vessels which only occasionally captured YMR. The vessel qualification criteria used in this analysis appear in Table C.2 and the distribution of tows by vessel and year is presented in Figure C.2. Once a vessel was selected, all data for the qualifying vessel were included, regardless of the number of trips in a year. Table C.2 shows the number of vessels used in this analysis and the fraction (83%) of the total catch represented in the core fleet. There was good vessel overlap across years (Figure C.2) in the fishery, where 21 of the 32 core vessels participated in the fishery for at least 20 years of the analysis.

Table C.2. Vessel qualification criteria used in CPUE analyses of stock by gear.

		Vessel selection criteria			Data set characteristics				
Analysis	Trawl Gear	N years	N trips	Minimum positive Records	N vessels	% total catch[1]	catch (t)	Total records	Positive records
totBC (3CD5ABCDE)	Bottom	5	10	100	32	83	26,499	134,199	37,038

[1] total catch calculated with all filters applied except for the vessel and depth restrictions

Table C.3 reports the explanatory variables offered to the model, based on the tow-by-tow information in each record, with the number of available categories varying as indicated in Table C.1, Table C.2 and Table C.3. Table C.4 summarises the core vessel data used in the analysis by calendar year, including the number of records (tows), the total hours fished and the associated YMR catch. This table also tracks the annual proportion of tows which did not report YMR.

Table C.3. Explanatory variables offered to the CPUE model, based on the tow-by-tow information.

Variable	Data type
Year	25 categories (calendar years)
Hours fished	continuous: 3rd order polynomial
Month	12 categories
DFO locality	Fishing locality areas identified by Rutherford (1995) (includes a final aggregated category, Table C.1)
Latitude	Latitude aggregated by 0.1° bands starting at 48°N (includes a final aggregated category, Table C.1)
Vessel	See Table C.2 for number of categories by analysis (no final aggregated category)
Depth	See Table C.1 for number of categories by analysis (no final aggregated category)
PFMC major area	7 categories: PMFC areas 3C, 3D, 5A, 5B, 5C, 5D, 5E

Table C.4. Summary data for the YMR bottom trawl fishery in totBC (3CD5ABCDE) by year for the core data set (after applying all data filters and selection of core vessels).

Year	Number vessels[1]	Number trips[1]	Number tows[1]	Number records[1]	Number records[2]	% zero records[2]	Total catch (t)[1]	Total hours[1]	CPUE (kg/h) (Eq. C.1)
1996	31	160	788	788	4,238	81.4	690.2	1,263	546.5
1997	31	284	1,529	1,529	5,477	72.1	1115.5	2,786	400.4
1998	30	342	2,005	2,005	6,411	68.7	1300.1	3,925	331.2
1999	29	380	1,952	1,952	6,702	70.9	1301.1	3,757	346.3
2000	30	418	2,363	2,363	7,427	68.2	1483.5	4,151	357.4
2001	30	400	2,235	2,235	6,917	67.7	1347.5	3,642	370.0
2002	30	450	2,213	2,213	7,465	70.4	1491.1	3,594	414.9
2003	30	461	2,247	2,247	7,311	69.3	1478.6	3,474	425.6
2004	30	407	2,045	2,045	7,007	70.8	1548.3	3,296	469.7
2005	28	396	1,880	1,880	7,564	75.1	1515.6	3,423	442.8
2006	27	364	1,920	1,920	6,362	69.8	1382.1	3,758	367.8
2007	27	310	1,744	1,744	5,688	69.3	994.5	3,273	303.9
2008	25	252	1,264	1,264	4,900	74.2	774.7	2,428	319.0
2009	25	282	1,586	1,586	5,289	70.0	1243.4	2,853	435.8
2010	24	251	1,607	1,607	5,364	70.0	970.2	3,167	306.3
2011	24	212	1,268	1,268	4,879	74.0	902.0	2,486	362.8
2012	23	186	1,239	1,239	4,338	71.4	700.9	2,496	280.8
2013	22	177	906	906	4,608	80.3	770.4	1,798	428.5
2014	23	171	754	754	4,248	82.3	605.0	1,405	430.8
2015	23	198	883	883	4,673	81.1	563.0	1,634	344.5
2016	18	205	1,159	1,159	4,143	72.0	765.3	2,330	328.4
2017	19	209	1,101	1,101	4,023	72.6	816.9	2,249	363.3
2018	16	162	973	973	3,586	72.9	794.4	1,926	412.4
2019	13	142	806	806	2,975	72.9	1017.7	1,430	711.6
2020	13	97	571	571	2,604	78.1	926.6	1,071	865.1

[1] calculated for tows with YMR catch >0; [2] calculated for all tows

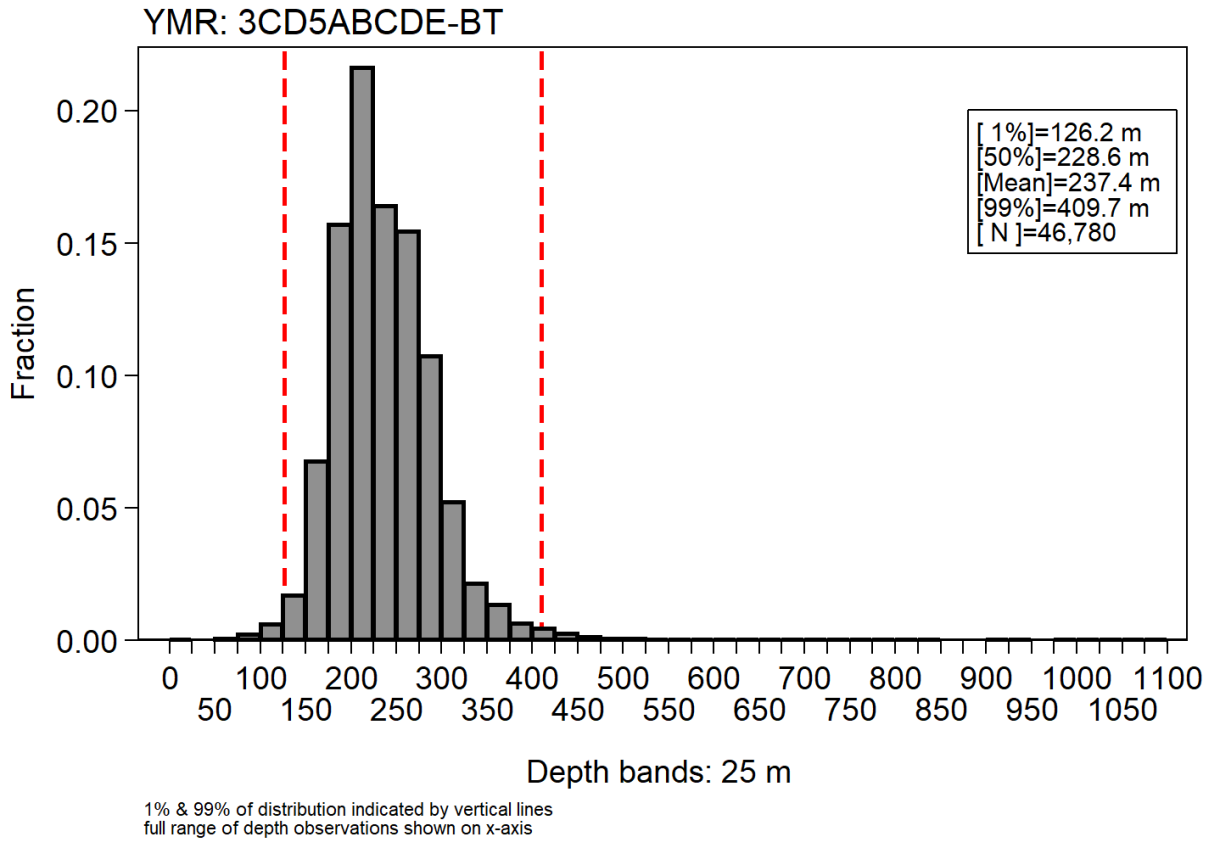

Figure C.1. Depth distribution of tows capturing YMR for the totBC (3CD5ABCDE) bottom trawl (BT) GLM analyses from 1996 to 2020 using 25 m intervals (each bin is labelled with the upper bound of the interval). Vertical lines indicate the 1% and 99% percentiles.

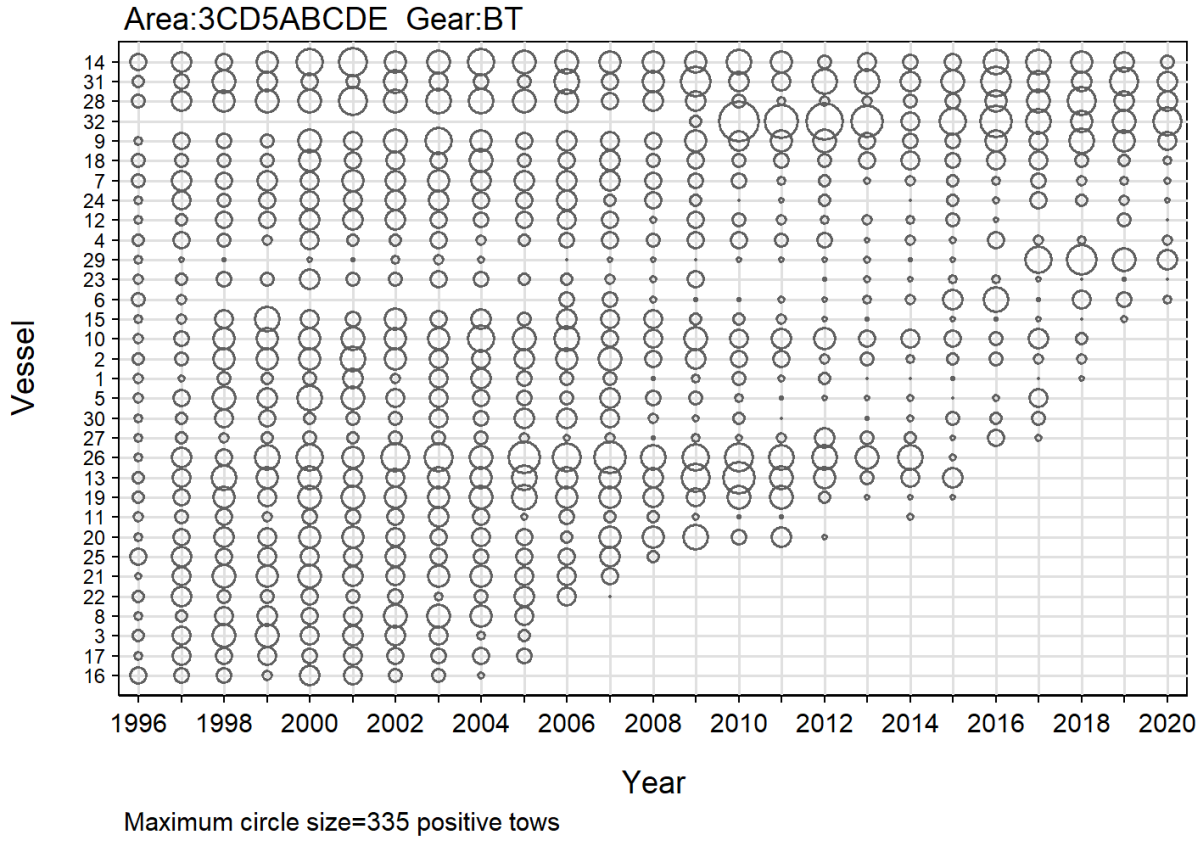

Figure C.2. Bubble plot showing vessel participation (number positive tows) by the core fleet in the totBC (3CD5ABCDE) BT GLM analyses. Vessels are coded in ascending order total effort by year.

C.4. RESULTS

C.4.1. totBC (3CD5ABCDE)

C.4.1.1. Bottom trawl fishery: positive lognormal model

A standardised lognormal General Linear Model (GLM) analysis was performed on positive catch records from the bottom trawl tow-by-tow data set generated as described in Section C.3. Eight explanatory variables (Table C.3) were offered to the model and `ln(catch)` was used as the dependent variable, where catch is the total by weight of landed plus discarded YMR in each record (tow) (Eq. C.3). The resulting CPUE index series is presented in Figure C.3.

The `[Year]` categorical variable was forced as the first variable in the model without regard to its effect on the model deviance. The remaining seven variables were offered sequentially, with a stepwise acceptance of the remaining variables with the best AIC. This process was continued until the improvement in the model R^2 was less than 1% (Table C.5). This model selected five of the seven remaining explanatory variables, including `[0.1°Latitude_bands]`, `[Depth]`, `[DFO locality]`, `[Vessel]`, and `[Month]` in addition to `[Year]`. The final lognormal model accounted for 30% of the total model deviance (Table C.5), with the year variable explaining less than 0.1% of the model deviance.

Model residuals showed a satisfactory fit to the underlying lognormal distributional assumption, with only some skewness in the body of the distribution and few deviations in the tails outside of +/- 2 standard errors (Figure C.4).

A stepwise plot showing the effect on the year indices as each explanatory variable was introduced into the model shows that the standardisation procedure made upward adjustments to the unstandardised series in the first six years of the series and a downward adjustment in 2020 after the introduction of the [DFO locality]variable, resulting in a U-shaped annual trend (Figure C.5).

*Table C.5. Order of acceptance of variables into the lognormal model of positive total mortalities (verified landings plus discards) of YMR totBC (3CD5ABCDE) bottom trawl fishery with the amount of explained deviance (R^2) for each variable. Variables accepted into the model are identified in bold with an *. [Year] was forced as the first variable.*

Variable	1	2	3	4	5	6	7
Year*	**0.0100**	-	-	-	-	-	-
0.1° Latitude bands*	0.1634	**0.1745**	-	-	-	-	-
Depth bands*	0.0519	0.0615	**0.2169**	-	-	-	-
DFO locality*	0.1623	0.1745	0.2174	**0.2612**	-	-	-
Vessel*	0.0458	0.0587	0.2013	0.2459	**0.2857**	-	-
Month*	0.0068	0.0176	0.1854	0.2227	0.2695	**0.2978**	-
PFMC major area	0.0705	0.0799	0.1865	0.2335	0.2643	0.2886	0.3010
Hours fished	0.0053	0.0147	0.1751	0.2175	0.2628	0.2876	0.2994
Improvement in deviance	0	0.1645	0.0424	0.0443	0.0245	0.0122	0.0032

CDI plots of the five explanatory variables introduced to the model in addition to [Year] show progressive impacts at the beginning of the series. There was adjustment to the first six years in the unstandardised series (Figure C.5) with the successive addition of the variables [0.1°Latitude_bands] (Figure C.6), [Depth_bands] (Figure C.7), [Vessel] (Figure C.9), and [Month] (Figure C.10). The variable [DFO locality] (Figure C.8) had little impact on the first six years of the series but was the cause of the sharp drop in the 2020 CPUE.

The lognormal year indices show a declining trend from the beginning of the series to about 2012, followed by a flattening of the series, with an upturn in the final two years of the series (Figure C.3). This model has reasonable diagnostics and shows reasonable changes from the unstandardised series.

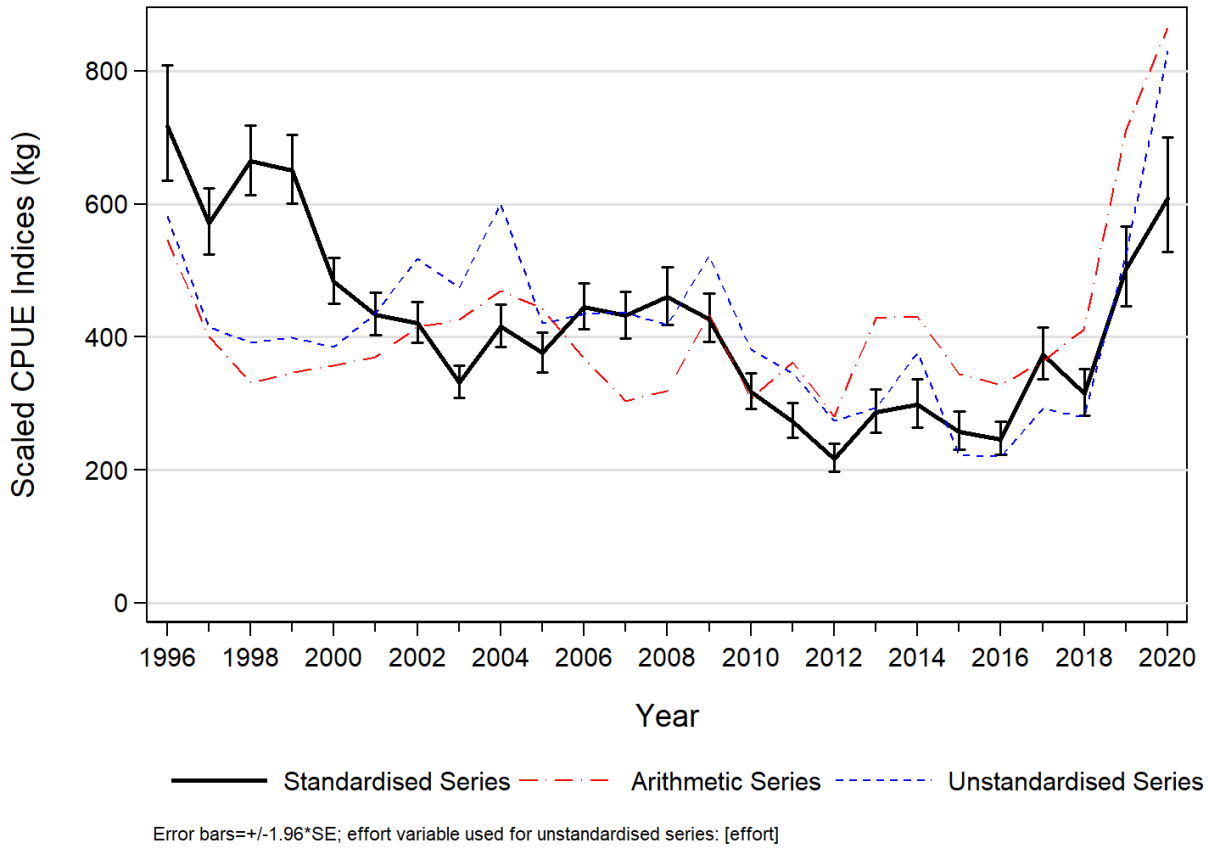

Figure C.3. Three positive catch CPUE series for YMR from 1996 to 2020 in the totBC (3CD5ABCDE) bottom trawl fishery. The solid line is the standardised CPUE series from the lognormal model (Eq. C.3). The arithmetic series (Eq. C.1) and the unstandardised series (Eq. C.2) are also presented. All three series have been scaled to same geometric mean.

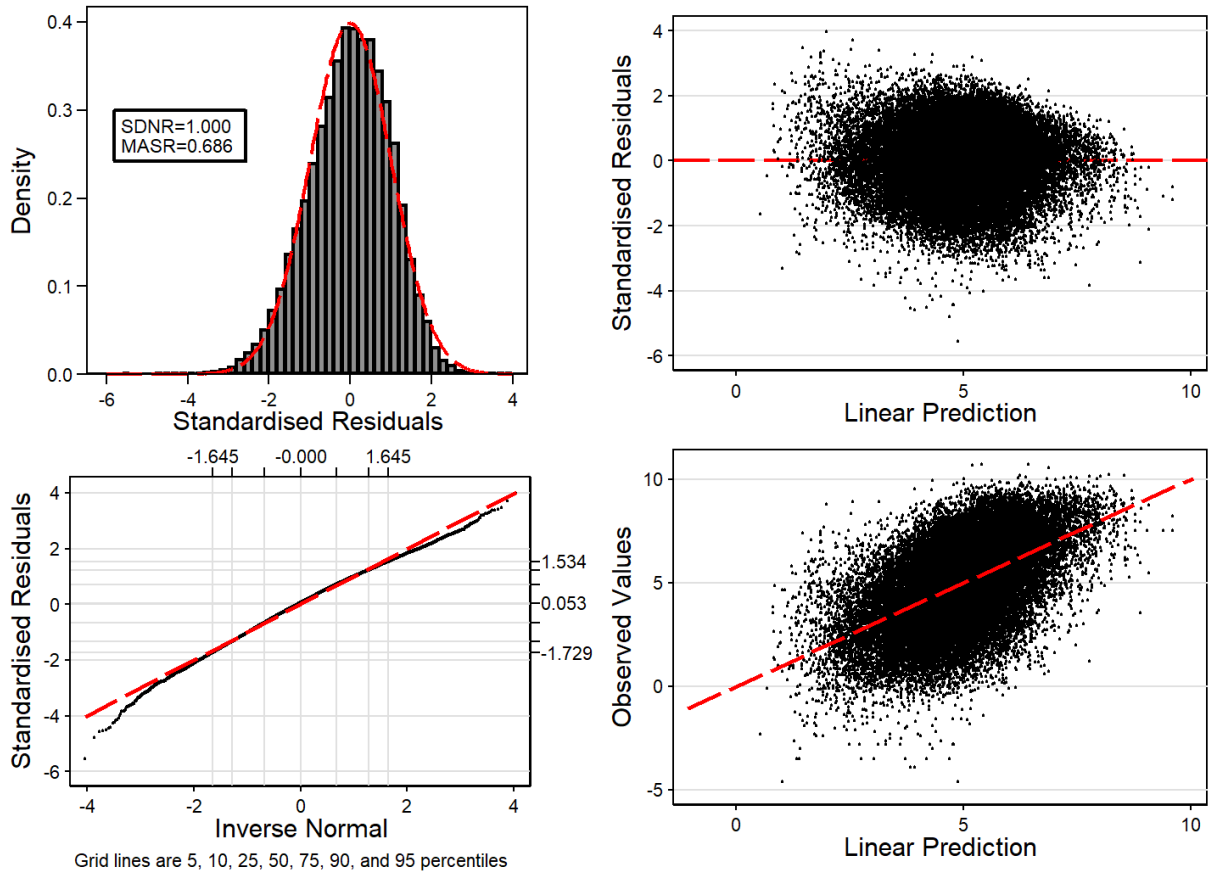

Figure C.4. Residual diagnostic plots for the GLM lognormal analysis for YMR in totBC (3CD5ABCDE) bottom trawl fishery. Upper left: histogram of the standardised residuals with overlaid lognormal distribution (SDNR = standard deviation of normalised residuals. MASR = median of absolute standardised residuals). Lower left: Q-Q plot of the standardised residuals with the outside horizontal and vertical lines representing the 5th and 95th percentiles of the theoretical and observed distributions. Upper right: standardised residuals plotted against the predicted CPUE. Lower right: observed CPUE plotted against the predicted CPUE.

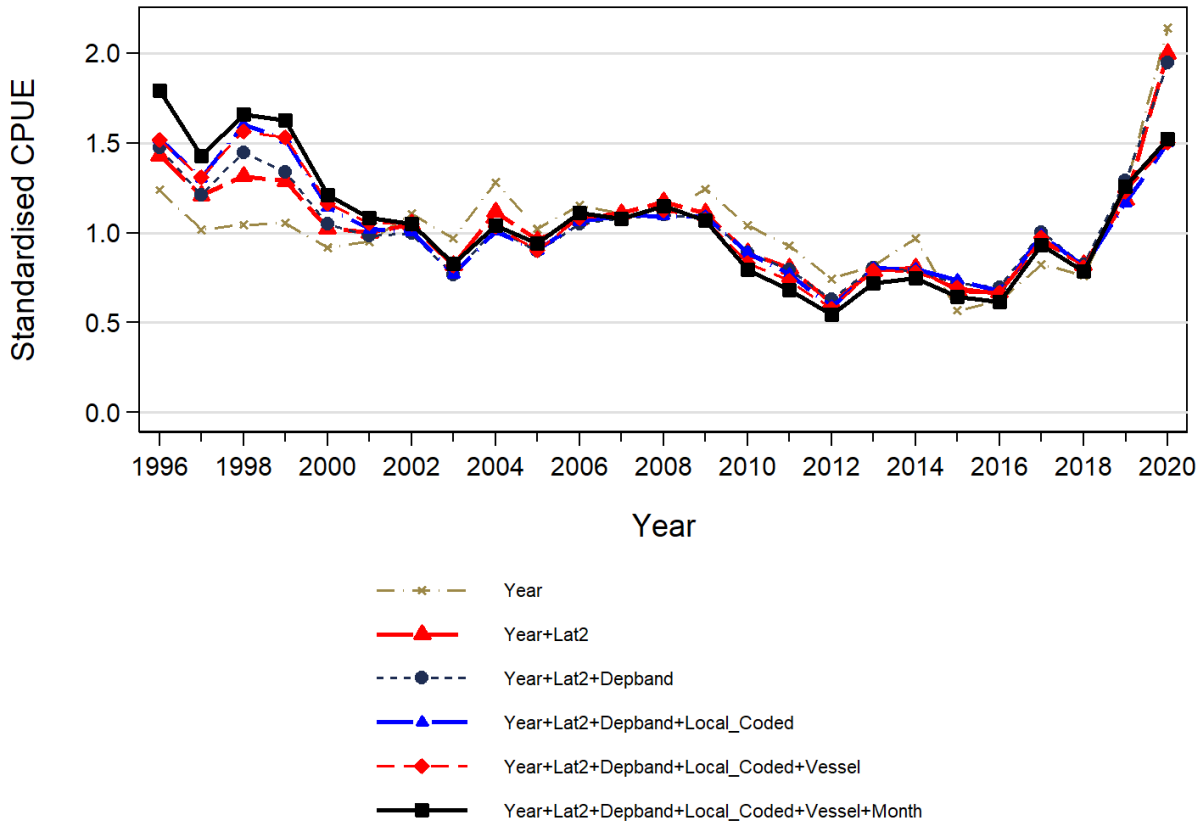

Figure C.5. Plot showing the year coefficients after adding each successive term of the standardised lognormal regression analysis for YMR in the totBC (3CD5ABCDE) bottom trawl fishery. The final model is shown with a thick solid black line. Each line has been scaled so that the geometric mean equals 1.0.

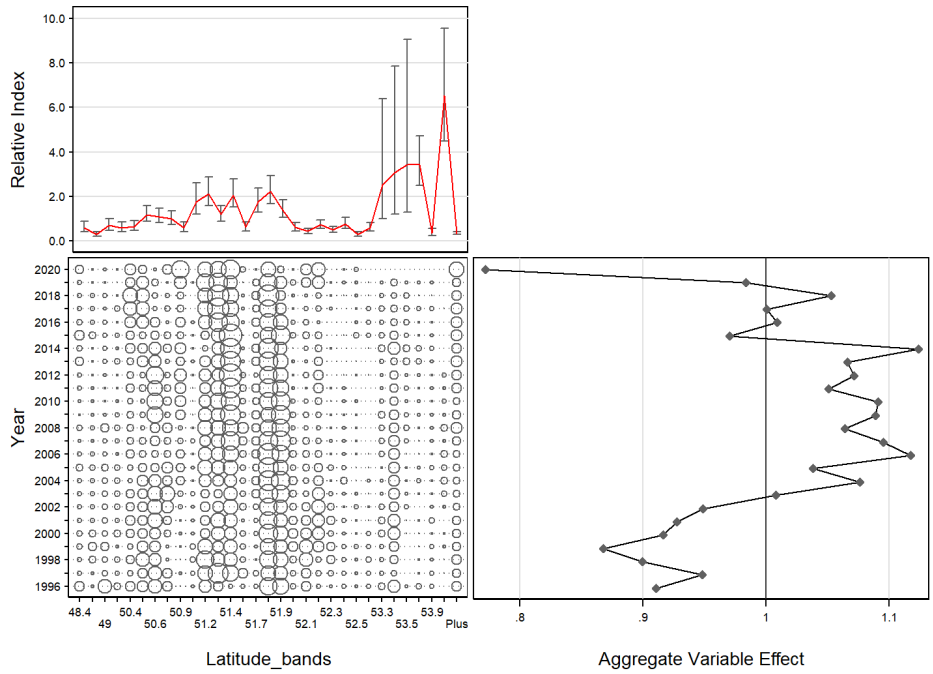

Figure C.6. CDI plot showing the effect of introducing the continuous variable [0.1°Latitude bands] to the lognormal regression model for YMR in the totBC (3CD5ABCDE) bottom trawl fishery. Each plot consists of subplots showing the effect by level of variable (top left), the relative distribution by year of variable records (bottom left), and the cumulative effect of variable by year (bottom right).

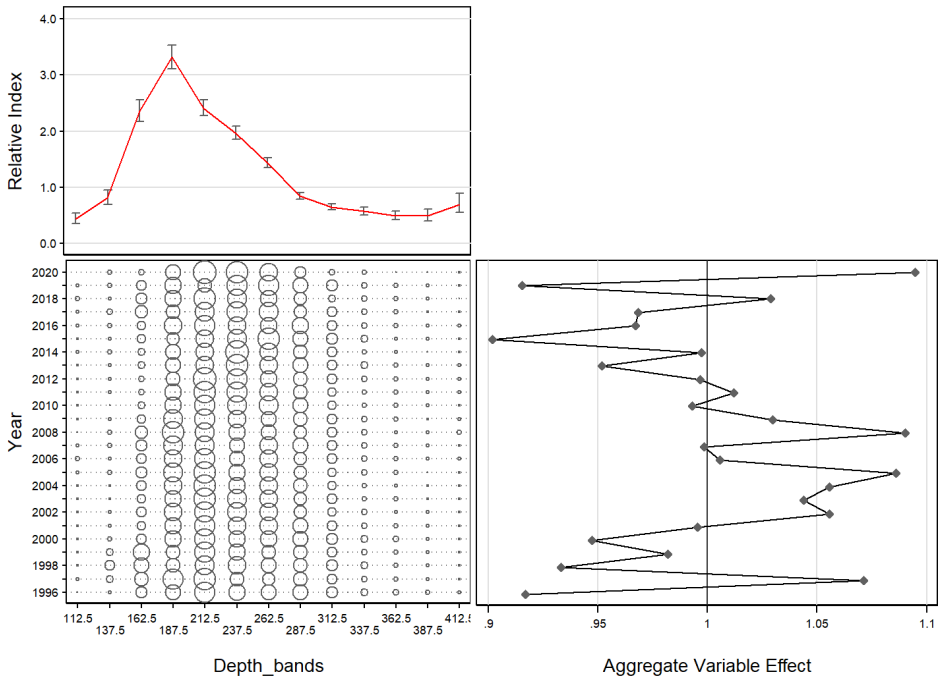

Figure C.7. CDI plot showing the effect of introducing the categorical variable [Depth bands] to the lognormal regression model for YMR in the totBC (3CD5ABCDE) bottom trawl fishery. Each plot consists of subplots showing the effect by level of variable (top left), the relative distribution by year of variable records (bottom left), and the cumulative effect of variable by year (bottom right).

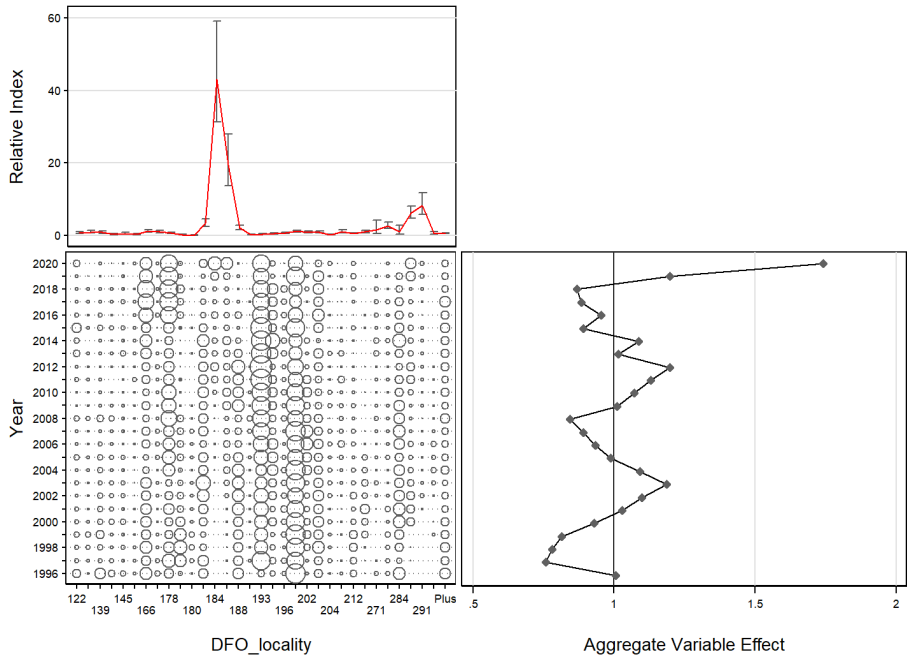

Figure C.8. CDI plot showing the effect of introducing the categorical variable [DFO locality] to the lognormal regression model for YMR in the totBC (3CD5ABCDE) bottom trawl fishery. Table C.6 provides the definitions for the coded values used for each locality in the above plot. Each plot consists of subplots showing the effect by level of variable (top left), the relative distribution by year of variable records (bottom left), and the cumulative effect of variable by year (bottom right).

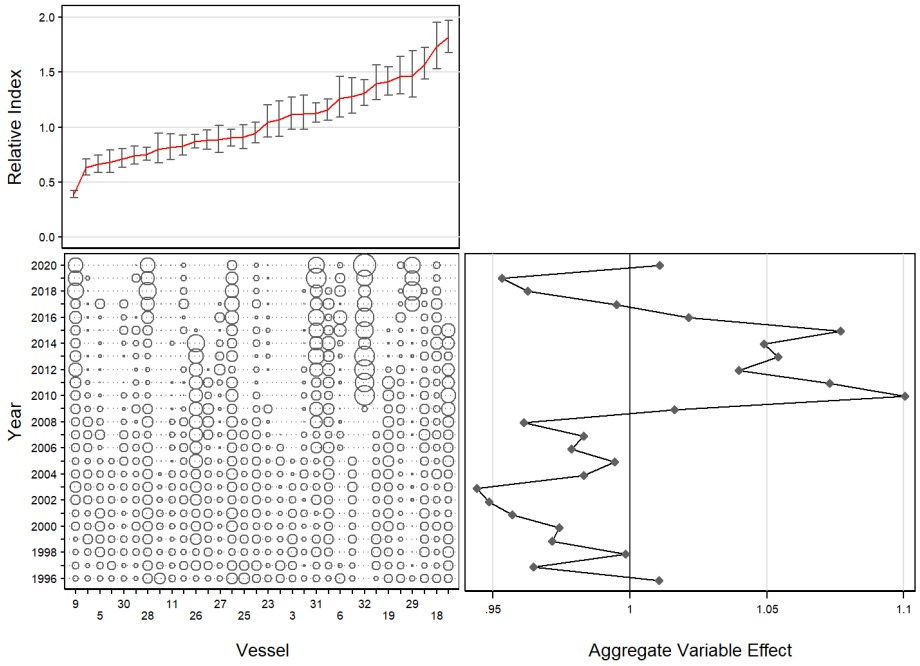

Figure C.9. CDI plot showing the effect of introducing the continuous variable [vessel] to the lognormal regression model for YMR in the totBC (3CD5ABCDE) bottom trawl fishery. Each plot consists of subplots showing the effect by level of variable (top left), the relative distribution by year of variable records (bottom left), and the cumulative effect of variable by year (bottom right).

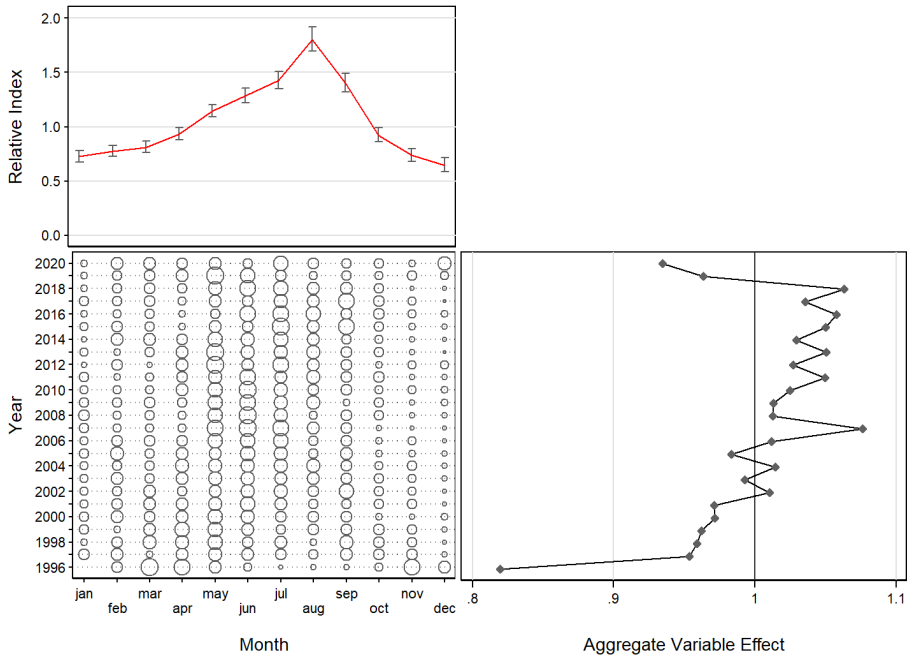

Figure C.10. CDI plot showing the effect of introducing the categorical variable [Month] to the lognormal regression model for YMR in the totBC (3CD5ABCDE) bottom trawl fishery. Each plot consists of subplots showing the effect by level of variable (top left), the relative distribution by year of variable records (bottom left), and the cumulative effect of variable by year (bottom right).

Table C.6. Definition of locality codes used in Figure C.8. Localities marked in grey (with asterisks) were removed for a sensitivity analysis described in Section C.6.

Code	PFMC Major	DFO Minor	Minor Name	Locality Name	Lognormal Index
122	3	23	Big Bank	Deep Big Bank/Barkley Canyon	0.726
138	3	24	Clayoquot Sd.	Father Charles Canyon	0.943
139	3	24	Clayoquot Sd.	Clayoquot Canyon	0.869
140	3	24	Clayoquot Sd.	South Estevan	0.333
145	4	25	Estevan-Esperanza Inlet	North Estevan	0.618
146	4	25	Estevan-Esperanza Inlet	Nootka	0.332
166	4	27	Quatsino Sd.	Quatsino Sound	1.181
177	5	11	Cape Scott-Triangle	Unknown	0.973
178	5	11	Cape Scott-Triangle	Triangle	0.638
179	5	11	Cape Scott-Triangle	Cape Scott Spit	0.230
180	5	11	Cape Scott-Triangle	Mexicana	0.069
*183	5	11	Cape Scott-Triangle	South Scott Islands	3.429
*184	5	11	Cape Scott-Triangle	W. Triangle (25 Mi.)	43.082
*187	5	11	Cape Scott-Triangle	South Triangle	19.575
188	5	11	Cape Scott-Triangle	Pisces Canyon	2.123
192	6	8	Goose Island Bank	NE Goose	0.229
193	6	8	Goose Island Bank	SE Goose	0.360
195	6	8	Goose Island Bank	SW Goose	0.560
196	6	8	Goose Island Bank	Mitchell's Gully	0.624
197	6	8	Goose Island Bank	SE Cape St. James	1.152
202	6	8	Goose Island Bank	SW Middle Bank	0.911
203	6	8	Goose Island Bank	Outside Cape St. James	0.966
204	6	8	Goose Island Bank	West Virgin Rocks	0.223
205	6	8	Goose Island Bank	Below Middle Bank	1.096
212	7	2	2B-East	South Morseby	0.573

Code	PFMC Major	DFO Minor	Minor Name	Locality Name	Lognormal Index
230	7	7	6-Central Morseby-Milbanke Sd.	Unknown	1.023
271	9	31	2A West - Rennell Sound	Rennell Sound	1.549
272	9	31	2A West - Rennell Sound	Frederick Island	2.620
284	9	31	2A West - Rennell Sound	South Hogback	1.080
*287	9	34	2B West - Anthony Island	Anthony Island	6.180
*291	9	34	2B West - Anthony Island	Flamingo Inlet	8.350
299	9	35	1 West - Langara	Rockpile-Langara	0.667

C.4.1.2. Bottom trawl fishery: binomial logit model

The same explanatory variables used in the lognormal model were offered sequentially to this model, beginning with the year categorical variable, until the improvement in the model R^2 was less than 1% (Table C.7). A binary variable which equalled 1 for positive catch tows and 0 for zero catch tows was used as the dependent variable. The final binomial model accounted for 44% of the total model deviance, with the year variable explaining <1% of the model deviance.

*Table C.7. Order of acceptance of variables into the binomial model of presence/absence of verified landings plus discards of YMR in totBC (3CD5ABCDE) bottom trawl fishery with the amount of explained deviance (R^2) for each variable. Variables accepted into the model are marked in bold with an *. Year was forced as the first variable.*

Variable	1	2	3	4	5	6
Year*	**0.0074**	-	-	-	-	-
DFO locality*	0.2814	**0.2867**	-	-	-	-
Depth bands*	0.2253	0.2352	**0.3983**	-	-	-
0.1° Latitude bands*	0.2543	0.2590	0.3305	**0.4223**	-	-
Month*	0.0176	0.0244	0.2973	0.4150	**0.4357**	-
Vessel	0.0248	0.0349	0.2931	0.4032	0.4267	0.4410
Hours fished	0.0057	0.0129	0.2881	0.3991	0.4229	0.4360
PFMC major area	0.1436	0.1488	0.2964	0.4023	0.4253	0.4393
Improvement in deviance	0	0.2792	0.1117	0.024	0.0134	0.0053

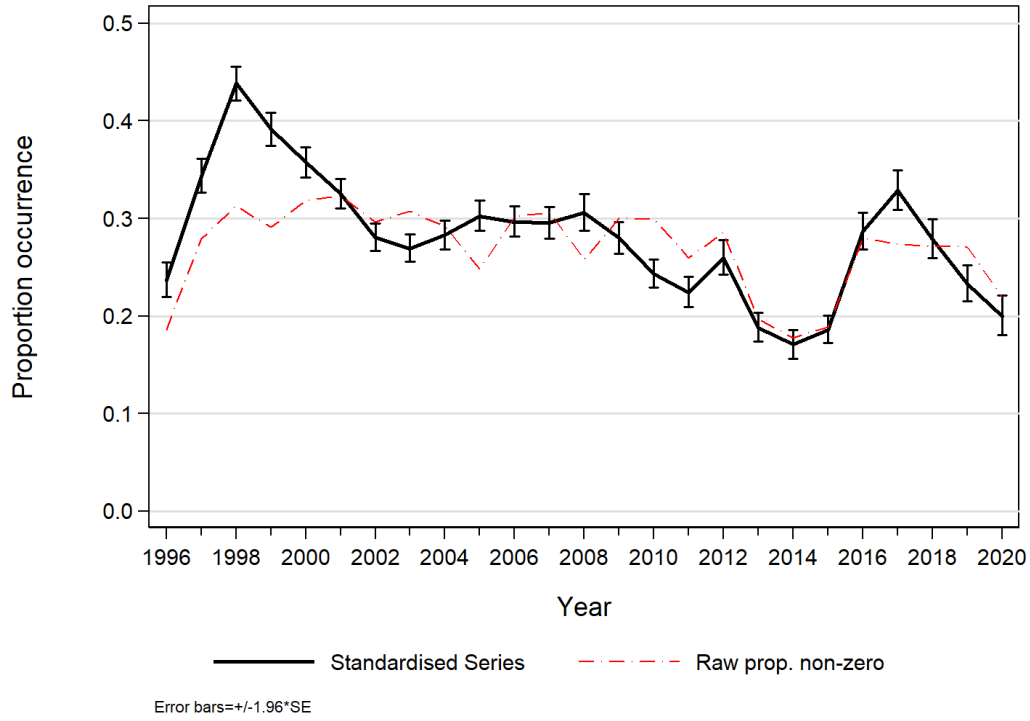

Figure C.11. Binomial index series for the YMR totBC (3CD5ABCDE) bottom trawl fishery analysis, also showing the trend in proportion of non-zero tows from the same data set.

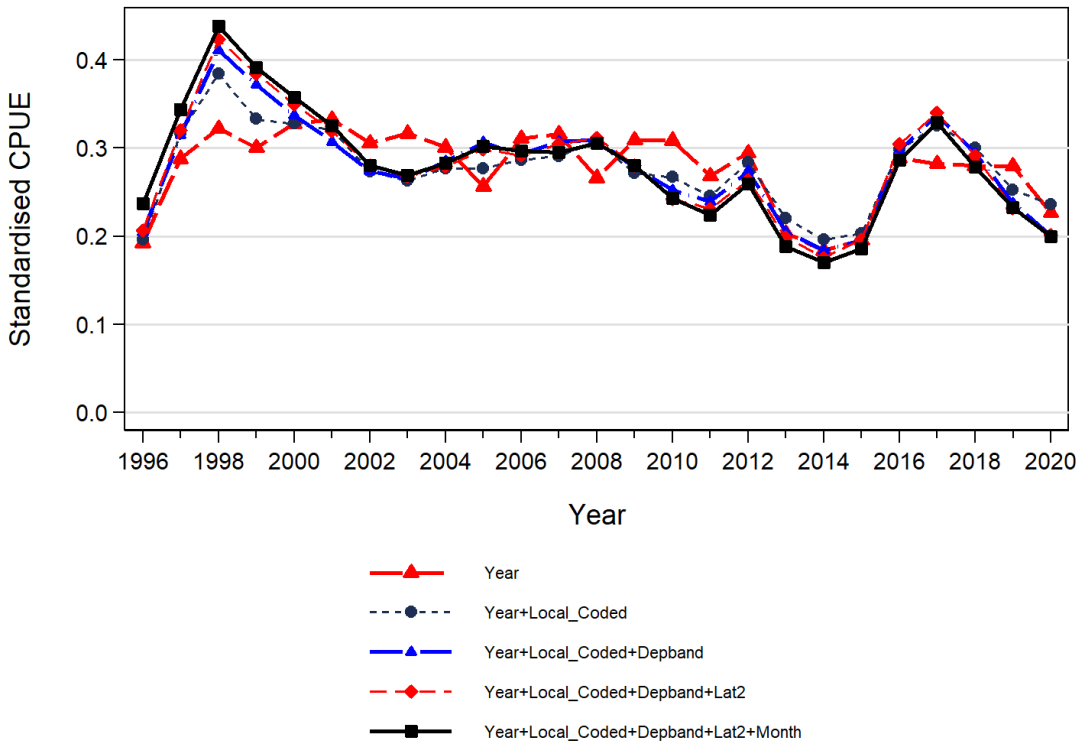

Figure C.12. Plot showing the year coefficients after adding each successive term of the standardised binomial regression analysis for YMR in the totBC (3CD5ABCDE) bottom trawl fishery. The final model is shown with a thick solid black line. Each line has been scaled so that the geometric mean equals 1.0.

The selected explanatory variables included [DFO locality] (Figure C.13), [Depth_bands] (Figure C.14), [0.1°Latitude_bands] (Figure C.15), and [Month] (Figure C.16), in addition to [Year]. This model showed an overall declining trend from 1998 to a low period extending from 2013 to 2015, followed by a short two year increase to 2017 and a subsequent decline which reached a level similar to that of 2013-2015 by 2020 (Figure C.11). The stepwise plot (Figure C.12), which shows the effect of adding each successive explanatory variable, indicates that there was little change to the unstandardised series except with the addition of the [DFO locality] variable, which changed the series from a flat to a declining series.

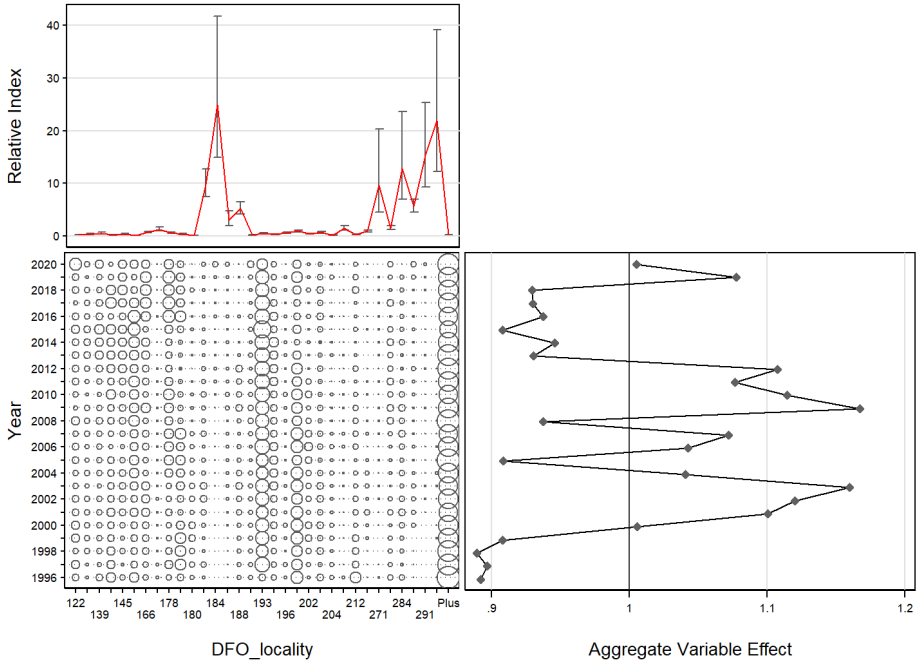

Figure C.13. CDI plot showing the effect of introducing the categorical variable [DFO locality] to the binomial regression model for YMR in the totBC (3CD5ABCDE) bottom trawl fishery. Table C.8 provides the definitions for the coded values used for each locality in the above plot. Each plot consists of subplots showing the effect by level of variable (top left), the relative distribution by year of variable records (bottom left), and the cumulative effect of variable by year (bottom right).

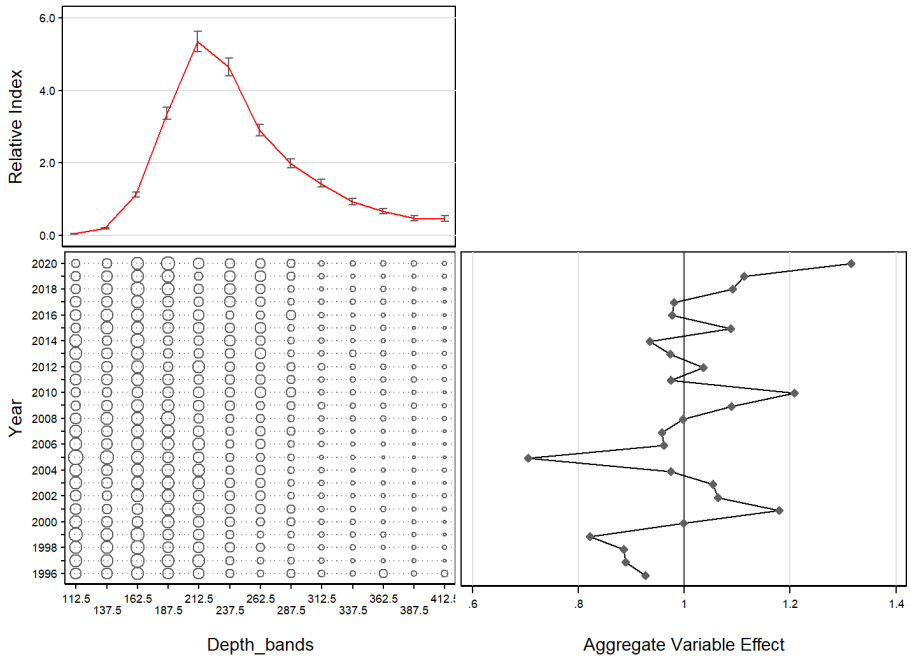

Figure C.14. CDI plot showing the effect of introducing the categorical variable [Depth bands] to the binomial regression model for YMR in the totBC (3CD5ABCDE) bottom trawl fishery. Each plot consists of subplots showing the effect by level of variable (top left), the relative distribution by year of variable records (bottom left), and the cumulative effect of variable by year (bottom right).

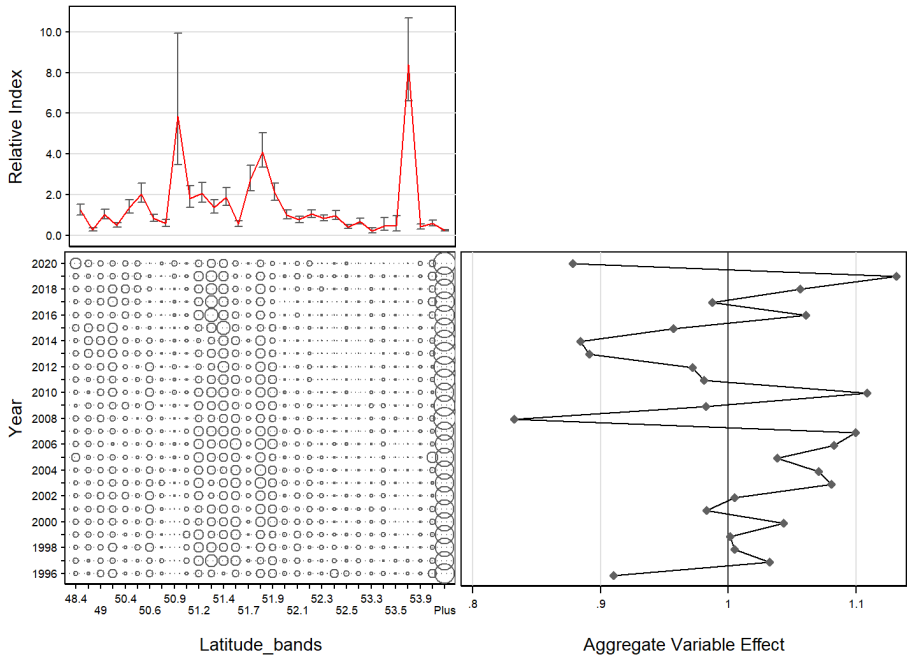

Figure C.15. CDI plot showing the effect of introducing the categorical variable [0.1° Latitude bands] to the binomial regression model for YMR in the totBC (3CD5ABCDE) bottom trawl fishery. Each plot consists of subplots showing the effect by level of variable (top left), the relative distribution by year of variable records (bottom left), and the cumulative effect of variable by year (bottom right).

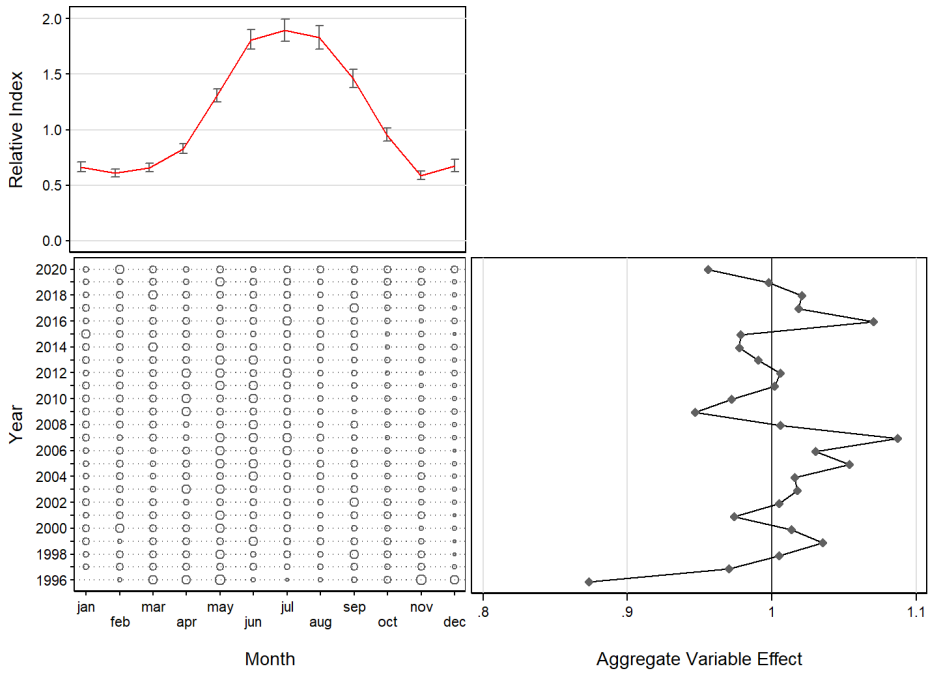

Figure C.16. CDI plot showing the effect of introducing the categorical variable [Month] to the binomial regression model for YMR in the totBC (3CD5ABCDE) bottom trawl fishery. Each plot consists of subplots showing the effect by level of variable (top left), the relative distribution of variable records by year (bottom left), and the cumulative effect of variable by year (bottom right).

Table C.8. Definition of locality codes used in Figure C.13. Localities marked in grey (with asterisks) were removed for a sensitivity analysis described in Section C.6.

Code	PFMC Major	DFO Minor	Minor Name	Locality Name	Binomial Index
122	3	23	Big Bank	Deep Big Bank/Barkley Canyon	0.249
138	3	24	Clayoquot Sd.	Father Charles Canyon	0.384
139	3	24	Clayoquot Sd.	Clayoquot Canyon	0.536
140	3	24	Clayoquot Sd.	South Estevan	0.199
145	4	25	Estevan-Esperanza Inlet	North Estevan	0.380
146	4	25	Estevan-Esperanza Inlet	Nootka	0.129
166	4	27	Quatsino Sd.	Quatsino Sound	0.719
177	5	11	Cape Scott-Triangle	Unknown	1.256
178	5	11	Cape Scott-Triangle	Triangle	0.591
179	5	11	Cape Scott-Triangle	Cape Scott Spit	0.367
180	5	11	Cape Scott-Triangle	Mexicana	0.115
*183	5	11	Cape Scott-Triangle	South Scott Islands	9.781
*184	5	11	Cape Scott-Triangle	W. Triangle (25 Mi.)	24.931
*187	5	11	Cape Scott-Triangle	South Triangle	3.102
*188	5	11	Cape Scott-Triangle	Pisces Canyon	5.221
192	6	8	Goose Island Bank	NE Goose	0.194
193	6	8	Goose Island Bank	SE Goose	0.485
195	6	8	Goose Island Bank	SW Goose	0.332
196	6	8	Goose Island Bank	Mitchell's Gully	0.590
197	6	8	Goose Island Bank	SE Cape St. James	0.947
202	6	8	Goose Island Bank	SW Middle Bank	0.416
203	6	8	Goose Island Bank	Outside Cape St. James	0.680
204	6	8	Goose Island Bank	West Virgin Rocks	0.149
205	6	8	Goose Island Bank	Below Middle Bank	1.461
212	7	2	2B-East	South Morseby	0.276
230	7	7	6-Central Morseby-Milbanke Sd.	Unknown	0.925
*271	9	31	2A West - Rennell Sound	Rennell Sound	9.647
272	9	31	2A West - Rennell Sound	Frederick Island	1.507
*284	9	31	2A West - Rennell Sound	South Hogback	12.838
*287	9	34	2B West - Anthony Island	Anthony Island	5.616
*291	9	34	2B West - Anthony Island	Flamingo Inlet	15.347
*299	9	35	1 West - Langara	Rockpile-Langara	21.871

C.4.1.3. Bottom trawl fishery: combined model

While the lognormal and binomial models show relatively similar overall declining trends over most of the period, the multiplicative nature of the combined model equation (Eq. C.4) results in a stronger declining trend from 1998 to 2015, followed by an uptick in the next two years of the series, and finally a levelling out after 2017 with the binomial and lognormal series trending in opposite directions in these years (Figure C.17).

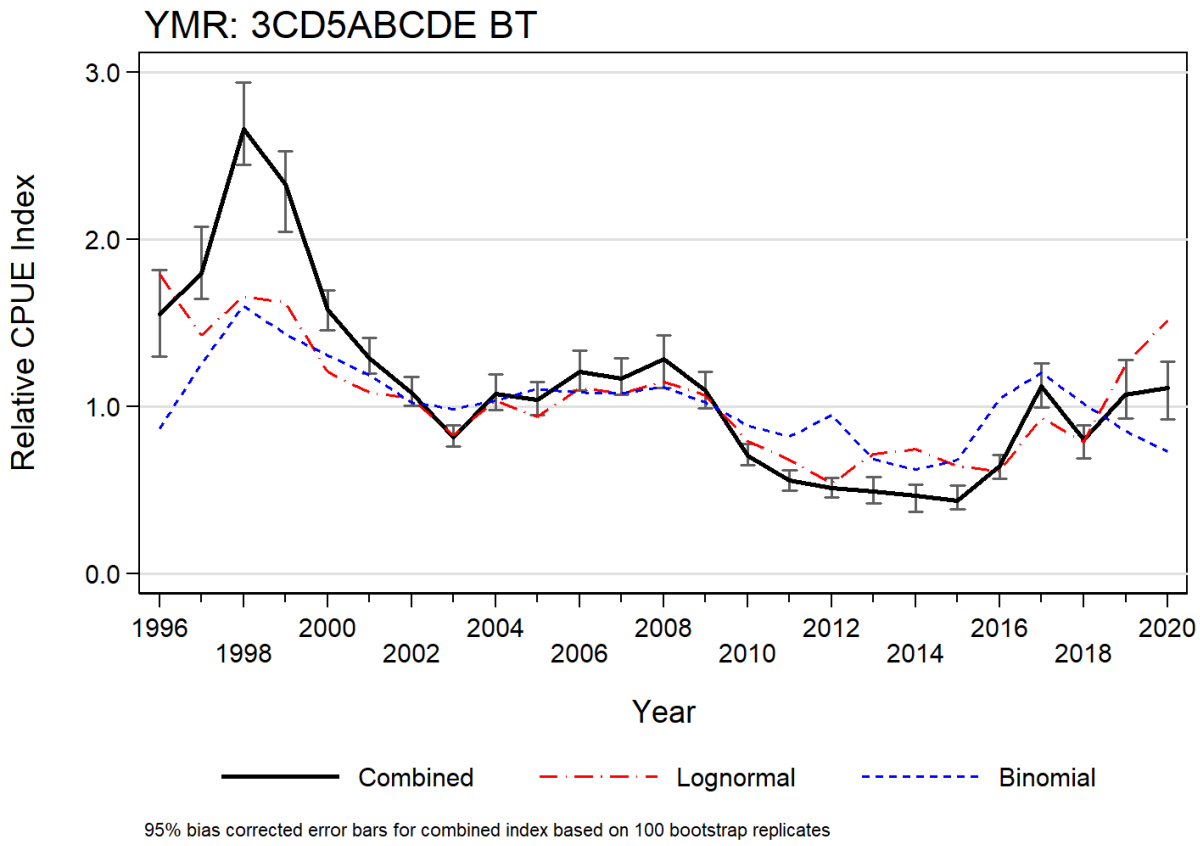

Figure C.17. Combined index series (Eq. C.4) for the totBC (3CD5ABCDE) bottom trawl fishery also showing the contributing lognormal and binomial index series. Confidence bounds based on 100 bootstrap replicates.

C.5. RELATIVE INDICES OF ABUNDANCE

Table C.9 summarises the suite of relative abundance indices and associated standard errors derived from this YMR CPUE analysis. The CPUE indices used in the age-structured stock assessment model appear as the delta-lognormal (combined) indices from the bottom trawl data (Figure C.17, Table C.9). The associated bootstrap standard errors (SE) were used as the initial CVs when fitting the stock assessment model.

Table C.9. Relative indices of annual CPUE from the arithmetic, unstandardised, lognormal models of non-zero bottom trawl catches of YMR in totBC (3CD5ABCDE). Also shown are the indices from the binomial model of presence/absence in this fishery and the combined delta-lognormal model (Eq. C.4). All indices are scaled so that their geometric means equal 1.0. Upper and lower 95% analytic confidence bounds and associated standard error (SE) are presented for the lognormal model, while bootstrapped (100 replicates) upper and lower 95% confidence bounds and the associated SE are presented for the combined model.

	Arithmetic	Geometric	Lognormal (Eq. C.3)				Binomial	Combined (Eq. C.4)			
Year	Index (Eq. C.1)	Index (Eq. C.2)	Index	Lower bound	Upper bound	SE	Index (Eq. C.3)	Index	Lower bound	Upper bound	SE
1996	1.366	1.455	1.791	1.588	2.020	0.0614	0.867	1.553	1.299	1.820	0.0903
1997	1.001	1.037	1.429	1.309	1.560	0.0447	1.258	1.798	1.645	2.080	0.0547
1998	0.828	0.979	1.659	1.535	1.794	0.0399	1.604	2.662	2.446	2.938	0.0487
1999	0.865	0.998	1.627	1.503	1.761	0.0405	1.433	2.332	2.046	2.531	0.0513
2000	0.893	0.963	1.209	1.125	1.298	0.0365	1.308	1.581	1.456	1.696	0.0470
2001	0.925	1.089	1.084	1.008	1.167	0.0375	1.190	1.291	1.198	1.410	0.0418
2002	1.037	1.295	1.052	0.977	1.131	0.0373	1.028	1.081	1.004	1.180	0.0417
2003	1.064	1.185	0.829	0.771	0.892	0.0373	0.986	0.817	0.763	0.890	0.0407
2004	1.174	1.501	1.039	0.963	1.121	0.0387	1.036	1.076	0.979	1.193	0.0463
2005	1.107	1.051	0.939	0.868	1.016	0.0402	1.107	1.040	0.950	1.148	0.0478
2006	0.919	1.086	1.113	1.030	1.203	0.0396	1.086	1.208	1.096	1.338	0.0508
2007	0.759	1.091	1.079	0.995	1.171	0.0415	1.081	1.167	1.074	1.288	0.0502
2008	0.797	1.045	1.150	1.046	1.264	0.0482	1.119	1.287	1.111	1.428	0.0635
2009	1.089	1.305	1.069	0.982	1.164	0.0433	1.025	1.096	0.992	1.209	0.0517
2010	0.766	0.953	0.795	0.730	0.865	0.0434	0.890	0.708	0.650	0.778	0.0510
2011	0.907	0.863	0.684	0.622	0.752	0.0483	0.821	0.561	0.501	0.623	0.0599
2012	0.702	0.685	0.543	0.493	0.598	0.0492	0.951	0.516	0.456	0.577	0.0603
2013	1.071	0.733	0.717	0.642	0.802	0.0570	0.688	0.494	0.420	0.581	0.0784
2014	1.076	0.941	0.746	0.661	0.842	0.0617	0.625	0.466	0.373	0.533	0.0850
2015	0.861	0.557	0.644	0.575	0.721	0.0575	0.680	0.438	0.388	0.531	0.0751
2016	0.821	0.550	0.616	0.557	0.681	0.0511	1.050	0.646	0.572	0.713	0.0601
2017	0.908	0.731	0.934	0.843	1.035	0.0523	1.204	1.124	0.994	1.259	0.0590
2018	1.031	0.699	0.788	0.705	0.879	0.0562	1.020	0.803	0.694	0.891	0.0677
2019	1.778	1.311	1.257	1.116	1.416	0.0607	0.853	1.072	0.931	1.279	0.0793
2020	2.162	2.074	1.520	1.319	1.750	0.0721	0.732	1.113	0.926	1.269	0.0785

C.6. COMPARISON OF CPUE SERIES WITH SYNOPTIC SURVEYS

C.6.1. Queen Charlotte Sound survey

Figure C.18 compares the totBC (3CD5ABCDE) combined CPUE series (Figure C.17, Table C.9) with the relative biomass series from the Queen Charlotte Sound synoptic survey (see Appendix B, Section B.4). This comparison seems reasonable, in spite of the very large error bars associated with this survey, with the CPUE series intersecting the range between survey error bars in nine of the ten indices (apart from the 2007 index). There is general agreement between the two series, given the high level of variability that seems to be associated with this survey.

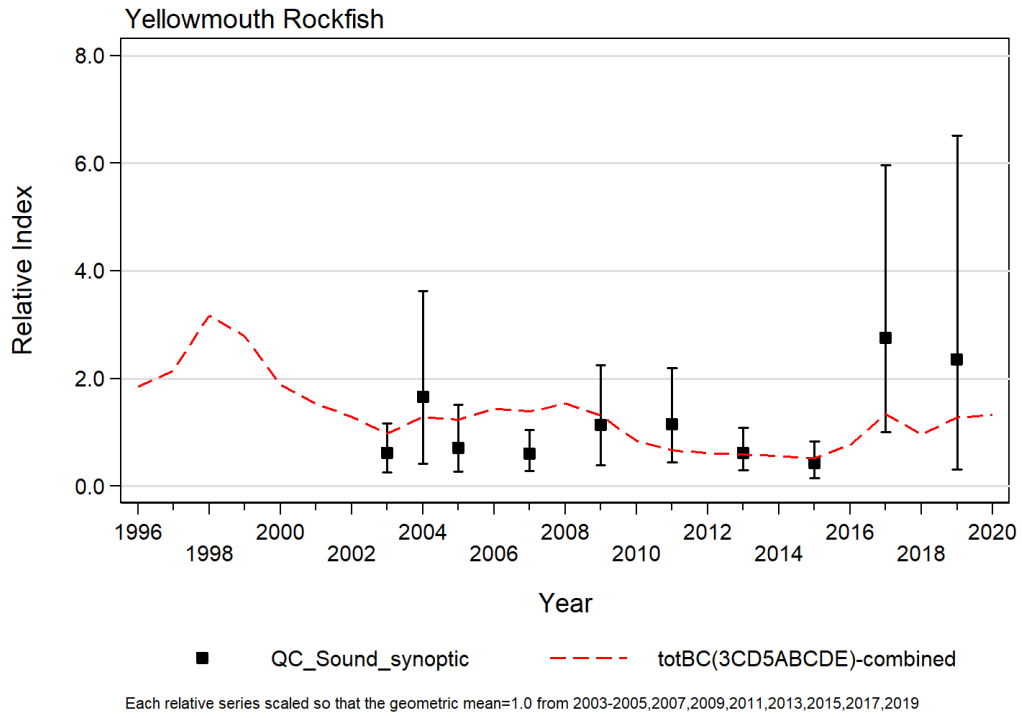

Figure C.18. Comparison of the Queen Charlotte Sound synoptic survey series with the CPUE index series (Eq. C.4) for the totBC (3CD5ABCDE) bottom trawl fishery. Survey confidence bounds based on 1000 bootstrap simulations.

C.6.2. West coast Vancouver Island survey

Figure C.19 compares the totBC (3CD5ABCDE) combined series (Figure C.17, Table C.9) with the relative biomass series from the west coast Vancouver Island synoptic survey (see Appendix B, Section B.5). This comparison seems poorer than for the QC Sound survey, with the 2016 and 2018 indices being the lowest in the series at a point when the CPUE series is climbing. The 2010 index is the highest in the series (and doesn't intersect the CPUE series) at a point when the CPUE series is declining. This series appears to be a poor match to the CPUE series, which isn't surprising given that the majority of the survey coverage is in habitat that appears to be less suitable for YMR (see distributional map A.1 in Appendix A).

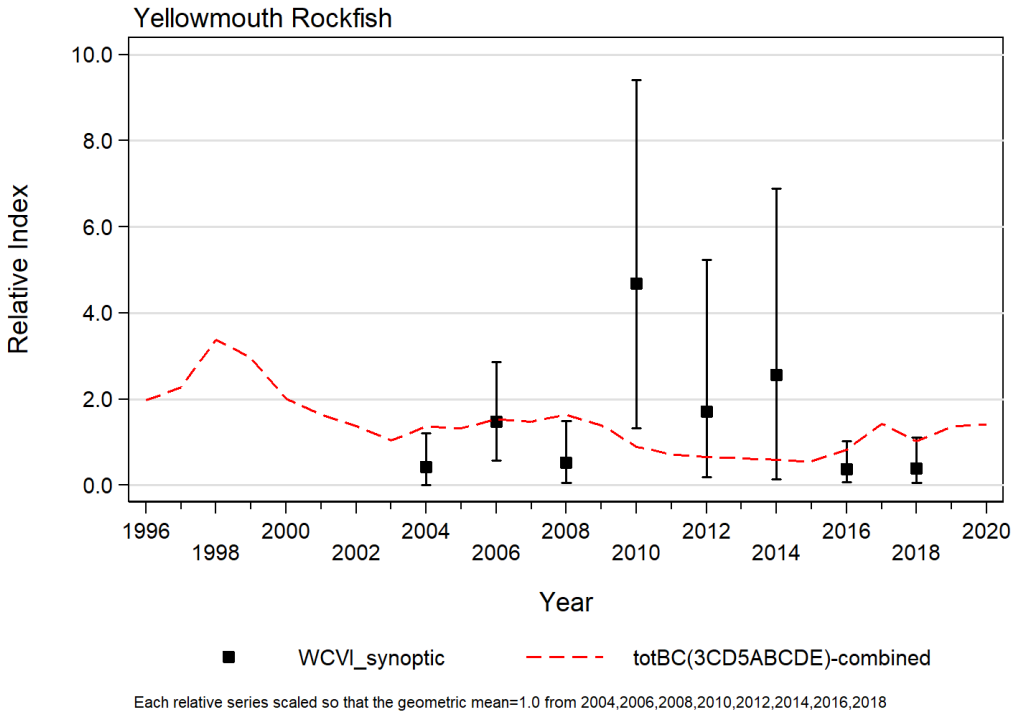

Figure C.19. Comparison of the west coast Vancouver Island synoptic survey series with the CPUE index series (Eq. C.4) for the totBC (3CD5ABCDE) bottom trawl fishery. Survey confidence bounds based on 1000 bootstrap simulations.

C.6.3. West coast Haida Gwaii survey

Figure C.20 compares the totBC (3CD5ABCDE) combined series (Figure C.17, Table C.9) with the relative biomass series from the west coast Haida Gwaii synoptic survey (see Appendix B, Section B.6). This comparison is intermediate between the two previous surveys, with the higher index values occurring at the end of series which is reasonably consistent with the CPUE series. However, the low survey index values at the beginning of the series are not consistent with the CPUE series. This comparison, as with the other two surveys, is hampered by the very large relative errors associated with YMR.

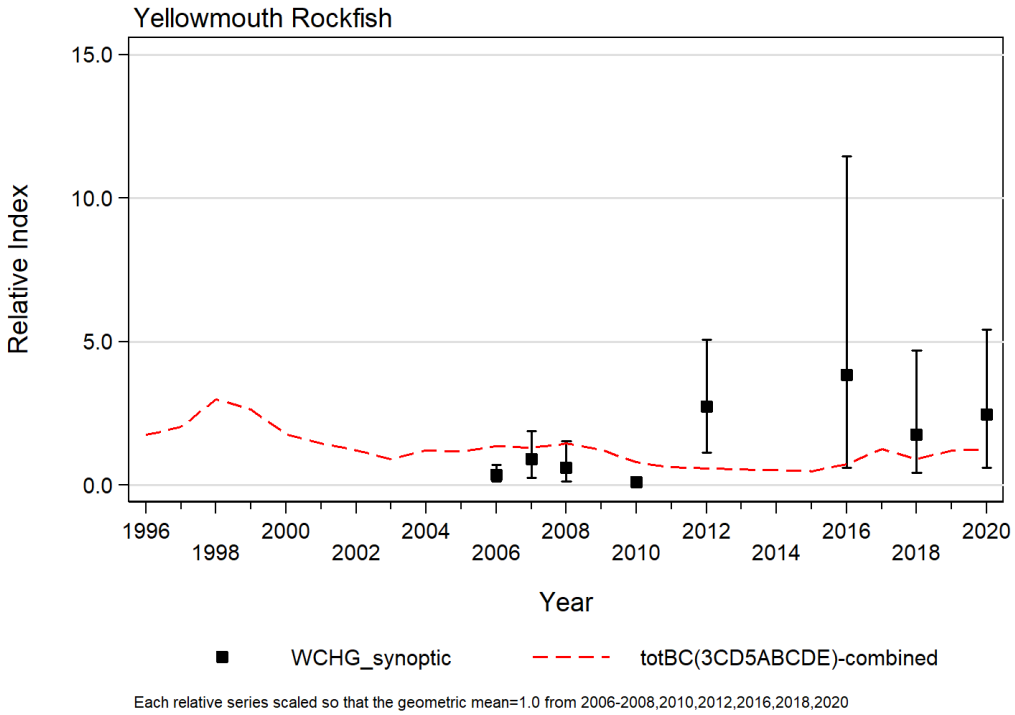

Figure C.20. Comparison of the west coast Haida Gwaii synoptic survey series with the CPUE index series (Eq. C.4) for the totBC (3CD5ABCDE) bottom trawl fishery. Survey confidence bounds based on 1000 bootstrap simulations.

C.7. COMPARISON OF CPUE SERIES WITH TWEEDIE CPUE MODEL

An analysis of the coastwide YMR catch/effort data based on an alternative model structure compared to the model described in Section C.2.2 was prepared for use in the YMR stock assessment (Sean Anderson, DFO Pacific Biological Station, pers. comm.). This model was based on the Tweedie distribution which can accommodate zero and positive tows in the same model, thus eliminating the necessity to estimate separate positive and logit models, combined using the delta-lognormal procedure (Eq. C.4). The procedure followed by the Tweedie model is documented in Anderson et al. (2019, Section D.3).

The Tweedie model is based on a similar set of filters as described in Section C.3, and consisted as follows:

area = "3CD5ABCDE"
year_range = c(1996, 2020)
lat_range = c(48, Inf)
min_positive_tows = 100
min_positive_trips = 10
min_yrs_with_trips = 5
lat_band_width = 0.1
depth_band_width = 25
gear = "bottom trawl"

The Tweedie model used random intercepts for vessel and locality while the delta-lognormal model treated these variables as factors. This set of filters resulted in a slightly different data set than that summarised in Table C.4, with 28 vessels compared to 32 as listed in Table C.2. We

used the Tweedie series with no [DFO locality x year] interactions because the sensitivity analyses detailed in Section C.8 below lead us to conclude that the estimated CPUE abundance series shows a consistent trend among the high and low abundance regions. Figure C.21 compares the totBC(3CD5ABCDE) combined CPUE series (Figure C.17, Table C.9) with the Tweedie series with no [DFO locality x year] interactions.

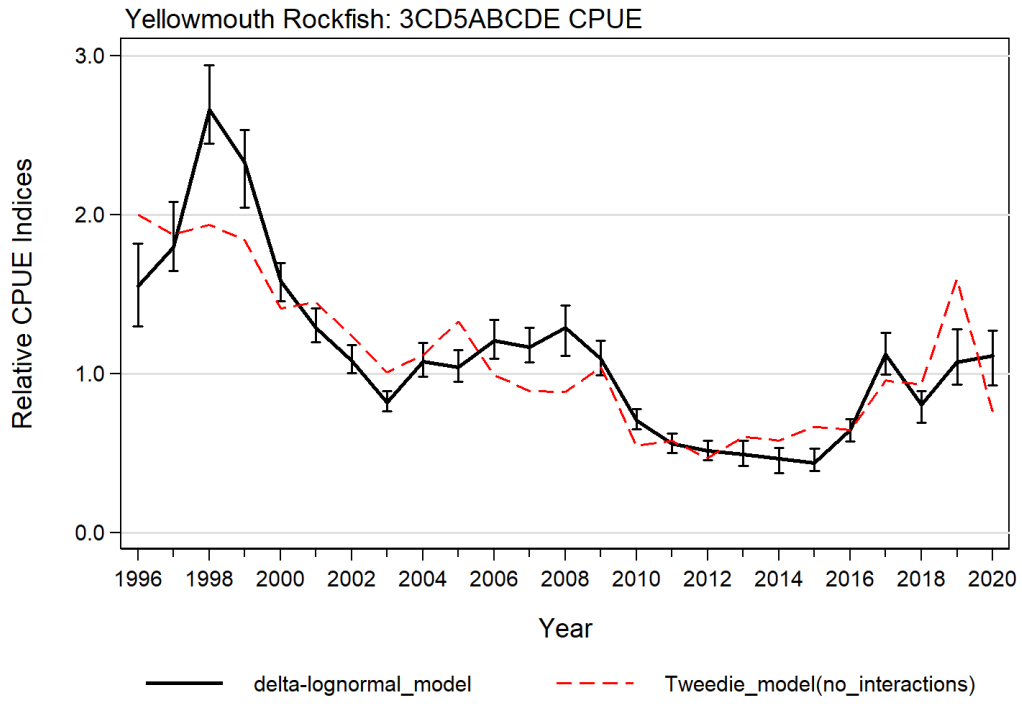

Figure C.21. Comparison of the delta-lognormal series (totBC(3CD5ABCDE)) with the Tweedie model used in Sensitivity run S04 (Sean Anderson, DFO Pacific Biological Station pers. comm.).

C.8. SENSITIVITY ANALYSES ON THE EFFECT OF DFO LOCALITIES

Two sensitivity analyses exploring the impact of removing DFO localities associated with high catch rates were performed to see the effect on the resulting combined analysis presented in Section C.5. The first analysis excluded the five DFO localities with the highest catch rates in the lognormal GLM. These DFO localities are marked in grey in Table C.6. Table C.10 presents the size of the dataset left after these DFO localities have been removed. A comparison of this table with the total dataset summarised in Table C.4 shows that this analysis retains much of the original data, with the same number of vessels, a similar number of trips and no apparent trend in the proportion of zero catches. When these data were put through the modelling steps described in Section C.2.2, the resulting standardisation was similar to the analysis which included all data, with perhaps less standardisation effect (see Figure C.22, top row). Because this analysis computes relative catch rates, some of the lognormal indices for the remaining DFO localities were now higher than estimated in the original model (Table C.11). However, the resulting annual index series differed little from the model which included all data (see Figure C.23, which excludes 5 DFO localities series).

Table C.10. Summary data for the YMR bottom trawl fishery in totBC (3CD5ABCDE) by year for the core data set (after applying all data filters and selection of core vessels) after removing the data for the five [DFO locality] marked in grey in Table C.6.

Year	Number vessels[1]	Number trips[1]	Number tows[1]	Number records[1]	Number records[2]	% zero records[2]	Total catch (t)[1]	Total hours[1]	CPUE (kg/h) (Eq. C.1)
1996	31	154	684	684	4,114	83.4	519.0	1,152	450.4
1997	31	278	1,331	1,331	5,262	74.7	802.4	2,509	319.8
1998	30	334	1,840	1,840	6,239	70.5	1,102.7	3,657	301.6
1999	29	365	1,803	1,803	6,541	72.4	1,076.0	3,551	303.0
2000	30	406	2,144	2,144	7,188	70.2	1,197.4	3,861	310.2
2001	30	382	1,933	1,933	6,572	70.6	977.4	3,260	299.9
2002	30	413	1,809	1,809	6,983	74.1	1,008.1	3,044	331.2
2003	30	410	1,736	1,736	6,729	74.2	877.0	2,799	313.4
2004	30	376	1,707	1,707	6,642	74.3	1,105.9	2,805	394.2
2005	28	368	1,597	1,597	7,244	78.0	1,179.2	2,945	400.5
2006	27	343	1,743	1,743	6,136	71.6	1,138.7	3,477	327.5
2007	27	295	1,568	1,568	5,462	71.3	817.6	3,013	271.4
2008	25	240	1,124	1,124	4,734	76.3	638.3	2,159	295.7
2009	24	249	1,309	1,309	4,941	73.5	966.8	2,370	407.9
2010	24	225	1,307	1,307	5,018	74.0	575.4	2,601	221.2
2011	24	195	1,038	1,038	4,582	77.3	586.7	2,045	286.9
2012	23	174	971	971	4,036	75.9	361.3	1,925	187.6
2013	22	162	770	770	4,437	82.6	433.7	1,545	280.7
2014	23	162	622	622	4,090	84.8	324.2	1,179	274.9
2015	23	192	814	814	4,584	82.2	333.8	1,519	219.7
2016	18	200	1,036	1,036	4,001	74.1	437.3	2,108	207.4
2017	19	204	1,026	1,026	3,943	74.0	491.7	2,123	231.6
2018	16	158	909	909	3,516	74.1	564.1	1,800	313.3
2019	13	137	723	723	2,881	74.9	749.9	1,284	583.9
2020	13	92	447	447	2,470	81.9	434.1	815	532.9

[1] calculated for tows with YMR catch >0; [2] calculated for all tows

Table C.11. Lognormal indices for the remaining DFO localities included in the model where the five localities with the highest catch rates had been excluded from the analysis.

Code	PFMC Major	DFO Minor	Minor Name	Locality Name	Lognormal Index
122	3	23	Big Bank	Deep Big Bank/Barkley Canyon	1.146
138	3	24	Clayoquot Sd.	Father Charles Canyon	1.503
139	3	24	Clayoquot Sd.	Clayoquot Canyon	1.370
140	3	24	Clayoquot Sd.	South Estevan	0.567
145	4	25	Estevan-Esperanza Inlet	North Estevan	1.013
146	4	25	Estevan-Esperanza Inlet	Nootka	0.492
166	4	27	Quatsino Sd.	Quatsino Sound	3.096
177	5	11	Cape Scott-Triangle	Unknown	1.398
178	5	11	Cape Scott-Triangle	Triangle	0.892
179	5	11	Cape Scott-Triangle	Cape Scott Spit	0.316
180	5	11	Cape Scott-Triangle	Mexicana	0.094
188	5	11	Cape Scott-Triangle	Pisces Canyon	5.758
192	6	8	Goose Island Bank	NE Goose	0.329
193	6	8	Goose Island Bank	SE Goose	0.534
195	6	8	Goose Island Bank	SW Goose	0.624
196	6	8	Goose Island Bank	Mitchell's Gully	0.770
197	6	8	Goose Island Bank	SE Cape St. James	1.380
202	6	8	Goose Island Bank	SW Middle Bank	1.019
203	6	8	Goose Island Bank	Outside Cape St. James	1.168
204	6	8	Goose Island Bank	West Virgin Rocks	0.320
205	6	8	Goose Island Bank	Below Middle Bank	1.410

Code	PFMC Major	DFO Minor	Minor Name	Locality Name	Lognormal Index
212	7	2	2B-East	South Morseby	0.963
230	7	7	6-Central Morseby-Milbanke Sd.	Unknown	1.792
271	9	31	2A West - Rennell Sound	Rennell Sound	2.624
272	9	31	2A West - Rennell Sound	Frederick Island	4.257
284	9	31	2A West - Rennell Sound	South Hogback	1.828
299	9	35	1 West - Langara	Rockpile-Langara	1.131

The second sensitivity analysis excluded a further four DFO localities which had the highest catch rates for the binomial GLM. These additional DFO localities are marked in grey in Table C.8 and resulted in a total of nine localities dropped. As for the previous analysis, a comparison of Table C.12 with the total dataset summarised in Table C.4 shows that considerable data still remained, again with the same number of vessels, a similar number of trips and no apparent trend in the proportion of zero catches. When these data were put through the modelling steps described in Section C.2.2, the resulting standardisation was again similar to that seen in the analyses which included all data, with the same amount of standardisation effect as in the first locality removal analysis (see Figure C.22, bottom row). Because this analysis computes relative catch rates, some of the binomial indices for the remaining DFO localities were now higher than estimated in the original model (Table C.13). The resulting annual index series showed more variability compared to the model which included all data or the model which dropped only five DFO localities (see Figure C.23, which excludes 9 DFO localities series). However, the overall trend was unchanged in all three models. This result implies that the underlying year effect as measured by these data is consistent across the entire coast, thereby reducing the potential for an interaction between area and year in this analysis.

Table C.12. Summary data for the YMR bottom trawl fishery in totBC (3CD5ABCDE) by year for the core data set (after applying all data filters and selection of core vessels) after removing the data for the nine [DFO locality] marked in grey in Table C.6.

Year	Number vessels[1]	Number trips[1]	Number tows[1]	Number records[1]	Number records[2]	% zero records[2]	Total catch (t)[1]	Total hours[1]	CPUE (kg/h) (Eq. C.1)
1996	31	147	623	623	4,004	84.4	454.8	1,064	427.4
1997	31	274	1,293	1,293	5,193	75.1	778.5	2,443	318.7
1998	30	326	1,765	1,765	6,146	71.3	1,014.7	3,521	288.1
1999	29	355	1,689	1,689	6,410	73.7	949.3	3,352	283.2
2000	30	386	1,860	1,860	6,886	73.0	881.9	3,457	255.1
2001	30	360	1,663	1,663	6,261	73.4	689.2	2,885	238.9
2002	30	378	1,545	1,545	6,667	76.8	749.7	2,714	276.3
2003	30	388	1,518	1,518	6,461	76.5	652.2	2,510	259.8
2004	30	356	1,495	1,495	6,408	76.7	920.2	2,542	362.0
2005	28	351	1,452	1,452	7,073	79.5	1,068.7	2,740	390.0
2006	27	322	1,547	1,547	5,913	73.8	986.1	3,227	305.6
2007	27	274	1,409	1,409	5,256	73.2	675.8	2,775	243.5
2008	25	221	1,032	1,032	4,599	77.6	587.7	2,047	287.2
2009	24	233	1,183	1,183	4,745	75.1	866.8	2,206	392.9
2010	24	211	1,199	1,199	4,859	75.3	510.0	2,453	207.9
2011	24	184	930	930	4,443	79.1	448.1	1,885	237.7
2012	23	166	860	860	3,912	78.0	249.2	1,769	140.9
2013	22	152	705	705	4,368	83.9	351.7	1,436	244.9
2014	23	145	535	535	3,968	86.5	213.8	1,031	207.3
2015	23	179	747	747	4,472	83.3	258.7	1,410	183.5
2016	18	189	983	983	3,917	74.9	390.1	2,023	192.8
2017	19	195	966	966	3,861	75.0	367.6	2,043	179.9
2018	16	149	871	871	3,453	74.8	518.3	1,740	297.8
2019	13	130	654	654	2,779	76.5	653.4	1,195	546.9
2020	13	91	400	400	2,387	83.2	394.0	709	555.7

[1] calculated for tows with YMR catch >0; [2] calculated for all tows

Table C.13. Lognormal indices for the remaining DFO localities included in the model where the nine localities with the highest catch rates in the binomial model had been excluded from the analysis.

Code	PFMC Major	DFO Minor	Minor Name	Locality Name	Binomial Index
122	3	23	Big Bank	Deep Big Bank/Barkley Canyon	0.626
138	3	24	Clayoquot Sd.	Father Charles Canyon	0.908
139	3	24	Clayoquot Sd.	Clayoquot Canyon	1.257
140	3	24	Clayoquot Sd.	South Estevan	0.484
145	4	25	Estevan-Esperanza Inlet	North Estevan	0.921
146	4	25	Estevan-Esperanza Inlet	Nootka	0.300
166	4	27	Quatsino Sd.	Quatsino Sound	1.666
177	5	11	Cape Scott-Triangle	Unknown	3.377
178	5	11	Cape Scott-Triangle	Triangle	1.488
179	5	11	Cape Scott-Triangle	Cape Scott Spit	0.902
180	5	11	Cape Scott-Triangle	Mexicana	0.278
192	6	8	Goose Island Bank	NE Goose	0.477
193	6	8	Goose Island Bank	SE Goose	1.251
195	6	8	Goose Island Bank	SW Goose	0.648
196	6	8	Goose Island Bank	Mitchell's Gully	1.258
197	6	8	Goose Island Bank	SE Cape St. James	1.838
202	6	8	Goose Island Bank	SW Middle Bank	0.828
203	6	8	Goose Island Bank	Outside Cape St. James	1.336
204	6	8	Goose Island Bank	West Virgin Rocks	0.383
205	6	8	Goose Island Bank	Below Middle Bank	2.950
212	7	2	2B-East	South Morseby	0.733
230	7	7	6-Central Morseby-Milbanke Sd.	Unknown	2.702
272	9	31	2A West - Rennell Sound	Frederick Island	3.535

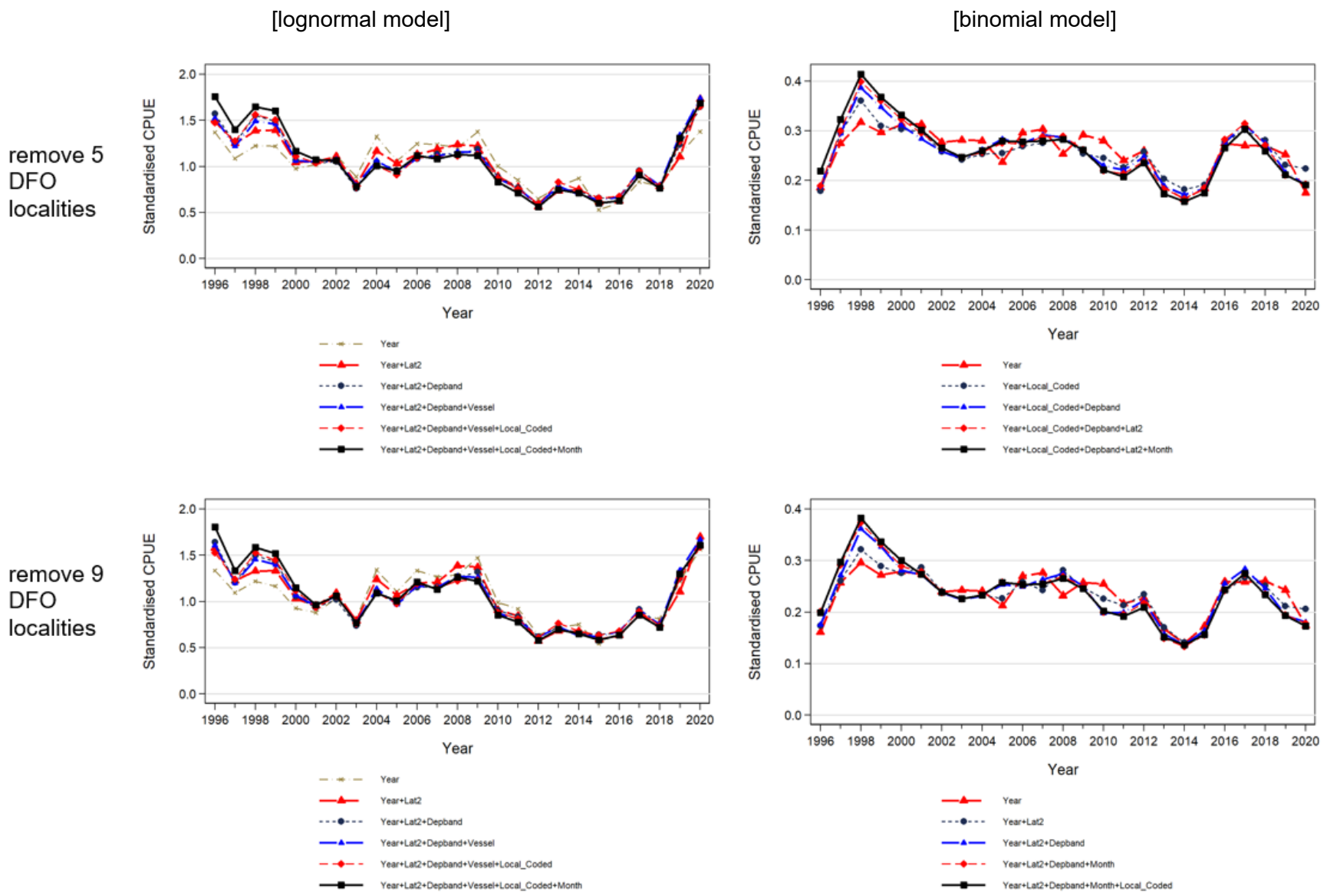

Figure C.22: Stepwise plots equivalent to those shown in Figure C.5 (lognormal model, left panels) and Figure C.12 (binomial model, right panels) showing the effect on the year indices with the addition of each explanatory variable accepted into the models after dropping the five [DFO locality] marked in grey in Table C.6 (top row) or dropping nine [DFO locality] marked in grey in Table C.8 (bottom row).

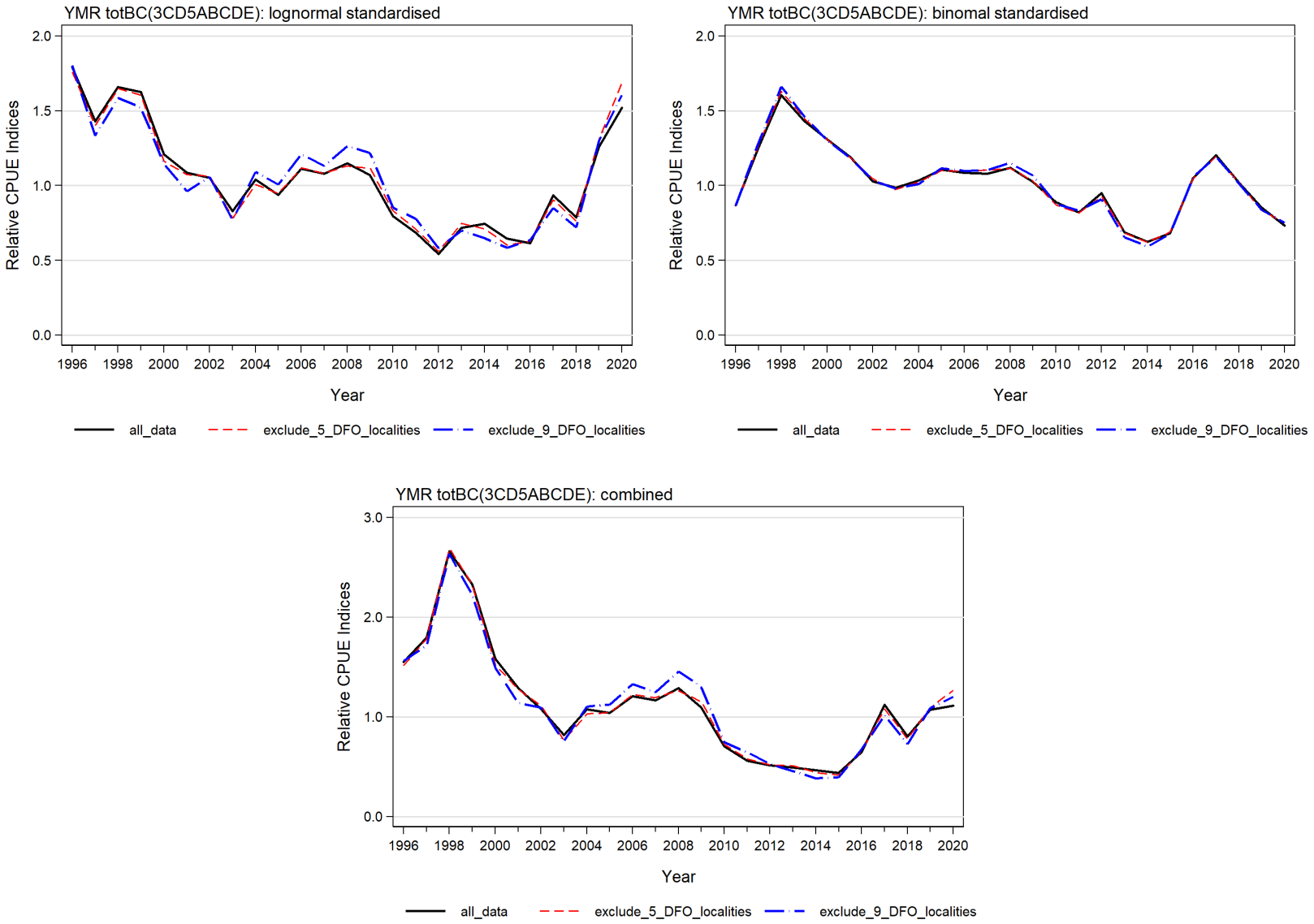

Figure C.23: Comparison plots showing the year index series from three YMR models: (top left) all data (Table C.4); (top right) exclude five DFO localities (Table C.10); (bottom) exclude nine DFO localities (Table C.10);

C.9. REFERENCES – CPUE

Anderson, S.C., Keppel, E.A., Edwards, A.M. 2019. A reproducible data synopsis for over 100 species of British Columbia groundfsh. DFO Can. Sci. Advis. Sec. Res. Doc. 2019/041. vii + 321 p.

Bentley, N., Kendrick, T.H., Starr, P.J., and Breen, P.A. 2012. Influence plots and metrics: tools for better understanding fisheries catch-per-unit-effort standardizations. ICES J. Mar. Sci. 69(1): 84-88.

Fletcher, D., Mackenzie, D., and Villouta, E. 2005. Modelling skewed data with many zeros: A simple approach combining ordinary and logistic regression. Environmental and Ecological Statistics12, 45–54.

Francis, R.I.C.C. 1999. The impact of correlations on standardised CPUE indices. N.Z. Fish. Ass. Res. Doc. 99/42: 30 pp. (Unpublished report held in NIWA library, Wellington, NZ)

Francis, R.I.C.C. 2001. Orange roughy CPUE on the South and East Chatham Rise. N.Z. Fish. Ass. Rep. 2001/26: 30 pp.

Quinn, T.R., and R.B. Deriso. 1999. Quantitative Fish Dynamics. Oxford University Press. 542 pp.

APPENDIX D. BIOLOGICAL DATA

This appendix describes analyses of biological data for Yellowmouth Rockfish (YMR) along the British Columbia (BC) coast. These analyses follow the methods adopted in previous rockfish stock assessments (e.g., Starr and Haigh 2021a), including length-weight relationships, von Bertalanffy growth models, maturity schedules, natural mortality, and age proportions for use in the YMR catch-at-age stock assessment model (Sections D.1 and D.2). As well, the data were investigated for possible differences between northern (5DE) and southern (3CD5ABC) regions (Section D.3) to determine if there was evidence that these regions should be treated as separate stocks. All biological analyses are based on YMR data extracted from the Fisheries and Oceans Canada (DFO) Groundfish database GFBioSQL on 2021-02-08 (98,011 records). General data selection criteria for most analyses are summarised in Table D.1, although data selection sometimes varied depending on the analysis.

Table D.1. Data selection criteria for analyses of biological data for allometric and growth analyses.

Field	Criterion	Notes
Trip type	`[trip_type] == c(2,3)`	Definition of research observations.
	`[trip_type] == c(1,4,5)`	Definition of commercial observations
Sample type	`[sample_type] == c(1,2,6,7,8)`	Only random or total samples.
Ageing method	`[agemeth] == c(3, 17) or == (0 & [year]>=1980) or == 1 for ages 1:3`	Break & burn|bake method unknown from 1980 on (assumed B&B) surface readings for young fish
Species category code	`[SPECIES_CATEGORY_CODE]==1 (or 3)`	1 = Unsorted samples 3 = Sorted (keeper) samples
Sex code	`[sex] == c(1,2)*`	Clearly identified sex (1=male or 2=female).
Area code	`[stock]` select stock area (coastwide)	PMFC major area codes 3:9

*GFBioSQL codes for `sex` (1=male, 2=female) are reversed in the model (1=female, 2=male).

D.1. LIFE HISTORY

D.1.1. Allometry – Weight vs. Length

A log-linear relationship with additive errors was fit to females (*s*=2), males (*s*=1), and combined to all valid weight and length data pairs i, $\{W_{is}, L_{is}\}$:

$$\ln\left(W_{is}\right) = \alpha_s + \beta_s \ln\left(L_{is}\right) + \varepsilon_{is}, \quad \varepsilon \sim N(0,\sigma^2) \quad \text{(D.1)}$$

where α_s and β_s are the intercept and slope parameters for each sex s.

Survey and commercial samples, regardless of gear type, were used independently to derive length-weight parameters for consideration in the model (Table D.2); however, only survey data coastwide were adopted for model use (Figure D.1, top panel). Commercial fishery weight data were not as abundant as those from research surveys and tended to represent a restricted range of weights compared to those from surveys (compare minimum, maximum and mean weights in Table D.2). It is also possible that the commercial weights were less precise than the survey weight data.

*Table D.2. Length-weight parameter estimates, standard errors (SE) and number of observations (n) for YMR (females, males and combined) from survey and commercial samples, regardless of gear type from 1988 to 2020. W_i = weight (kg) of specimen i, W_{pred} = predicted weight from fitted data set. (**S**): survey data; (**C**): commercial data.*

Stock	Sex	n	ln(*a*)	SE ln(*a*)	*b*	SE *b*	mean W_i	SD W_i	min W_i	max W_i	mean W_{pred}
YMR	F	4,796	-11.757	0.016	3.183	0.004	1.186	0.572	0.010	4.110	1.144
CST	M	4,878	-11.950	0.014	3.241	0.004	1.122	0.571	0.008	2.708	1.093
(**S**)	F+M	9,679	-11.854	0.011	3.212	0.003	1.153	0.572	0.008	4.110	1.118
YMR	F	1,829	-11.164	0.080	3.033	0.021	1.510	0.346	0.388	2.600	1.315
CST	M	2,101	-11.415	0.082	3.101	0.022	1.441	0.297	0.428	2.345	1.257
(**C**)	F+M	3,929	-11.268	0.057	3.062	0.015	1.474	0.323	0.388	2.600	1.289
YMR	F	1,204	-11.106	0.057	3.011	0.015	1.478	0.531	0.210	4.110	1.290
5DE	M	1,140	-11.457	0.055	3.111	0.015	1.402	0.502	0.240	2.708	1.234
(**S**)	F+M	2,345	-11.246	0.040	3.052	0.011	1.440	0.518	0.210	4.110	1.262
YMR	F	429	-10.762	0.126	2.921	0.033	1.484	0.376	0.594	2.578	1.192
5DE	M	625	-11.406	0.116	3.097	0.031	1.421	0.334	0.455	2.225	1.162
(**C**)	F+M	1,055	-11.037	0.087	2.997	0.023	1.447	0.353	0.455	2.578	1.182
YMR	F	3,595	-11.822	0.018	3.200	0.005	1.086	0.552	0.010	2.551	1.086
3CD5ABC	M	3,744	-11.996	0.016	3.253	0.004	1.035	0.564	0.008	2.632	1.038
(**S**)	F+M	7,341	-11.910	0.012	3.227	0.003	1.060	0.559	0.008	2.632	1.062
YMR	F	1,402	-11.386	0.098	3.094	0.026	1.519	0.336	0.388	2.600	1.391
3CD5ABC	M	1,474	-11.406	0.110	3.100	0.029	1.450	0.280	0.428	2.345	1.320
(**C**)	F+M	2,876	-11.387	0.073	3.095	0.019	1.484	0.311	0.388	2.600	1.358

D.1.2. Growth – Length vs. Age

Otolith age data were available from both surveys and commercial fishing trips; however, data from the surveys were used in determining the growth function used in the model. Of the 16,733 records with age data, all records had concurrent lengths, and 6,464 records were suitable for growth analysis after qualifying by sex (female|male), trip type (research|surveys), sample type (random), and ageing methodology. The majority of these ages were determined using the break-and-burn (B&B) method (MacLellan 1997). The growth model below uses 3,241 female specimens and 3,223 male specimens; Table D.3 summarises the availability of all YMR otoliths.

Growth was formulated as a von Bertalanffy model where lengths by sex, L_{is}, for fish $i = 1,\ldots,n_s$ are given by:

$$L_{is} = L_{\infty s}\left[1 - e^{-\kappa_s\left(a_{is} - t_{0s}\right)}\right] + \varepsilon_{is}, \quad \varepsilon \sim N\left(0, \sigma^2\right) \qquad \text{(D.2)}$$

where for each sex s,

$L_{\infty s}$ = the average length at maximum age of an individual,

κ_s = growth rate coefficient, and

t_{0s} = age at which the average size is zero.

The negative log likelihood for each sex s, used for minimisation is:

$$\ell\left(L_\infty, \kappa, t_0, \sigma\right) = n\ln\left(\sigma\right) + \frac{\sum_i^n \left(L_i - L_i\right)^2}{2\sigma^2}, \qquad i = 1,\ldots,n.$$

D.1.2.1. Maximum Likelihood Estimation

Various maximum likelihood estimation (MLE) fits were made for the length vs. age data. One growth model (von Bertalanffy) was used on the full set of research|survey data (Figure D.2) and the four primary surveys used in this assessment (Figure D.3) – QCS synoptic, WCVI synoptic, WCHG synoptic, and GIG historical (see Table D.4 for all parameter fits). Figure D.4 shows cumulative length frequencies the synoptic surveys using paired years. The QCS survey tended to capture smaller fish than the other two surveys.

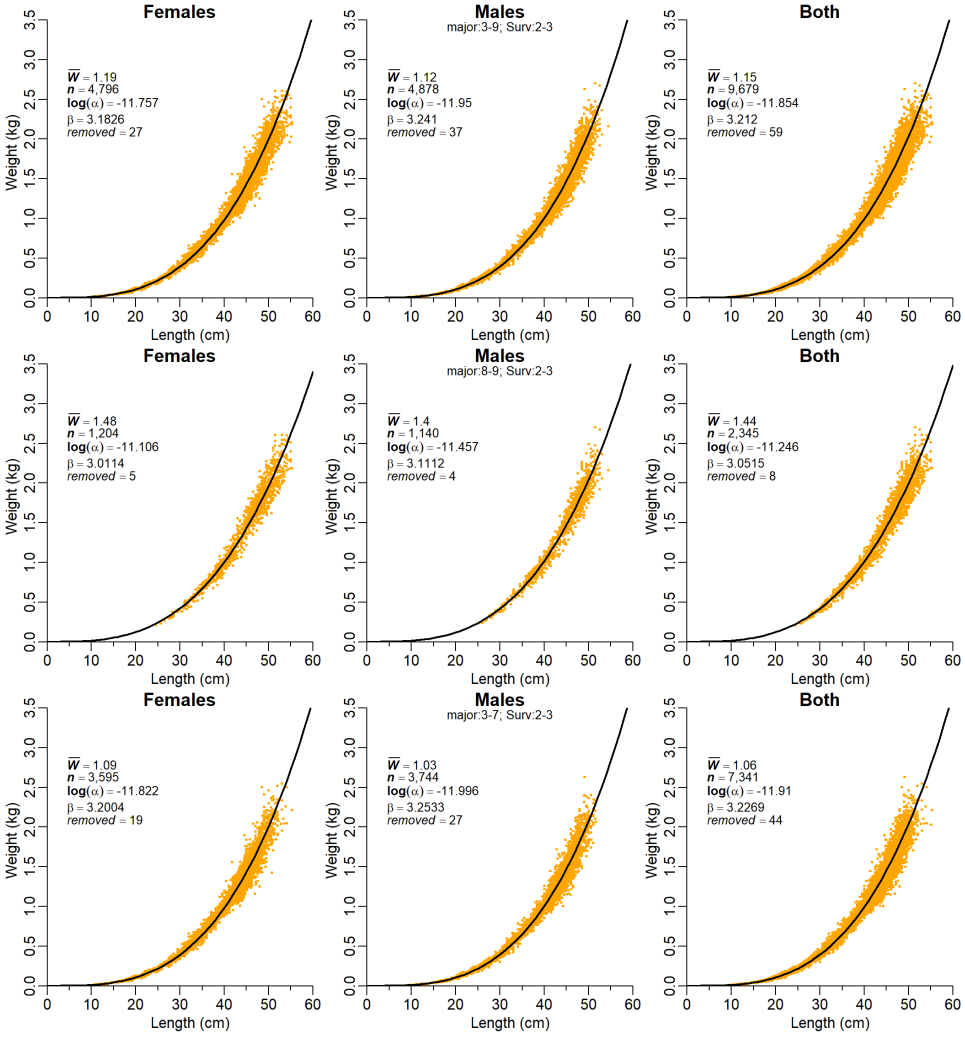

Figure D.1. Length-weight relationship for YMR – (top) coastwide survey data, (middle) 5DE survey data, (bottom) 3CD5ABC survey data. Records with absolute value of standardised residuals >3 (based on a preliminary fit) were dropped.

Table D.3. Number of YMR specimen otoliths aged by various methods. Number of samples appear in parentheses and are not additive between the sexes (i.e. otoliths by sex usually come from the same sample). The 'Charter' samples are from research surveys conducted on commercial vessels. These otoliths were collected over the period 1965 to 2019.

Trip Type	Activity	Age method	Female	Male	Unknown
Non-obs domestic	commercial	break & burn	1448 (52)	1385 (52)	---
Research	survey	surface read	36 (2)	28 (2)	---
Research	survey	break & burn	515 (32)	634 (33)	---
Charter	survey	surface read	6 (4)	8 (3)	---
Charter	survey	break & burn	2720 (170)	2581 (167)	5 (5)
Obs domestic	commercial	surface read	5 (2)	5 (1)	---
Obs domestic	commercial	thin section	43 (1)	50 (3)	---
Obs domestic	commercial	break & burn	3399 (140)	3854 (140)	11 (8)

Table D.4. Age-length parameter estimates for YMR (females, males, and both combined) from fits using the von Bertalanffy growth model (Quinn and Deriso 1999) using specimens from research and surveys combined as well as for specific surveys (north to south: WCHG = west coast Haida Gwaii, QCS = Queen Charlotte Sound, GIG = Goose Island Gully, WCVI = west coast Vancouver Island).

MLE Model	Data Source	Sex	n	Linf (cm)	K	t_0 (cm)
YMR vonB	research+surveys	Female	3200	48.2	0.1157	-2.46
		Male	3163	46.7	0.1288	-2.00
		Both	6362	47.4	0.1227	-2.18
YMR vonB	WCHG synoptic	Female	925	49.7	0.1109	-2.51
		Male	887	47.8	0.1283	-1.75
		Both	1812	48.8	0.1190	-2.14
YMR vonB	QCS synoptic	Female	1276	46.4	0.1256	-2.01
		Male	1240	45.1	0.1394	-1.61
		Both	2517	45.8	0.1322	-1.80
YMR vonB	GIG historical	Female	404	47.0	0.1248	-2.33
		Male	371	46.1	0.0802	-10
		Both	774	46.4	0.1060	-4.96
YMR vonB	WCVI synoptic	Female	284	49.5	0.1296	-2.35
		Male	356	47.8	0.1410	-2.24
		Both	639	48.4	0.1413	-2.01

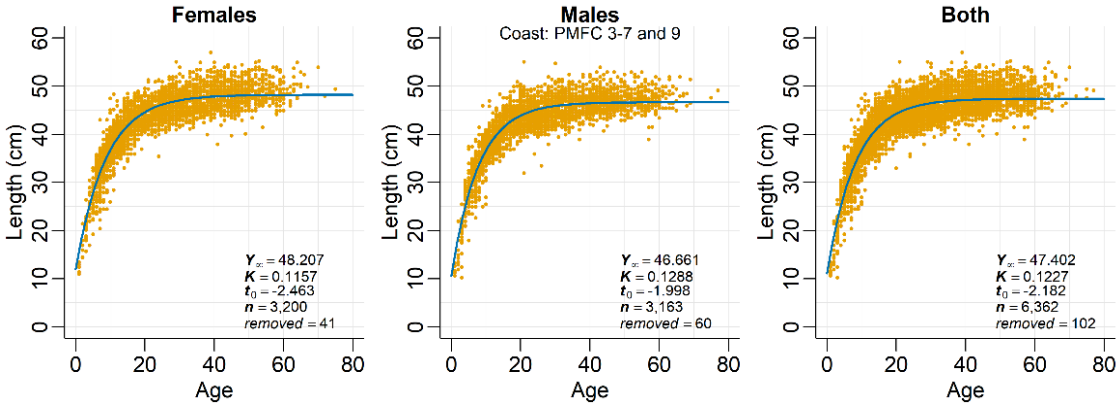

Figure D.2. Growth specified by age-length relationship: von Bertalanffy fits to YMR coastwide using data from research and surveys. Ages were determined by break-and-burn otoliths and surface-read otoliths from ages 1 to 3. Records with absolute value of standardised residuals >3 (based on a preliminary fit) were dropped.

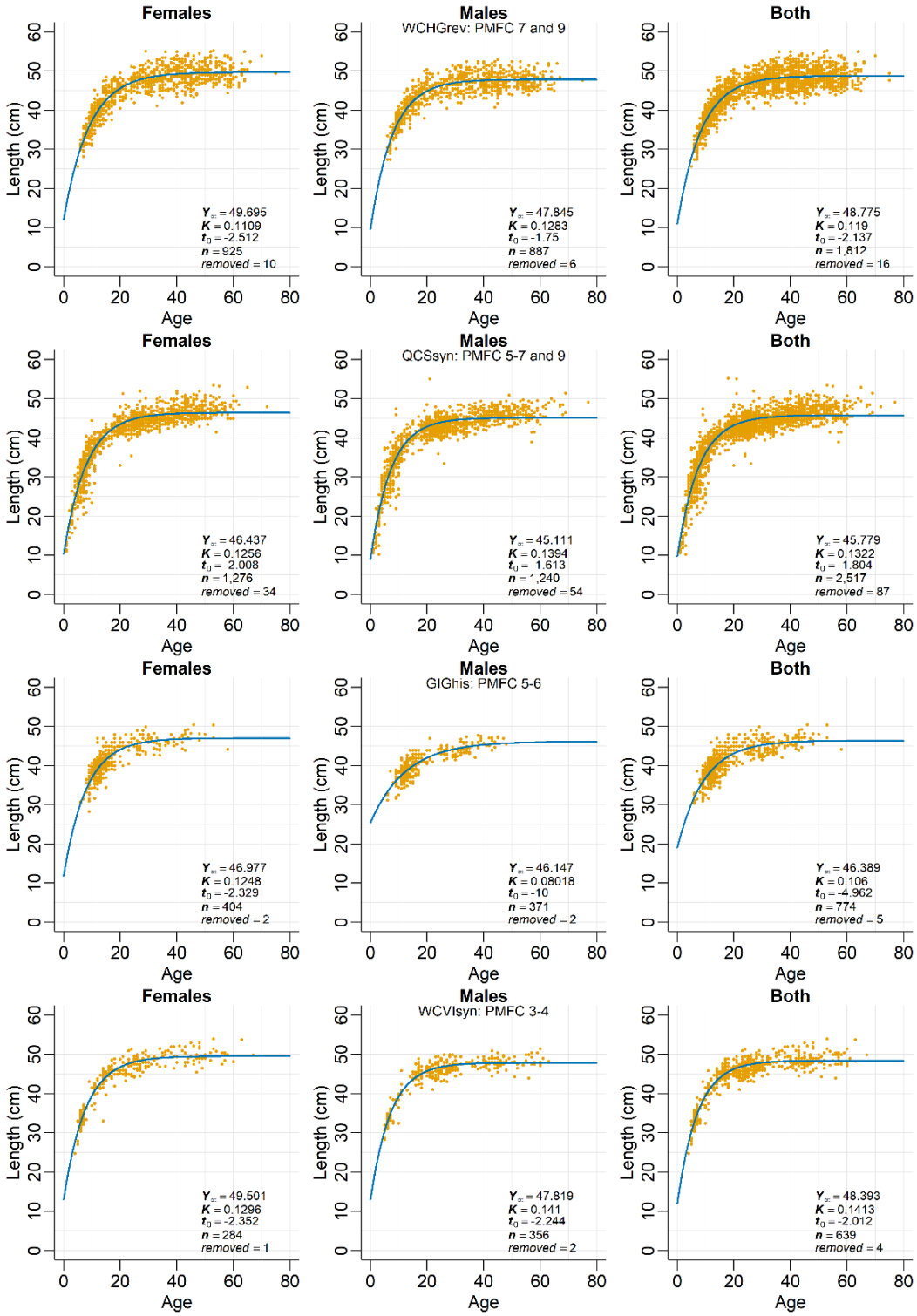

Figure D.3. Growth specified by age-length relationship: von Bertalanffy fits to YMR from four surveys: WCHG synoptic, QCS synoptic, GIG historical, and WCVI synoptic. See caption in Figure D.2 for additional details.

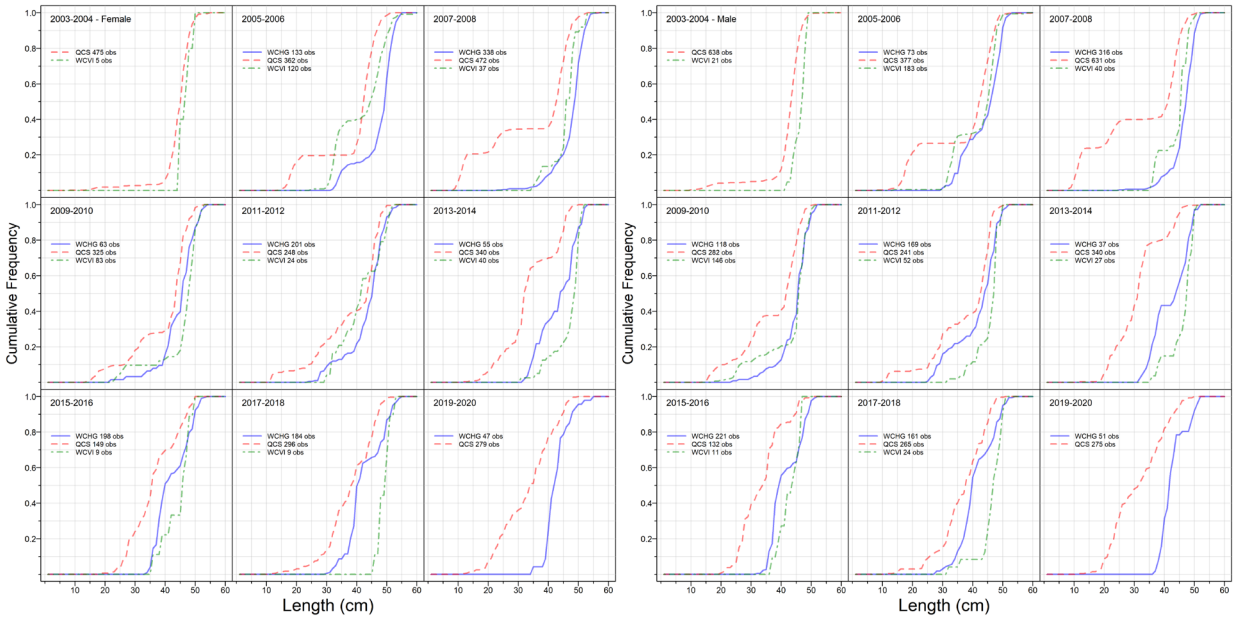

Figure D.4. Cumulative length frequencies for females (left) and males (right) comparing synoptic surveys occurring every two years. WCHG = west coast Haida Gwaii, QCS = Queen Charlotte Sound, WCVI = west coast Vancouver Island.

D.1.3. Maturity

This analysis was based on all "staged" (examined for maturity status) females in the DFO GFBioSQL database. Maturity codes for YMR in the database (Table D.5) come from `MATURITY_CONVENTION_CODE = 1`, which describes 7 maturity conditions for Rockfish (1977+).

Table D.5. GFBio maturity codes for rockfish, including BC rockfish.

Code	Female	Male
1	Immature - translucent, small	Immature - translucent, string-like
2	Maturing - small yellow eggs, translucent or opaque	Maturing - swelling, brown-white
3	Mature - large yellow eggs, opaque	-
4	Fertilized - large, orange-yellow eggs, translucent	Mature - large white, easily broken
5	Embryos or larvae - includes eyed eggs	Ripe - running sperm
6	Spent - large flaccid red ovaries; maybe a few larvae	Spent - flaccid, red
7	Resting - moderate size, firm, red-grey ovaries	Resting - ribbon-like, small brown

Mature (stage 3) YMR females start appearing in August and are most abundant during the months of December through February, with fertilised females peaking in March followed by embryo-bearing fish in April (Figure D.5). Ideally, lengths- and ages-at-maturity are calculated at times of peak development stages (males: insemination season, females: parturition season; Westrheim 1975). However, all months were used in creating the maturity curve because these data provided cleaner fits than using a subset of months. This required combining commercial and research data because most of the research data do not extend into the late autumn, winter and early spring months.

For the maturity analysis, all stages 3 and higher were assumed to be mature, and a maturity ogive was fit to the filtered data using a double-normal model:

$$m_{as} = \begin{cases} e^{-(a-v_s)^2/\rho_{sL}}, & a \le v_s \\ 1, & a > v_s \end{cases} \qquad \text{(D.3)}$$

where, m_{as} = maturity at age a for sex s (combined),

v_s = age of full maturity for sex s,

ρ_{sL} = variance for the left limb of the maturity curve for sex s.

To estimate a maturity ogive, the biological data records (recs) were qualified as follows:

• stocks – YMR coastwide	major = 3:9	98,011 recs
• ageing method (see note below)	ameth = c(0,1,3,17)	16,550 recs
• sample type – total catch/random	stype = c(1,2,6,7)	16,478 recs
• sex – females only	sex = 2	8,055 recs
• maturity codes for rockfish	mats = c(1:7)	6,271 recs
• ogive age limits	age = c(0,60)	5,420 recs
• trip type – survey + commercial	ttype = 1:5	5,420 recs
• month – all months	month = 1:12	5,420 recs

Generally, rockfish biological analyses use ages from otoliths processed and read using the 'break and burn' procedure (ameth=3) or coded as 'unknown' (ameth=0) but processed in 1980 or later. There is also a method termed 'break and bake' (ameth=17); however, no YMR were processed using this technique. Additionally, rockfish otoliths aged 1-3 y are sometimes processed using surface readings (ameth=1) because the ageing lab finds this technique more reliable than B&B for very young fish; see Table D.3 for YMR otoliths processed.

The above qualification yielded 5420 YMR female specimens from research surveys and the commercial fishery with maturity readings and valid ages. (The commercial fishery lacked data for YMR ages younger than 8 to determine ogives separately from survey data.) Mature specimens comprised those coded 3 to 7 for rockfish (Table D.5). The empirical proportion of mature females at each age was calculated (Figure D.6). A double-normal function (Eq. D.3) was fitted to the observed proportions mature at ages 1 to 60 to smooth the observations and determine an increasing monotonic function for use in the stock assessment model (Figure D.6). Additionally, a logistic function used by Vivian Haist (VH) for length models in New Zealand rock lobster assessments (Haist et al. 2009) was used to compare with the double normal model.

Following a procedure adopted by Stanley et al. (2009) for Canary Rockfish (*S. pinniger*), the proportions mature for young ages fitted by Eq. D.3 were not used because the fitted line may overestimate the proportion of mature females (Figure D.6). Therefore, the maturity ogive used in the stock assessment models (columns marked 'Mod m_a' in Table D.6) set proportion mature to zero for ages 1 to 4, then switched to the fitted monotonic function for ages 5 to 16. All ages from 17 were forced to 1 (fully mature). This strategy follows previous BC rockfish stock assessments where it was recognised that younger ages are not well sampled and those that are, tend to be larger and more likely to be mature. The function of this ogive in the stock assessment model is to calculate the spawning biomass used in the Beverton-Holt stock recruitment function, and is treated as a constant known without error. The ages at 50% and full maturity are estimated from the double-normal fit at 11 y and 16.8 y, respectively.

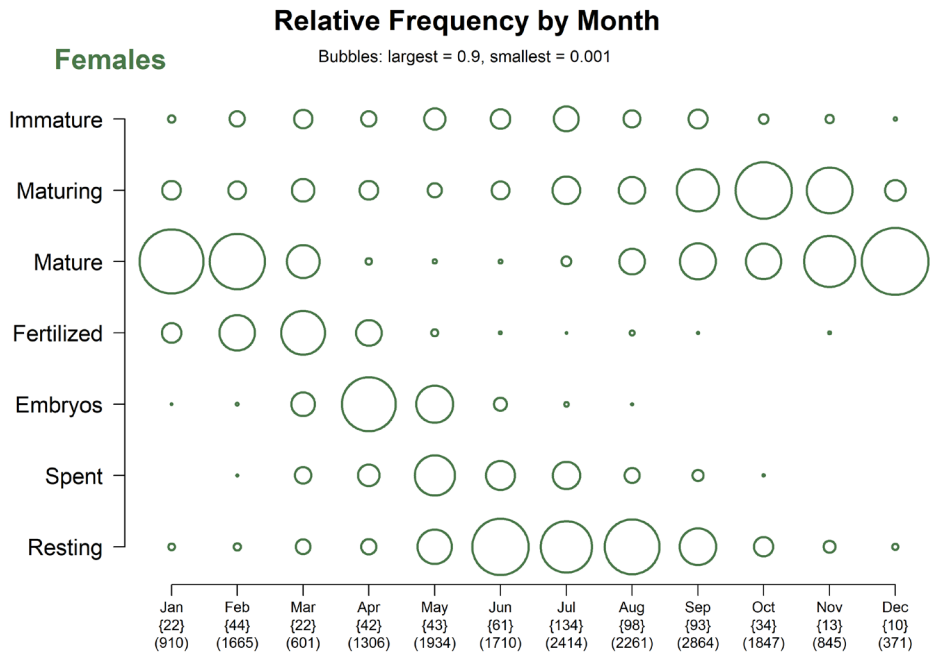

Figure D.5. Relative frequency of maturity codes by month for YMR females. Data include maturities from commercial and research specimens. Frequencies are calculated among each maturity category for every month.

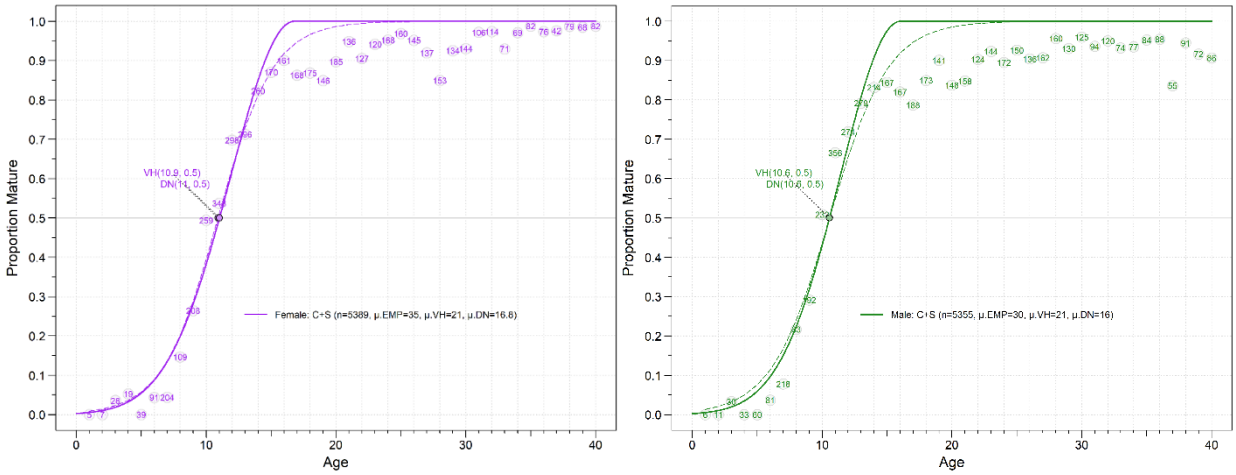

Figure D.6. Maturity ogives for YMR females (left) and males (right). Solid line shows double-normal (DN) curve fit; dashed line shows logistic model fit (VH = Vivian Haist); numbers in circles denote number of female specimens used to calculate the input proportions-mature (EMP =empirical). Estimated ages at 50% maturity are indicated near the median line; ages at full maturity (µ.VH, µ.DN) are displayed in the legend.

Table D.6. Proportion YMR females mature by age (m_a) used in the catch-age model ('Mod' column). Maturity stages 1 and 2 were assumed to be immature fish and all other staged fish (stages 3 to 7) were assumed to be mature. EMP = empirical, BL = binomial logit, VH =logistic used by Vivian Haist, DN = double normal (Eq.D.3), Mod = used in population model.

Age	# Fish	EMP m_a	BL m_a	VH m_a	DN m_a	Mod m_a
1	5	0	0.1020	0.0090	0.0055	0
2	7	0	0.1242	0.0144	0.0104	0
3	28	0.0357	0.1504	0.0229	0.0188	0
4	19	0.0526	0.1810	0.0364	0.0328	0
5	39	0	0.2163	0.0572	0.0549	0.0549
6	91	0.0440	0.2563	0.0888	0.0880	0.0880
7	204	0.0441	0.3008	0.1355	0.1352	0.1352
8	109	0.1468	0.3494	0.2012	0.1994	0.1994
9	208	0.2644	0.4014	0.2883	0.2819	0.2819
10	259	0.4942	0.4557	0.3943	0.3822	0.3822
11	348	0.5374	0.5111	0.5114	0.4970	0.4970
12	298	0.6980	0.5662	0.6272	0.6198	0.6198
13	296	0.7128	0.6197	0.7300	0.7414	0.7414
14	260	0.8231	0.6705	0.8130	0.8505	0.8505
15	170	0.8706	0.7175	0.8748	0.9357	0.9357
16	161	0.9006	0.7603	0.9183	0.9873	0.9873
17	168	0.8631	0.7984	0.9475	1	1
18	175	0.8686	0.8318	0.9667	1	1
19	146	0.8493	0.8606	0.9790	1	1
20	185	0.8973	0.8851	0.9868	1	1
25	160	0.9688	0.9590	0.9988	1	1
30	144	0.9306	0.9861	0.9999	1	1
35	82	0.9878	0.9954	1.0000	1	1
40	82	0.9878	0.9985	1.0000	1	1

D.1.4. Natural Mortality

Based on a previous stock assessment of YMR (Edwards et al. 2012), estimates of natural mortality (*M*) from an Awatea-fitted model were 0.0595 (0.0544, 0.0648) for females and 0.0559 (0.0507, 0.0613) for males. In the DFO database GFBioSQL, the maximum age for YMR is 99 years, which suggests an *M* value ranging from 0.047 to 0.055, depending on the method (Table D.8). At age 50 (~0.95 quantile), the estimate *M* value range from 0.092 to 0.11 (Table D.8), which far exceeds the estimates from the previous assessment.

The Hoenig (1983) estimator describes an exponential decay LN(k) = -Z t_L, where Z = natural mortality, t_L = longevity of a stock, and k = proportion of animals that are still alive at t_L. Quinn and Deriso (1999) popularised this estimator by re-arranging Hoenig's equation and setting k=0.01 (as originally suggested by Hoenig):

$$M = -\ln(0.01) \,/\, t_{\max} \qquad \text{(D.4)}$$

Then et al. (2015) revisited various natural mortality estimators and recommended the use of an updated Hoenig estimator based on nonlinear least squares:

$$M = 4.899\, t_{\max}^{-0.916} \qquad \text{(D.5)}$$

where t_{max} = maximum age.

During the review process for Redstripe Rockfish (DFO 2022), one of the principal reviewers, Vladlena Gertseva (2018, Northwest Fisheries Science Center, National Oceanic and Atmospheric Administration [NOAA], pers. comm.), noted that Then et al. (2015) did not consistently apply a log transformation. In real space, one might expect substantial

heteroscedasticity in both the observation and process errors associated with the relationship of M to t_{max}. Re-evaluating the data used in Then et al. (2015) by fitting the one-parameter t_{max} model using a log-log transformation (such that the slope is forced to be -1 in the transformed space, as in Hamel 2015), Gertseva recalculated the point estimate for M as:

$$M = 5.4 / t_{\max} \qquad \text{(D.6)}$$

In past CSAS Regional Peer Review meetings, participants have been averse to adopting a maximum age that comes from a single, usually isolated individual, preferring instead to observe the tail distribution of ages (Figure D.7). For YMR, this suggests that ages 50 and above might be more appropriate. Using ages 50 to 90 at 10 y increments (~0.95-0.99 quantiles), Table D.8 calculates possible M values based on the Hoenig (1983) and Vladlena Gertseva estimators (2018, Northwest Fisheries Science Center, National Oceanic and Atmospheric Administration [NOAA], pers. Comm).

In preliminary trials using SS, estimating M using revised data from surveys and the commercial fleet proved to be untenable. The MPD estimate for females was 0.072 and the MCMC estimate was 0.071 (0.060, 0.082); however, the estimates of R0 were unrealistically high and the MCMC simulation procedure did not converge. Therefore, based on Table D.8, the previous YMR assessment, and numerous trial runs for this assessment, we opted to fix M values to span a feasible set: $M \in \{0.04, 0.045, 0.05, 0.055, 0.06\}$.

Table D.7. 99th percentile of age by year, YMR species category (determined from GMU spatial definition) and commercial/research category. Also shown are the number of samples and number of otoliths used when calculating the 99th percentile. Dash '--' indicates no data.

	Number samples (# otoliths)								99th percentile (age)							
	Commercial				Research				Commercial				Research			
Year	3C	3D5AB	5CD	5E	3C	3D5AB	5CD	5E	3C	3D5AB	5CD	5E	3C	3D5AB	5CD	5E
1965	--	--	--	--	1 (36)	--	--	--	--	--	--	--	32.3	--	--	--
1967	--	--	--	--	--	1 (28)	--	--	--	--	--	--	--	31.0	--	--
1978	--	--	--	1 (95)	--	--	--	--	--	--	--	31.1	--	--	--	--
1979	--	2 (200)	--	4 (394)	1 (85)	2 (199)	--	3 (279)	--	70.0	--	32.2	56.6	31.0	--	29.2
1980	--	--	--	7 (698)	--	--	--	--	--	--	--	33.0	--	--	--	--
1990	--	6 (240)	1 (53)	3 (199)	--	--	--	--	--	41.0	80.3	43.0	--	--	--	--
1991	--	5 (245)	--	--	--	--	--	--	--	40.0	--	--	--	--	--	--
1992	--	9 (297)	--	--	--	--	--	--	--	43.3	--	--	--	--	--	--
1993	--	7 (373)	1 (61)	--	--	--	--	3 (152)	--	58.0	47.6	--	--	--	--	42.5
1994	--	4 (229)	--	--	--	7 (135)	--	--	--	44.7	--	--	--	52.0	--	--
1995	--	8 (304)	--	--	--	8 (449)	--	--	--	48.0	--	--	--	44.5	--	--
1996	--	5 (312)	--	--	5 (50)	2 (40)	--	2 (94)	--	43.0	--	--	17.5	45.1	--	46.4
1997	--	--	--	--	--	--	1 (50)	7 (262)	--	--	--	--	--	--	48.0	52.8
1998	--	9 (361)	--	2 (80)	--	--	--	--	--	51.4	--	48.0	--	--	--	--
1999	--	9 (393)	2 (94)	--	--	--	--	--	--	49.2	48.0	--	--	--	--	--
2000	--	3 (155)	2 (102)	2 (140)	--	--	--	--	--	60.9	53.0	51.2	--	--	--	--
2001	--	4 (235)	3 (184)	2 (111)	--	--	--	--	--	51.7	51.0	54.0	--	--	--	--
2002	--	6 (374)	1 (23)	2 (127)	--	--	--	--	--	51.0	51.0	55.2	--	--	--	--
2003	--	6 (318)	2 (91)	--	--	15 (238)	4 (12)	--	--	52.0	57.0	--	--	57.9	42.7	--
2004	--	--	--	--	--	1 (26)	--	--	--	--	--	--	--	60.0	--	--
2005	--	8 (317)	1 (65)	--	--	5 (145)	2 (35)	--	--	50.0	59.0	--	--	59.5	85.6	--
2006	--	--	--	--	3 (101)	4 (199)	--	2 (118)	--	--	--	--	60	58.0	--	53.8
2007	--	7 (351)	1 (48)	--	--	5 (189)	3 (143)	3 (168)	--	56.5	56.0	--	--	58.1	56.6	61.3
2008	--	--	--	--	--	1 (56)	--	4 (171)	--	--	--	--	--	50.9	--	59.0
2009	--	7 (389)	--	--	--	14 (350)	1 (31)	--	--	59.1	--	--	--	54.0	56.1	--
2010	--	6 (276)	3 (128)	--	--	4 (108)	--	5 (153)	--	58.3	59.5	--	--	59.9	--	60.0
2011	--	5 (204)	2 (101)	2 (102)	--	9 (247)	2 (50)	--	--	60.0	60.0	62.0	--	58.6	7.5	--
2012	--	5 (283)	--	--	1 (1)	1 (27)	--	9 (257)	--	53.2	--	--	23	59.2	--	60.4
2013	--	2 (98)	--	1 (63)	--	10 (278)	5 (121)	--	--	44.1	--	64.1	--	57.5	44.6	--
2014	1 (35)	2 (100)	--	--	--	1 (35)	--	3 (77)	27.0	50.0	--	--	--	51.5	--	63.0
2015	--	3 (171)	--	1 (61)	--	3 (83)	2 (57)	--	--	58.6	--	63.2	--	45.4	9.9	--
2016	--	5 (258)	--	--	--	--	--	12 (350)	--	52.4	--	--	--	--	--	64.5
2017	--	6 (301)	1 (50)	--	--	15 (353)	2 (45)	--	--	61.0	59.1	--	--	60.5	10.6	--
2018	--	1 (47)	2 (104)	--	--	--	--	7 (222)	--	41.1	65.0	--	--	--	--	66.0
2019	--	3 (160)	--	--	--	7 (184)	2 (44)	--	--	50.0	--	--	--	65.5	4.0	--
Total	1 (35)	143 (6991)	22 (1104)	27 (2070)	11 (273)	115 (3369)	24 (588)	60 (2303)	27.0	51.8	57.4	48.8	37.9	53.0	36.6	54.9

Table D.8. Estimates of YMR natural mortality using equations based on fish longevity. Various upper ages > 0.95 quantile up to the observed t_{max} = 99y are used to illustrated the variability in M based on alternative 'maximum' ages. Empirical cumulative distribution function (ecdf) was used to estimate quantiles for various ages: in R, ecdf_fun = function(x,pc) ecdf(x)(pc).

Age	Quantile from ecdf	Hoenig (1983) M=-LN(0.01)/tmax	Gertseva (2018) M=5.4/tmax
50	0.9529909	0.0921	0.1080
60	0.9935347	0.0768	0.0900
70	0.9991541	0.0658	0.0771
80	0.9996979	0.0576	0.0675
90	0.9999396	0.0512	0.0600
99	1	0.0465	0.0545

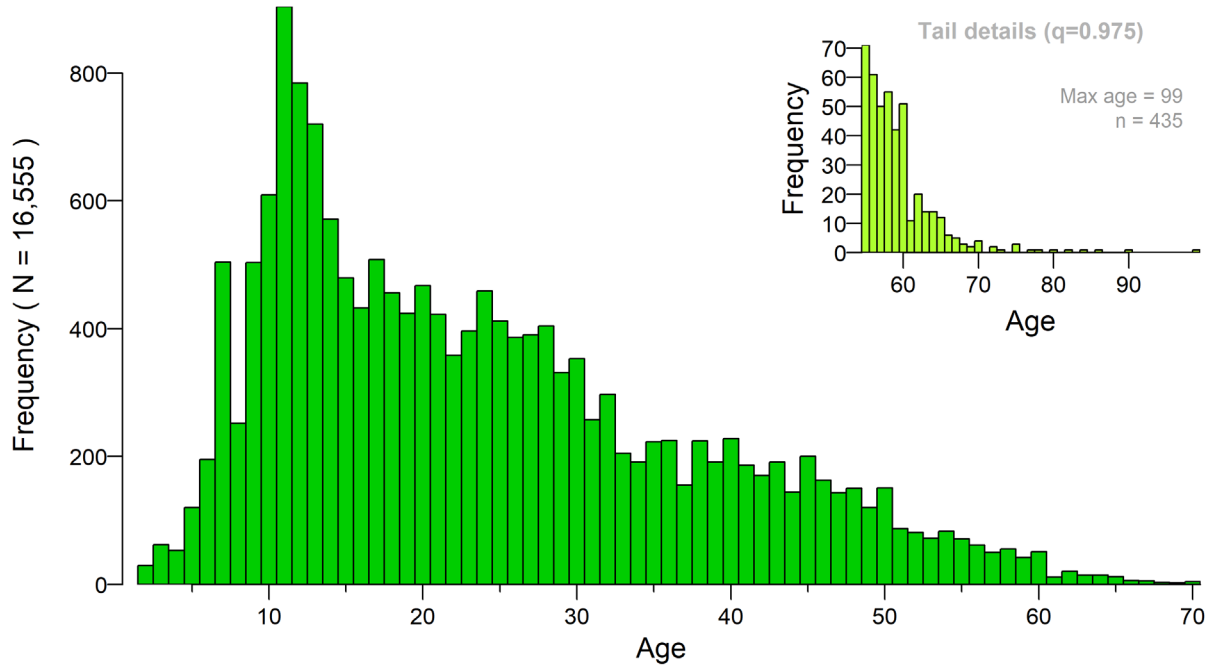

Figure D.7. Distribution of YMR female + male ages; inset shows details for ages >=55 y old, which is the 0.975 quantile of the complete age data set.

D.1.5. Generation Time

Generation time t_G is assumed to be the average age of adults (males and females) in the population, and takes the form:

$$t_G = k + \frac{1}{e^M - 1} \qquad \text{(D.7)}$$

where k = age at 50% maturity,

M = instantaneous rate of natural mortality.

COSEWIC uses a rough approximation to generation time:

$$t_G = k + \frac{1}{M} \qquad \text{(D.8)}$$

From Section D.1.3, k = 11.0 y for YMR females. If we assume that M = 0.055 (using oldest age in Table D.8), then the COSEWIC estimate of generation time t_G = 29.2 y for the coastwide stock. For simplicity, we adopt t_G = 30 years, which was the generation time used in the 2011 YMR stock assessment (Edwards et al. 2012).

D.2. WEIGHTED AGE PROPORTIONS

This section summarises a method for representing commercial and survey age structures in the stock assessment model for a given species (herein called 'target') through weighting observed age frequencies x_a or proportions x'_a by catch‖density in defined strata (h). (Throughout this section, the symbol '‖' is used to delimit parallel values for commercial and survey analyses, respectively, as the mechanics of the weighting procedure are similar for both. The symbol can be read 'or', e.g., catch or density.) For commercial samples, these strata comprise quarterly periods within a year, while for survey samples, the strata are defined by longitude, latitude, and depth boundaries unique to each survey series. A two-tiered weighting system is used as follows:

Within each stratum h, commercial age samples were identified by trip (usually one sample per trip[14]) and the age frequencies per trip were weighted by the target catch weight (tonnes) of the tows that were sampled to yield one weighted age frequency per stratum (quarter). For each year, the quarterly age frequencies were then weighted by the quarterly fishery catch of the target. If a quarter had not been sampled, it was not used in the weighting for the year. For example, if samples of the target were missing in Oct-Dec 2018, only the first three quarters of target catch would be used to prorate three quarterly age frequencies in 2018, resulting in a single age frequency for the year.

Annual survey ages were weighted similarly. Each sampled tow in a survey stratum was weighted by the tow's target catch density (t/km^2) to yield a single weighted age frequency per stratum. As above, not all survey strata had age samples and so weighted age frequencies by sampled stratum were weighted by the appropriate stratum area (km^2). For example, if only shallow strata were sampled for age, the deep strata areas were not used to prorate the shallow-strata age frequencies. As for commercial ages, the two-tiered weighting scheme yielded one age frequency per survey year.

Ideally, sampling effort would be proportional to the amount of the target caught, but this is not usually the case. Personnel can control the sampling effort on surveys more than on board commercial vessels, but the relative catch among strata over the course of a year or survey cannot be known with certainty until the events have occurred. Therefore, the stratified weighting scheme outlined above and detailed below attempts to adjust for unequal sampling effort among strata.

For simplicity, the weighting of age frequencies x_a is used for illustration, unless otherwise specified. The weighting occurs at two levels: h (quarters for commercial ages, strata for survey ages) and i (years if commercial, total stratum area if survey). Notation is summarised in Table D.9.

[14] Samples were combined, weighted by the tow weight, for trips with more than one sample to give a single age frequency for each trip.

Table D.9. Equations for weighting age frequencies or proportions; (c) = commercial, (s) = survey.

Indices

Symbol	Description
a	age class (1 to A, where A is an accumulator age-class)
d	(c) trip ID as sample unit (usually one sample per trip) (s) sample ID as sample unit (usually one sample per survey tow)
h	(c) calendar year quarter (1 to 4), 91.5 days each (s) survey stratum (area-depth combination)
i	(c) calendar year (1977 to present) (s) single survey ID in survey series (e.g., 2003 QCS Synoptic)

Data

Symbol	Description
x_{adhi}	observations-at-age a for sample unit d in quarter‖stratum h of year‖survey i
x'_{adhi}	proportion-at-age a for sample unit d in quarter‖stratum h of year‖survey i
C_{dhi}	(c) commercial catch (tonnes) of the target for sample unit d in quarter h of year i (s) density (t/km^2) of the target for sample unit d in stratum h of survey i
C'_{dhi}	C_{dhi} as a proportion of total catch‖density $C_{hi} = \sum_d C_{dhi}$
y_{ahi}	weighted age frequencies at age a in quarter‖stratum h of year‖survey i
K_{hi}	(c) total commercial catch (t) of the target in quarter h of year i (s) stratum area (km^2) of stratum h in survey i
K'_{hi}	K_{hi} as a proportion of total catch‖area $K_i = \sum_h K_{hi}$
p_{ai}	weighted frequencies at age a in year‖survey i
p'_{ai}	weighted proportions at age a in year‖survey i

For each quarter‖stratum h, sample unit frequencies x_{ad} are weighted by sample unit catch‖density of the target species. (For commercial ages, trip is used as the sample unit, though at times one trip may contain multiple samples. In these instances, multiple samples from a single trip will be merged into a single sample unit.) Within any quarter‖stratum h and year‖survey i there is a set of sample catches‖densities C_{dhi} that can be transformed into a set of proportions:

$$C'_{dhi} = C_{dhi} \Big/ \sum_d C_{dhi} \,. \qquad \text{(D.9)}$$

The proportion C'_{dhi} is used to weight the age frequencies x_{adhi} summed over d, which yields weighted age frequencies by quarter‖stratum for each year‖survey:

$$y_{ahi} = \sum_d \left(C'_{dhi} x_{adhi} \right). \quad \text{(D.10)}$$

This transformation reduces the frequencies x from the originals, and so y_{ahi} is rescaled (multiplied) by the factor

$$\sum_a x_{ahi} \Big/ \sum_a y_{ahi} \quad \text{(D.11)}$$

to retain the original number of observations. (For proportions x' this is not needed.) Although this step is performed, it is strictly not necessary because at the end of the two-step weighting, the weighted frequencies are transformed to represent proportions-at-age.

At the second level of stratification by year‖survey i, the annual proportion of quarterly catch (t) for commercial ages or the survey proportion of stratum areas (km^2) for survey ages is calculated

$$K'_{hi} = K_{hi} \Big/ \sum_h K_{hi} \qquad \text{(D.12)}$$

to weight y_{ahi} and derive weighted age frequencies by year‖survey:

$$p_{ai} = \sum_h \left(K'_{hi} y_{ahi} \right). \qquad \text{(D.13)}$$

Again, if this transformation is applied to frequencies (as opposed to proportions), it reduces them from the original, and so p_{ai} is rescaled (multiplied) by the factor

$$\sum_a y_{ai} \Big/ \sum_a p_{ai} \qquad \text{(D.14)}$$

to retain the original number of observations.

Finally, the weighted frequencies are transformed to represent proportions-at-age:

$$p'_{ai} = p_{ai} \Big/ \sum_a p_{ai} \,. \qquad \text{(D.15)}$$

If initially we had used proportions x'_{adhi} instead of frequencies x_{adhi}, the final transformation would not be necessary; however, its application does not affect the outcome.

The choice of data input (frequencies x vs. proportions x') can sometimes matter: the numeric outcome can be very different, especially if the input samples comprise few observations. Theoretically, weighting frequencies emphasises our belief in individual observations at specific ages while weighting proportions emphasises our belief in sampled age distributions. Neither method yields inherently better results; however, if the original sampling methodology favoured sampling few fish from many tows rather than sampling many fish from few tows, then weighting frequencies probably makes more sense than weighting proportions. In this assessment, age frequencies x are weighted.

D.2.1. Commercial Ages

For the YMR stock, sampled age frequencies (AF) from the commercial fisheries (primarily bottom and midwater trawl) were combined; the shrimp trawl data were not used. Therefore, the model was run assuming a joint selectivity for all fishing methods (the catch data were also combined into a single fishery).

The 2018 stock assessment of Redstripe Rockfish (Starr and Haigh, 2021a) did not separate sorted (by size or sex) and unsorted samples when introducing proportions-at-age into the model. This practice was also followed for the 2019 BOR stock assessment after exploratory runs using only sorted and only unsorted samples were examined. Usually the sorted samples occur earlier in the time series than do the unsorted samples. Consequently, dropping sorted samples loses information about early recruitment strength. This stock assessment uses combined sorted and unsorted samples for YMR AFs.

Table D.10. Commercial trip quarterly data from the 'Trawl+' fishery used to weight YMR proportions-at-age: number of sampled trips, YMR catch (t) by sampled trip and by all trips.

REBS north Trawl Fishery

Year	# Trips | # Samples				Sampled catch (t)				Fishery catch (t)			
	Q1	Q2	Q3	Q4	Q1	Q2	Q3	Q4	Q1	Q2	Q3	Q4
1978	---	1 | 1	---	---	---	2.95	---	---	86	266	552	311
1979	3 | 3	3 | 3	---	---	42.78	2.50	---	---	142	240	56	---
1980	---	2 | 2	3 | 3	2 | 2	---	56.44	57.31	54.76	---	227	224	97
1990	7 | 7	3 | 3	---	---	78.60	58.35	---	---	355	826	437	62
1991	4 | 4	---	1 | 1	---	50.95	---	4.54	---	414	482	241	105
1992	6 | 6	1 | 1	2 | 2	---	52.08	1.36	7.95	---	349	606	408	140
1993	2 | 2	5 | 5	---	1 | 1	12.37	16.14	---	5.90	388	369	149	259
1994	---	1 | 1	1 | 1	2 | 2	---	6.81	14.97	14.30	382	254	172	436
1995	4 | 4	---	3 | 3	1 | 1	42.68	---	16.03	3.39	484	470	420	31
1996	4 | 4	1 | 1	---	---	68.18	15.03	---	---	526	628	119	149
1998	4 | 5	3 | 3	2 | 2	1 | 1	70.37	36.14	23.52	6.02	464	663	529	203
1999	3 | 3	6 | 6	2 | 2	---	18.02	27.89	2.24	---	410	642	480	223
2000	1 | 1	3 | 3	3 | 3	---	1.82	27.92	11.13	---	672	651	634	130
2001	2 | 2	3 | 3	4 | 4	---	9.95	8.26	6.74	---	448	579	562	267
2002	---	4 | 4	4 | 4	1 | 1	---	24.35	21.28	4.54	535	579	738	189
2003	---	3 | 3	3 | 3	2 | 2	---	14.96	20.69	15.96	466	588	559	317
2005	---	2 | 2	5 | 5	2 | 2	---	4.46	22.65	33.11	445	545	761	228
2007	---	5 | 5	3 | 3	---	---	20.65	5.32	---	179	484	618	80
2009	3 | 3	1 | 1	3 | 3	---	8.81	0.04	22.52	---	259	483	723	132
2010	---	4 | 5	2 | 3	1 | 1	---	42.29	18.58	24.49	193	340	475	180
2011	---	5 | 5	2 | 2	2 | 2	---	26.18	25.95	38.99	227	335	519	146
2012	1 | 1	2 | 2	1 | 1	1 | 1	3.61	8.22	12.60	21.09	84	372	501	238
2013	1 | 1	1 | 1	---	1 | 1	11.95	23.89	---	8.88	93	456	580	190
2014	1 | 1	2 | 2	---	---	0.84	1.79	---	---	328	413	537	95
2015	2 | 2	1 | 1	---	1 | 1	2.63	9.46	---	1.45	92	382	530	191
2016	1 | 1	---	4 | 4	---	6.58	---	31.01	---	223	273	458	201
2017	4 | 4	1 | 1	2 | 2	---	18.02	43.02	8.36	---	363	482	474	70
2018	2 | 2	1 | 1	---	---	1.83	1.35	---	---	230	546	337	94
2019	2 | 2	1 | 1	---	---	6.36	0.67	---	---	229	609	478	194

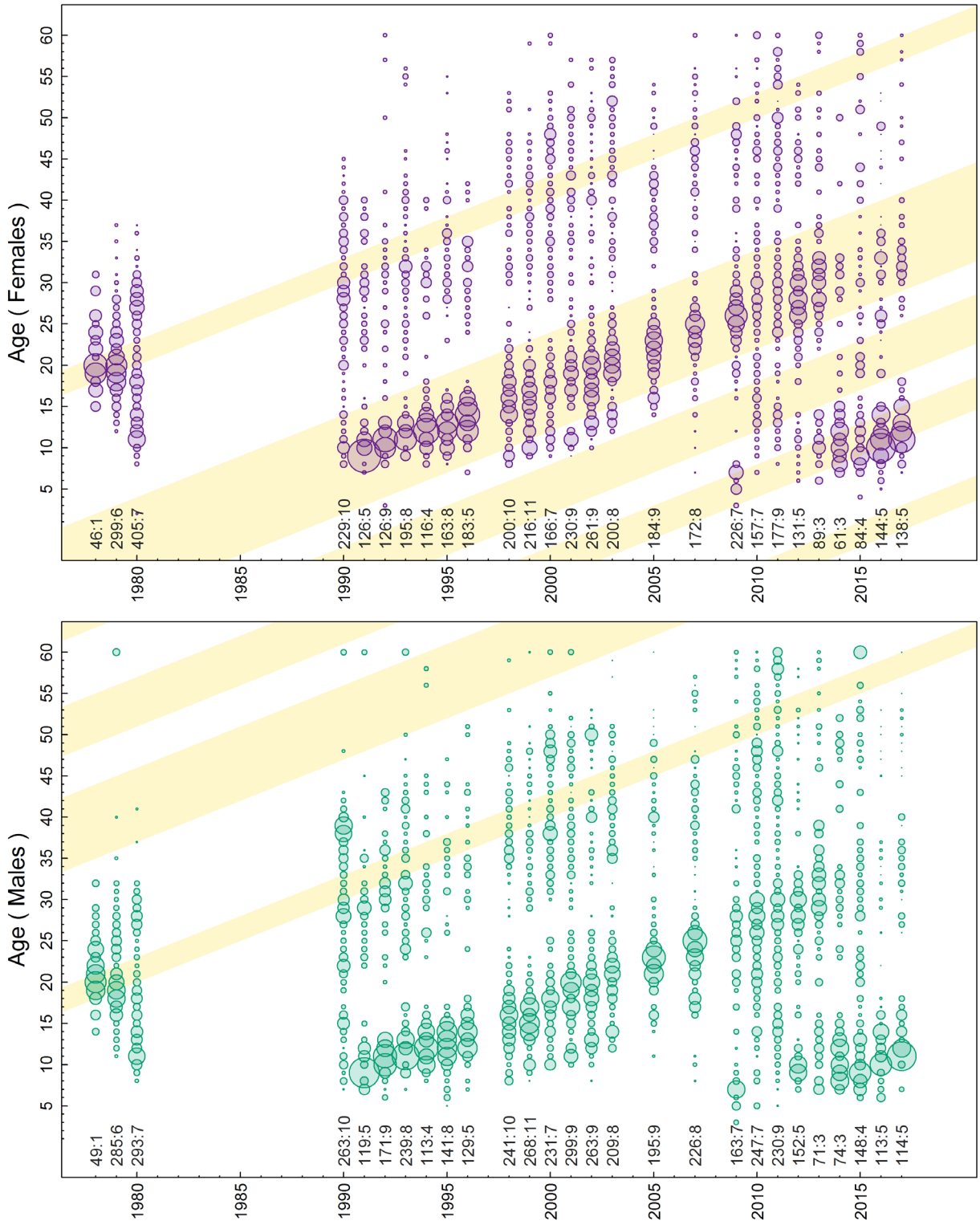

Figure D.8. Proportions-at-age for YMR caught by commercial trawl gear (left) and gear other than trawl (right) calculated as age frequencies weighted by trip catch within quarters and commercial catch within years. Diagonal shaded bands indicate cohorts that were born when the mean Pacific Decadal Oscillation was positive. Numbers displayed along the bottom axis indicate number of fish aged and number of samples (colon delimited) by year.

D.2.2. Research/Survey Ages

Age data for YMR from the surveys cover years from 1979 to 2019 (Table D.11). Age cohort patterns are discernible, which is not always the case for other rockfish sampled by surveys.

The coastwide YMR stock is covered by four surveys:

- QCS Synoptic (9 years) from 2003-2019 (Figure D.9);
- WCVI Synoptic (7 years) in 1996 and from 2004-2014 (Figure D.10);
- WCHG Synoptic (9 years) in 1997 and from 2006-2018 (Figure D.11);
- GIG Historical (3 years) in 1979 and 1994-95 (Figure D.12);

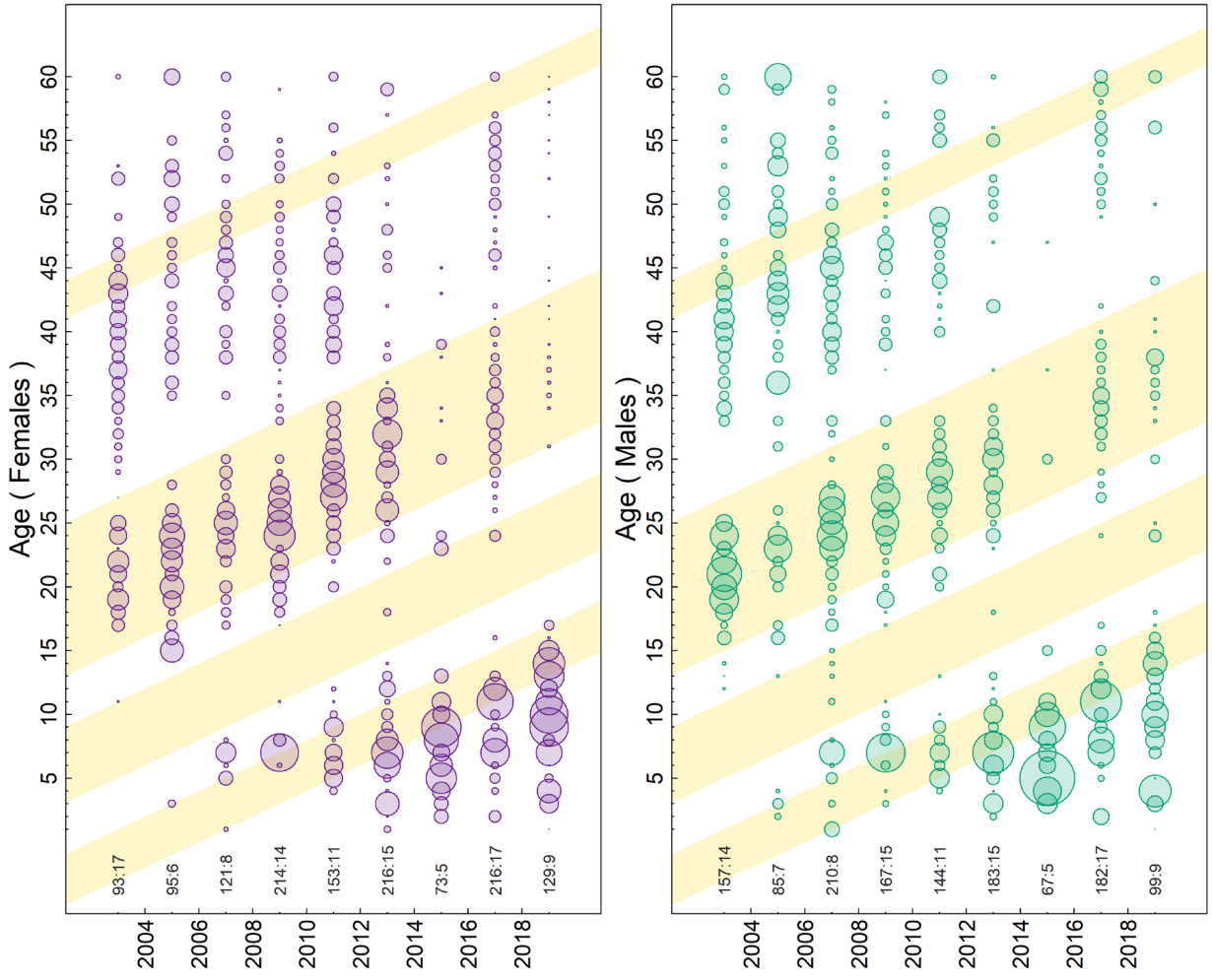

Figure D.9. QCS Synoptic (2003-2019) – proportions-at-age based on age frequencies weighted by mean fish density within strata and by total stratum area within survey (Table D.11). See Figure D.8 for details on diagonal shaded bands and displayed numbers.

Table D.11. Number of YMR age samples (s) collected from surveys and YMR density (d=kg/km^2) by survey stratum identifier (h); stratum area is shown in parentheses.

Year	Survey Strata						
QCS	h=18 (5012 km^2)	h=19 (5300 km^2)	h=20 (2640 km^2)	h=21 (528 km^2)	h=22 (1740 km^2)	h=23 (3928 km^2)	h=24 (3664 km^2)
2003	-	s=2, d=1.460	s=7, d=1.379	-	-	-	s=10, d=0.864
2005	-	-	s=2, d=1.880	-	s=1, d=0.013	s=3, d=0.371	s=1, d=0.620
2007	-	s=1, d=0.434	s=2, d=1.408	-	s=1, d=0.051	s=2, d=0.058	s=2, d=1.262
2009	-	s=2, d=0.286	s=7, d=1.928	s=2, d=1.358	s=1, d=0.044	s=2, d=4.851	s=1, d=0.363
2011	-	s=1, d=1.747	s=6, d=2.773	-	-	s=1, d=1.328	s=3, d=1.319
2013	s=1, d=0.589	s=3, d=1.431	s=5, d=0.884	-	-	s=2, d=0.882	s=4, d=1.023
2015	-	-	s=3, d=1.645	-	-	s=2, d=0.476	-
2017	-	s=2, d=3.713	s=9, d=1.800	-	-	s=2, d=0.319	s=4, d=10.339
2019	-	s=2, d=5.737	s=5, d=8.550	-	-	s=2, d=0.283	-
WCVI	h=67 (708 km^2)	h=68 (572 km^2)	h=118 (1207 km^2)	h=119 (497 km^2)	-	-	-
1996	-	-	s=1, d=0.078	s=6, d=4.334	-	-	-
2004	s=1, d=0.393	-	-	-	-	-	-
2006	s=7, d=0.579	-	-	-	-	-	-
2008	s=1, d=1.206	-	-	-	-	-	-
2010	s=4, d=2.060	-	-	-	-	-	-
2012	s=1, d=0.606	s=1, d=3.187	-	-	-	-	-
2014	s=1, d=3.309	-	-	-	-	-	-
WCHG	h=114 (1244 km^2)	h=115 (892 km^2)	h=126 (1266 km^2)	h=151 (1076 km^2)	h=152 (1004 km^2)	-	-
1997	s=5, d=4.019	s=3, d=1.234	-	-	-	-	-
2006	-	-	s=2, d=1.427	-	-	-	-
2007	-	-	-	s=3, d=4.390	-	-	-
2008	-	-	-	s=4, d=2.950	-	-	-
2010	-	-	-	s=5, d=0.600	-	-	-
2012	-	-	-	s=8, d=7.124	s=1, d=5.400	-	-
2014	-	-	-	s=3, d=8.518	-	-	-
2016	-	-	-	s=10, d=1.588	s=2, d=16.237	-	-
2018	-	-	-	s=7, d=5.480	-	-	-
GIG	h=0 (3408 km^2)	h=121 (1166 km^2)	h=122 (1677 km^2)	h=124 (686 km^2)	h=138 (1190 km^2)	h=139 (1023 km^2)	h=186 (1199 km^2)
1979	s=2, d=30.652	-	-	-	-	-	-
1994	-	-	-	-	s=1, d=6.514	s=2, d=1.263	s=1, d=0.668
1995	-	s=2, d=15.793	s=2, d=12.118	s=1, d=4.799	-	-	-

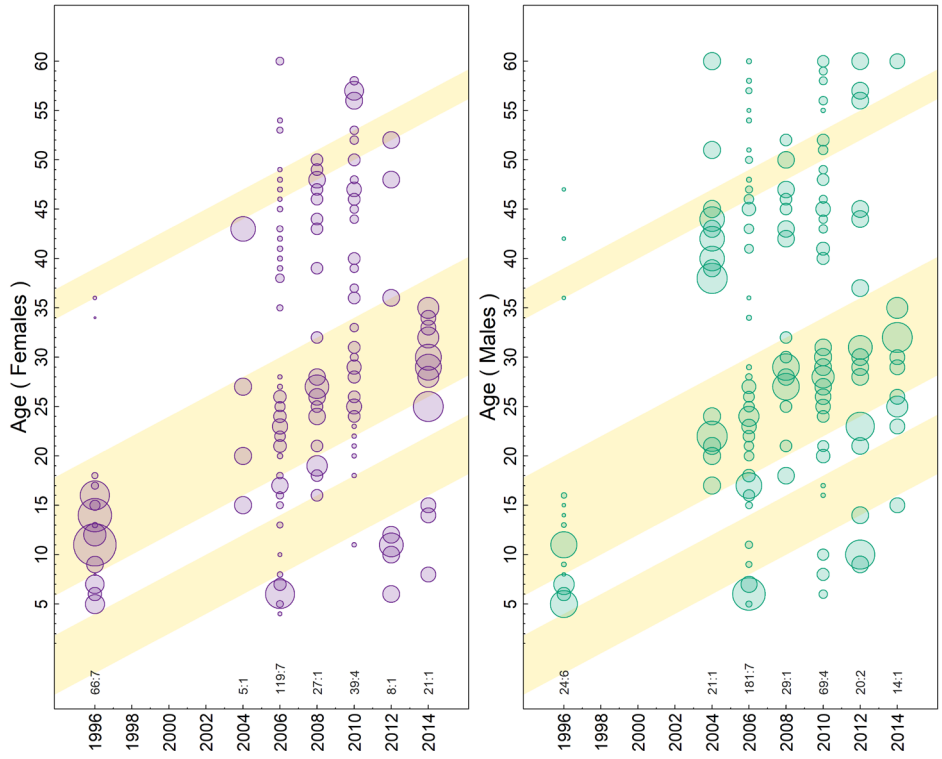

Figure D.10. WCVI Synoptic (2004 on) and WCVI rockfish (1996) – proportions-at-age: see Table D.11 and Figure D.8 for details.

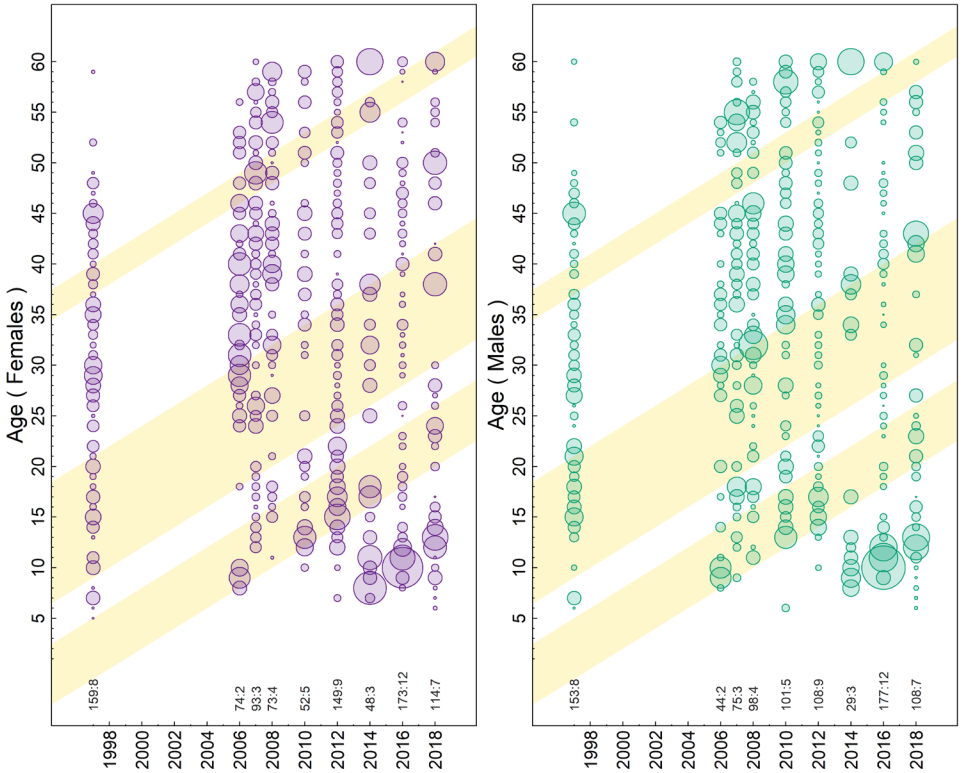

Figure D.11. WCHG Synoptic (2006 on) and WCQCI rockfish (1997) – proportions-at-age: see Table D.11 and Figure D.8 for details.

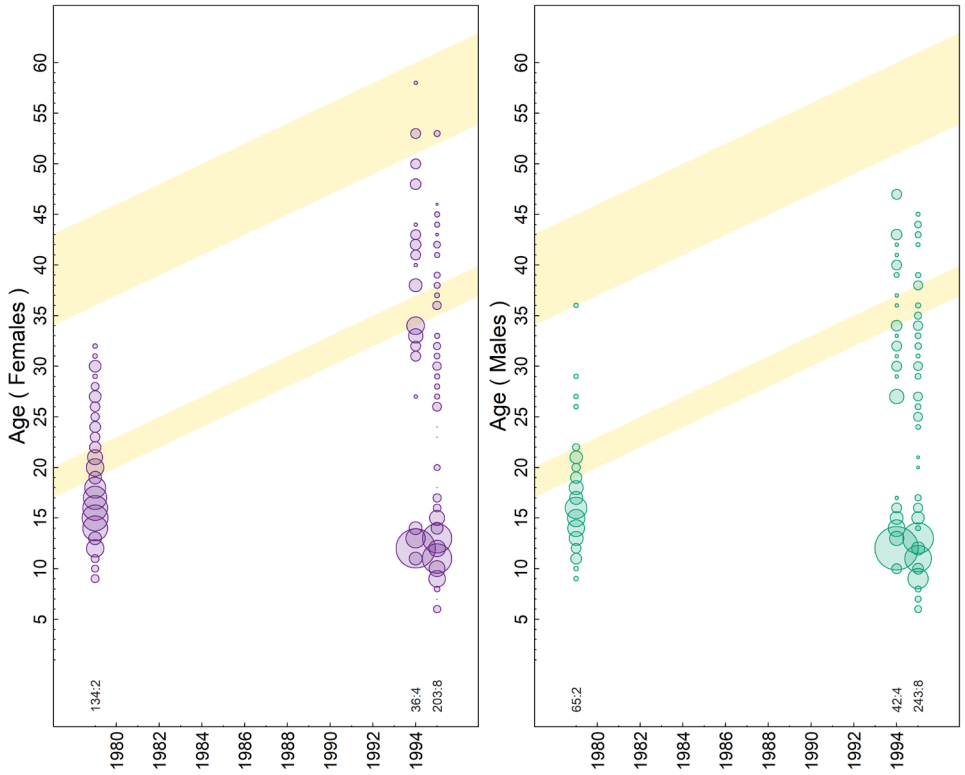

Figure D.12. GIG Historical survey – proportions-at-age: see Table D.11 and Figure D.8 for details.

D.2.3. Ageing Error

Accounting for ageing error in stock assessments helps to identify episodic recruitment events. Figure D.13 suggests that YMR ages determined by primary readers are produced fairly consistently by secondary readers when performing spot-check analyses; however, there are some large deviations which become more extreme at older ages. Therefore, the base case population model for YMR uses an ageing error (AE) vector of standard deviations that is calculated from the CV of observed lengths-at-age (Figure D.14, Table D.12). Explicitly, the ageing error vector used was the standard deviation for each age determined as the CV of lengths at each age multiplied by the corresponding age:

$$\sigma_a = (\sigma_{L_a} / \mu_{L_a})\ a$$

In the SS' data file, ages start at 0 and end at *A* (60 for YMR), which means A+1 entries are needed. In the ageing error section of the data file, we specified ages 0.5 to 60.5 with the entries of σ_a from Table D.12 for ages 1 to 61.

Ageing error is more typically estimated using statistical models that use multiple age readings from individual fish to derive a classification matrix that defines the probability of assigning an observed age to a fish based on its true age (Richards et al. 1992). True ages are not known but can be considered the most probable value for the observed ages with a degree of imprecision depicted using normal, exponential, or age reader error (Richards et al. 1992). We did not explore the statistical estimation of ageing error in this assessment.

Table D.12. Calculating ageing error (AE) vector (shaded column) for use in SS from CVs of observed lengths-at age L_a, where n_{L_a} = number of lengths observed at each age a, μ_{L_a} = mean length at age, σ_{L_a} = standard deviation of mean length at age, $\mathrm{CV}_{L_a} = \sigma_{L_a} / \mu_{L_a}$, and $\mathrm{AE} = \sigma_a = a\ \mathrm{CV}_{L_a}$.

a	n_{L_a}	μ_{L_a}	σ_{L_a}	CV_{L_a}	σ_a	a	n_{L_a}	μ_{L_a}	σ_{L_a}	CV_{L_a}	σ_a
1	5	12.3	1.037	0.200	0.200	31	127	46.0	2.234	0.049	1.506
2	14	16.2	2.765	0.171	0.341	32	141	46.5	2.271	0.049	1.564
3	42	20.9	1.673	0.080	0.240	33	96	46.3	2.960	0.064	2.110
4	51	26.5	3.373	0.127	0.508	34	95	46.4	2.707	0.058	1.986
5	91	28.8	3.759	0.130	0.652	35	90	46.7	2.405	0.051	1.802
6	174	32.3	4.868	0.151	0.905	36	82	46.9	2.554	0.054	1.959
7	293	32.5	3.047	0.094	0.655	37	65	46.5	2.307	0.050	1.834
8	182	34.6	3.607	0.104	0.835	38	62	47.7	3.045	0.064	2.425
9	255	36.8	3.143	0.085	0.768	39	61	47.5	2.823	0.059	2.317
10	302	37.7	2.665	0.071	0.707	40	68	48.3	2.528	0.052	2.092
11	331	38.7	2.102	0.054	0.598	41	55	48.0	2.953	0.062	2.522
12	297	39.9	1.964	0.049	0.590	42	67	47.8	2.172	0.045	1.908
13	198	40.6	1.798	0.044	0.575	43	81	48.4	2.218	0.046	1.972
14	138	41.0	2.227	0.054	0.761	44	51	48.3	2.527	0.052	2.302
15	111	41.8	2.289	0.055	0.821	45	78	47.8	2.273	0.048	2.138
16	75	42.7	2.491	0.058	0.933	46	73	48.1	2.117	0.044	2.023
17	103	44.1	2.318	0.053	0.894	47	55	47.9	1.729	0.036	1.698
18	63	43.5	4.328	0.100	1.791	48	78	48.1	2.410	0.050	2.406
19	39	44.4	2.286	0.051	0.978	49	55	47.7	2.201	0.046	2.260
20	60	44.5	2.820	0.063	1.268	50	72	48.5	2.317	0.048	2.388
21	74	45.2	2.048	0.045	0.952	51	51	47.5	2.310	0.049	2.480
22	60	44.7	1.775	0.040	0.873	52	54	47.9	2.856	0.060	3.100
23	75	45.2	2.729	0.060	1.389	53	47	48.4	2.607	0.054	2.854
24	114	45.4	2.457	0.054	1.298	54	52	48.2	2.257	0.047	2.528
25	96	45.4	2.409	0.053	1.326	55	51	47.6	1.970	0.041	2.276
26	132	45.7	2.002	0.044	1.140	56	47	48.0	2.278	0.047	2.658
27	145	45.7	2.196	0.048	1.298	57	40	47.3	2.675	0.057	3.221
28	178	46.0	2.133	0.046	1.300	58	51	47.6	2.387	0.050	2.905
29	148	45.7	2.148	0.047	1.363	59	32	47.7	2.500	0.052	3.091
30	181	46.0	1.995	0.043	1.301	60	38	47.4	1.929	0.041	2.442
-	-	-	-	-	-	61	72	48.5	2.531	0.052	3.182

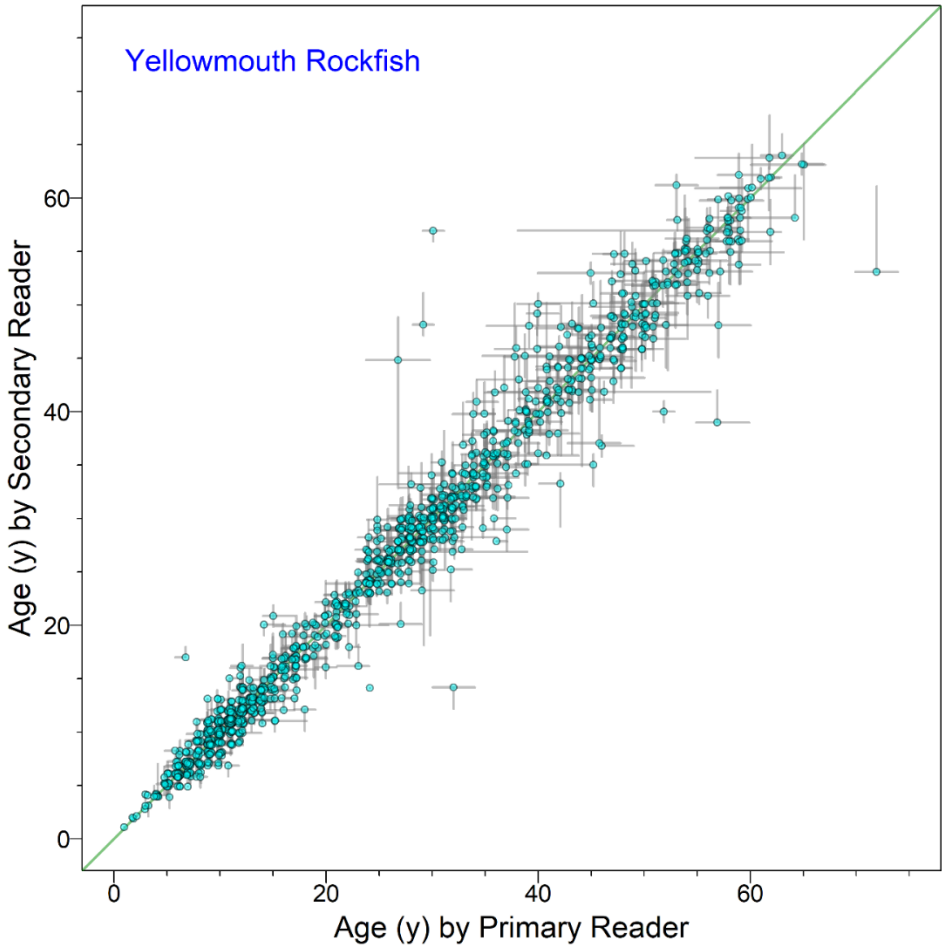

Figure D.13. Ageing error of YMR specified as the range between minimum and maximum age (grey bars) determined by primary and secondary readers for each accepted age (points). The data are jittered using a random uniform distribution between -0.25 and 0.25 y.

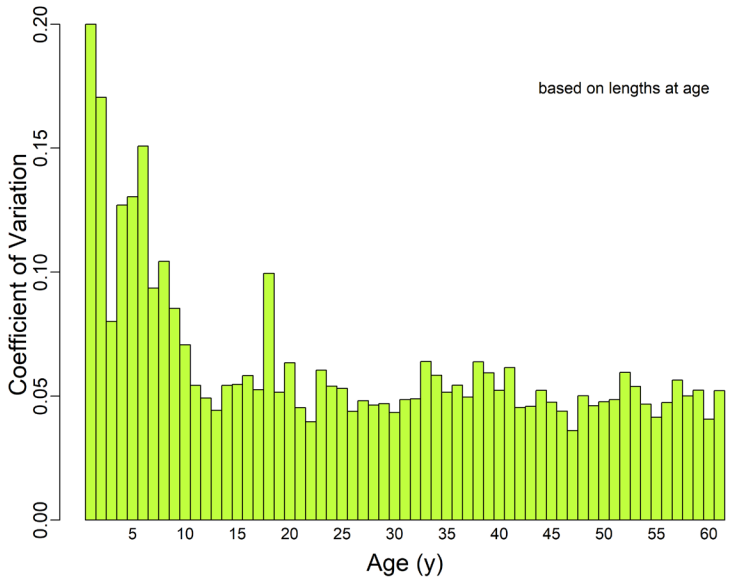

Figure D.14. Coefficient of variation (CV) of observed YMR lengths-at-age.

D.3. STOCK STRUCTURE

D.3.1. Stock Definition

At present, there is no genetic information to delineate separate stocks for YMR. The coastwide distribution of catch over 25 years suggests two potential stocks – a northern one in PMFC 5DE and a southern on in 3CD5ABC (Figure D.15).

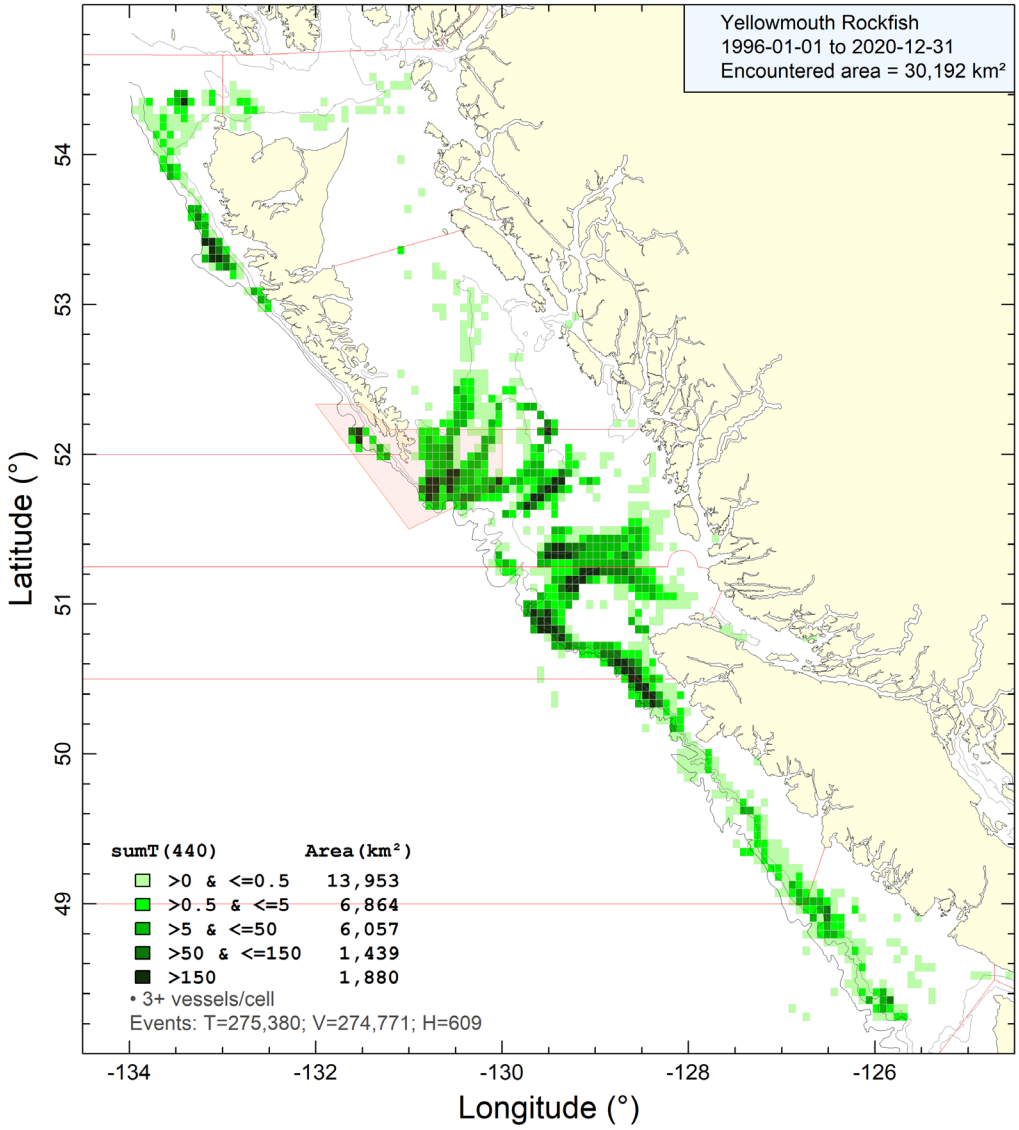

Figure D.15. Coastwide distribution of YMR catch by the trawl fleet from 1996 to 2020.

The areal separation for YMR identified in Figure D.15 also aligns with previous stock assessments of other rockfish (Starr and Haigh, 2021 a,b). This separation may be caused by the North Pacific Current bifurcation (Pickard and Emery 1982, Freeland 2006, Cummins and Freeland 2007, Batten and Freeland 2007) whereby free-swimming larvae from the two regions are kept separated.

D.3.2. Fish Length Distributions

Simple comparisons of commercial length distributions by stock from the trawl fisheries show no evidence that length frequency distributions were markedly different by capture method when combined across all areas (Figure D.16). All gear types detected a drop in mean age in 2013-14, although the lower end of the age range for midwater trawl tows appears to dip below the lower end of the bottom trawl age range in some years (2013, 2015) while there is little difference at the lower end of the age range in other years (2005, 2007, 2016, 2017)(Figure D.17). What is more striking is the consistent difference at the upper end of the age range, whereby the bottom trawl data consistently have older YMR than seen in the midwater samples. While these differences may be sufficient to treat midwater trawl as a separate fishery, there are inadequate data to characterise the midwater fishery as well as the observation that this fishery overall accounts for 16% of the annual catch of YMR from 1996 to 2020. Consequently, we chose to combine the AF data from midwater trawl gear with the bottom trawl data.

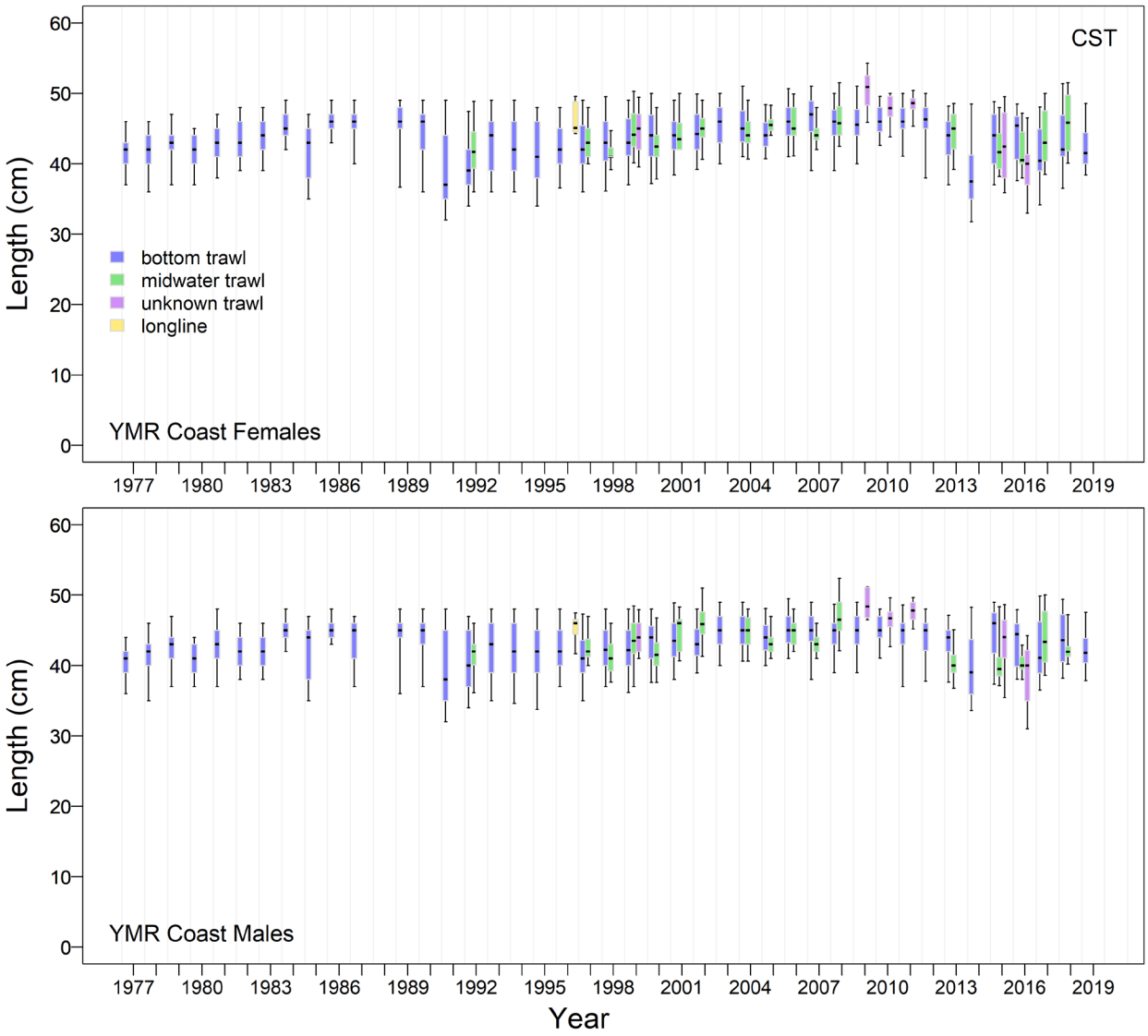

Figure D.16. Comparison of annual distributions of YMR length by sex among gear types in the commercial fisheries. Boxplot quantiles: 0.05, 0.25, 0.5, 0.75, 0.95.

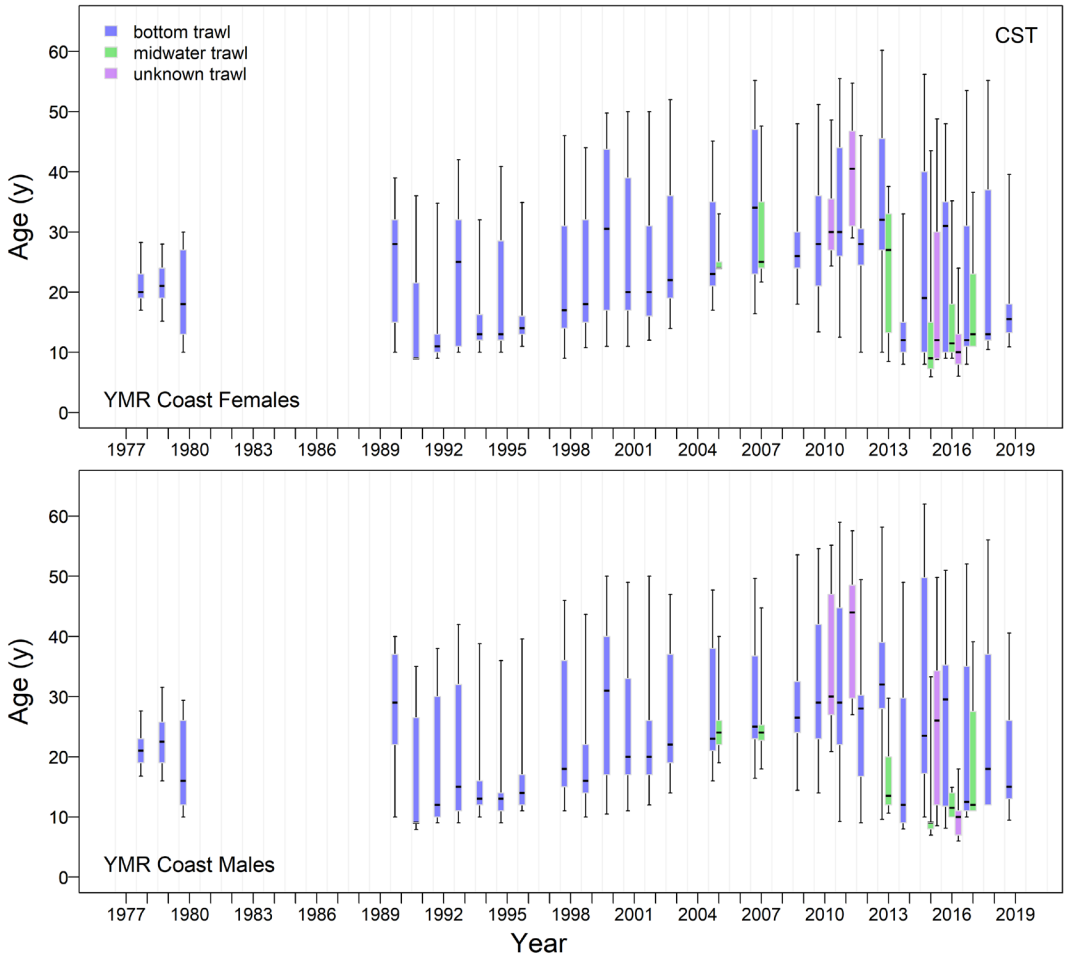

Figure D.17. Comparison of annual distributions of YMR age by sex among gear types in the commercial fisheries. Boxplot quantiles: 0.05, 0.25, 0.5, 0.75, 0.95.

The distributions of commercial lengths (Figure D.18) and ages (Figure D.19) along the coast compared with a northern subset (PMFC areas 5DE) and a southern subset (PMFC areas 3CD5ABC) show some differences by coastal region, with the northern (5DE) samples having older fish in both sexes than seen in the more southern fish. However, there are relatively few samples from 5DE and this combined area accounts for only a relatively small fraction of the annual YMR catch (about 12% averaged over the period 1996–2020). We chose to go ahead with a single area model representing the entire coast because the differences among the two regions were not consistent in all years. There also were no 5DE samples between 2002 and 2012 and after 2015 (Figure D.19).

The distribution of lengths from a variety of surveys (Figure D.20) show inter-survey differences in mean length that likely stem from survey selectivity differences, perhaps influenced by depth:

- the two outer coast synoptic surveys (WCVI and WCHG) appear to catch larger fish than either the QCS synoptic (central coast) or the HS synoptic (north coast) surveys;
- the HS survey catches small fish consistently, while the QCS survey catches the greatest size range;
- the longline surveys catch large fish while the acoustic survey tends to see mid-range fish.

- four of six surveys show similar YMR length distributions with QCS synoptic catching smaller fish on average and the Shrimp trawl survey catching much smaller (and younger) fish.

Some of these patterns are also reflected by age ranges in the catch by the three primary synoptic surveys, with the QCS survey catching the youngest age range, followed by the WCVI survey catching an intermediate age range and the WCHG survey catching the oldest YMR in most years (Figure D.21). These differences mirror the observations from the commercial fishery (Figure D.19).

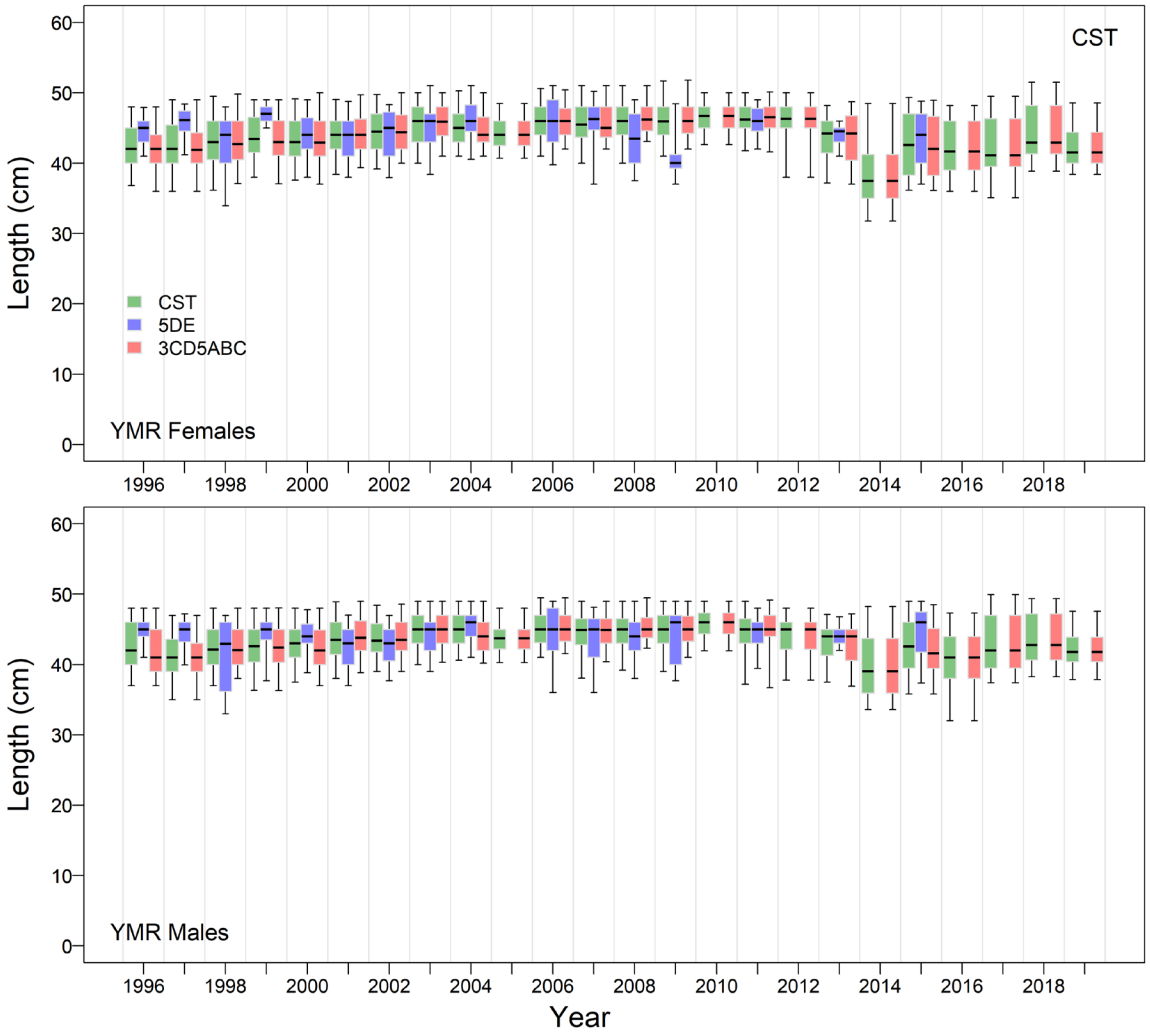

Figure D.18. Comparison of annual distributions of YMR length along the BC coast with northern (5DE) and southern (3CD5ABC) areas in the commercial fisheries. Boxplot quantiles: 0.05, 0.25, 0.5, 0.75, 0.95.

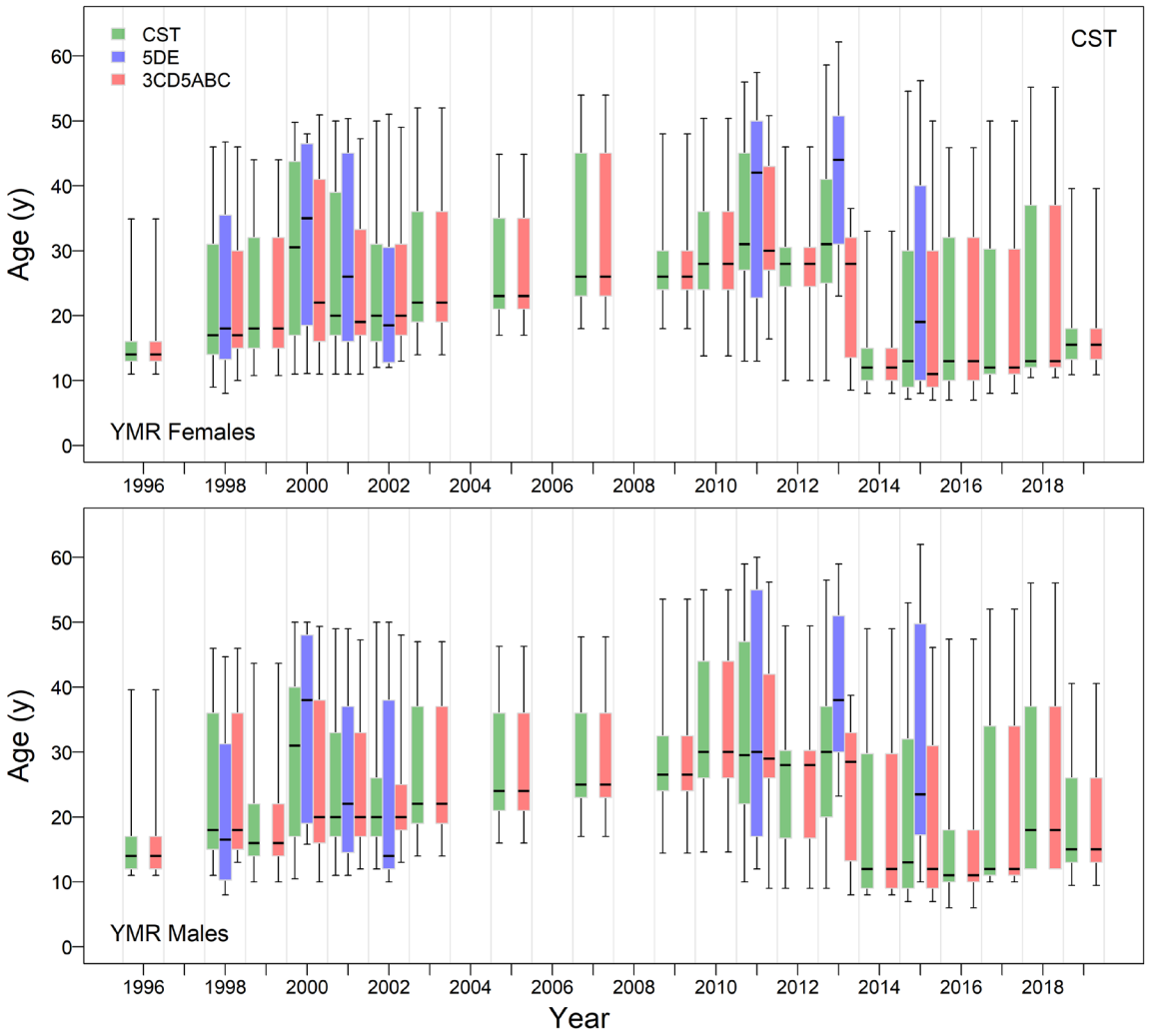

Figure D.19. Comparison of annual distributions of YMR age along the BC coast with northern (5DE) and southern (3CD5ABC) areas in the commercial fisheries. Boxplot quantiles: 0.05, 0.25, 0.5, 0.75, 0.95.

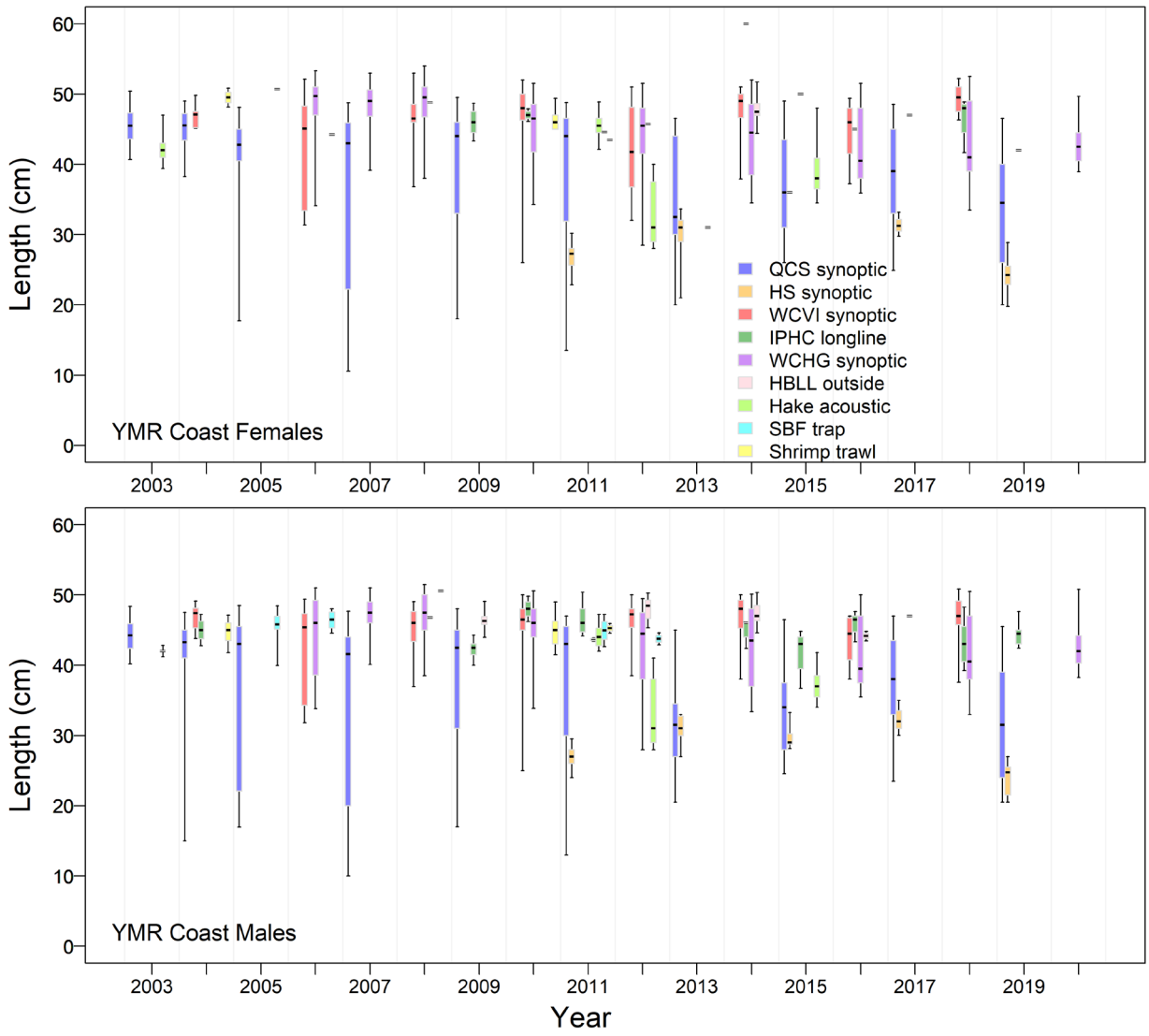

Figure D.20. Comparison of annual distributions of YMR length among nine surveys (five trawl, two longline, one trap, and one acoustic). Boxplot quantiles: 0.05, 0.25, 0.5, 0.75, 0.95.

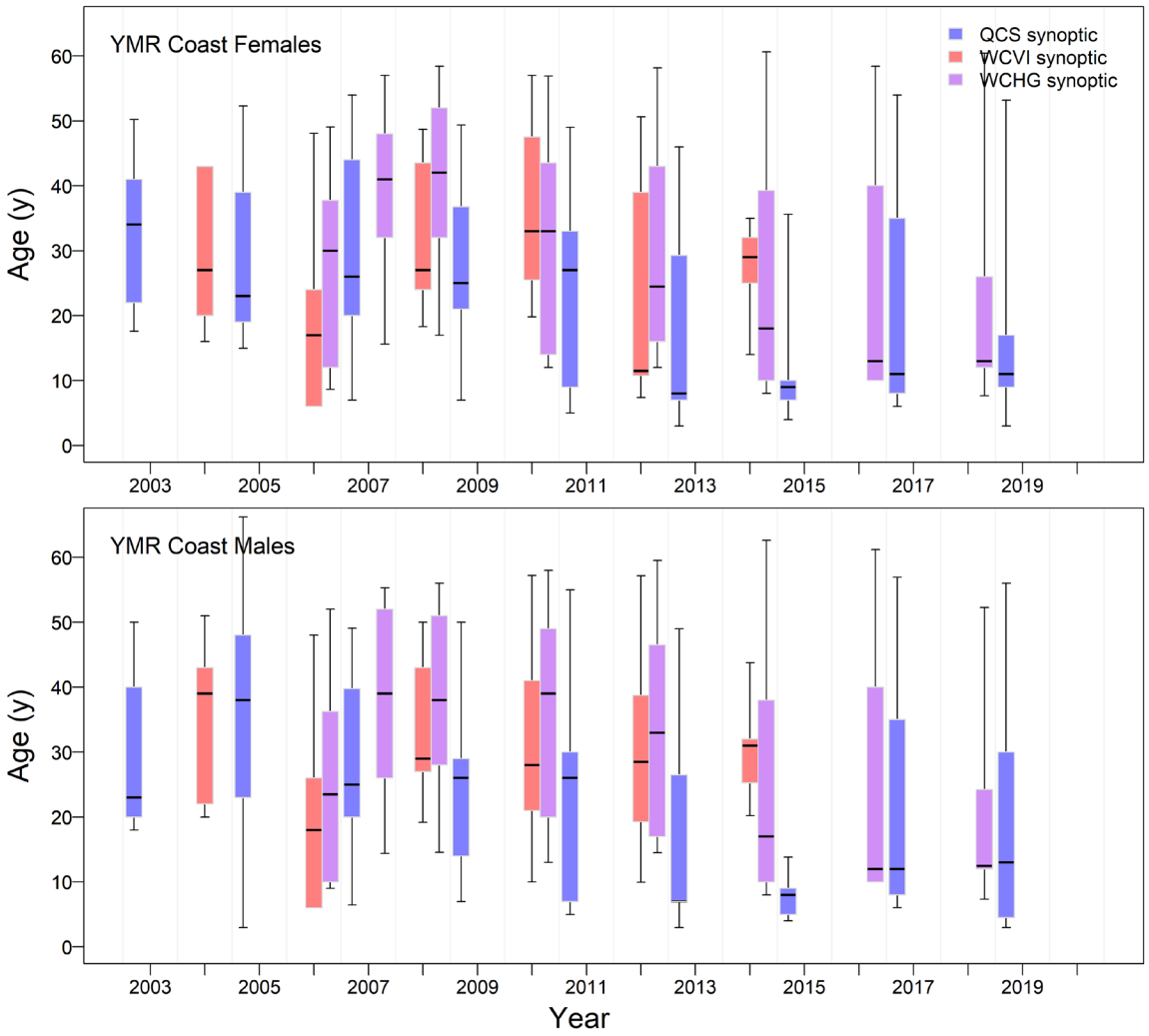

Figure D.21. Comparison of annual distributions of YMR age among three bottom trawl synoptic surveys. Boxplot quantiles: 0.05, 0.25, 0.5, 0.75, 0.95.

D.3.3. Comparison of Growth Models

A comparison of growth models[15] between various regional groups using commercial length-age data (Figure D.22) shows the following trends:

- female estimates of L-infinity are larger than for males;
- males and females from southern regional groupings (3CD5AB, 3CD5ABC) estimate larger L-infinities than those from the north (5E, 5CE);
- coastwide L-infinity estimates lie in between northern and southern sizes.
- estimates of k largely overlap, lying between 0.08 and 0.10 and show no regional trend.

In contrast, samples from surveys show the opposite trend: with both sexes estimating larger L-infinities in the north than in the south (Figure D.23); females L-infinity estimates are larger than

[15]Random effects model that incorporates ageing error provided by Sean Anderson (2019, DFO Groundfish, pers. comm.), which is evaluated by the R package `rstan` to derive MCMC samples (Stan Development Team 2020). Note differences were minor between models with ageing error and without.

for males. There will be selectivity differences between the commercial fleet and the survey rather than regional differences.

The growth model estimates from the commercial fishery lack small fish and consequently are not as well-determined as those from the research surveys (see Figure D.24).

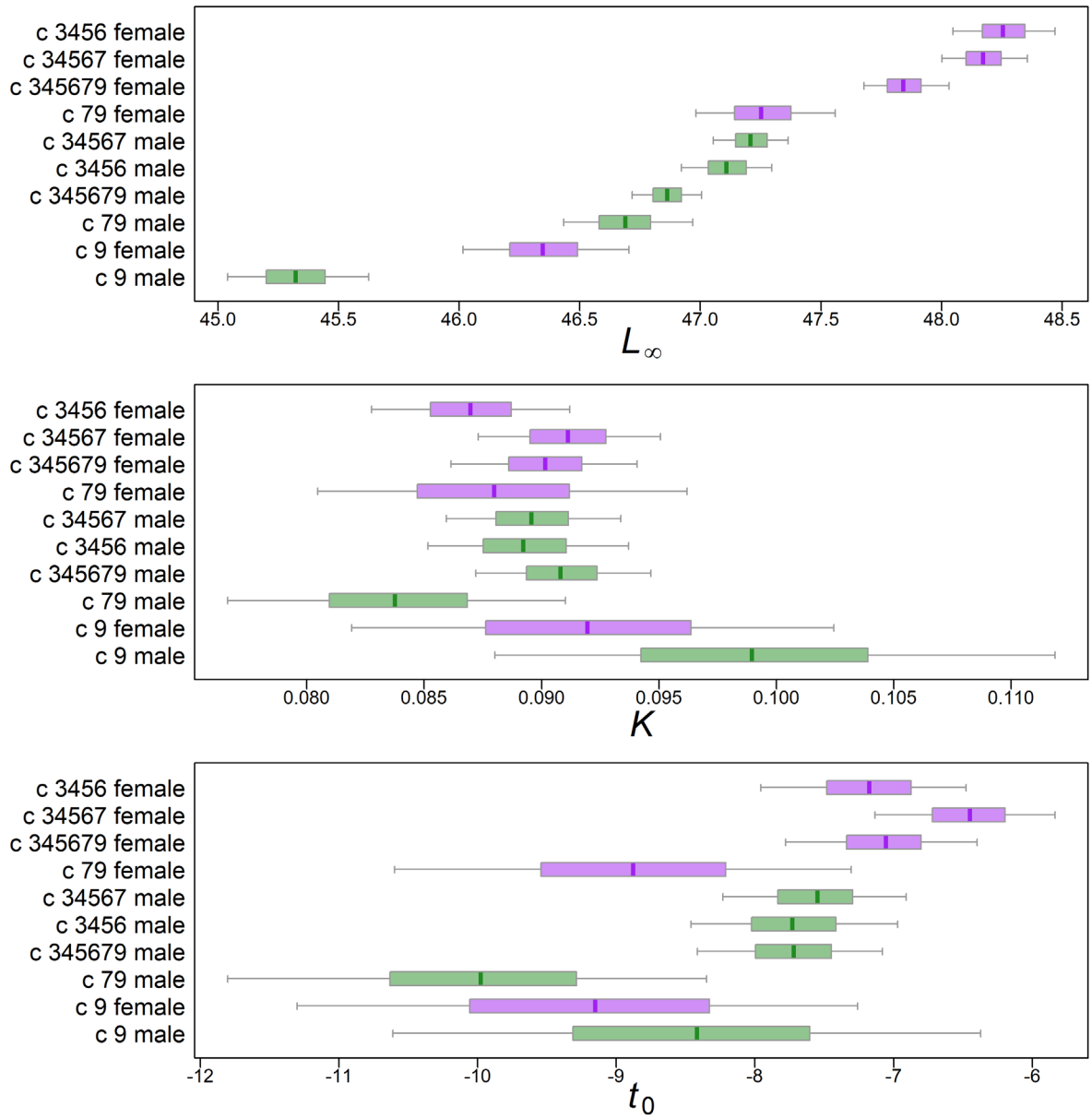

Figure D.22. MCMC samples (4 chains, 500 each) for von Bertalanffy parameters using commercial length-age data by area (various combinations of PMFC areas: 3=3C, 4=3D, 5=5A, 6=5B, 7=5C and 9=5E). Boxplots (purple = female, green = male) show 0.05, 0.25, 0.5, 0.75, and 0.95 quantiles.

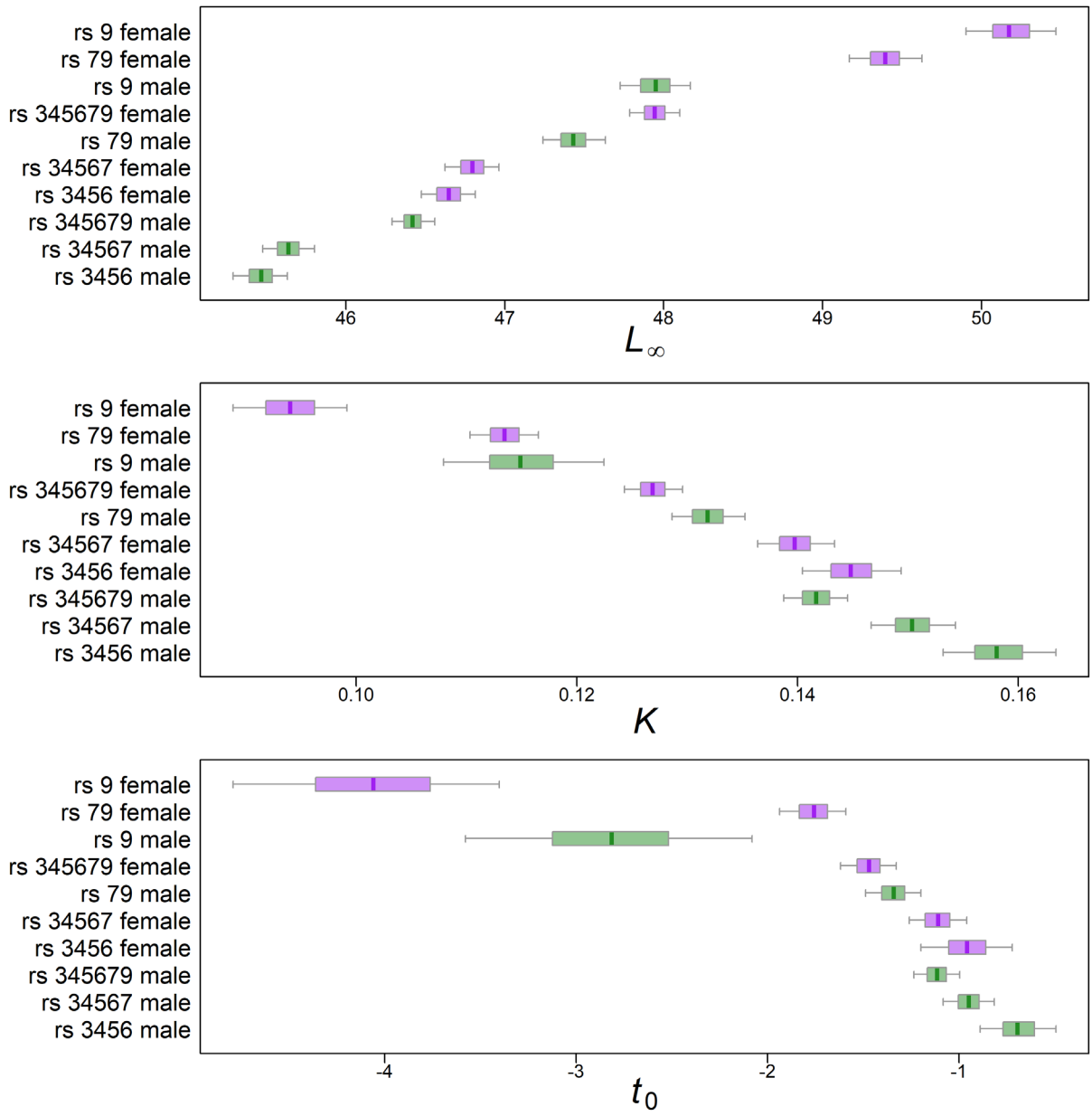

Figure D.23. MCMC samples (4 chains, 500 each) for von Bertalanffy parameters using research/survey length-age data by area (various combinations of PMFC areas: 3=3C, 4=3D, 5=5A, 6=5B, 7=5C and 9=5E). Boxplots (purple = female, green = male) show 0.05, 0.25, 0.5, 0.75, and 0.95 quantiles.

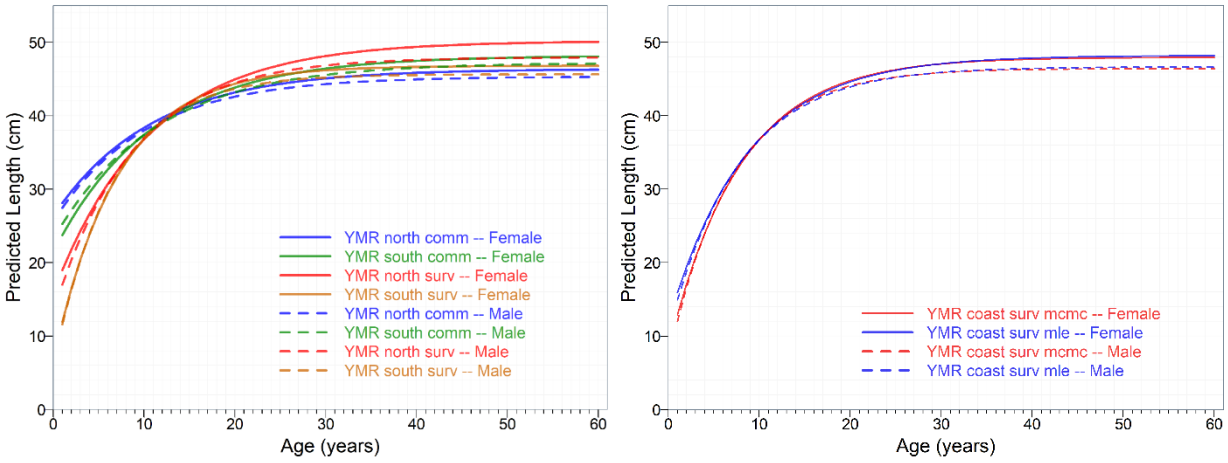

Figure D.24. Left: von Bertalanffy fits using median parameter estimates from the rstan model fit to survey YMR length-age data by region (north=5E vs. south=3CD5ABC) and fleet (commercial vs. survey) using random effects (RE) ageing error (CVs of length-at-age). Right: comparison of von Bertalanffy fits via rstan (medians MCMC RE ageing error) with MLE fits for coastwide YMR survey data.
Line type indicates sex (solid=female, dashed=male) for both panels.
Line colour (left) indicates region by fleet (blue=north commercial, green=south commercial, red=north survey, orange=south survey); line colour (right) indicates model (red=rstan MCMC RE, blue=MLE).

D.4. REFERENCES – BIOLOGY

Batten, S.D., and Freeland, H.J. 2007. Plankton populations at the bifurcation of the North Pacific Current. Fisheries Oceanography 16(6): 536-546.

Cummins, P.F., and Freeland, H.J. 2007. Variability of the North Pacific Current and its bifurcation. Progress in Oceanography 75(2): 253-265.

DFO. 2022. Proceedings of the Pacific regional peer review of the Redstripe Rockfish (*Sebastes proriger*) stock assessment for British Columbia in 2018; June 13-14, 2018; Greg Workman (ed). DFO Can. Sci. Advis. Sec. Proceed. Ser. In Press

Edwards, A.M., Haigh, R., and Starr, P.J. 2012. Stock assessment and recovery potential assessment for Yellowmouth Rockfish (*Sebastes reedi*) along the Pacific coast of Canada. DFO Can. Sci. Advis. Sec. Res. Doc. 2012/095. iv + 188 p.

Freeland, H.J. 2006. What proportion of the North Pacific Current finds its way into the Gulf of Alaska? Atmosphere-Ocean 44(4): 321-330.

Haist, V., Breen, P.A., and Starr, P.J. 2009. A multi-stock, length-based assessment model for New Zealand rock lobster (*Jasus edwardsii*). N.Z. J. Mar. Freshw. Res. 43: 355-371.

Hamel, O.S. 2015. A method for calculating a meta-analytical prior for the natural mortality rate using multiple life history correlates. ICES J. Mar. Sci. 72(1): 62-69.

Hoenig, J.M. 1983. Empirical use of longevity data to estimate mortality rates. Fish. Bull. 82(1): 898-903.

MacLellan, S.E. 1997. How to age rockfish (*Sebastes*) using *S. alutus* as an example – the otolith burnt section technique. Can. Tech. Rep. Fish. Aquat. Sci. 2146: 39 p.

Pickard, G.L., and Emery, W.J. 1982. Descriptive Physical Oceanography, an Introduction. Pergamon Press, Oxford UK, 4th (SI) enlarged ed.

Quinn, T.J.I., and Deriso, R.B. 1999. Quantitative Fish Dynamics. Oxford University Press, New York, NY.

Richards, L.J., Schnute, J.T., Kronlund, A.R., and Beamish, R.J. 1992. Statistical models for the analysis of ageing error. Can. J. Fish. Aquat. Sci. 49(9). 1801-1815.

Stan Development Team. 2020. RStan: the R interface to Stan. R package version 2.21.2.

Stanley, R.D., Starr, P., and Olsen, N. 2009. Stock assessment for Canary rockfish (*Sebastes pinniger*) in British Columbia waters. DFO Can. Sci. Advis. Sec. Res. Doc. 2009/013: xxii + 198 p.

Starr, P.J., and Haigh, R. 2021a. Redstripe Rockfish (*Sebastes proriger*) stock assessment for British Columbia in 2018. DFO Can. Sci. Advis. Sec. Res. Doc. 2021/014: vii + 340 p.

Starr, P.J., and Haigh, R. 2021b. Walleye Pollock (*Theragra chalcogramma*) stock assessment for British Columbia in 2017. DFO Can. Sci. Advis. Sec. Res. Doc. 2021/004. viii+294 p.

Then, A.Y., Hoenig, J.M., Hall, N.G., and Hewitt, D.A. 2015. Evaluating the predictive performance of empirical estimators of natural mortality rate using information on over 200 fish species. ICES J. Mar. Sci. 72(1): 82-92.

Westrheim, S. 1975. Reproduction, Maturation, and Identification of Larvae of some Sebastes (Scorpaenidae) Species in the Northeast Pacific Ocean. J. Fish. Res. Bd. Can. 32: 2399-2411.

APPENDIX E. MODEL EQUATIONS

E.1. INTRODUCTION

The 2021 stock assessment of Yellowmouth Rockfish (YMR) adopts Stock Synthesis 3 (SS), version 3.30.17.01 (2021-06-15), which is a statistical age-structured population modelling framework (Methot and Wetzel 2013) that uses ADMB's power for Bayesian estimation of population trajectories and their uncertainties. The Stock Synthesis Development Team at NOAA (National Oceanic and Atmospheric Administration, U.S. Dept. Commerce) provides executables and documentation on how to run SS, and the SS source code is available on GitHub.

Previously, YMR was assessed using a simpler age-structured model called 'Awatea', which is a version of Coleraine (Hilborn et al. 2003) that was developed and maintained by Allan Hicks (then at Univ. Washington, now at IPHC). Both Awatea and SS are platforms for implementing the Automatic Differentiation Model Builder software (ADMB Project 2009), which provides (a) maximum posterior density estimates using a function minimiser and automatic differentiation, and (b) an approximation of the posterior distribution of the parameters using the Markov Chain Monte Carlo (MCMC) method, specifically using the Hastings-Metropolis algorithm (Gelman et al. 2004).

Awatea has been used in the following BC stock age-structured assessments since 2007:

- 2020 – Rougheye/Blackspotted Rockfish complex in PMFC areas 5DE and 3CD5AB (Starr and Haigh 2022*b*),
- 2019 – Bocaccio for the coast of BC (Starr and Haigh 2022*a*),
- 2019 – Widow Rockfish for the coast of BC (Starr and Haigh 2021*a*),
- 2018 – Redstripe Rockfish in PMFC areas 5DE and 3CD5ABC (Starr and Haigh 2021*b*),
- 2017 – Pacific Ocean Perch (POP) in Queen Charlotte Sound (Haigh et al. 2018),
- 2014 – Yellowtail Rockfish for the coast of BC (DFO 2015),
- 2013 – Silvergray Rockfish along the Pacific coast of Canada (Starr et al. 2016),
- 2013 – Rock Sole in BC (Holt et al. 2016),
- 2012 – POP off the west coast of Vancouver Island (Edwards et al. 2014*b*),
- 2012 – POP off the west coast of Haida Gwaii (Edwards et al. 2014*a*),
- 2011 – Yellowmouth Rockfish along the Pacific coast of Canada (Edwards et al. 2012*a*),
- 2010 – POP in Queen Charlotte Sound (Edwards et al. 2012*b*);
- 2009 – Canary Rockfish in BC update (DFO 2009*b*);
- 2007 – Canary Rockfish in BC (Stanley et al. 2009).

The chief strength of Coleraine|Awatea is the use of a robust likelihood formulation proposed by Fournier et al. (1998) for the composition data by sex and age (or length). The robust normal model was used over the more traditional multinomial error model because it reduced the influence of observations with standardised residuals > 3 standard deviations (Fournier et al. 1990). Fournier et al. (1990) identified two types of deviations:

- type I – occasional occurrence of an event of very low probability; and
- type II – probability of observing an event with higher frequency than normal in the population (e.g., school of young fish).

Their robustified likelihood function reduces both types of deviations.

SS offers two error models: the Multinomial and a compound Dirichlet-multinomial. The latter can estimate effective sample sizes that are similar to iterative reweighting methods, but without

requiring multiple iterations of running the assessment model (Thorson et al. 2017). At the time of the stock assessment, SS did not offer Fournier's robustified normal likelihood function.

The data inputs to SS comprise four files – `'starter.ss'`, `'data.ss'`, `'control.ss'`, and `'forecast.ss'` – instead of a single file used by Awatea. Parameter control and priors appear in the `control` file, and data appear in the `data` file; these files can be named anything the user wishes because the `starter` file specifies their names. The names for the `starter` and `forecast` files must remain invariant. Unlike Awatea, which requires specifying an input file from the command line (e.g. `'awatea -ind fielname.txt'`), calling SS is done by typing only `'ss'` because the software assumes the presence of the four files above. The options in SS for fitting the data are more complex than those for Awatea and offer a greater degree of flexibility; however, this flexibility requires a steep learning curve.

In this assessment, we used the Multinomial distribution for fitting age frequencies (AF) despite the benefits of using the Dirichlet-multinomial because, in early trials, we saw no real improvement to AF residual fits which required manual reweighting. Consequently, this assessment retained a manual weighting scheme for abundance and composition data, described in Section E.6.2..

Running of SS is streamlined using custom R code (archived on the GitHub site 'PBS Software as `PBSsynth`'), which relies heavily on code provided by the R packages '`PBSawatea`', '`r4ss`' (Taylor et al. 2020), and '`adnuts`' (Monnahan 2018). Figures and tables of output were automatically produced in R, an environment for statistical computing and graphics (R Core Team 2021). The R function `Sweave` (Leisch 2002) automatically collates, via LaTeX, the large amount of figures and tables into `'pdf'` files for model runs and Appendix F.

Methot and Wetzel (2013) provide details of the SS model in their Appendix A. Below are selected details of the age-structured model, the Bayesian procedure, the reweighting scheme, the prior distributions, and the methods used for calculating reference points and performing projections.

E.2. MODEL ASSUMPTIONS

The **assumptions** of the model are:

1. The assessed BC population of Yellowmouth Rockfish (YMR) comprised a single stock in combined PMFC areas 3CD5ABCDE.
2. Annual catches were taken by one fishery: 'Trawl+', which denoted a combined fishery dominated by trawl gear (bottom and midwater), with additional (minor) catch coming from other fisheries (halibut longline, sablefish trap, lingcod & salmon troll, and rockfish hook & line). The annual catch was known without error and occurred in the middle of each year.
3. The Beverton-Holt stock-recruitment relationship was time-invariant, with a log-normal error structure.
4. Selectivity was different among fleets (fishery and surveys) but the same between sexes, and remained invariant over time. Selectivity parameters were estimated when ageing data were available.
5. Natural mortality M was fixed at five values (0.04, 0.045, 0.05, 0.055, 0.06) for females and males, and held invariant over time.
6. Growth parameters were fixed and invariant over time.

7. Maturity-at-age parameters for females were fixed and invariant over time. Male maturity did not need to be considered, because it was assumed that there were always sufficient mature males. The mature male population is not tracked by this model, with spawning biomass expressed as mature females only.
8. Recruitment at age 0 was 50% females and 50% males.
9. Recruitment standard deviation (σ_R) was fixed at 0.9.
10. Only fish ages determined using the preferred otolith break-and-burn methodology (MacLellan 1997) were used because ages determined by surface ageing methods (chiefly before 1978) were biased (Beamish 1979). Surface ageing was deemed suitable for very young rockfish (ages 1-3).
11. An ageing error (AE) vector based on CVs of observed lengths-at-age was used.
12. Commercial samples of catch-at-age in a given 3-month period within a year were representative of the fishery in that quarter-year if there were $\geq$2 samples in that year.
13. Relative abundance indices were proportional to the vulnerable biomass at the mid point of the year, after half the catch and half the natural mortality had been removed.
14. The age composition samples came from the middle of the year after half the catch and half the natural mortality had been removed.

E.3. MODEL NOTATION AND EQUATIONS

Model notation is given in Table E.1, the model equations in Tables E.2 and E.3, and description of prior distributions for estimated parameters in Table E.4. The model description is divided into the deterministic components, stochastic components and Bayesian priors. Full details of notation and equations are given after the tables.

The deterministic components in Table E.2 iteratively calculate numbers of fish in each age class (and of each sex) through time, while allowing for the commercial catch data, weight-at-age and maturity data, and known fixed values for all parameters.

Given that values are not known (or assumed fixed) for all parameters, many need to be estimated, and stochasticity needs to be added to recruitment. This is accomplished by the stochastic components given in Table E.3.

Incorporation of the prior distributions for estimated parameters gives the full Bayesian implementation, the goal of which is to minimise the objective function $\mathcal{F}(\boldsymbol{\Theta})$ given by (E.52). This function is derived from the deterministic, stochastic and prior components of the model.

Table E.1. Notation for the SS catch-at-age model (continued overleaf). The assessment model uses only 'cohorts' (age-classes by year) even though SS recognises finer subdivisions of time called 'morphs' (seasons), which can be further characterised by 'platoons' (rates of growth).

Symbol	Description and units
	Indices (all subscripts)
a	▸ age class, where $a = 1, 2, 3, ...A$, and ▹ a' = reference age near youngest age well-represented in data; ▹ a'' = reference age near oldest age well-represented in data
l	▸ length bin, where $l = 1, 2, 3, ...\Lambda$, and Λ is the bin index of the largest length; ▹ L' = reference length for a'; ▹ L'' = reference length for a''; ▹ $\breve{L}_l$, $\mathring{L}_l$ = minimum and middle length of length bin l, respectively
t	▸ model year, where $t = 1, 2, 3, ...T$, corresponds to actual years: 1935, ..., 2022, and $t = 0$ represents unfished equilibrium conditions
g	▸ index for series (abundance|composition) data: 1 – Trawl+ Fishery|CPUE (commercial data) 2 – QCS Synoptic trawl survey series 3 – WCVI Synoptic trawl survey series 4 – WCHG Synoptic trawl survey series 5 – GIG Historical trawl survey series
s	▸ sex, 1=females, 2=males
	Index ranges
A	▸ accumulator age-class, $A \in \{60\}$
G	▸ number of fleets (fisheries and surveys)
Λ	▸ number of length bins
T	▸ number of model years, $T = 88$
$\mathbf{T}_g$	▸ sets of model years for survey abundance indices from series g, listed here for clarity as actual years (subtract 1934 to give model year t): $\mathbf{T}_1$ = {1996, ..., 2020} $\mathbf{T}_2$ = {2003:2005, 2007, 2009, 2011, 2013, 2015, 2017, 2019} $\mathbf{T}_3$ = {2006:2008, 2010, 2012, 2016, 2018, 2020} $\mathbf{T}_4$ = {2004, 2006, 2008, 2010, 2012, 2014, 2016, 2018} $\mathbf{T}_5$ = {1967, 1969, 1971, 1973, 1976:1977, 1984, 1994}
$\mathbf{U}_g$	▸ sets of model years with proportion-at-age data for series g: $\mathbf{U}_1$ = {1979:1980, 1990:1996, 1998:2003, 2005, 2007, 2009:2019} $\mathbf{U}_2$ = {2003, 2005, 2007, 2009, 2011, 2013, 2015, 2017, 2019} $\mathbf{U}_3$ = {1996, 2006, 2010, 2012} $\mathbf{U}_4$ = {1997, 2006:2008, 2010, 2012, 2014, 2016, 2018} $\mathbf{U}_5$ = {1979, 1994:1995}
	Data and fixed parameters
$\widetilde{a}_a$	▸ age after bias adjustment for age a (used in ageing error)
ξ_a	▸ standard deviation for age a (used in ageing error)
p_{atgs}	▸ observed weighted proportion of fish from series g in each year $t \in \mathbf{U}_g$ that are age-class a and sex s; so $\Sigma_{a=1}^{A}\Sigma_{s=1}^{2} p_{atgs} = 1$ for each $t \in \mathbf{U}_g$; in SS: ▹ p_l = observed proportion in length bin l;

Symbol	Description and units
	▹ p_a = observed proportion in age a; and
	▹ p_z = observed proportion by size in length bin l;
	▹ YMR only uses p_a
n_{tg}	▸ specified sample size that yields corresponding p_{atgs}
$\widetilde{n}_{tg}$	▹ effective sample size based on $\widehat{p}_{atgs}$
C_{tg}	▸ observed catch biomass (tonnes) in year $t = 1, 2, ..., T-1$
τ_{tg}	▸ standard deviation of C_{tgs}
d_{tg}	▸ discarded catch biomass (tonnes) in year t
δ_{tg}	▸ standard deviation of d_{tg}
δ'_{tg}	▸ user-specified standard deviation offset to add to δ_{tg}
w_{as}	▸ average weight (kg) of individual of age-class a of sex s from fixed parameters
$\overline{w}_{tg}$	▸ mean body weight (kg) by year (t) and fleet (g)
ψ_{tg}	▸ standard deviation of $\overline{w}_{tg}$
ψ'_{tg}	▸ user-specified standard deviation offset to add to ψ_{tg}
m_a	▸ proportion of age-class a females that are mature, fixed from data
I_{tg}	▸ biomass estimates (tonnes) from surveys $g = 2, ..., 5$, for year $t \in \mathbf{T}_g$, tonnes
κ_{tg}	▸ standard deviation of I_{tg}
κ'_{tg}	▸ user-specified standard deviation offset added to κ_{tg}
σ_R	▸ standard deviation parameter for recruitment process error, $\sigma_R = 0.9$
ϵ_t	▸ recruitment deviations arising from process error
b_t	▸ recruitment bias adjustment parameter:
	▹ ranges from 1 (data-rich years) to 0 (data-poor years)
$\widehat{x}$	▸ estimated values of observed data x (generalised)
	Estimated parameters
$\boldsymbol{\Theta}$	▸ set of estimated parameters:
R_0	▸ virgin recruitment of age-0 fish (numbers of fish, 1000s)
M_s	▸ natural mortality rate for sex $s = 1, 2$ (fixed at five values)
h	▸ steepness parameter for Beverton-Holt recruitment (fixed at 0.7)
q_g	▸ catchability for fleets ($g = 1, ..., 5$)
β_{itg}	▸ double-normal parameters for females ($s = 1$), where i=$1, ..., 6$ for the six β parameters that determine selectivity S_{atgs} for year t and series g=$1, ..., 5$, using joiner functions j_{1atgs} and j_{2atgs} for ascending- and descending-limb functions π_{1atgs} and π_{2atgs}, respectively, where γ_{1tgs} and γ_{2tgs} describe exponential terms
Δ_{itg}	▸ shift in vulnerability for males ($s = 2$), where subscripts itg are the same as those for β
	Derived states
N_{ats}	▸ number of age-class a fish (1000s) of sex s at the start of year t
B_t	▸ spawning biomass (tonnes mature females) at the start of year t
B_0	▸ virgin spawning biomass (tonnes mature females) at the start of year 0
R_t	▸ recruitment of age-0 fish (numbers of fish, 1000s) in year t
ρ_t	▹ recruitment deviations (log thousands age-0 fish) in year t
V_{tg}	▸ vulnerable biomass (tonnes, females + males) in the middle of year t
$\mathcal{B}_{tg}$	▸ mid-season retained dead biomass (tonnes, females + males)
F_{tg}	▸ instantaneous fishing mortality rate for time period t by fishery g

Symbol	Description and units
	▹ hybrid method uses Pope's approximation and Baranov's equation
	▹ calculations facilitated by temporary variables $\mathcal{T}_{tg}$ and joiners $\mathcal{J}_{tg}$
Z_{ats}	▸ total mortality rate (natural & fishing) for time period t and sex s
	Likelihood components
$\mathcal{L}_{1g}(\mathbf{\Theta}\|\{\widehat{I}_{tg}\})$	▸ log-likelihood component: CPUE or abundance index
$\mathcal{L}_{2g}(\mathbf{\Theta}\|\{d_{tg}\})$	▸ log-likelihood component: discard biomass
$\mathcal{L}_{3g}(\mathbf{\Theta}\|\{\overline{w}_{tg}\})$	▸ log-likelihood component: mean body weight
$\mathcal{L}_{4g}(\mathbf{\Theta}\|\{l_{tg}\})$	▸ log-likelihood component: length composition
$\mathcal{L}_{5g}(\mathbf{\Theta}\|\{a_{tg}\})$	▸ log-likelihood component: age composition
$\mathcal{L}_{6g}(\mathbf{\Theta}\|\{z_{tg}\})$	▸ log-likelihood component: generalised size composition
$\mathcal{L}_{7g}(\mathbf{\Theta}\|\{C_{tg}\})$	▸ log-likelihood component: initial equilibrium catch
$\mathcal{L}_{R}(\mathbf{\Theta}\|\{R_{tg}\})$	▸ log-likelihood component: recruitment deviations
$\mathcal{L}_{\phi_j}(\mathbf{\Theta}\|\{\phi_j\})$	▸ log-likelihood component: parameter priors
$\mathcal{L}_{P_t}(\mathbf{\Theta}\|\{P_t\})$	▸ log-likelihood component: random parameter deviations (if time-varying)
$\mathcal{L}(\mathbf{\Theta})$	▸ total log-likelihood
	Prior distributions and objective function
$\phi_j(\mathbf{\Theta})$	▸ prior distribution for parameter j
$\phi(\mathbf{\Theta})$	▸ joint prior distribution for all estimated parameters
$\mathcal{F}(\mathbf{\Theta})$	▸ objective function to be minimised

Table E.2. Deterministic components. Using the catch, weight-at-age and maturity data, with fixed values for all parameters, the initial conditions are calculated from (E.1)-(E.6), and then state dynamics are iteratively calculated through time using the main equations (E.7), selectivity functions (E.8)-(E.14), and the derived states (E.15)-(E.33). Estimated observations for survey biomass indices and proportions-at-age can then be calculated using (E.36) and (E.37). In Table E.3, the estimated observations of these are compared to data.

Deterministic components

Initial conditions ($t = 0$; $s = 1, 2$)

$$N_{a0s} = 0.5R_0 e^{-aM_s} \; ; \quad 0 \le a \le 3A\text{-}1 \tag{E.1}$$

$$N_{A0s} = \sum_{a=A}^{3A-1} N_{a0s} + \left(N_{3A-1,0s}\, e^{-M_{as}}\right) / \left(1 - e^{-M_{as}}\right) \tag{E.2}$$

$$B_0 = B_1 = \sum_{a=1}^{A} w_{as} m_{as} N_{a0s} \; ; \quad s{=}1 \;\; (\text{female}) \tag{E.3}$$

$$L_{a0s} = \begin{cases} \breve{L}_1 + \left(a/a'\right)\left(L'_s - \breve{L}_1\right) & ; \;\; a \le a' \\ L_{\infty s} + \left(L'_s - L_{\infty s}\right) e^{-k_s(a-a')} & ; \;\; a' < a \le A\text{-}1 \end{cases} \tag{E.4}$$

$$\text{where} \;\; L_{\infty s} = L'_s + \left(L''_s - L'_s\right)\left[1 - e^{-k_s(a''-a')}\right] \tag{E.5}$$

$$L_{A0s} = \frac{\sum_{a=A}^{2A}\left[e^{-0.2(a-A-1)}\right]\left[L_{As} + (a/A - 1)(L_{\infty s} - L_{A0s})\right]}{\sum_{a=A}^{2A} e^{-0.2(a-A-1)}} \tag{E.6}$$

State dynamics ($2 \le t \le T$; $s = 1, 2$)

$$N_{ats} = \begin{cases} cR_{0t} & ; \;\; a = 0, c = \text{proportion female} \\ N_{a-1,t-1,s}\, e^{-Z_{a,t-1,s}} & ; \;\; 1 \le a \le A\text{-}1 \\ N_{A-1,t-1,s}\, e^{-Z_{A-1,t-1,s}} + N_{A,t-1,s}\, e^{-Z_{A,t-1,s}} & ; \;\; a = A \end{cases} \tag{E.7}$$

Selectivity Pattern 20 ($g = 1, ..., 5$)

$$S_{atgs} = \pi_{1atgs}(1 - j_{1atgs}) + j_{1atgs}\left[(1 - j_{2atgs}) + j_{2atgs}\pi_{2atgs}\right] \tag{E.8}$$

$$j_{1atgs} = 1 \,/\, \left[1 + e^{-20(a-\beta_{1tgs})/(1+|a-\beta_{1tgs}|)}\right] \; ; \quad \beta_{1tgs} = \text{first age when } S_{tgs}{=}1 \tag{E.9}$$

$$j_{2atgs} = 1 \,/\, \left[1 + e^{-20(a-a^{\star}_{tgs})/(1+|a-a^{\star}_{tgs}|)}\right] \; ; \quad a^{\star}_{tgs} = \text{last age when } S_{tgs}{=}1 \tag{E.10}$$

$$a^{\star}_{tgs} = \beta_{1tgs} + (0.99A - \beta_{1tgs})/(1 + \beta_{2tgs}) \; ; \quad \text{assuming age bin = 1y} \tag{E.11}$$

$$\pi_{1atgs} = \left(\frac{1}{1 + e^{-\beta_{5tgs}}}\right)\left(\frac{1}{1 - \left(1 + e^{-\beta_{5tgs}}\right)}\right)\left(\frac{e^{-(a-\beta_{1tgs})^2/e^{\beta_{3tgs}}} - \gamma_{1tgs}}{1 - \gamma_{1tgs}}\right) \tag{E.12}$$

$$\pi_{2atgs} = 1 + \left[\left(\frac{1}{1 + e^{-\beta_{6tgs}}}\right) - 1\right]\left(\frac{e^{-(a-a^{\star}_{tgs})/e^{\beta_{4tgs}}} - 1}{\gamma_{2tgs} - 1}\right) \tag{E.13}$$

$$\gamma_{1tgs} = e^{-(1-\beta_{1tgs})^2/e^{\beta_{3tgs}}} \; ; \quad \gamma_{2tgs} = e^{-(A-a^{\star}_{tgs})^2/e^{\beta_{4tgs}}} \tag{E.14}$$

Deterministic components

Derived states ($1 \le t \le T-1$)

$$L_{ats} = L_{a-1,t-1,s} + \left(L_{a-1-k,t-1,s} - L_{\infty s} \right) \left(e^{-k_s} - 1 \right); \quad a < A \tag{E.15}$$

$$L_{Ats} = \frac{N_{A-1,ts}\overline{L}_{Ats} + N_{Ats}\left[L_{Ats} - \left(L_{Ats} + L_{\infty s} \right) \left(e^{-k_s} - 1 \right) \right]}{N_{A-1,ts} + N_{Ats}} \tag{E.16}$$

$$\overline{L}_{ats} = L_{ats} + \left(L_{ats} - L_{\infty s} \right) \left(e^{-0.5k_s} - 1 \right) \tag{E.17}$$

$$\alpha_{ats} = \begin{cases} \overline{L}_{ats}\nu'_s \,|\, a_{ts}\nu'_s & ; \; a \le a' \\ \overline{L}_{ats}\left[\nu'_s + (\overline{L}_{ats}\text{-}L'_s)/(L''_s\text{-}L'_s)(\nu''_s\text{-}\nu'_s)\right] \,| \\ \quad a_{ts}\nu'_s\left[\nu'_s + (a_{ts}\text{-}a'_s)/(a''_s\text{-}a'_s)(\nu''_s\text{-}\nu'_s)\right] & ; \; a' < a < a'' \\ \overline{L}_{ats}\nu''_s \,|\, a_{ts}\nu''_s & ; \; a'' \le a \end{cases} \tag{E.18}$$

$$\varphi_{lats} = \begin{cases} \Phi\left[(\breve{L}_l - \overline{L}_{ats})/\alpha_{ats}\right] & ; \; l = 1 \\ \Phi\left[(\breve{L}_{l+1} - \overline{L}_{ats})/\alpha_{ats}\right] - \Phi\left[(\breve{L}_l - \overline{L}_{ats})/\alpha_{ats}\right] & ; \; 1 < l < L \\ 1 - \Phi\left[(\breve{L}_l - \overline{L}_{ats})/\alpha_{ats}\right] & ; \; l = L \end{cases} \tag{E.19}$$

$w_{ls} = a_s \mathring{L}_l^{b_s}$; $\mathring{L}_l$ = mid-size of length bin l (E.20)

$f_a = \sum_{l=1}^{\Lambda} \varphi_{las} m_l o_l w_{ls}$; s=1, m=maturity, o=eggs/kg (E.21)

$Z_{ats} = M_{as} \sum_{g \in 1} \left(S_{atgs} F_{tg} \right)$; F_{tg} = apical fishing mortality rate (E.22)

$$\mathcal{T}_{1tg} = C_{tg}/(\widehat{\mathcal{B}}_{tg} + 0.1C_{tg}) \; ; \; \mathcal{J}_{1tg} = 1/\left[1 + e^{30(\mathcal{T}_{1tg}-0.95)}\right] \; ; \; \mathcal{T}_{2tg} = \mathcal{J}_{1tg}\mathcal{T}_{1tg} + 0.95(1 - \mathcal{J}_{1tg}) \tag{E.23}$$

$$F_{1tg} = -\log\left(1 - \mathcal{T}_{2tg}\right) \tag{E.24}$$

$$\widehat{C}_t = \sum_{g \in 1} \sum_{s=1}^{2} \sum_{a=0}^{A} \frac{F_{1tg}}{Z_{ats}} w_{as} N_{ats} S_{atgs} \lambda_{ats} \; ; \quad \lambda_{ats} = \left(1 - e^{-Z_{ats}}\right)/\left(Z_{ats}\right) \tag{E.25}$$

$$\overrightarrow{Z}_t = C_t/(\widehat{C}_t + 0.0001) \; ; \; Z'_{ats} = M_{as} + \overrightarrow{Z}_t(Z_{ats} - M_{as}) \; ; \; \lambda'_{ats} = (1 - e^{-Z'_{ats}})/(Z'_{ats}) \tag{E.26}$$

$$\mathcal{T}_{3tg} = \sum_{s=1}^{2} \sum_{a=0}^{A} w_{as} N_{ats} S_{atgs} \lambda'_{ats} \tag{E.27}$$

$$F_{2tg} = C_{tg}/(\mathcal{T}_{3tg} + 0.0001) \; ; \quad \mathcal{J}_{2tg} = 1/\left[1 + e^{30(F_{2tg}-0.95F_{\max})}\right] \tag{E.28}$$

$F_{tg} = \mathcal{J}_{2tg}F_{2tg} + (1 - \mathcal{J}_{2tg})F_{\max}$; updated estimate of F using hybrid method above (E.29)

$$C_{ats} = \sum_{g \in 1} \frac{F_{tg}}{Z'_{ats}} w_{as} N_{ats} S_{atgs} \lambda'_{ats} \tag{E.30}$$

$B_t = \sum_{a=0}^{A} N_{ats} f_a$; s=1, f=fecundity (E.31)

$$V_{tg} = \sum_{s=1}^{2} \sum_{a=1}^{A} e^{-M_s/2} w_{as} N_{ats} S_{atgs} \; ; \quad g \in \{1\}, \; u_{tg} = C_{tg}/V_{tg}, \; u_{atgs} = u_{tg} S_{atgs} \tag{E.32}$$

Deterministic components

$$R_t = \frac{4hR_0B_{t-1}}{(1-h)B_0 + (5h-1)B_{t-1}} \quad \left(\equiv \frac{B_{t-1}}{\alpha + \beta B_{t-1}}\right) \tag{E.33}$$

Ageing error

$$\Phi(x|\mu,\sigma) = \frac{1}{\sqrt{2\pi}} \int_{-\infty}^{(x-\mu)/\sigma} e^{-(t^2/2)}\, dt \quad \text{cumulative normal distribution} \tag{E.34}$$

$$\Psi_a = \begin{cases} \Phi\left(\frac{a-\widetilde{a}_a}{\xi_a}\right) & ;\ a = 1 \\ \Phi\left(\frac{a+1-\widetilde{a}_a}{\xi_a}\right) - \Phi\left(\frac{a-\widetilde{a}_a}{\xi_a}\right) & ;\ 1 < a < A \\ 1 - \Phi\left(\frac{A-\widetilde{a}_a}{\xi_a}\right) & ;\ a = A \end{cases} \tag{E.35}$$

Estimated observations

$$\widehat{I}_{tg} = q_g \sum_{s=1}^{2} \sum_{a=1}^{A} e^{-M_s/2}(1 - u_{ats}/2) w_{as} S_{ags} N_{ats}\,; \quad t \in \mathbf{T}_g,\ g = 1, ..., 5 \tag{E.36}$$

$$\widehat{p}_{atgs} = \frac{e^{-M_s/2}(1 - u_{ats}/2) S_{ags} N_{ats}}{\sum_{s=1}^{2} \sum_{a=1}^{A} e^{-M_s/2}(1 - u_{ats}/2) S_{ags} N_{ats}};\ 1 \le a \le A,\ t \in \mathbf{U}_g,\ g=1,...,5,\ s=1,2 \tag{E.37}$$

Table E.3. Stochastic components. Calculation of likelihood function $\mathcal{L}(\boldsymbol{\Theta})$ for stochastic components of the model in Table E.2, and resulting objective function $f(\boldsymbol{\Theta})$ to be minimised.

Stochastic components

Estimated parameters

$$\boldsymbol{\Theta} = \{R_0; q_{1,\ldots,5}; \mu_{1,\ldots,5}, \pi_{\mathrm{T}1,\ldots,5}, v_{\mathrm{L}1,\ldots,5L}, v_{\mathrm{R}1,\ldots,5}, \pi_{\mathrm{F}1,\ldots,5}\} \tag{E.38}$$

Recruitment deviations

$$\rho_{t+1} = \log R_{t+1} - \log B_t + \log(\alpha + \beta B_t) + 0.5 b_t \sigma_R^2 + \epsilon_t \; ; \quad \epsilon_t \sim \mathcal{N}(0, \sigma_R^2), \; 1 \le t \le T\text{-}1 \tag{E.39}$$

$$\text{where } b_t = \begin{cases} 0 & ; \; t \le t_1^b \\ b_{\max}\left[1 - (t - t_1^b)/(t_2^b - t_1^b)\right] & ; \; t_1^b < t < t_2^b \\ b_{\max} & ; \; t_2^b \le t \le t_3^b \\ b_{\max}\left[1 - (t_3^b - t)/(t_4^b - t_3^b)\right] & ; \; t_3^b < t < t_4^b \\ 0 & ; \; t_4^b \le t \end{cases} \tag{E.40}$$

Log-likelihood components (⊛ active, ◁ inactive)

$$\circledast \; \mathcal{L}_{1g}(\boldsymbol{\Theta}|\{\widehat{I}_{tg}\}) = \sum_{t \epsilon \mathbf{T}_g} \left[\frac{(\log I_{tg} - \log(q_g B_{tg}))^2}{2\kappa_{tg}^2} + \kappa'_{tg} \log \kappa_{tg} \right] \tag{E.41}$$

$$\triangleleft \; \mathcal{L}_{2g}(\boldsymbol{\Theta}|\{d_{tg}\}) = \sum_{t=1}^{T} 0.5(\mathrm{df}_g + 1) \log \left[\frac{1 + (d_{tg} - \widehat{d}_{tg})^2}{\mathrm{df}_g \delta_{tg}^2} \right] + \delta'_{tg} \log \delta_{tg} \tag{E.42}$$

$$\triangleleft \; \mathcal{L}_{3g}(\boldsymbol{\Theta}|\{\overline{w}_{tg}\}) = \sum_{t=1}^{T} 0.5(\mathrm{df}_{\overline{w}} + 1) \log \left[\frac{1 + (\overline{w}_{tg} - \widehat{\overline{w}}_{tg})^2}{\mathrm{df}_{\overline{w}} \psi_{tg}^2} \right] + \psi'_{tg} \log \psi_{tg} \tag{E.43}$$

$$\triangleleft \; \mathcal{L}_{4g}(\boldsymbol{\Theta}|\{l_{tg}\}) = \textstyle\sum_{t \epsilon \mathbf{U}_g} \sum_{s=1}^{2} \sum_{l=1}^{L} n_{tgs} \, p_{ltgs} \, \log\left(p_{ltgs} / \widehat{p}_{ltgs}\right) \text{; composition option 1} \tag{E.44}$$

$$\circledast \; \mathcal{L}_{5g}(\boldsymbol{\Theta}|\{a_{tg}\}) = \textstyle\sum_{t \epsilon \mathbf{U}_g} \sum_{s=1}^{2} \sum_{a=1}^{A} n_{tgs} \, p_{atgs} \, \log\left(p_{atgs} / \widehat{p}_{atgs}\right) \text{; composition option 2} \tag{E.45}$$

$$\triangleleft \; \mathcal{L}_{6g}(\boldsymbol{\Theta}|\{z_{tg}\}) = \textstyle\sum_{t \epsilon \mathbf{U}_g} \sum_{s=1}^{2} \sum_{z=1}^{\Lambda} n_{tgs} \, p_{ztgs} \, \log\left(p_{ztgs} / \widehat{p}_{ztgs}\right) \text{; composition option 3} \tag{E.46}$$

$$\circledast \; \mathcal{L}_{7g}(\boldsymbol{\Theta}|\{C_{tg}\}) = \textstyle\sum_{t=1}^{T} \left[\log C_{tg} - \log(\widehat{C}_{tg} + 1\mathrm{e}\text{-}6)\right]^2 / \, 2\tau_{tg}^2 \tag{E.47}$$

$$\circledast \; \mathcal{L}_R(\boldsymbol{\Theta}|\{R_t\}) = 0.5 \textstyle\sum_{t=1}^{T} (\widetilde{R}_t^2 / \sigma_R^2) + b_t \log \sigma_R^2 \tag{E.48}$$

$$\circledast \; \mathcal{L}_{\phi_j}(\boldsymbol{\Theta}|\{\phi_j\}) = 0.5 \left[(\phi_j - \mu_{\phi_j})/\sigma_{\phi_j}\right]^2 \quad \text{; normal prior distributions for parameter } j \tag{E.49}$$

$$\circledast \; \mathcal{L}_{\phi_j}(\boldsymbol{\Theta}|\{\phi_j\}) = 0.5 \left[(\log \phi_j - \mu_{\phi_j})/\sigma_{\phi_j}\right]^2 \quad \text{; lognormal prior distributions for parameter } j \tag{E.50}$$

$$\triangleleft \; \mathcal{L}_{P_j}(\boldsymbol{\Theta}|\{P_{jt}\}) = (1/2\sigma_P^2) \textstyle\sum_{t=1}^{T} \widetilde{P}_{jt}^2 \quad \text{; for time-varing parameters, if any} \tag{E.51}$$

Objective function

$$\mathcal{F}(\boldsymbol{\Theta}) = \sum_{i=1}^{7} \sum_{g=1}^{G} \omega_{ig} \mathcal{L}_{ig} + \omega_R \mathcal{L}_R + \sum_{\phi} \omega_\phi \mathcal{L}_\phi + \sum_{P} \omega_P \mathcal{L}_P \quad ; \omega = \text{weighting factors for each } \mathcal{L} \tag{E.52}$$

Table E.4. Details for estimation of parameters, including prior distributions with corresponding means and standard deviations, bounds between which parameters are constrained, and initial values to start the minimisation procedure for the MPD (mode of the posterior density) calculations. For uniform prior distributions, the bounds completely parameterise the prior. In SS, an analytical solution for q is calculated when the parameter is allowed to 'float'.

Parameter	Phase	Prior distribution	Mean, SD	Bounds	Initial value
YMR offshore					
$\log R_0$	1	normal	8, 8	[1, 16]	8
M_1, M_2	-	fixed	–	–	{0.04 to 0.06 by 0.005}
h	-	fixed	–	–	0.7
$\log q_{1,...,5}$	-	analytic	-3, 6	[-15, 15]	-3
μ_1	3	normal	10.7, 2.14	[1, 40]	10.7
μ_2	3	normal	15.6, 3.12	[1, 40]	15.6
μ_3	3	normal	15.4, 3.08	[1, 40]	15.4
μ_4	3	normal	10.8, 2.16	[1, 40]	10.8
μ_5	3	normal	17.4, 3.48	[1, 40]	17.4
$\log v_{\mathrm{L}1}$	4	normal	1.6, 0.32	[-15, 15]	1.6
$\log v_{\mathrm{L}2}$	4	normal	3.72, 0.744	[-15, 15]	3.72
$\log v_{\mathrm{L}3}$	4	normal	3.44, 0.688	[-15, 15]	3.44
$\log v_{\mathrm{L}4}$	4	normal	2.08, 0.416	[-15, 15]	2.08
$\log v_{\mathrm{L}5}$	4	normal	4.6, 0.92	[-15, 15]	4.6
$\Delta_{1,...,5}$	-	fixed	–	[-20, 20]	0

E.4. DESCRIPTION OF DETERMINISTIC COMPONENTS

Notation (Table E.1) and set up of the deterministic components (Table E.2) are described below. Acronyms: SS = Stock Synthesis, AW = Awatea, AF = age frequencies|proportions, YMR = Yellowmouth Rockfish.

E.4.1. Age classes

Index (subscript) a represents age classes, going from 1 to the accumulator age class A of 60. Age class $a = 5$, for example, represents fish aged 4-5 years (which is the usual, though not universal, convention, Caswell 2001), and so an age-class 1 fish was born the previous year. The variable N_{ats} is the number of age-class a fish of sex s at the *start* of year t, so the model is run to year T which corresponds to the beginning of year 2022.

E.4.2. Years

Index t represents model years, going from 1 to $T = 88$, and $t = 0$ represents unfished equilibrium conditions. The actual year corresponding to $t = 1$ is 1935, and so model year $T = 88$ corresponds to 2022. The interpretation of year depends on the model's derived state or data input:

- beginning of year: N_{ats}, B_t, R_t
- middle of year: C_{tg}, V_{tg}, F_{tg}, u_{tg}, $\widehat{I}_{tg}$, $\widehat{p}_{atgs}$

E.4.3. Commercial Data

As described in Appendix A, the commercial catch was reconstructed back to 1918 for five fisheries – (1) trawl, (2) halibut longline, (3) sablefish trap|logline, (4) dogfish|lingcod|salmon troll, and (5) hook & line rockfish outside – all excluding PMFC area 4B (Strait of Georgia). In this assessment, one fishery was used – 'Trawl+' (comprising the five fisheries). The dominance of catch by the trawl fishery was so large (>99%) that catches from all fisheries were combined to form a single fishery. Given the negligible catches in the early years, the model was started in 1935, and catches prior to 1935 were not considered. The time series for catches by fishery are denoted C_{tg} and include retained and discarded catches (either observed or reconstructed). The set $\mathbf{U}_{1,...,5}$ (Table E.1) gives the years of available ageing data from the commercial fishery. The proportions-at-age values are given by p_{atgs} with observed sample size n_{tg}, where $g = 1$ corresponds to the commercial data. These proportions are the weighted proportions calculated using the stratified weighting scheme, described in Appendix D, that adjusts for unequal sampling effort across temporal and spatial strata.

E.4.4. Survey Data

Survey data from fleets g=$2, ..., 5$ were used, as described in detail in Appendix B. For the BC coast, indices g denote the surveys g=2: Queen Charlotte Sound (QCS) Synoptic; g=3: West Coast Vancouver Island (WCVI) Synoptic; g=4: West Coast Haida Gwaii (WCHG) Synoptic; g=5: Goose Island Gully (GIG) Historical. The years for which data were available for each survey are given in Table E.1; $\mathbf{T}_g$ corresponds to years for the survey biomass estimates I_{tg} (and corresponding standard deviations κ_{tg}), and $\mathbf{U}_g$ corresponds to years for proportion-at-age data p_{atgs} (with observed sample sizes n_{tg}). Note that sample size refers to the number of samples, where each sample comprises specimens, typically ~30-350 fish.

E.4.5. Sex

A two-sex model was used, with subscript s=1 for females and s=2 for males (note that these subscripts are the reverse of the codes used in the GFBioSQL database). Ageing data were partitioned by sex, as were the weights-at-age inputs. Selectivities and natural mortality were specified by sex.

E.4.6. Weights-at-age

The weights-at-age w_{as} were assumed fixed over time and were based on sex-specific allometric (length-weight) and growth (age-length) model parameters derived from the biological data; see Appendix D for details.

E.4.7. Maturity of females

The proportion of age-class a females that are mature is m_a, and was assumed to be fixed over time; see Appendix D for details.

E.4.8. Initial conditions

An unfished equilibrium situation at the beginning of the reconstruction was assumed because there was no evidence of significant removals prior to 1935. The initial conditions (E.1) and (E.2) were obtained by setting $R_t = R_0$ (virgin recruitment), $N_{ats} = N_{a1s}$ (equilibrium condition) and $u_{ats} = 0$ (no fishing). The virgin spawning biomass B_0 was obtained from (E.3). The initial lengths were set using the growth equations of Schnute (1981) (E.4)-(E.6).

E.4.9. State dynamics

The core of the model is the set of dynamic equations (E.7) for the estimated number N_{ats} of age-class a fish of sex s at the start of year t. The proportion of female new recruits c in Equation (E.7) was set to 0.5. Equation (E.7) calculates the numbers of fish in each age class (and of each sex) that survive to the following year, where Z_{ats} represents the total mortality rate, which in this case comprises natural mortality M and fishing mortality F. The accumulator age class A retains survivors from this class in following years.

Natural mortality M_s was fixed for males and females in this assessment, except for sensitivity run S02. This parameter enters the equations in the form e^{-M_s} as the proportion of unfished individuals that survive the year.

E.4.10. Selectivities

Separate selectivities were modelled for each of the five fleets ($g = 1$ for the fishery and $g = 2, ..., 5$ for the surveys) using SS' selectivity pattern 20 for females (Equations E.8-E.14) and selectivity option 3 for males (although YMR male selectivity was fixed to be the same as that for females in this assessment). Note that 'log' herein refers to natural logarithms. Pattern 20 describes double normal selectivity for females where the parameters are:

1. β_{1g} – age at which selectivity first reaches maximum selectivity (usually 1):
   - SS: beginning age (year) for the plateau;
   - AW: age of full selectivity (μ_g) for females;
2. β_{2g} – used to generate a logistic between peak (β_{1g}) and maximum age (A) that determines width of top plateau ($a_g^\star - \beta_{1g}$), where $a_g^\star$ is the final age of the top plateau;
3. β_{3g} – used to determine width of the ascending limb of double normal curve:
   - SS: determines slope of ascending limb by tweaking its variance;
   - AW: log of variance for left limb ($v_{\mathrm{L}g}$) of selectivity curve;
4. β_{4g} – used to determine width of the descending limb of double normal curve:
   - SS: determines slope of descending limb by tweaking its variance;
   - AW: log of variance for right limb ($v_{\mathrm{R}g}$) of selectivity curve;
5. β_{5g} – determines initial selectivity by generating a logistic between 0 and 1 at first age;
   - where selectivity $S_{a=1,g} = 1/(1 + e^{-\beta_{5g}})$; however,
   - use -999 to ignore initial selectivity algorithm and decay small fish selectivity using β_{3g};
6. β_{6g} – determines final selectivity by generating a logistic between 0 and 1 at final age bin;
   - where selectivity $S_{Ag} = 1/(1 + e^{-\beta_{6g}})$.

Option 3 for pattern 20 describes male selectivity as offsets to female selectivity, where parameters are:

1. Δ_{1g} = male peak offset (Δ_g in AW) added to the first selectivity parameter, β_{1g} (μ_g in AW);
2. Δ_{2g} = male width offset (log width) added to the third selectivity parameter, β_{3g} ($v_{\mathrm{L}g}$ in AW);
3. Δ_{3g} = male width offset (log width) added to the fourth selectivity parameter, β_{4g} ($v_{\mathrm{R}g}$ in AW);
4. Δ_{4g} = male plateau offset added to the sixth selectivity parameter, β_{6g};
5. Δ_{5g} = male apical selectivity for males (usually 1 but could be different than that for females).

Dome selectivity only occurs under three conditions:

- the width of the top plateau (between β_{1g} and $a_g^\star$) must be less than $A - \beta_{1g}$;
- the steepnees of the descending limb (controlled by β_{4g}) must not be too shallow; and
- the final selectivity (controlled by β_{6g}) must be less than peak selectivity (usually 1).

Generally for males, the same selectivity function is used except that some of the selectivity parameters (β_{ig} for $i \in \{1, 3, 4, 6\}$) may be shifted if male AF data are sufficiently different from female AF data. For YMR, $\Delta_{1,2,3,4}$ were fixed to 0, i.e., male selectivity was assumed to be the same as that for females.

For YMR offshore, two of the six selectivity priors (β_{1g} and β_{3g}) were estimated using normal priors, while the other four were fixed to values that maintained maximum selectivity for ages older than $\beta_{1g} \vee \mu_g$ (i.e., no dome-selectivity). We used informative priors to ensure that the survey selectivities remained in an appropriate range, given the sparse and contradictory nature of the survey AF data. Although we use informative priors for the trawl AF data, we could have used a uniform prior, given the strong signal observed in all model fits to these data. The prior means were set to mean values derived from the MCMC posterior medians from the previous POP stock assessments, matching each survey from the appropriate stock assessment. These priors were assigned moderately tight bounds (CV=20%). The MCMC posteriors for these YMR offshore selectivity parameters varied little among all the stock assessments (except when given high weights) and showed acceptable posterior diagnostics.

E.4.11. Derived states

The spawning biomass (biomass of mature females, in tonnes) B_t at the start of year t is calculated in (E.31) by multiplying the numbers of females N_{at1} by fecundity f_a (E.21), which is a function of a length-age matrix φ_{lats} (E.19), the maturity ogive (m_l), egg production (o_l), and weights-at-length w_{l1} (E.20).

The fishing mortality rate F_{tg} (E.29) is derived through an iterative process to fit observed catches closely rather than removing the catches by subtraction. A mid-season harvest rate is calculated using Pope's approximation (Pope 1972), which is then converted to an instantaneous F using the Baranov equation (Baranov 1918). Each fleet's approximate F is repeated iteratively several times (usually three to four) using the Newton-Rhapson procedure until its value yields a close match to the observed catches by the fleet. Details can be found in Methot and Wetzel (2013).

Although SS does not report vulnerable biomass *per se*, equation (E.32) provides an equation from Awatea for V_{tg} mid-year. Assuming that C_{tg} is taken mid-year, the harvest rate is simply C_{tg}/V_{tg}. Further, for year t, the proportion u_{tg} of age-class a and sex s fish that are caught in fishery g can be calculated by multiplying the commercial selectivities S_{atgs} and the ratio u_t (E.32).

E.4.12. Stock-recruitment function

A Beverton-Holt recruitment function is used, parameterised in terms of steepness, h, which is the proportion of the long-term unfished recruitment obtained when the stock abundance is reduced to 20% of the virgin level (Mace and Doonan 1988; Michielsens and McAllister 2004). Awatea uses a prior on h taken from Forrest et al. (2010), where shape parameters for a beta distribution are $\alpha = (1-h)B_0/(4hR_0)$ and $\beta = (5h-1)/4hR_0$ (Hilborn et al. 2003; Michielsens and McAllister 2004). Substituting these into the Beverton-Holt equation, $R_t = B_{t-1}/(\alpha + \beta B_{t-1})$, where R_0 is the virgin recruitment, R_t is the recruitment in year t, B_t is the spawning biomass at the start of year t, and B_0 is the virgin spawning biomass. Stock Synthesis offers several

recruitment options including Ricker, Beverton-Holt, and a three-parameter survivorship-based function suitable for low-fecundity species (Taylor et al. 2013); however, h was fixed to 0.7 (except for one sensitivity run) in this assessment as the stock was never seriously depleted.

E.4.13. Fitting to data

Model estimates of the survey biomass indices I_{tg} are denoted $\widehat{I}_{tg}$ and are calculated in (E.36). The estimated numbers N_{ats} are multiplied by the natural mortality term $e^{-M_s/2}$ (that accounts for half of the annual natural mortality), the term $1 - u_{ats}/2$ (that accounts for half of the commercial catch), weights-at-age w_{as} (to convert to biomass), and selectivity S_{ags}. The sum (over ages and sexes) is then multiplied by the catchability parameter q_g to give the model biomass estimate $\widehat{I}_{tg}$.

The estimated proportions-at-age $\widehat{p}_{atgs}$ are calculated in (E.37). For a particular year and gear type, the product $e^{-M_s/2}(1 - u_{ats}/2)S_{ags}N_{ats}$ gives the relative expected numbers of fish caught for each combination of age and sex. Division by $\sum_{s=1}^{2}\sum_{a=1}^{A} e^{-M_s/2}(1 - u_{ats}/2)S_{ags}N_{ats}$ converts these to estimated proportions for each age-sex combination, such that $\sum_{s=1}^{2}\sum_{a=1}^{A}\widehat{p}_{atgs} = 1$.

Ageing error (AE) in this stock assessment was applied using SS' vector-style inputs of bias and precision. The bias vector used was 0.5 to 60.5 at increments of 1 year for ages 0 through 60, which in SS signifies no age bias. The precision vector for ages 0 through 60 was estimated as the standard deviation of ages 1 through 61 calculated from the CVs of lengths-at-age: $\sigma_a = a(\sigma_{L_a}/\mu_{L_a})$, where $a = 1, ..., 61$. Using these vectors, SS applies a cumulative normal distribution for each age to calculate the frequency of expected age given a mean assigned age and standard deviation (see E.35).

> *"SS never adjusts input data. Rather, it adjusts expected values for data to take into account known factors that influenced the creation of the observations. So, ageing error is applied to a modeled distribution of true ages (after selectivity has taken a subset from the population) to create a new distribution of ages that includes the influence of ageing error."*
>
> – Richard Methot, 2021, *pers. comm.*

E.5. DESCRIPTION OF STOCHASTIC COMPONENTS

E.5.1. Parameters

The set $\boldsymbol{\Theta}$ gives the parameters that are estimated. The estimation procedure is described in the Bayesian Computations section below.

E.5.2. Recruitment deviations

For recruitment, a log-normal process error is assumed, such that the stochastic version of the deterministic stock-recruitment function (E.33) is

$$R_t = \frac{B_{t-1}}{\alpha + \beta B_{t-1}} e^{-0.5 b_t \sigma_R^2 + \epsilon_t} \tag{E.53}$$

where $\epsilon_t \sim \mathcal{N}(0, \sigma_R^2)$, and the bias-correction term $-b_t\sigma_R^2/2$ term in (E.5.2.) ensures that the mean of the recruitment deviations equals 0. This then gives the recruitment deviation equation (E.39) and log-likelihood function (E.48). In this assessment, the value of σ_R was fixed at 0.9 based on values used in recent BC rockfish stock assessments. Other assessments have used σ_R = 0.6 following an assessment of Silvergray Rockfish (Starr et al. 2016) in which the authors

stated that the value was typical for marine 'redfish' (Mertz and Myers 1996). An Awatea model of Rock Sole used σ_R = 0.6 (Holt et al. 2016), citing that it was a commonly used default for finfish assessments (Beddington and Cooke 1983). In recent BC rockfish assessments, we have adopted σ_R = 0.9 based on an empirical model fit consistent with the age composition data for 5ABC POP (Edwards et al. 2012*b*). A study by Thorson et al. (2014) examined 154 fish populations and estimated σ_R = 0.74 (SD=0.35) across seven taxonomic orders; the marginal value for Scorpaeniformes was σ_R=0.78 (SD=0.32) but was only based on 7 stocks.

E.5.3. Log-likelihood functions

The objective funtion function $\mathcal{F}(\boldsymbol{\Theta})$ (E.52) comprises a weighted sum of individual likelihood components that can include:

- $\mathcal{L}_{I_g}$ (E.41) – CPUE or abundance index by fleet
- $\mathcal{L}_{d_g}$ (E.42) – discarded biomass by fleet
- $\mathcal{L}_{\widehat{w}_g}$ (E.43) – mean body weight by fleet
- $\mathcal{L}_{l_g}$ (E.44) – length composition by fleet
- $\mathcal{L}_{a_g}$ (E.45) – age composition by fleet
- $\mathcal{L}_{z_g}$ (E.46) – mean size-at-age by fleet
- $\mathcal{L}_{C_g}$ (E.47) – catch by fleet
- $\mathcal{L}_R$ (E.48) – recruitment deviations
- $\mathcal{L}_{\phi_j}$ (E.49) to (E.50) – parameter priors
- $\mathcal{L}_{P_j}$ (E.51) – random parameter deviations

See Methot and Wetzel (2013) and Methot et al. (2020) for more likelihood options and details.

E.6. BAYESIAN COMPUTATIONS

Estimation of parameters compares the estimated (model-based) observations of survey biomass indices and proportions-at-age with the data, and minimises the recruitment deviations. This is done by minimising the objective function $f(\boldsymbol{\Theta})$, which equation (E.52) shows is the negative of the sum of the total log-likelihood function comprising the logarithmic components (E.41)-(E.51).

The procedure for the Bayesian computations is as follows:

1. minimise the objective function $f(\boldsymbol{\Theta})$ to give estimates of the mode of the posterior density (MPD) for each parameter:
   - this is done in phases,
   - a reweighting procedure is performed;
2. generate samples from the joint posterior distributions of the parameters using Monte Carlo Markov Chain (MCMC) procedure, starting the chains from the MPD estimates.

E.6.1. Phases

The MPD estimates were obtained by minimising the objective function $f(\boldsymbol{\Theta})$, from the stochastic (non-Bayesian version) of the model. The resulting estimates were then used to initiate the chains for the MCMC procedure for the full Bayesian model.

Simultaneously estimating all the estimable parameters for complex nonlinear models is ill advised, and so ADMB allows some of the estimable parameters to be kept fixed during the initial part of the optimisation process ADMB Project (2009). Some parameters are estimated in phase 1, then some further ones in phase 2, and so on. The order (if estimated) typically used by the BC Offshore Rockfish assessment team is:

phase 1: virgin recruitment R_0 and survey catchabilities $q_{2,...,5}$
(although the q fit herein adopts a 'float' option, which calculates an analytical solution);
phase 2: recruitment deviations ϵ_t (held at 0 in phase 1);
phase 3: natural mortality M_s and age of full selectivity for females β_{1g} for g=$1, ..., 5$;
phase 4: additional selectivity parameters β_{ng} for n=$2, ..., 6$ and g=$1, ..., 5$;
phase 5: steepness h.

E.6.2. Reweighting

Sample sizes are used to calculate the variance for a data source and are useful to indicate the relative differences in uncertainty across years within each data source. However, sample size may not represent the relative difference in the variance between different data sources (usually abundance vs. composition). Therefore, the relative weights for each data source in an integrated stock assessment should be adjusted to reflect the information content of each, while retaining the relative differences across years. This can be accomplished by applying adjustment factors to abundance and composition data to weight either data source up or down relative to the other. Rockfish stock assessments using the Awatea model since 2011 have adopted the Francis (2011) reweighting approach – adding series-specific process error to abundance index CVs on the first reweight, and iteratively reweighting age frequency (composition data) sample size by mean age on the first and subsequent reweights.

E.6.2.1. Abundance

For abundance data (survey indices, commercial CPUE indices), Francis (2011) recommends reweighting observed coefficients of variation, c_0, by first adding process error c_p ~ 0.2 to give a reweighted coefficient of variation

$$c_1 = \sqrt{c_0^2 + c_\mathrm{p}^2}\ . \tag{E.54}$$

Survey abundance indices for YMR exhibited high relative error, and so no additional error c_p was added to these indices.

A procedure was developed for estimating process error c_p to add to the commercial CPUE using a spline-smoother analysis. Francis (2011), citing Clark and Hare (2006), recommends using a smoothing function to determine the appropriate level of process error to add to CPUE data, with the goal of finding a balance between rigorously fitting the indices while not removing the majority of the signal in the data. An arbitrary sequence of length 50, comprising degrees of freedom (DF, ν_i), where $i = 2, ..., N$ and N = number of CPUE values U_t from $t = 1996, ..., 2020$, was used to fit the CPUE data with a spline smoother. At $i = N$, the spline curve fit the data perfectly and the residual sum of squares (RSS, ρ_N) was 0. Using spline fits across a range of trial DF ν_i, values of RSS ρ_i formed a logistic-type curve with an inflection point at $i = k$ (Figure E.1). The difference between point estimates of ρ_i (proxy for the slope δ_i) yielded a concave curve with a minimum δ_i, which occurred close to the inflection point k. At the inflection point k, ν_k= 2.449 for YMR offshore, corresponding to ρ_k= 3.118, which was converted to c_p= 0.3296 using:

$$c_\mathrm{p} = \sqrt{\frac{\rho_k}{N-2}}\ \left[\frac{1}{N}\sum_{t=1996}^{2020} U_t\right]^{-1}\ . \tag{E.55}$$

For each model run, the abundance index CVs were adjusted on the first reweight only using the process error c_p = 0.3296, 0, 0, 0, and 0 along the BC coast (g=1,...,5).

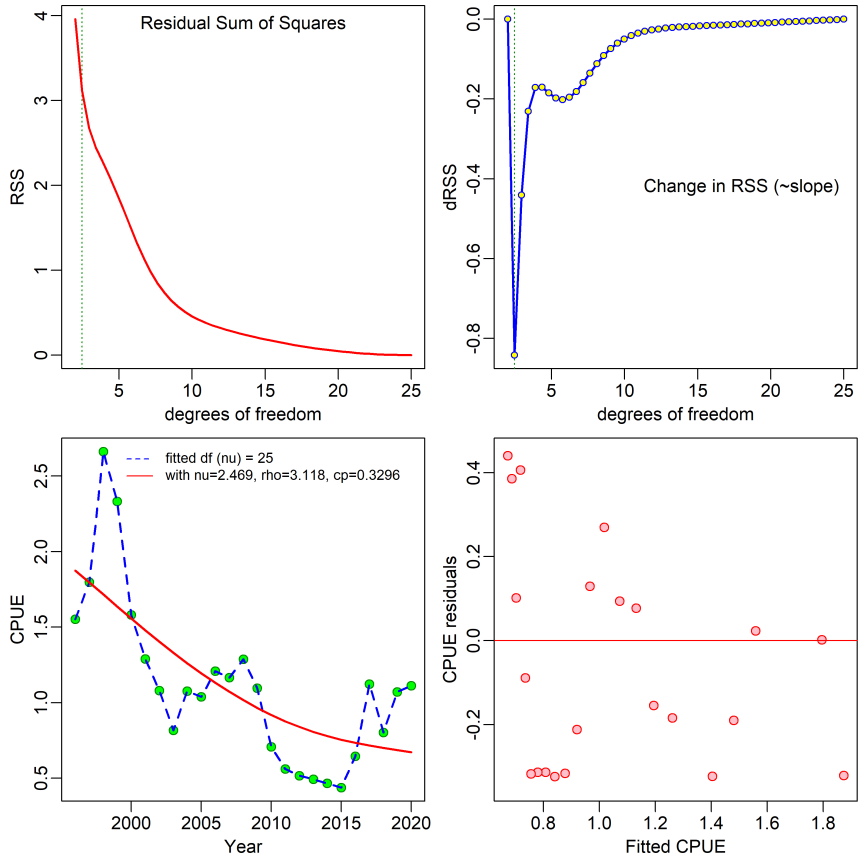

Figure E.1. Estimating process error to add to commercial CPUE data: top left – residual sum of squares (RSS) from spline-smoother at various degrees of freedom; top right – slope of RSS (~ first derivative), vertical dotted line at DF where slope is at a minimum; bottom left – CPUE index data with spline-fitted DF (dashed blue curve) and DF=2.469 (solid red curve); bottom right – standardised residual fit.

E.6.2.2. Composition

YMR model fits using the Francis weighting procedure (Francis 2011) led to assessment outcomes which were not credible, with the MCMC posterior distributions giving high probabilities for equilibrium initial stock sizes (B_0) greater than 100,000 metric tonnes and posterior tails that exceeded 1,000,000 tonnes (typically associated with high values of M). These estimated stock sizes greatly exceeded the B_0 base case estimates made for the same stock by Edwards et al. (2012*a*) and also exceeded the equivalent B_0 estimates for Pacific Ocean Perch, the *Sebastes* species with the acknowledged largest population in BC waters. The underlying reason for these high probabilities for large YMR stock size lies in the uninformative nature of the survey biomass estimates, which showed little contrast and have high relative errors (Tables B.4, B.7, B.10, B.13, Appendix B). Even adding a CPUE series with greater contrast and somewhat lower relative error did not solve the problem of long tails associated with very large biomass estimates.

Experimentation with alternative weights for the age frequency data led to the conclusion that assessment outcomes that gave results that were more consistent with Edwards et al. (2012*a*), and which seemed to be in a credible range, could be obtained by giving higher weight to the commercial trawl age frequency data. The Francis (2011) procedure was designed to downweight composition data so that survey and CPUE biomass series predominate. However,

this procedure failed for the 2021 YMR stock assessment because of the uninformative nature of the survey biomass index series.

Arbitrary upweighting of the commercial age frequency data on the order of four to six times the original sample sizes resulted in model estimates that were more in keeping with expected outcomes. However, while these increased weights solved the problem of long tails for very large stock sizes, they were *ad hoc* and had no theoretical basis. A commonly used alternative method was adopted based on a procedure suggested in the SS manual under "Guidance on Population Dynamics Modelling, Data Weighting", which compares the harmonic mean of effective sample sizes to the arithmetic mean of observed samples sizes:

> *"Effective sample size is calculated from fit of observed to expected length or age compositions. Tuning algorithm is intended to make the arithmetic mean of the input sample size equal to the harmonic mean of the effective sample size (McAllister and Ianelli 1997)"*
>
> – Methot et al. (2021), *Data Weighting*

Stewart and Hamel (2014) used this harmonic mean method to conclude that sample sizes for composition data are often 2-4 times the number of hauls per trip. Generally, greater numbers of samples with fewer specimens are prefereable to fewer numbers of samples with more specimens.

SS calculates effective samples sizes (E.6.2.2.) and the R package `r4ss` (Taylor et al. 2020) reports the ratio of the harmonic mean of these effective sample sizes $\widetilde{n}_{tg}$ relative to the original mean sample size n_{tg} for each fleet g (Figure E.2).

Each model run reported in this stock assessment was fit twice. The first run provided an initial fit to the data from which we calculated the "harmonic mean ratio" (E.6.2.2.). The second model run used this ratio (w_1) to weight the commercial trawl age frequency data, as well as adding process error to the CPUE series (see Section E.6.2.2.). We only used the harmonic mean ratio for the commercial age data and deliberately downweighted the survey age data ($w_{2,3,4,5}$=0.25) for reasons described in Section 8.1.1. The MPD fit from this weighted second run was then used as the initial model for the MCMC simulation procedure.

$$\widetilde{n}_{tg} = \frac{\sum_{a=1}^{A} \widehat{p}_{atg}\left(1-\widehat{p}_{atg}\right)}{\sum_{a=1}^{A}\left(p_{atg}-\widehat{p}_{atg}\right)} \tag{E.56}$$

$$w_g = \frac{\sum_t N_g/(1/\widetilde{n}_{tg})}{\sum_t n_{tg}/N_g} \;; \quad N_g = \text{number years with AF data in fleet } g \tag{E.57}$$

E.6.3. Prior distributions

Descriptions of the prior distributions for the estimated parameters (without including recruitment deviations) are given in Table E.4. A wide normal prior $\mathcal{N}$(8,8) was used for R_0; this provided more stability in the model than using a uniform prior without affecting the estimation process. Selectivity priors were normal with means based on median values from MCMC posteriors from previous POP stock assessments, matching each survey, and with CVs of 20%. Selectivity is discussed more fully in Section E.4.10. Steepness was not estimated in this model, but was fixed at h=0.7. Catchability parameters q_g were determined analytically by SS (using `float=1`). Natural mortality was fixed in the base component runs from 0.04 to 0.06; however, a sensitivity anlysis used a normal prior of $\mathcal{N}$(0.05,0.01) when estimating this parameter.

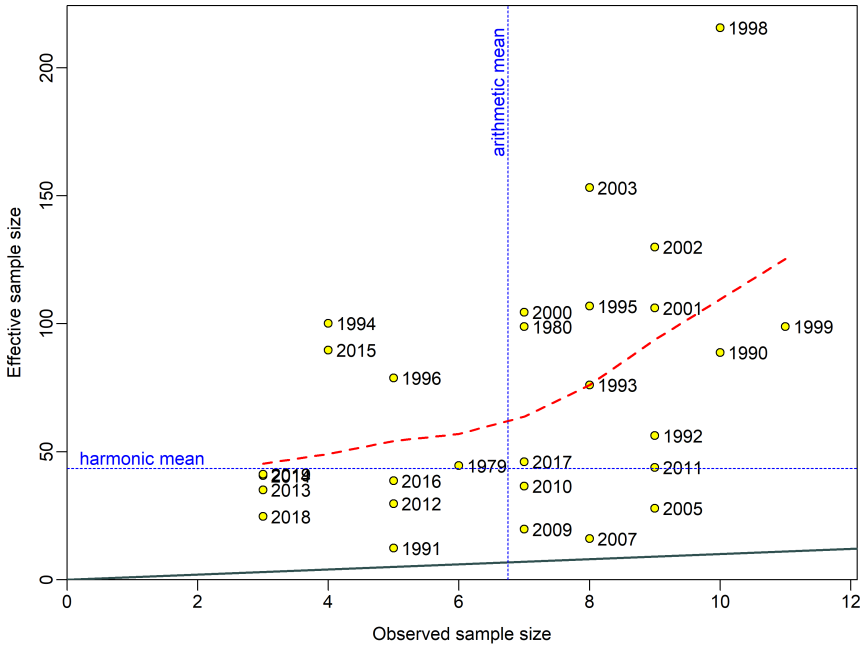

Figure E.2. Unweighted Trawl+ AF – harmonic mean of effective sample size vs. arithmetic mean of adjusted sample size. The goal of weighting composition data is to adjust the arithmetic mean of the observed sample size to be approximately equal to the harmonic mean of the effective sample size (i.e., nudge the solid grey line to run through the intersection of the blue dotted lines).

E.6.4. MCMC properties

The MCMC procedure used the 'no U-turn sampling' (NUTS) algorithm (Monnahan and Kristensen 2018; Monnahan et al. 2019) to produce 4000 iterations, parsing the workload into 8 parallel chains (using the R package `snowfall`, Knaus 2015) of 500 iterations each, discarding the first 250 iterations and saving the last 250 samples per chain. The parallel chains were then merged for a total of 2000 samples for use in the MCMC analysis.

E.7. REFERENCES POINTS, PROJECTIONS AND ADVICE TO MANAGERS

Advice to managers is given with respect to a suite of reference points. The first set is based on MSY (maximum sustainable yield) and includes the provisional reference points of the DFO Precautionary Approach (DFO 2006, 2009*a*), namely $0.4B_{\mathrm{MSY}}$ and $0.8B_{\mathrm{MSY}}$ (and also provided are B_{MSY} and u_{MSY}, which denote the estimated equilibrium spawning biomass and harvest rate at MSY, respectively). A second set of reference points, the current spawning biomass B_{2022} and harvest rate u_{2021}, is used to show the probability of the stock size increasing from the current female spawning biomass or decreasing from the current harvest rate. A third set of reference points, $0.2B_0$ and $0.4B_0$, is based on the estimated unfished equilibrium spawning biomass B_0. See main text for further discussion.

The probability $\mathrm{P}(B_{2022} > 0.4B_{\mathrm{MSY}})$ is calculated as the proportion of the 10,000 MCMC samples for which $B_{2022} > 0.4B_{\mathrm{MSY}}$ (and similarly for the other biomass-based reference points). For harvest rates, the probability $\mathrm{P}(u_{2021} < u_{\mathrm{MSY}})$ is calculated so that both B- and u-based stock status indicators (and projections when $t = 2023, ..., 2032$) state the probability of being in a 'good' place.

Projections were made for 11 years starting with the biomass for the start of 2022. The user of SS should be aware that all derived values are for a start-of-year time period. Therefore, if the end year in the data file is specified as 2021, derived quantities like spawning biomass B_t are estimated to start of year 2021. By default, SS will project forward at least one year so that catch in 2021 can be applied and derived quantities will be generated for 2022 (one-year forecast). Therefore, in the file `forecast.ss`, a user needs to specify the current year plus any additional forecast years (e.g., a 10-yr forecast would need 11 specified catches from 2022 to 2033). Additionally, if a user needs generational forecasts (e.g, three YMR generations = 90 years), then 91 forecast years need to be specified before any MCMC runs are attempted. In this working paper, our 10-y projection included the current year (start of 2022) so we effectively only have 9 years of projection.

A range of constant catch strategies were used, from 0 to 3000 t at 500 (or 250) t increments (the average catch from 2016 to 2020 was 1272 t along the BC coast). For each strategy, projections were performed for each of the 10,000 MCMC samples (resulting in posterior distributions of future spawning biomass). Recruitments were randomly calculated using (E.33) (i.e. based on lognormal recruitment deviations from the estimated stock-recruitment curve), using randomly generated values of $\epsilon_t \sim \text{Normal}(0, \sigma_R^2)$. Unfortunately, SS calculates projected recruitment deviations at the time of the MCMC runs and so we were not able to change the catch policy after the MCMCs had been performed. In Awatea, the `-mceval` switch can generate a user-specified time series of $\{\epsilon_t\}$ for each of the MCMC samples, which means that catch policies can vary in the number of years projected forward.

E.8. REFERENCES – MODEL RESULTS

ADMB Project. 2009. AD Model Builder: Automatic Differentiation Model Builder. Developed by David Fournier and freely available from admb-project.org.

Baranov, F.I. 1918. "On the question of the biological basis of fisheries: on the question of the dynamics of the fishing industry", (translated from Russian by W.E. Ricker 1945). Izvestiya Otdela Rybovodstva I Nauchno-promyslovykh Issledovanii 1. 81–128.

Beamish, R.J. 1979. New information on the longevity of Pacific ocean perch (*Sebastes alutus*). Can. J. Fish. Aquat. Sci. 36(11). 1395–1400.

Beddington, J.R. and Cooke, J.G. 1983. The potential yield of fish stocks. FAO Fish. Tech. Paper 242. v + 47 p.

Caswell, H. 2001. Matrix Population Models: Construction, Analysis and Interpretation. Sinauer Associates, Massachusetts.

Clark, W.G. and Hare, S.R. 2006. Assessment and management of Pacific halibut: data, methods, and policy. Sci. Rep. 83, International Pacific Halibut Commission, Seattle, WA.

DFO. 2006. A harvest strategy compliant with the precautionary approach. DFO Can. Sci. Advis. Sec. Sci. Advis. Rep. 2006/023. 7 p.

DFO. 2009*a*. A fishery decision-making framework incorporating the Precautionary Approach.

DFO. 2009*b*. Stock assessment update for British Columbia Canary Rockfish. DFO Can. Sci. Advis. Sec. Sci. Resp. 2009/019. 39 p.

DFO. 2015. Yellowtail Rockfish (*Sebastes flavidus*) stock assessment for the coast of British Columbia, Canada. DFO Can. Sci. Advis. Sec. Sci. Advis. Rep. 2015/010. 14 p.

Edwards, A.M., Haigh, R. and Starr, P.J. 2014*a*. Pacific Ocean Perch (*Sebastes alutus*) stock assessment for the north and west coasts of Haida Gwaii, British Columbia. DFO Can. Sci. Advis. Sec. Res. Doc. 2013/092. vi + 126 p.

Edwards, A.M., Haigh, R. and Starr, P.J. 2014*b*. Pacific Ocean Perch (*Sebastes alutus*) stock assessment for the west coast of Vancouver Island, British Columbia. DFO Can. Sci. Advis. Sec. Res. Doc. 2013/093. vi + 135 p.

Edwards, A.M., Haigh, R. and Starr, P.J. 2012*a*. Stock assessment and recovery potential assessment for Yellowmouth Rockfish (*Sebastes reedi*) along the Pacific coast of Canada. DFO Can. Sci. Advis. Sec. Res. Doc. 2012/095. iv + 188 p.

Edwards, A.M., Starr, P.J. and Haigh, R. 2012*b*. Stock assessment for Pacific ocean perch (*Sebastes alutus*) in Queen Charlotte Sound, British Columbia. DFO Can. Sci. Advis. Sec. Res. Doc. 2011/111. viii + 172 p.

Forrest, R.E., McAllister, M.K., Dorn, M.W., Martell, S.J.D. and Stanley, R.D. 2010. Hierarchical Bayesian estimation of recruitment parameters and reference points for Pacific rockfishes (*Sebastes* spp.) under alternative assumptions about the stock-recruit function. Can. J. Fish. Aquat. Sci. 67. 1611–1634.

Fournier, D.A., Hampton, J. and Sibert, J.R. 1998. MULTIFAN-CL: a length-based, age-structured model for fisheries stock assessment, with application to South Pacific albacore, *Thunnus alalunga*. Can. J. Fish. Aquat. Sci. 55(9). 2105–2116.

Fournier, D.A., Sibert, J.R., Majkowski, J. and Hampton, J. 1990. MULTIFAN a likelihood-based method for estimating growth parameters and age composition from multiple length frequency data sets illustrated using data for southern bluefin tuna (*Thunnus maccoyii*). Can. J. Fish. Aquat. Sci. 47(2). 301–317.

Francis, R.I.C.C. 2011. Data weighting in statistical fisheries stock assessment models. Can. J. Fish. Aquat. Sci. 68(6). 1124–1138.

Gelman, A., Carlin, J.B., Stern, H.S. and Rubin, D.B. 2004. Bayesian Data Analysis, 2nd edition. Chapman and Hall/CRC, New York.

Haigh, R., Starr, P.J., Edwards, A.M., King, J.R. and Lecomte, J.B. 2018. Stock assessment for Pacific Ocean Perch (*Sebastes alutus*) in Queen Charlotte Sound, British Columbia in 2017. DFO Can. Sci. Advis. Sec. Res. Doc. 2018/038. v + 227 p.

Hilborn, R., Maunder, M., Parma, A., Ernst, B., Payne, J. and Starr, P. 2003. Coleraine: A generalized age-structured stock assessment model. User's manual version 2.0. University of Washington Report SAFS-UW-0116. Tech. rep., University of Washington.

Holt, K.R., Starr, P.J., Haigh, R. and Krishka, B. 2016. Stock assessment and harvest advice for Rock Sole (*Lepidopsetta* spp.) in British Columbia. DFO Can. Sci. Advis. Sec. Res. Doc. 2016/009. ix + 256 p.

Knaus, J. 2015. snowfall: Easier cluster computing (based on snow). R package version 1.84-6.1.

Leisch, F. 2002. Sweave: dynamic generation of statistical reports using literate data analysis. In W. Härdle and B. Rönz, eds., Compstat 2002 - Proceedings in Computational Statistics, p. 575–580. Physica Verlag, Heidelberg.

Mace, P.M. and Doonan, I.J. 1988. A generalized bioeconomic simulation for fish population dynamics. NZ Fish. Assess. Res. Doc. 88/4. 51 p.

MacLellan, S.E. 1997. How to age rockfish (*Sebastes*) using *S. alutus* as an example – the otolith burnt section technique. Can. Tech. Rep. Fish. Aquat. Sci. 2146. 39 p.

McAllister, M.K. and Ianelli, J.N. 1997. Bayesian stock assessment using catch-age data and the sampling – importance resampling algorithm. Can. J. Fish. Aquat. Sci. 54(2). 284–300.

Mertz, G. and Myers, R. 1996. Influence of fecundity on recruitment variability of marine fish. Can. J. Fish. Aquat. Sci. 53(7). 1618–1625.

Methot, R.D., Wetzel, C.R., Taylor, I.G. and Doering, K. 2020. Stock Synthesis: User Manual Version 3.30.16. Tech. rep., NOAA Fisheries, Seattle WA, USA, September 1, 2020.

Methot, R.D., Wetzel, C.R., Taylor, I.G., Doering, K.L. and Johnson, K.F. 2021. Stock Synthesis: User Manual Version 3.30.18. Tech. rep., NOAA Fisheries, Seattle WA, USA, October 1, 2021.

Methot, R.D. and Wetzel, C.R. 2013. Stock Synthesis: A biological and statistical framework for fish stock assessment and fishery management. Fish. Res. 142. 86–99.

Michielsens, C.G.J. and McAllister, M.K. 2004. A Bayesian hierarchical analysis of stock-recruit data: quantifying structural and parameter uncertainties. Can. J. Fish. Aquat. Sci. 61(6). 1032–1047.

Monnahan, C.C. 2018. adnuts: No-U-Turn MCMC Sampling for ADMB Models. R package ver. 1.1.2.

Monnahan, C.C., Branch, T.A., Thorson, J.T., Stewart, I.J. and Szuwalski, C.S. 2019. Overcoming long Bayesian run times in integrated fisheries stock assessments. ICES J. Mar. Sci. 76(6). 1477–1488.

Monnahan, C.C. and Kristensen, K. 2018. No-U-turn sampling for fast Bayesian inference in ADMB and TMB: Introducing the adnuts and tmbstan R packages. PLoS ONE 13(5). e0197,954.

Pope, J.G. 1972. An investigation of the accuracy of virtual population analysis using cohort analysis. Int. Comm. Northwest Atl. Fish. Res. Bull. 9. 65–74.

R Core Team. 2021. R: A Language and Environment for Statistical Computing. R Foundation for Statistical Computing, Vienna, Austria.

Schnute, J.T. 1981. A versatile growth model with statistically stable parameters. Can. J. Fish. Aquat. Sci. 38(9). 1128–1140.

Stanley, R.D., Starr, P. and Olsen, N. 2009. Stock assessment for Canary Rockfish (*Sebastes pinniger*) in British Columbia waters. DFO Can. Sci. Advis. Sec. Res. Doc. 2009/013. xxii + 198 p.

Starr, P.J. and Haigh, R. 2021*a*. Widow Rockfish (*Sebastes entomelas*) stock assessment for British Columbia in 2019. DFO Can. Sci. Advis. Sec. Res. Doc. 2021/039. vi + 238 p.

Starr, P.J. and Haigh, R. 2022*a*. Bocaccio (*Sebastes paucispinis*) stock assessment for British Columbia in 2019, including guidance for rebuilding plans. DFO Can. Sci. Advis. Sec. Res. Doc. 2022/001. vii + 292 p.

Starr, P.J. and Haigh, R. 2022*b*. Rougheye/Blackspotted Rockfish (*Sebastes aleutianus / melanostictus*) stock assessment for British Columbia in 2020. DFO Can. Sci. Advis. Sec. Res. Doc. 2022/20. vii + 385 p.

Starr, P.J. and Haigh, R. 2021*b*. Redstripe Rockfish (*Sebastes proriger*) stock assessment for British Columbia in 2018. DFO Can. Sci. Advis. Sec. Res. Doc. 2021/014. vii + 340 p.

Starr, P.J., Haigh, R. and Grandin, C. 2016. Stock assessment for Silvergray Rockfish (*Sebastes brevispinis*) along the Pacific coast of Canada. DFO Can. Sci. Advis. Sec. Res. Doc. 2016/042. vi + 170 p.

Stewart, I.J. and Hamel, O.S. 2014. Bootstrapping of sample sizes for length- or age-composition data used in stock assessments. Can. J. Fish. Aquat. Sci. 71(4). 581–588.

Taylor, I.G., Gertseva, V., Methot., R.D. and Maunder, M.N. 2013. A stock-recruitment relationship based on pre-recruit survival, illustrated with application to spiny dogfish shark. Fish. Res. 142. 15–21.

Taylor, I.G., Stewart, I.J., Hicks, A.C., Garrison, T.M., Punt, A.E., Wallace, J.R., Wetzel, C.R., Thorson, J.T., Takeuchi, Y., Ono, K., Monnahan, C.C., Stawitz, C.C., A'mar, Z.T., Whitten, A.R., Johnson, K.F., Emmet, R.L., Anderson, S.C., Lambert, G.I., Stachura, M.M., Cooper, A.B., Stephens, A., Klaer, N.L., McGilliard, C.R., Mosqueira, I., Iwasaki, W.M., Doering, K., Havron, A.M., Vaughan, N. and Denson, L.S. 2020. r4ss: R Code for Stock Synthesis. R package ver. 1.40.1.

Thorson, J.T., Jensen, O.P. and Zipkin, E.F. 2014. How variable is recruitment for exploited marine fishes? A hierarchical model for testing life history theory. Can. J. Fish. Aquat. Sci. 71(7). 973–983.

Thorson, J.T., Johnson, K.F., Methot, R.D. and Taylor, I.G. 2017. Model-based estimates of effective sample size in stock assessment models using the Dirichlet-multinomial distribution. Fish. Res. 192. 84–93.

APPENDIX F. MODEL RESULTS

F.1. INTRODUCTION

This appendix describes results for a coastwide stock of Yellowmouth Rockfish (YMR, *Sebastes reedi*) that spans the outer BC coast in PMFC areas 3CD5ABCDE. Broadly, the results include:

- mode of the posterior distribution (MPD) calculations to compare model estimates to observations,
- Markov chain Monte Carlo (MCMC) simulations to derive posterior distributions for the estimated parameters for a composite base case,
- MCMC diagnostics for the component runs of the composite base case, and
- a range of sensitivity model runs, including MCMC diagnostics.

Note that MCMC diagnostics are rated using the following subjective criteria:

- Good – no trend in traces, split-chains align, no autocorrelation
- Marginal – trace trend temporarily interrupted, split-chains somewhat frayed, some autocorrelation
- Poor – trace trend fluctuates substantially or shows a persistent increase/decrease, split-chains differ from each other, substantial autocorrelation
- Unacceptable – trace trend shows a persistent increase/decrease that has not levelled, split-chains differ markedly from each other, persistant autocorrelation

The final advice consists of a composite base case which provides the primary guidance. A range of sensitivity runs are presented to show the effect of some of the main modelling assumptions. Estimates of major quantities and advice to management (decision tables) are presented here and in the main text.

F.2. YELLOWMOUTH COASTWIDE (3CD5ABCDE)

The base case for YMR BC was selected from model runs 77, 71, 75, 72, and 76 and pooled. Important decisions made during the assessment of YMR BC included:

- fixed natural mortality M to five levels: 0.04, 0.045, 0.05, 0.055, and 0.06 for a total of five reference models using one axis of uncertainty:
  - B1: R77 (M=0.04)
  - B2: R71 (M=0.045)
  - B3: R75 (M=0.05)
  - B4: R72 (M=0.055)
  - B5: R76 (M=0.06)
- assumed two sexes (females, males);
- set plus age class A to 60 years;
- assumed one commercial fishery dominated by trawl (bottom + midwater), with minor removals by halibut longline, sablefish trap, lingcod longline, inshore longline, and salmon troll, pooled into a single catch series with associated age frequency (AF) data drawn from the trawl fishery;
- used one commercial bottom trawl fishery abundance index series (bottom trawl CPUE index, 1996–2020);
- used four survey abundance index series (QCS Synoptic, WCVI Synoptic, WCHG Synoptic, and GIG Historical), with age frequency (AF) data;

- assumed a wide (weak) normal prior $\mathcal{N}(8, 8)$ on $\log R_0$ to help stabilise the model;
- used informed normal priors for the two selectivity parameters (μ_g, $v_{g\text{L}}$, see Appendix E) for all fleets (fishery and surveys), and set the male selectivity offset (Δ_g) to 0;
- estimated recruitment deviations from 1950 to 2012;
- applied abundance reweighting: added CV process error to index CVs, c_p=0.3296 for the commercial CPUE series and c_p=0 for the surveys (see Appendix E);
- applied composition reweighting: adjusted AF effective sample sizes using a harmonic mean ratio method (see Appendix E) based on McAllister and Ianelli (1997);
- fixed the standard deviation of recruitment residuals (σ_R) to 0.9;
- used an ageing error vector based on the CV of observed lengths at age, described in Appendix D, Section D.2.3 and plotted in Figure D.26 (left panel).

Five fixed M values produced five separate model runs, with the respective posterior distributions pooled as a composite base case used to provide advice to managers. The central run of the composite base case (Run75: M=0.05, CPUE c_p=0.3296) was used as a reference case against which 14 sensitivity runs were compared.

All model runs were reweighted (i) once for abundance, by adding process error c_p to the commercial CPUE (no additional error was added to the survey indices because observed error was already high), and (ii) once for composition (effective sample size for AF data) using the harmonic mean ratio procedure outlined in Appendix E. The process error added to the commerical CPUE was based on a spline analysis (Appendix E).

F.2.1. YMR – Central Run MPD

The modelling procedure first determines the best fit (MPD) to the data by minimising the negative log likelihood. Because the YMR BC composite base case examined five models, only the central run (M=0.05, CPUE c_p=0.3296, trawl AFs adjusted by harmonic mean ratio) is presented as an example to show the fits to the data and to present MPD diagnostics (Table F.1). Each MPD run is used as the respective starting point for the MCMC simulations.

The following plot references apply to the central run.

- Figure F.2 – model fits to the CPUE and survey indices across observed years;
- Figures F.3-F.11 – model fits (lines=predicted) to the female and male age frequency data (bars=observed) for the fishery and four survey data sets;
- Figures F.4-F.12 – standardised residuals of model fits to the female and male age frequency data for the fishery and four survey data sets;
- Figure F.13 – harmonic mean of effective sample size vs. arithmetic mean of observed sample size;
- Figure F.14 – model estimates of mean age compared to the observed mean ages;
- Figure F.15 – estimated gear selectivities, together with the ogive for female maturity;
- Figure F.16 – spawning biomass time series and spawning biomass depletion;
- Figure F.17 – the recruitment time series and recruitment deviations.

The model fits to the survey abundance indices were generally satisfactory (Figures F.2, although various indices were missed entirely (2013 QCS, 2010 WCVI, 2012 WCHG, 1994 GIG). The fit to the commercial CPUE indices showed a downward trend from 1996 to 2010 and remained fairly flat thereafter. None of the indices were missed, largely due to adding process error of 33%. Likelihood profile analysis indicated that the CPUE index series was the only abundance series that provided information on stock size.

Only the commercial AF were used to estimate recruitments. This was done by upweighting the commercial AF data using the harmonic mean ratio of the effective sample size to the arithmetic mean of the observed sample size. These values tended to be large (>6), giving a high weight to these data. The AF data for the surveys were deliberately given very low weights (0.25). This was done to eliminate any impact on the recruitment estimates from these data, while still estimating a realistic selectivity function. The reason for this approach was that quality of the survey AF data seemed low, given the inconsistencies in the apparent year class strength between survey years and between sexes within the same survey year.

The harmonic mean of effective sample size vs. the arithmetic mean of observed sample size (Figure F.13) shows ratios of 6.3, 3.6, 3.2, 4.6, and 6.7 for the five fleets for the central run. The base component runs all use harmonic mean ratios calculated for the fishery AFs (6.22 for R77, 6.28 for R71, 6.32 for R75, 6.36 for R72, and 6.39 for R76) and downweighted all the survey AFs using the ratio 0.25 (Table F.2). The resulting model estimates of mean age matched the adjusted mean ages very well, even for the downweighted survey AF data (Figure F.14).

Fits to the commercial trawl fishery age frequency data were excellent, with the model tracking year classes consistently across the 41 year time span represented by the commercial AF data (Figure F.3). There are some large departures at various age classes (standardised residuals>2 (Figure F.4), but that is not surprising given the large number of age-year categories to fit (there are 1680 categories=28 y times 60 ages). Residuals by year show that there are about 9-10 age-year categories in the 1990s that are greater than 2 and four greater than 3. The 1952 and 1982 cohorts show a few residuals greater than 2 as well; however, almost all the age residuals are below 2. Fits to AFs from the three synoptic surveys and the GIG historical survey were mixed as expected, given the low weight used to fit these data (Figures F.5–F.12).

The survey selectivity parameter estimates did not move very far from the priors, which differed by survey (Figure F.1). However, the parameter estimates for the commercial trawl fishery moved well away from the prior, indicating the presence of a strong signal from the data. The maturity ogive, generated from an externally fitted model (see Appendix D), was situated to the right of the commercial fishery selectivity function, indicating that sub-mature fish are harvested by this fishery. The survey selectivity functions were also situated to the left of the maturity function, indicating that the surveys are sampling sub-mature year classes.

The spawning biomass (female) trajectory for the central run lies between 12,000 and 40,000 tonnes and reached the lowest point in the trajectory in 2013 or 2014 and has since increased, with the lowest point just below $0.5B_0$ (Figure F.16).

The recruitment estimates showed four large events in 1952, 1961, 1982, and 2006 (Figure F.17). These events appear to be well defined in the data, with the definition greatly improved after the implementation of ageing error based on CVs of length-at-age (see Sensitivity section). The model estimated two periods of prolonged below average recruitment deviations, the first between 1970 and 1980 and the second between 1990 and 2000. The four recruitment ‘spikes’ corresponded to recruitments around three times the long-term average recruitment

F.2.1.1. Central run MPD tables

Table F.1. Central Run 75: Priors and MPD estimates for estimated parameters. Prior information – distributions: 0 = uniform, 2 = beta, 6 = normal

Parameter	Phase	Range	Type	(Mean,SD)	Initial	MPD
LN(R0)	1	(1, 16)	6	(8, 8)	8	8.062
mu(1) TRAWL+	3	(1, 40)	6	(10.7, 2.14)	10.7	11.645
varL(1) TRAWL+	4	(-15, 15)	6	(1.6, 0.32)	1.6	2.073
mu(2) QCS	3	(1, 40)	6	(15.6, 3.12)	15.6	13.599
varL(2) QCS	4	(-15, 15)	6	(3.72, 0.744)	3.72	3.915
mu(3) WCVI	3	(1, 40)	6	(15.4, 3.08)	15.4	13.738
varL(3) WCVI	4	(-15, 15)	6	(3.44, 0.688)	3.44	3.820
mu(4) WCHG	3	(1, 40)	6	(10.8, 2.16)	10.8	10.834
varL(4) WCHG	4	(-15, 15)	6	(2.08, 0.416)	2.08	2.017
mu(5) GIG	3	(1, 40)	6	(17.4, 3.48)	17.4	15.753
varL(5) GIG	4	(-15, 15)	6	(4.6, 0.92)	4.6	4.828

F.2.1.2. Central run MPD figures

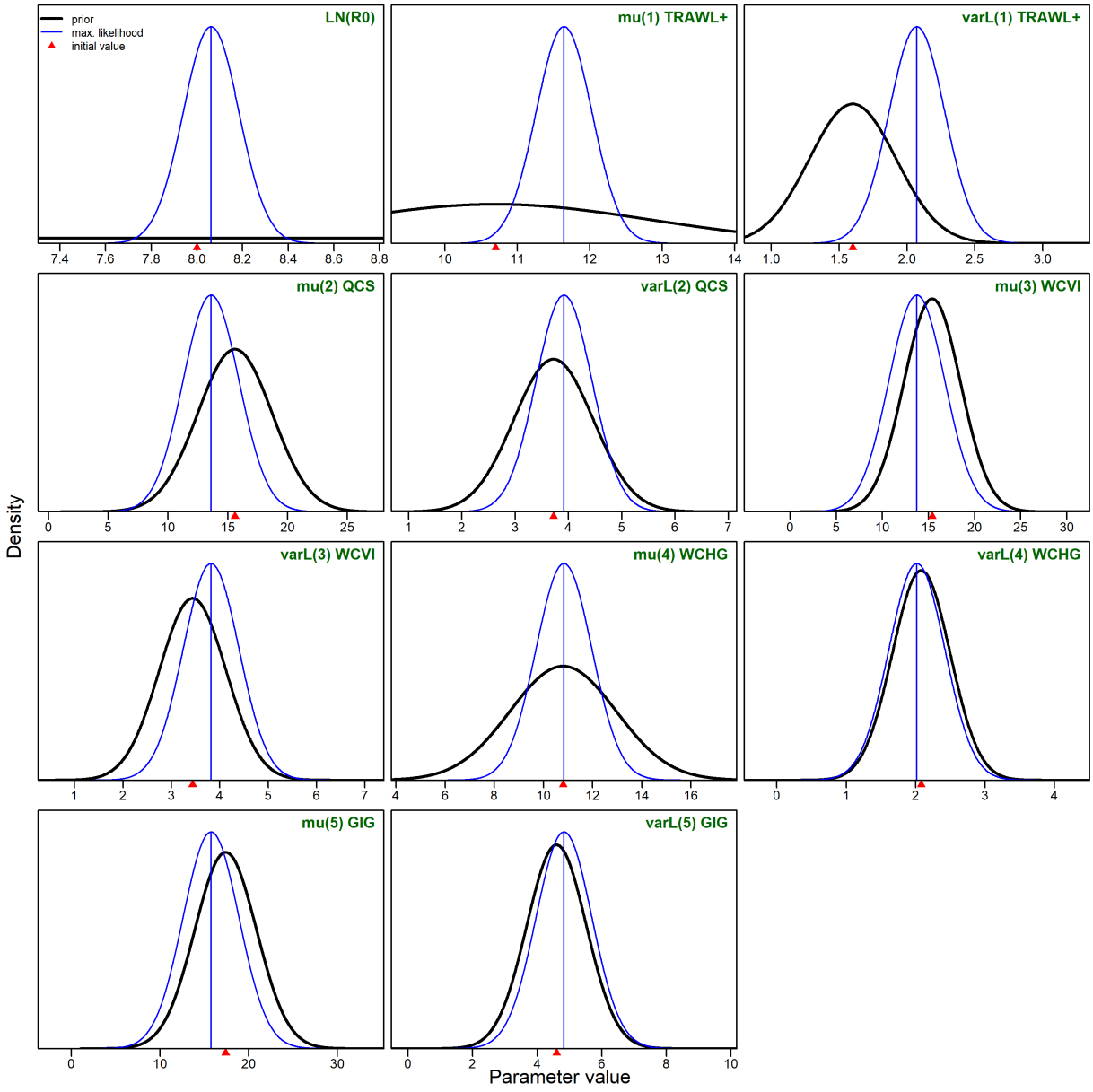

Figure F.1. Central Run 75: Likelihood profiles (thin blue curves) and prior density functions (thick black curves) for the estimated parameters. Vertical lines represent the maximum likelihood estimates; red triangles indicate initial values used in the minimization process.

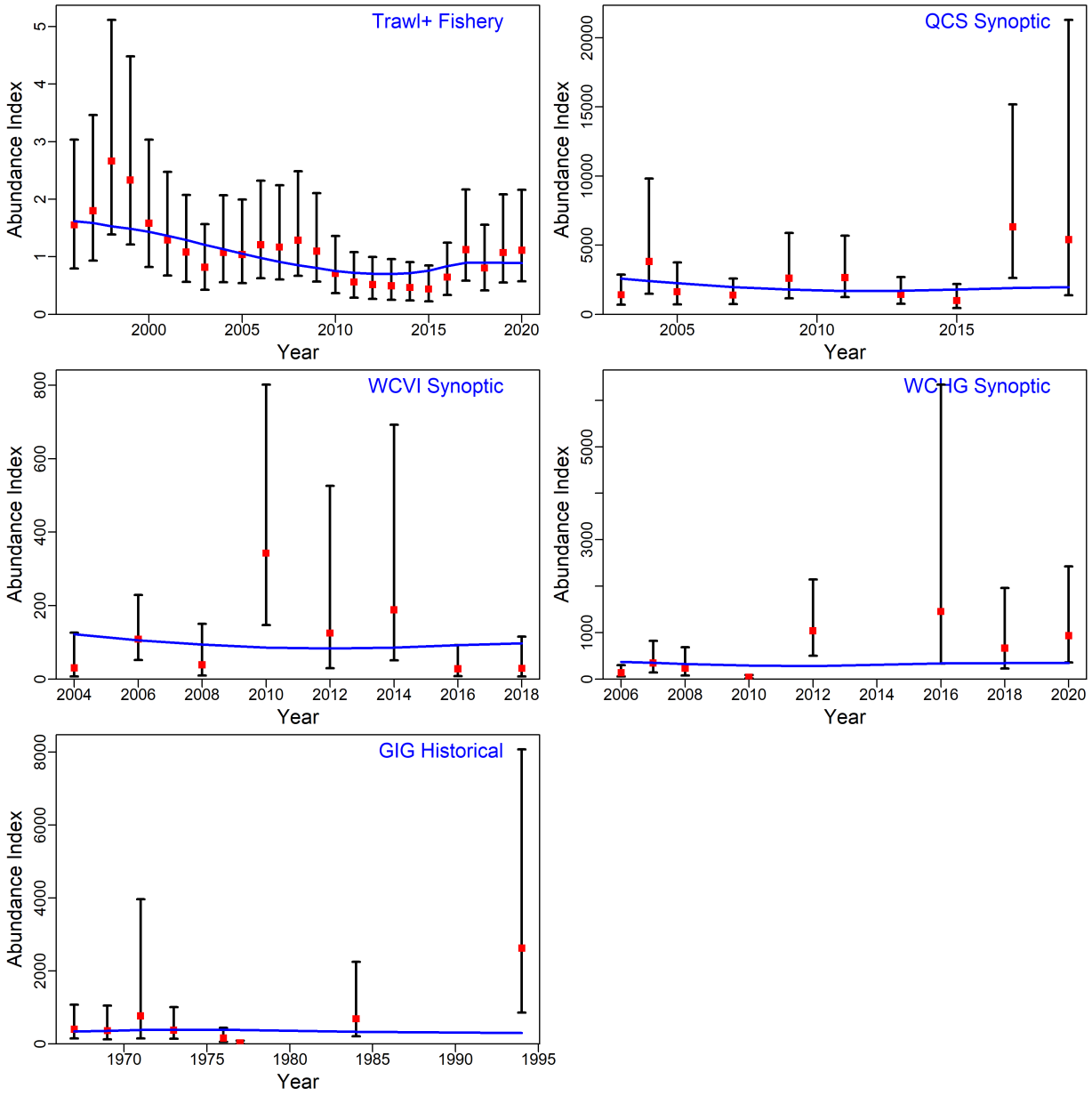

Figure F.2. Central Run 75: Survey index values (points) with 95% confidence intervals (bars) and MPD model fits (curves) for the fishery-independent survey series.

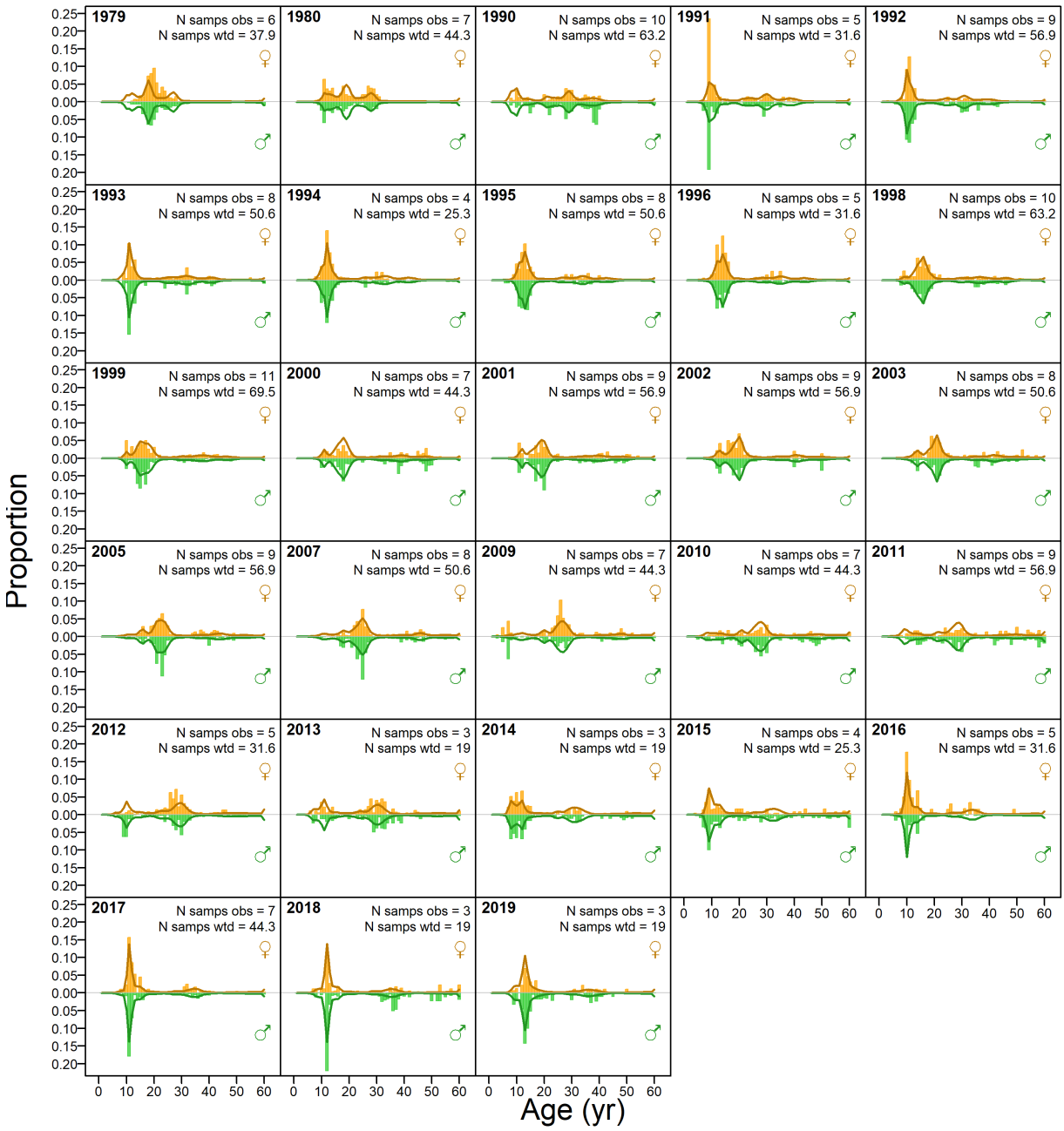

Figure F.3. Central Run 75: Trawl+ Fishery proportions-at-age (bars=observed, lines=predicted) for females and males combined.

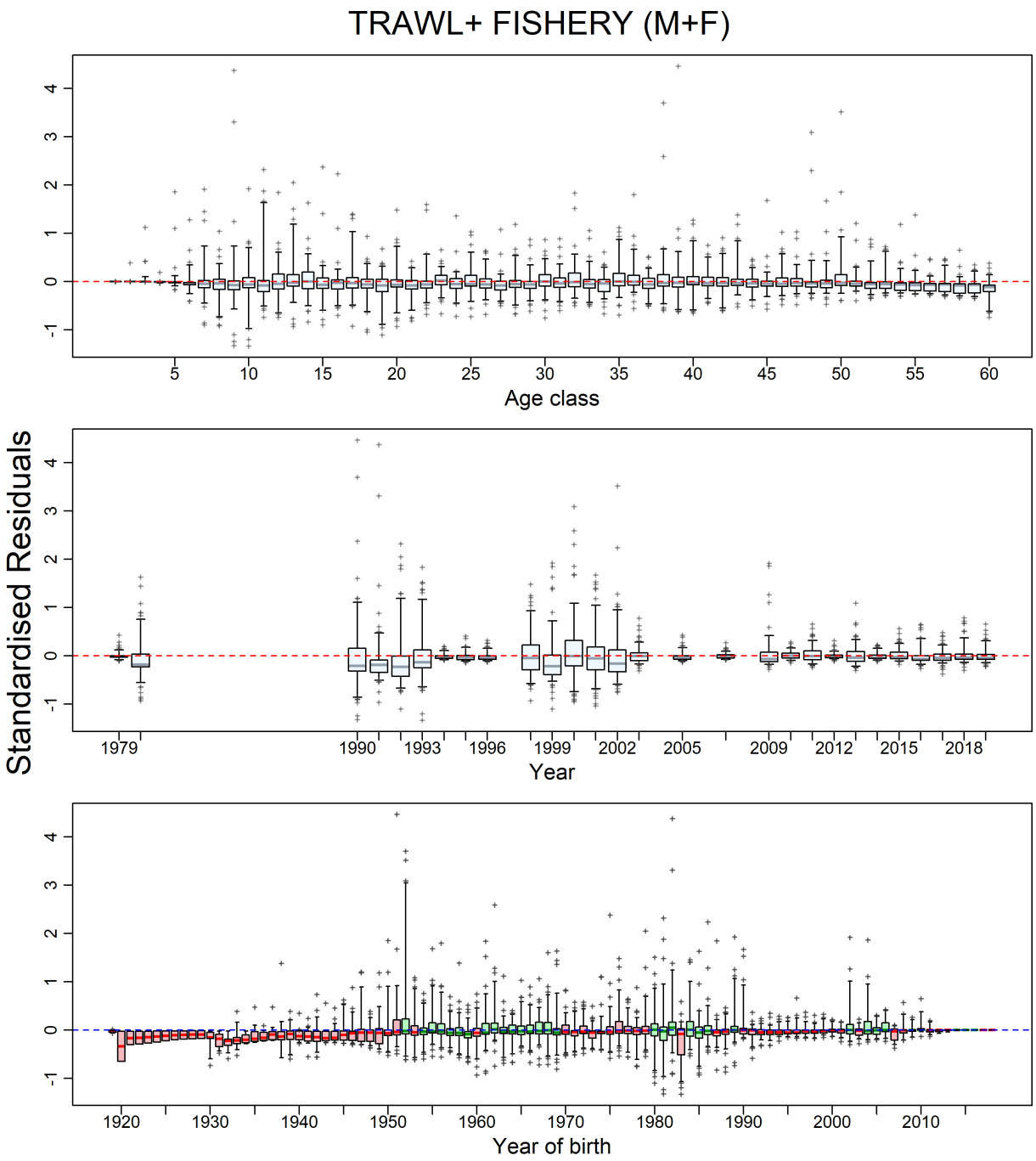

Figure F.4. Central Run 75: Trawl+ Fishery residuals of model fits to proportion-at-age data. Vertical axes are standardised residuals. Boxplots in threes panels show residuals by age class, by year of data, and by year of birth (following a cohort through time). Cohort boxes are coloured green if recruitment deviations in birth year are positive, red if negative. Boxes give quantile ranges (0.25-0.75) with horizontal lines at medians, vertical whiskers extend to the the 0.05 and 0.95 quantiles, and outliers appear as plus signs.

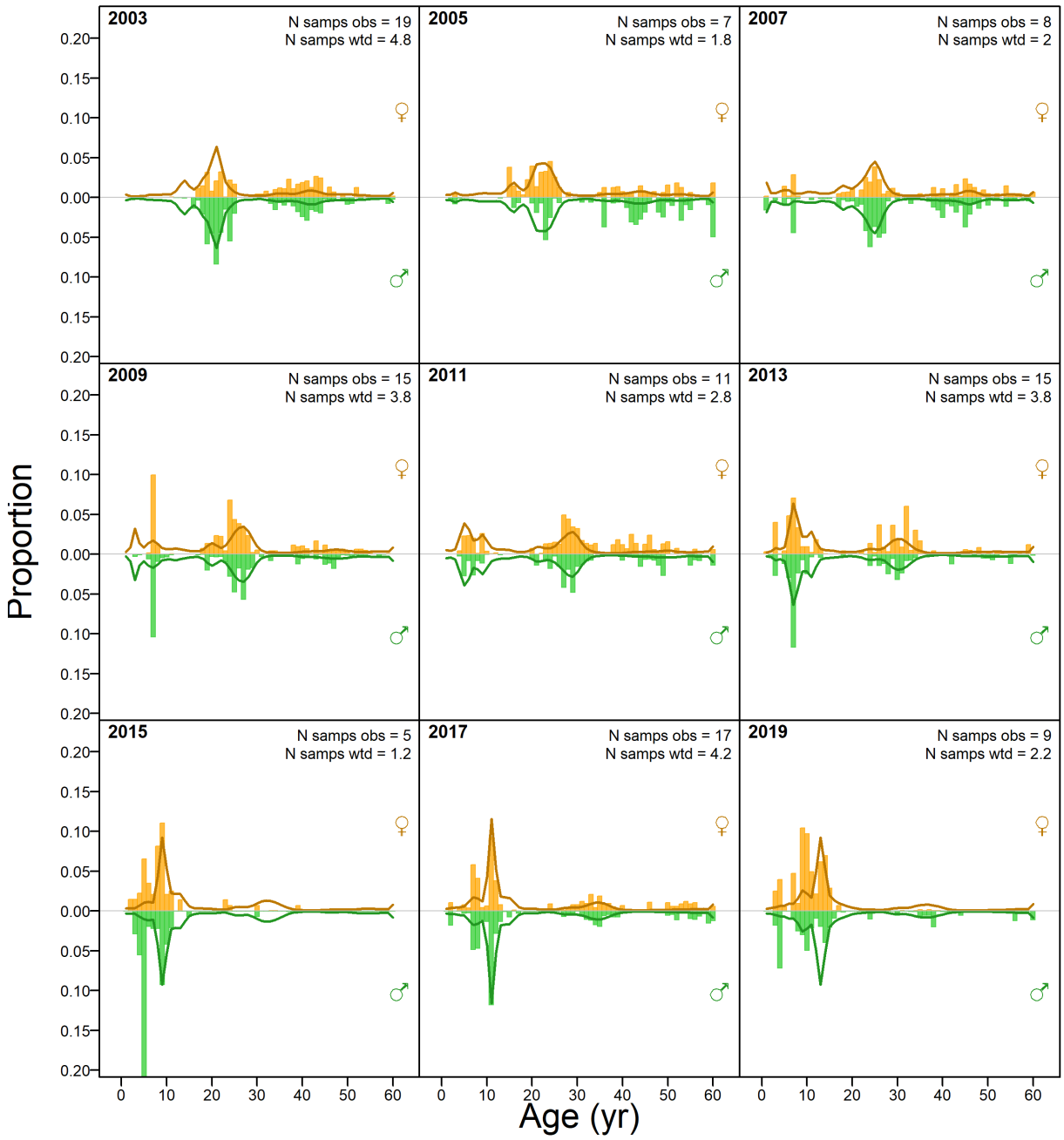

Figure F.5. Central Run 75: QCS Synoptic survey proportions-at-age (bars=observed, lines=predicted) for females and males combined.

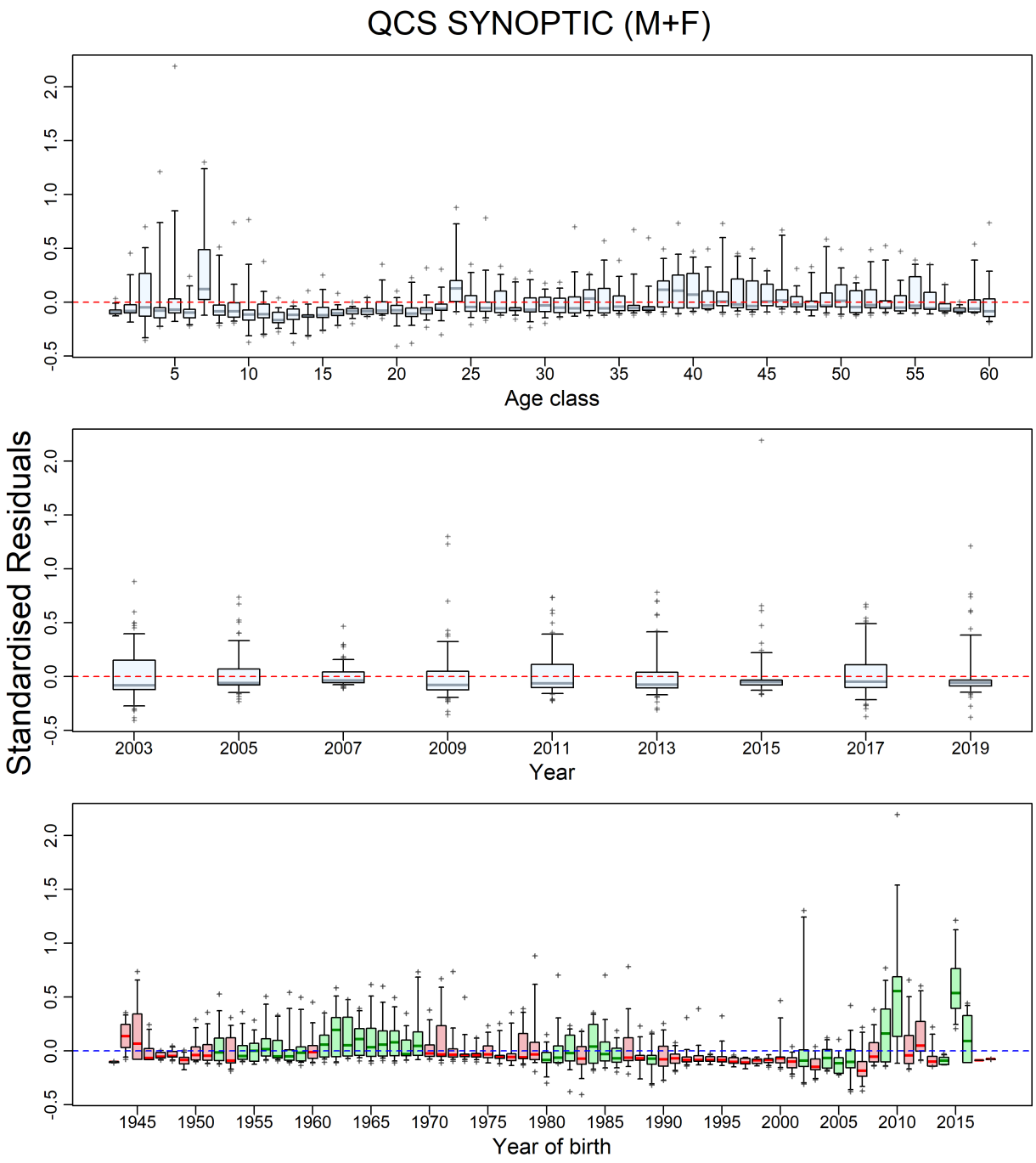

Figure F.6. Central Run 75: QCS Synoptic survey residuals of model fits to proportion-at-age data. See Fig. F.4 caption for plot details.

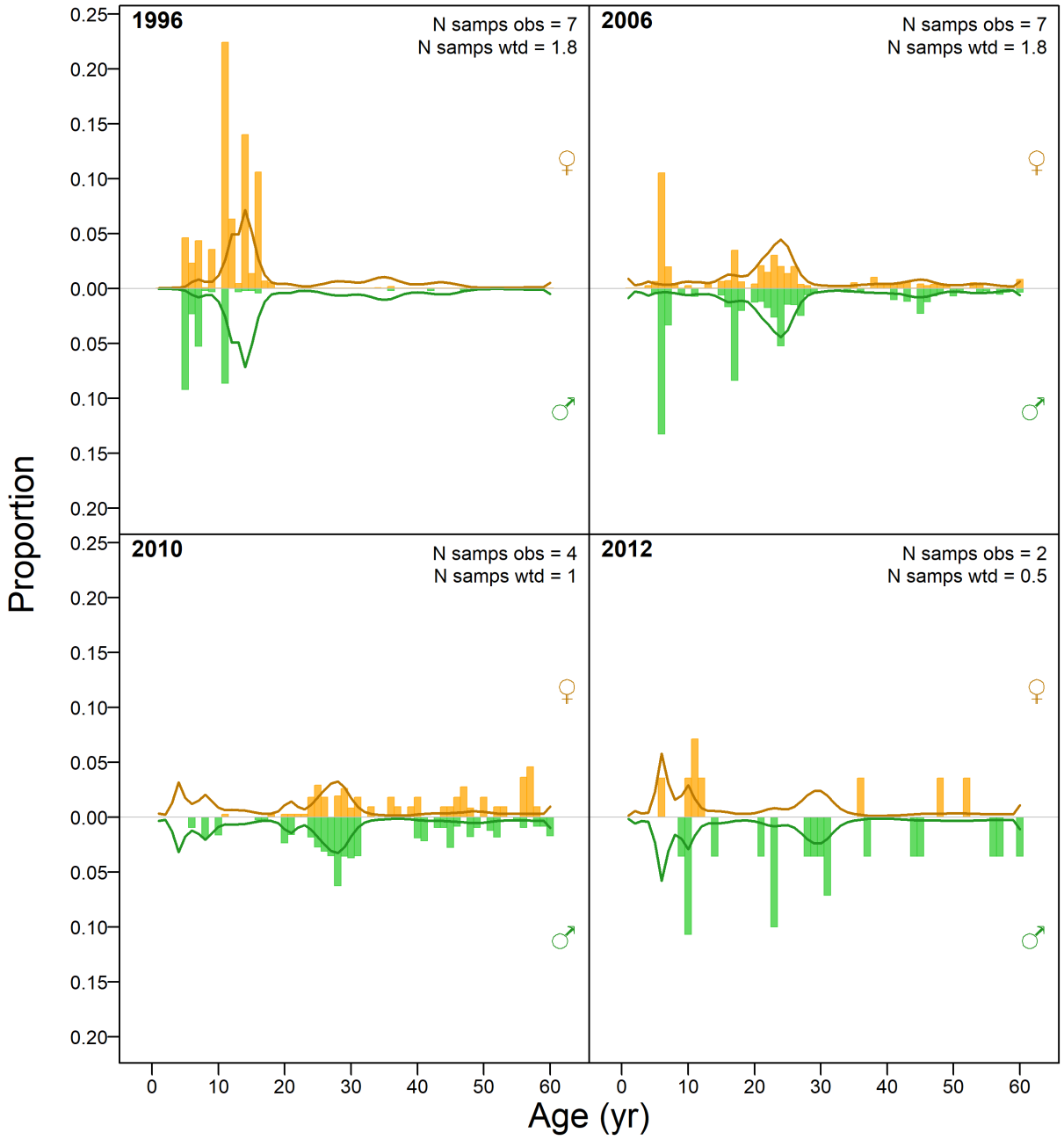

Figure F.7. Central Run 75: WCVI Synoptic survey proportions-at-age (bars=observed, lines=predicted) for females and males combined.

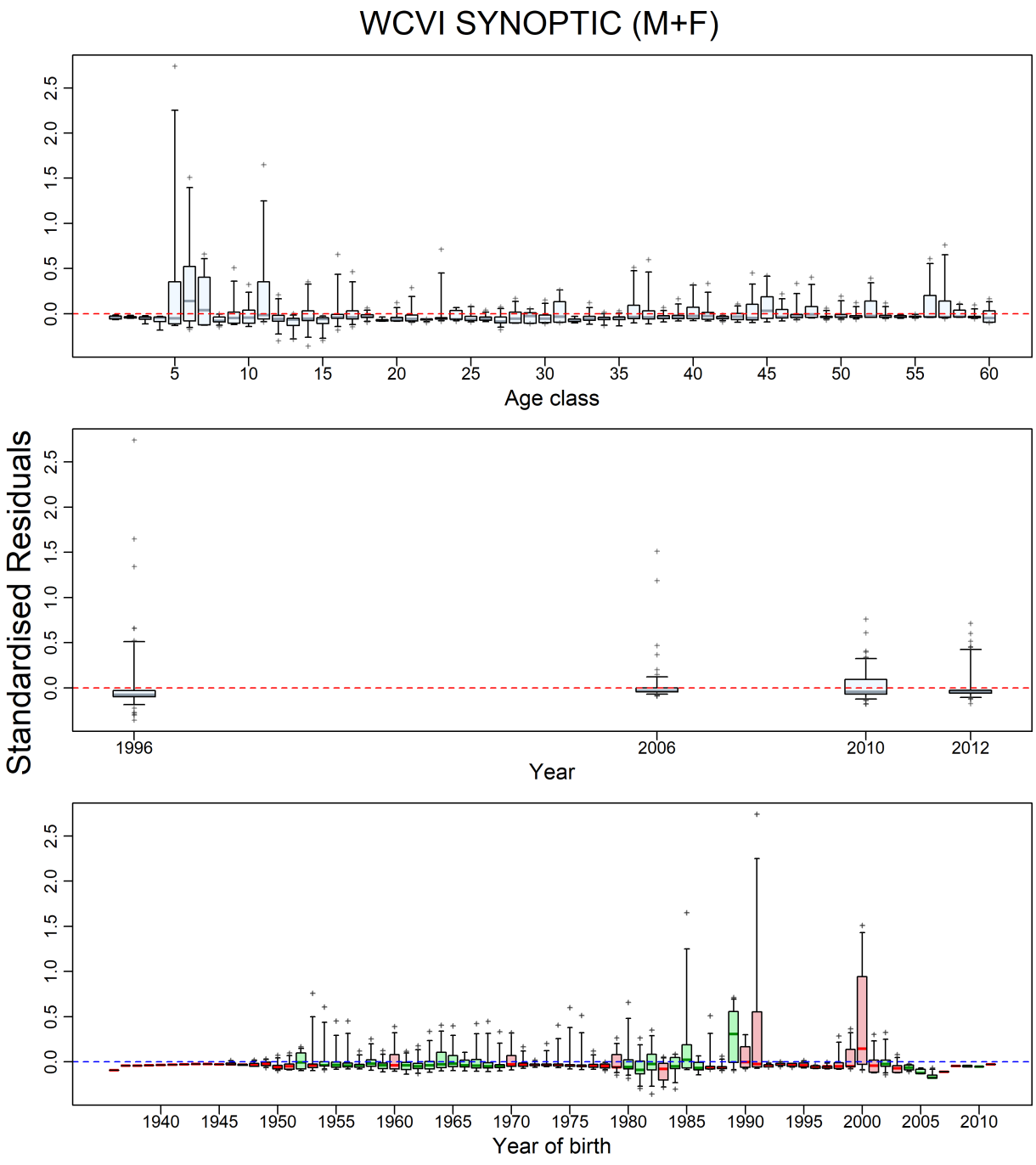

Figure F.8. Central Run 75: WCVI Synoptic survey residuals of model fits to proportion-at-age data. See Fig. F.4 caption for plot details.

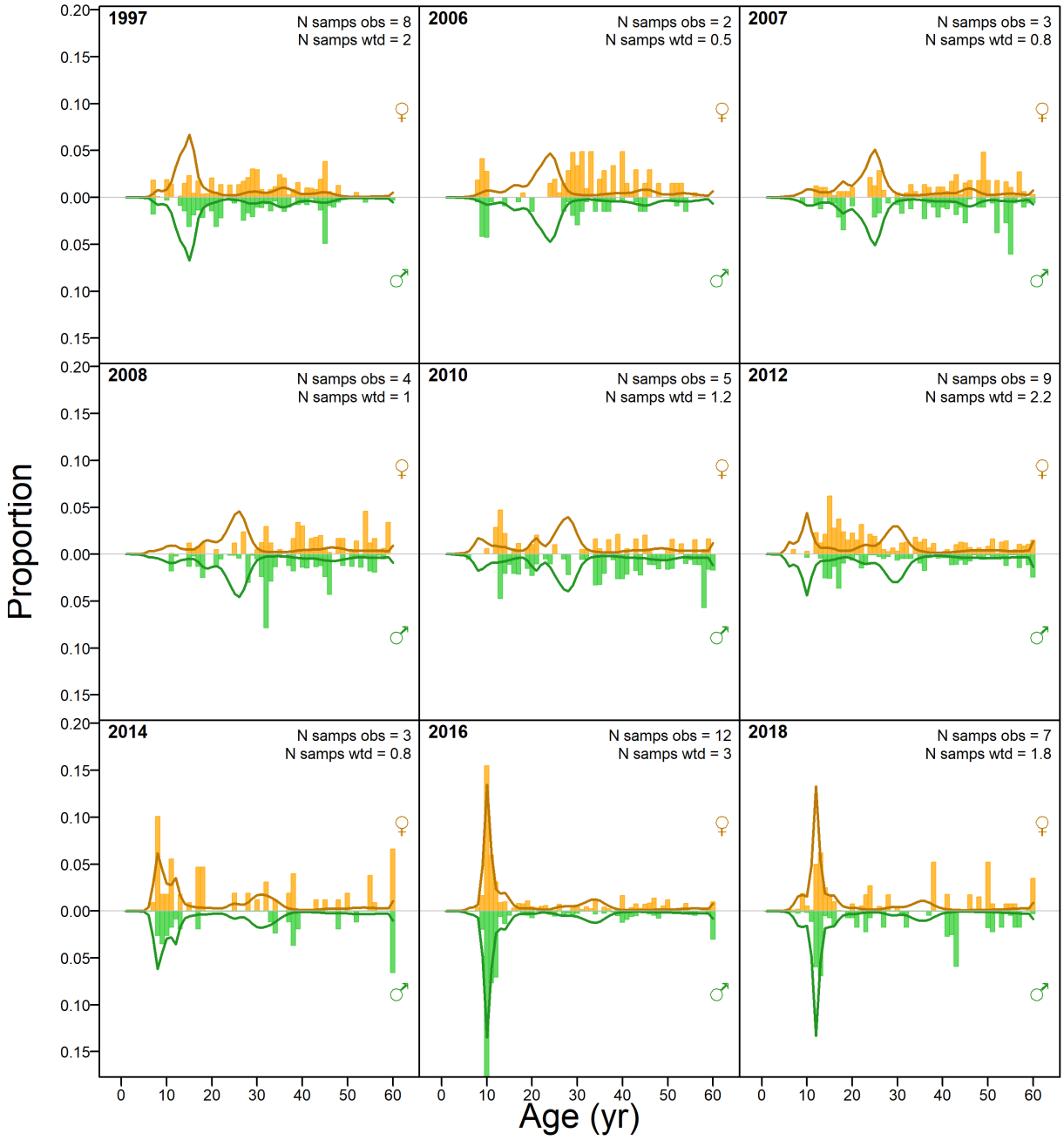

Figure F.9. Central Run 75: WCHG Synoptic survey proportions-at-age (bars=observed, lines=predicted) for females and males combined.

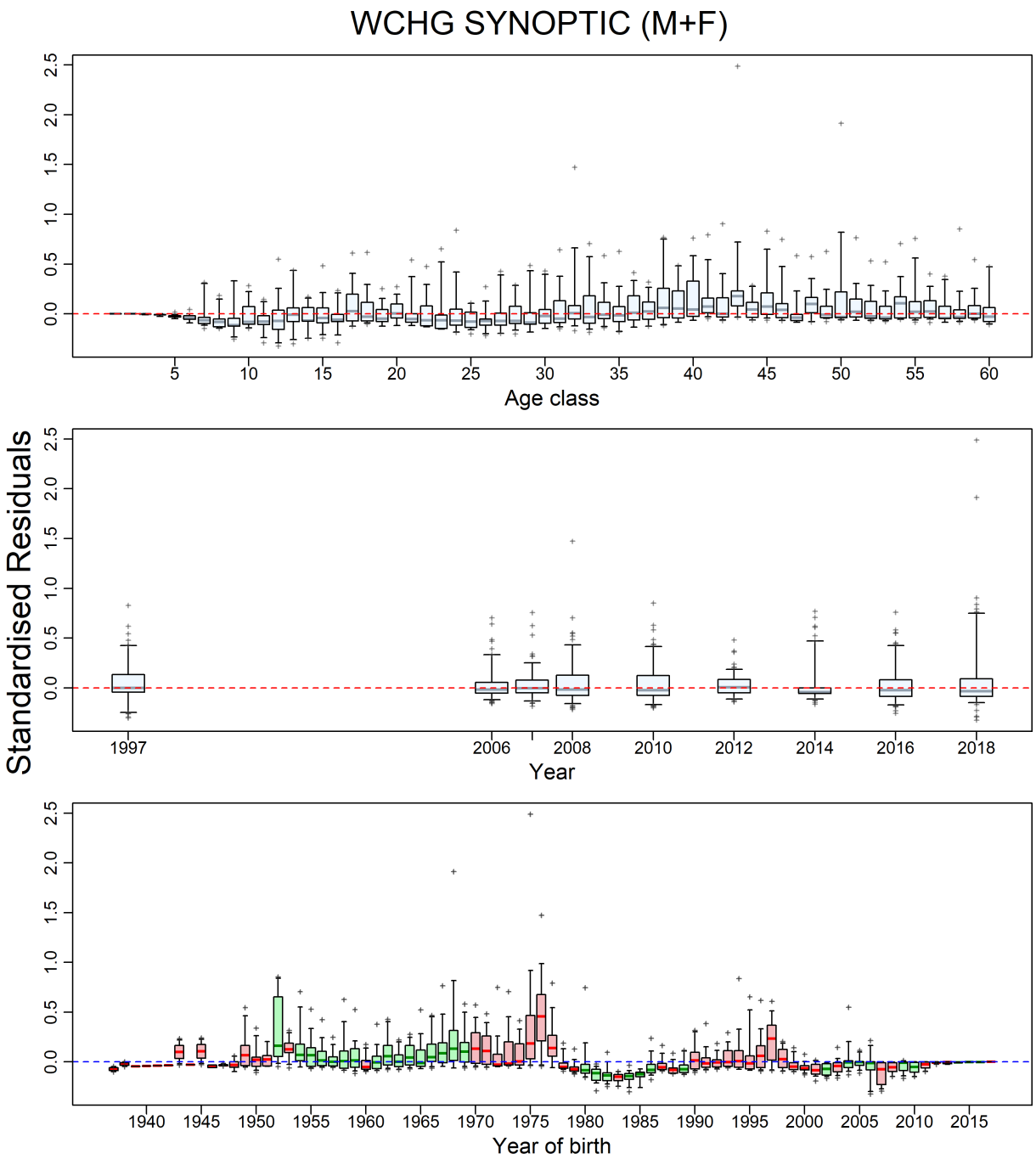

Figure F.10. Central Run 75: WCHG Synoptic survey residuals of model fits to proportion-at-age data. See Fig. F.4 caption for plot details.

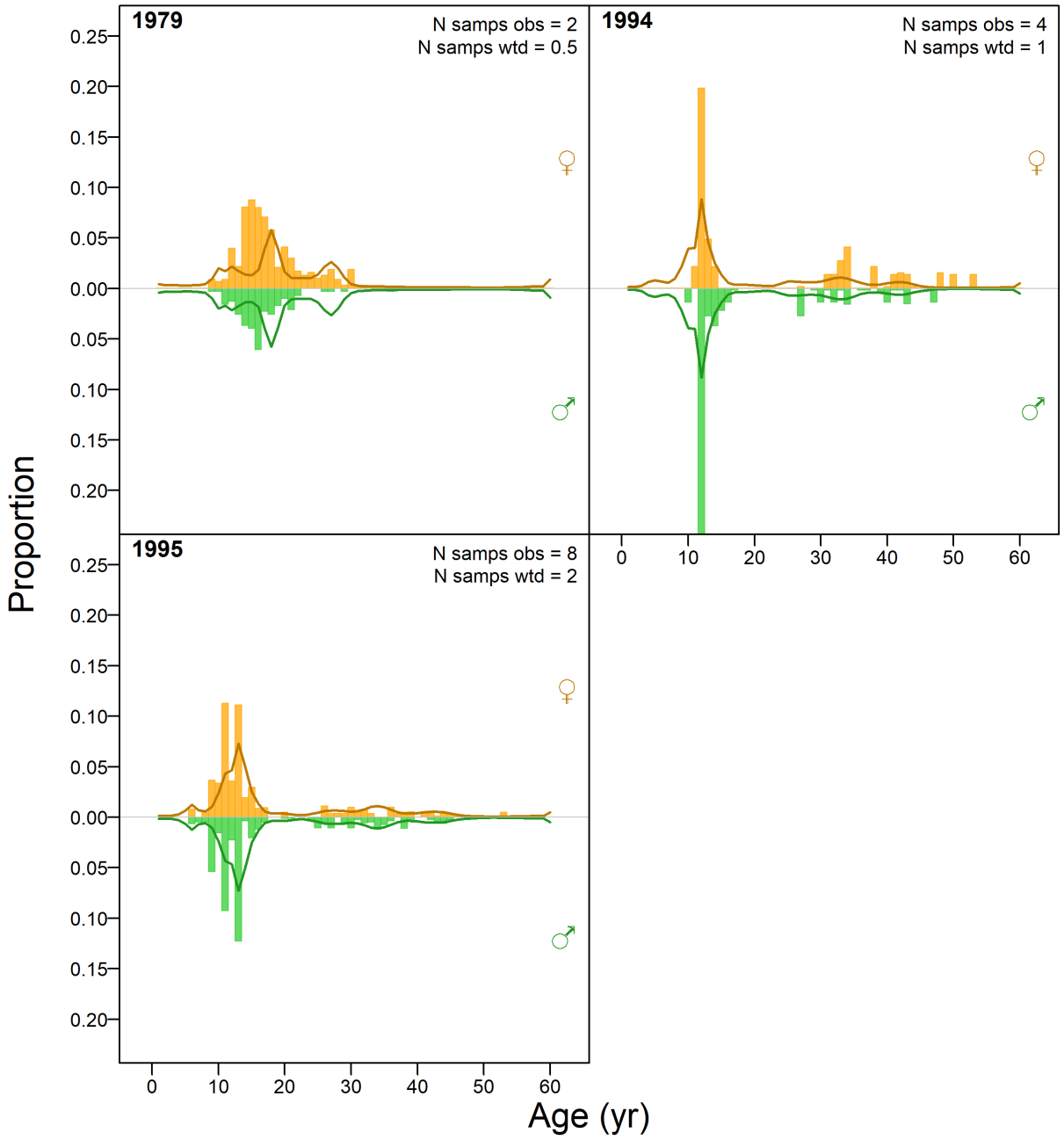

Figure F.11. Central Run 75: GIG Hisorical survey proportions-at-age (bars=observed, lines=predicted) for females and males combined.

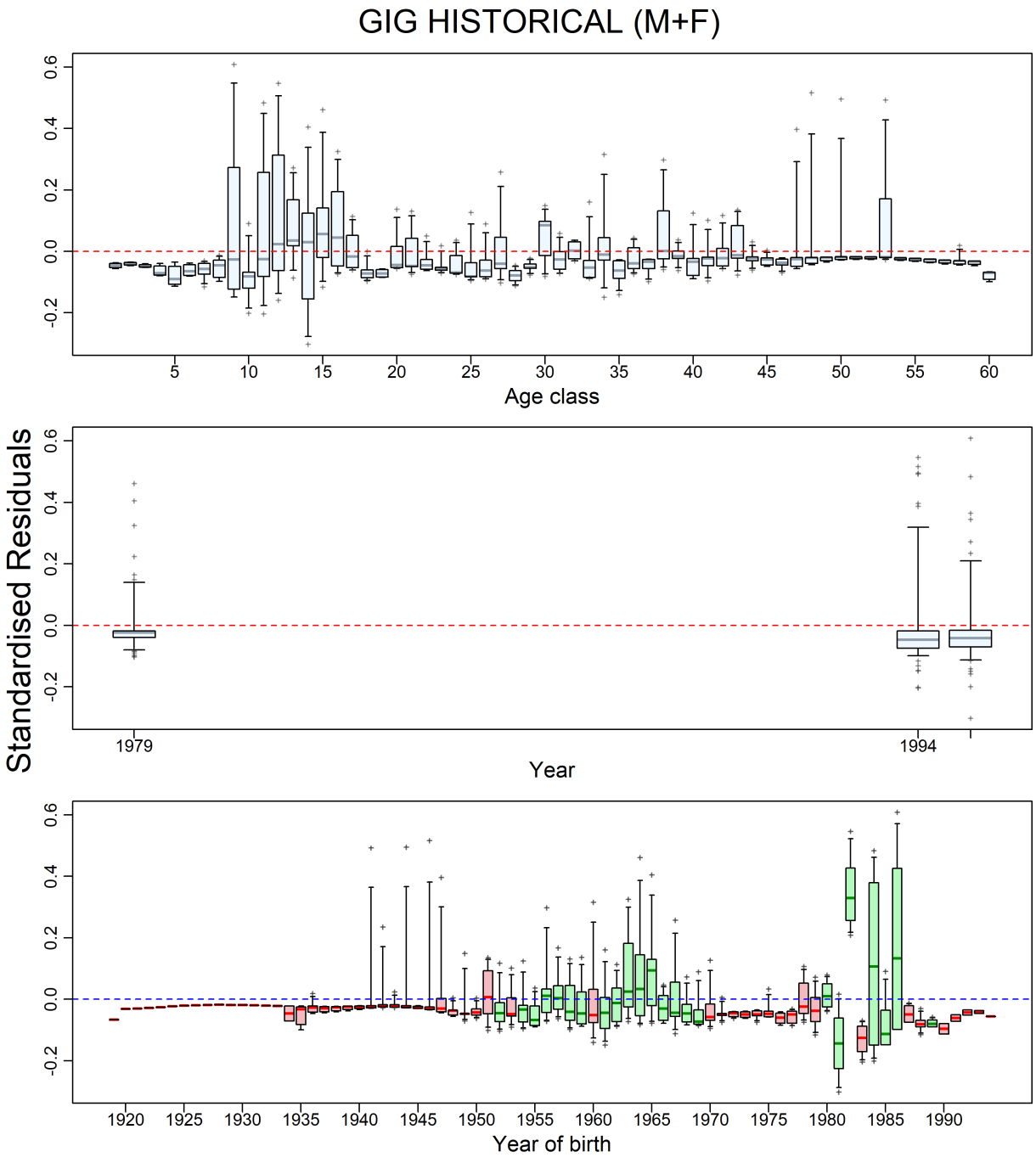

Figure F.12. Central Run 75: GIG Historical survey residuals of model fits to proportion-at-age data. See Fig. F.4 caption for plot details.

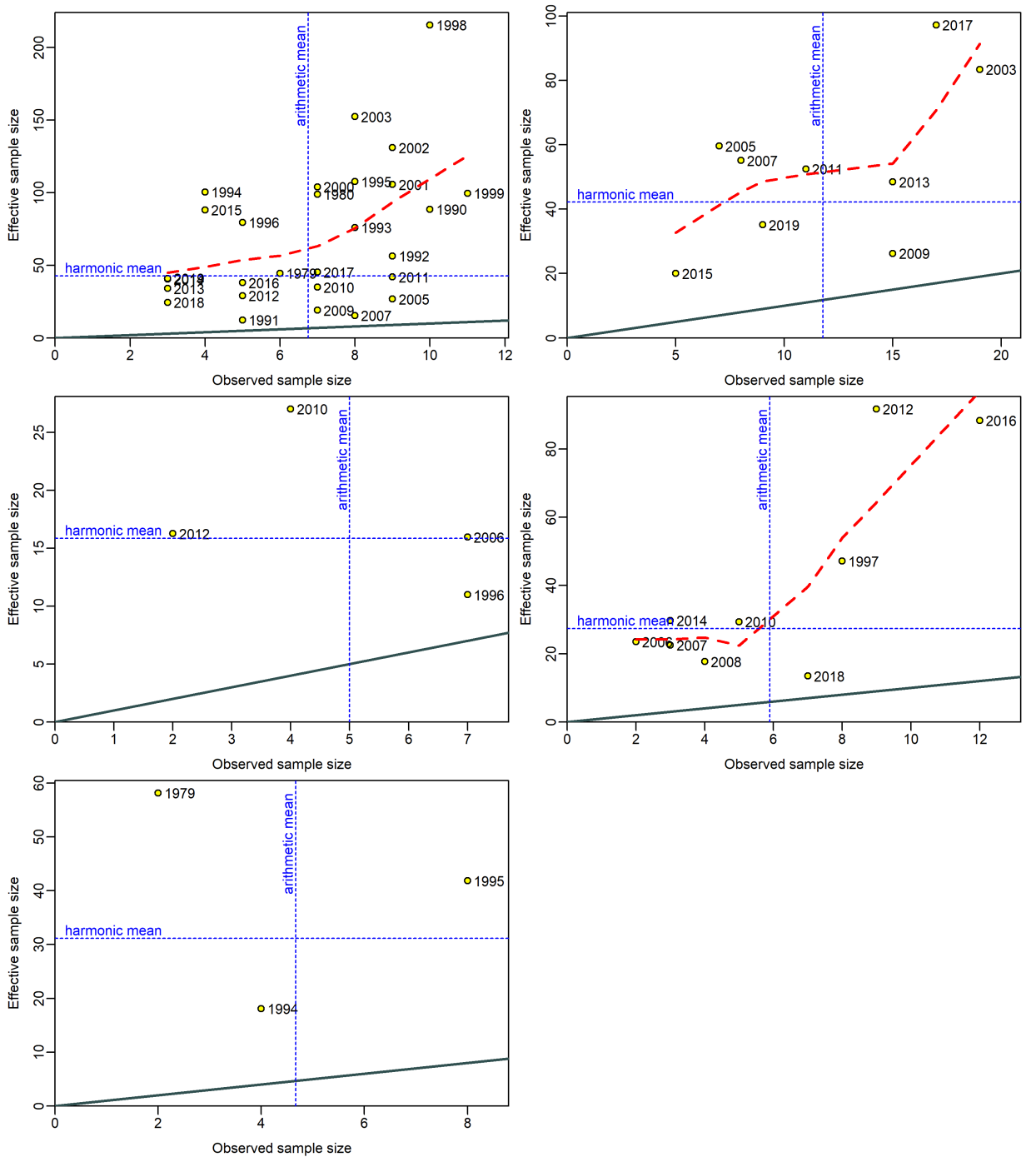

Figure F.13. Central Run 75: Harmonic mean of effective sample size (horizontal dashed line) vs. arithmetic mean of observed sample size (vertical dashed line) for unweighted AFs. Solid line shows 1:1 relationship; red dashed curve shows first-order polynomial regression fit.

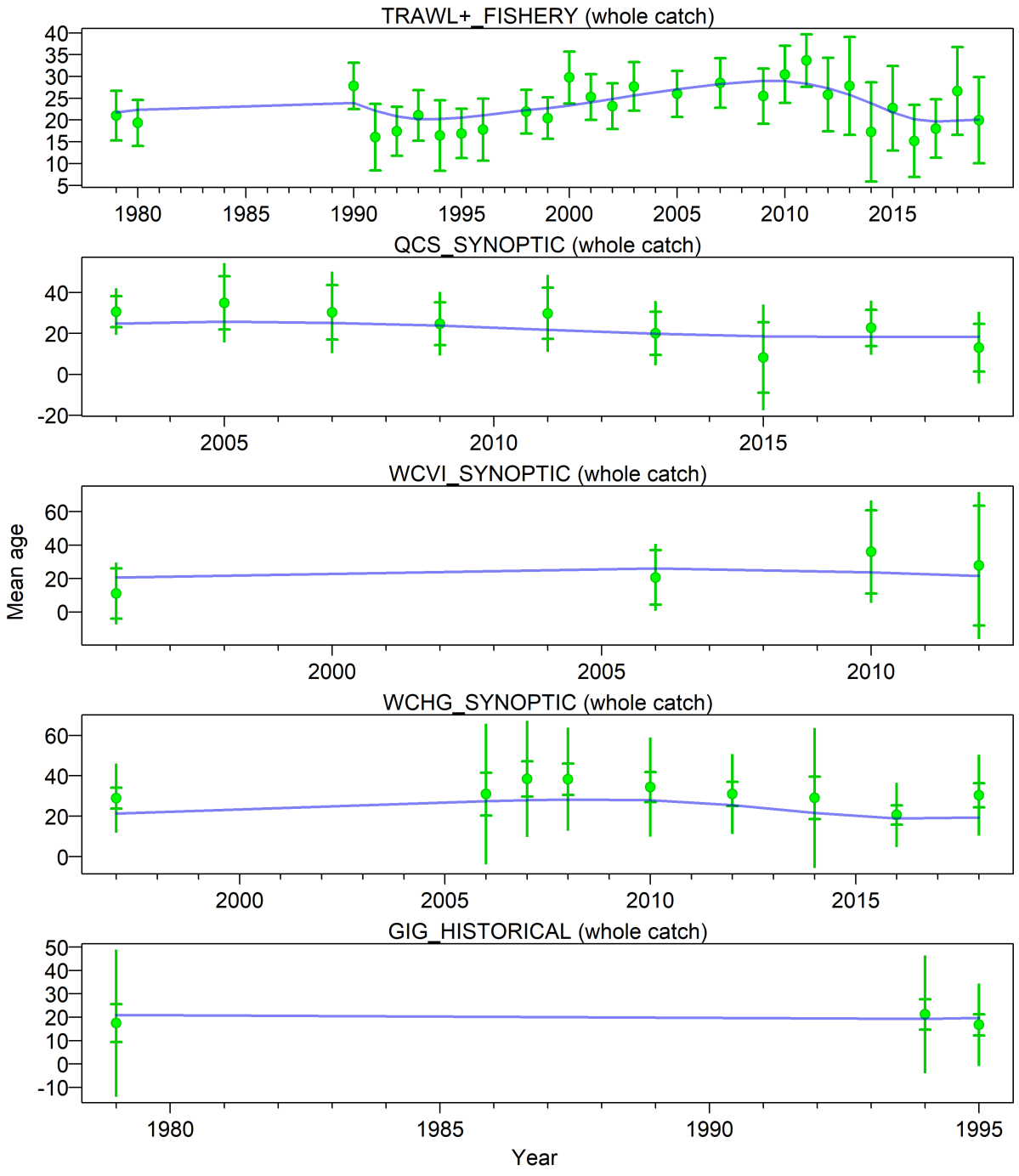

Figure F.14. Central Run 75: Mean ages each year for the weighted data (solid green circles) where vertical bars denote the range of the data and cross bars denote ~95% confidence intervals associated with adjusted sample sizes; model estimates of mean age appear as blue lines.

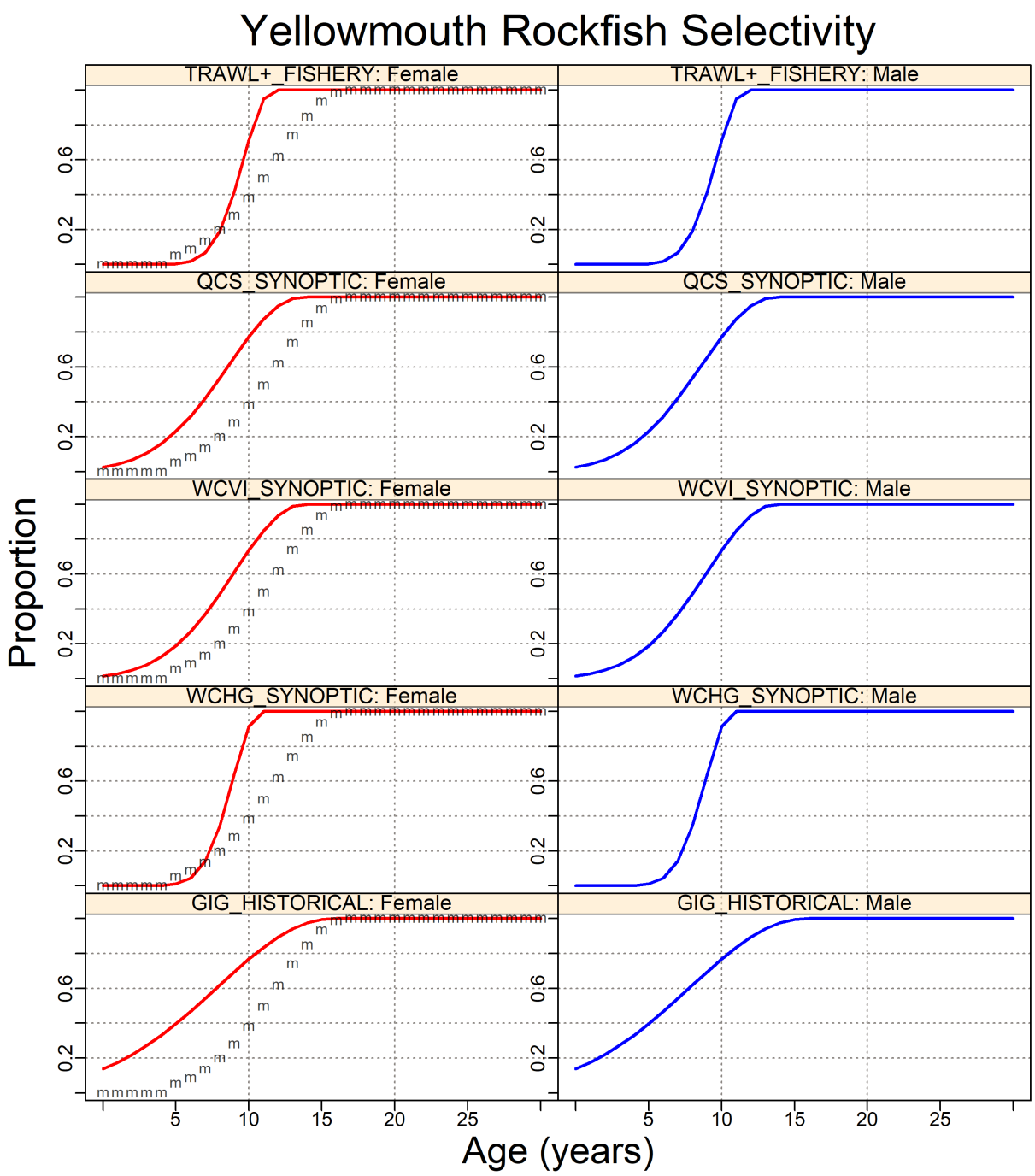

Figure F.15. Central Run 75: Selectivities for commercial fleet catch and surveys (all MPD values), with maturity ogive for females indicated by 'm'.

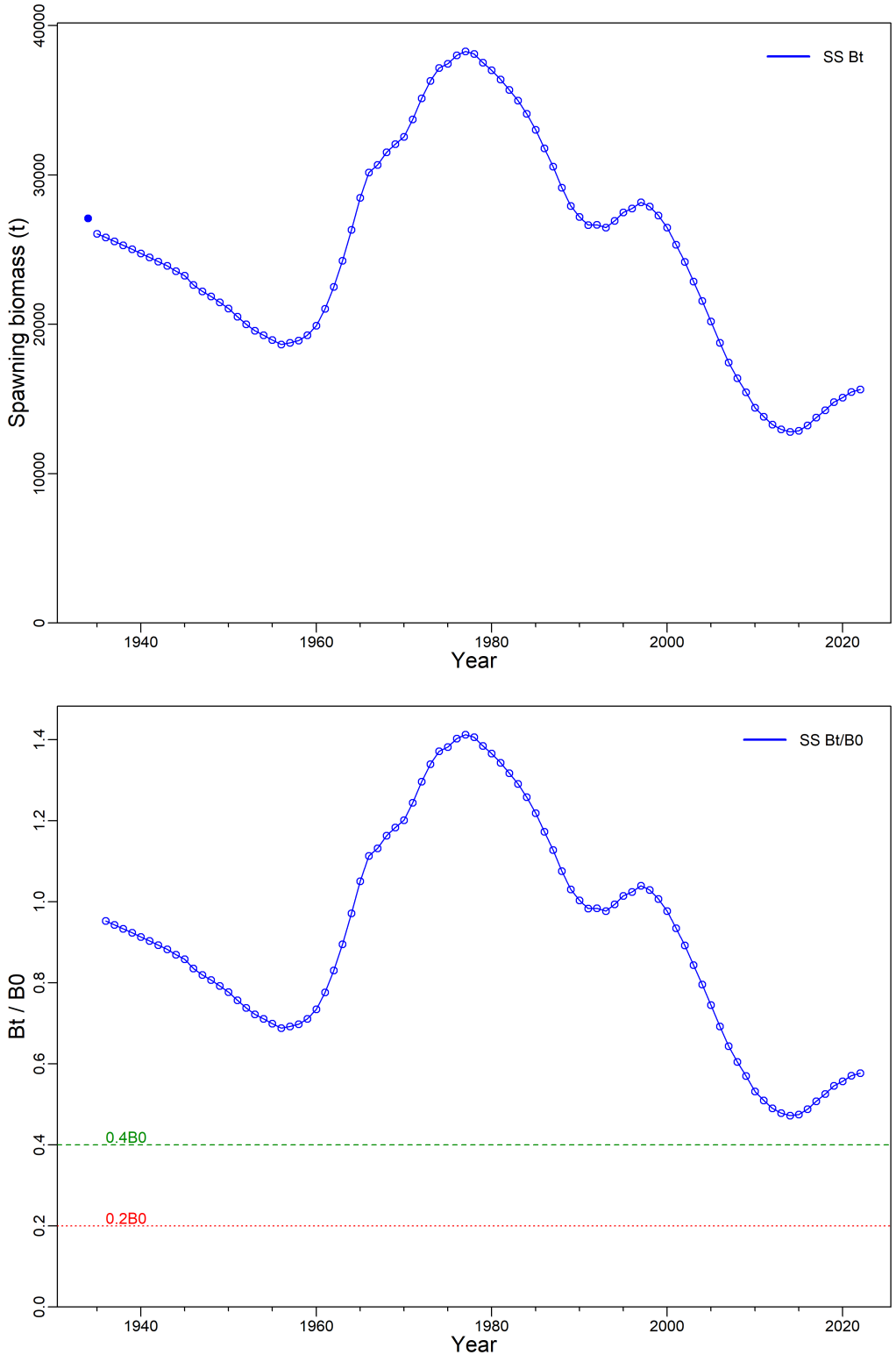

Figure F.16. Central Run 75: Spawning biomass – (top) B_t (tonnes, mature females) over time; (bottom) B_t relative to unfished equilbrium spawning biomass B_0. Blue line designates SS fit for 2022.

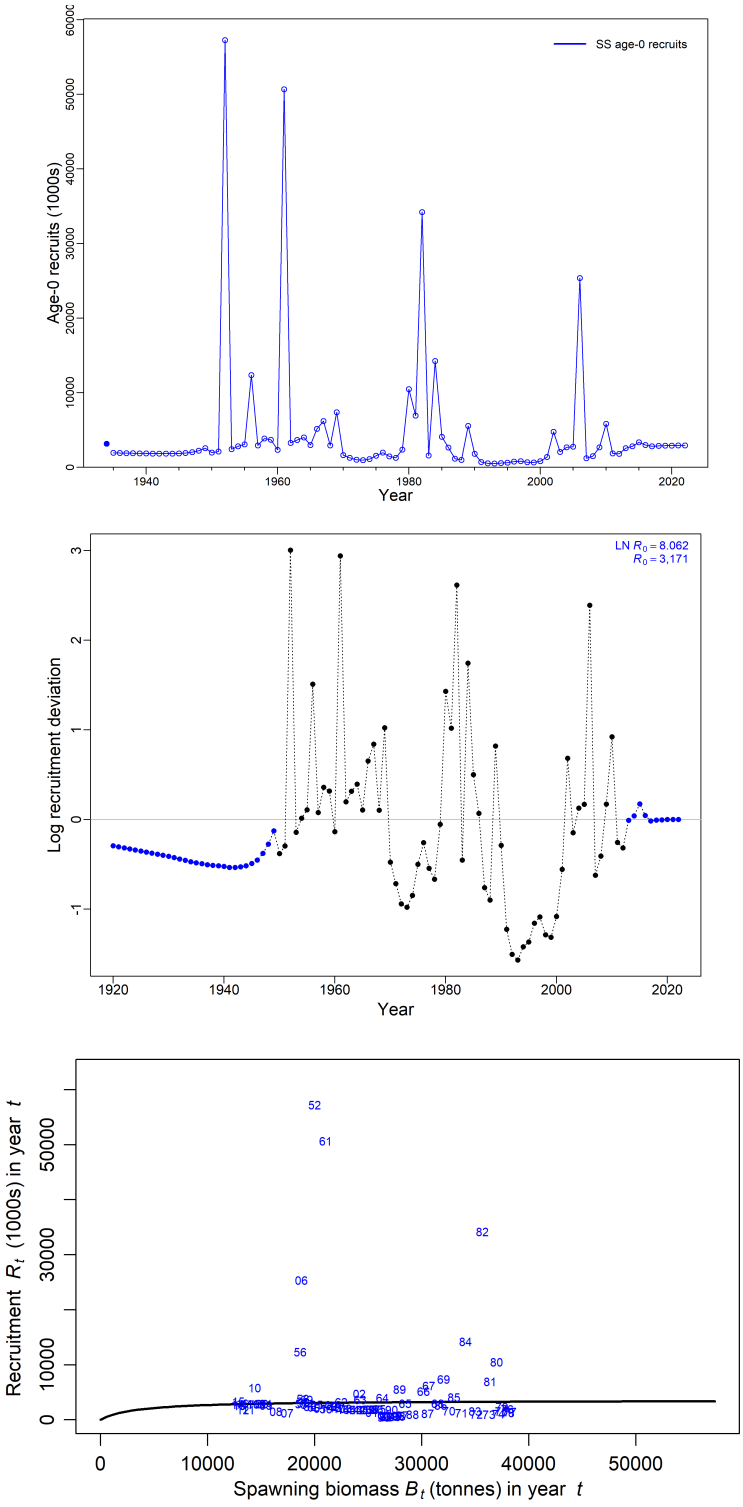

Figure F.17. Central Run 75: Recruitment – (top) thousands of age-0 fish from 1935 to 2022; (middle) log of annual recruitment deviations ϵ_t, where bias-corrected multiplicative deviation is $e^{\epsilon_t - \sigma_R^2/2}$ and $\epsilon_t \sim Normal(0, \sigma_R^2)$; (bottom) deterministic stock-recruit relationship (black curve) and observed values (labelled by year of spawning).

F.2.2. YMR – Central Run MCMC

The MCMC procedure used the 'no U-turn sampling' (NUTS) algorithm (Monnahan and Kristensen 2018; Monnahan et al. 2019) to produce 4,000 iterations, parsing the workload into 8 parallel chains (Knaus 2015) of 500 iterations each, discarding the first 250 iterations and saving the last 250 samples per chain. The parallel chains were then merged for a total of 2,000 samples for use in the MCMC analysis.

The MCMC plots show:

- Figure F.18 – traces for 2,000 samples of the primary estimated parameters;
- Figure F.19 – split-chain diagnostic plots for the primary estimated parameters;
- Figure F.20 – auto-correlation diagnostic plots for the primary estimated parameters;
- Figure F.21 – marginal posterior densities for the primary parameters compared to their respective prior density functions.

MCMC traces for the central run (M=0.05) showed acceptable convergence properties (no trend with increasing sample number) for the estimated parameters (Figure F.18), as did diagnostic analyses that split the posterior samples into three equal consecutive segments (Figure F.19) and checked for parameter autocorrelation out to 60 lags (Figure F.20). Most of the parameter medians did not move far from their initial MPD estimates (Figure F.21).

F.2.2.1. Central run figures

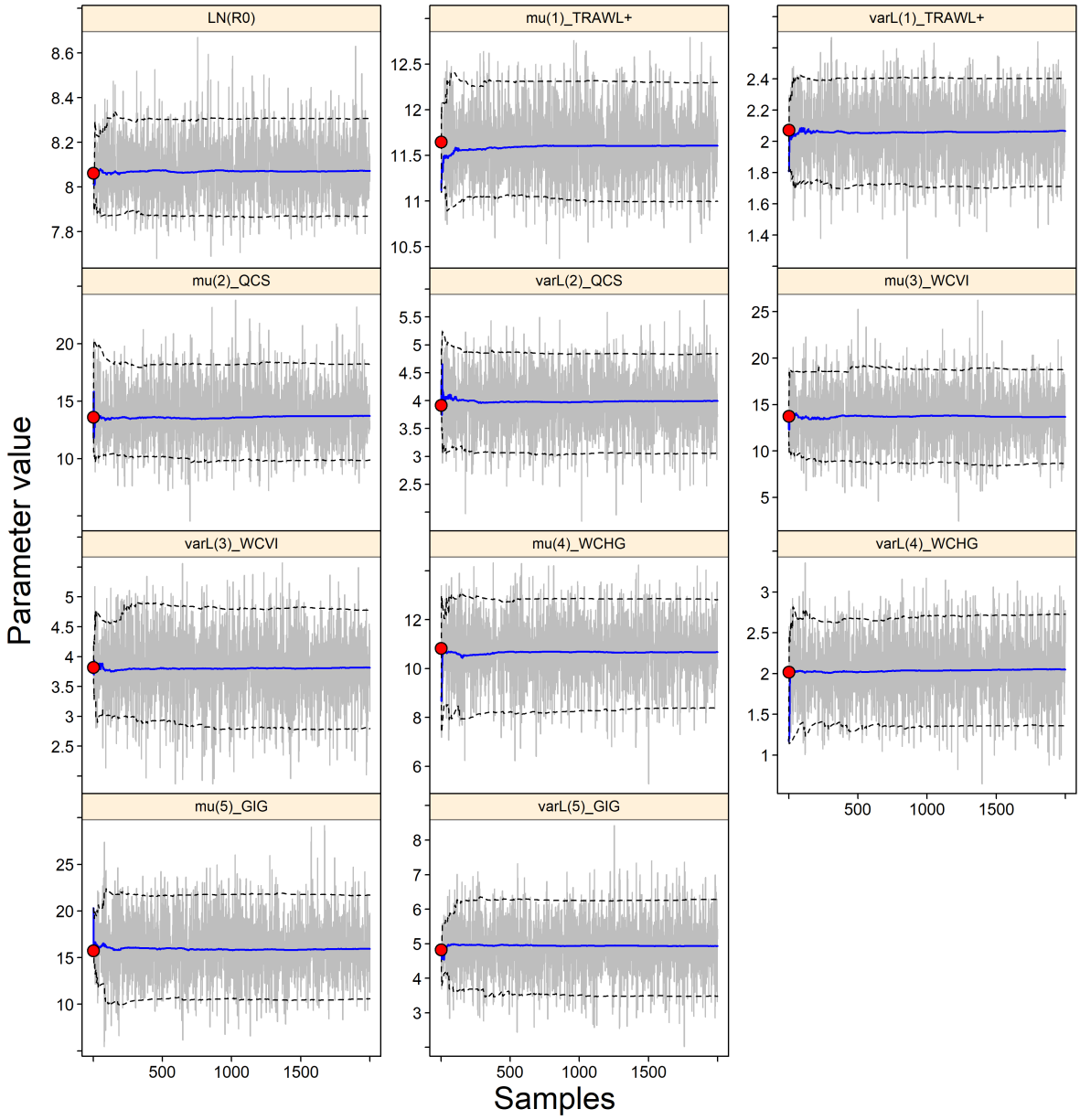

Figure F.18. Central Run 75: MCMC traces for the estimated parameters. Grey lines show the 2,000 samples for each parameter, solid lines show the cumulative median (up to that sample), and dashed lines show the cumulative 0.05 and 0.95 quantiles. Red circles are the MPD estimates. For parameters other than M (if estimated), subscripts 1-5 correspond to SS fleets (one fishery and four surveys).

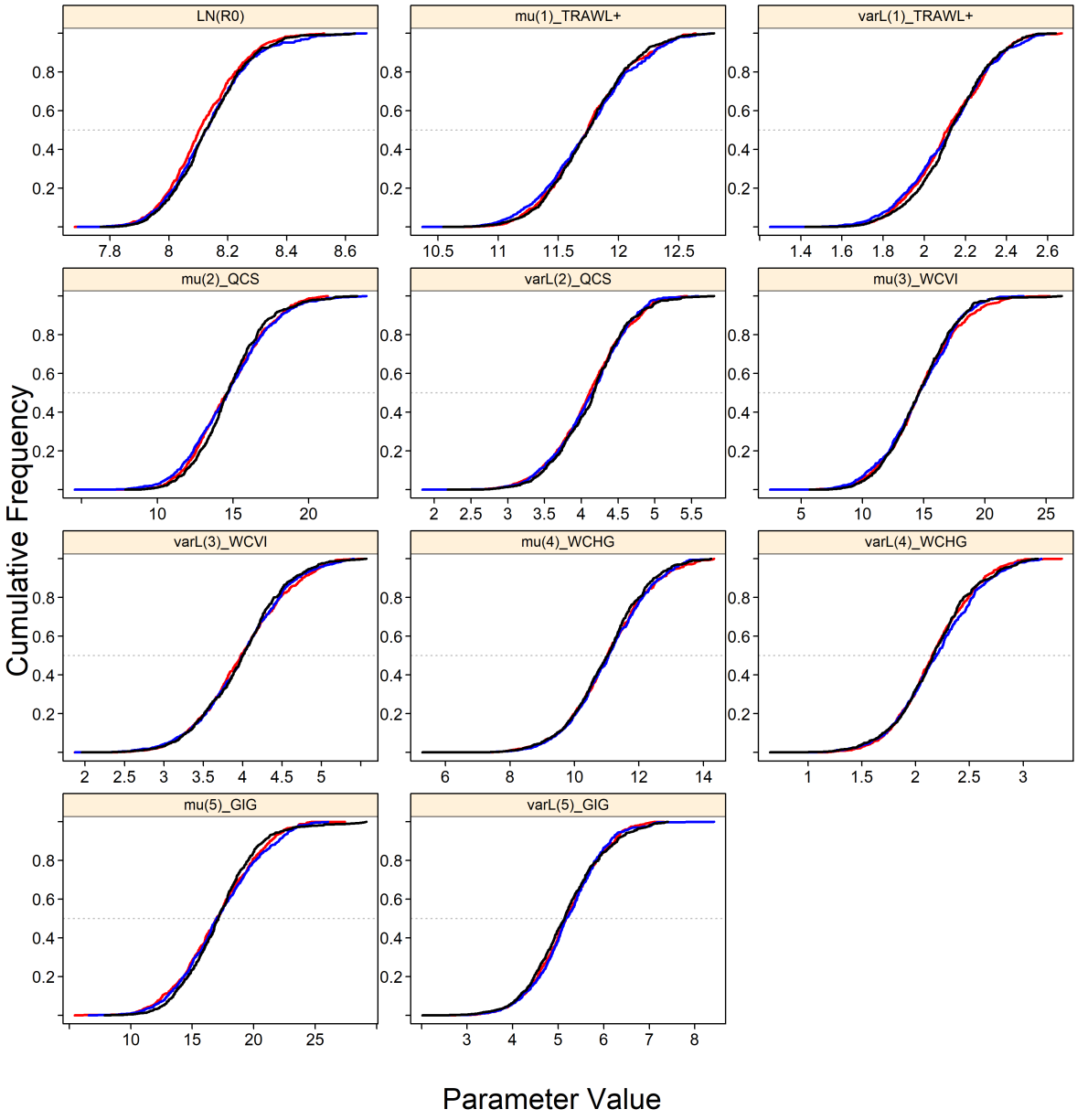

Figure F.19. Central Run 75: Diagnostic plot obtained by dividing the MCMC chain of 2,000 MCMC samples into three segments, and overplotting the cumulative distributions of the first segment (red), second segment (blue) and final segment (black).

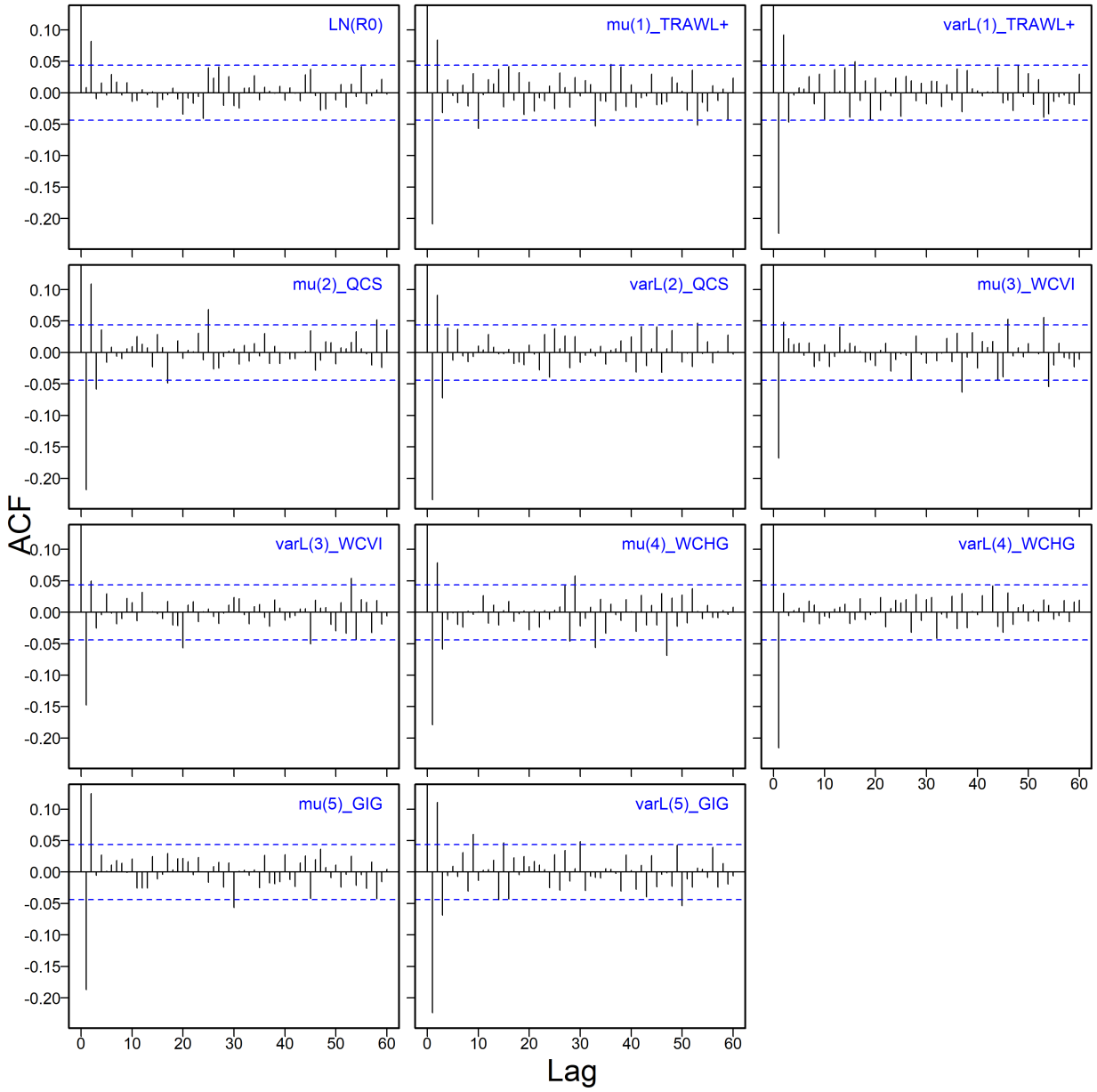

Figure F.20. Central Run 75: Autocorrelation plots for the estimated parameters from the MCMC output. Horizontal dashed blue lines delimit the 95% confidence interval for each parameter's set of lagged correlations.

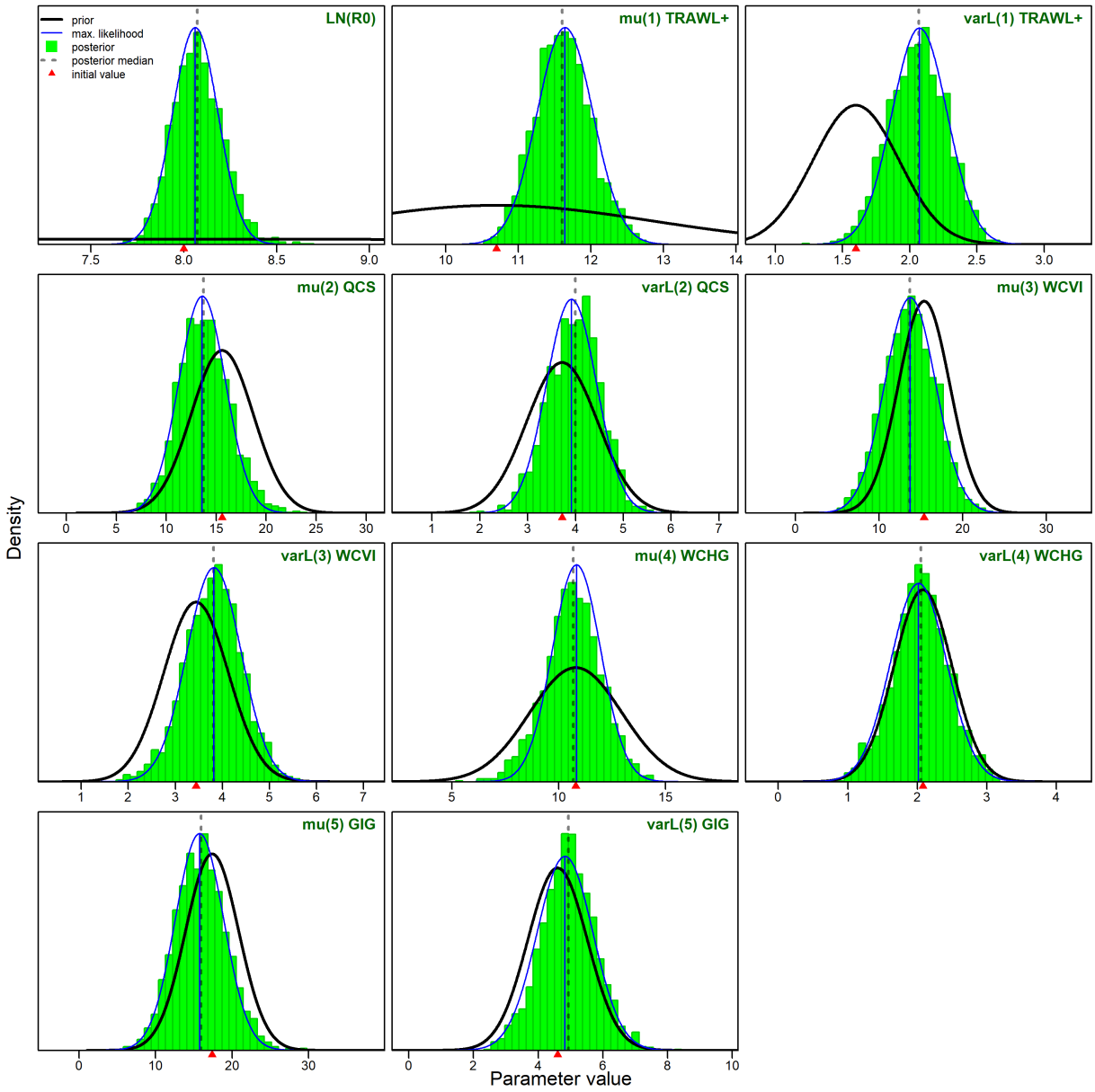

Figure F.21. Central Run 75: Posterior distribution (vertical green bars), likelihood profile (thin blue curve), and prior density function (thick black curve) for estimated parameters. Vertical dashed line indicates the MCMC posterior median; vertical blue line represents the MPD; red triangle indicates initial value for each parameter.

F.2.3. YMR – Composite Base Case

The composite base case examined five runs which spanned one axis of uncertainty (M) for this stock assessment:

- **B1** (Run77) – fixed $M_{1,2}$ = 0.04;
- **B2** (Run71) – fixed $M_{1,2}$ = 0.045;
- **B3** (Run75) – fixed $M_{1,2}$ = 0.05;
- **B4** (Run72) – fixed $M_{1,2}$ = 0.055;
- **B5** (Run76) – fixed $M_{1,2}$ = 0.06.

All component runs used CPUE c_{p}=0.3296, no added process error on survey indices, ageing error based on CVs of length-at-age, and AF sample reweighting using the harmonic mean ratio method specific to each model run. The 2,000 MCMC samples from each of the above runs were pooled to create a composite posterior of 10,000 samples, which was used to estimate population status and to provide advice to managers.

Composite base case median parameter estimates appear in Table F.3, and derived quantities at equilibrium and associated with maximum sustainable yield (MSY) and B_0 appear in Table F.4. The differences among the component base runs are summarised by various figures:

- Figure F.22 – MCMC traces of R_0 for the 5 candidate base runs;
- Figure F.23 – three chain segments of R_0 MCMC chains;
- Figure F.24 – autocorrelation plots for R_0 MCMC output;
- Figure F.25 – quantile plots of parameter estimates from 5 component base runs;
- Figure F.26 – quantile plots of selected derived quantities from 5 component base runs.

In this stock assessment, projections extend to 2032. Projections out to 3 generations (90 years), where one generation was determined to be 30 years (see Appendix D), were not completed due to technical reasons associated with the new model framework (SS) and time constraints; however, the stock status of YMR in the Healthy zone does not warrant such projections at this time. Various model trajectories and final stock status for the composite base case appear in the figures:

- Figure F.27 – estimates of spawning biomass B_t (tonnes) from pooled model posteriors spanning 1935-2112;
- Figure F.28 – estimates of spawning biomass relative to B_0 (top panel) and B_{MSY} (bottom panel) from pooled model posteriors;
- Figure F.29 – estimates of exploitation rate u_t (top panel) and u_t/u_{MSY} (bottom panel) from pooled model posteriors;
- Figure F.30 – estimates of recruitment R_t (1000s age-0 fish, top panel) and recruitment deviations (bottom panel) from pooled model posteriors;
- Figure F.31 – phase plot through time of median B_t/B_{MSY} and u_t/u_{MSY} relative to DFO's Precautionary Approach (PA) provisional reference points;
- Figure F.32 – YMR BC stock status at beginning of 2022.

The five component runs demonstrated acceptable MCMC diagnostics for most of the parameters.

Unlike the 2011 YMR stock assessment (Edwards et al. 2012), we were not able to estimate M reliably in this assessment. The inability of the SS platform to estimate M appeared to be due to the different distributional assumption used by this model to fit the AF data. An unreported model

run using Awatea with data updated to the end of 2020 successfully estimated M, giving MCMC estimates of 0.057 (0.053, 0.061) and 0.056 (0.052, 0.060) for females and males respectively. While these estimates were below the lower end of the range for externally estimated M (see Appendix D, section D.1.4), model behaviour for the SS model when M>0.06 appeared to be unstable and the MCMC diagnostics were unacceptable. Natural mortality appears to be the most important component of uncertainty in this stock assessment. Consequently, a composite base case was constructed by assembling model runs which spanned a plausible range of M values for this stock as well as providing acceptable fits and MCMC diagnostics. Various other sources of uncertainty were explored in sensitivity runs based on central run 75.

The composite base case, comprising five pooled MCMC runs, was used to calculate a set of parameter estimates (Table F.3) and derived quantities at equilibrium and those associated with MSY (Table F.4). Figure F.25 shows the distribution of all the estimated parameters. In most cases, the component runs had parameter estimates with overlapping distributions. Equilibrium recruitment in 1935 (R_0) varied with M, increasing as M increased. The selectivity parameters differed little among the five M estimates.

Similar to the parameter distributions, those for derived quantities (Figure F.26) varied by M. Not surprisingly, B_0, MSY, B_{MSY}, u_{MSY}, and current stock status relative to B_0 increased with increasing M. The ratio of B_{MSY}/B_0 remained constant but uncertainty around the median estimate expanded. Given a catch of 1057 t/y in 2021, the apparent harvest rates become lower because estimated spawning biomass (and consequently vulnerable biomass) increases.

The composite base case population trajectory from 1935 to 2022 and projected biomass to 2032 (Figure F.27), assuming a constant catch policy of 1057 t/y, estimates median spawning biomass B_t in t=1935, 2022, and 2032 to be 26,385, 18,001, and 17,040 tonnes, respectively. Figure F.28 indicates that the median stock biomass will remain above the USR for the next 10 years at annual catches equal to the 2022 catch. Exploitation rates have largely stayed below u_{MSY} for much of the fishery's history (Figure F.29). Recruitment of age-0 fish shows four main recruitment events in 1952, 1962, 1982, and 2006 (Figure F.30).

A phase plot of the time-evolution of spawning biomass and exploitation rate by the modelled fishery in MSY space (Figure F.31) suggests that the stock is firmly in the Healthy zone, with a current position at B_{2022}/B_{MSY} = 2.394 (1.535, 3.727) and u_{2021}/u_{MSY} = 0.508 (0.202, 1.001). The current-year stock status figure (Figure F.32) shows the position of the composite base case in DFO's Healthy zone, and demonstrates how the individual component runs contribute to the composite base case. Values of M higher than 0.06 will push the stock status further into the Healthy zone.

F.2.3.1. Base case tables

Table F.2. Age frequency weights used for the five base component runs.

Base	Run	Trawl	QCS	WCVI	WCHG	GIG
B1	R77	6.219091	0.25	0.25	0.25	0.25
B2	R71	6.277630	0.25	0.25	0.25	0.25
B3	R75	6.321921	0.25	0.25	0.25	0.25
B4	R72	6.363513	0.25	0.25	0.25	0.25
B5	R76	6.389239	0.25	0.25	0.25	0.25

Table F.3. Composite base case: the 0.05, 0.25, 0.5, 0.75, and 0.95 quantiles for pooled model parameters (defined in Appendix E) from MCMC estimation of five component model runs of 2,000 samples each.

Parameter	5%	25%	50%	75%	95%
$\log R_0$	7.525	7.774	8.070	8.411	8.820
μ_1 (TRAWL+)	10.98	11.34	11.60	11.88	12.28
μ_2 (QCS)	10.07	12.09	13.65	15.38	17.99
μ_3 (WCVI)	8.951	11.64	13.67	15.68	18.61
μ_4 (WCHG)	8.474	9.900	10.72	11.52	12.75
μ_5 (GIG)	10.67	13.61	15.85	18.21	21.68
$\log v_{\text{L1}}$ (TRAWL+)	1.703	1.917	2.063	2.203	2.394
$\log v_{\text{L2}}$ (QCS)	3.056	3.622	3.982	4.342	4.829
$\log v_{\text{L3}}$ (WCVI)	2.812	3.427	3.837	4.225	4.784
$\log v_{\text{L4}}$ (WCHG)	1.376	1.772	2.046	2.314	2.707
$\log v_{\text{L5}}$ (GIG)	3.463	4.358	4.934	5.518	6.352

Table F.4. Composite base case: the 0.05, 0.25, 0.5, 0.75, and 0.95 quantiles of MCMC-derived quantities from 10,000samples pooled from 5 component runs. Definitions are: B_0 – unfished equilibrium spawning biomass (mature females), B_{2022} – spawning biomass at the end of 2022, u_{2021} – exploitation rate (ratio of total catch to vulnerable biomass) in the middle of 2021, u_{max} – maximum exploitation rate (calculated for each sample as the maximum exploitation rate from 1935-2022), B_{MSY} – equilibrium spawning biomass at MSY (maximum sustainable yield), u_{MSY} – equilibrium exploitation rate at MSY, All biomass values (and MSY) are in tonnes. For reference, the average catch over the last 5 years (2016-2020) was 1272 t.

Quantity	5%	25%	50%	75%	95%
B_0	20,898	23,707	26,386	30,528	41,314
B_{2022}	10,070	13,848	18,001	24,978	42,533
B_{2022}/B_0	0.4446	0.5708	0.6922	0.8417	1.080
u_{2021}	0.01012	0.01697	0.02357	0.03048	0.04154
u_{max}	0.02686	0.03845	0.04837	0.05730	0.06531
MSY	695.7	845.4	1,039	1,327	1,919
B_{MSY}	6,063	6,894	7,656	8,810	11,938
$0.4B_{\text{MSY}}$	2,425	2,758	3,063	3,524	4,775
$0.8B_{\text{MSY}}$	4,850	5,515	6,125	7,048	9,550
B_{2022}/B_{MSY}	1.535	1.969	2.394	2.905	3.727
B_{MSY}/B_0	0.2702	0.2847	0.2917	0.2971	0.3036
u_{MSY}	0.04063	0.04356	0.04636	0.04893	0.05117
u_{2021}/u_{MSY}	0.2019	0.3471	0.5082	0.7066	1.001

Table F.5. Log likelihood (LL) values reported by component base runs for survey indices, age composition (AF), recruitment, and total (not all LL components reported here)

Run	M	CPUE	QCS	WCVI	WCHG	GIG	Index	AF	Recruit	Total
R77	0.040	-18.4	1.28	7.86	20.4	14.3	25.4	454	47.5	638
R71	0.045	-18.3	1.06	7.90	20.0	14.4	25.1	456	43.5	637
R75	0.050	-18.1	0.870	7.92	19.7	14.5	24.9	456	41.9	635
R72	0.055	-17.8	0.703	7.93	19.4	14.5	24.8	457	40.8	635
R76	0.060	-17.4	0.555	7.94	19.1	14.6	24.8	458	39.9	634

Table F.6. Component base case runs: model parameter MPDs (delimited by '|') and MCMC medians (with 0.05 and 0.95 quantile limits) for each of the five component model runs of 2,000 samples each.

Par	B1 (R77)	B2 (R71)	B3 (R75)	B4 (R72)	B5 (R76)
$\log R_0$	|7.59| 7.60 (7.43,7.77)	|7.83| 7.83 (7.63,8.03)	|8.06| 8.07 (7.87,8.31)	|8.30| 8.34 (8.10,8.66)	|8.57| 8.64 (8.34,9.12)
μ_1	|11.6| 11.6 (11.0,12.2)	|11.6| 11.6 (11.0,12.3)	|11.6| 11.6 (11.0,12.3)	|11.6| 11.6 (11.0,12.3)	|11.6| 11.6 (11.0,12.3)
μ_2	|13.5| 13.4 (10.1,17.6)	|13.5| 13.5 (10.1,18.1)	|13.6| 13.7 (9.88,18.2)	|13.7| 13.7 (10.1,18.1)	|13.7| 13.8 (10.2,17.9)
μ_3	|13.6| 13.7 (9.04,18.4)	|13.7| 13.6 (8.87,18.5)	|13.7| 13.7 (8.65,18.7)	|13.8| 13.7 (9.19,18.6)	|13.8| 13.7 (8.87,18.8)
μ_4	|10.8| 10.7 (8.48,12.7)	|10.8| 10.7 (8.41,12.8)	|10.8| 10.7 (8.39,12.8)	|10.8| 10.7 (8.48,12.8)	|10.9| 10.8 (8.63,12.7)
μ_5	|15.9| 15.7 (10.6,21.5)	|15.7| 15.8 (10.5,21.9)	|15.8| 15.9 (10.6,21.7)	|15.8| 15.9 (10.8,21.7)	|15.8| 15.8 (10.9,21.5)
$\log v_{\text{L1}}$	|2.08| 2.07 (1.70,2.39)	|2.08| 2.06 (1.71,2.40)	|2.07| 2.07 (1.71,2.40)	|2.07| 2.06 (1.70,2.40)	|2.06| 2.06 (1.70,2.38)
$\log v_{\text{L2}}$	|3.94| 3.99 (3.05,4.83)	|3.92| 3.97 (3.06,4.86)	|3.92| 4.00 (3.06,4.84)	|3.91| 3.98 (3.03,4.80)	|3.90| 3.98 (3.11,4.78)
$\log v_{\text{L3}}$	|3.83| 3.87 (2.79,4.81)	|3.82| 3.85 (2.85,4.82)	|3.82| 3.81 (2.79,4.78)	|3.82| 3.82 (2.83,4.80)	|3.81| 3.84 (2.80,4.74)
$\log v_{\text{L4}}$	|2.02| 2.06 (1.39,2.67)	|2.02| 2.06 (1.39,2.70)	|2.02| 2.05 (1.36,2.73)	|2.02| 2.03 (1.39,2.73)	|2.02| 2.03 (1.37,2.73)
$\log v_{\text{L5}}$	|4.85| 4.92 (3.45,6.36)	|4.83| 4.94 (3.47,6.39)	|4.83| 4.93 (3.48,6.29)	|4.83| 4.95 (3.54,6.35)	|4.83| 4.92 (3.42,6.41)

Table F.7. Component base case runs: MCMC median (with 0.05 and 0.95 quantile limits) for derived model quantities for each of the five component model runs of 2,000 samples each.

Quantity	B1 (R77)	B2 (R71)	B3 (R75)	B4 (R72)	B5 (R76)
B_0	23,422 (19,803,27,792)	24,560 (20,305,29,781)	26,065 (21,402,32,811)	28,934 (22,862,40,191)	33,671 (25,045,54,967)
B_{2022}	12,371 (8,582,18,089)	14,846 (9,942,22,439)	18,027 (11,714,29,058)	23,006 (14,262,41,213)	30,144 (17,377,64,795)
B_{2022}/B_0	0.53 (0.38,0.73)	0.61 (0.44,0.84)	0.69 (0.50,0.95)	0.80 (0.56,1.1)	0.90 (0.65,1.2)
u_{2021}	0.034 (0.024,0.049)	0.028 (0.019,0.041)	0.023 (0.015,0.035)	0.018 (0.011,0.029)	0.014 (0.0068,0.024)
u_{MSY}	0.062 (0.055,0.069)	0.056 (0.047,0.063)	0.048 (0.038,0.056)	0.040 (0.029,0.049)	0.032 (0.020,0.043)
MSY	755 (636,892)	883 (723,1,073)	1,040 (849,1,311)	1,260 (997,1,735)	1,585 (1,180,2,554)
B_{MSY}	6,824 (5,742,8,061)	7,137 (5,843,8,679)	7,593 (6,199,9,590)	8,380 (6,616,11,553)	9,663 (7,175,15,600)
$0.4B_{\text{MSY}}$	2,730 (2,297,3,225)	2,855 (2,337,3,471)	3,037 (2,480,3,836)	3,352 (2,647,4,621)	3,865 (2,870,6,240)
$0.8B_{\text{MSY}}$	5,459 (4,594,6,449)	5,710 (4,675,6,943)	6,074 (4,959,7,672)	6,704 (5,293,9,242)	7,730 (5,740,12,480)
B_{2022}/B_{MSY}	1.8 (1.3,2.5)	2.1 (1.5,2.9)	2.4 (1.7,3.3)	2.7 (2.0,3.8)	3.1 (2.3,4.3)
B_{MSY}/B_0	0.29 (0.28,0.30)	0.29 (0.27,0.30)	0.29 (0.27,0.30)	0.29 (0.27,0.30)	0.29 (0.26,0.31)
u_{MSY}	0.041 (0.040,0.041)	0.044 (0.043,0.044)	0.046 (0.046,0.047)	0.049 (0.049,0.049)	0.051 (0.051,0.051)
u_{2021}/u_{MSY}	0.85 (0.60,1.2)	0.65 (0.44,0.94)	0.51 (0.32,0.76)	0.38 (0.22,0.59)	0.27 (0.13,0.46)

F.2.3.2. Base case figures

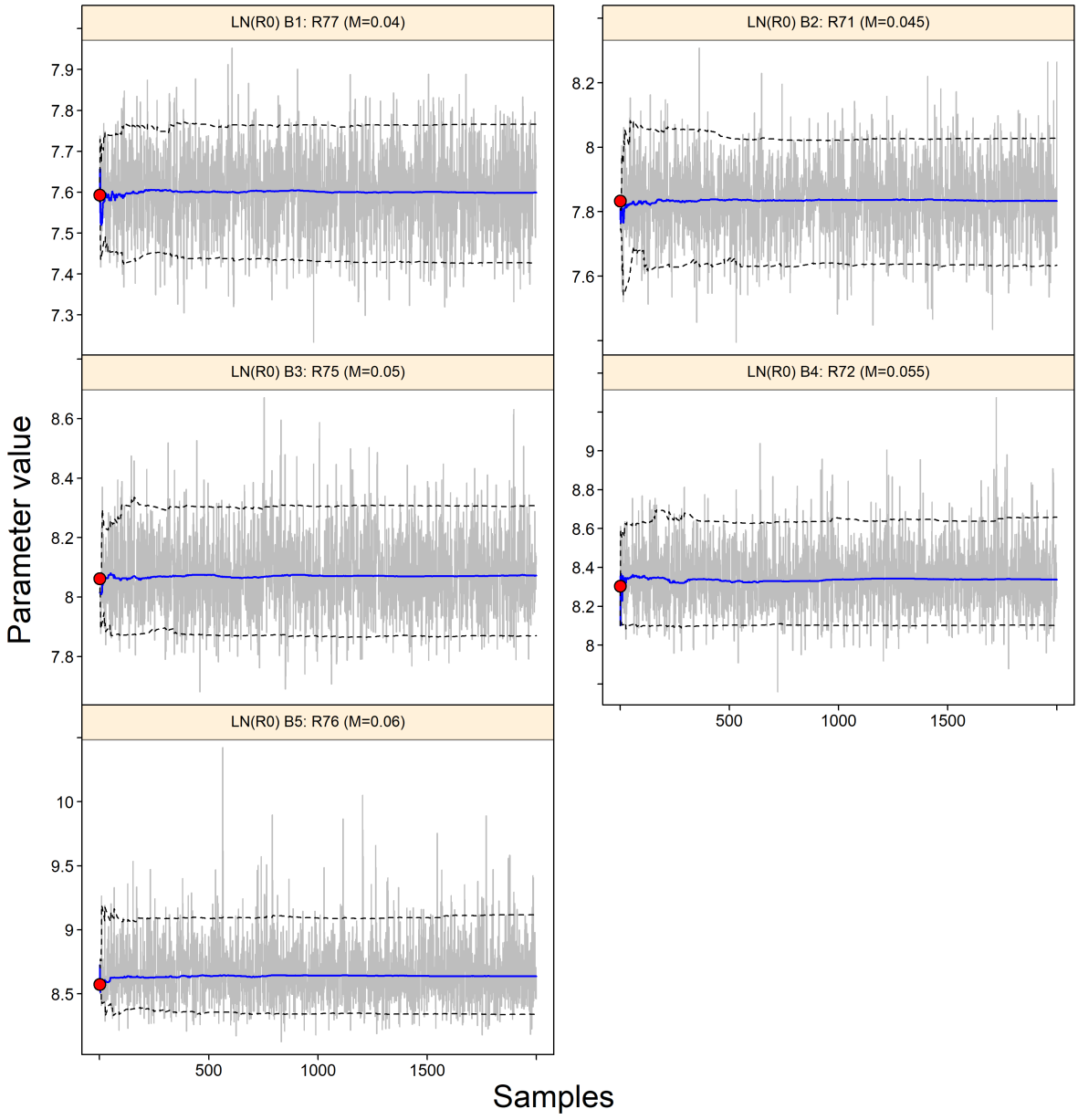

Figure F.22. Composite base case component runs: MCMC traces of R_0 for the 5 candidate base runs. Grey lines show the 2,000 samples for the R_0 parameter, solid lines show the cumulative median (up to that sample), and dashed lines show the cumulative 0.05 and 0.95 quantiles. Red circles are the MPD estimates.

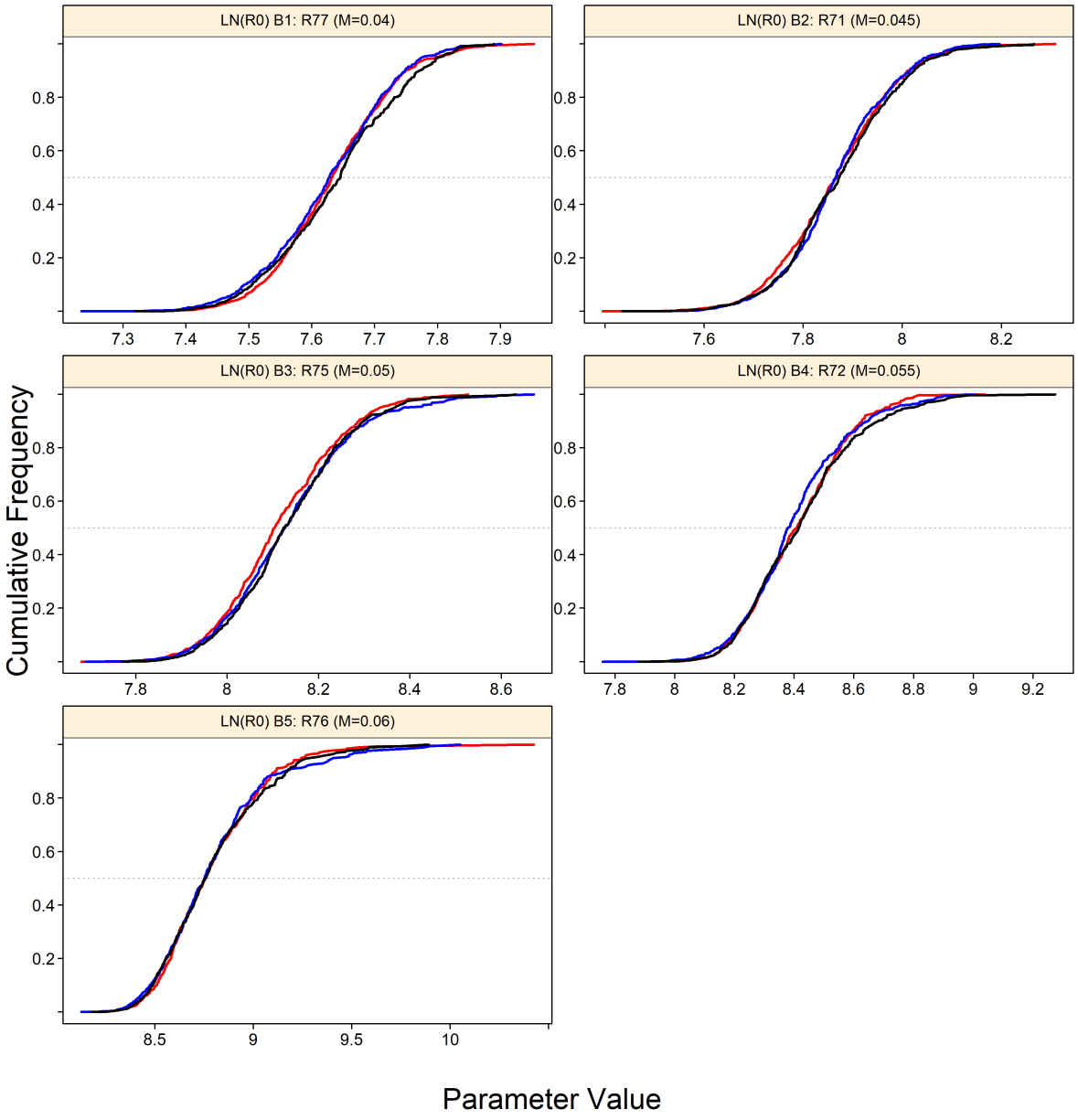

Figure F.23. Composite base case component runs: diagnostic plots obtained by dividing the R_0 MCMC chains of 2,000 MCMC samples into three segments, and overplotting the cumulative distributions of the first segment (red), second segment (blue) and final segment (black).

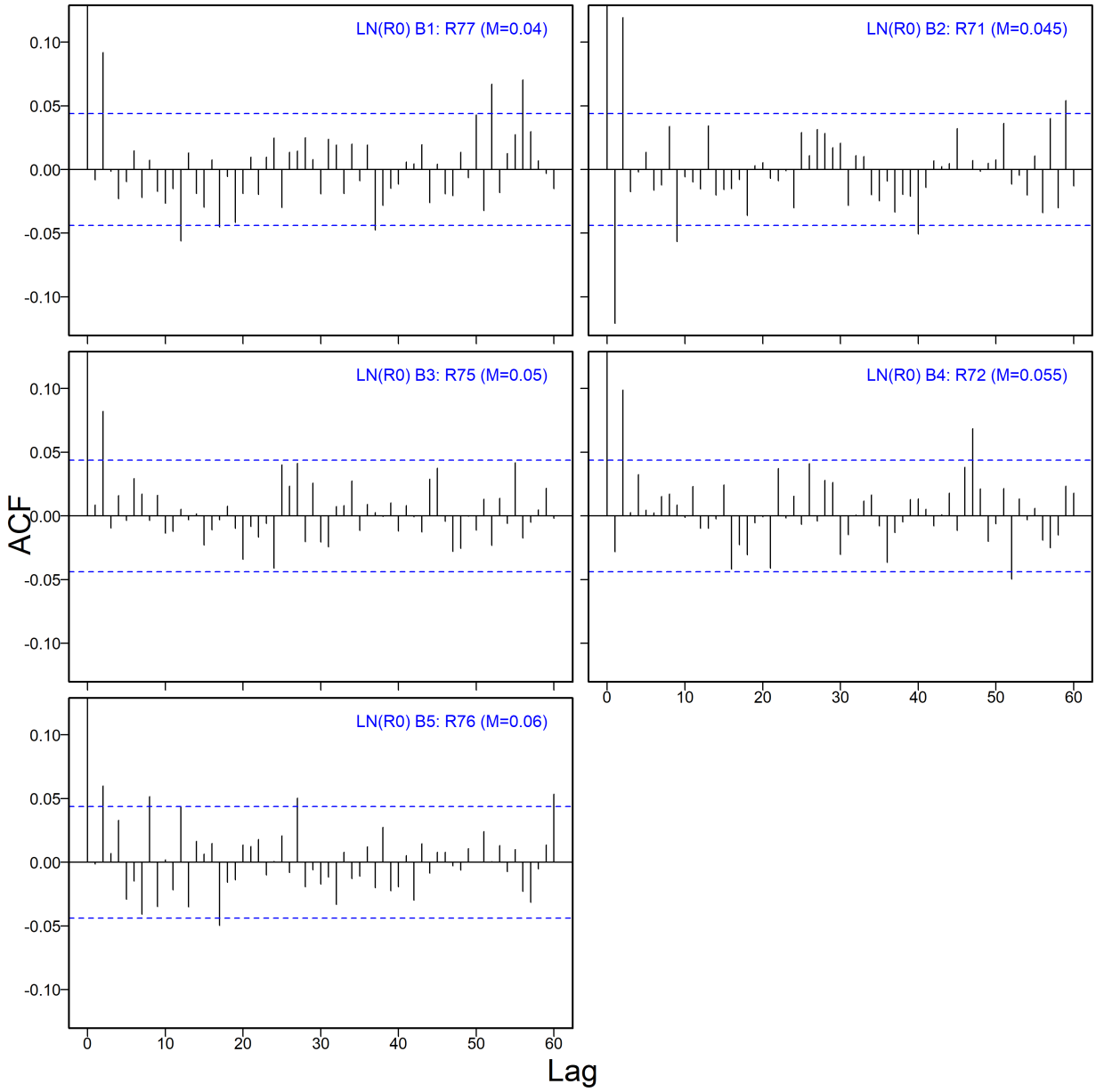

Figure F.24. Composite base case component runs: autocorrelation plots for the R_0 parameters from the MCMC output. Horizontal dashed blue lines delimit the 95% confidence interval for each parameter's set of lagged correlations.

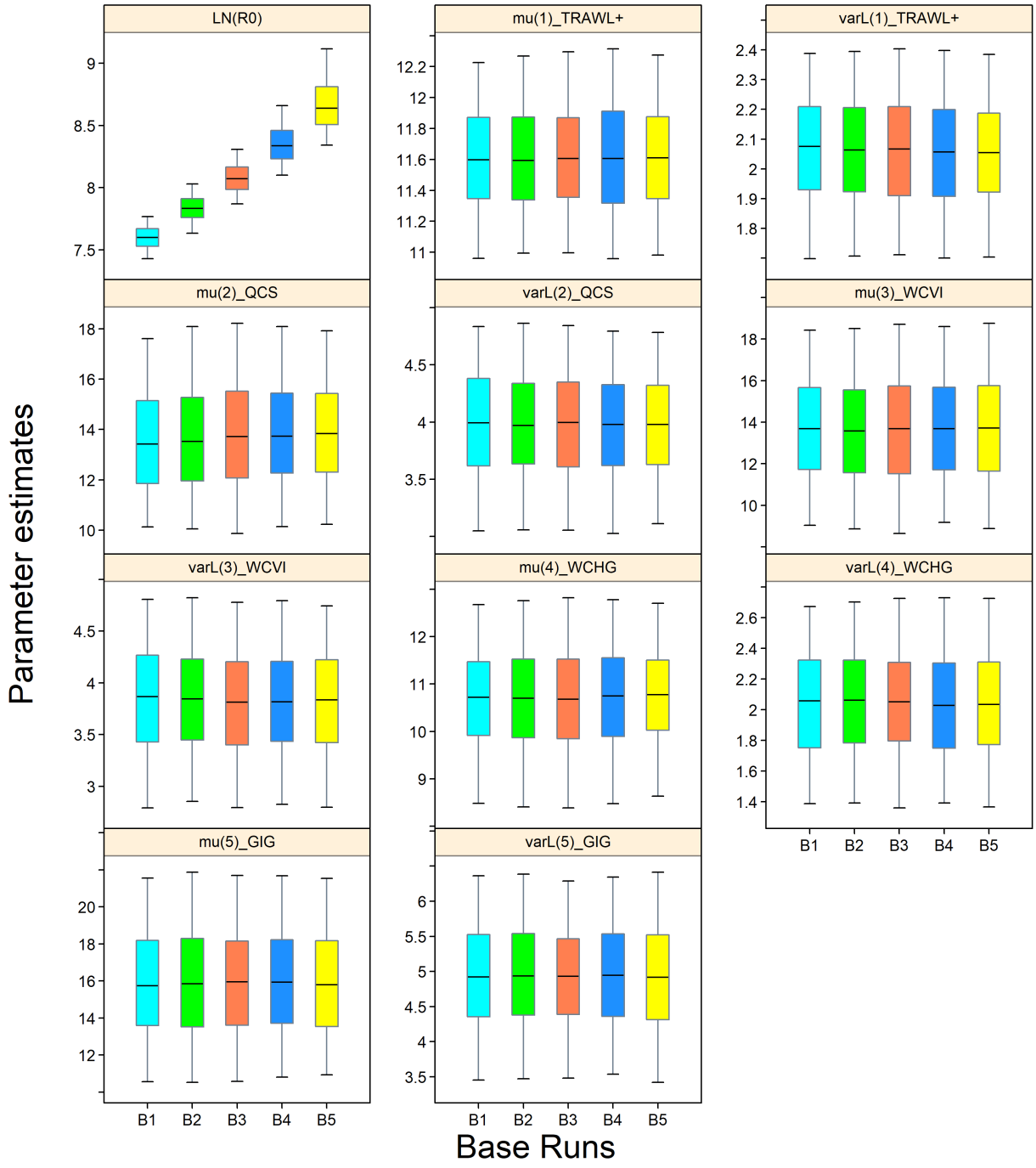

Figure F.25. Composite base case: quantile plots of the parameter estimates from 5 component runs of the base case, where each box denotes various M values (0.04, 0.045, 0.05, 0.055, 0.06). The boxplots delimit the 0.05, 0.25, 0.5, 0.75, and 0.95 quantiles.

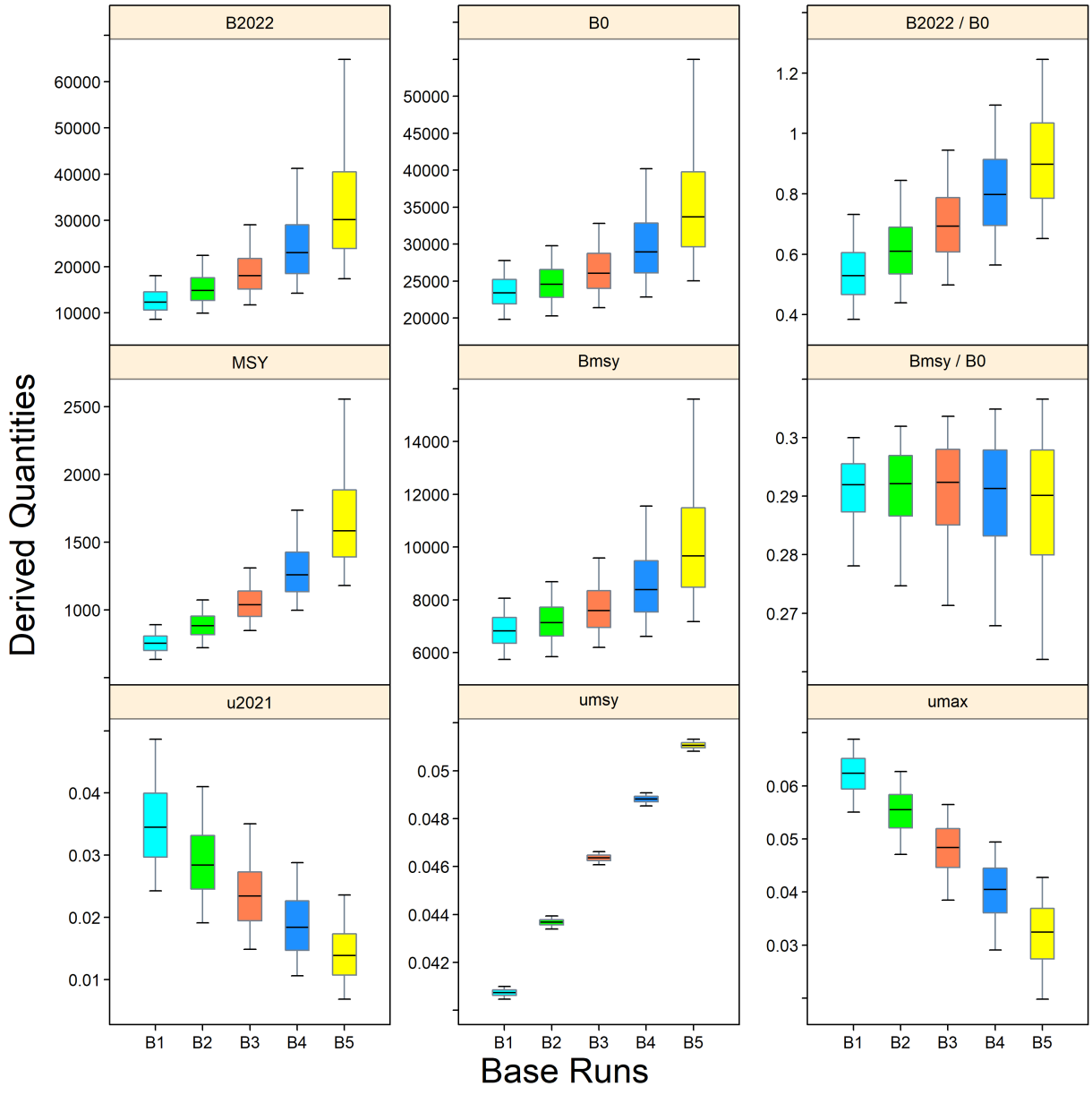

Figure F.26. Composite base case: quantile plots of selected derived quantities (B_{2022}, B_0, B_{2022}/B_0, MSY, B_{MSY}, B_{MSY}/B_0, u_{2021}, u_{MSY}, u_{max}) from 5 component runs of the base case, where each box denotes various M values (0.04, 0.045, 0.05, 0.055, 0.06). The boxplots delimit the 0.05, 0.25, 0.5, 0.75, and 0.95 quantiles.

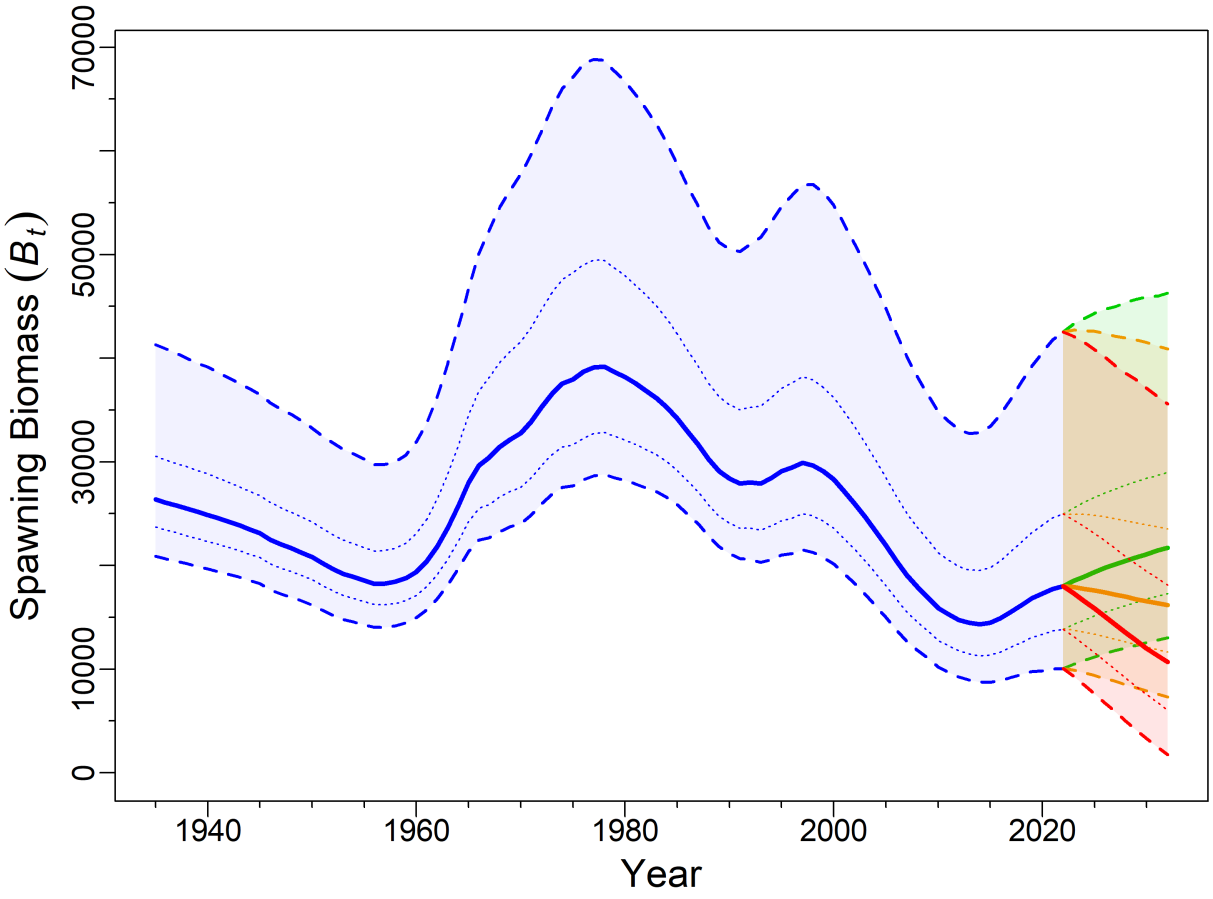

Figure F.27. Composite base case: estimates of spawning biomass B_t (tonnes) from pooled model posteriors. The median biomass trajectory appears as a solid curve surrounded by a 90% credibility envelope (quantiles: 0.05-0.95) in light blue and delimited by dashed lines for years t=1935:2022; projected biomass appears in light red for years t=2023:2032. Also delimited is the 50% credibility interval (quantiles: 0.25-0.75) delimited by dotted lines. The horizontal dashed lines show the median LRP and USR.

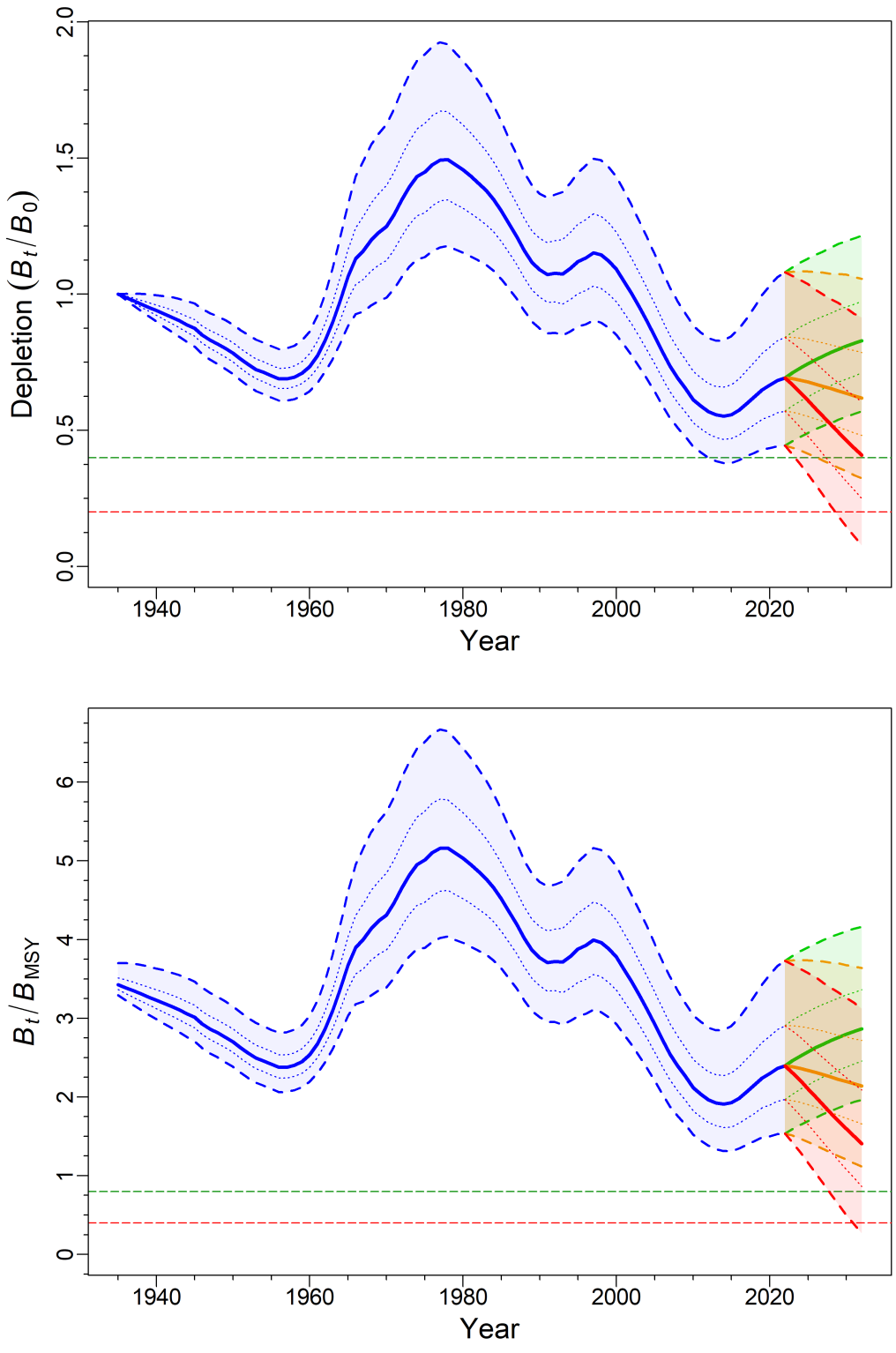

Figure F.28. Composite base case: estimates of spawning biomass B_t relative to (top) B_0 and (bottom) B_{MSY} from pooled model posteriors. The horizontal dashed lines show 0.2B_0 & 0.4B_0 (top) and 0.4B_{MSY} & 0.8B_{MSY} (bottom). See Fig. F.27 caption for envelope details.

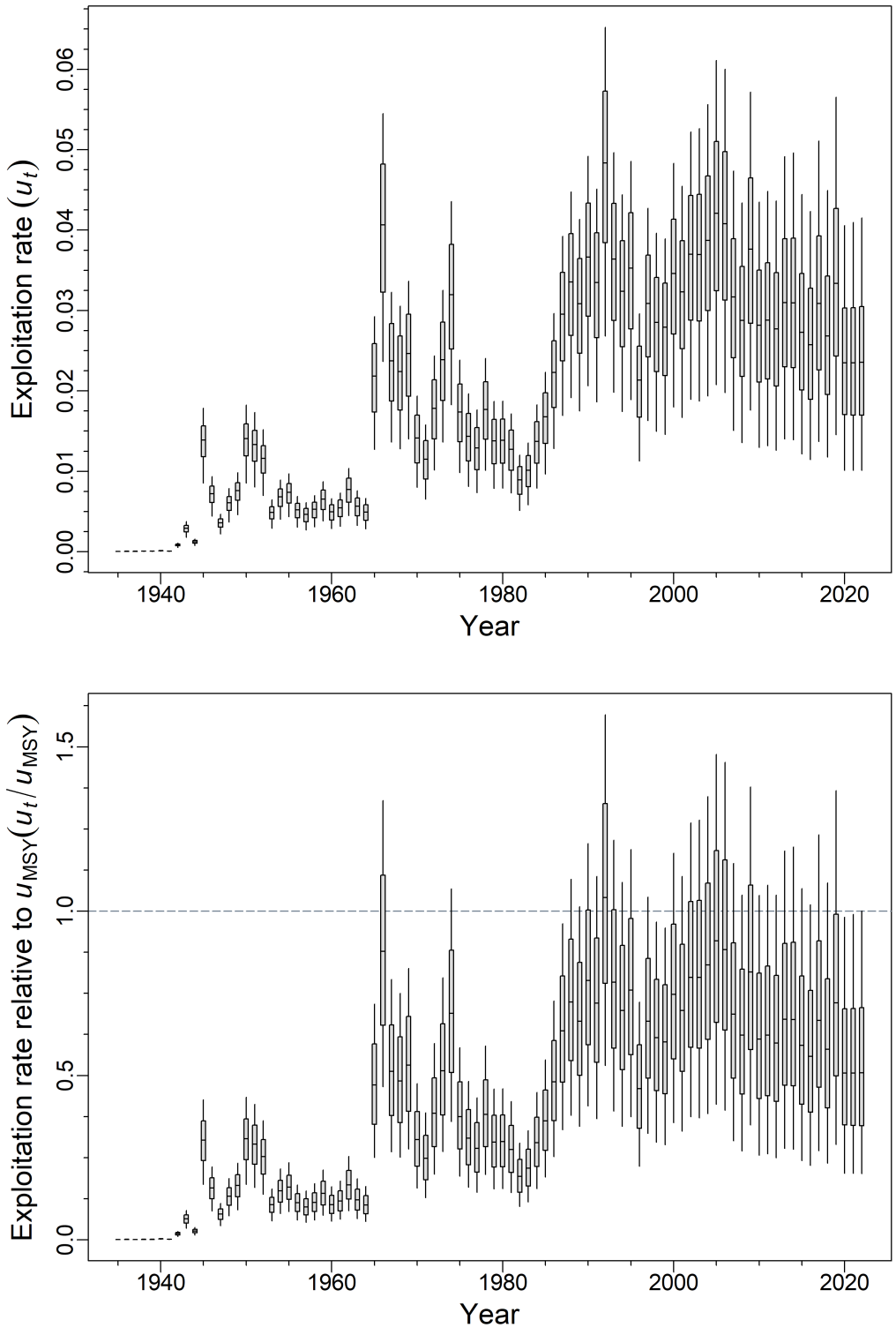

Figure F.29. Composite base case: posterior distribution of (top) exploitation trajectory u_t and (bottom) exploitation relative to u_{MSY}.

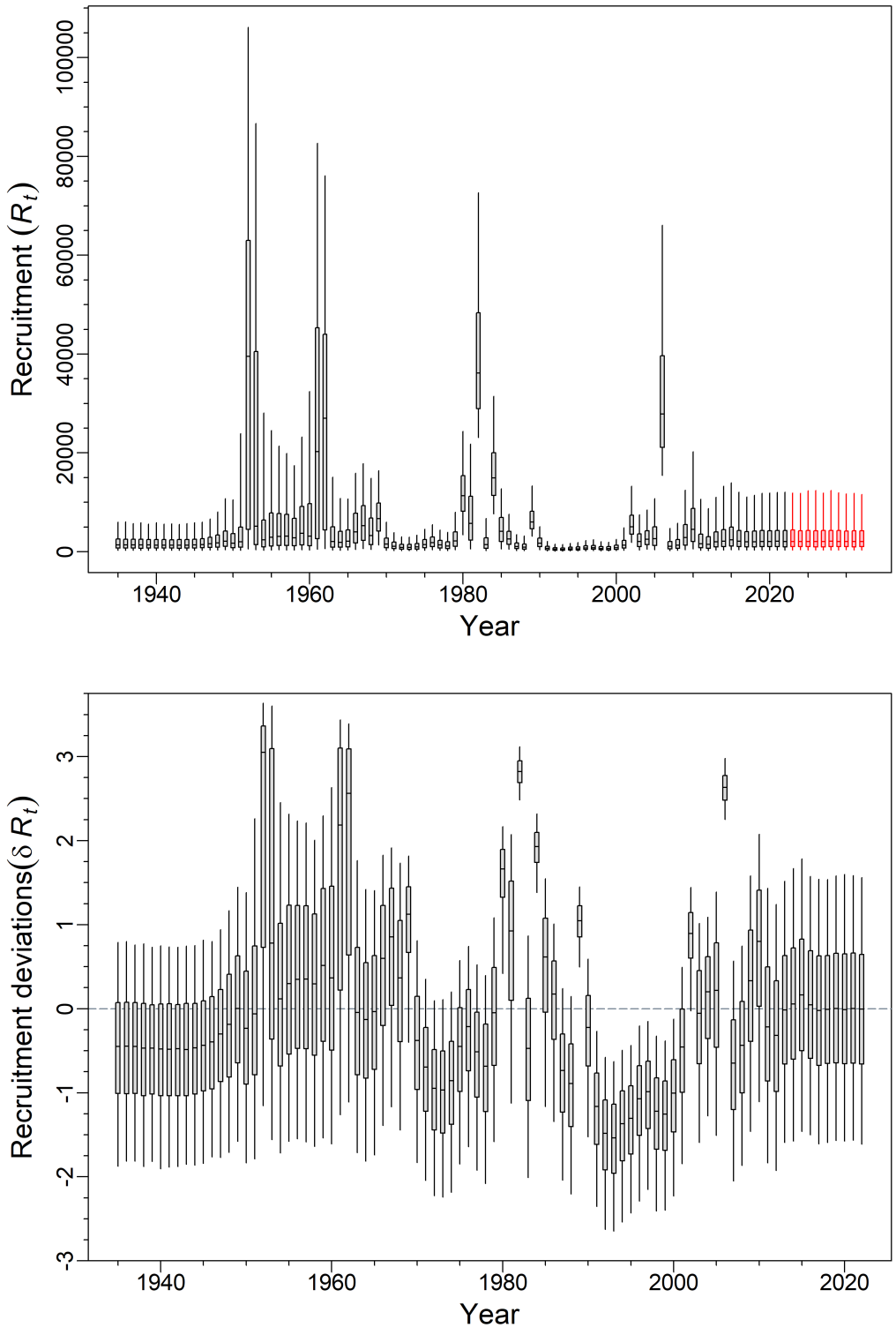

Figure F.30. Composite base case: posterior distribution of (top) recruitment trajectory (1000s of age-0 fish) and (bottom) recruitment deviation trajectory.

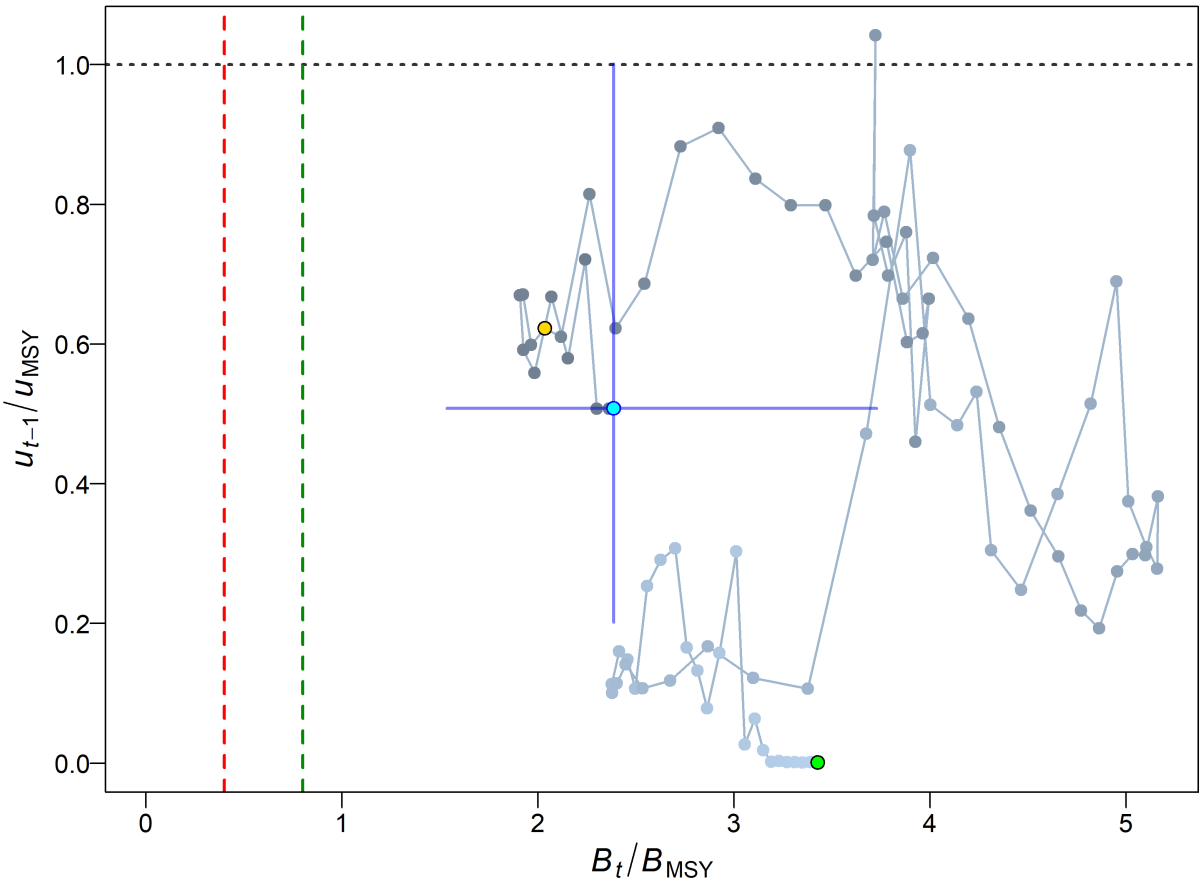

Figure F.31. Composite base case: phase plot through time of the medians of the ratios B_t/B_{MSY} (the spawning biomass in year t relative to B_{MSY}) and u_{t-1}/u_{MSY} (the exploitation rate in year $t-1$ relative to u_{MSY}) for one fishery (trawl+). The filled green circle is the equilibtium starting year (1935). Years then proceed along lines gradually darkening from light grey, with the final year (2022) as a filled cyan circle, and the blue cross lines represent the 0.05 and 0.95 quantiles of the posterior distributions for the final year. Red and green vertical dashed lines indicate the PA provisional limit and upper stock reference points (0.4, 0.8 B_{MSY}), and the horizontal grey dotted line indicates u at MSY.

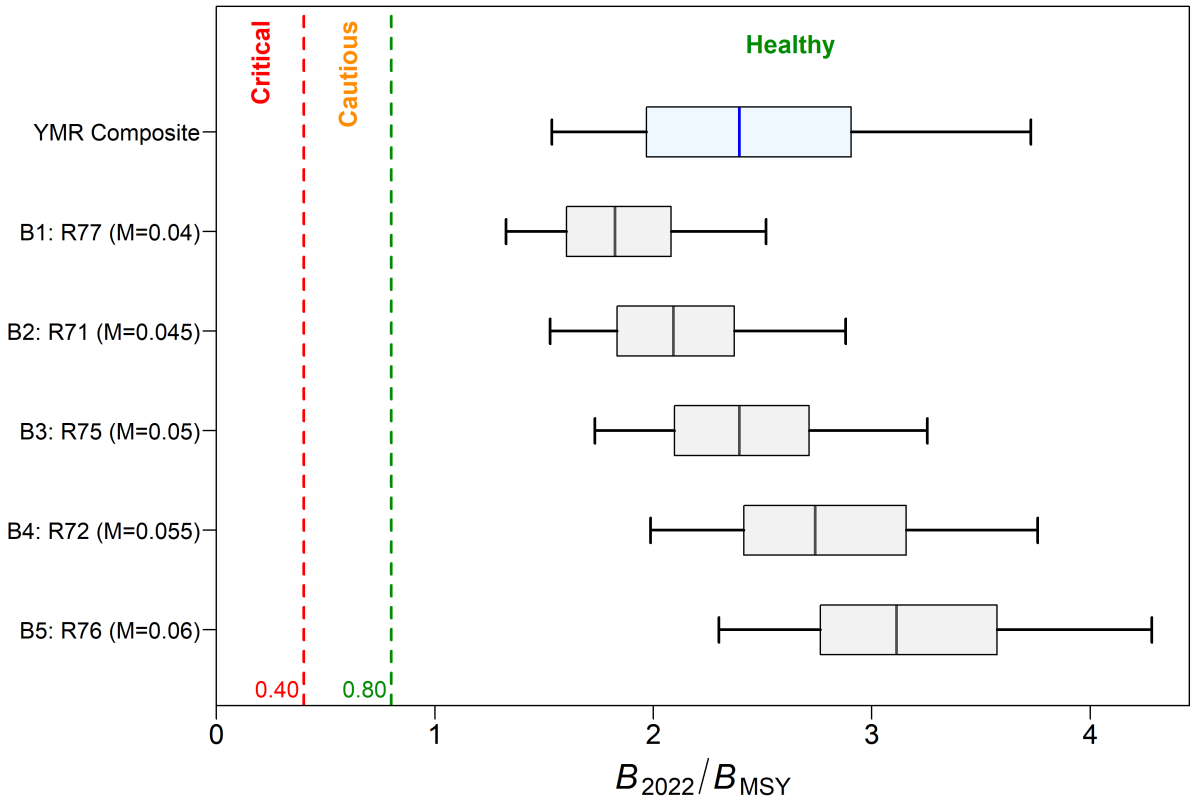

Figure F.32. Composite base case: stock status at beginning of 2022 relative to the PA provisional reference points of $0.4B_{MSY}$ and $0.8B_{MSY}$ for a base case comprising 5 model runs. The top quantile plot shows the composite distribution and below are the 5 contributing runs. Quantile plots show the 0.05, 0.25, 0.5, 0.75, and 0.95 quantiles from the MCMC posteriors.

F.2.4. YMR – Decision Tables

Table F.8. YMR BC: decision table for the limit reference point $0.4B_{MSY}$ featuring current- and 10-year projections for a range of **constant catch** *strategies (in tonnes). Values are P$(B_t > 0.4B_{MSY})$, i.e. the probability of the spawning biomass (mature females) at the start of year t being greater than the limit reference point. The probabilities are the proportion (to two decimal places) of the 10000 MCMC samples for which $B_t > 0.4B_{MSY}$. For reference, the average catch over the last 5 years (2016-2020) was 1272 t.*

CC	2022	2023	2024	2025	2026	2027	2028	2029	2030	2031	2032
0	1	1	1	1	1	1	1	1	1	1	1
500	1	1	1	1	1	1	1	1	1	1	1
750	1	1	1	1	1	1	1	1	1	1	1
1000	1	1	1	1	1	1	1	1	1	1	1
1250	1	1	1	1	1	1	1	1	1	1	1
1500	1	1	1	1	1	1	1	1	>0.99	>0.99	>0.99
2000	1	1	1	1	1	>0.99	>0.99	>0.99	>0.99	0.99	0.98
2500	1	1	1	1	>0.99	>0.99	>0.99	0.99	0.97	0.95	0.92
3000	1	1	1	1	>0.99	0.99	0.98	0.95	0.91	0.87	0.81

Table F.9. YMR BC: decision table for the upper stock reference point $0.8B_{MSY}$ featuring current- and 10-year projections for a range of **constant catch** *strategies (in tonnes), such that values are P$(B_t > 0.8B_{MSY})$. For reference, the average catch over the last 5 years (2016-2020) was 1272 t.*

CC	2022	2023	2024	2025	2026	2027	2028	2029	2030	2031	2032
0	1	1	1	1	1	1	1	1	1	1	1
500	1	1	1	1	1	1	1	1	1	1	1
750	1	1	1	1	1	1	1	>0.99	>0.99	>0.99	>0.99
1000	1	1	1	1	1	>0.99	>0.99	>0.99	>0.99	>0.99	>0.99
1250	1	1	1	1	>0.99	>0.99	>0.99	>0.99	>0.99	>0.99	0.99
1500	1	1	1	>0.99	>0.99	>0.99	>0.99	0.99	0.99	0.98	0.98
2000	1	1	>0.99	>0.99	>0.99	0.99	0.98	0.97	0.95	0.92	0.90
2500	1	1	>0.99	>0.99	0.99	0.97	0.94	0.91	0.87	0.82	0.78
3000	1	1	>0.99	0.99	0.97	0.93	0.88	0.82	0.76	0.70	0.64

Table F.10. YMR BC: decision table for the reference point B_{MSY} featuring current- and 10-year projections for a range of **constant catch** *strategies (in tonnes), such that values are P$(B_t > B_{MSY})$. For reference, the average catch over the last 5 years (2016-2020) was 1272 t.*

CC	2022	2023	2024	2025	2026	2027	2028	2029	2030	2031	2032
0	1	1	1	1	1	1	1	1	1	1	1
500	1	>0.99	>0.99	>0.99	>0.99	>0.99	>0.99	>0.99	>0.99	>0.99	>0.99
750	1	>0.99	>0.99	>0.99	>0.99	>0.99	>0.99	>0.99	>0.99	>0.99	>0.99
1000	1	>0.99	>0.99	>0.99	>0.99	>0.99	>0.99	>0.99	0.99	0.99	0.99
1250	1	>0.99	>0.99	>0.99	>0.99	>0.99	0.99	0.99	0.98	0.98	0.97
1500	1	>0.99	>0.99	>0.99	0.99	0.99	0.98	0.97	0.97	0.95	0.94
2000	1	>0.99	>0.99	0.99	0.98	0.97	0.94	0.92	0.89	0.86	0.83
2500	1	>0.99	0.99	0.98	0.96	0.92	0.88	0.83	0.78	0.74	0.69
3000	1	>0.99	0.99	0.96	0.92	0.86	0.80	0.73	0.67	0.61	0.55

Table F.11. YMR BC: decision table for the reference point u_{MSY} featuring current- and 10-year projections for a range of **constant catch** *strategies, such that values are P$(u_t < u_{MSY})$. For reference, the average catch over the last 5 years (2016-2020) was 1272 t.*

CC	2021	2022	2023	2024	2025	2026	2027	2028	2029	2030	2031
0	0.95	1	1	1	1	1	1	1	1	1	1
500	0.95	1	1	1	1	1	1	1	1	1	1
750	0.95	>0.99	>0.99	>0.99	>0.99	>0.99	>0.99	>0.99	>0.99	0.99	0.99
1000	0.95	0.96	0.96	0.96	0.95	0.95	0.94	0.94	0.94	0.93	0.93
1250	0.95	0.87	0.86	0.85	0.84	0.83	0.82	0.81	0.80	0.79	0.78
1500	0.95	0.74	0.73	0.71	0.70	0.69	0.67	0.66	0.65	0.64	0.62
2000	0.95	0.52	0.50	0.48	0.47	0.45	0.43	0.42	0.41	0.39	0.38
2500	0.95	0.36	0.35	0.33	0.31	0.29	0.28	0.27	0.25	0.24	0.23
3000	0.95	0.25	0.23	0.22	0.20	0.19	0.18	0.16	0.15	0.14	0.13

Table F.12. YMR BC: decision table for the reference point B_{2022} featuring current- and 10-year projections for a range of **constant catch** *strategies, such that values are P$(B_t > B_{2022})$. For reference, the average catch over the last 5 years (2016-2020) was 1272 t.*

CC	2022	2023	2024	2025	2026	2027	2028	2029	2030	2031	2032
0	0	0.99	0.98	0.97	0.96	0.95	0.94	0.94	0.93	0.93	0.93
500	0	0.89	0.83	0.80	0.77	0.75	0.73	0.72	0.71	0.70	0.69
750	0	0.72	0.64	0.61	0.58	0.55	0.53	0.52	0.51	0.50	0.49
1000	0	0.51	0.44	0.42	0.39	0.37	0.36	0.35	0.34	0.33	0.32
1250	0	0.34	0.29	0.28	0.26	0.24	0.23	0.22	0.21	0.20	0.20
1500	0	0.22	0.19	0.18	0.17	0.16	0.15	0.14	0.13	0.13	0.12
2000	0	0.10	0.09	0.08	0.07	0.07	0.06	0.06	0.06	0.05	0.05
2500	0	0.05	0.04	0.04	0.04	0.03	0.03	0.03	0.03	0.03	0.02
3000	0	0.02	0.02	0.02	0.02	0.02	0.02	0.02	0.01	0.01	0.01

Table F.13. YMR BC: decision table for the reference point u_{2021} featuring current- and 10-year projections for a range of **constant catch** *strategies, such that values are P$(u_t < u_{2021})$. For reference, the average catch over the last 5 years (2016-2020) was 1272 t.*

CC	2021	2022	2023	2024	2025	2026	2027	2028	2029	2030	2031
0	0	1	1	1	1	1	1	1	1	1	1
500	0	1	1	1	1	1	1	1	1	1	1
750	0	1	1	1	1	1	1	1	1	1	>0.99
1000	0	1	0.99	0.91	0.80	0.71	0.64	0.59	0.55	0.51	0.48
1250	0	0	0	<0.01	<0.01	<0.01	0.01	0.01	0.01	0.02	0.02
1500	0	0	0	0	<0.01	<0.01	<0.01	<0.01	<0.01	<0.01	<0.01
2000	0	0	0	0	0	0	0	<0.01	<0.01	<0.01	<0.01
2500	0	0	0	0	0	0	0	0	0	<0.01	<0.01
3000	0	0	0	0	0	0	0	0	0	0	0

Table F.14. YMR BC: decision table for an alternative reference point $0.2B_0$ featuring current- and 10 year projections for a range of **constant catch** *strategies, such that values are P$(B_t > 0.2B_0)$. For reference, the average catch over the last 5 years (2016-2020) was 1272 t.*

CC	2022	2023	2024	2025	2026	2027	2028	2029	2030	2031	2032
0	1	1	1	1	1	1	1	1	1	1	1
500	1	1	1	1	1	1	1	1	1	1	1
750	1	1	1	1	1	1	1	1	1	1	1
1000	1	1	1	1	1	1	1	>0.99	>0.99	>0.99	>0.99
1250	1	1	1	1	1	>0.99	>0.99	>0.99	>0.99	>0.99	>0.99
1500	1	1	1	1	>0.99	>0.99	>0.99	>0.99	>0.99	0.99	0.99
2000	1	1	1	>0.99	>0.99	>0.99	0.99	0.98	0.97	0.95	0.93
2500	1	1	1	>0.99	>0.99	0.98	0.96	0.94	0.90	0.87	0.82
3000	1	1	>0.99	>0.99	0.98	0.96	0.92	0.86	0.81	0.75	0.69

Table F.15. YMR BC: decision table for an alternative reference point $0.4B_0$ featuring current- and 10 year projections for a range of **constant catch** *strategies, such that values are P$(B_t > 0.4B_0)$. For reference, the average catch over the last 5 years (2016-2020) was 1272 t.*

CC	2022	2023	2024	2025	2026	2027	2028	2029	2030	2031	2032
0	0.98	0.99	0.99	>0.99	>0.99	>0.99	>0.99	>0.99	>0.99	>0.99	>0.99
500	0.98	0.98	0.98	0.99	0.99	0.99	0.99	0.99	0.99	0.99	0.99
750	0.98	0.98	0.98	0.98	0.98	0.98	0.97	0.97	0.97	0.97	0.97
1000	0.98	0.98	0.97	0.97	0.97	0.96	0.96	0.95	0.94	0.93	0.93
1250	0.98	0.98	0.97	0.96	0.95	0.94	0.93	0.91	0.90	0.89	0.87
1500	0.98	0.97	0.96	0.95	0.93	0.92	0.89	0.87	0.85	0.83	0.81
2000	0.98	0.97	0.95	0.92	0.88	0.85	0.81	0.77	0.73	0.69	0.66
2500	0.98	0.96	0.92	0.88	0.82	0.77	0.71	0.66	0.60	0.55	0.51
3000	0.98	0.95	0.90	0.83	0.76	0.69	0.61	0.54	0.49	0.44	0.40

Table F.16. YMR BC: decision table for COSEWIC reference criterion A2 'Endangered' featuring current- and 10-year projections and for a range of **constant catch** *strategies, such that values are P$(B_t > 0.5B_0)$. For reference, the average catch over the last 5 years (2016-2020) was 1272 t.*

CC	2022	2023	2024	2025	2026	2027	2028	2029	2030	2031	2032
0	0.88	0.91	0.93	0.94	0.95	0.96	0.97	0.98	0.98	0.99	0.99
500	0.88	0.89	0.90	0.91	0.91	0.92	0.92	0.92	0.92	0.92	0.92
750	0.88	0.89	0.89	0.89	0.88	0.88	0.88	0.88	0.88	0.87	0.87
1000	0.88	0.88	0.87	0.86	0.86	0.84	0.84	0.83	0.82	0.81	0.80
1250	0.88	0.87	0.85	0.84	0.82	0.81	0.79	0.77	0.75	0.73	0.72
1500	0.88	0.86	0.84	0.82	0.79	0.76	0.74	0.71	0.69	0.66	0.64
2000	0.88	0.84	0.80	0.76	0.72	0.68	0.63	0.59	0.55	0.52	0.49
2500	0.88	0.83	0.77	0.71	0.65	0.58	0.53	0.49	0.45	0.41	0.37
3000	0.88	0.81	0.73	0.65	0.57	0.51	0.45	0.40	0.35	0.31	0.28

Table F.17. YMR BC: decision table for COSEWIC reference criterion A2 'Threatened' featuring current- and 10-year projections and for a range of **constant catch** *strategies, such that values are P$(B_t > 0.7B_0)$. For reference, the average catch over the last 5 years (2016-2020) was 1272 t.*

CC	2022	2023	2024	2025	2026	2027	2028	2029	2030	2031	2032
0	0.48	0.53	0.56	0.59	0.63	0.66	0.68	0.71	0.73	0.75	0.77
500	0.48	0.51	0.52	0.53	0.55	0.55	0.56	0.57	0.58	0.59	0.59
750	0.48	0.50	0.50	0.51	0.51	0.51	0.51	0.51	0.51	0.51	0.51
1000	0.48	0.49	0.49	0.48	0.48	0.47	0.46	0.45	0.45	0.44	0.43
1250	0.48	0.48	0.47	0.46	0.44	0.43	0.42	0.41	0.39	0.38	0.37
1500	0.48	0.47	0.45	0.43	0.41	0.39	0.38	0.36	0.34	0.33	0.31
2000	0.48	0.45	0.42	0.39	0.36	0.33	0.30	0.28	0.26	0.24	0.23
2500	0.48	0.44	0.39	0.35	0.31	0.28	0.25	0.22	0.20	0.18	0.16
3000	0.48	0.42	0.37	0.31	0.27	0.23	0.20	0.18	0.15	0.13	0.12

F.2.4.1. GMU – Guidance for setting TACs

Decision tables for the composite base case provide advice to managers as probabilities that current and projected biomass B_t ($t = 2022, ..., 2032$) will exceed biomass-based reference points (or that projected exploitation rate u_t will fall below harvest-based reference points) under constant catch (CC) policies. Note that years for biomass-based reference points refer to the start of years, whereas years for harvest-based reference points refer to years prior to the start ($\sim$mid-year). Decision tables in the document (all under a constant catch policy):

- Table F.8 – probability of B_t exceeding the LRP, P$(B_t > 0.4B_{\text{MSY}})$;
- Table F.9 – probability of B_t exceeding the USR, P$(B_t > 0.8B_{\text{MSY}})$;
- Table F.10 – probability of B_t exceeding biomass at MSY, P$(B_t > B_{\text{MSY}})$;
- Table F.11 – probability of u_t falling below harvest rate at MSY, P$(u_t < u_{\text{MSY}})$;
- Table F.12 – probability of B_t exceeding current-year biomass, P$(B_t > B_{2022})$;
- Table F.13 – probability of u_t falling below current-year harvest rate, P$(u_t < u_{2021})$;
- Table F.14 – probability of B_t exceeding a non-DFO 'soft limit', P$(B_t > 0.2B_0)$;
- Table F.15 – probability of B_t exceeding a non-DFO 'target' biomass, P$(B_t > 0.4B_0)$;

MSY-based reference points estimated within a stock assessment model can be highly sensitive to model assumptions about natural mortality and stock recruitment dynamics (Forrest et al. 2018). As a result, other jurisdictions use reference points that are expressed in terms of B_0 rather than B_{MSY} (e.g., N.Z. Min. Fish. 2011), because B_{MSY} is often poorly estimated as it depends on estimated parameters and a consistent fishery (although B_0 shares several of these same problems). Therefore, the reference points of $0.2B_0$ and $0.4B_0$ are also presented here. These are default values used in New Zealand respectively as a 'soft limit', below which management action needs to be taken, and a 'target' biomass for low productivity stocks, a mean around which the biomass is expected to vary. The 'soft limit' is equivalent to the upper stock reference (USR, $0.8B_{\text{MSY}}$) in the provisional DFO Sustainable Fisheries Framework while a 'target' biomass is not specified by the provisional DFO SFF. Additionally, results are provided comparing projected biomass to B_{MSY} and to current spawning biomass B_{2022}, and comparing projected harvest rate to current harvest rate u_{2021}.

COSEWIC indicator A1 is reserved for those species where the causes of the reduction are clearly reversible, understood, and ceased. Indicator A2 is used when the population reduction

may not be reversible, may not be understood, or may not have ceased. The 2011 Yellowmouth Rockfish recovery potential analysis (Edwards et al. 2012) placed YMR into category A2b (where the 'b' indicates that the designation was based on 'an index of abundance appropriate to the taxon'). Under A2, a species is considered Endangered or Threatened if the decline has been >50% or >30% below B_0, respectively.

Additional short-term tables for COSEWIC's A2 criterion:

- Table F.16 – probability of B_t exceeding 'Endangered' status (P($B_t > 0.5B_0$);
- Table F.17 – probability of B_t exceeding 'Threatened' status (P($B_t > 0.7B_0$).

F.2.5. YMR – Sensitivity Analysis

Fourteen sensitivity analyses were run (with full MCMC simulations) relative to the central run (Run75: M=0.05, CPUE c_{p}=0.3296) to test the sensitivity of the outputs to alternative model assumptions:

- **S01** (Run78) – add 1997 index to WCHG survey series: (label: "add 1997 WCHG index");
- **S02** (Run79) – estimate M using a normal prior: $\mathcal{N}(0.05, 0.01)$ (label: "estimate M");
- **S03** (Run80) – drop commercial CPUE series (label: "drop CPUE");
- **S04** (Run81) – use CPUE series fitted by Tweedie distribution (label: "Tweedie CPUE");
- **S05** (Run82) – reduce std.dev. of recr. residuals σ_R from 0.9 to 0.6 (label: "sigmaR=0.6");
- **S06** (Run83) – increase std.dev. of recr. residuals σ_R from 0.9 to 1.2 (label: "sigmaR=1.2");
- **S07** (Run84) – reduce commercial catch for 1965-1995 by 33% (label: "reduce catch 33%");
- **S08** (Run85) – increase comm. catch for 1965-1995 by 50% (label: "increase catch 50%");
- **S09** (Run86) – upweight QCS AF samples by 3.5 (label: "upweight QCS AF");
- **S10** (Run87) – delay recruitment deviations from 1950 to 1970 (label: "start Rdevs in 1970");
- **S11** (Run88) – remove ageing error based on CVs of length-at-age (label: "no ageing error");
- **S12** (Run91) – reduce steepness from h=0.7 to h=0.5 (label: "steepness h=0.5");
- **S13** (Run92) – double 2021 catch from 1057 t to 2114 t (label: "double 2021 catch");
- **S14** (Run93) – use AE based on ageing precision (label: "AE from age readers").

All sensitivity runs were reweighted once for: (i) abundance, by adding process error to the commercial CPUE (except for S04 because error was already high), and (ii) composition, by multiplying the trawl AF sample size by a harmonic mean ratio procedure (Appendix E, Table F.18). The process error added to the commercial CPUE for all sensitivities (except S04) was the same as that adopted in the central run B3 (R75) (CPUE=0.3296), based on a spline analysis (Appendix E). No additional process error was added to survey indices because observed error was already high.

The MPD (mode of the posterior distribution) 'best fit' was used as the starting point for a Bayesian search across the joint posterior distributions of the parameters using the Monte Carlo Markov Chain (MCMC) method. Unlike previous BC rockfish assessments, which used a random walk Metropolis procedure, sensitivity runs (as for the base components) were evaluated using a "No U-Turn Sampling" (NUTS) procedure to reduce the evaluation time from days to hours. All sensitivity runs, except for S02 (estimate M), were judged to have converged for the NUTS algorithm using 8 parallel chains of 500 each and discarding the first 250 from each. The remaining 8 sets of 250 samples were merged to yield 2,000 samples per sensitivity run. Using a higher numbers of simulations with thinning did not improve the fit to S02 (estimate M), although it did remove autocorrelation.

The differences among the sensitivity runs (including the central run) are summarised in tables of median parameter estimates (Table F.19) and median MSY-based quantities (Table F.20). Sensitivity plots appear in:

Table F.18. Age frequency weights used for the central run (B3) and fourteen sensitivity runs.

Sens	Run	Trawl	QCS	WCVI	WCHG	GIG
B3	R75	6.321921	0.25	0.25	0.25	0.25
S01	R78	6.325070	0.25	0.25	0.25	0.25
S02	R79	6.408812	0.25	0.25	0.25	0.25
S03	R80	10.279413	0.25	0.25	0.25	0.25
S04	R81	10.440879	0.25	0.25	0.25	0.25
S05	R82	6.449762	0.25	0.25	0.25	0.25
S06	R83	6.222421	0.25	0.25	0.25	0.25
S07	R84	6.253996	0.25	0.25	0.25	0.25
S08	R85	6.389155	0.25	0.25	0.25	0.25
S09	R86	6.321921	3.50	0.25	0.25	0.25
S10	R87	5.997195	0.25	0.25	0.25	0.25
S11	R88	5.241267	0.25	0.25	0.25	0.25
S12	R91	6.326616	0.25	0.25	0.25	0.25
S13	R92	6.358515	0.25	0.25	0.25	0.25
S14	R93	6.055056	0.25	0.25	0.25	0.25

- Figure F.33 – trace plots for chains of R_0 MCMC samples;
- Figure F.34 – diagnostic split-chain plots for R_0 MCMC samples;
- Figure F.35 – diagnostic autocorrelation plots for R_0 MCMC sample;
- Figure F.36 – trajectories of median B_t (tonnes);
- Figure F.37 – trajectories of median B_t/B_0;
- Figure F.38 – trajectories of median recruitment deviations;
- Figure F.39 – trajectories of median recruitment R_t (1000s age-0 fish);
- Figure F.40 – trajectories of median exploitation rate u_t;
- Figure F.41 – quantile plots of selected parameters for the sensitivity runs;
- Figure F.42 – quantile plots of selected derived quantities for the sensitivity runs;
- Figure F.43 – stock status plots of B_{2022}/B_{MSY}.

F.2.5.1. Sensitivity diagnostics

The diagnostic plots (Figures F.33 to F.35) suggest that eight sensitivity runs exhibited good MCMC behaviour, four were fair, one was poor, and one was unacceptable with little credibility.

- Good – no trend in traces, split-chains align, no autocorrelation:
  - S01 (add 1997 WCHG index)
  - S04 (Tweedie CPUE)
  - S06 (sigmaR=1.2)
  - S07 (reduce catch 33%)
  - S08 (increase catch 50%)
  - S12 (steepness h=0.5)
  - S13 (double 2021 catch)
  - S14 (AE from age readers)
- Fair – trace trend temporarily interrupted, split-chains somewhat frayed, some autocorrelation:
  - S03 (drop CPUE)

    - S05 (sigmaR=0.6)
    - S09 (upweight QCS AF)
    - S11 (no ageing error)
- Poor – trace trend fluctuates substantially or shows a persistent increase/decrease, split-chains differ from each other, substantial autocorrelation:
    - S10 (start Rdevs in 1970)
- Unacceptable – trace trend shows a persistent increase/decrease that has not levelled, split-chains differ markedly from each other, persistent autocorrelation:
    - S02 (estimate M)

The run that estimated M (S02) may not have converged and the unacceptable diagnostics suggested instability in the model. Additionally, the posterior for M_1 (females), 0.070 (0.060, 0.078), moved well above the prior $\mathcal{N}(0.05, 0.01)$. While a higher M may be suitable for this species, it was not supported by the available data while using the SS modelling platform.

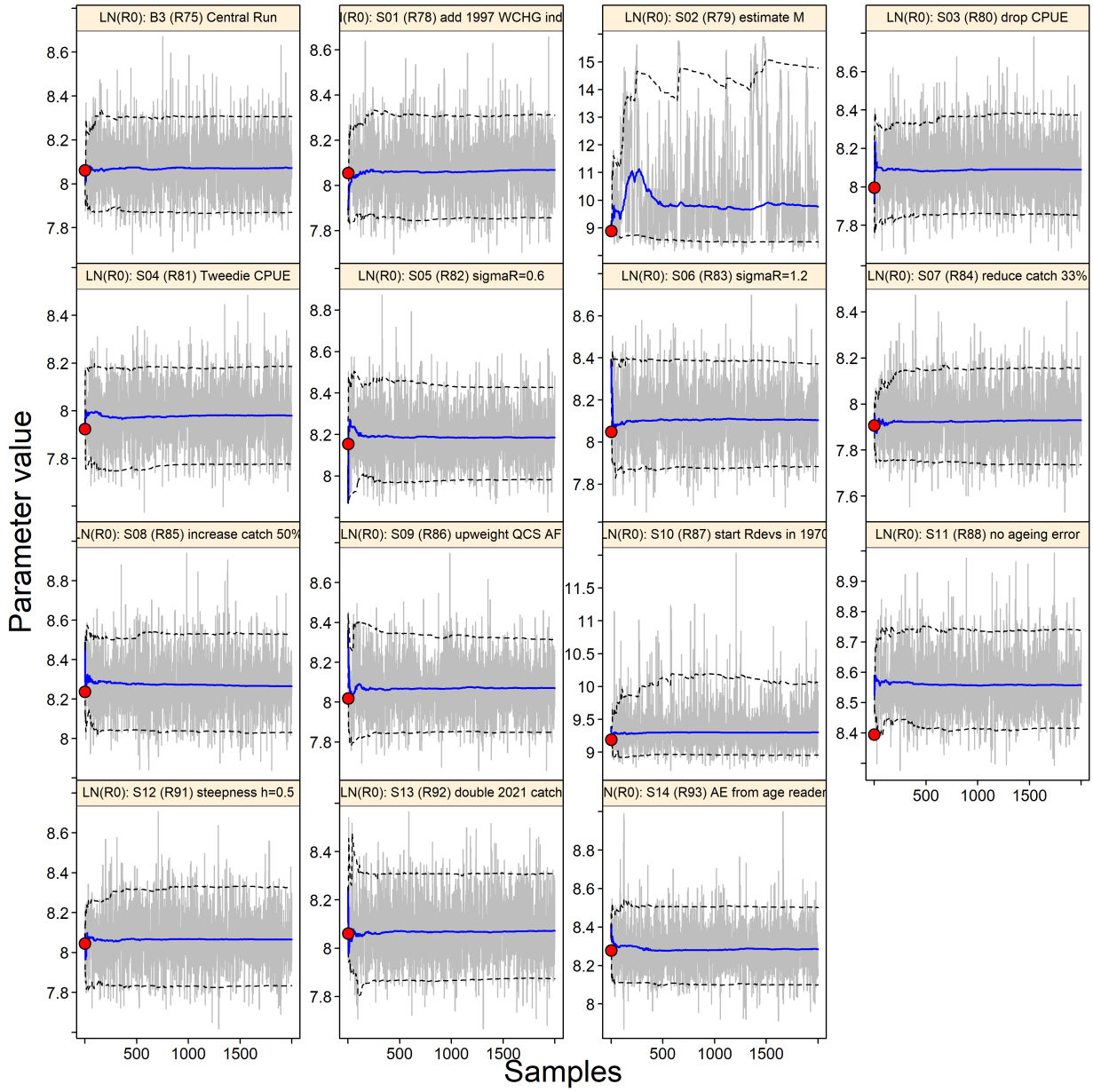

Figure F.33. YMR sensitivity R_0: MCMC traces for the estimated parameters. Grey lines show the 2,000 samples for each parameter, solid blue lines show the cumulative median (up to that sample), and dashed lines show the cumulative 0.05 and 0.95 quantiles. Red circles are the MPD estimates.

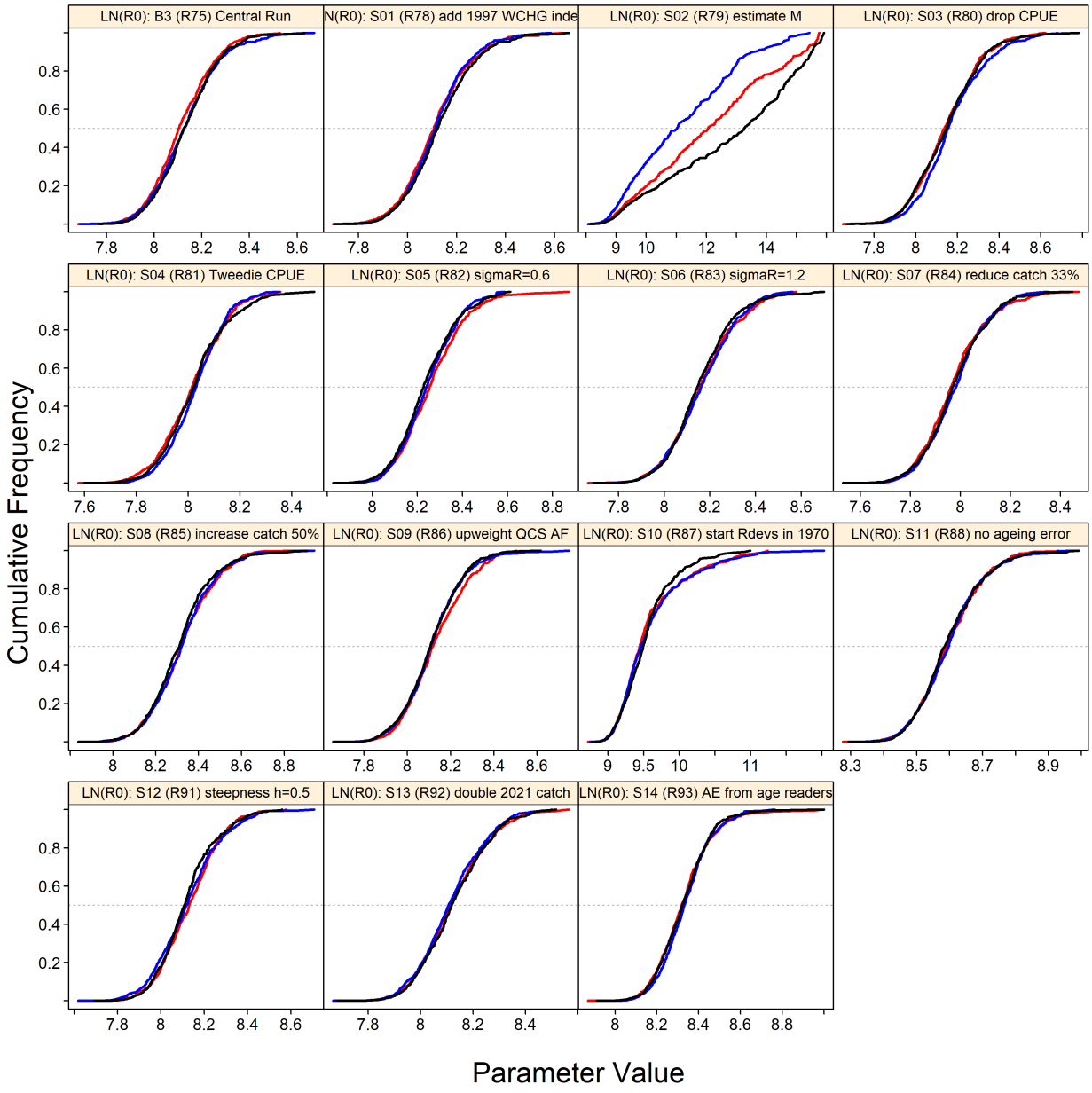

Figure F.34. YMR sensitivity R_0: diagnostic plots obtained by dividing the MCMC chain of 2,000 MCMC samples into three segments, and overplotting the cumulative distributions of the first segment (red), second segment (blue) and final segment (black).

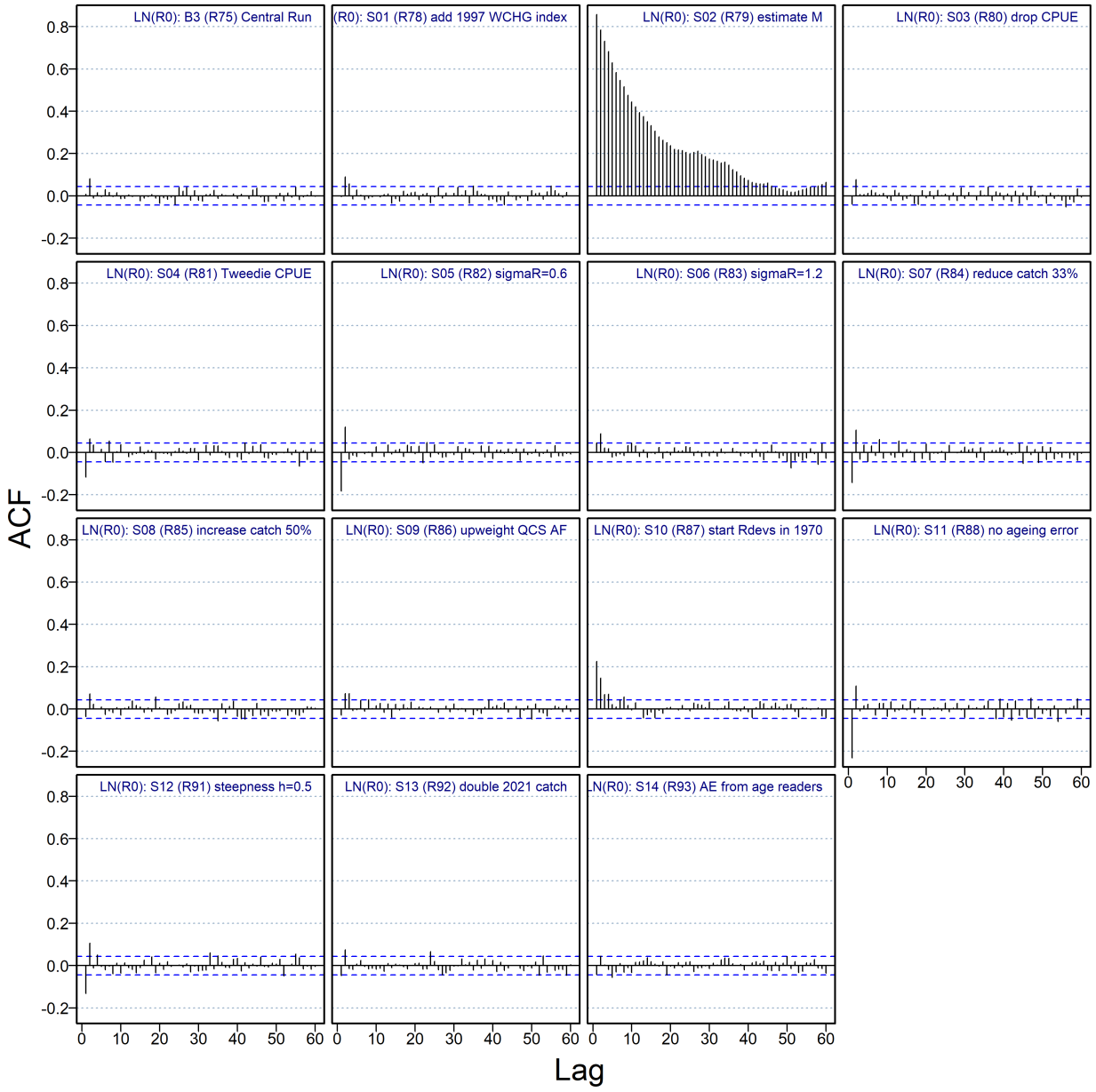

Figure F.35. YMR sensitivity R_0: autocorrelation plots for the estimated parameters from the MCMC output. Horizontal dashed blue lines delimit the 95% confidence interval for each parameter's set of lagged correlations.

F.2.5.2. Sensitivity comparisons

The trajectories of the B_t medians relative to B_0 (Figure F.37) indicate that most sensitivities followed the trajectory of the central run with some variation, while three scenarios departed markedly (S02, S10, S11). Although estimating M (S02) followed the trajectory of the central run, it remained consistently above the latter and resulted in one of the most optimistic scenarios. However, it is likely that this run did not converge and these results should be interpreted with caution.

The most pessimistic run was the one without ageing error (AE) corrections (S11), followed by the run using an alternative AE based on CVs of age calculated from otolith readers' estimates of precision (S14), suggesting that accounting for ageing error is important to remove bias, in both cases negative. The trajectory of the AE run using CVs of age (S14) lies in between the run with no AE (S11) and the central run (B3) for the base case, which uses AE based on CVs of length-at age.

While S11 and S14 estimated higher B_0 values (median = 41,400 t and 32,150 t, respectively) compared to the central run (median = 26,000 t), the median estimates of current stock status relative to B_0 were lower (S11=0.39, S14=0.55, B3=0.69). The higher B_0 suggests that the runs using absent/weaker AE adjustments were estimating more productive stocks (the median MSY values are 62% and 24% greater than the central run estimate; Table F.20). However, what is more likely, is that these models were trading off initial equilibrium biomass and strong early recruitments to get the best fit to the data. Figure F.36 shows this, with the two runs with alternative AE assumptions (S11 and S14) starting off at levels higher than B3 (median B_0: S11=41,767, S14=32,151, B3=26,065; Table F.20), but between 1970 and 1980 all three models converged to similar levels of absolute biomass after the constraint of data took effect. The S11 and S14 runs adjusted the initial biomass and early recruitments to get a better fit to the data, given the different AE assumptions. By the time the three model trajectories reached 2022, they estimated similar levels of median female spawning biomass: S11=16,389, S14=18,482, B3=18,027 (Table F.20). The lower estimate for B_{2022} by S11 (compared to B3 and S14) is explained by the low recruitment deviations estimated by this model in the late 1990s. The use (or lack) of ageing error (AE), showed that this process had an important impact on model results. The model with no ageing error (S11) estimated recruitment peaks spread broadly across adjacent years, while a strong AE assumption (B3, central run) concentrated recruitment into single years. The intermediate AE assumption (S14) lay between the two extremes of S11 and B3, with the first two recruitment peaks spread less broadly across years than in S11. This issue emerged as a potential axis of uncertainty during the RPR review and should be explored in future assessments. The authors chose the strong AE assumption because the single-year recruitment events were consistent with expected rockfish life history patterns.

The run that estimated recruitment deviations starting in 1970 rather than 1950 (S10) followed a path well below the central run before trending up to an estimate for current (2022) stock status that was higher than the run that estimated M. The reason for this result can be seen in Figure F.38, where run S10 estimated the highest recruitment deviations of all the runs during the low period in the late 1990s. Run S10 then estimated higher recruitment deviations in the following years compared to most of the other runs. This compensatory behaviour is responsible for the very optimistic stock status estimated by this run. S10 also estimated an unrealistically high level of female spawning biomass compared to all other runs, save S02 (Figure F.36).

Dropping the CPUE series (S03) resulted in higher estimates for current status; however, this run increased the fishery AF weight because the dominant uncertainty in S03 was the high relative

error associated with the surveys. The harmonic mean ratio procedure increased the weight associated with the fishery AF data (Table F.18) because the effective sample size associated with these data was relatively informative compared to the other data in the model.

Run S09, which upweighted the QC Sound survey AFs, illustrates why we chose to downweight the available survey age frequency data. This run estimated an age at maximum selectivity that was shifted downward by three years compared to the central run (S09 median μ_2=10.8, B3 median μ_2=13.7; Table F.19). By adjusting the selectivity function to the left, this model estimated two very large recent year classes (in 2010 and 2015) that were absent in all the other model runs (Figures F.39 & F.38). These strong year classes resulted in a very optimistic estimate of current stock status (median=0.75B_0), which would likely propagate into optimistic projections. While these year classes may in fact exist, it seemed unwise to allow these few uncertain observations in a single survey to drive such a high degree of optimism.

Parameter estimates varied little among sensitivity runs (Figure F.41), with the exception of S02 (estimating M) and S09 (upweighting the QCS survey AFs). Derived quantities based on MSY (Figure F.42) exhibited unrealistically high values of MSY and B_0 for S02 and S10 (delayed estimation of recruitment deviations).

The stock status (B_{2022}/B_{MSY}) for the sensitivities (Figure F.43) are all in the DFO Healthy zone, including the most pessimistic S11 run that does not correct for ageing error.

Table F.19. YMR BC: median values of MCMC samples for the primary estimated parameters, comparing the central run to 14 sensitivity runs (2,000 samples each). C =Central, R = Run, S = Sensitivity. Numeric subscripts other than those for R_0 and M indicate the following gear types g: 1 = Bottom Trawl CPUE, 2 = QCS Synoptic, 3 = WCVI Synoptic, 4 = WCHG Synoptic, and 5 = GIG Historical. Sensitivity runs: S01 = add 1997 WCHG index, S02 = estimate M, S03 = drop CPUE, S04 = Tweedie CPUE, S05 = sigmaR=0.6, S06 = sigmaR=1.2, S07 = reduce catch 33%, S08 = increase catch 50%, S09 = upweight QCS AF, S10 = start Rdevs in 1970, S11 = no ageing error, S12 = steepness h=0.5, S13 = double 2021 catch, S14 = AE from age readers

Par	B3(R75)	S01(R78)	S02(R79)	S03(R80)	S04(R81)	S05(R82)	S06(R83)	S07(R84)	S08(R85)	S09(R86)	S10(R87)	S11(R88)	S12(R91)	S13(R92)	S14(R93)
$\log R_0$	8.073	8.067	9.767	8.090	7.979	8.186	8.104	7.929	8.265	8.070	9.302	8.558	8.066	8.072	8.284
μ_1	11.61	11.60	11.59	11.72	11.79	11.54	11.64	11.62	11.58	11.32	11.70	11.75	11.59	11.59	11.81
μ_2	13.72	13.58	13.87	13.76	13.67	13.78	13.71	13.63	13.73	10.79	14.21	13.74	13.72	13.68	13.70
μ_3	13.68	13.52	13.80	13.72	13.65	13.59	13.80	13.52	13.68	13.89	14.03	13.59	13.72	13.68	13.85
μ_4	10.68	10.74	10.71	10.75	10.74	10.76	10.68	10.73	10.77	10.59	10.83	10.69	10.74	10.73	10.75
μ_5	15.94	15.78	15.76	15.68	15.83	15.84	15.94	15.88	15.83	15.99	15.80	16.02	15.89	15.84	15.91
$\log v_{\mathrm{L}1}$	2.067	2.063	2.038	2.152	2.172	2.038	2.072	2.061	2.055	1.956	2.063	2.197	2.061	2.062	2.180
$\log v_{\mathrm{L}2}$	3.996	3.972	3.950	3.990	4.004	4.029	3.970	3.988	3.991	3.193	4.027	3.977	3.999	3.991	3.979
$\log v_{\mathrm{L}3}$	3.814	3.847	3.833	3.832	3.829	3.838	3.840	3.827	3.842	3.756	3.823	3.833	3.842	3.827	3.837
$\log v_{\mathrm{L}4}$	2.050	2.040	2.046	2.044	2.046	2.054	2.060	2.041	2.047	2.055	2.046	2.055	2.045	2.044	2.061
$\log v_{\mathrm{L}5}$	4.929	4.908	4.927	4.935	4.954	4.910	4.898	4.983	4.965	4.939	4.882	4.906	4.919	4.941	4.916
M_1	—	—	0.07010	—	—	—	—	—	—	—	—	—	—	—	—
M_2	—	—	0.06822	—	—	—	—	—	—	—	—	—	—	—	—

Table F.20. YMR BC: medians of MCMC-derived quantities from the central run and 14 sensitivity runs (2,000 samples each) from their respective MCMC posteriors. Definitions are: B_0 – unfished equilibrium spawning biomass (mature females), B_{2022} – spawning biomass at the end of 2022, u_{2022} – exploitation rate (ratio of total catch to vulnerable biomass) in the middle of 2022, u_{max} – maximum exploitation rate (calculated for each sample as the maximum exploitation rate from 1935 to 2022), MSY – maximum sustainable yield at equilibrium, B_{MSY} – equilibrium spawning biomass at MSY, u_{MSY} – equilibrium exploitation rate at MSY, All biomass values (and MSY) are in tonnes. Sensitivity runs: S01 = add 1997 WCHG index, S02 = estimate M, S03 = drop CPUE, S04 = Tweedie CPUE, S05 = sigmaR=0.6, S06 = sigmaR=1.2, S07 = reduce catch 33%, S08 = increase catch 50%, S09 = upweight QCS AF, S10 = start Rdevs in 1970, S11 = no ageing error, S12 = steepness h=0.5, S13 = double 2021 catch, S14 = AE from age readers

Quantity	B3(R75)	S01(R78)	S02(R79)	S03(R80)	S04(R81)	S05(R82)	S06(R83)	S07(R84)	S08(R85)	S09(R86)	S10(R87)	S11(R88)	S12(R91)	S13(R92)	S14(R93)
B_0	26,065	25,959	76,859	26,252	23,561	29,859	26,421	22,621	31,784	26,118	93,667	41,767	26,063	26,114	32,151
B_{2022}	18,027	17,578	93,063	22,521	17,071	21,577	17,537	16,126	21,845	20,296	111,764	16,389	18,271	17,558	18,482
B_{2022}/B_0	0.693	0.682	1.21	0.869	0.730	0.720	0.665	0.713	0.694	0.780	1.19	0.391	0.697	0.676	0.577
u_{2022}	0.0234	0.0240	0.00457	0.0195	0.0249	0.0200	0.0235	0.0262	0.0194	0.0184	0.00395	0.0241	0.0234	0.0472	0.0223
u_{max}	0.0484	0.0490	0.0119	0.0444	0.0495	0.0449	0.0493	0.0450	0.0626	0.0443	0.0181	0.0501	0.0477	0.0495	0.0485
MSY	1,040	1,034	4,294	1,056	947	1,163	1,073	901	1,261	1,033	3,561	1,684	709	1,038	1,286
B_{MSY}	7,593	7,553	21,976	7,725	6,919	8,498	7,836	6,579	9,210	7,579	25,939	12,344	9,575	7,587	9,382
$0.4B_{\text{MSY}}$	3,037	3,021	8,790	3,090	2,768	3,399	3,134	2,631	3,684	3,032	10,376	4,938	3,830	3,035	3,753
$0.8B_{\text{MSY}}$	6,074	6,043	17,581	6,180	5,535	6,798	6,269	5,263	7,368	6,063	20,751	9,875	7,660	6,070	7,506
B_{2022}/B_{MSY}	2.39	2.34	4.22	2.95	2.49	2.53	2.24	2.46	2.39	2.69	4.30	1.32	1.91	2.33	1.98
B_{MSY}/B_0	0.292	0.292	0.290	0.295	0.294	0.285	0.299	0.293	0.291	0.291	0.277	0.297	0.370	0.292	0.294
u_{MSY}	0.0464	0.0464	0.0550	0.0463	0.0464	0.0463	0.0464	0.0464	0.0464	0.0462	0.0464	0.0463	0.0281	0.0464	0.0464
u_{2022}/u_{MSY}	0.505	0.517	0.0827	0.420	0.537	0.432	0.507	0.565	0.418	0.398	0.0850	0.520	0.833	1.02	0.482

Table F.21. Log likelihood (LL) values reported by central and sensitivity runs for survey indices, age composition (AF), recruitment, and total (not all LL components reported here)

Sen.Run	Label	CPUE	QCS	WCVI	WCHG	GIG	Index	AF	Recruit	Total
S00 (R75)	central run	-18.1	0.870	7.92	19.7	14.5	24.9	456	41.9	635
S01 (R78)	add 1997 WCHG index	-18.1	0.909	7.92	19.1	14.5	24.3	456	42.0	635
S02 (R79)	estimate M	-17.0	0.425	7.94	18.9	14.6	24.9	457	39.3	635
S03 (R80)	drop CPUE	0	0.659	7.94	19.2	14.3	42.2	706	51.8	912
S04 (R81)	Tweedie CPUE	-22.5	0.957	7.95	19.7	14.5	20.7	715	52.2	900
S05 (R82)	sigmaR=0.6	-16.8	0.610	7.75	19.4	14.2	25.2	483	55.5	675
S06 (R83)	sigmaR=1.2	-18.5	0.934	8.03	19.7	14.6	24.7	442	39.6	619
S07 (R84)	reduce catch 33%	-18.4	1.12	7.89	20.1	13.7	24.4	452	42.4	630
S08 (R85)	increase catch 50%	-17.4	0.572	7.94	19.2	15.4	25.8	460	42.9	640
S09 (R86)	upweight QC AF	-18.5	0.681	7.84	20.0	14.4	24.4	627	51.0	818
S10 (R87)	start Rdevs in 1970	-8.07	-0.807	8.25	16.4	12.1	27.9	540	21.0	701
S11 (R88)	no ageing error	-17.9	0.964	7.82	19.9	14.5	25.3	387	35.1	560
S12 (R91)	steepness h=0.5	-18.0	0.927	7.88	19.8	14.5	25.0	457	42.3	636
S13 (R92)	double 2021 catch	-18.1	0.872	7.92	19.7	14.5	24.9	459	42.0	638
S14 (R93)	AE from age readers	-17.9	0.735	7.95	19.4	14.4	24.7	443	40.7	621

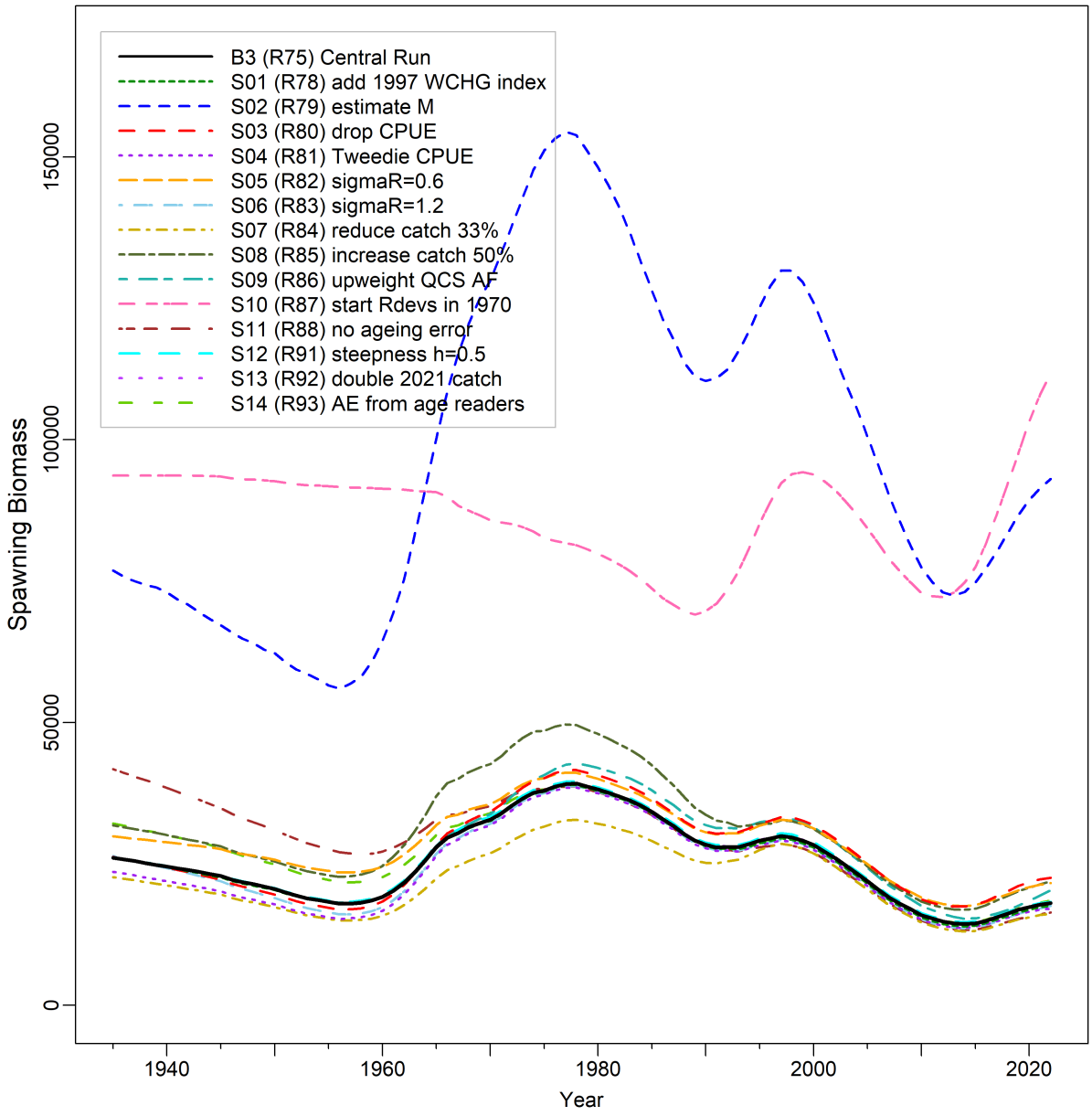

Figure F.36. YMR sensitivity: model trajectories of median spawning biomass (tonnes) for the central run of the composite base case and 14 sensitivity runs.

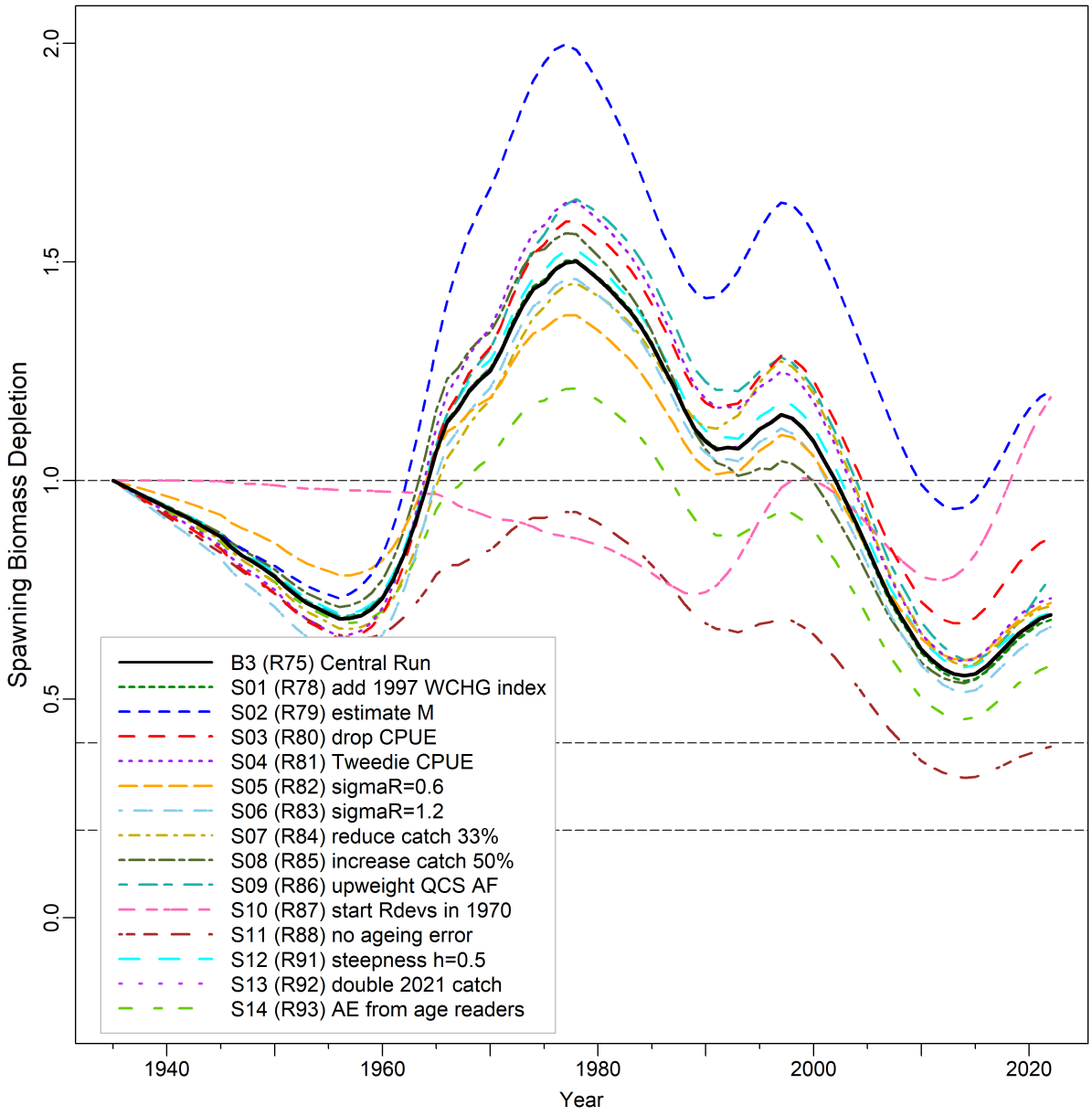

Figure F.37. YMR sensitivity: model trajectories of median spawning biomass as a proportion of unfished equilibrium biomass (B_t/B_0) for the central run of the composite base case and 14 sensitivity runs. Horizontal dashed lines show alternative reference points used by other jurisdictions: 0.2B_0 (~DFO's USR), 0.4B_0 (often a target level above B_{MSY}), and B_0 (equilibrium spawning biomass).

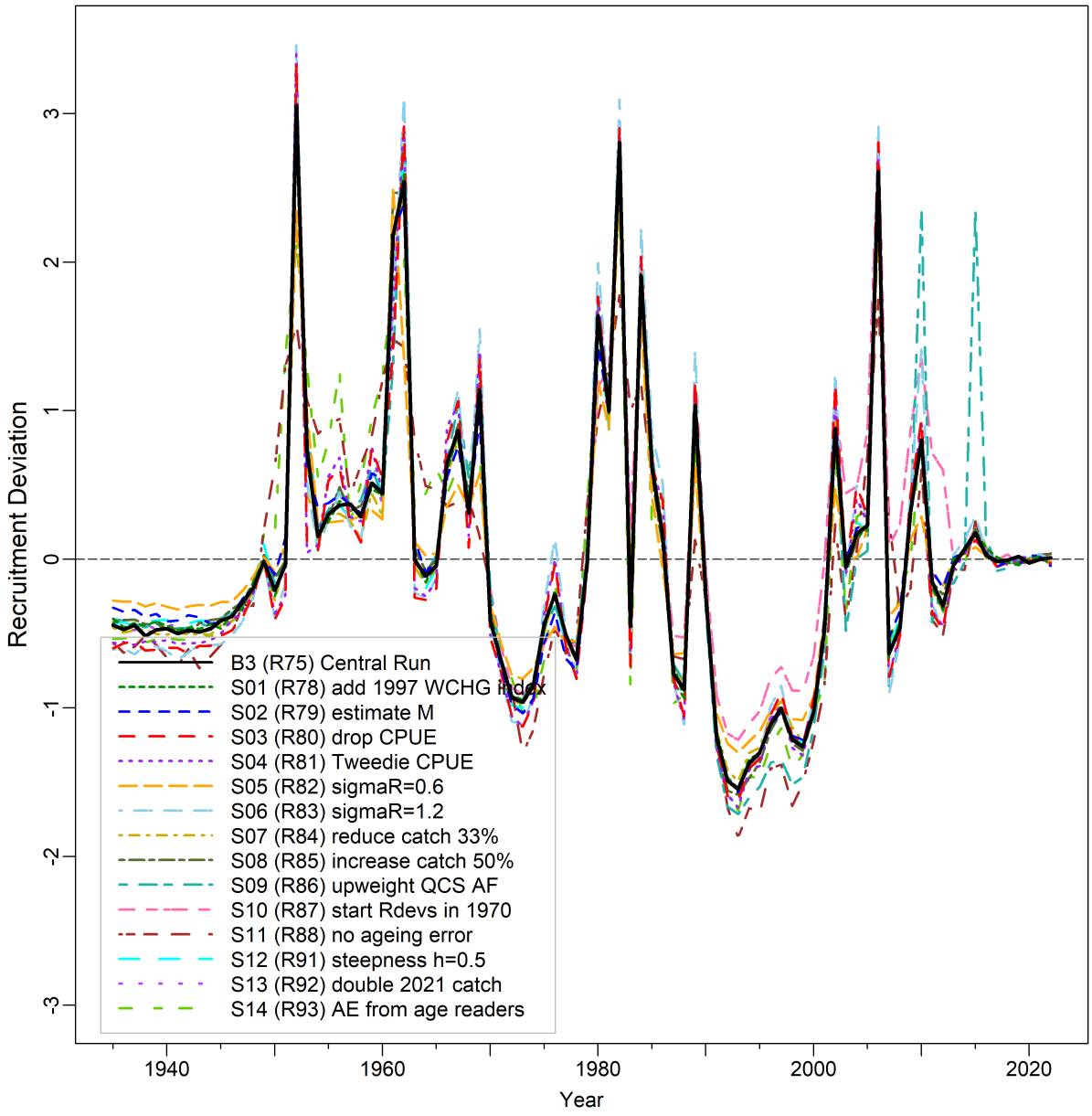

Figure F.38. YMR sensitivity: model trajectories of median recruitment deviations for the central run of the composite base case and 14 sensitivity runs.

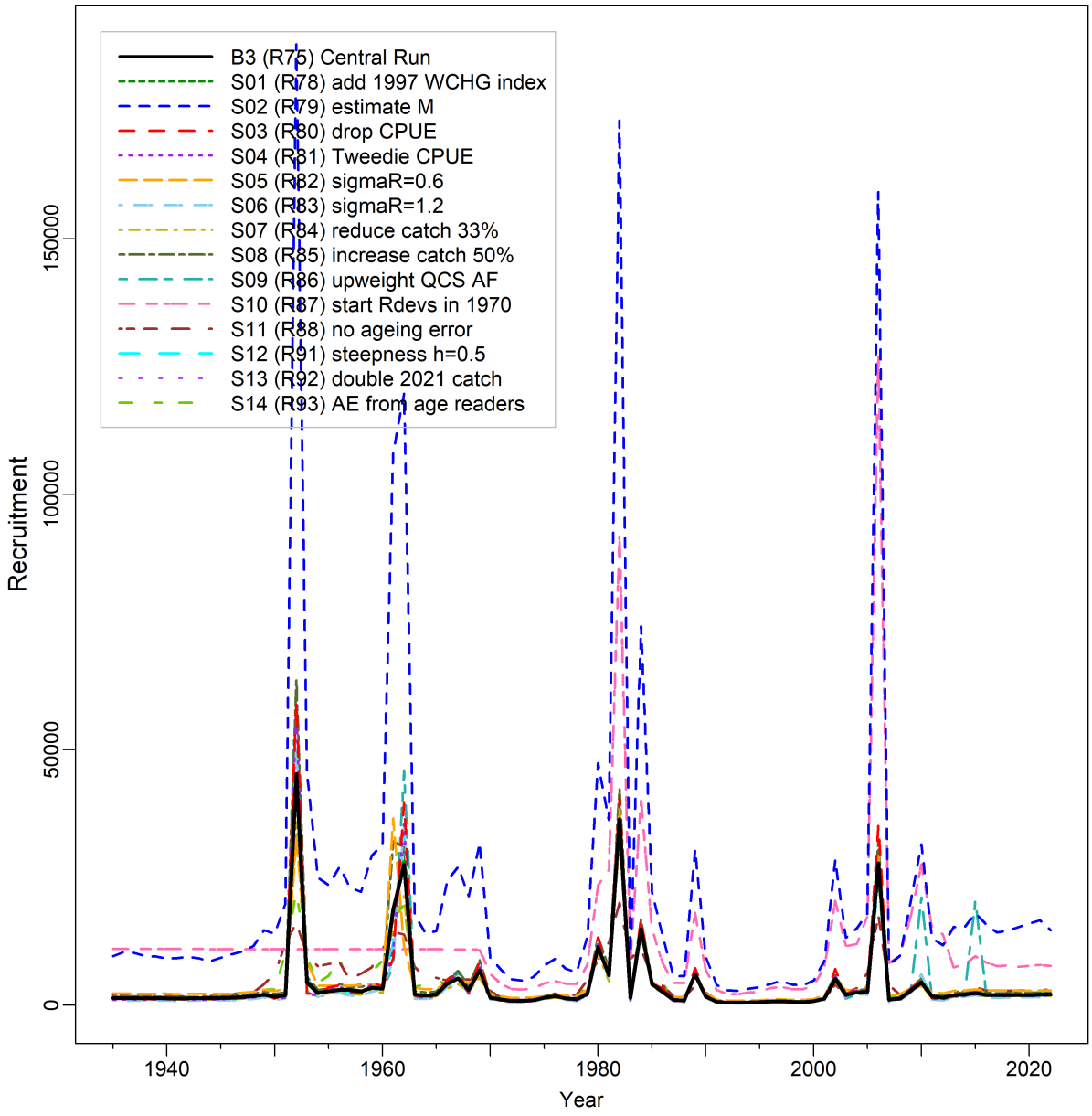

Figure F.39. YMR sensitivity: model trajectories of median recruitment of one-year old fish (R_t, 1000s) for the central run of the composite base case and 14 sensitivity runs.

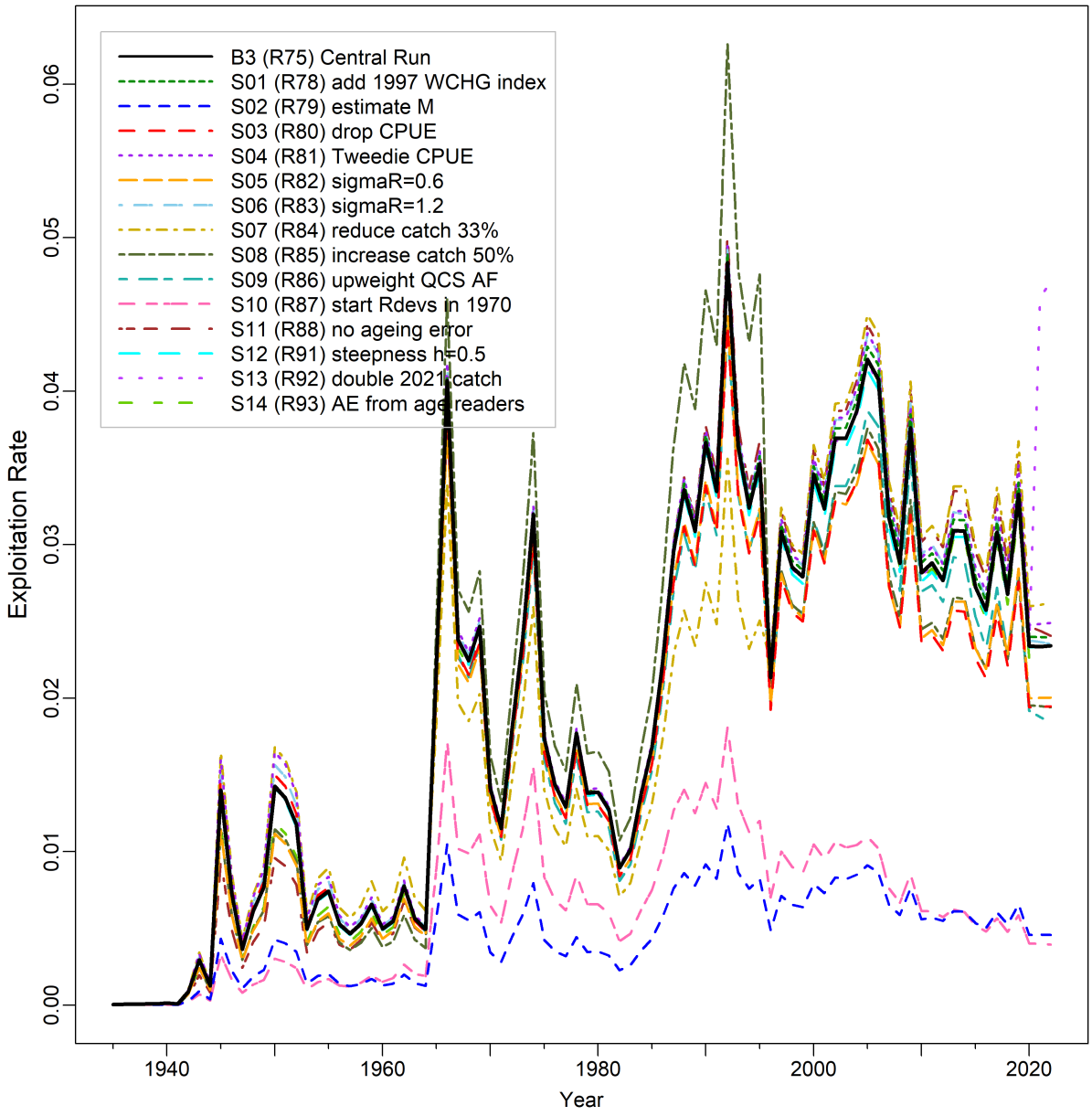

Figure F.40. YMR sensitivity: model trajectories of median exploitation rate of vulnerable biomass (u_t) for the central run of the composite base case and 14 sensitivity runs.

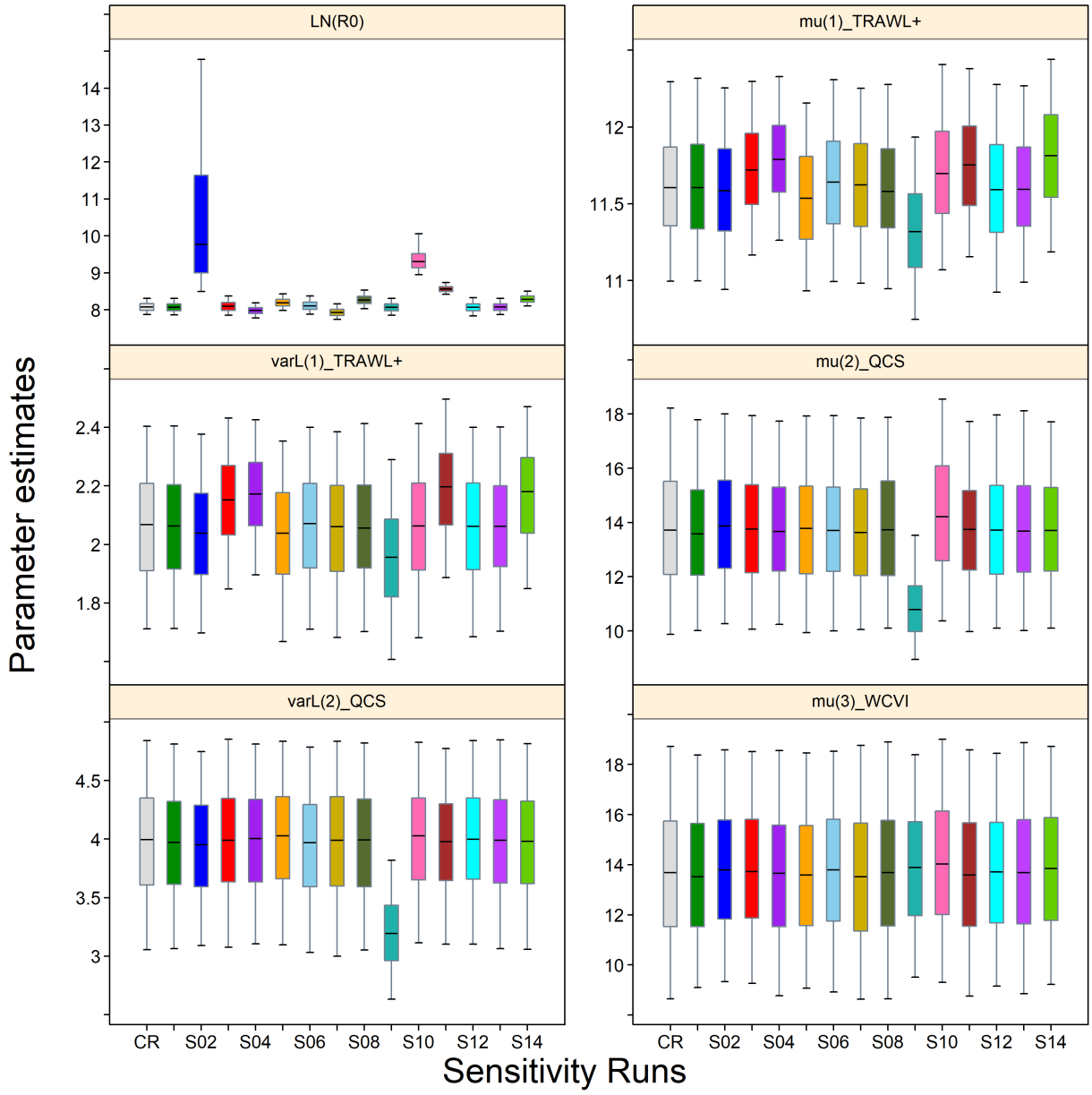

Figure F.41. YMR sensitivity: quantile plots of selected parameter estimates ($\log R_0$, $\mu_{g=1,2,3}$, $\log v_{Lg=1,2}$) comparing the central run with 14 sensitivity runs. See text on sensitivity numbers. The boxplots delimit the 0.05, 0.25, 0.5, 0.75, and 0.95 quantiles; outliers are excluded.

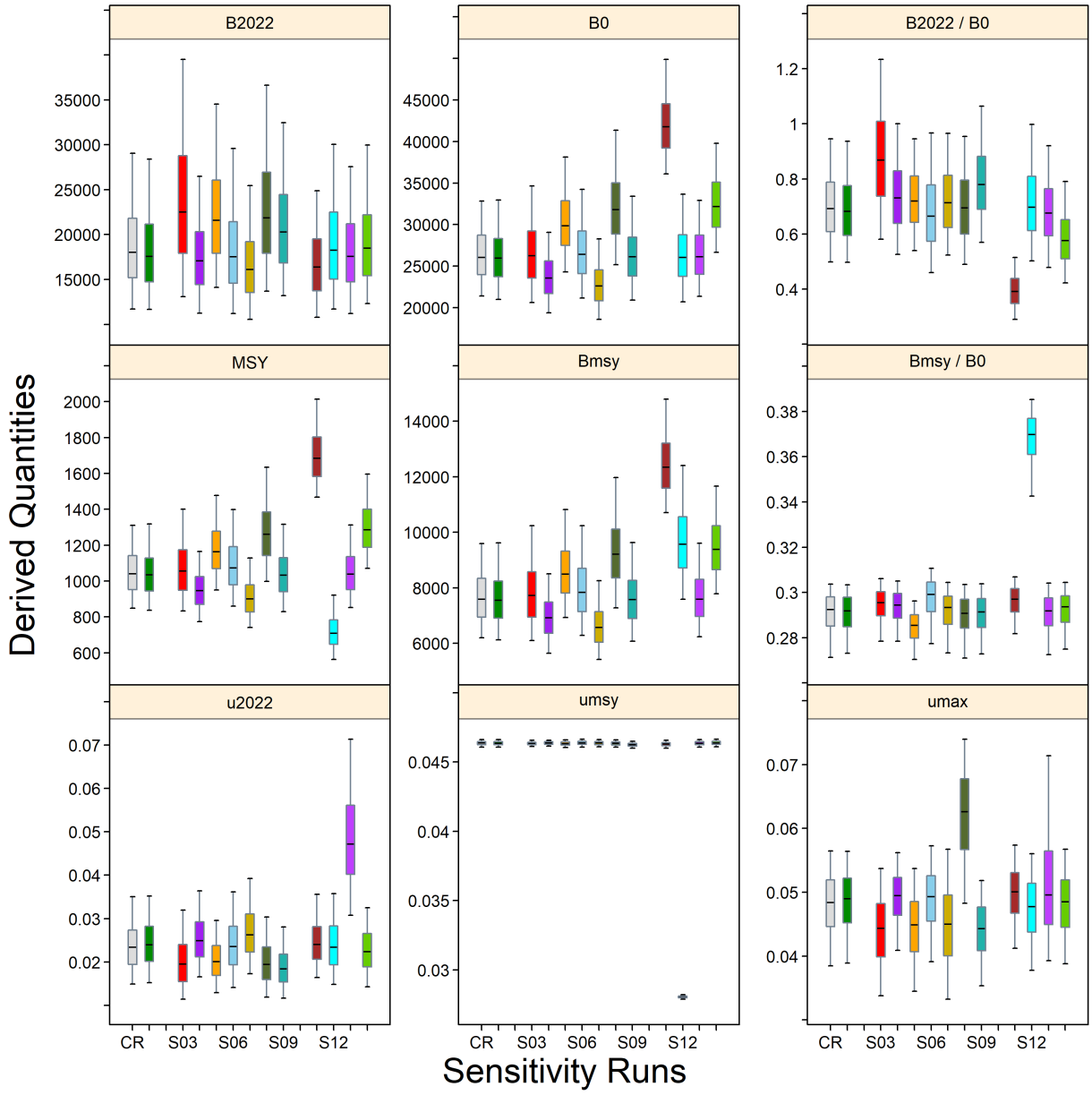

Figure F.42. YMR sensitivity: quantile plots of selected derived quantities (B_{2022}, B_0, B_{2022}/B_0, MSY, B_{MSY}, B_{MSY}/B_0, u_{2021}, u_{MSY}, u_{max}) comparing the central run with 12 sensitivity runs (S02 and S10 omitted because biomass scale overwhelms that of the others, see Table F.20). See text on sensitivity numbers. The boxplots delimit the 0.05, 0.25, 0.5, 0.75, and 0.95 quantiles; outliers are excluded.

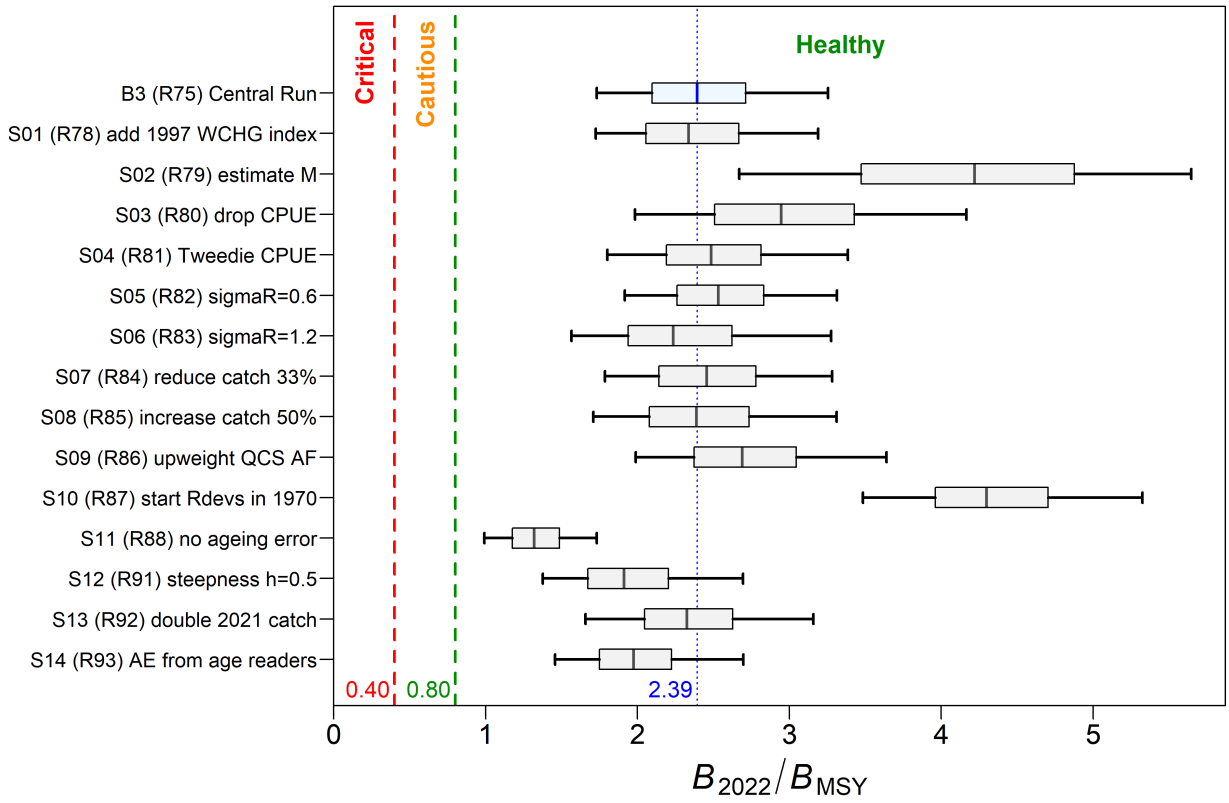

Figure F.43. YMR sensitivity: stock status at beginning of 2022 relative to the DFO PA provisional reference points of 0.4B_{MSY} and 0.8B_{MSY} for the central run of the composite base case (Run75) and 14 sensitivity runs. Vertical dotted line uses median of the central run to faciliate comparisons with sensitivity runs. Boxplots show the 0.05, 0.25, 0.5, 0.75, and 0.95 quantiles from the MCMC posterior.

F.3. REFERENCES – MODEL RESULTS

Edwards, A.M., Haigh, R. and Starr, P.J. 2012. Stock assessment and recovery potential assessment for Yellowmouth Rockfish (*Sebastes reedi*) along the Pacific coast of Canada. DFO Can. Sci. Advis. Sec. Res. Doc. 2012/095. iv + 188 p.

Forrest, R.E., Holt, K.R. and Kronlund, A.R. 2018. Performance of alternative harvest control rules for two Pacific groundfish stocks with uncertain natural mortality: bias, robustness and trade-offs. Fish. Res. 206. 259–286.

Knaus, J. 2015. snowfall: Easier cluster computing (based on snow). R package version 1.84-6.1.

McAllister, M.K. and Ianelli, J.N. 1997. Bayesian stock assessment using catch-age data and the sampling – importance resampling algorithm. Can. J. Fish. Aquat. Sci. 54(2). 284–300.

Monnahan, C.C., Branch, T.A., Thorson, J.T., Stewart, I.J. and Szuwalski, C.S. 2019. Overcoming long Bayesian run times in integrated fisheries stock assessments. ICES J. Mar. Sci. 76(6). 1477–1488.

Monnahan, C.C. and Kristensen, K. 2018. No-U-turn sampling for fast Bayesian inference in ADMB and TMB: Introducing the adnuts and tmbstan R packages. PLoS ONE 13(5). e0197,954.

N.Z. Min. Fish. 2011. Operational Guidelines for New Zealand's Harvest Strategy Standard. Ministry of Fisheries, New Zealand.

APPENDIX G. ECOSYSTEM INFORMATION

This appendix describes ecosystem information relevant to Yellowmouth Rockfish (YMR, GFBioSQL code '440') along the British Columbia (BC) coast. Some of these analyses compare a northern population (PMFC areas 5DE) with a southern one (PMFC areas 3CD5ABC); however, the stock assessment treats the coastwide population of YMR as a single stock. The information in this appendix provides information that might be useful to other agencies and supports the interpretation of YMR spatial and biological information.

G.1. SPATIAL DISTRIBUTION

Data for spatial analyses of YMR were extracted from the SQL DFO databases 'PacHarvest[16]' and 'GFFOS[17]' on Jan 25, 2021. Some of the analyses below are designed to facilitate the reporting of findings to COSEWIC (Committee on the Status of Endangered Wildlife in Canada), regardless of its assessed status.

Yellowmouth Rockfish is ubiquitous along the BC coast, with CPUE hotspots in the three gullies of Queen Charlotte Sound, off NW Vancouver Island , and off Rennell Sound (Figure G.1). Densities appear to be low off the west coast of Vancouver Island south of Brooks Peninsula and in Hecate Strait. Broadly, the 'extent of occurrence' (EO) for YMR covers 114,943 km^2 (on water and excluding seamounts data) using historical fishing events (1982-2020) to determine a convex hull envelope (Figure G.2). Of the bottom trawl tows capturing YMR, 98% of the tows have starting depths between 130 m and 402 m (Figure G.3). By region, these boundaries deepen to 199-466 m in the north (5DE, Figure G.4) but remain similar at 127-391 m in the south (3CD5ABC, Figure G.5). Using the coastwide YMR bottom-tow depth range as a proxy for suitable YMR benthic habitat, a refined estimate of EO is 44,654 km^2 in BC's Exclusive Economic Zone (Figure G.6). To estimate the 'area of occupancy' (AO), the catch of YMR was located within a grid comprising 4 km^2 cells (2km × 2km), and the cells occupied by YMR were summed to estimate an AO of 13,652 km^2 along the BC coast spanning 25 years (Figure G.7). An alternative depiction of YMR catch is summarised by fishery in DFO fishing localities – Trawl (Figure G.8), Halibut (Figure G.9), Sablefish (Figure G.10), Dogfish/Lingcod (Figure G.11), and H&L Rockfish (Figure G.12).

[16] PacHarvest (or PacHarv) was the DFO database, managed by the Pacific region's Groundfish Section, housing the trawl fishery's observer data from 1996 to 2007. Fisherlogs were also added to PacHarvest and all records (observer and fisher) were reconciled with the official landings from the dockside monitoring program.

[17] GFFOS is the Groundfish interface to DFO's current database platform for catch statistics called 'Fishery Operation System'. Groundfish catch records from the H&L fisheries were switched to GFFOS in 2006 while those from the trawl fisheries were switched to GFFOS in 2007.

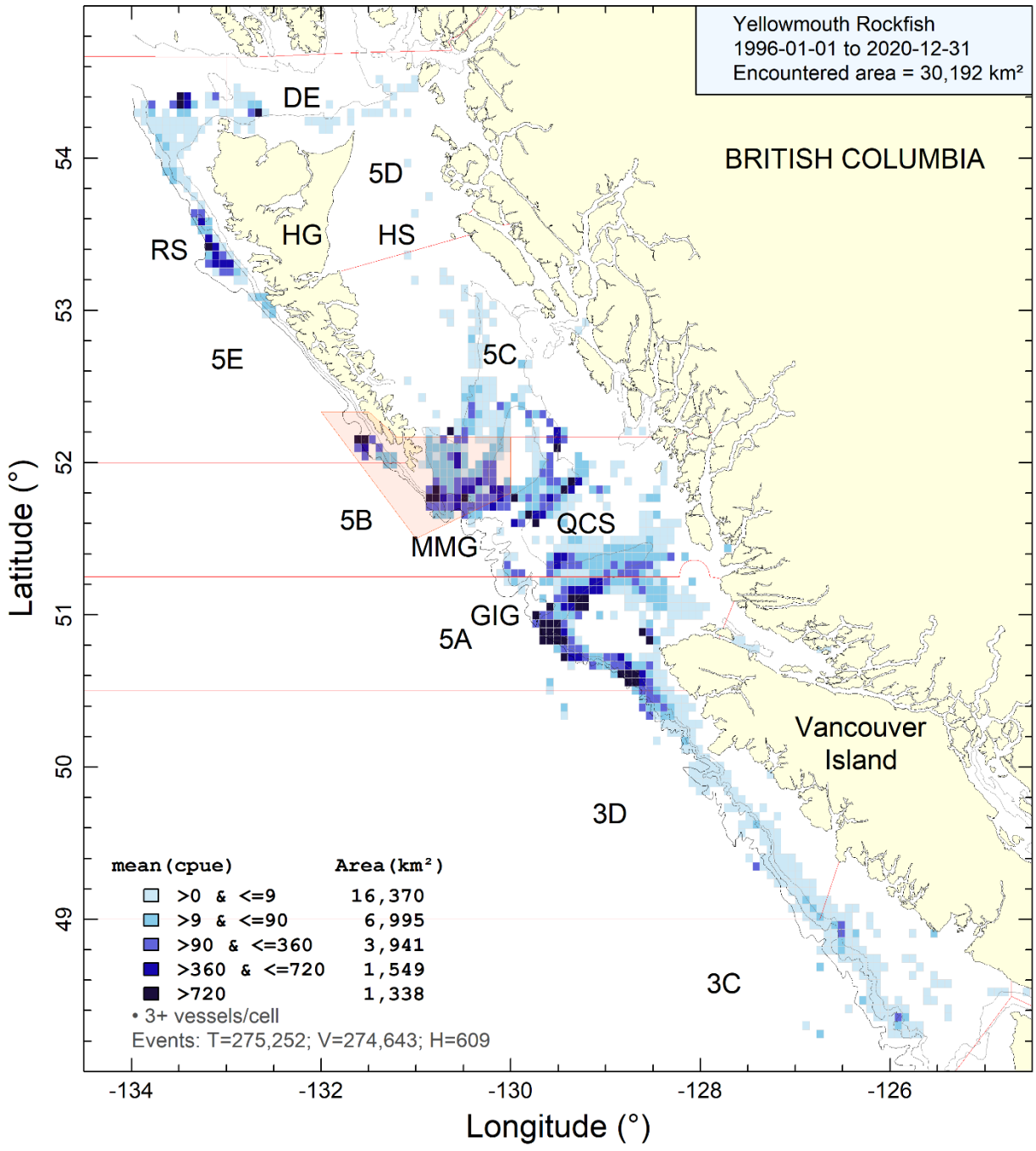

Figure G.1. CPUE density of YMR from trawl tows (bottom and midwater) occurring from 1996 to 2020. DE = Dixon Entrance, GIG = Goose Island Gully, HG = Haida Gwaii, HS = Hecate Strait, MMG = Moresby and Mitchell's Gullies, QCS = Queen Charlotte Sound, RS = Rennell Sound. Shaded polygon shows the extension of area 5C for managing Pacific Ocean Perch and Yellowmouth Rockfish, primarily to capture Moresby Gully as a single management unit.

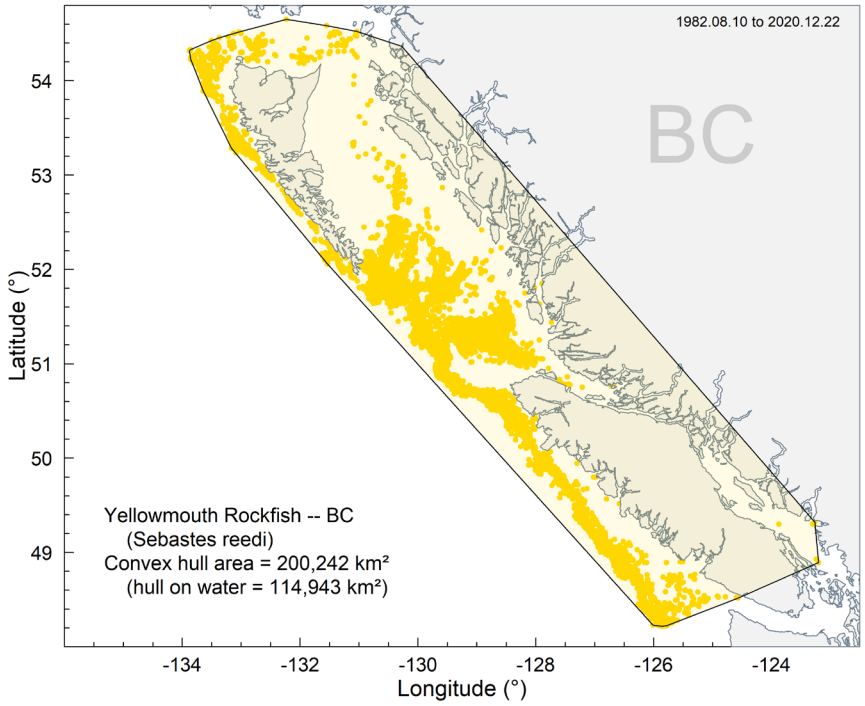

Figure G.2. Extent of Occurrence as a convex hull surrounding fishing events that caught YMR along the BC coast; the shading within the hull on water covers 114,943 km^2.

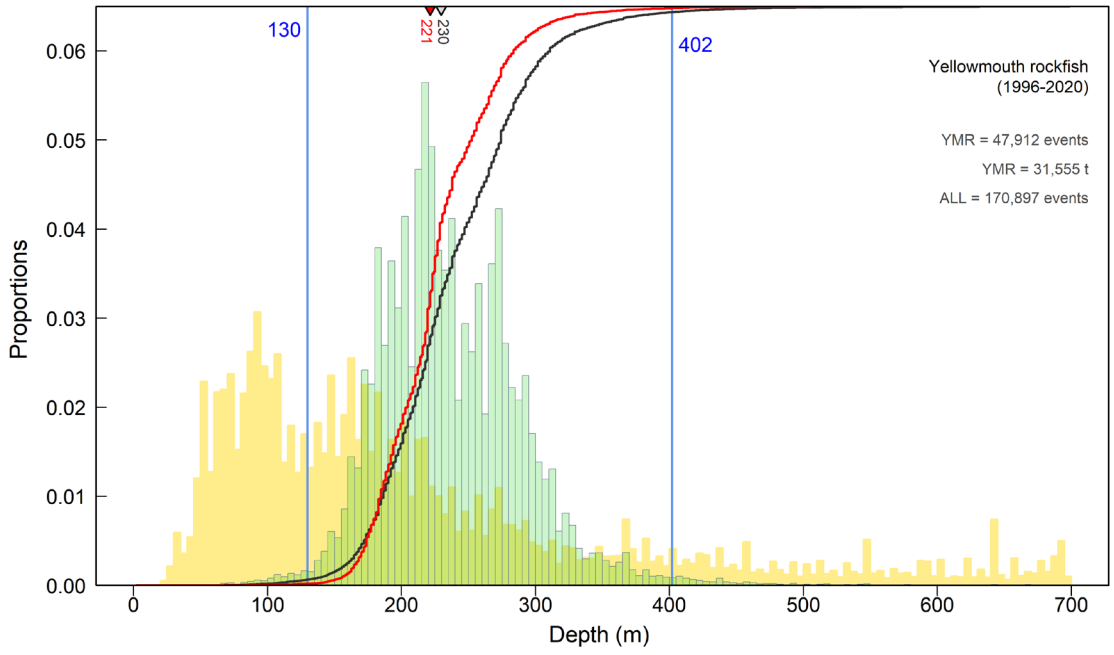

Figure G.3. YMR coastwide – Depth frequency of bottom trawl tows (green histogram) that captured YMR from commercial logs (1996-2020 in PacHarvest and GFFOS) in PMFC areas 3CD5ABCDE. The vertical solid lines denote the 0.01 and 0.99 quantiles. The black curve shows the cumulative frequency of tows that encounter YMR while the red curve shows the cumulative catch of YMR at depth (scaled from 0 to 1). The median depths of YMR encounters (inverted grey triangle) and of cumulative catch (inverted red triangle) are indicated along the upper axis. The yellow histogram in the background reports the relative trawl effort on all species offshore down to 1000 m.

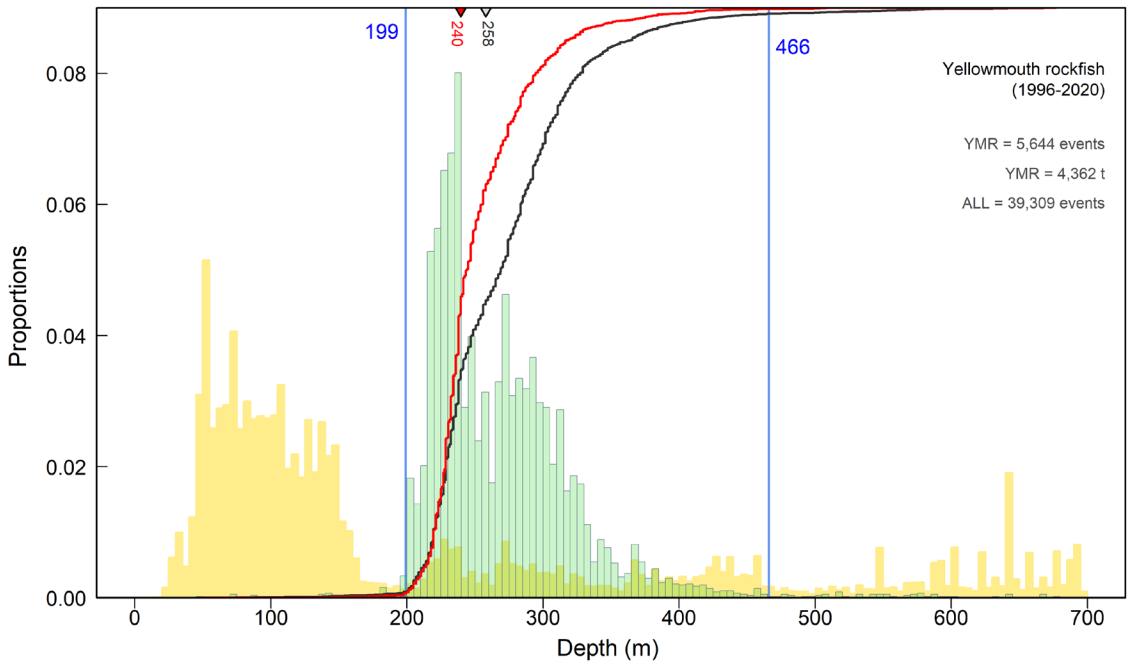

Figure G.4. YMR north – Depth frequency of bottom trawl tows (green histogram) that captured YMR from commercial logs (1996-2020 in PacHarvest and GFFOS) in PMFC areas 5DE. See Figure G.2 caption for additional details.

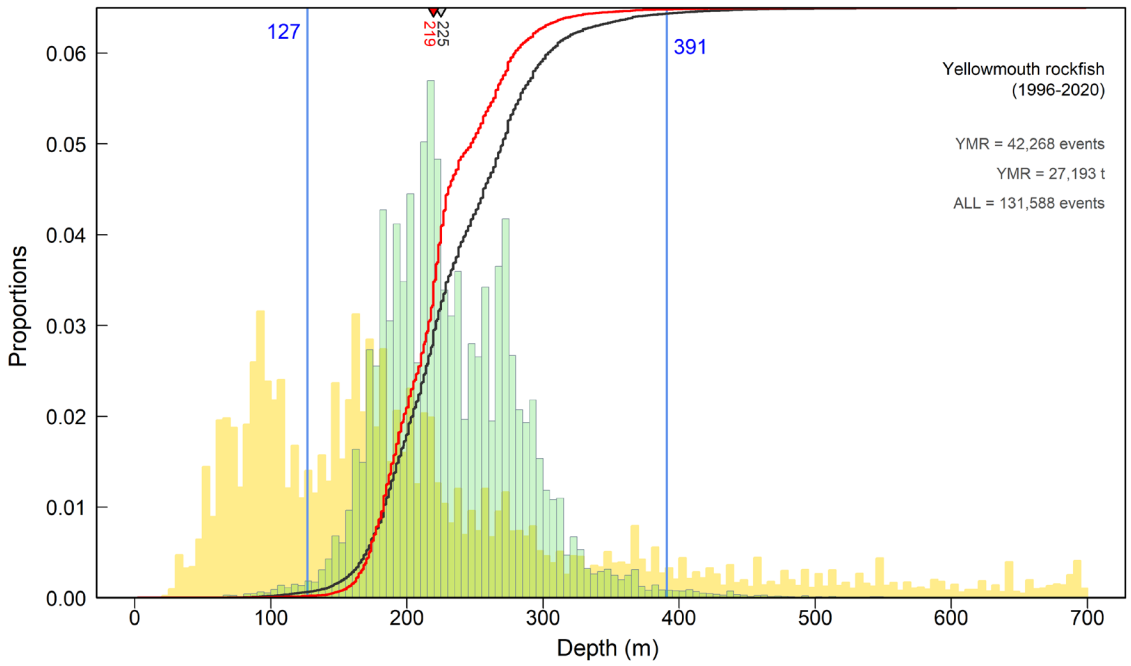

Figure G.5. YMR south – Depth frequency of bottom trawl tows (green histogram) that captured YMR from commercial logs (1996-2020 in PacHarvest and GFFOS) in PMFC areas 3CD5ABC. See Figure G.2 caption for additional details.

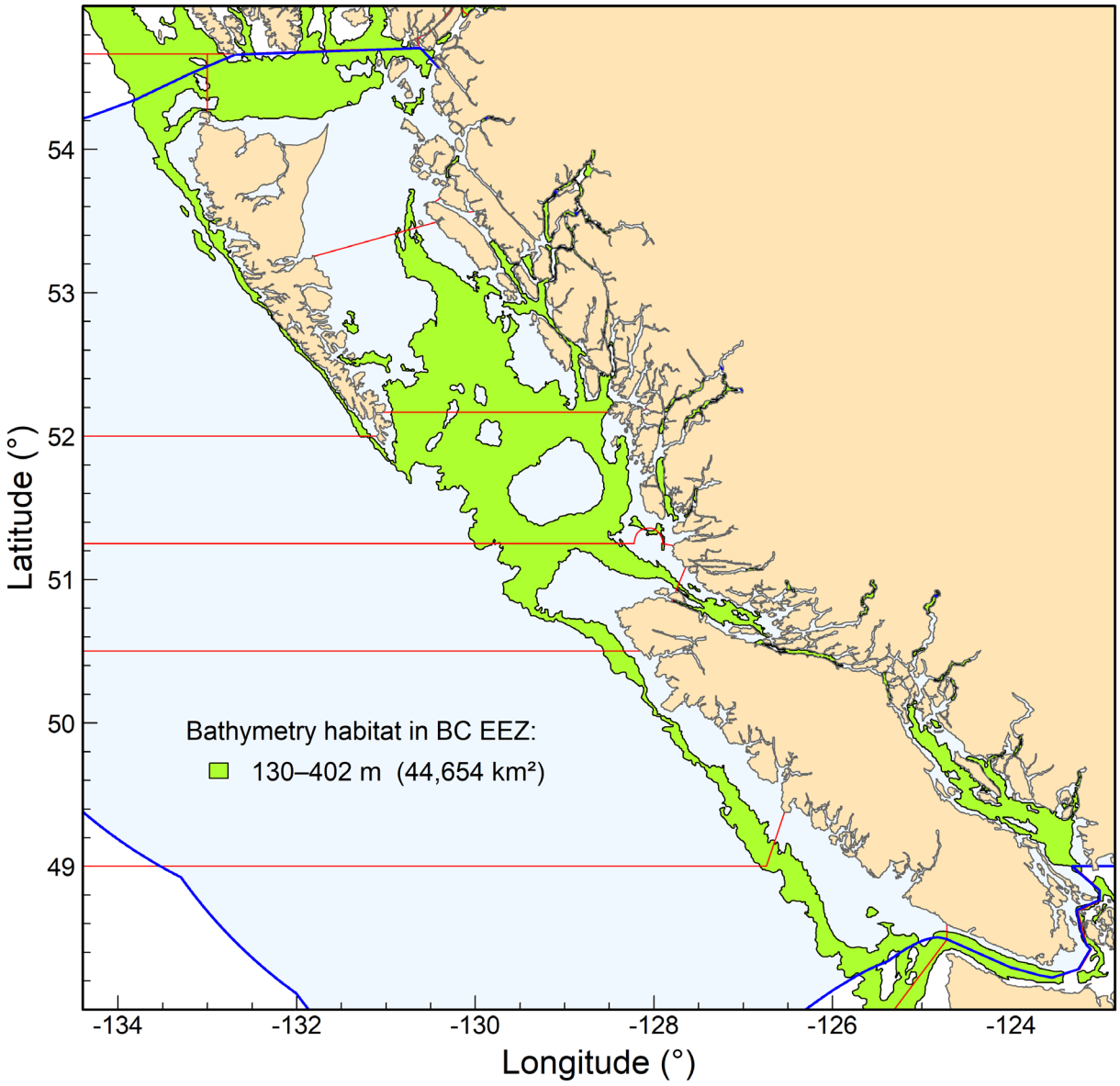

Figure G.6. Highlighted bathymetry (green) between 130 and 402 m serves as a proxy for benthic habitat along the BC coast for YMR. The green highlighted region within Canada's exclusive economic zone (EEZ, blue highlighted area) covers 44,654 km^2. The boundaries in red delimit PMFC areas.

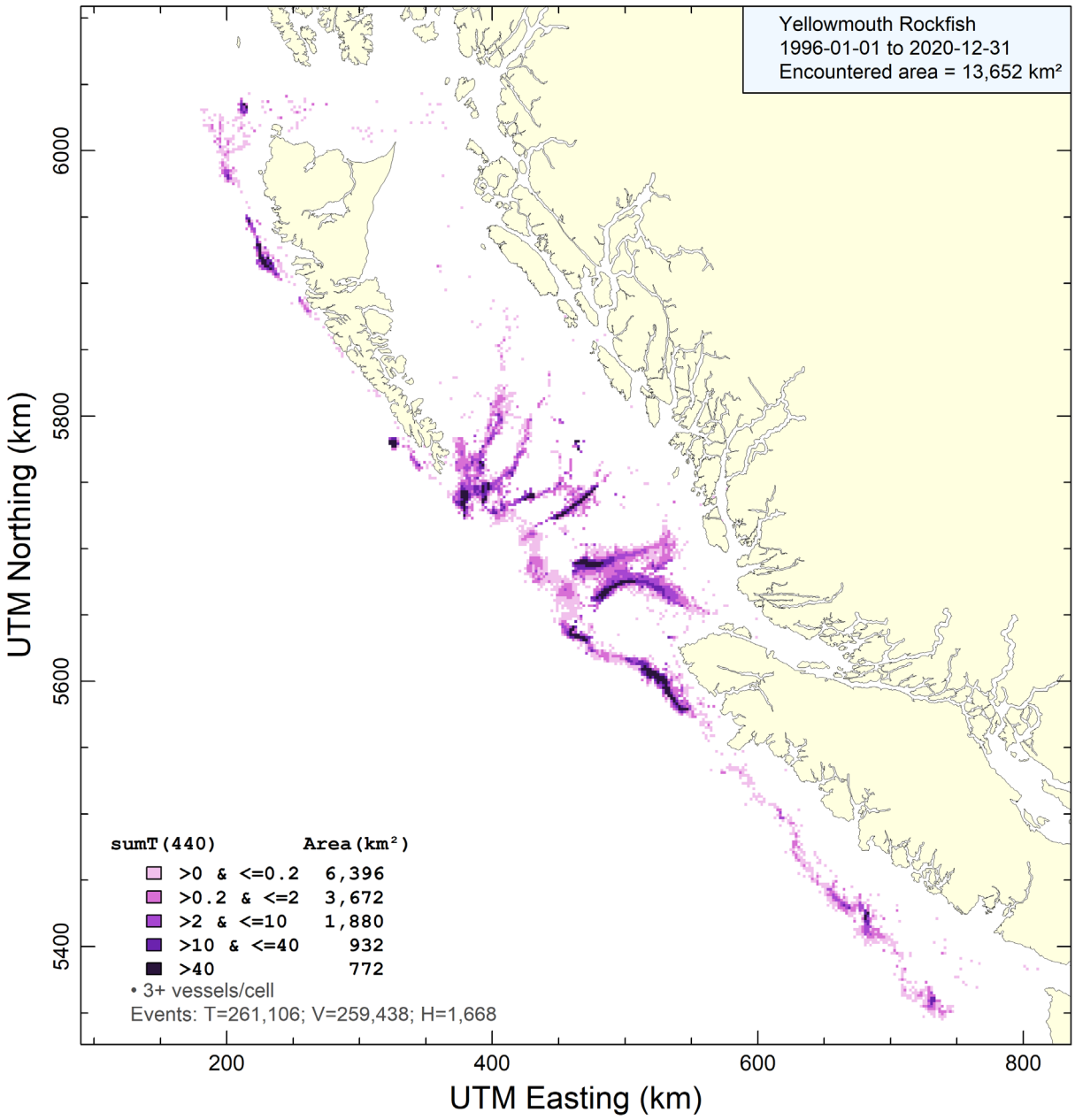

Figure G.7. Area of Occupancy (AO) determined by bottom trawl capture of YMR in grid cells 2km × 2km. Cells with fewer than three fishing vessels are excluded. The estimated AO is 13,652 km^2 along the BC coast.

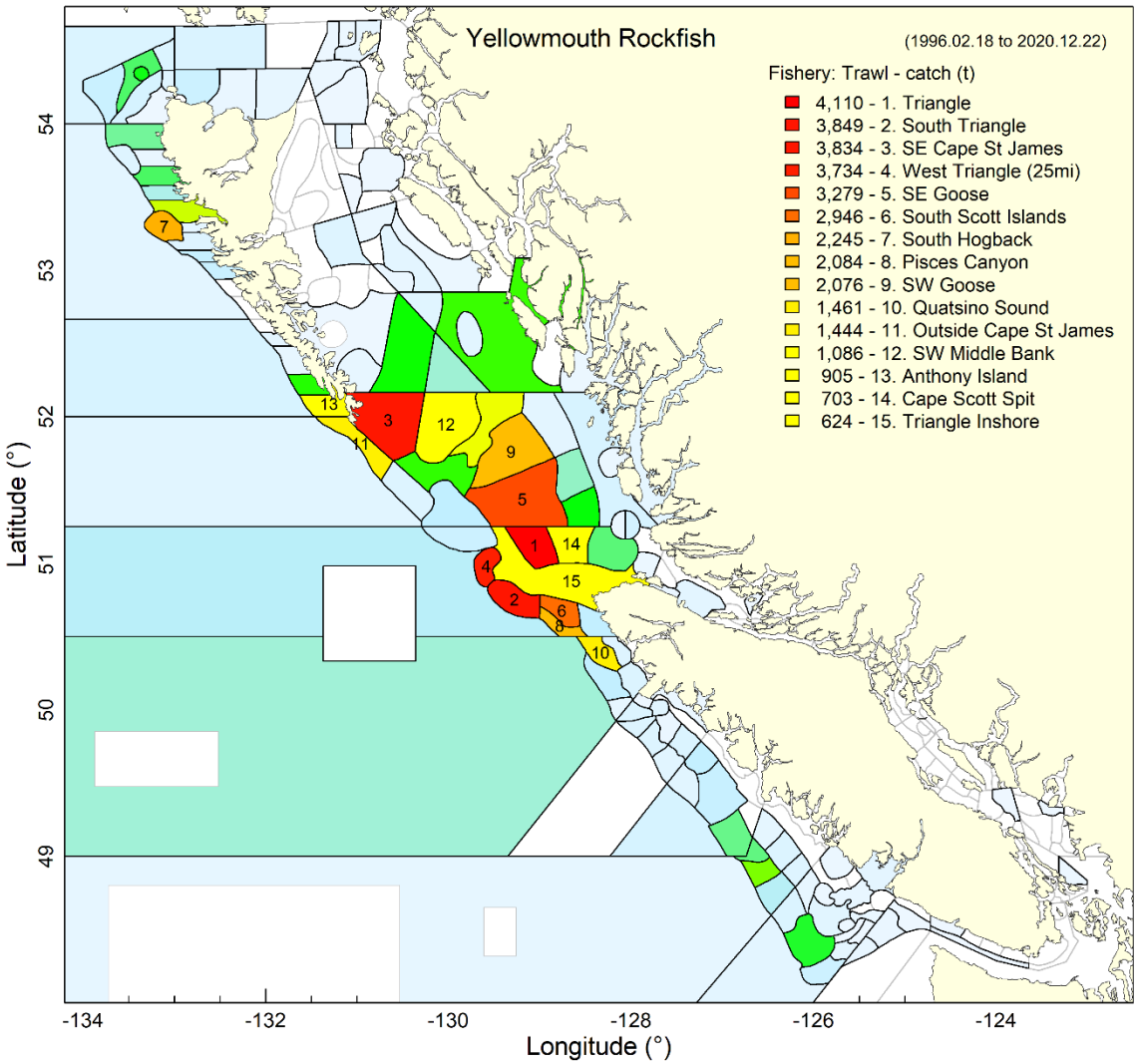

Figure G.8. YMR Trawl – Top 15 fishing localities by total catch (tonnes) where YMR was caught by the trawl fishery. All shaded localities indicate areas where YMR was encountered from 1996 to 2020, ranging from relatively low numbers in cool blue, through the spectrum, to relatively high catches in red. Seamount catches are excluded.

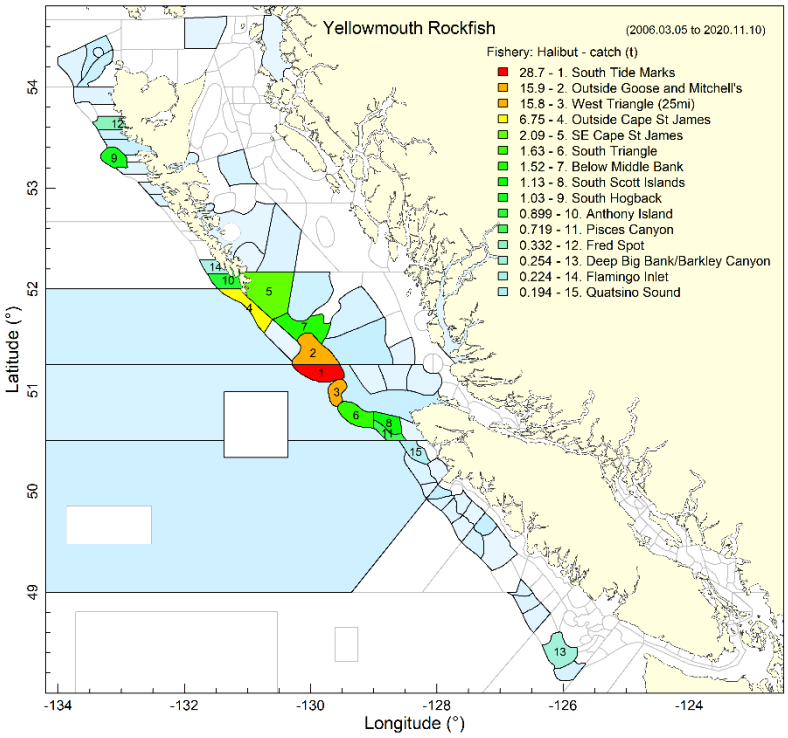

Figure G.9. YMR Halibut – Top 15 fishing localities by total catch (tonnes) where YMR was caught by the halibut fishery. See Figure G.8 caption for further details.

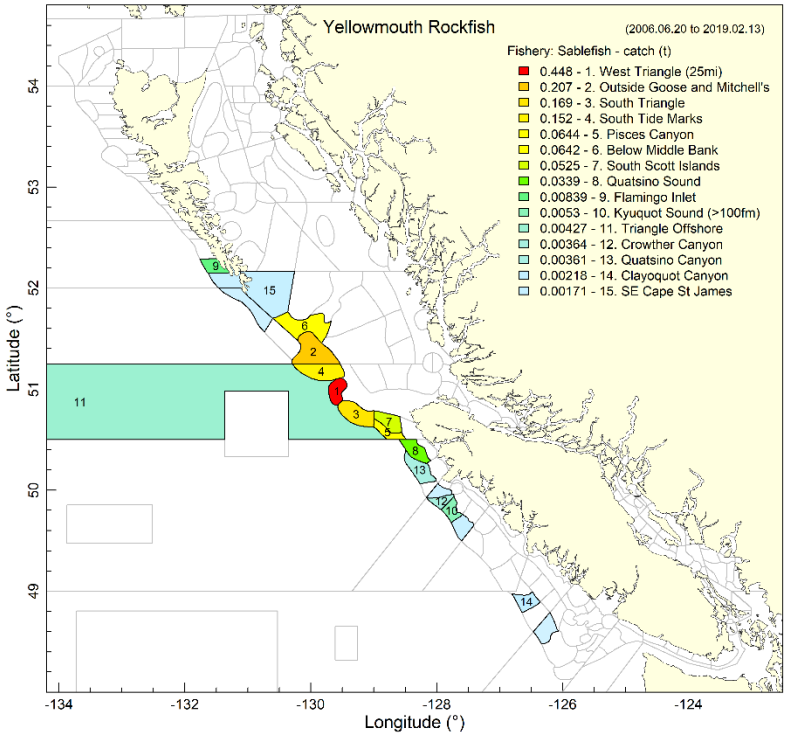

Figure G.10. YMR Sablefish – Top 15 fishing localities by total catch (tonnes) where YMR was caught by the sablefish fishery. See Figure G.8 caption for further details.

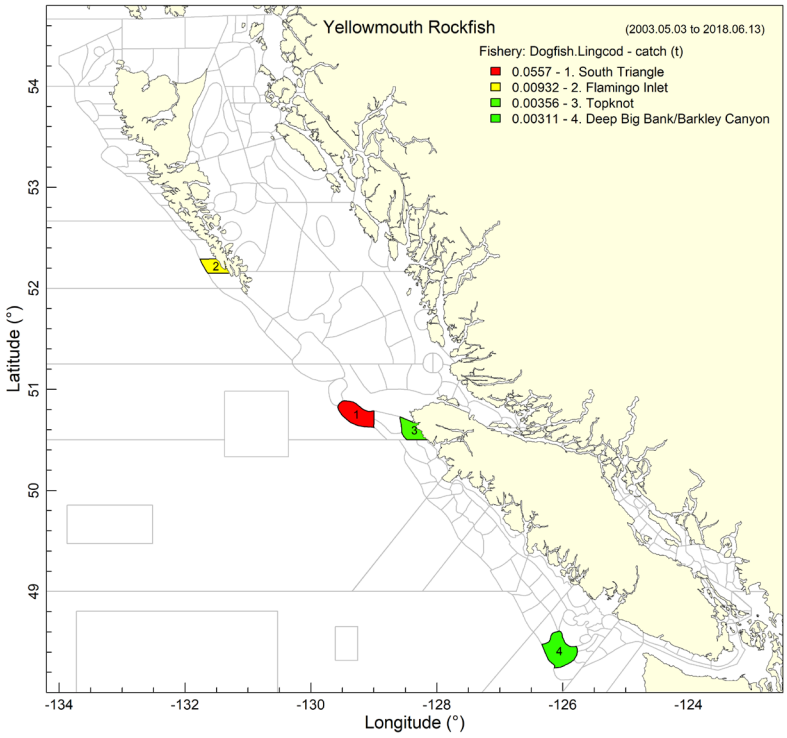

Figure G.11. YMR Dogfish/Lingcod – Top 15 fishing localities by total catch (tonnes) where YMR was caught by the dogfish/lingcod (formerly Schedule II) fishery. See Figure G.8 caption for further details.

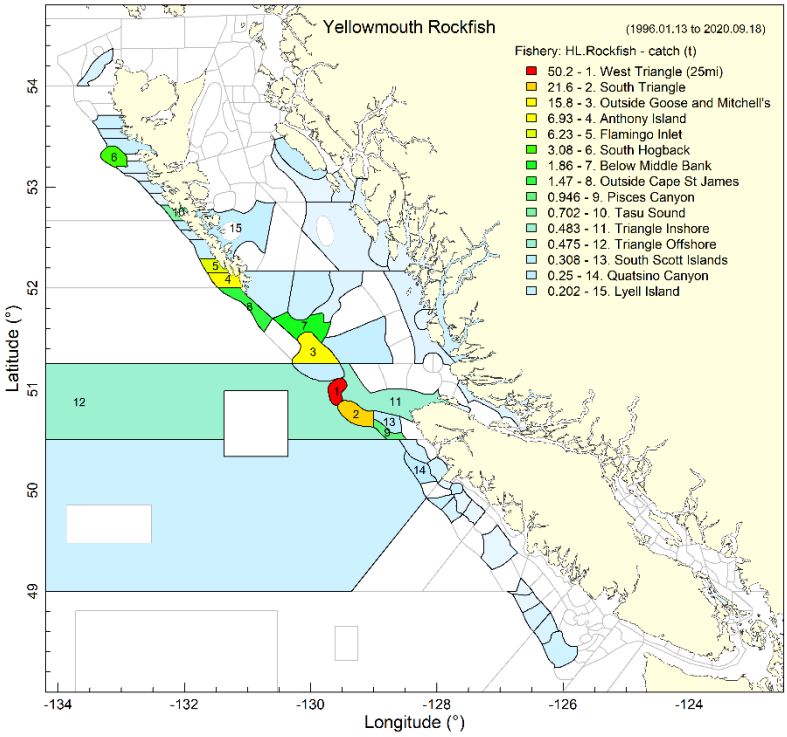

Figure G.12. YMR H&L Rockfish – Top 15 fishing localities by total catch (tonnes) where YMR was caught by the hook and line rockfish (Outside H&L, formerly ZN) fishery. See Figure G.8 caption for further details.

G.2. CONCURRENT SPECIES

Species caught concurrently in coastwide bottom trawl tows that captured at least one YMR specimen comprised, by region:

- Coastal BC (3CD+5ABCDE):
  23% Pacific Ocean Perch, 20% Arrowtooth Flounder, 9% Yellowtail Rockfish,
  6% Yellowmouth Rockfish, and 6% Dover Sole by weight (Table G.1, Figure G.13);
- North (5DE):
  43% POP, 15% Rougheye/Blackspotted Rockfish, 10% Silvergray Rockfish,
  7% Yellowmouth Rockfish, and 6% Redstripe Rockfish (Table G.2, Figure G.14);
- South (3CD5ABC):
  species mix was similar to that for the coast (Table G.3, Figure G.15).

The other gear type that intercepts YMR on a regular basis is midwater trawl (hook and line and trap gears catching YMR are dominated by Pacific Halibut [55%] and Sablefish [96%]). Of the midwater trawl events capturing at least one YMR specimen, catches comprised

- Pacific Hake (coast: 83%, 5DE: 61%, 3CD5AB: 84%),
- Yellowtail Rockfish(coast: 6%, 5DE: 4%, 3CD5AB: 6%),
- Widow Rockfish (coast: 5%, 5DE: 19%, 3CD5AB: 5%), and
- Walleye Pollock (coast: 2%, 5DE: 9%, 3CD5AB: 1%),

amongst others (see Tables G.1-G.3 and Figures G.13-G.15).

To explore how YMR coastwide is associated with other rockfish in bottom trawl tows, 28 rockfish species caught by YMR bottom trawl gear were grouped by `clara` (clustering large applications) using R's package cluster (Maechler et al. 2018). The top ten rockfish species in terms of total catch summed over the period 1996–2020 for each fishery are listed in Table G.1.

The cluster analysis on commercial bottom trawl catch (Figure G.16, see caption for species abbreviations) shows that the primary group featuring YMR (red) also includes POP and SST. These three species commonly co-occur in trawl tows, and the cluster occurs primarily in the three major gullies of Queen Charlotte Sound (Moresby, Mitchell's, and Goose Island, from north to south). The remaining clusters have decreasing associations with YMR; however, they highlight triplets of species that characterise BC waters, at least through the lens of the commercial fishery. A secondary cluster (orange) represented by QBR-RSR-RBR is found in shallower waters of Hecate Strait and Goose Island Bank. The remaining four groups are dominated by other rockfish species: group 3 (yellow, SGR) occurs in the central coast region; group 4 (light green, YTR) inhabits shelf regions, group 5 (dark green, SST) occurs in deeper regions along the shelf-slope boundary, and group 6 (blue, CAR) is scattered in shallow areas, primarily off WCVI.

Table G.1. YMR coastwide – Top 10 species by catch weight (sum of landed + discarded 1996-2020) that co-occur in YMR fishing events by gear type in PMFC areas 3CD5ABCDE (Figure G.13). Rockfish species of interest to COSEWIC appear in red font, target species (occur in every tow) appear in blue font.

Code*	Species	Latin Name	Catch (tonnes)	Catch (%)	∑Catch (%)
Gear:	**Bottom Trawl**				
396	Pacific Ocean Perch	*Sebastes alutus*	114,749	23.2	23.2
602	Arrowtooth Flounder	*Atheresthes stomias*	98,891	20.0	43.2
418	Yellowtail Rockfish	*Sebastes flavidus*	45,201	9.15	52.4
440	Yellowmouth Rockfish	*Sebastes reedi*	31,837	6.44	58.8
626	Dover Sole	*Microstomus pacificus*	29,538	5.98	64.8
405	Silvergray Rockfish	*Sebastes brevispinis*	29,111	5.89	70.7
439	Redstripe Rockfish	*Sebastes proriger*	16,392	3.32	74.0
437	Canary Rockfish	*Sebastes pinniger*	15,195	3.08	77.1
467	Lingcod	*Ophiodon elongatus*	12,893	2.61	79.7
044	Spiny Dogfish	*Squalus acanthias*	10,437	2.11	81.8
Gear:	**Hook and Line****				
614	Pacific Halibut	*Hippoglossus stenolepis*	50,719	54.8	54.8
455	Sablefish	*Anoplopoma fimbria*	12,065	13.0	67.9
394	Rougheye/Blackspotted	*S. aleutianus/melanostictus*	6,410	6.93	74.8
044	Spiny Dogfish	*Squalus acanthias*	6,093	6.59	81.4
059	Longnose Skate	*Raja rhina*	3,823	4.13	85.5
401	Redbanded Rockfish	*Sebastes babcocki*	3,504	3.79	89.3
467	Lingcod	*Ophiodon elongatus*	3,087	3.34	92.6
442	Yelloweye Rockfish	*Sebastes ruberrimus*	1,765	1.91	94.6
403	Shortraker Rockfish	*Sebastes borealis*	941	1.02	95.6
405	Silvergray Rockfish	*Sebastes brevispinis*	917	0.99	96.6
Gear:	**Midwater Trawl**				
225	Pacific Hake	*Merluccius productus*	542,671	83.4	83.4
418	Yellowtail Rockfish	*Sebastes flavidus*	36,279	5.58	89.0
417	Widow Rockfish	*Sebastes entomelas*	31,932	4.91	93.9
228	Walleye Pollock	*Theragra chalcogramma*	15,211	2.34	96.3
439	Redstripe Rockfish	*Sebastes proriger*	5,659	0.87	97.1
440	Yellowmouth Rockfish	*Sebastes reedi*	5,155	0.79	97.9
396	Pacific Ocean Perch	*Sebastes alutus*	5,044	0.78	98.7
437	Canary Rockfish	*Sebastes pinniger*	1,802	0.28	99.0
405	Silvergray Rockfish	*Sebastes brevispinis*	1,119	0.17	99.2
044	Spiny Dogfish	*Squalus acanthias*	1,102	0.17	99.3
Gear:	**Trap*****				
455	Sablefish	*Anoplopoma fimbria*	5,945	96.3	96.3
394	Rougheye/Blackspotted	*S. aleutianus/melanostictus*	84	1.37	97.7
614	Pacific Halibut	*Hippoglossus stenolepis*	84	1.35	99.0
602	Arrowtooth Flounder	*Atheresthes stomias*	33	0.54	99.6
044	Spiny Dogfish	*Squalus acanthias*	9	0.15	99.7
401	Redbanded Rockfish	*Sebastes babcocki*	8	0.13	99.9
467	Lingcod	*Ophiodon elongatus*	4	0.06	99.9
403	Shortraker Rockfish	*Sebastes borealis*	1	0.01	99.9
451	Shortspine Thornyhead	*Sebastolobus alascanus*	1	0.01	99.9
97A	Octopus	Octopoda	0	0.01	99.9

*COSEWIC species in {‘027’, ‘034’, ‘394’, ‘410’, ‘424’, ‘435’, ‘437’, ‘440’, ‘442’, ‘453’}
**YMR with 16th highest catch in YMR hook and line events, representing 0.20% by catch weight.
***YMR does not appear in the top 20 species for trap events.

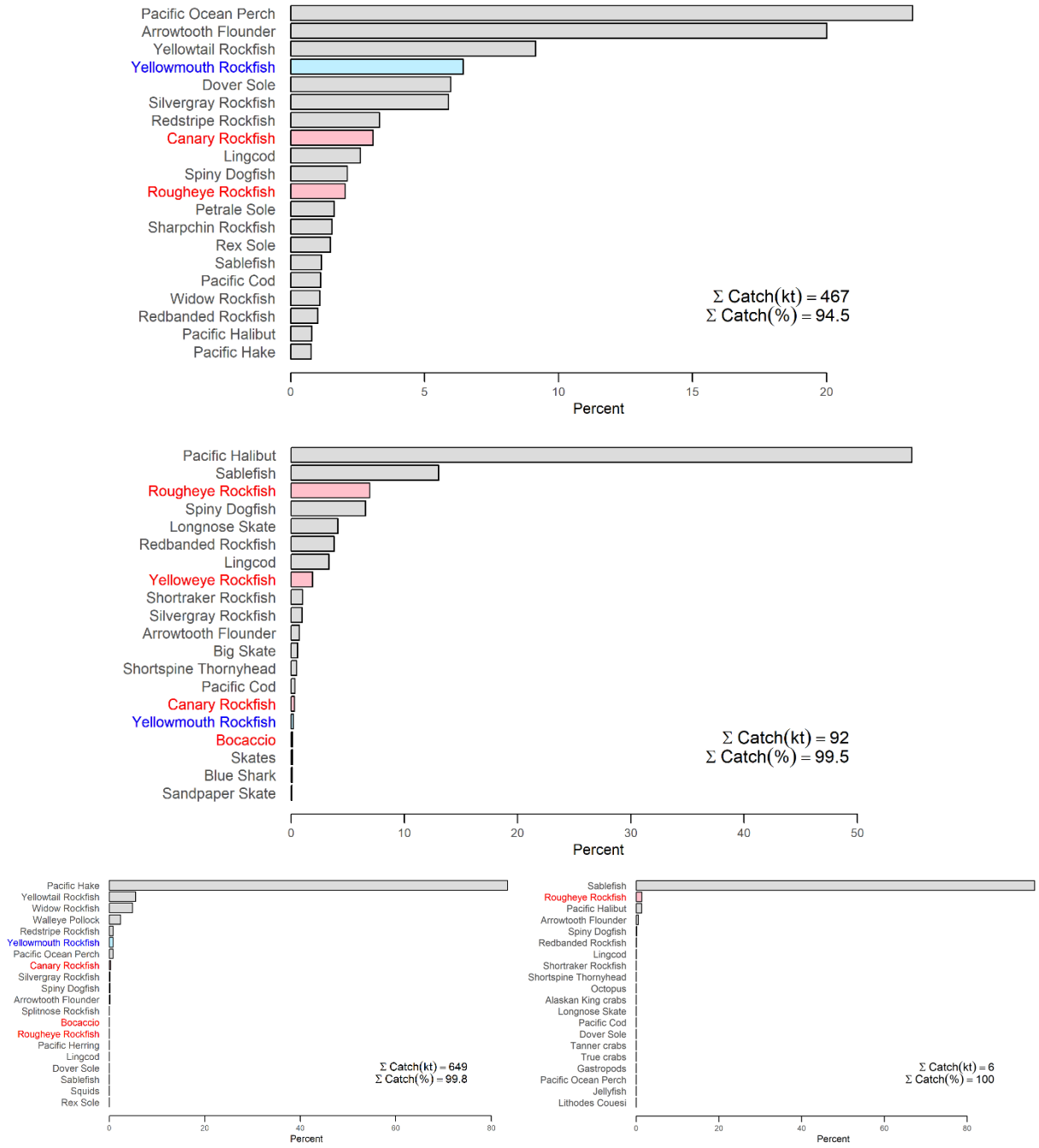

Figure G.13. YMR coastwide – Distribution of catch weights summed over the period Feb 1996 to Dec 2020 for important finfish species from fishing events in GFFOS (includes PacHarv) that caught at least one YMR in PMFC areas 3CD5ABCDE. The four panels correspond to various gear types – bottom trawl (top), hook and line (middle), midwater trawl (bottom left), and trap (bottom right). Fishing events were selected over a depth range between 130 and 402 m (the 0.01 and 0.99 quantile range, see Figure G.3). Relative concurrence is expressed as a percentage by species relative to the total catch weight summed over all finfish species in the specified period. Assessment species appear in blue; COSEWIC species appear in red.

Table G.2. YMR north – Top 10 species by catch weight (sum of landed + discarded from 1996 to 2020) that co-occur in YMR fishing events by gear type in PMFC areas 5DE (Figure G.14). Rockfish species of interest to COSEWIC appear in red font, target species (which occur in every tow) appear in blue font.

Code*	Species	Latin Name	Catch (tonnes)	Catch (%)	∑Catch (%)
Gear:	**Bottom Trawl**				
396	Pacific Ocean Perch	*Sebastes alutus*	25,391	42.8	42.8
394	Rougheye/Blackspotted	*S. aleutianus/melanostictus*	8,938	15.1	57.9
405	Silvergray Rockfish	*Sebastes brevispinis*	5,877	9.91	67.8
440	Yellowmouth Rockfish	*Sebastes reedi*	4,336	7.31	75.1
439	Redstripe Rockfish	*Sebastes proriger*	3,342	5.64	80.7
602	Arrowtooth Flounder	*Atheresthes stomias*	2,604	4.39	85.1
626	Dover Sole	*Microstomus pacificus*	2,046	3.45	88.6
417	Widow Rockfish	*Sebastes entomelas*	1,383	2.33	90.9
451	Shortspine Thornyhead	*Sebastolobus alascanus*	952	1.61	92.5
607	Petrale Sole	*Eopsetta jordani*	710	1.20	93.7
Gear:	**Hook and Line****				
614	Pacific Halibut	*Hippoglossus stenolepis*	16,747	58.1	58.1
394	Rougheye/Blackspotted	*S. aleutianus/melanostictus*	4,807	16.7	74.7
455	Sablefish	*Anoplopoma fimbria*	3,123	10.8	85.6
059	Longnose Skate	*Raja rhina*	844	2.93	88.5
401	Redbanded Rockfish	*Sebastes babcocki*	689	2.39	90.9
403	Shortraker Rockfish	*Sebastes borealis*	584	2.03	92.9
044	Spiny Dogfish	*Squalus acanthias*	427	1.48	94.4
467	Lingcod	*Ophiodon elongatus*	324	1.12	95.5
451	Shortspine Thornyhead	*Sebastolobus alascanus*	259	0.90	96.4
405	Silvergray Rockfish	*Sebastes brevispinis*	240	0.83	97.3
Gear:	**Midwater Trawl**				
225	Pacific Hake	*Merluccius productus*	2,857	60.9	60.9
417	Widow Rockfish	*Sebastes entomelas*	888	18.9	79.9
228	Walleye Pollock	*Theragra chalcogramma*	440	9.38	89.2
418	Yellowtail Rockfish	*Sebastes flavidus*	199	4.24	93.5
396	Pacific Ocean Perch	*Sebastes alutus*	125	2.67	96.1
394	Rougheye/Blackspotted	*S. aleutianus/melanostictus*	48	1.03	97.2
439	Redstripe Rockfish	*Sebastes proriger*	34	0.72	97.9
440	Yellowmouth Rockfish	*Sebastes reedi*	27	0.57	98.5
405	Silvergray Rockfish	*Sebastes brevispinis*	26	0.56	99.0
437	Canary Rockfish	*Sebastes pinniger*	20	0.42	99.4
Gear:	**Trap*****				
455	Sablefish	*Anoplopoma fimbria*	4,639	96.6	96.6
394	Rougheye/Blackspotted	*S. aleutianus/melanostictus*	93	1.93	98.5
602	Arrowtooth Flounder	*Atheresthes stomias*	37	0.77	99.3
614	Pacific Halibut	*Hippoglossus stenolepis*	26	0.54	99.9
467	Lingcod	*Ophiodon elongatus*	1	0.02	99.9
044	Spiny Dogfish	*Squalus acanthias*	1	0.02	99.9
403	Shortraker Rockfish	*Sebastes borealis*	1	0.02	99.9
ZAD	Tanner crabs	*Chionoecetes*	1	0.01	99.9
VMD	Scarlet King Crab	*Lithodes couesi*	0	0.01	99.9
451	Shortspine Thornyhead	*Sebastolobus alascanus*	0	0.01	99.9

*COSEWIC species in {'027', '034', '394', '410', '424', '435', '437', '440', '442', '453'}
**YMR with 19th highest catch in YMR hook and line events, representing 0.06% by catch weight.
***YMR does not appear in the top 20 species for trap events.

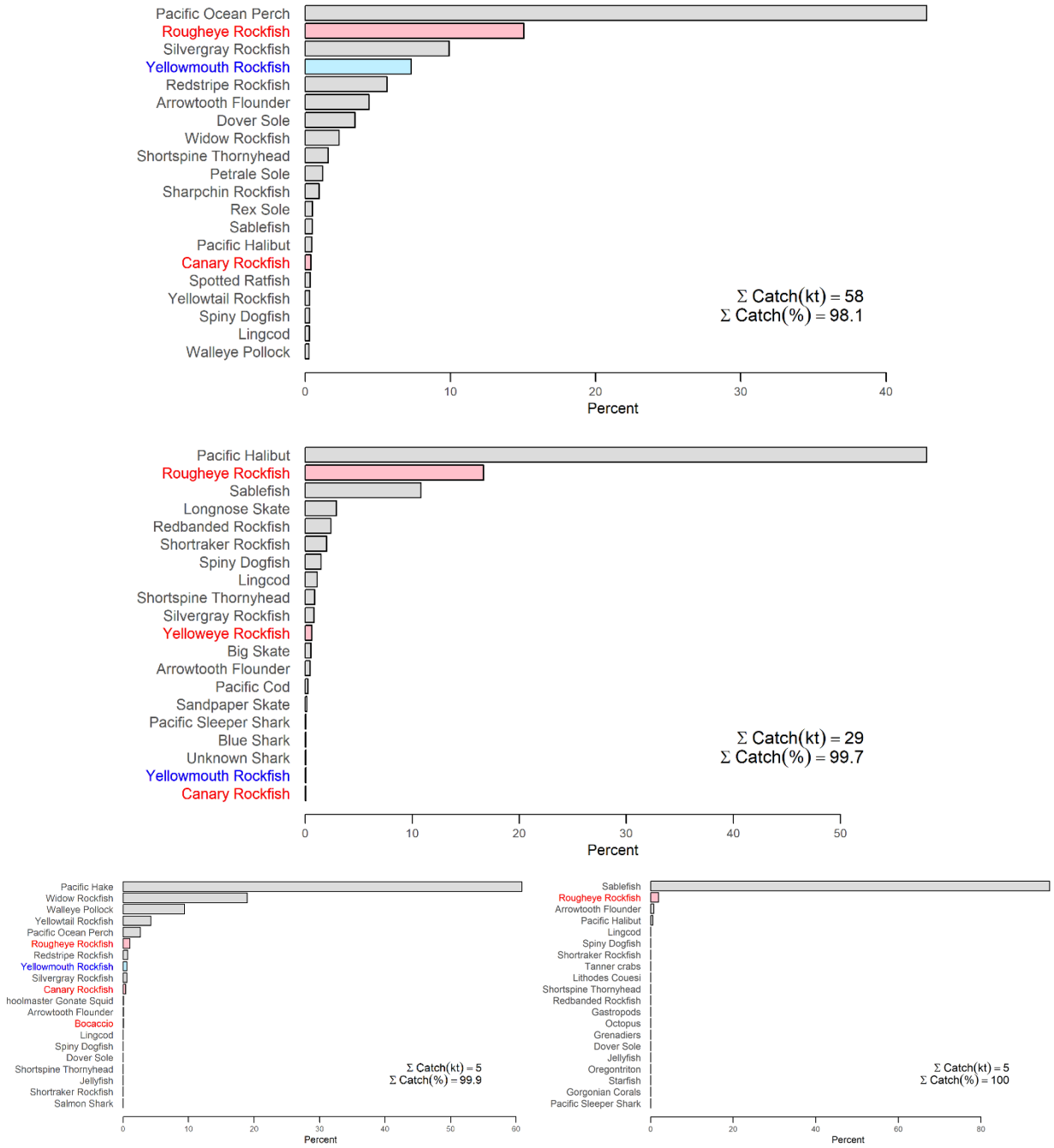

Figure G.14. YMR north – Distribution of catch weights summed over the period Feb 1996 to Dec 2020 for important finfish species from fishing events in GFFOS (includes PacHarv) that caught at least one YMR in PMFC areas 5DE between 199 and 466 m for gears bottom trawl (top) , hook and line (middle), midwater trawl (bottom left), and trap (bottom right). See Figure G.13 caption for further details.

Table G.3. YMR south – Top 10 species by catch weight (sum of landed + discarded from 1996 to 2020) that co-occur in YMR fishing events by gear type in PMFC areas 3CD5ABC (Figure G.15). Rockfish species of interest to COSEWIC appear in red font, target species (which occur in every tow) appear in blue font.

Code*	Species	Latin Name	Catch (tonnes)	Catch (%)	∑Catch (%)
Gear:	**Bottom Trawl**				
396	Pacific Ocean Perch	*Sebastes alutus*	89,320	21.7	21.7
602	Arrowtooth Flounder	*Atheresthes stomias*	89,024	21.6	43.3
418	Yellowtail Rockfish	*Sebastes flavidus*	44,599	10.8	54.1
440	Yellowmouth Rockfish	*Sebastes reedi*	27,494	6.67	60.7
405	Silvergray Rockfish	*Sebastes brevispinis*	23,186	5.62	66.4
626	Dover Sole	*Microstomus pacificus*	17,154	4.16	70.5
437	Canary Rockfish	*Sebastes pinniger*	15,023	3.64	74.2
467	Lingcod	*Ophiodon elongatus*	13,112	3.18	77.4
439	Redstripe Rockfish	*Sebastes proriger*	13,065	3.17	80.5
044	Spiny Dogfish	*Squalus acanthias*	9,961	2.42	82.9
Gear:	**Hook and Line****				
614	Pacific Halibut	*Hippoglossus stenolepis*	32,753	52.9	52.9
455	Sablefish	*Anoplopoma fimbria*	9,564	15.4	68.3
044	Spiny Dogfish	*Squalus acanthias*	5,662	9.14	77.5
059	Longnose Skate	*Raja rhina*	2,935	4.74	82.2
401	Redbanded Rockfish	*Sebastes babcocki*	2,782	4.49	86.7
467	Lingcod	*Ophiodon elongatus*	2,496	4.03	90.8
394	Rougheye/Blackspotted	*S. aleutianus/melanostictus*	1,526	2.46	93.2
442	Yelloweye Rockfish	*Sebastes ruberrimus*	1,138	1.84	95.1
602	Arrowtooth Flounder	*Atheresthes stomias*	514	0.83	95.9
405	Silvergray Rockfish	*Sebastes brevispinis*	463	0.75	96.6
Gear:	**Midwater Trawl**				
225	Pacific Hake	*Merluccius productus*	536,310	84.3	84.3
418	Yellowtail Rockfish	*Sebastes flavidus*	37,287	5.86	90.2
417	Widow Rockfish	*Sebastes entomelas*	31,703	4.98	95.1
228	Walleye Pollock	*Theragra chalcogramma*	7,067	1.11	96.3
439	Redstripe Rockfish	*Sebastes proriger*	5,785	0.91	97.2
440	Yellowmouth Rockfish	*Sebastes reedi*	5,143	0.81	98.0
396	Pacific Ocean Perch	*Sebastes alutus*	4,834	0.76	98.7
437	Canary Rockfish	*Sebastes pinniger*	1,891	0.30	99.0
044	Spiny Dogfish	*Squalus acanthias*	1,125	0.18	99.2
405	Silvergray Rockfish	*Sebastes brevispinis*	1,073	0.17	99.4
Gear:	**Trap*****				
455	Sablefish	*Anoplopoma fimbria*	3,437	97.0	97.0
614	Pacific Halibut	*Hippoglossus stenolepis*	56	1.57	98.6
394	Rougheye/Blackspotted	*S. aleutianus/melanostictus*	17	0.47	99.0
602	Arrowtooth Flounder	*Atheresthes stomias*	16	0.44	99.5
044	Spiny Dogfish	*Squalus acanthias*	7	0.20	99.7
401	Redbanded Rockfish	*Sebastes babcocki*	7	0.19	99.9
467	Lingcod	*Ophiodon elongatus*	3	0.07	99.9
403	Shortraker Rockfish	*Sebastes borealis*	1	0.01	99.9
97A	Octopus	Octopoda	0	0.01	99.9
451	Shortspine Thornyhead	*Sebastolobus alascanus*	0	0.01	100.0

*COSEWIC species in {‘027’, ‘034’, ‘394’, ‘410’, ‘424’, ‘435’, ‘437’, ‘440’, ‘442’, ‘453’}
**YMR with 16th highest catch in YMR hook and line events, representing 0.27% by catch weight.
***YMR with 15th highest catch in YMR trap events, representing 0.003% by catch weight.

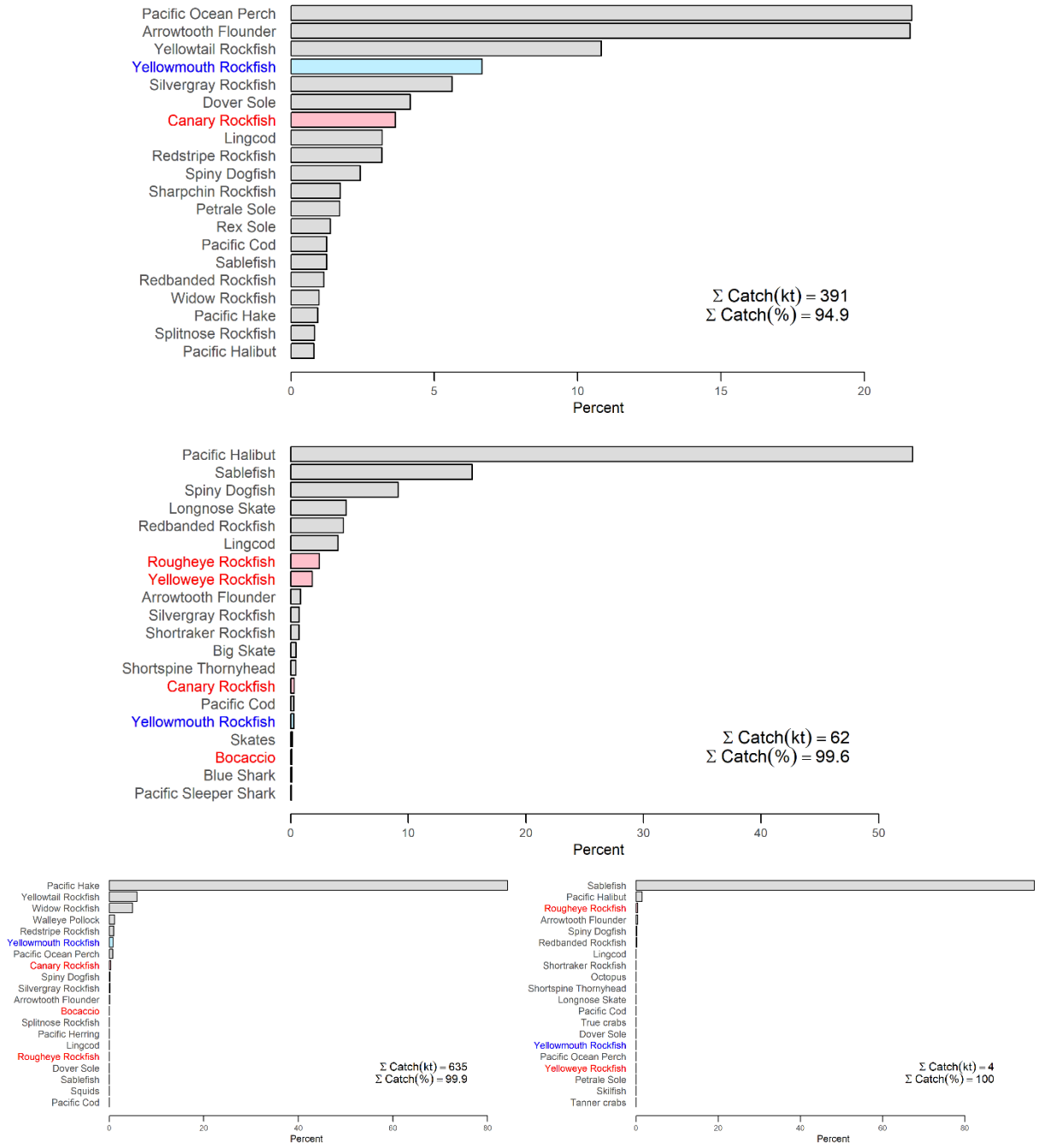

Figure G.15. YMR south – Distribution of catch weights summed over the period Feb 1996 to Dec 2020 for important finfish species from fishing events in GFFOS (includes PacHarv) that caught at least one YMR in PMFC areas 3CD5ABC between 127 and 391 m for gears bottom trawl (top) , hook and line (middle), midwater trawl (bottom left), and trap (bottom right). See Figure G.13 caption for further details.

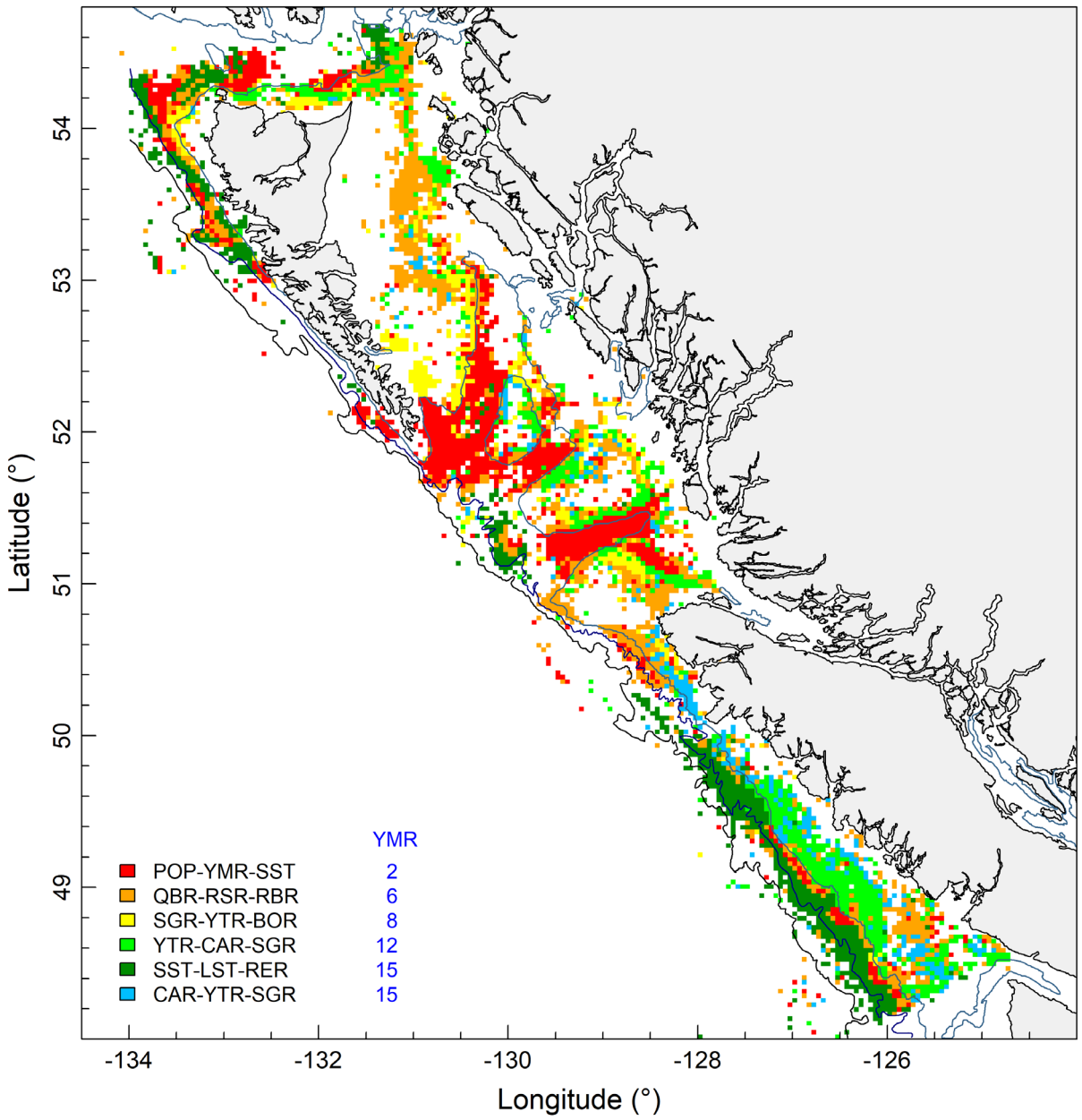

Figure G.16. Groups of rockfish in bottom trawl tows (28 species from 1996-2021) identified by clara (clustering large applications) in R's package 'cluster' (Maechler et al. 2018). Isobaths trace the 200, 1000, and 1800 m depth contours. The legend identifies six clusters represented by the top three species comprising the medoids; the clusters are ordered by the contribution of Yellowmouth Rockfish (YMR) to each medoid, where YMR's rank in the medoid is displayed as blue numbers. Species codes: BOR = Bocaccio, CAR = Canary Rockfish, LST =Longspine Thornyhead, POP =Pacific Ocean Perch, QBR = Quillback Rockfish, RBR = Redbanded Rockfish, RER = Rougheye/ Blackspotted Rockfish complex, RSR = Redstripe Rockfish, SGR = Silvergray Rockfish, SST =Shortspine Thornyhead, and YTR =Yellowtail Rockfish.

G.3. TROPHIC INTERACTIONS

Fu et al (2017) used an ecosystem model (OSMOSE: Object-oriented Simulator of Marine Ecosystems Exploitation) to explore predator-prey interactions in a previously-defined ecosystem called PNCIMA[18]. The study used 10 key populations and 19 background taxa, one of which included YMR in the slope rockfish category; POP was treated as a separate background taxon. The OSMOSE model focused on a pelagic group of species that included Pacific Herring, Walleye Pollock, and Pacific Cod; however, the model could be applied to other functional groups.

GFBioSQL only reports one instance of euphausiids in the stomach contents of YMR. Assuming that YMR may occupy a similar niche as POP, the latter's stomach contents included 97 instances of euphausiids and at least one of the following: invertebrates, jellyfish, shrimps, squids, lanternfish, and Pacific Herring. Love et al. (2002) reported that POP eats copepods, krill, mysids, amphipods, and midwater fish; they are preyed upon by Albacore Tuna and Northern Fur Seals.

Whipps et al. (2003) attempted to characterise a *Mycobacterium* species isolated from the kidney and spleen of YMR and POP; however the genetic markers they used were not sufficiently specific enough to reveal positive species identification. The closest association was *M. montefiorense*, a species found in Moray Eels in Florida.

G.4. ENVIRONMENTAL EFFECTS

There are few (if any) studies that directly link YMR to environmental effects through indicators such as sea surface temperature or upwelling strength. The last assessment of POP (Haigh et al. 2018) attempted to tie environmental indicators (nine climatic and environmental indices) to POP recruitment, but none of them appeared to exert a strong influence.

G.5. ADVICE FOR MANAGERS

There is potential for environmental indicators to be incorporated into stock assessment models. Andrew Edwards (pers. comm., PBS Nanaimo, 2021) secured three years funding for a project entitled 'Incorporating environmental information into management advice by understanding historical declines of Pacific Herring and recent increases of Bocaccio'. It will build on work in Edwards et al. (2017) and Haigh et al. (2018) while using the framework of the Gulf of St. Lawrence Ecosystem Approach project. While this does not affect YMR, *per se*, its application could be transferable.

The modelling software Stock Synthesis (SS) has a rudimentary method for including environmental effects in the stock-recruitment function (Methot Jr et al. 2021). However, the SS authors provide the following advice: 'The preferred approach to including environmental effects on recruitment is not to use the environmental effect in the direct calculation of the expected level of recruitment. Instead, the environmental data would be used as if it were a survey observation of the recruitment deviation.

[18] Pacific North Coast Integrated Management Area – encompasses Queen Charlotte Sound, Hecate Strait, Dixon Entrance , and the west coast of Haida Gwaii.

G.6. REFERENCES – ECOSYSTEM

Edwards, A.M., Haigh, R., Tallman, R., Swain, D.P., Carruthers, T.R., Cleary, J.S., Stenson, G., and Doniol-Valcroze, T. 2017. Proceedings of the Technical Expertise in Stock Assessment (TESA) National Workshop on 'Incorporating an ecosystem approach into single-species stock assessments', 21-25 November 2016, Nanaimo, British Columbia. Can. Tech. Rep. Fish. Aquat. Sci. 3213. vi + 53 p.

Fu, C., Olsen, N., Taylor, N., Grüss, A., Batten, S., Liu, H., Verley, P., and Shin, Y.J. 2017. Spatial and temporal dynamics of predator-prey species interactions off western Canada. ICES J. Mar. Sci. 74(8). 2107-2119.

Haigh, R., Starr, P.J., Edwards, A.M., King, J.R., and Lecomte, J.B. 2018. Stock assessment for Pacific Ocean Perch (*Sebastes alutus*) in Queen Charlotte Sound, British Columbia in 2017. DFO Can. Sci. Advis. Sec. Res. Doc. 2018/038: v + 227 p.

Love, M.S., Yoklavich, M., and Thorsteinson, L. 2002. The Rockfishes of the Northeast Pacific. University of California Press, Berkeley and Los Angeles, California.

Maechler, M., Rousseeuw, P., Struyf, A., Hubert, M., and Hornik, K. 2018. cluster: Cluster Analysis Basics and Extensions. R package version 2.0.7-1.

Methot Jr, R.D., Wetzel, C.R., Taylor, I.G., Doering, K.L., and Johnson, K.F. 2021. Stock Synthesis: User Manual Version 3.30.17. NOAA Fisheries, Seattle WA, USA, June 11, 2021.

Whipps, C.M., Watral, V.G., and Kent, M.L. 2003. Characterization of a *Mycobacterium* sp. in rockfish, *Sebastes alutus* (Gilbert) and *Sebastes reedi* (Westrheim & Tsuyuki), using rDNA sequences. J. Fish Dis. 26(4). 241-245.

APPENDIX H. BRIDGING ANALYSIS

H.1. INTRODUCTION

The Regional Peer Review (RPR) meeting held on 8-9 September 2021 (DFO 2021) requested more documentation of the relationship between the 2011 Yellowmouth Rockfish (YMR) stock assessment (Edwards et al. 2012) and the revised Stock Synthesis 3 (SS) stock assessment presented in 2021. The first stock assessment was modelled using Awatea, a modified version of Coleraine (Hilborn et al. 2003), with the two stock assessment platforms providing what appeared to be substantially different results. Unfortunately, because of difficulties from working in the new environment of the SS platform, the authors concentrated on obtaining credible results for this stock assessment rather than tracing an orderly progression from the previous to the current software platform. Once credible results were obtained from the SS platform, the authors were able to operate the Awatea platform using the same updated data as those used in the SS platform. The authors prepared some comparisons which were presented at the September 2021 RPR meeting that helped understand the difference between the two models. This Appendix documents those comparisons with the accompanying explanations.

H.2. METHODS

We attempted to retrospectively fit a version of Awatea that resembled as much as possible the Central Run (Run75), one of the runs comprising the composite base case which had been accepted at the RPR meeting. The specifications chosen for this analysis have been summarised in Table H.1, with many of the assumptions listed in this table consistent between the two models. However, some key assumptions were unavoidably different given the software implementations available on each platform.

The most serious divergence was the different distributional assumption used to fit the age frequency compositional data, with Awatea only providing the option of the robust normal distribution (Fournier et al. 1998) while SS used either the multinomial or the compound Dirichlet-multinomial approximation (Methot et al. 2021). This difference appeared to be crucial, because it was not possible to use comparable methods to weight the age-frequency data Table H.1. We attempted to implement the ‘harmonic mean ratio’ procedure used in the SS stock assessment in Awatea, with weights set to 6.32 for the commercial age frequencies (AF) and 0.25 for the survey AF. However, the resulting model estimates were not credible and are not reported here. Instead, we chose to use the Francis mean-age weighting procedure (Francis 2011) for the Awatea model, which was consistent with recent Awatea rockfish stock assessments (e.g., Starr and Haigh 2021; using the following AF weights: commercial 1.84, QCS 0.70, WCVI 0.36, WCHG 1.21, and GIG 3.23).

Several other differences affected this comparison, but only one is likely consequential, which was the different implementation of ageing error in these two platforms. This was a function of the design of the two stock assessment platforms, which implement different approaches to this problem. The consequence of this difference is that we were only able to generate approximately comparable approaches for this analysis. Two additional differences lie in the range of years used to specify the log R_0 parameter and how the CPUE and survey scaling parameters (q) were handled. Regarding the range of years used to estimate R_0, the SS platform had much greater flexibility, while the Awatea platform by default used the entire time series, a feature that is not available for modification without a coding change. However, while it is not possible to fully understand the effect of this difference, we believe that it is likely of lesser consequence compared to the difference in the assumed distribution used to fit the age frequency data. Finally, there should be almost no difference in the two approaches used to

handle the survey and CPUE q values, except that the estimation procedure used in Awatea should introduce more variability into the overall model estimates. The option to solve q analytically was not available in Awatea. Finally, the weighting difference described in the previous paragraph may lead to some differences in the estimation of year class strength, with the SS model deliberately downweighting the survey AF data while the survey AF data were allowed greater relative weight in the Awatea model.

H.3. MPD COMPARISONS

A comparison between the two models of the fits to the four survey series Figure H.1and to the CPUE series (Figure H.2) showed no strong difference in how these two models deal with these observations. The fits to the age frequency data (Figure H.3, Figure H.4) showed a bit more difference, with the SS fits possibly superior to the Awatea fits. These differences were not great and were unlikely to lead to major differences between the two platforms. One major difference was clear: the absolute magnitude of the standardised residuals was much larger for the SS model fits, with values up to 4 for SS while there was only one value greater than 2 for Awatea (Figure H.4).

Comparisons of the recruitment deviation estimates (Figure H.5) and of the spawning biomass trajectories (Figure H.6) showed clear differences between the inferences made from the data by these two stock assessment platforms, with SS making tighter estimates of year class strength, especially before 1980. For instance, SS estimated a strong year class of age-0 fish in 1952 while Awatea estimated a smaller year class of age-1 fish in 1953, and on average, generally stronger year classes than SS throughout this early period. This is not surprising, given that Awatea estimated a larger log R_0 and consequently a larger B_0 than did SS (Table H.2). The Awatea platform estimated a higher average recruitment than did the SS platform (Table H.2), which is evident in Figure H.6, with the Awatea biomass trajectory starting at a much higher level in 1935 than did the SS model. However, both models converged around 1965, with each showing a strong peak near 1980 and roughly the same trajectory after the peak. Both models ended in 2022 near the same level of absolute biomass. One interpretation of this outcome is that, while there is uncertainty about the size of the initial biomass and its subsequent trajectory, this uncertainty diminishes once the quantity of age frequency data improves and there are biomass indices available to inform the model. Before that, it is the model assumptions that are driving the biomass interpretation.

H.4. MCMC COMPARISONS

Both models had acceptable MCMC diagnostics, indicating that the MCMC simulations had converged with the traces showing no overall trend (Figure H.7), the partial cumulative parameter distributions had acceptable overlap (Figure H.8) and there was little evidence of autocorrelation in the parameters (Figure H.9).

Apart from the difference in the estimate of log R_0, Table H.2 shows some differences in the selectivity parameter estimates for the five fleets. The parameter estimates for μ (age at maximum selectivity) for the TRAWL+ fishery were reasonably similar between the two platforms with some relatively minor differences in the log v_L parameter (standard deviation of the left side selectivity). This is the data set with the most composition data and which was given the most weight in the reconstruction, so it is expected that the estimates are similar. There are greater differences in the parameter estimates for the surveys, particularly for the WCVI synoptic survey, where the estimates for μ and log v_L were considerably different (Table H.2). However, these surveys were given very low weight in the SS reconstruction so it is less surprising that the models will interpret the data differently, especially since the weights were applied differently in the two models.

Figure H.10 compares the median recruitments, showing that the SS platform estimated a very large recruitment in 1952 for which there was no equivalent in the Awatea reconstruction. This difference is likely the result of the fact that Awatea estimated a larger initial biomass than did SS, so a large 1952 recruitment was needed in the SS reconstruction to match the catch history in the mid-1960s as well as the older age proportions in the age frequency data while this was unnecessary in the Awatea reconstruction. Both platforms estimated a large recruitment in 1961, which, when combined with the large 1952 recruitment estimated by SS, allowed both reconstructions to estimate similar peak biomass levels in 1978 (Figure H.11: 1978 median biomass SS=39,200 t; 1978 median biomass Awatea=39,700 t). The two median biomass trajectories had converged by 1967 and appeared to track each other closely from then on, up to the end of the reconstruction in 2022, with considerable overlap among the respective credibility intervals (Figure H.11). However, when this same trajectory was provided in terms of B_0 (Figure H.12), the model reconstructions appeared to be very different, with Awatea showing much lower levels of relative biomass than that estimated by SS. However, the similarity between the two models in terms of absolute biomass from the mid-1960s to the end of the reconstruction corroborates the conclusions made from the MPD comparisons: while the distributional assumption used to fit the compositional data led to a considerably different estimate of initial biomass, the correspondence in the biomass trajectories from the mid-1960s indicated that the two models appeared to be interpreting the data similarly from that point on. The difference in stock status and overall productivity (as shown by the larger estimate of MSY made by Awatea – see Table H.2) was likely the result of the model assumptions, not the data. Fortunately, both model platforms indicated that the current biomass is above the DFO reference levels of $0.4B_{MSY}$ and $0.8\ B_{MSY}$ (Table H.2) with a high probability, resulting in consistent management advice offered by either model platform.

Aside from differences in model platforms, the stock assessment also identified ageing error assumptions as another source of uncertainty (Figure H.13). Depending on the degree to which AFs were adjusted to reflect uncertainty (i.e., strong ageing error adjustment produced distinct single-year high-recruitment events while no ageing error smeared recruitment events out to adjacent cohort years), the estimates of initial equilibrium biomass change whereas the final-year estimates remain similar. This will have implications for reference points, and should be kept in mind when conducting future stock assessments.

Table H.1. Specifications for the two runs: SS central run (Run 75.01) and Awatea equivalent (Run75.01).

Key Assumption	**SS central run (Run75.01)**	**Awatea (Run75.01)**
natural mortality (M)	0.05	0.05
fixed steepness (h)	0.7	0.7
assumed two sexes (females, males)	X	X
accumulator age class	60	60
one commercial fishery dominated by trawl (bottom + midwater), with minor removals by halibut longline, sablefish trap, lingcod longline, inshore longline, and salmon troll, pooled into a single catch series with associated age frequency (AF) data drawn from the trawl fishery	X	X
one commercial bottom trawl fishery abundance index series (bottom trawl CPUE index, 1996–2020)	X	X
used 4 survey abundance index series (QCS Synoptic, WCVI Synoptic, WCHG Synoptic, and GIG Historical), with age frequency (AF) data	X	X
wide normal prior $N(8,8)$ on log R_0	X	X
used informed normal priors for the two selectivity parameters (μ_g, v_{gL}) for all fleets (fishery and surveys), and set the male selectivity offset(Δ_g) to 0 (Appendix E)	X	X
estimated recruitment deviations	1950 to 2012	1935 to 2020
fixed standard deviation of recruitment residuals (σ_R)	0.9	0.9

Key Assumption	SS central run (Run75.01)	Awatea (Run75.01)
applied abundance reweighting: added CV process error to index CVs, c_p =0.3296 for the commercial CPUE series and c_p =0 for the surveys (Appendix E);	X	X
applied composition reweighting	harmonic mean ratio method (see Appendix E)	Francis (2011) method T8
ageing error vector based on the CV of observed lengths	Appendix D.2.3	approximated
survey and CPUE scaling parameters (q)	factored out analytically	estimated
downweight the survey age frequency data so that they are used to estimate selectivity but to not contribute to the estimates of year class strength	X	not done

Table H.2. MCMC parameter and derived parameter estimates for the two stock assessment platforms.

Parameters	**SS Run75.01**			**AW Run75.01**		
	0.05	**0.5**	**0.95**	**0.05**	**0.5**	**0.95**
log R_0	7.870	8.073	8.307	8.281	8.385	8.519
μ_1(TRAWL+)	11.0	11.6	12.3	10.7	11.4	12.2
log v_{L1}(TRAWL+)	1.71	2.07	2.40	1.15	1.61	2.03
μ_2(QCS)	9.9	13.7	18.2	10.1	14.0	19.4
log v_{L2}(QCS)	3.06	4.00	4.84	2.52	3.54	4.38
μ_3(WCVI)	8.6	13.7	18.7	13.8	17.6	20.8
log v_{L3}(WCVI)	2.79	3.81	4.78	2.34	3.37	4.20
μ_4(WCHG)	8.4	10.7	12.8	10.2	11.2	12.5
log v_{L4}(WCHG)	1.36	2.05	2.73	1.29	1.88	2.41
μ_5(GIG)	10.6	15.9	21.7	11.6	14.1	18.2
log v_{L5}(GIG)	3.48	4.93	6.29	2.97	4.08	5.24

Derived Parameters	**SS Run75.01**			**AW Run75.01**		
	0.05	**0.5**	**0.95**	**0.05**	**0.5**	**0.95**
B_0	21,402	26,065	32,811	35,661	39,576	45,255
B_{2022}	11,714	18,027	29,058	11,945	17,222	25,180
B_{2022}/B_0	0.481	0.664	0.904	0.333	0.438	0.565
u_{2021}	0.015	0.023	0.035	0.020	0.030	0.042
B_{MSY}	6,075	7,548	9,569	9,943	11,046	12,649
MSY	834	1,031	1,311	1,335	1,485	1,694
u_{MSY}	0.046	0.046	0.047	0.060	0.064	0.066
B_{2022}/B_{MSY}	1.732	2.394	3.255	1.186	1.570	2.013
u_{2021}/u_{MSY}	0.325	0.504	0.751	0.320	0.466	0.669
$P(B_{2022} > 0.4B_{MSY})$	-	1.0	-	-	1.0	-
$P(B_{2022} > 0.8B_{MSY})$	-	1.0	-	-	1.0	-

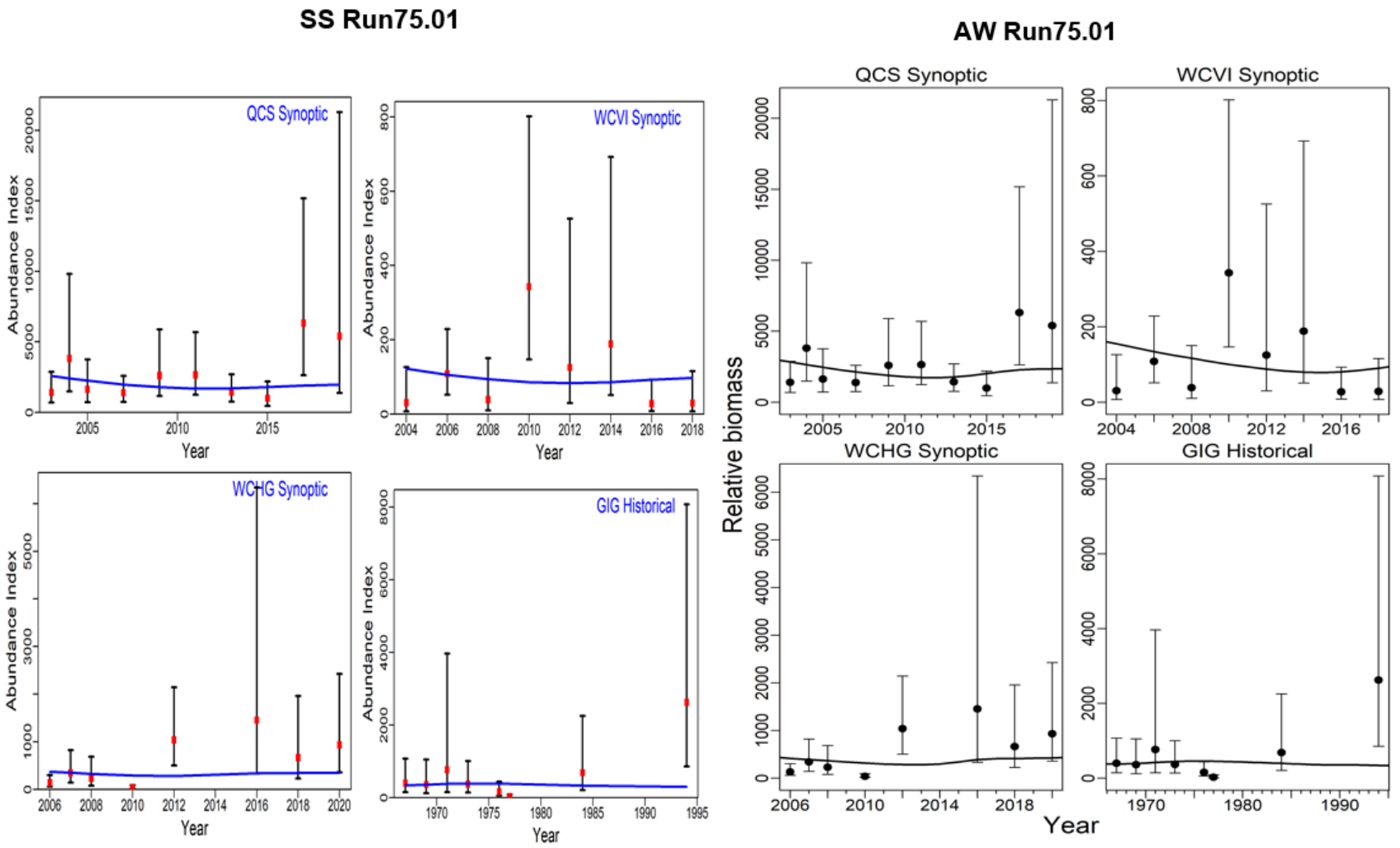

Figure H.1. Comparison of the MPD model fits to the four survey series, with the SS fits shown in the first two columns on the left and the Awatea fits in the final two columns on the right.

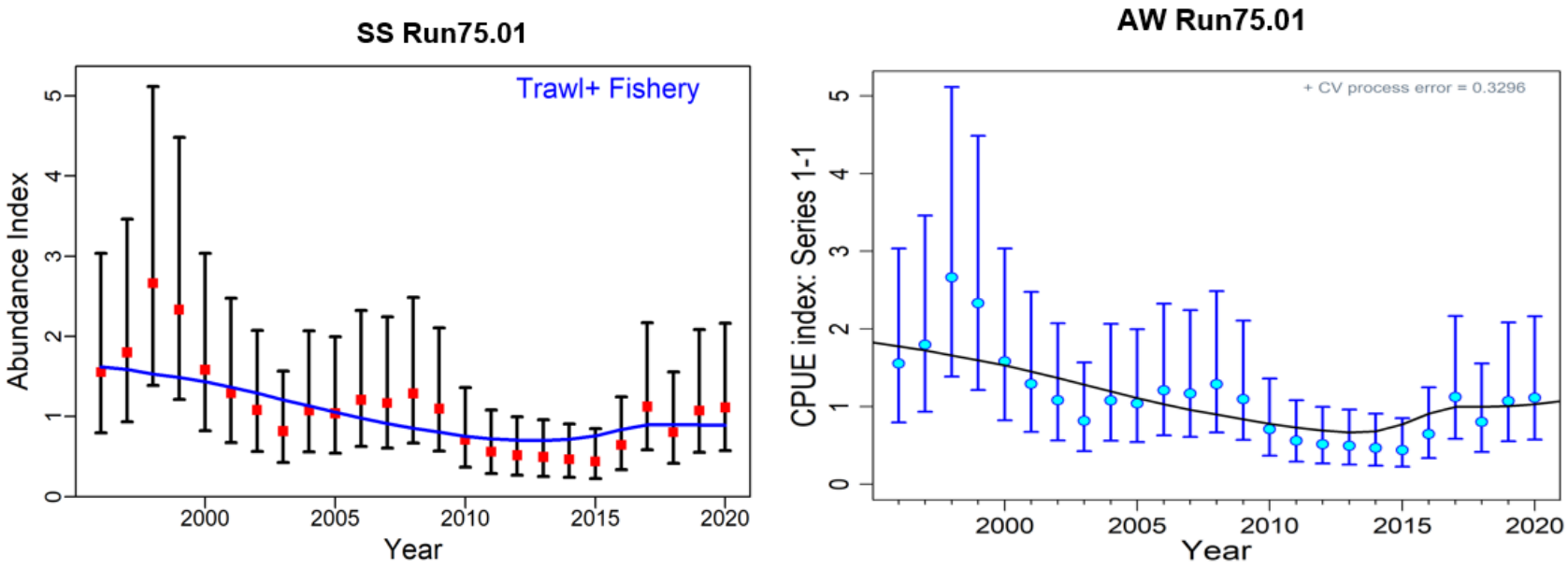

Figure H.2. Comparison of the MPD model fits to the CPUE series, with the SS fit shown on the left and the Awatea fit on the right.

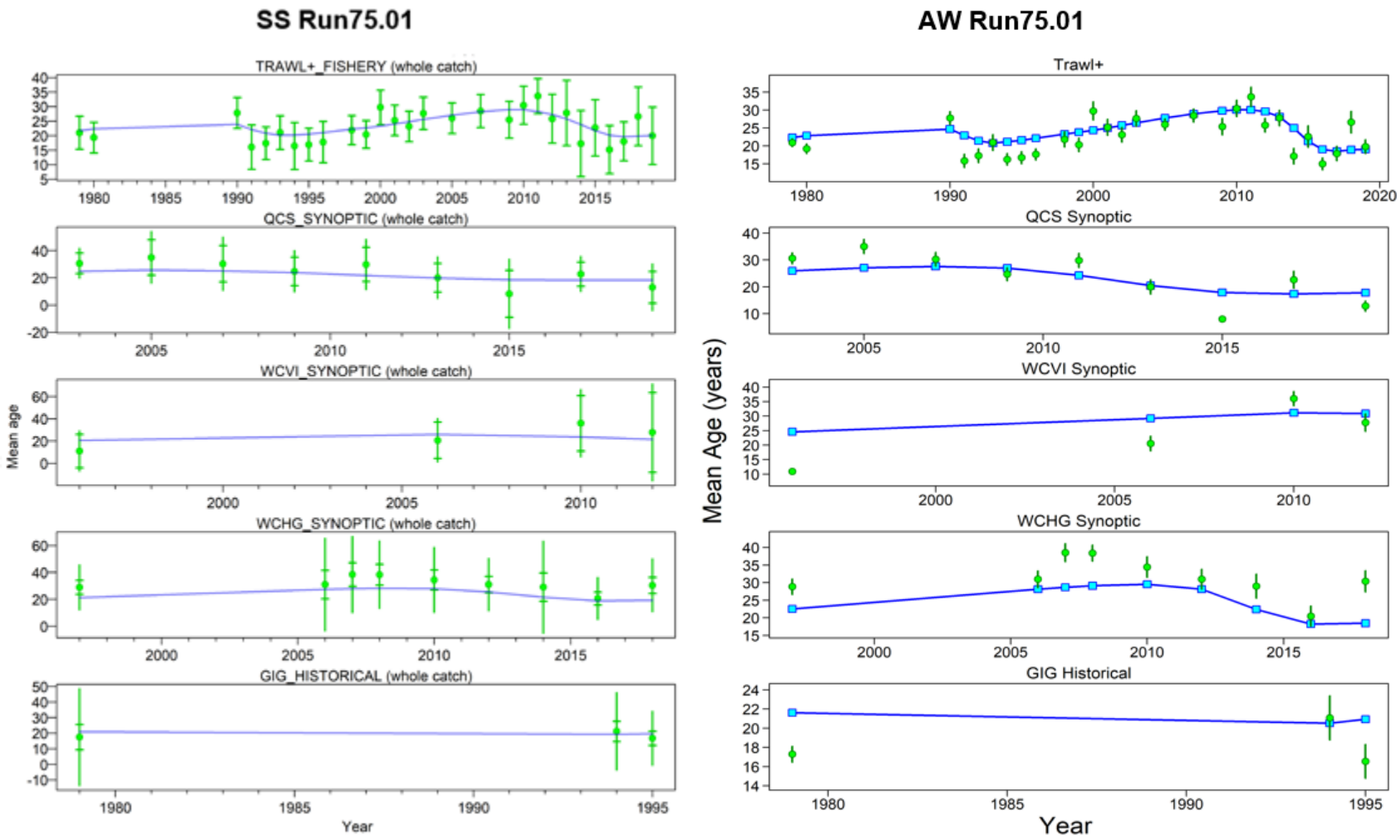

Figure H.3. Comparison of the MPD model estimates of mean age by year for each set of age frequency data, with the SS estimates shown on the left and the Awatea estimates on the right.

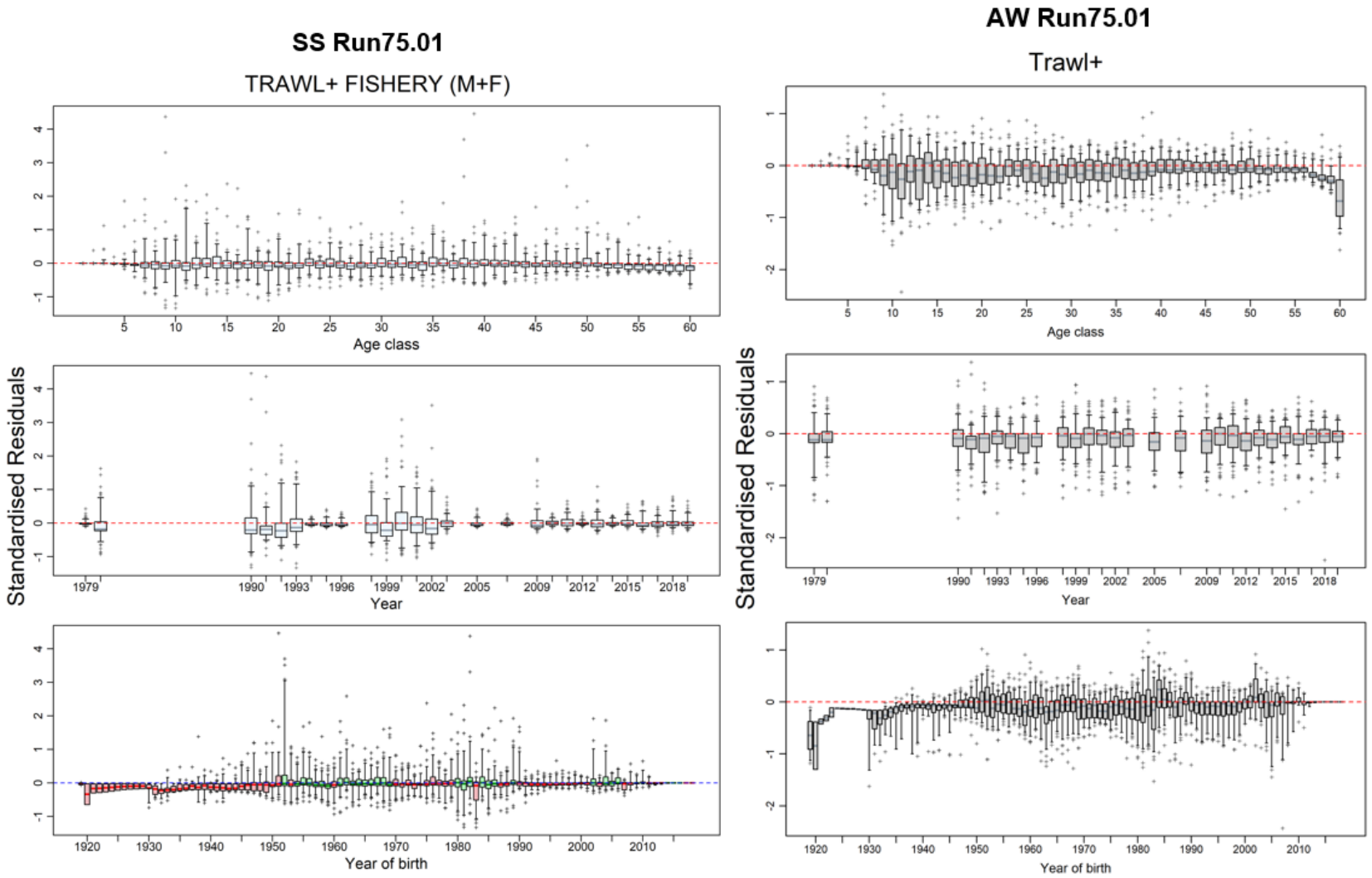

Figure H.4. Comparison of the MPD residuals from the fits to the TRAWL+ fishery age frequency data, with the SS residuals shown on the left and the Awatea residuals on the right.

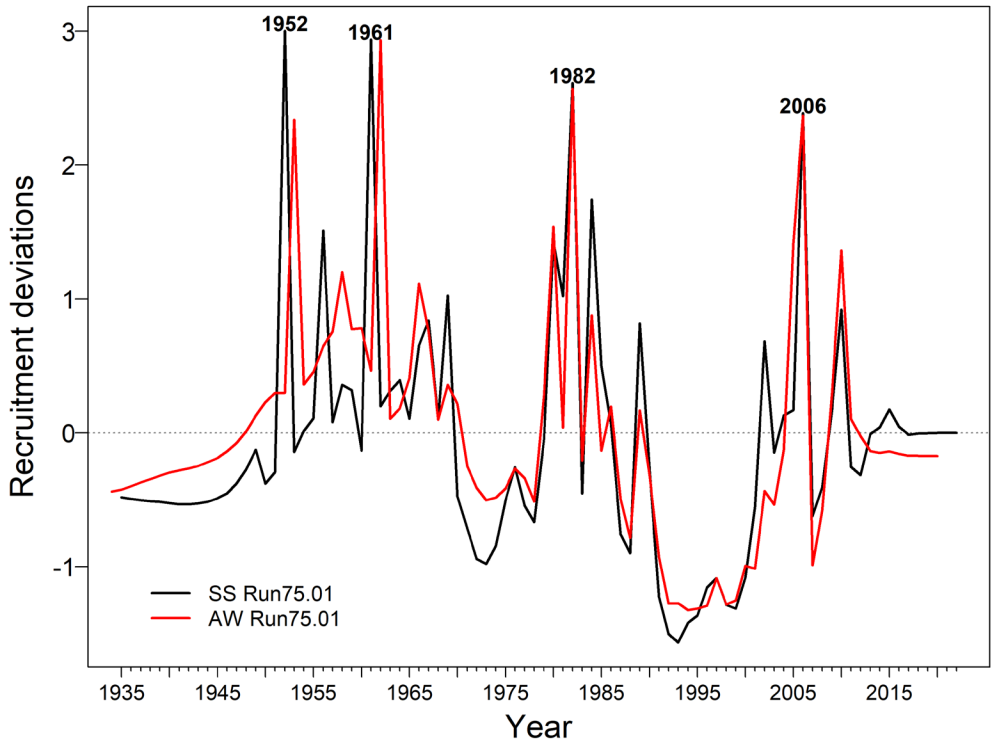

Figure H.5. Overlay comparison of the MPD recruitment deviations estimated by each model.

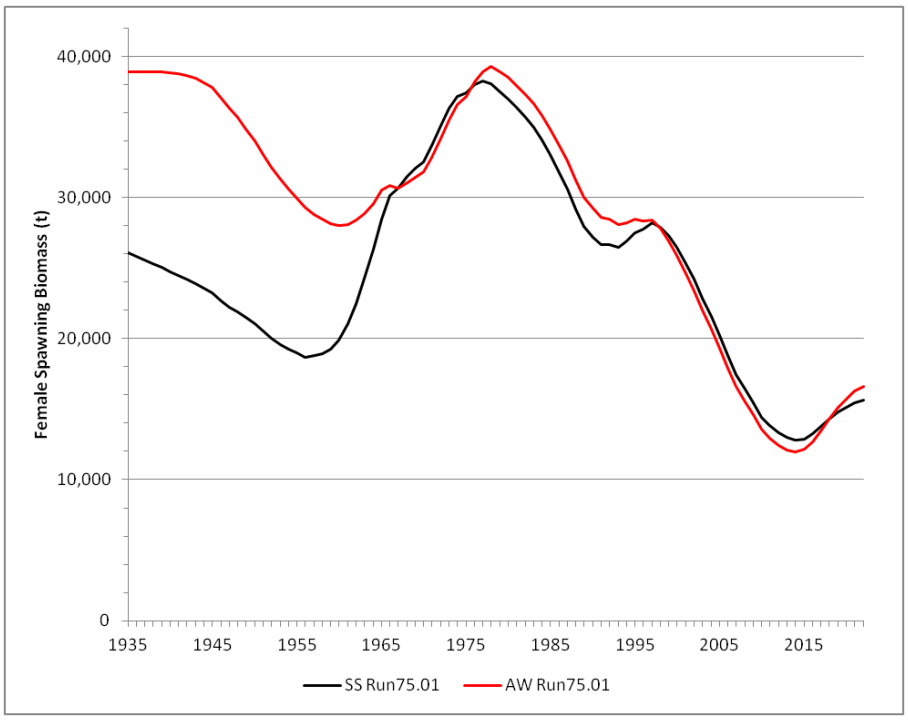

Figure H.6. Overlay comparison of the MPD female spawning biomass trajectories estimated by each model.

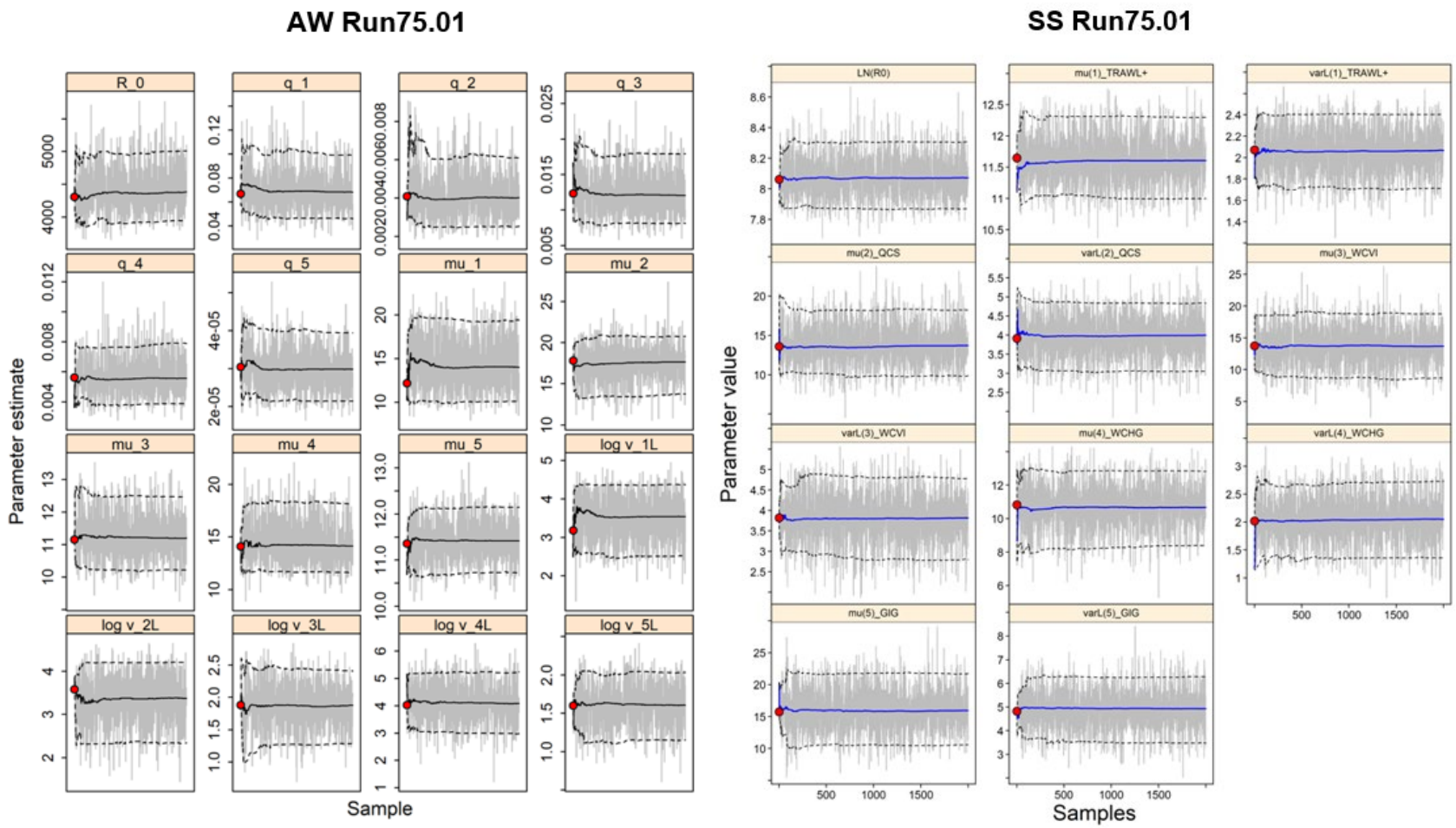

Figure H.7. Comparison of the MCMC traces for the main model parameters, with the SS3 traces shown on the left and the Awatea traces on the right.

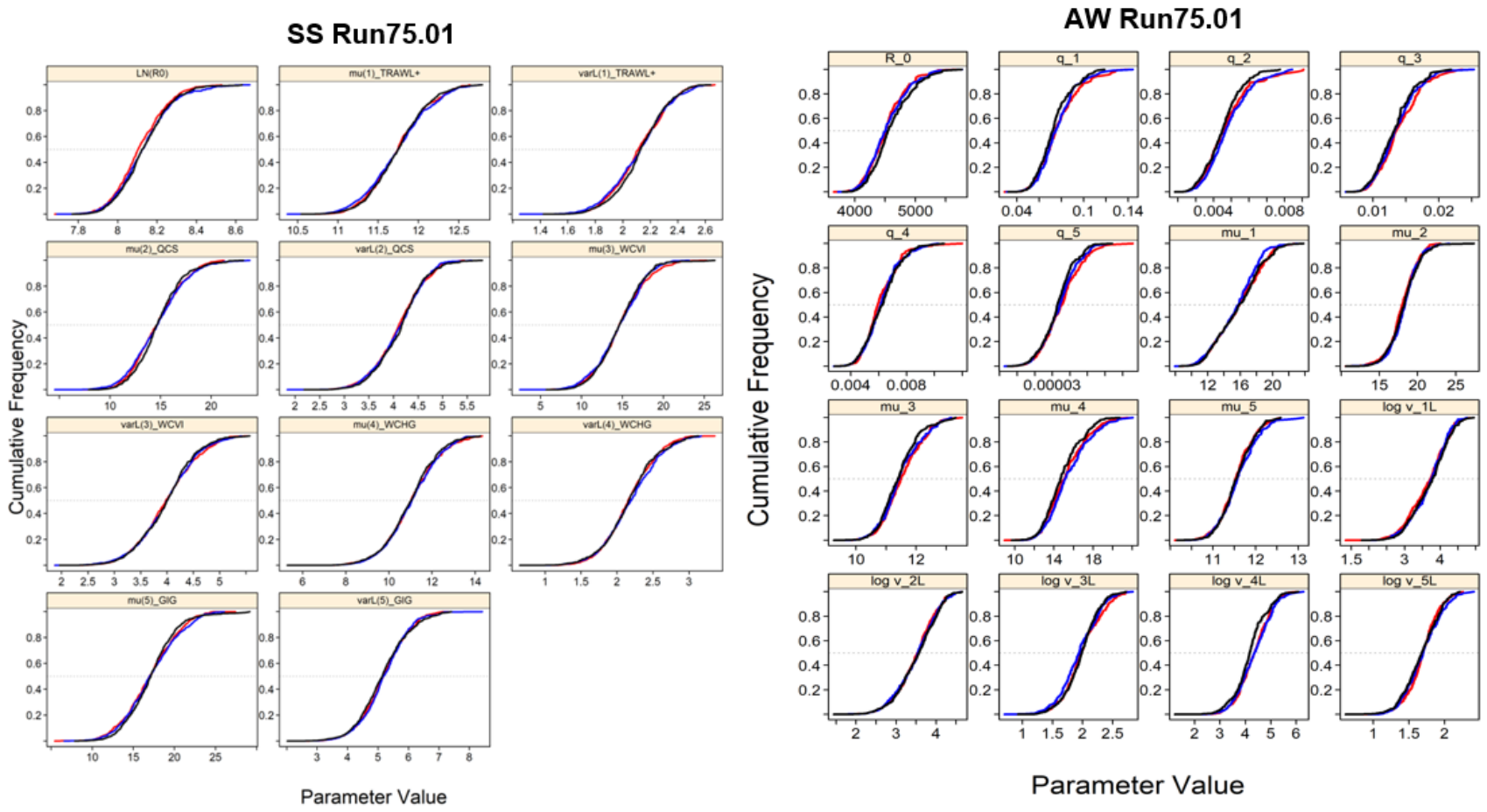

Figure H.8. Comparison of the cumulative distributions of the MCMC traces split into three parts, with the first segment (red),second segment (blue) and final segment (black), with the SS3 cumulative distributions shown on the left and the Awatea cumulative distributions on the right.

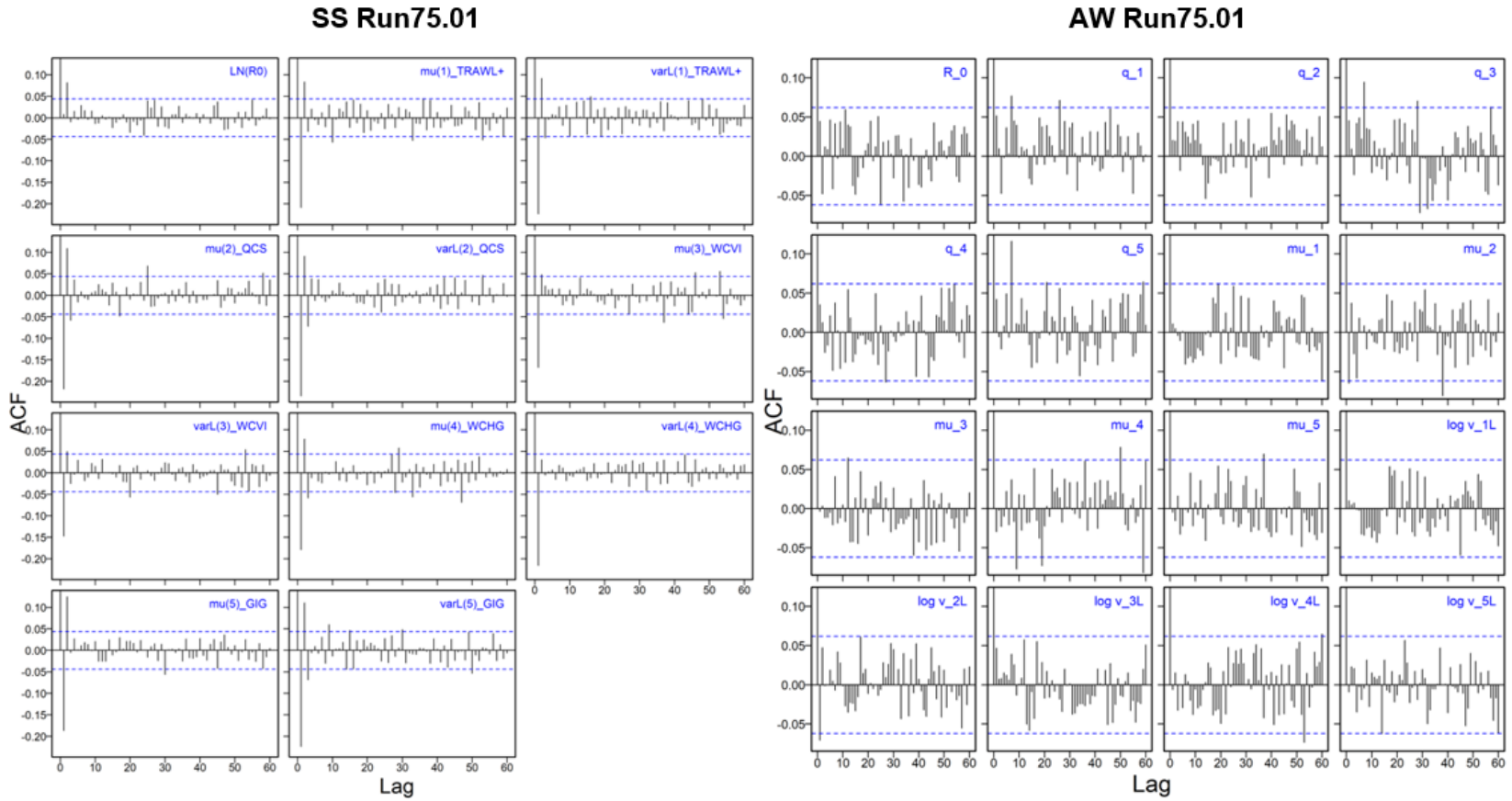

Figure H.9. Comparison of the main parameter autocorrelations from the MCMC traces, with the SS results shown on the left and the Awatea results on the right.

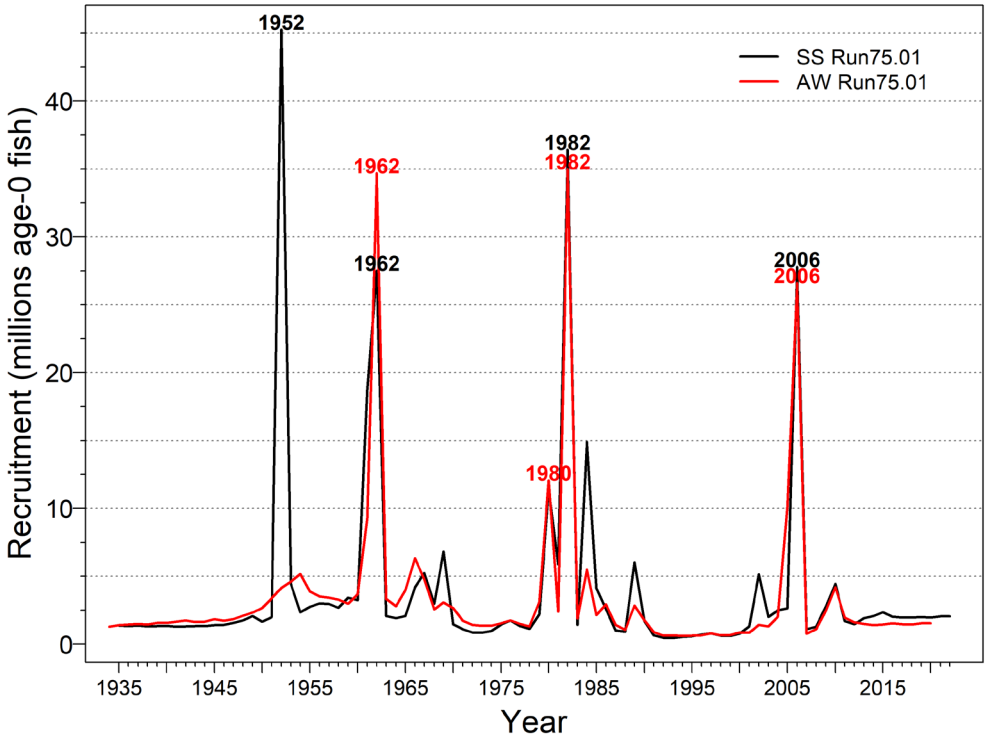

Figure H.10. Overlay comparison of the median MCMC recruitments estimated by each model (SS = Stock Synthesis 3, AW = Awatea).

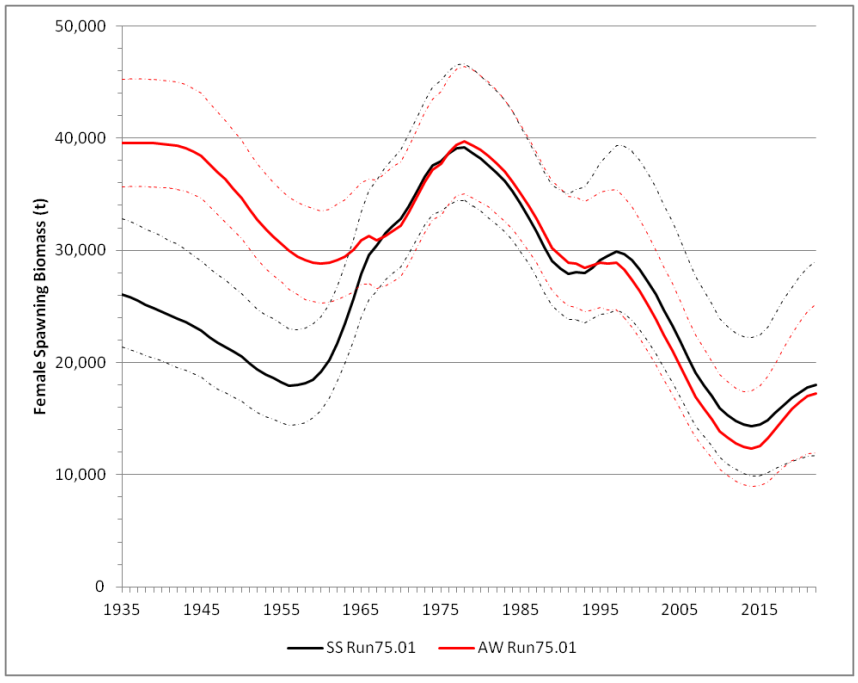

Figure H.11. Overlay comparison of the MCMC female spawning biomass trajectories (in tonnes) estimated by each model: solid lines depict the respective posterior medians and the black/red dashed lines show the 90% credibility interval for each model.

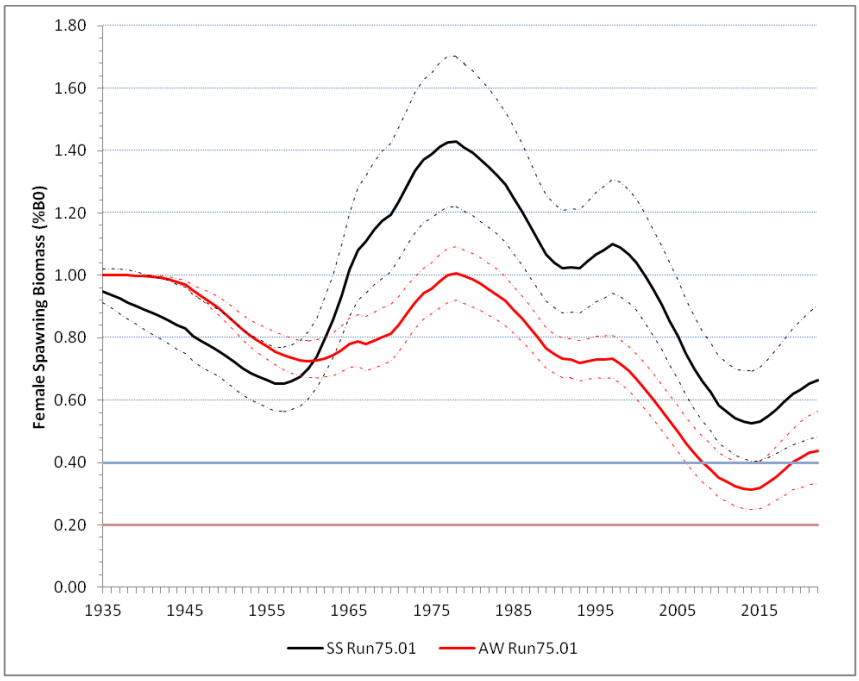

Figure H.12. Overlay comparison of the MCMC female spawning biomass trajectories (relative to B_0) estimated by each model: solid lines depict the respective posterior medians and the black/red dashed lines show the 90% credibility interval for each model. Also shown are the New Zealand default target biomass for low productivity stocks of $0.4B_0$ and the "soft limit" of $0.2B_0$.

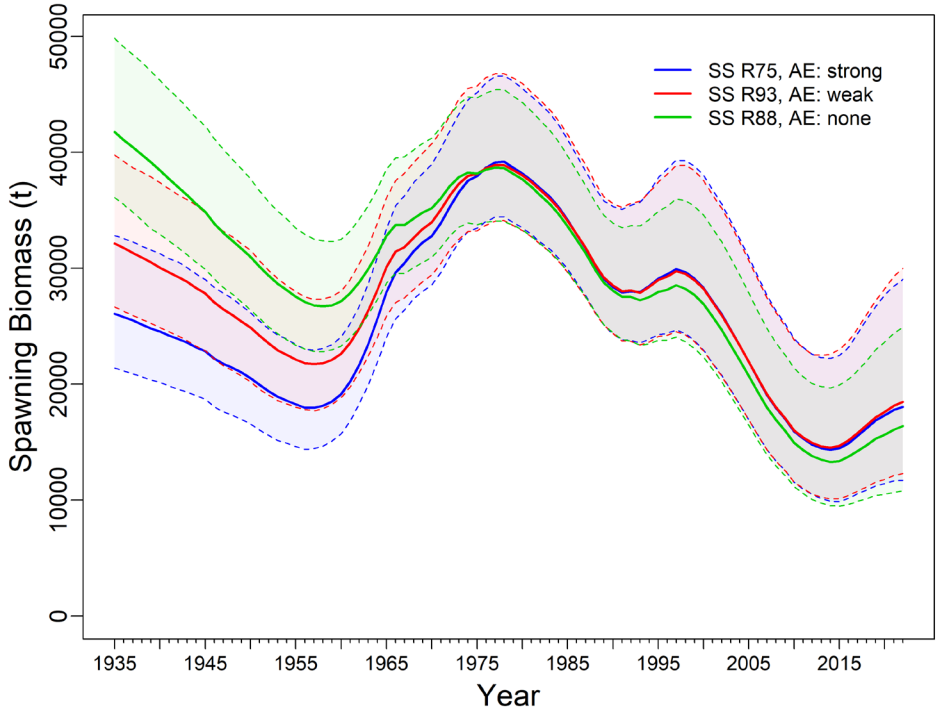

Figure H.13. Comparison of MCMC female spawning biomass trajectories from three SS runs with different ageing error (AE) scenarios:R75 with strong AE based on CVs of length-at-age, R93 with weak AE based on CVs of age based on age readers' determination of age, and R88 with no ageing error. Solid lines depict medians, dashed lines depict 0.05 and 0.95 quantiles.

H.5. REFERENCES – BRIDGING ANALYSIS

DFO. 2022. Proceedings of the Pacific regional peer review on Yellowmouth Rockfish (*Sebastes reedi*) stock assessment for British Columbia in 2021; September 8-9, 2021. DFO Can. Sci. Advis. Sec. Proceed. Ser. 2022/003.

Edwards, A.M., Haigh, R., and Starr, P.J. 2012. Stock assessment and recovery potential assessment for Yellowmouth Rockfish (*Sebastes reedi*) along the Pacific coast of Canada. DFO Can. Sci. Advis. Sec. Res. Doc. 2012/095: iv + 188 p.

Fournier, D.A, Hampton, J., and Sibert, J.R. 1998. MULTIFAN-CL: a length-based, age-structured model for fisheries stock assessment, with applications to South Pacific albacore, *Thunnus alalunga*. Can. J. Fish. Aquat. Sci. 55:1-12.

Francis, R.I.C.C. 2011. Data weighting in statistical fisheries stock assessment models. Can. J. Fish. Aquat. Sci. 68(6): 1124–1138.

Hilborn, R., Maunder, M., Parma, A., Ernst, B., Payne, J., and Starr, P. 2003. Coleraine: A generalized age-structured stock assessment model. User's manual version 2.0. University of Washington Report SAFS-UW-0116. Tech. rep., University of Washington.

Methot Jr, R.D., Wetzel, C.R., Taylor, I.G., Doering, K.L., and Johnson, K.F. 2021. Stock Synthesis User Manual, version 3.30.17. NOAA Fisheries, Seattle WA. iv + 233 p.

Starr, P.J., and Haigh, R. 2021. Redstripe Rockfish (*Sebastes proriger*) stock assessment for British Columbia in 2018. DFO Can. Sci. Advis. Sec. Res. Doc. 2021/014: vii + 340 p.